SHIMADZU

Excellence in Science
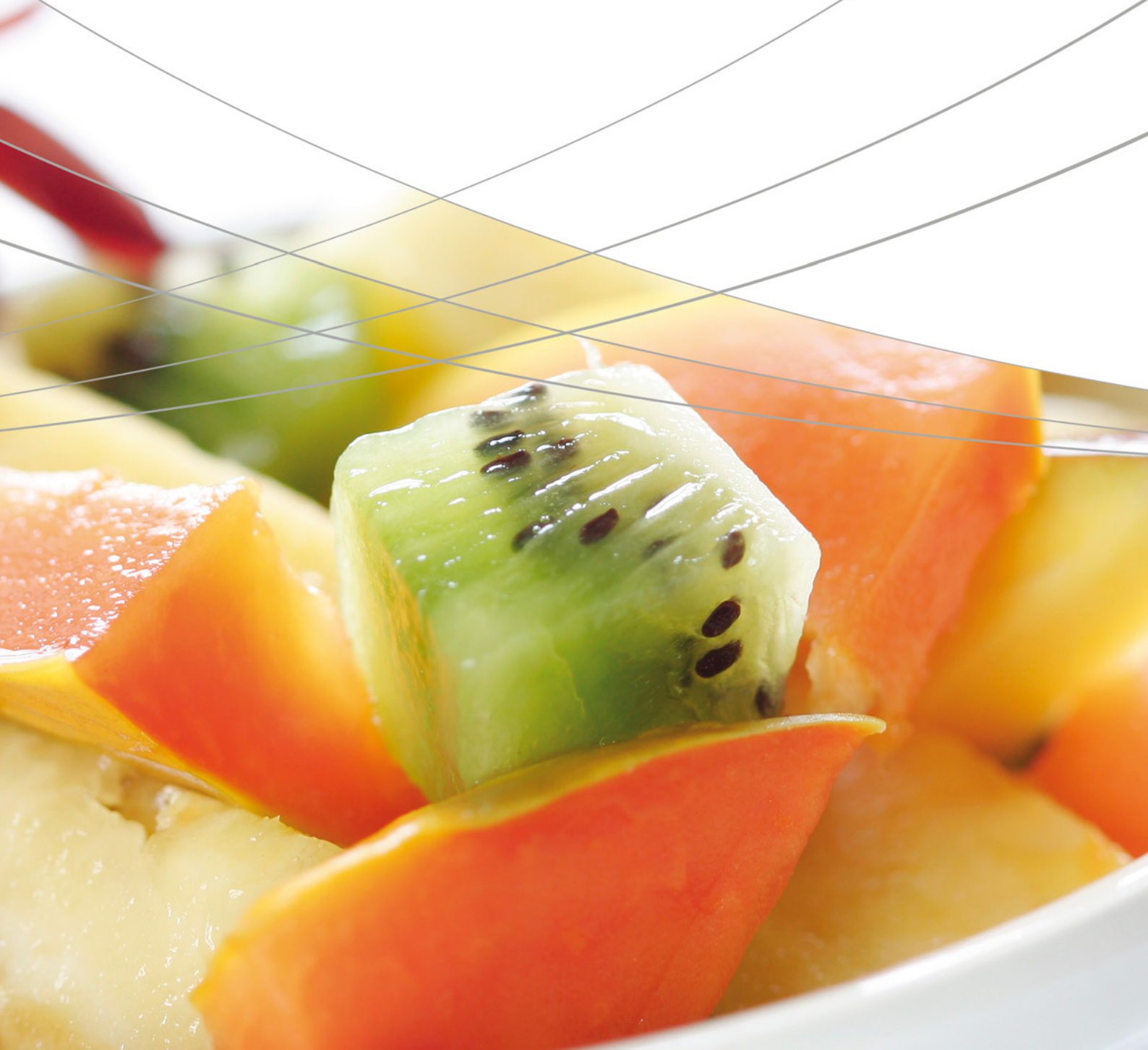
Application Handbook

Food, Beverages, Agriculture

Release 2

Food, Beverages and Agriculture

Regarding food, water, beverages and agricultural cropland, the increasing world population is one of the biggest challenges of mankind. How can access be provided to sufficient and safe food as well as clean water? How can crop failure be prevented? Can new food sources be explored?

In industrial nations, the percentage of convenience food has been increasing. How can new ingredients be discovered to replace existing ones regarding calories, fat and flavoring substance in order to support a healthier life?

Food and beverages industries

In food and beverages industries, analytical instrumentation methods are essential to ensure high product quality during several steps in the production process, such as quality control of raw materials (e.g. natural products) as well as their treatment during and after production. Whether it is the analysis of degradation of edible oils or the vitamins in baby food, the quantification of food additives or pesticide residues, the quality control of packing materials concerning color and possible contaminants or the determination of distinct aromas found in natural products – the demands of high-throughput food and beverage QA/QC laboratories require high-speed and high-quality analysis.

The quality of food is not only about its ingredients and raw materials, but also about its texture which complements the experience in the moment of consumption. Crispness, gumminess, softness/hardness are all important properties which enhance the taste sensation when people eat.

Agriculture

While the agriculture industry undergoes a shift from natural crop development to the use of biological agents, the fundamental mission of the industry remains the same: providing the world with healthy products. To ensure the health of crops, reliable instruments are needed that provide accurate, timely data on such critical areas as water supply, soil composition and animal feeds.

Nutraceuticals

The natural products industry has undergone a tremendous amount of growth in the last decade. With this dynamic growth, there has been a surge of regulations to monitor the development process and ensure the safety of the end product, e.g. regarding herbs, botanicals, supplements and organic foods.

Shimadzu's broad range of analytical instruments provide the food, beverages and agricultural industries with leading technologies in chromatography (GC, UHPLC), mass spectrometry (GC-MS, LC-MS, MALDI), sum parameter (TOC), spectroscopy (UV-Vis, FTIR, AAS, ICP-OES, EDX) and material testing. Based on most modern hardware and software, Shimadzu's systems can be used in highly regulated environments and are compliant with regulations such as FDA 21 CFR Part 11 and GLP.

www.shimadzu.eu/food-beverages-agriculture

Contents

![Shimadzu logo] SHIMADZU
Excellence in Science

1. Chromatography

1. Chromatography

1.1 Gas Chromatography

Chromatographic separation and analysis of volatile and semi volatile components in food, beverages, liquors as well as packing materials are used for food packaging. Gas chromatography is a key technique in qualitative and/or quantitative analysis of food composition, natural products, food additives, flavor and aroma compounds and contaminants such as pesticides and environmental pollutants.

No. 10   High-sensitivity analysis of impurities in gas (food additives)

SHIMADZU
Excellence in Science

Application Data Sheet	GC Gas Chromatograph
No.10	# High-Sensitivity Analysis of Impurities in Gas (1)

Gases used in a variety of fields, such as industrial, medical, and food, typically have to meet the established quality standards, which vary according to the application. This requires performing gas purity tests. The Shimadzu Tracera high-sensitivity gas chromatograph is equipped with a barrier discharge ionization detector (BID) that permits the simultaneous high-sensitivity analysis of inorganic gases and lower hydrocarbons.

This data sheet introduces the impurity analysis of ethylene and carbon dioxide food additives using Tracera.

Analysis Examples

1. Analysis of Impurities in Ethylene

Ethylene is an important chemical used as feedstock in a variety of applications and its purity is essential. Fig. 1 shows an ethylene chromatograph. H_2 (30 ppm), CO (2 ppm), CO_2 (15 ppm), and CH_4 (30 ppm) were detected as trace impurities.
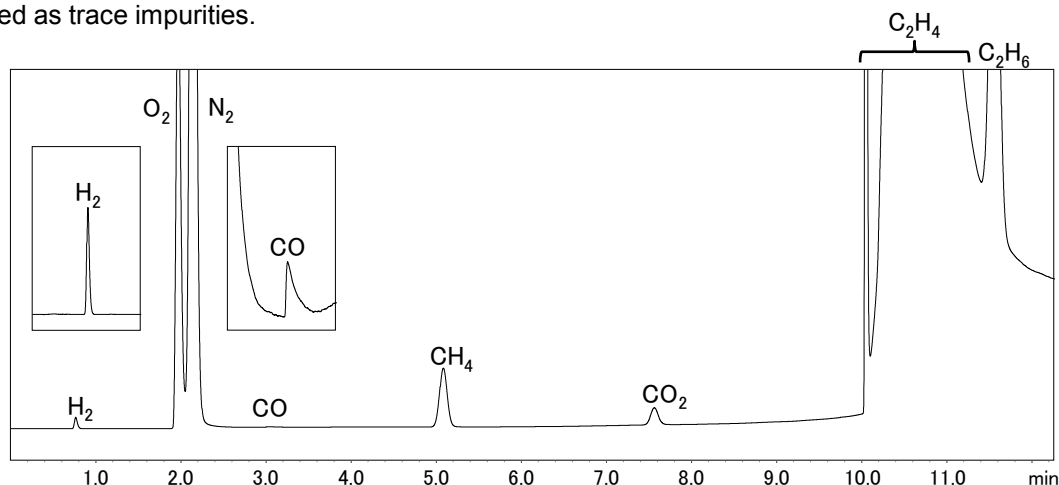
Fig. 1: Chromatograph of Impurities in Ethylene   Note: With baseline correction

2. Impurity Analysis of Carbon Dioxide Food Additive

Quality standards have been established for carbon dioxide gas used as food additives to ensure that it contains no components harmful to human health.
Fig. 2 shows the chromatogram of a carbon dioxide food additive. Trace impurities of CH_4 (2.2 ppm) and C_2H_4 (1.5 ppm) were detected.

Fig. 2: Chromatograph of Impurities in Carbon Dioxide Food Additive

Note: With baseline correction

Instruments Used

Gas Chromatograph	Tracera (GC-2010 Plus A + BID-2010 Plus)
Gas Sampler	MGS-2010
Software	GCsolution
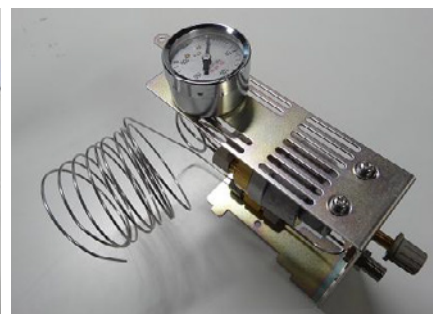
Valve Assembly   Manual Flow Controller for Purging

Fig. 3: Shimadzu Tracera High-Sensitivity Gas
           Chromatograph

Fig. 4: MGS-2010 Gas Sampler

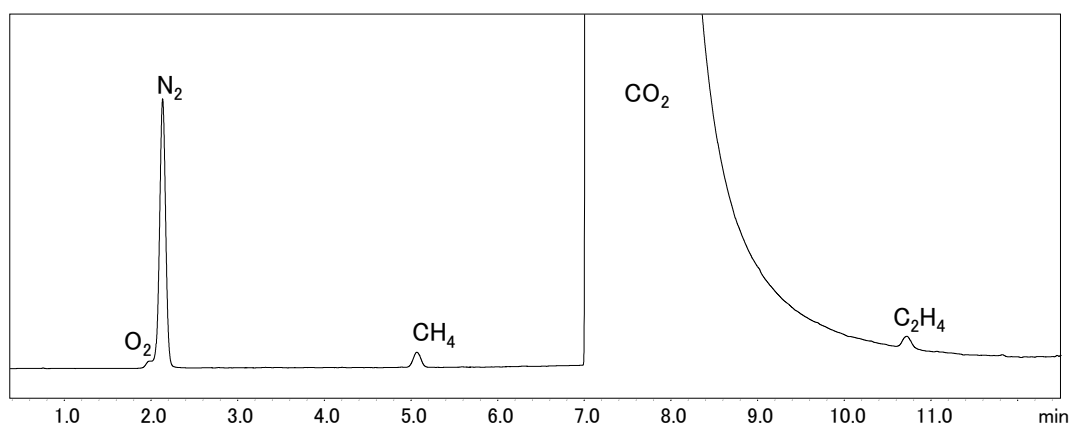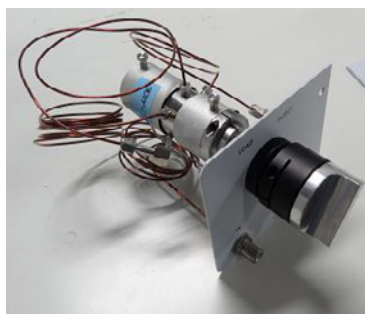The MGS-2010 is a manual gas sampler for the GC-2010 Plus. It is equipped with a purge mechanism to reduce leakage of ambient air into the device. Using the helium-purged MGS-2010 to inject the sample gas when analyzing atmospheric components such as O_2 and N_2 with Tracera can reduce contamination from atmospheric air.

Analytical Conditions

Column	Micropacked ST
Column temp.	35 °C (2.5 min) – 20 °C /min - 250 °C (0 min) - 15 °C /min - 270 °C (5.42 min) Total: 20 min
Carrier gas	He
Carrier gas control	Pressure
Pressure program	250 kPa (2.5 min) – 15 kPa/min – 400 kPa (7.5 min) (He)
Injection mode	Split (1:5)
Injection port temp.	150 °C
Detector temp.	280 °C
Discharge gas	He: 70 mL/min
Injection volume	1 mL

SHIMADZU

Shimadzu Corporation

www.shimadzu.com/an/

1. Chromatography

1.2 Liquid Chromatography

HPLC and UHPLC systems are able to quantitatively analyze substances in mixtures containing multiple ingredients by separating and detecting target substances. They are also used to purify specific substances once they are separated. Shimadzu offers a wide variety of application-specific systems, such as automated sample pretreatment systems for amino acid analysis or on-line sample trapping for quantification of residual pesticides.

HPLC-SEG-01	UHPLC assay for stevia glycosides
HPLC-SEG-02	UHPLC assay for polyphenols, methylxan thines, sweeteners, flavouring substances and some common preservatives as present in dark chocolate products
HPLC-SEG-03	Comprehensive HPLC analysis of alkaloids and permitted additives in dark chocolate products
L435	Quantitation by HPLC and identification by LC/MS for total aflatoxins in food
L434	UF-Amino station LC/MS ultra fast amino acid analysis system (part 2)
L441	High speed, high resolution analysis (part 46) analysis of pre-column derivatized biogenic amines by the Nexera SIL-30AC autosampler
L467	Analysis of sugars in orange juice and grape juice by Prominence-i and differential refractive index detector
L471	Comprehensive two-dimensional analysis of polyphenols in red wine using Nexera-e coupled with SPD-M30A
L474	Analysis of oligosaccharides in japanese sake using ELSD-LT II
L481	Analysis of sugars and sugar alcohols in energy drink by Prominence-i with RID-20A
L437	High speed, high resolution analysis (part 45) analysis of pre-column derivatized amino acids by the Nexera SIL-30AC autosampler (part 2)
L484	Analysis of nivalenol and deoxynivalenol in wheat using Prominence-i
L491	Comprehensive 2D separation of carotenoids in red chili pepper by the Nexera-e system
L492	Comprehensive 2D separation of triglycerides in vegetable oil with ELSD/LCMS-IT-TOF detection
L497	Using the Nexera UC online SFE-SFC-MS system to analyze residual pesticides in agricultural products
L498	Analysis of cyanide ion and cyanogen chloride in mineral water by post-column ion chromatography
L501	Analysis of vitamin E in a commercial supplement by offline SFE-SFC-PDA
L502	Analysis of residual pesticides in agricultural products using Nexera UC off-line SFE-GC/MS system

![SHIMADZU]

Application Note

High Performance Liquid Chromatography

No. HPLC_SEG_01

UHPLC assay for stevia glycosides
Gesa J. Schad, SEG

■ Keywords:

UHPLC, Nexera X2, Stevia Glycosides

■ Introduction:

With today's growing health awareness, there is an increasing interest in sugar substitutes in various areas of the food industry. Stevia, the natural alternative to artificial sweeteners, extracted from the Stevia rebaudiana plant has just recently been approved for use in the EU. Rebaudioside A is largely enriched in commercial Stevia products, while natural extract contains Stevioside as the major component. Hence, an HPLC assay for quality control purposes, must be able to clearly separate this critical peak pair.

■ Analytical Conditions:

System configuration:

A Shimadzu Nexera X2 UHPLC system was used consisting of two quaternary solvent pumps (LC-30AD) with two 5 channel degassers (DGU-20A5R), an autosampler (SIL-30AC), and a column oven (CTO-20AC). The system was also equipped with an SPD-M30A photo diode array detector.

Method:

Column: ACE Excel 2 Super C18, 150 x 2.1 mm
Mobile Phase: 10 mM NaH2PO4, pH 2.8 A: in H_2O
and B: in MeCN/H_2O (80:20 v/v)
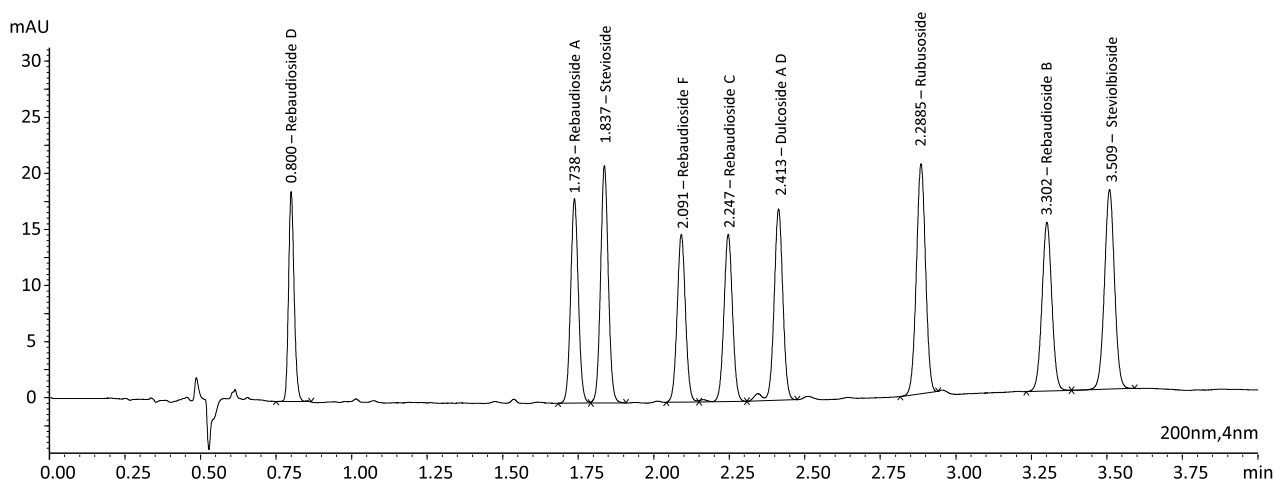Gradient: 39.5 – 48 % B: in 4 min
Cycle time: 7 min Flow rate: 0.6 mL/min
Temperature: 50 °C Injection Volume: 1 µL
Sample: 0.04 mg/mL of each compound in MeCN/H_2O (6:94)

■ Chromatogram

■ Conclusion /Result

A robust, selective, and sensitive separation of nine stevia glycosides in less than a third of the time of the JECFA approved assay was established successfully within two working days.

SHIMADZU

Application Note

No. HPLC_SEG_02

High Performance Liquid Chromatography

UHPLC assay for polyphenols, methylxanthines, sweeteners, flavouring substances and some common preservatives as present in dark chocolate products
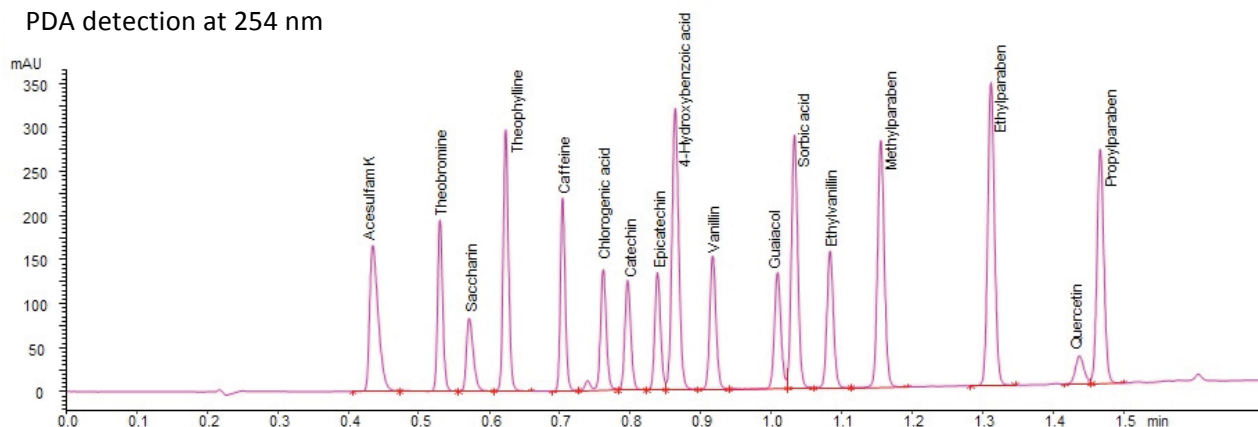
Gesa J. Schad, SEG

■ Keywords:

UHPLC, Nexera X2, polyphenols, sweeteners, methylxanthines, chocolate

■ Introduction:

Apart from the well-known negative effects of any high fat, high sugar food product, there is also evidence of health benefits related to chocolate consumption. These positive effects such as lowering blood pressure, antioxidant properties, reduction in the risk of cardiovascular disorder and increasing the cognitive abilities are all attributed to the flavanoid content, which is only relevant in dark chocolate products (≥ 40 % cocoa). However, a high cocoa and therefore flavanoid content comes with an even higher amount of less desirable alkaloids, namely the stimulants caffeine and thebromine. In addition to the natural products found in cocoa beans there is a large number of permitted additives that can be added to chocolate products to alter the taste, texture or expiry date, like artificial or natural sweeteners, flavouring compounds or preservatives. In order to monitor the composition and therefore quality of cocoa containing food an analytical method needs to enable individual quantification of any of these possible ingredients.

■ Analytical Conditions:

System configuration:

A Shimadzu Nexera X2 UHPLC system was used consisting of two quaternary solvent pumps (LC-30AD) with two 5 channel degassers (DGU-20A5R), an autosampler (SIL-30AC), and a column oven (CTO-20AC). The system was also equipped with an SPD-M30A photo diode array detector.

Method:

Column: ACE Excel 2 C18-Amide, 100 x 2.1 mm

Mobile Phase: 10 mM $HCOONH_4$, pH 2.8 A: in H_2O and B: in $MeCN/H_2O$ (90:10 v/v)

Gradient: 5 – 85 % B in 1.5 min

Cycle time: 2 min   Flow rate: 1.2 mL/min

Temperature: 42 °C   Injection Volume: 2 µL

Sample: ~ 0.05 mg/mL of each compound in $MeCN/H_2O$ (5:95)

■ Conclusion /Result

A robust, fast and sensitive UHPLC method for the simultaneous separation of polyphenols, methylxanthines, sweeteners, flavouring substances and preservatives in dark chocolate products has been developed.

■ Chromatogram

PDA detection at 254 nm

SHIMADZU

Application Note

No. HPLC_SEG_03

High Performance Liquid Chromatography

Comprehensive HPLC analysis of alkaloids and permitted additives in dark chocolate products

G.J. Schad, SEG

■ **Keywords:**

Nexera-e, comprehensive LC, polyphenols, sweeteners, methylxanthines, chocolate

■ **Introduction:**

A comprehensive two-dimensional LC method for the simultaneous determination of polyphenols, methylxanthines, sweeteners, flavouring substances, as well as some common preservatives has been developed. Instead of employing various methods for the different groups of substances, this multidimensional approach allows for screening of all the compounds of interest in one single run, by using a combination of two reversed phase analyses with the largely different selectivity of an ODS column in the first and an amide type bonded phase in the second dimension. This online 2D approach offers enhanced resolving power compared to a one dimensional run by employing two successive separations, with different selectivity in a single analysis.

■ **Analytical Conditions:**

System configuration:

A Shimadzu Nexera-e 2D UHPLC system was used consisting of four binary solvent pumps (LC-30AD) with one 3 channel (DGU-20A3R) and a 5 channel degasser (DGU-20A5R), an autosampler (SIL-30AC), and a column oven (CTO-20AC) equipped with two 6-port-2-position valves (FCV-32AH) connected with two 20 µl sample loops. The system was also equipped with an SPD-M30A photo diode array detector.

1st dimension method:

Column: ACE 3 Super-C18, 150 x 1 mm, 3 µm

Mobile Phase: 10 mM $HCOONH_4$, pH 2.8 A: in H_2O and B: in MeOH/H_2O (90:10 v/v)
Gradient: 25 – 100 % B in 60 min
Cycle time: 90 min Flow rate: 0.01 mL/min
Temperature: 42 °C Injection Volume: 10 µL
Sample: ~ 0.05 mg/mL of each compound in MeCN/H2O (5:95)

2nd dimension method:

Column: ACE Excel 2 C18-Amide, 100 x 2.1 mm

Mobile Phase: 10 mM $HCOONH_4$, pH 2.8 A: in H_2O and B: in MeCN/H_2O (90:10 v/v)
Gradient: 5 – 85 % B in 1.5 min
Cycle time: 2 min Flow rate: 1.2 mL/min
Temperature: 42 °C Loop size: 20 µL

■ **Chromatogram**
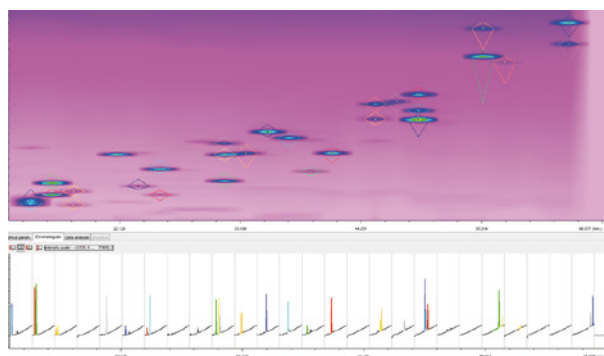
■ **Conclusion /Result**

After separate optimisation of the two gradient methods, 26 compounds of interest (see compound list) with large differences in structure and physicochemical properties could be separated and quantified in one two-dimensional LCxLC separation. In the chromatogram below the 2D plot the peaks separated in one chosen modulation time can be identified. Integration

contours and peaks in the chromatogram are colour coded for clarification.

Compound list
Acesulfam K
Theobromine
4-Hydroxybenzaldehyde
Sorbic acid
Quercetin
Methylparaben
Ethylparaben
Propylparaben
Catechin
4-Hydroxybenzoic acid
Ethylvanillin
Theophylline
Epicatechin
Vanillic acid
Aspartam
Guaiacol
Coumarin
Eugenol
Chlorogenic acid
Caffeine
Vanillin
Quinine sulfate
Benzoic acid
Vanillylmandelic acid

⊕ **SHIMADZU**

SHIMADZU
Excellence in Science

Application News

No.L435

High Performance Liquid Chromatography

Quantitation by HPLC and Identification by LC/MS for Total Aflatoxins in Food

Aflatoxins are mycotoxins that are extremely carcinogenic and acutely toxic. In Japan, foods in which the total aflatoxins (sum of B_1, B_2, G_1 and G_2 aflatoxins) are detected at levels exceeding 10 μg/kg are in violation of Article 6, Item 2 of the Food Sanitation Act[1].
Previously, in Application News articles L422, L428 and L430, we introduced examples of simultaneous analysis of these 4 substances (B_1, B_2, G_1 and G_2) using HPLC and UHPLC. In accordance with the test method[2] specified in the notification of August 16, 2011, after pretreatment using an immunoaffinity column, we conducted (1) quantitation using an HPLC system compliant with the test method, (2) identification using a LC/MS system compliant with the test method, and (3) rapid quantitation and identification using the Nexera UHPLC. Here, we present these analyses in addition to the results of the validation.

■ Total Aflatoxins Test Flow

Fig. 1 shows the complete workflow, including sample preparation, for total aflatoxins according to the specified test method (HPLC or LC/MS), and Fig. 2 shows the structures of those aflatoxins. For processed foods and spices, after extraction with a solution containing an organic solvent, the aflatoxins are purified using an immunoaffinity column (IAC). The fluorescence intensity of aflatoxins B_1 and G_1 is increased by following pretreatment procedure (A) with trifluoroacetic acid (TFA), and quantitative testing is carried out using an HPLC with an RF-20Axs fluorescence detector. If the aflatoxins are detected at a level greater than the reference value, it is re-dissolved in mobile phase without TFA derivatization after drying the purified solution eluted from IAC (pretreatment procedure (B)), and identification of the contained aflatoxins is carried out by LC/MS.
Among the properties of aflatoxins is their susceptibility to degradation when exposed to ultraviolet light, and their tendency in aqueous solution to adsorb to glass surfaces. Therefore, when conducting analysis, it is necessary to use silanized, amber glass vials or polypropylene vials to prevent reduced recoveries. Also, for analysis of actual samples, it is recommended to clean the column after each analysis with mobile phase containing a higher concentration of organic solvent than that used for the analysis.
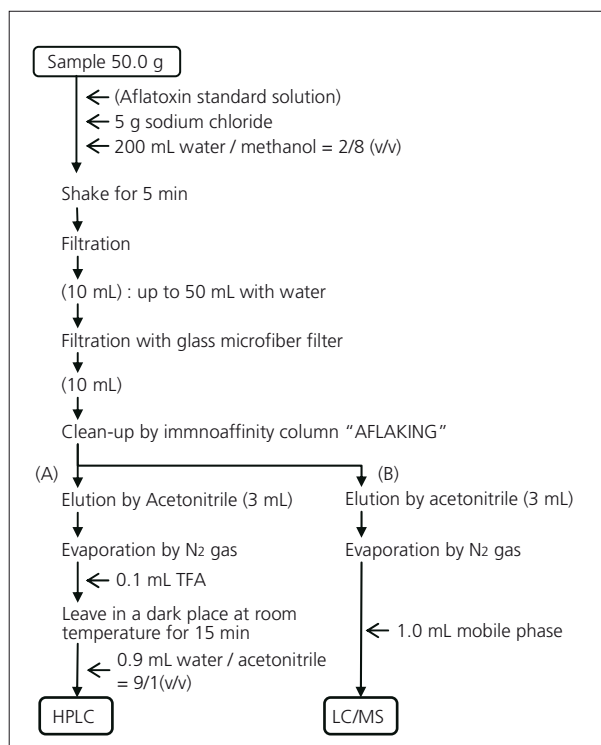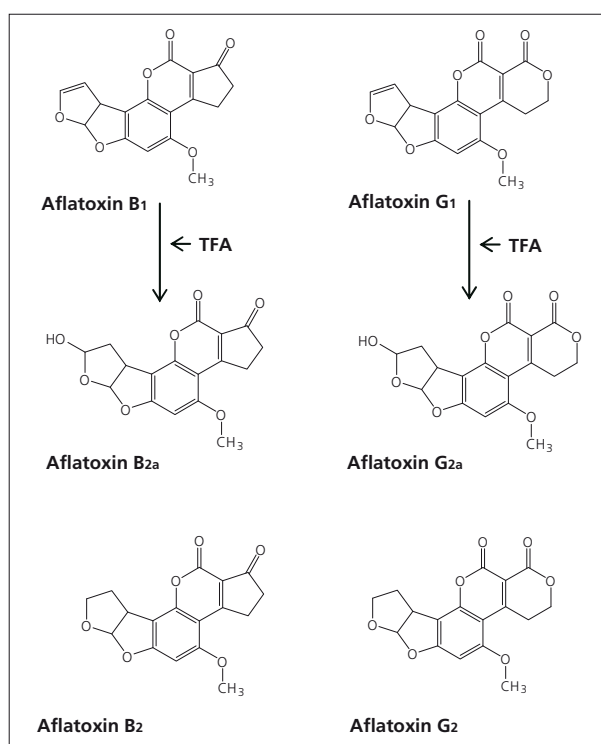

Fig. 1 Total Aflatoxin Test Workflow

Fig. 2 Structures of Aflatoxins

■ (1) Quantitation by HPLC –Accuracy and Precision–

Aflatoxins in commercially available roasted peanuts were processed according to procedure (A) in Fig 1, and analysis was conducted by HPLC using the test method to verify the recovery (accuracy) and repeatability (precision). The analytical conditions are shown in Table 1.
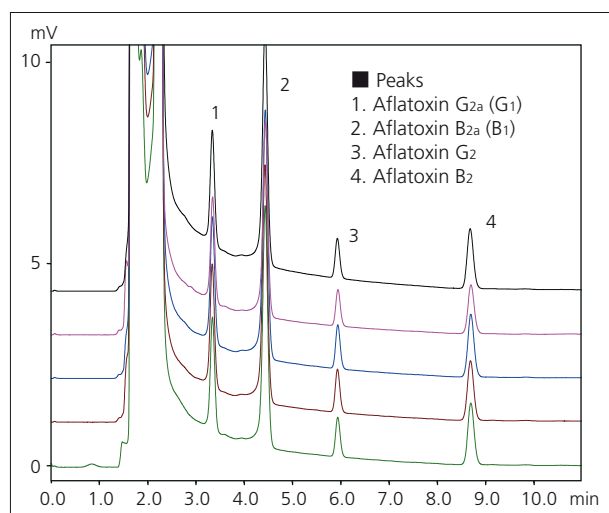
The roasted peanuts were spiked with aflatoxin B_1 and G_1 at a concentration of 0.8 µg/kg each, and aflatoxin B_2 and G_2 at a concentration of 0.2 µg/kg each (total aflatoxins: 2 µg/kg). The accuracy and precision with respect to each substance in repeat testing (n = 5) are shown in Table 2. Accuracy of 76–100 % was obtained that satisfied the criteria of the specified reference value in the guideline (70–110 %). In addition, the precision obtained was 5.7–9.6 %, which also met the specified reference value (less than 20 %).

Table 1 Analytical Conditions

Column	: Shim-pack FC-ODS (150 mmL. × 4.6 mmI.D., 3 µm)
Mobile Phase	: Water / Methanol / Acetonitrile = 6/3/1 (v/v/v)
Flow Rate	: 0.8 mL/min
Column Temp.	: 40 °C
Detection	: RF-20Axs, Ex at 365 nm, Em at 450 nm
RF Cell	: Conventional cell
Cell Temp.	: 25 °C
Injection Volume	: 20 µL

Table 2 Accuracy and Precision of Quantitation by HPLC

	Aflatoxin B_1	Aflatoxin B_2	Aflatoxin G_1	Aflatoxin G_2
Recovery (%)	79	90	76	100
%RSD	9.6	8.9	7.3	5.7

Fig. 3 Chromatograms of Roasted Peanuts Spiked with Aflatoxins (Quantitation by HPLC)

■ (2) Identification Testing by LC/MS

Commercially available roasted peanuts that were not spiked with the aflatoxin standard solution were subjected to dry processing according to procedure (B) in Fig. 1, and a matrix sample solution (blank) was prepared by dissolving the residue in 1 mL of 10 % acetonitrile solution. The matrix sample solution and aflatoxin standard solution were mixed 1:1, and standard addition matrix samples were prepared at 0.05, 0.25, 0.5, 2.5 and 5 µg/L, respectively (equivalent

to 0.2, 1, 2, 10, 20 µg/kg, respectively). Analyses (n = 6) were then conducted using the LCMS-8030 triple stage LC/MS/MS. Fig. 4 shows the MRM* chromatograms obtained from analysis of the 0.5 µg/L standard addition matrix sample, and Table 3 and Table 4 show the analytical conditions. The LCMS-8030 clearly demonstrated sufficient sensitivity to conduct identification testing.

*MRM...Multiple Reaction Monitoring
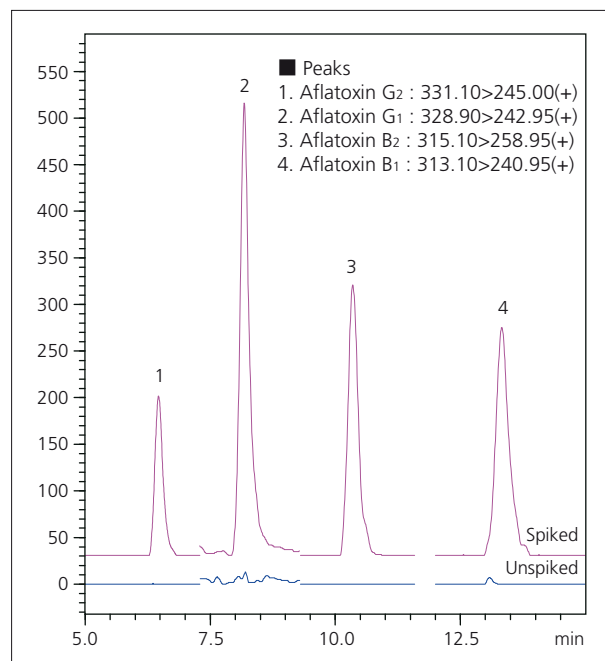
Fig. 4 MRM Chromatograms of Roasted Peanuts Matrix (Upper) Spiked, (Lower) Unspiked

Table 3 Analytical Conditions

[HPLC]	
Column	: Shim-pack FC-ODS (150 mmL. × 2.0 mmI.D., 3 µm)
Mobile Phase	: 10 mmol/L Ammonium acetate water / Methanol = 3/2 (v/v)
Flow Rate	: 0.2 mL/min
Column Temp.	: 40 °C
Injection Volume	: 6 µL
[MS]	
Probe Voltage	: +4.5 kV ESI-positive mode
Nebulizing Gas Flow	: 3 L/min
Drying Gas Flow	: 15 L/min
DL Temp.	: 250 °C
Heat Block Temp.	: 400 °C

Table 4 MRM Mode Parameters

Compound	Transition	Dwell time (ms)	CE (V)	Resolution (Q1, Q3)
Aflatoxin B_1	313.10 > 240.95	200	-40	Unit
Aflatoxin B_2	315.10 > 258.95	200	-33	Unit
Aflatoxin G_1	328.90 > 242.95	200	-30	Unit
Aflatoxin G_2	331.10 > 245.00	200	-32	Unit

In addition, to evaluate the validity of the standard addition method for quantitation of aflatoxins, we checked the linearity of the calibration curves of spiked matrix samples, in addition to the repeatability. Fig. 5 shows the calibration curves, and Table 5 shows the average area and repeatability of the peaks corresponding to 0.25, 0.5 and 5 µg/L. Excellent linearity was obtained over the range of 0.05–5 µg/L, with a coefficient of determination greater than $R^2 = 0.999$, and good repeatability was also confirmed. As a result, identification testing was confirmed to be possible using the LCMS-8030, and quantitation using calibration curves of matrix samples spiked with standards was also confirmed to be effective.

Fig. 6 shows an example of the quantitative testing results obtained using the Shimadzu Nexera UHPLC after conducting pretreatment of aflatoxin-added roasted peanuts according to Fig. 1 (B), and Table 6 shows the analytical conditions. The roasted peanuts were spiked with aflatoxins B_1 and G_1 at 2.4 µg/kg each, and aflatoxins B_2 and G_2 at 0.6 µg/kg each. The accuracy and precision obtained for each substance in repeat analysis (n = 5) are shown in Table 7. Accuracy of 76–80 % and precision of 4.5–6.5 % were obtained, that satisfied the criteria of the specified reference value in the guideline.

In addition to the extremely good sensitivity of this analytical method as shown in Application News L422 and L430, it was confirmed that this method is effective for rapid quantitative testing of aflatoxins.

Fig. 5 Calibration Curves of Matrix Samples Spiked with Aflatoxins (Roasted Peanuts, 0.05–5 µg/L)
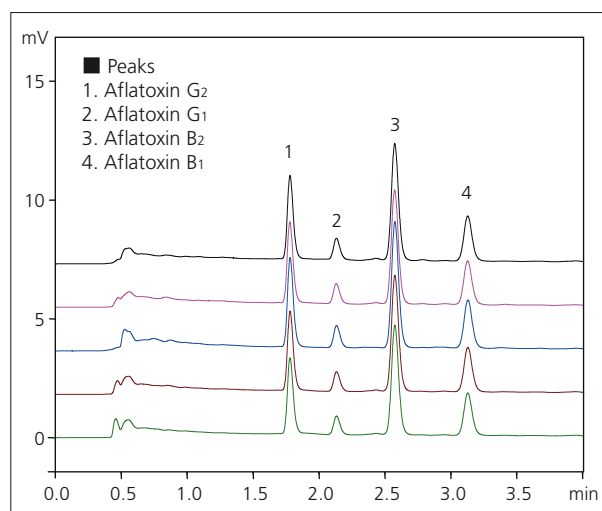
Fig. 6 Chromatograms of Roasted Peanuts Spiked with Aflatoxins (Direct Detection) (10 µL Injected)

Table 5 Average and Repeatability of Peak Area (n = 6)

	0.25 µg/L		0.5 µg/L		5 µg/L	
	Area	%RSD	Area	%RSD	Area	%RSD
Aflatoxin B_1	1010	6.37	2033	3.92	22936	1.49
Aflatoxin B_2	3156	1.87	6481	5.09	66012	0.54
Aflatoxin G_1	2209	6.07	4517	3.74	45841	1.45
Aflatoxin G_2	2296	5.96	4749	4.74	47250	0.83

Table 6 Analytical Conditions

Column	: Shim-pack XR-ODS II (100 mmL. × 3.0 mmI.D., 2.2 µm)
Mobile Phase	: Water / Methanol / Acetonitrile = 6/3/1 (v/v/v)
Flow Rate	: 1.0 mL/min
Column Temp.	: 50 °C
Detection	: RF-20Axs, Ex. at 365 nm, Em. at 450 nm
RF Cell	: Conventional cell
Cell Temp.	: 25 °C
Injection Volume	: 10 µL

■ (3) Rapid Quantitation and Identification by Nexera UHPLC with LCMS-8030

Although TFA derivatization is specified in the quantitative test by HPLC according to the official test method, if the obtained value for total aflatoxins exceeds the reference value, follow-up analysis is required. The additional pretreatment is done without TFA derivatization (in Fig. 1 (B) for LC/MS analysis). However, if detection with sufficient sensitivity is achieved through direct detection (without TFA derivatization) as specified in the quantitative test, sample preparation, quantitative testing and identification can all be done using just the procedure of Fig. 1 (B). As a result, such a complicated pretreatment procedure does not need to be repeated. Furthermore, UHPLC what enables the high-throughput analysis brings even greater efficiency of the test for total aflatoxin.
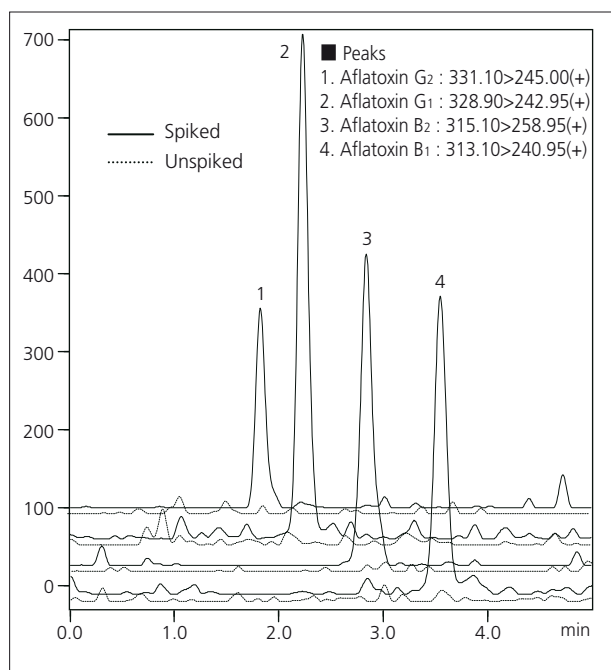
Table 7 Accuracy and Precision of Quantitation by UHPLC without Derivatization

	Aflatoxin B_1	Aflatoxin B_2	Aflatoxin G_1	Aflatoxin G_2
Recovery (%)	76	77	77	80
%RSD	4.5	5.1	6.1	6.5

Furthermore, since the LCMS-8030 is an LC/MS/MS that supports UHPLC, when used in combination with the high-speed analysis offered with the above-mentioned Nexera, rapid identification of aflatoxins becomes possible.

Fig. 7 shows the MRM chromatograms generated using high-speed analysis of the same sample of Fig. 4 using the analytical conditions of Table 8 and Table 9. All 4 aflatoxins eluted within 4 minutes, and identification was clearly obtained with sufficient sensitivity even under such high-speed conditions.

Fig. 8 shows the calibration curves generated using the same HPLC analytical conditions (Fig. 5) and matrix samples spiked with aflatoxins. Excellent linearity was obtained over the range of 0.05–25 µg/L, with a coefficient of determination greater than $R^2 = 0.999$. The peak area repeatability (%RSD, n = 6) obtained for each of the aflatoxin matrix samples at a concentration of 0.25 µg/L was B_1: 14.24 %, B_2: 5.33 %, G_1: 5.45 % and G_2: 18.9 %, demonstrating good repeatability even when using high-speed analysis.

Table 9 MRM Mode Parameters

Compound	Transition	Dwell time (ms)	CE (V)	Resolution (Q1, Q3)
Aflatoxin B_1	313.10 > 240.95	100	-40	Unit
Aflatoxin B_2	315.10 > 258.95	100	-33	Unit
Aflatoxin G_1	328.90 > 242.95	100	-30	Unit
Aflatoxin G_2	331.10 > 245.00	100	-32	Unit
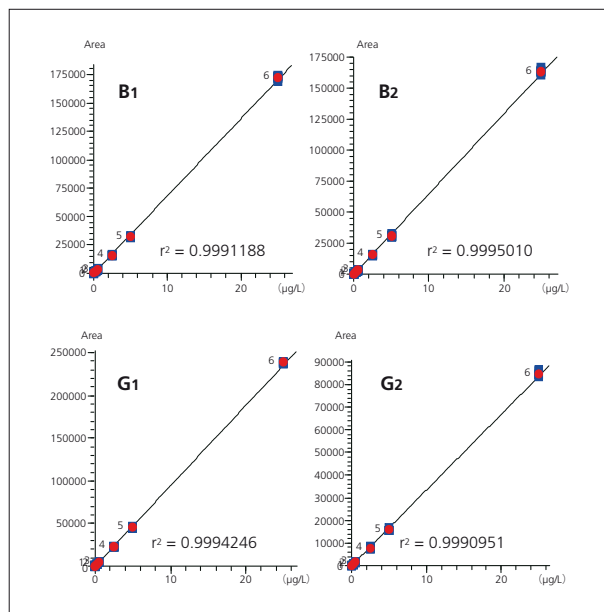
Fig. 8 Calibration Curves of Matrix Samples Spiked with Aflatoxins (Roasted Peanuts, 0.05–25 µg/L)

[References]
1) Handling of Foods Containing Aflatoxins (Japanese Ministry of Health, Labour and Welfare, Dept. of Food Safety Issue 0331 No. 5, March 31, 2011)
2) Test Method for Total Aflatoxins (Dept. of Food Safety Issue 0816 No. 1, August 16, 2011)

Peaks
1. Aflatoxin G_2 : 331.10>245.00(+)
2. Aflatoxin G_1 : 328.90>242.95(+)
3. Aflatoxin B_2 : 315.10>258.95(+)
4. Aflatoxin B_1 : 313.10>240.95(+)

Spiked
Unspiked

Fig. 7 MRM Chromatograms of Roasted Peanuts (Upper, Solid Line) Spiked, (Lower, Broken Line) Unspiked

Table 8 Analytical Conditions

[HPLC]
Column : Shim-pack XR-ODS Ⅱ (100 mmL. × 2.0 mmI.D., 2.2 µm)
Mobile Phase : 10 mmol/L Ammonium acetate water / Methanol = 3/2 (v/v)
Flow Rate : 0.45 mL/min
Column Temp. : 50 °C
Injection Volume : 6 µL
[MS]
Probe Voltage : +4.5 kV ESI-Positive mode
Nebulizing Gas Flow : 3 L/min
Drying Gas Flow : 15 L/min
DL Temp. : 250 °C
Heat Block Temp. : 400 °C

SHIMADZU

Shimadzu Corporation

www.shimadzu.com/an/

SHIMADZU
Excellence in Science

Application News

No.L434

High Performance Liquid Chromatography

UF-Amino Station LC/MS Ultra Fast Amino Acid Analysis System (Part 2)
Improved Sample Analysis Reliability

Analysis of amino acids is typically a time-consuming process, and although this analysis can be speeded up using HPLC or UHPLC for reversed phase pre-column derivatization of the amino acids, the reliability of the results can be adversely affected with samples containing complex matrices, such as biological or food samples. This can be due to insufficient separation of the impurities from amino acids or separation among the amino acids in the sample.

The new UF-Amino Station, a dedicated amino acid analysis system, adopts a mass spectrometer for detection. Mass spectrometry can provide excellent detection selectivity and highly reliable analysis even when the sample contains many components of interest or a complex matrix. Furthermore, the automated derivatization processing provided with the autosampler also contributes to improved reliability of quantitative values.

Here, we introduce the features of the UF-Amino Station that demonstrate its power in actual sample analysis.

■ Superior Selectivity with LC/MS Detection

Fig. 1 shows the results of analysis of amino acids in commercially available skim milk by the UV detection with pre-column derivatization using phenyl isothiocyanate (PITC) as a derivatization reagent (upper) and by using the UF-Amino Station (lower). If amino acids derivatized using PITC are analyzed using the same separation time as that using the UF-Amino Station, inadequate separation among amino acids or between contaminants and target amino acids may occur, adversely affecting the quantitative results. This is due mainly to the selectivity of the UV detection method, and even in the chromatogram of Fig. 1 (upper part), when the analysis time is the same as that using the UF-Amino Station, adequate separation is clearly jeopardized due to the contaminants. However, because the UF-Amino Station adopts an LC/MS as the detector, of each amino acid is conducted using a separate mass chromatogram (Fig. 1 (lower part)). This high detection selectivity minimizes the effects of amino acid interaction and the overlapping of amino acid and contaminant peaks in the quantitative results. The analytical conditions associated with the data of Fig. 1 are shown in Table 1.
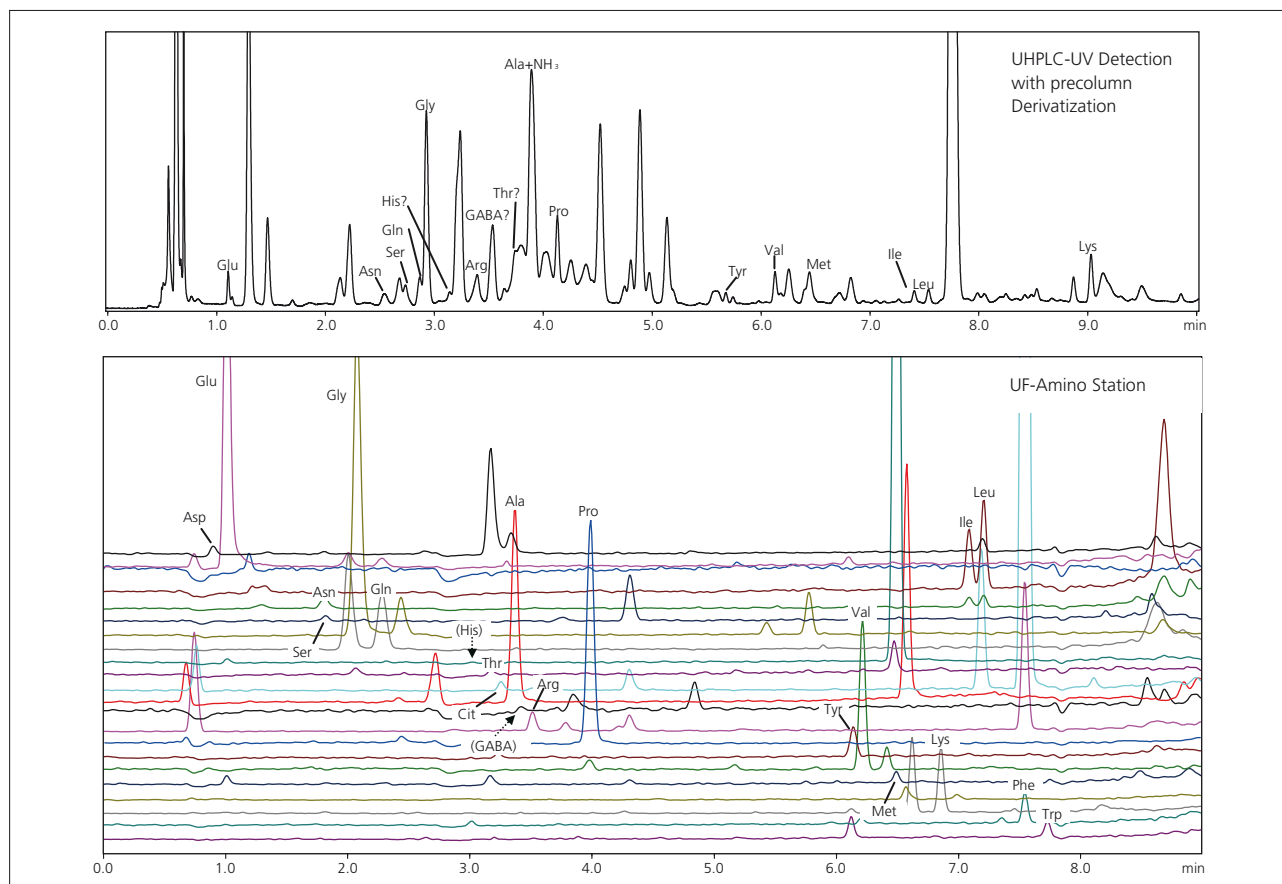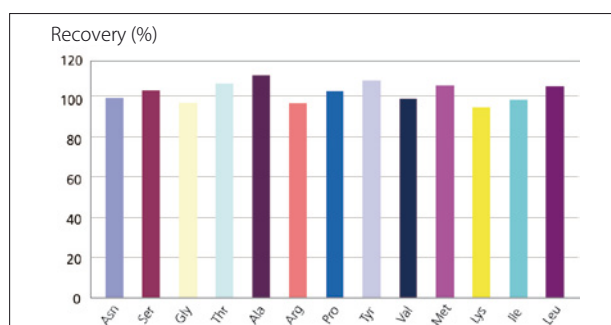

Fig. 1　Analysis of Amino Acids in Skim Milk: (Upper) UV Detection with PTC-Pre-Column Derivatization, (Lower) UF-Amino Station

Fig. 2 shows the results of amino acid recovery analysis of the same commercially available skim milk of Fig. 1, spiked with a standard solution of amino acids, this time using the UF-Amino Station. Preparation was conducted according to the specified method, which included deproteinization of the skim milk by dissolving it in heated water and adding acetonitrile, addition of amino acid standard solution, and addition of internal standard solution, etc. Analysis was conducted using the UF-Amino Station. The excellent recoveries shown in Fig. 2 demonstrate the high quantitative reliability that can be obtained even with a sample containing a highly complex matrix, such as that of nonfat dry milk.

Also, as introduced in Application News No. L433, the UF-Amino Station automates the derivatization of amino acids with the pretreatment feature provided in the SIL-20AC$_{PT}$ autosampler. This feature not only improves analysis efficiency, but also boosts the repeatability of the derivatization process, thus contributing to significantly higher precision.

Table 1 Analytical Conditions

[UHPLC, UV Detection with PTC-Precolumn Derivatization]
Column   : Shim-pack XR-ODS (100 mm L. × 3.0 mm I.D., 2.6 µm)
Mobile Phase   : (Potassium) phosphate buffer (pH 7.0) and Acetonitrile, Gradient Elution
Flowrate   : 0.9 mL/min
Column Temp.   : 40 °C
Reaction Reagent : Phenyl Isothiocyanate
Detection   : SPD-20AV at 254 nm with Semi-micro Cell
[UF-Amino Station]
Refer to *Application News No. L433*

Fig. 2 Recovery of Amino Acids in Skim Milk

■ **Biological Sample Applications**

Biological samples also contain many impurities which often can adversely affect the reliability of quantitative values when using UV detection with pre-column derivatization. Fig. 3 shows the results of the analysis of amino acids in a commercially available serum-free culture medium and rat plasma using the UF-Amino Station. In both samples, all components are clearly separated without any interference effects, clearly demonstrating that the UF-Amino Station is applicable for accurate analysis of amino acids in biological samples.

Serum-Free Culture
(Data provided by Ajinomoto Co., Inc.)
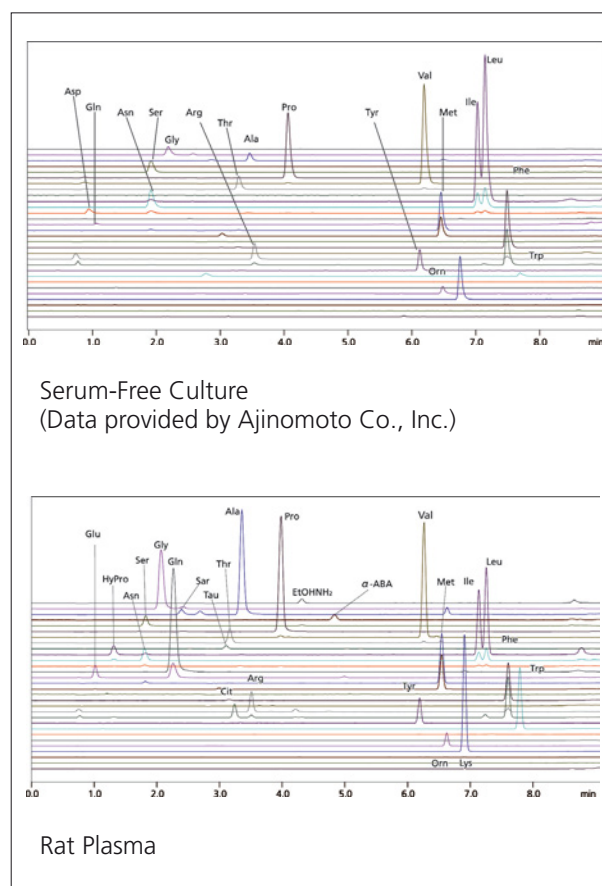
Rat Plasma

Fig. 3 Biological Sample Applications:
(Upper) Serum-Free Culture, (Lower) Rat Plasma

SHIMADZU

Shimadzu Corporation

www.shimadzu.com/an/

SHIMADZU
Excellence in Science

Application News

High Performance Liquid Chromatography

High Speed, High Resolution Analysis (Part 46) Analysis of Pre-Column Derivatized Biogenic Amines by the Nexera SIL-30AC Autosampler

No.L449

Biogenic amines are produced naturally by the enzymatic decarboxylation of amino acids in beverages and food. Biogenic amines such as these are also used as an indicator of food spoilage. Histamine, a substance that can cause allergy-like food poisoning, must not exceed 50 ppm in food in general according to FDA standards, 100 ppm in marine products in the EU, and 400 ppm in fish sauce according to the Codex International Food Standards. In addition, biogenic amines such as cadaverine and tyramine appear to intensify the allergy-like food toxicity of histamine.

In Application News articles L432 and L437, we introduced examples of the pretreatment functions of the SIL-30AC autosampler in the analysis of fluorescence-derivatized amino acids using o-phthalaldehyde (OPA). Here, we introduce an example of the analysis of fluorescent amines that were derivatized with OPA.

■ Simultaneous Determination of 7 Biogenic Amines

With this method, the pretreatment functions of the Nexera SIL-30AC autosampler were utilized to conduct automated derivatization of the amines using OPA. Table 1 shows the derivatization reagents used with this method, and Fig. 1 shows the reagent addition and mixing settings that were used for automated derivatization using the Nexera SIL-30AC autosampler. The analytical conditions that were used are shown in Table 2, and the chromatogram obtained from analysis of a standard solution is shown in Fig. 2. In addition to automating the derivatization step, the overall analysis time can be further shortened by using the overlapping injection feature that was introduced in Application News L437. This allows the next sample in the sequence to be derivatized and loaded into the needle for injection immediately after the analysis of the current sample is complete.

Table 1 Derivatization Reagents (10 mg/L each)

- Mercaptopropionic Acid Solution (MPA solution)
  3-Mercaptopropionic Acid 10 µL in 0.1 mol/L Borate Buffer (pH 9.2) 10 mL
- o - Phthalaldehyde Solution (OPA solution)
  o - Phthalaldehyde 10 mg in 0.1 mol/L Borate Buffer (pH 9.2) 10 mL
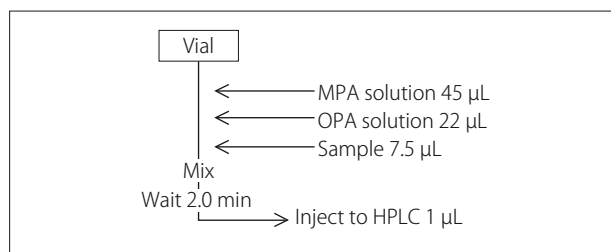
Fig. 1 Flowchart of Derivatization with SIL-30AC

Table 2 Analytical Conditions

Column	: Shim-pack XR-ODSⅢ (75 mm L. × 2.0 mm I.D., 1.6 µm)
Mobile Phase	: A : 100 mmol/L Acetate (Sodium) Buffer (pH 4.7)
	B : Acetonitrile
Time Program	: B.Conc. 15 % (0 min) →30 % (3 min) →40 % (8 min)
	→15 % (8.01-11 min)
Flowrate	: 0.5 mL/min
Column Temp.	: 40 °C
Injection Vol.	: 1 µL
Detection	: RF-20A$_{XS}$ Ex. at 330 nm, Em. at 440 nm
Cell Temp.	: 30 °C
Flow Cell	: Semi-micro cell

■Peaks
1. Histamine, 2. Agmatine, 3. Tyramine, 4. Tryptamine,
5. Putrescine, 6. Phenethylamine, 7. Cadaverine
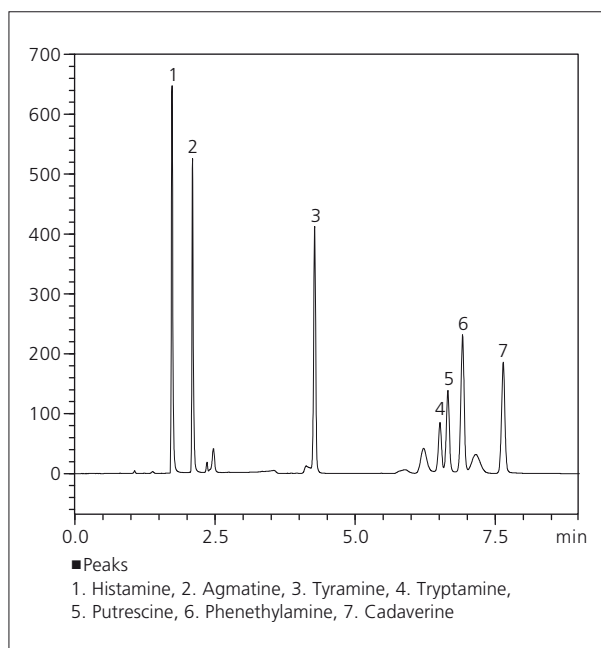
Fig. 2 Chromatogram of Standard Solution of 7 Biogenic Amines (10 mg/L each)

■ Linearity and Repeatability

The calibration curves generated using amine concentrations from 0.1 to 100 mg/L showed excellent linearity with a coefficient of determination (R^2) greater than 0.999 for all components. Table 3 shows the repeatability of retention times and area values obtained from repeated injections of 7 amines (n=6).

Table 3 Repeatability

	R.T. %RSD	Area %RSD
Histamine	0.067	0.70
Agmatine	0.055	0.72
Tyramine	0.037	0.60
Tryptamine	0.035	0.88
Putrescine	0.037	0.61
Phenethylamine	0.036	0.37
Cadaverine	0.030	0.84

■ Analysis of Foods and Beverages

Figs. 3 to 6 show the results of analysis of commercially available beer, wine, pork, and tuna samples. The beer and wine were passed through a 0.22 μm membrane filter, and then used as sample solutions. The pork and tuna were first stored at 37 °C for 24 hours to accelerate the production of amines. Then, 0.5 mol/L aqueous trichloroacetic acid solution was added to the homogenized samples, and following centrifugation, the supernatants were neutralized with 0.3 mol/L aqueous sodium hydroxide solution, and then passed through a 0.22 μm membrane filter to serve as sample solutions.

Fig. 4 Chromatogram of Wine
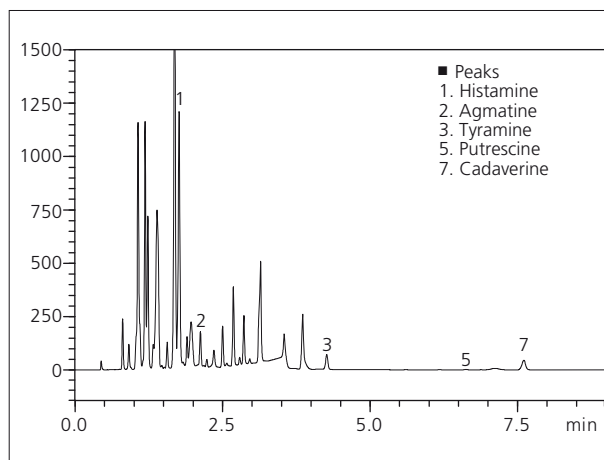
Fig. 5 Chromatogram of Pork
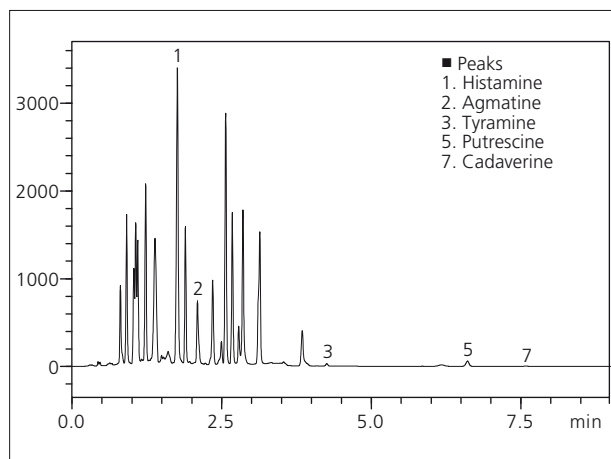
Fig. 3 Chromatogram of Beer

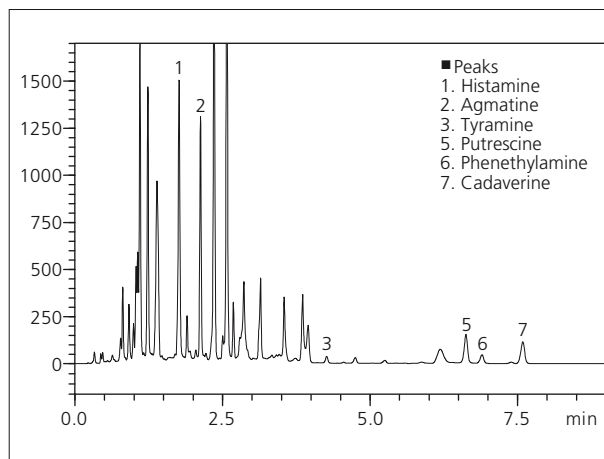**Fig. 6 Chromatogram of Tuna**

SHIMADZU

Shimadzu Corporation

www.shimadzu.com/an/

SHIMADZU
Excellence in Science
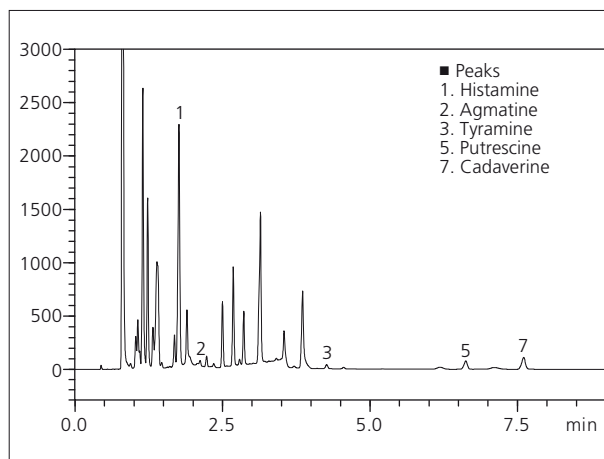
Application News

No.L467

High Performance Liquid Chromatography

Analysis of Sugars in Orange Juice and Grape Juice by Prominence-i and Differential Refractive Index Detector

As sugars display little ultraviolet absorption, a differential refractive index detector or an evaporative light scattering detector is used for their detection.

The new Prominence-i integrated high-performance liquid chromatograph can be connected to the RID-10A differential refractive index detector. Since the column oven can accommodate a 30-cm column for use in sugar analysis (ligand exchange column), and the temperature can be controlled up to 85 °C, it therefore supports applications that require a long column and high column temperature.

Here, we introduce an example of sugar analysis in juices using the Prominence-i with the RID-10A.

Table 1 Analytical Conditions

Column	: Shim-pack SCR-101N (300 mm L. × 7.9 mm I.D., 10 μm)
Mobile Phase	: Water
Flowrate	: 0.6 mL/min
Column Temp.	: 80 °C
Injection Volume	: 10 μL
Detection	: RID-10A
	Polarity +, Cell temp. 40 °C, Response 1.5 sec

■ Analysis of Sugar Standard Solution

Fig. 1 shows the results of analysis of a standard mixture of four sugars (maltotriose, sucrose, glucose, fructose) using a 10 μL injection (each at 20 g/L). The analytical conditions were as shown in Table 1. For the analytical column, we used the Shim-pack SCR-101N, a specialized sugar-analysis column that supports both the gel filtration and ligand exchange modes.

■ Linearity

Fig. 2 shows the linearity obtained using the conditions listed in Table 1. Calibration curves were generated for the four sugars using concentrations ranging from 0.4 to 20 g/L, and the mean area value obtained from each set of the three repeat measurements. Excellent linearity was obtained, with a coefficient of determination greater than $R^2=0.9999$ for all of the substances.
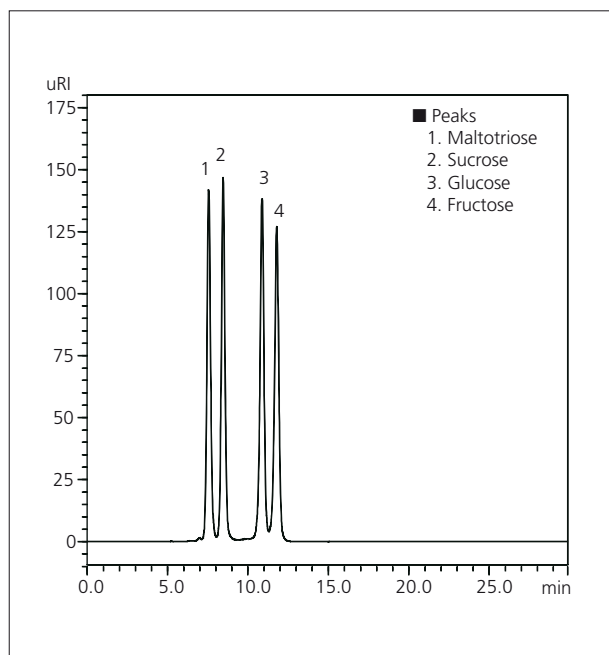
Fig. 1 Chromatogram of a Standard Mixture of Four Sugars (20 g/L each, 10 μL injected)
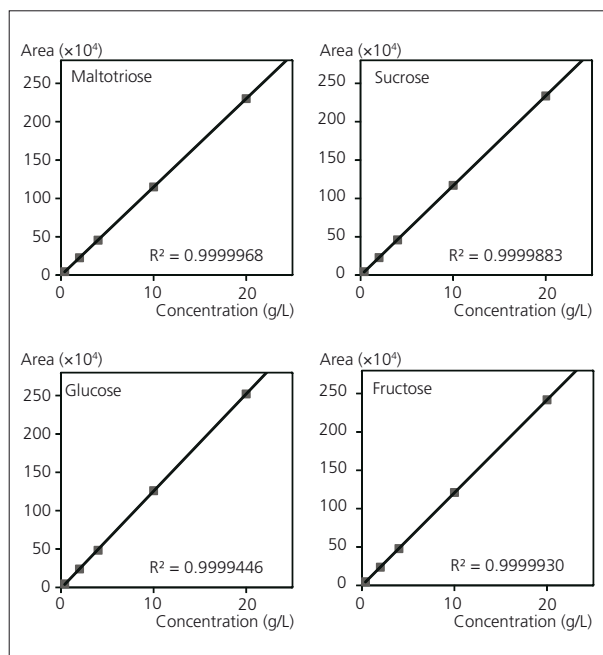
Fig. 2 Calibration Curves of a Standard Mixture of 4 Sugars (0.4 - 20 g/L, 10 μL injected)

■ Analysis of Orange Juice

Fig. 3 and 4 show the chromatograms obtained from analysis of Orange Juice A and Orange Juice B, respectively. Both Orange Juice A and B were diluted with water to obtain 10-fold dilutions, respectively, and after filtering the solutions through a 0.2 μm membrane filter, 10 μL each was injected. The analytical conditions used were the same as those shown in Table 1.

Sucrose, glucose and fructose were detected in both types of orange juice. Table 3 shows the content values for the respective sugars detected in the juices.

Table 3 Content of Each Sugar in Orange Juices

	Content (g/L)	
	Orange juice A	Orange juice B
Sucrose	36	36
Glucose	25	28
Fructose	27	34
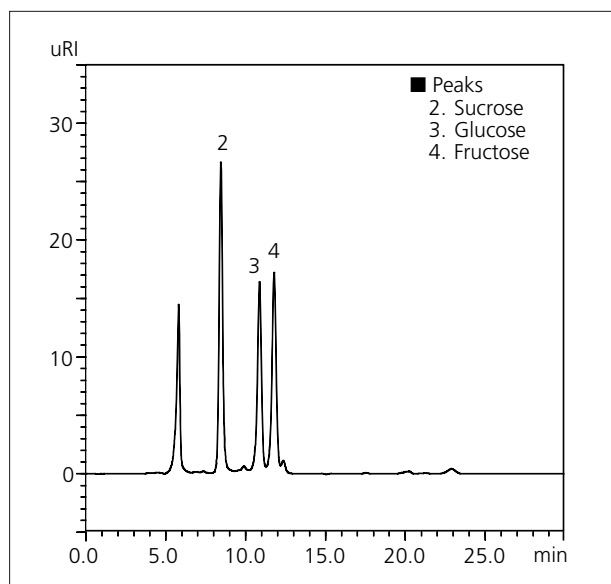
Fig. 3 Chromatogram of Orange Juice A (10 μL injected)

■ Analysis of Grape Juice

Fig. 4 shows a chromatogram obtained from analysis of grape juice. The grape juice was diluted with water to obtain a 10-fold dilution, and after filtering the solution through a 0.2 μm membrane filter, 10 μL of the prepared sample was injected. The analytical conditions used were the same as those shown in Table 1.

Glucose and fructose were detected in the grape juice. Table 4 shows the content values of the detected sugars.

Table 4 Content of Each Sugar in Grape Juice

	Content (g/L)
Glucose	50
Fructose	56
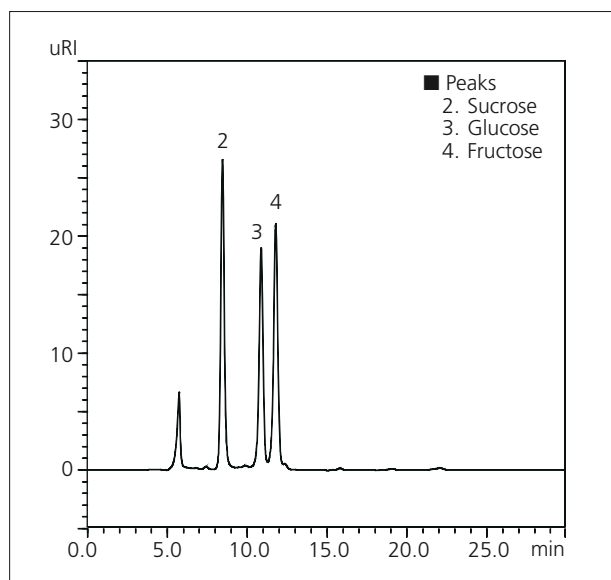
Fig. 4 Chromatogram of Orange Juice B (10 μL injected)
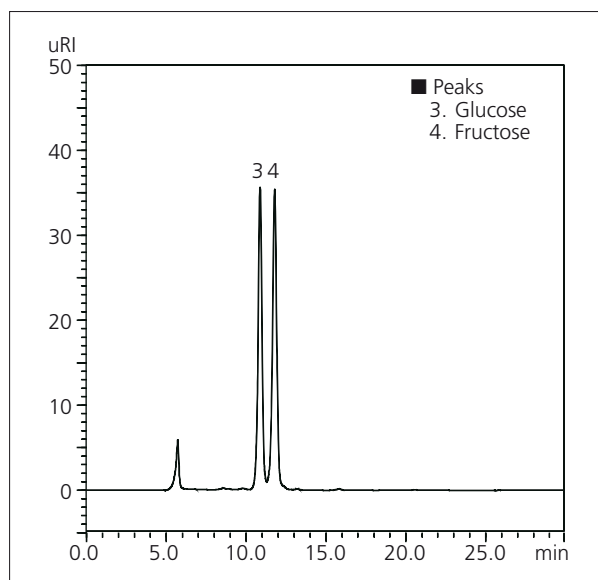
Fig. 5 Chromatogram of Grape Juice (10 μL injected)

SHIMADZU

Shimadzu Corporation

www.shimadzu.com/an/

SHIMADZU
Excellence in Science

Application News

High Performance Liquid Chromatography

Comprehensive Two-Dimensional Analysis of Polyphenols in Red Wine Using Nexera-e Coupled with SPD-M30A

No.L471

Phenolic compounds are created as secondary metabolites in plants. In many cases, their structures contain multiple aromatic rings and a hydroxyl group. These polyphenols are known to display antioxidant effects, and are said to be effective in preventing arteriosclerosis and cerebral infarction. Red wine is known to contain large amounts of polyphenols, including flavonoids and phenolic acids, and in recent years has attracted considerable attention due to the health benefits associated with these substances. Regarding the analysis of polyphenols in red wine, separation and quantitation of these polyphenols by simultaneous analysis using HPLC is difficult due to the presence of many coexisting substances. The Nexera-e comprehensive two-dimensional liquid chromatograph can be very effective for such an analysis.

■ **Comprehensive Two-Dimensional Separation with SPD-M30A at Appropriate Wavelengths for Respective Analytes**

By using the Nexera-e with a photodiode array detector (PDA), a target component can be separated from a complicated mixture of coexisting substances, and then quantitated, all in a single analysis. In the analysis, assuming ethyl gallate, tyrosol and rutin as the target compounds, the ChromSquare dedicated software was applied to generate a contour plot using the respective optimal wavelengths, thereby permitting both separation and quantitation. Fig. 1 shows the contour plots at the respective optimal wavelengths, along with the 1D and 2D gradient profiles generated using the auto-gradient feature.
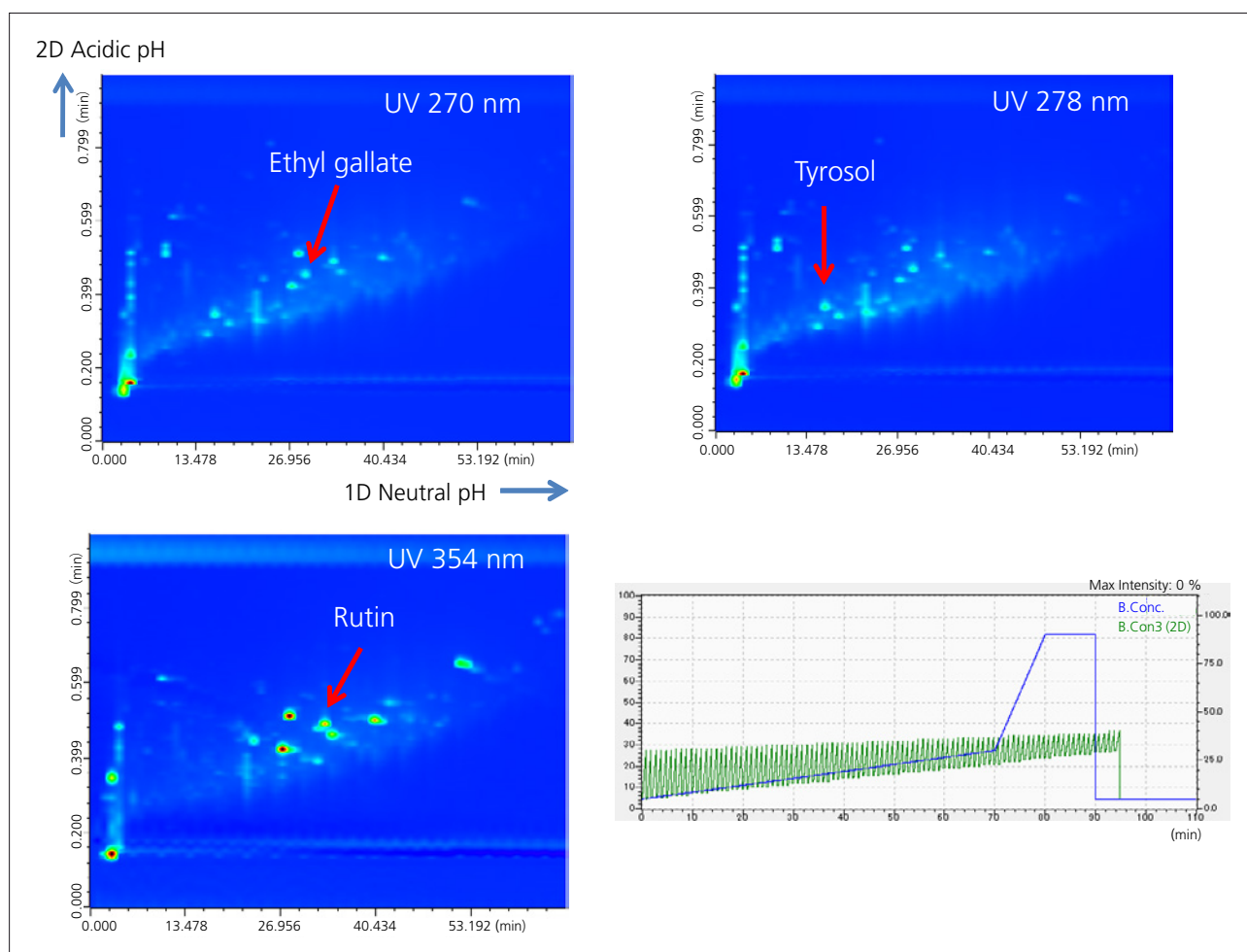
Fig. 1 Comparison of Comprehensive-2D Separation of Commercial Red Wine with Appropriate Wavelength Obtained Using "Auto-Gradient" Profile Feature

■ Quantitation of Ethyl Gallate, Rutin, and Tyrosol in Red Wine

The analytical conditions are shown in Table 1. We attempted to conduct separation by reversed-phase × reversed phase using a neutral phosphate buffer solution in the 1st dimension, and an acidic phosphate buffer solution in the 2nd dimension.

The calibration curve for each substance was generated using 6 concentrations in the range of 5 - 250 mg/L. The red wine sample was filtered through a 0.22 μm membrane filter, and then injected. Fig. 2 shows the calibration curve for ethyl gallate. Also, Table 2 shows the repeatability of the total and 2D retention times, respectively, for the three analytes, the blob area repeatability values corresponding to the peak areas, the calibration curve coefficient of determination (R^2) values, and the respective quantitation values.

Table 1 Analytical Conditions

1D Column	: Shim-pack XR-ODS Ⅱ (100 mm L. × 1.5 mm I.D., 2.2 μm)
Mobile Phase	: A : 10 mM (sodium) phosphate buffer pH = 6.8
	B : acetonitrile
Flowrate	: 0.05 mL/min
Time Program	: B Conc. 5 % (0 min) → 30 % (70 min) → 90 % (80 min) → 90 % (90 min)
	→ 5 % (90.1 min) → STOP (110 min)
Column Temp.	: 40 °C
Injection Vol.	: 3 μL
Loop Vol.	: 50 μL (Modulation time: 60 sec)
2D Column	: Kinetex XB-C18 (50 mm L. × 3 mm I.D., 2.6 μm)
Mobile Phase	: A : 10 mM (sodium) phosphate buffer pH = 2.6
	B : acetnitrile
Flowrate	: 2 mL/min
Time Program	: Auto-gradient: Initial. B Conc. 5 % (0 min) → 30 % (0.75 min) → 5 % (0.76 min)
	→ STOP (1 min)
	Final. B Conc. 30 % (0 min) → 40 % (0.75 min) → 30 % (0.76 min) → STOP (1 min)
	The initial and final B Conc. were changed in a stepwise manner.
Detector	: SPD-M30A photodiode array detector (high sensitivity cell 1 μL, wavelength = 270 nm, 278 nm, 354 nm)
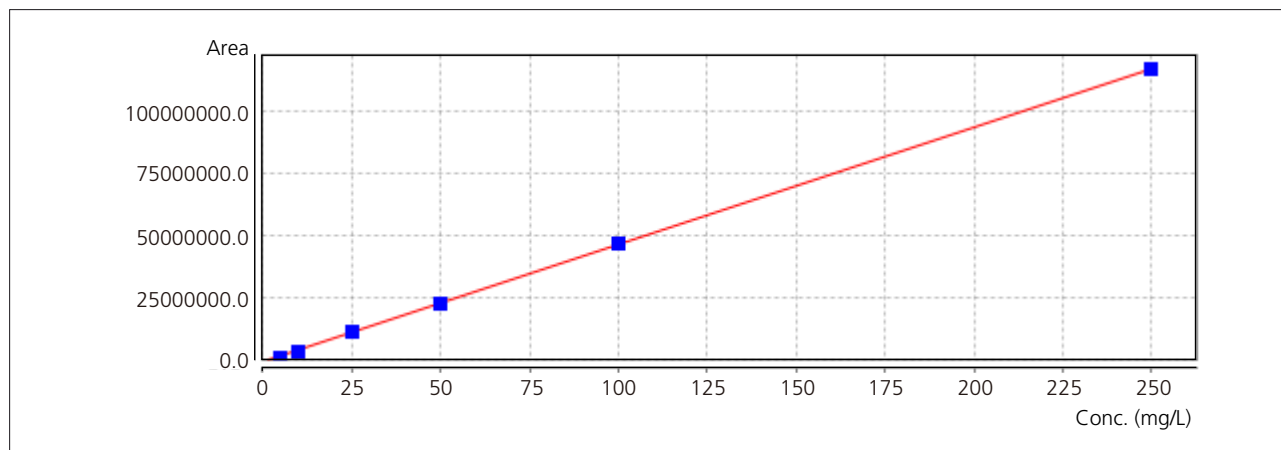
Fig. 2 Calibration Curve for Ethyl Gallate

Table 2 Repeatability of Retention Time and Blob Area (%RSD, n = 5), R^2 Value and Concentration (mg/L)

Compound	Total retention time	Retention time (2D)	Area		R squared	Concentration
Tyrosol	0.007	0.159	2.7		0.999804	101.5
Ethyl gallate	0.007	0.49	3.8		0.999864	15.1
Rutin	0.007	0.52	4.1		0.998805	14.2

SHIMADZU

Shimadzu Corporation

www.shimadzu.com/an/

SHIMADZU
Excellence in Science

Application News

No.L474

High Performance Liquid Chromatography

Analysis of Oligosaccharides in Japanese Sake Using an Evaporative Light Scattering Detector

An evaporative light scattering detector (ELSD) is an HPLC detector often called a "universal" detector because it can detect almost all non-volatile sample components, including those that do not absorb light. Although a differential refractive index detector (RID) can also be used for analysis of compounds with no chromophore, the ELSD removes any potential interference from the solvent peak that is eluted at the column void volume because detection occurs after volatilization and evaporation of the mobile phase. In addition, an ELSD detector has an advantage over an RID with its capability for analysis using gradient elution conditions.

Here we introduce an example of analysis of oligosaccharides in Japanese sake using the Nexera-i integrated high-performance liquid chromatograph, which includes a built-in UV detector. The ELSD-LT II evaporative light scattering detector was connected directly to the Nexera-i through an A/D acquisition board.

■ Analysis of a Standard Mixture of Isomaltooligosaccharides

A differential refractive index detector is typically used in the analysis of sugars, but it is limited because gradient elution cannot be used, therefore resulting in longer run times. Fig. 1 shows the chromatogram obtained from the analysis of a standard mixture of isomaltooligosaccharides using isocratic conditions, and Table 1 shows the analytical conditions that were used.

Table 1 Analytical Conditions: Isocratic Elution

Column	: Asahipak NH$_2$P-50 4E (250 mm L. × 4.6 mm I.D.)
Mobile Phase	: A: 10 mM Ammonium Acetate Buffer
	B : Acetonitrile
	Isocratic
	B 70 %
Flowrate	: 1.0 mL/min
Column Temp.	: 40 °C
Detection	: ELSD-LT II
	Temperature : 40 °C
	Gain : 7
	Nebulizer Gas : N$_2$
	Gas Pressure : 350 kPa

Under isocratic conditions, components that have long retention times tend to have broader peak shapes and diminished sensitivity because of the less intense response. Fig. 2 shows an example where a gradient was used for the same sample. The analytical conditions are described in Table 2. Using gradient elution with the ELSD permits separation of many components with high sensitivity because the narrower peaks produce a much higher signal.

Table 2 Analytical Conditions: Gradient Elution

Column	: Asahipak NH$_2$P-50 4E (250 mm L. × 4.6 mm I.D.)
Mobile Phase	: A : 10 mM Ammonium Acetate Buffer
	B : Acetonitrile
	Linear Gradient
	B 70 % → 40 %, 25 min
Flowrate	: 1.0 mL/min
Column Temp.	: 40 °C
Detection	: ELSD-LT II
	Temperature : 40 °C
	Gain : 7
	Nebulizer Gas : N$_2$
	Gas Pressure : 350 kPa

Peaks
1. Glucose
2. Isomaltose
3. Panose

Fig. 1 Standard Solution of Isomaltooligosaccharides: Isocratic Elution

Peaks
1. Glucose
2. Maltose
3. Isomaltose
4. Panose
5. Isomaltotriose
6. Isomaltotetraose
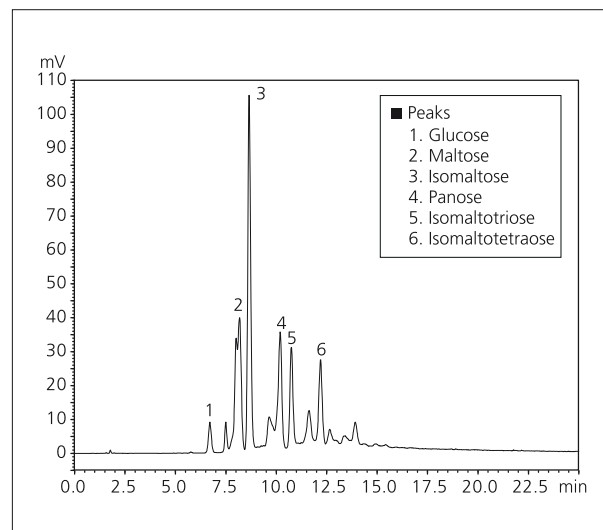
Fig. 2 Standard Solution of Isomaltooligosaccharides: Gradient Elution

■ **Quantitative Analysis of Oligosaccharides Included in Sake**

We used the ELSD to conduct quantitative analysis of glucose, isomaltose and panose that are present in sake. Pretreatment of the sake sample was performed according to the steps shown in Fig. 3. The calibration curves that were generated based on standard samples analyzed using the analytical conditions shown in Table 2 are shown in Fig. 4. Because the ELSD is not a spectroscopic detector, it does not obey Beer's law with a linear correlation between absorbance and concentration. Instead, a log-log plot of peak area and analyte quantity produces a linear response. Within the concentration range including 100, 200, 400, 1000, and 2000 mg/L (for glucose, 200, 400, 800, 2000, 4000 mg/L), excellent linearity was obtained with R^2 greater than 0.999. Fig. 5 shows the chromatogram of sake obtained using the conditions shown in Table 2. The quantitation results calculated using the calibration curves generated using the standard samples are shown in Table 3.

Sake 1 mL ← Water 1 mL
↓ ← Acetonitrile 3 mL
Mixing
↓
Filtration (0.2 µm membrane filter)
↓
HPLC 5 µL inj.
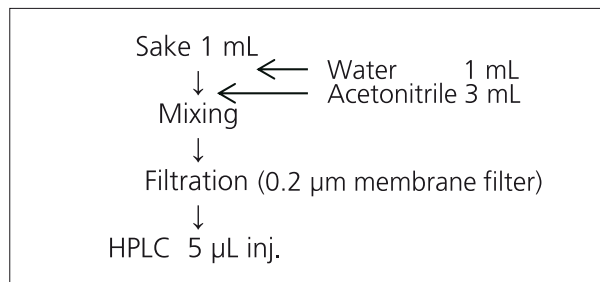
Fig. 3 Pretreatment of Sake
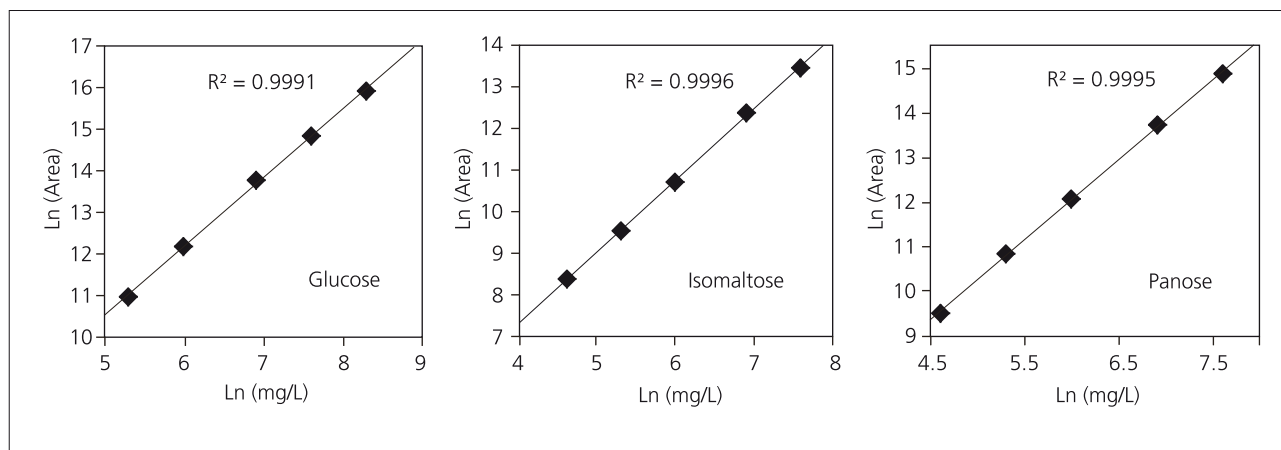
Fig. 4 Calibration Curves (Each injection 5 µL)
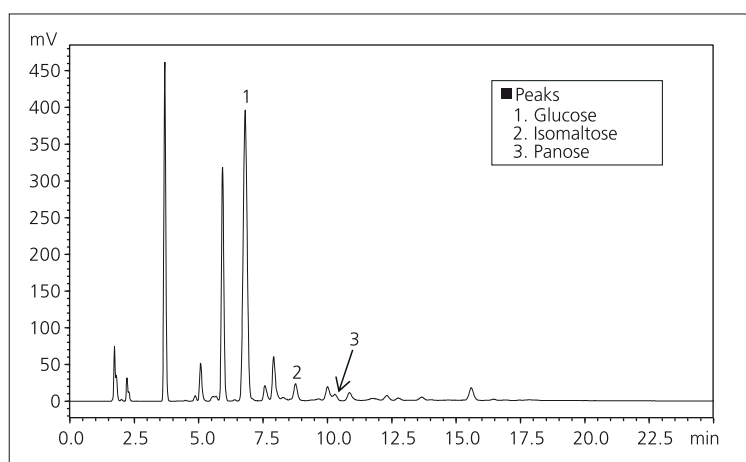
Fig. 5 Chromatogram of Sake

Table 3 Quantitation Results and Repeatability (n = 3) of Oligosaccharides in Japanese Sake

	Area	%RSD	Conc.
Glucose	432×10^4	0.6	13110 mg/L
Isomaltose	228×10^3	2.1	5130 mg/L
Panose	909×10^2	5.9	1410 mg/L

Note: The listed concentrations are the values obtained after converting the results obtained from the 5 µL measurement samples to the undiluted source solution.

SHIMADZU

Shimadzu Corporation

www.shimadzu.com/an/

SHIMADZU
Excellence in Science

Application News

No.L481

High Performance Liquid Chromatography

Analysis of Sugars and Sugar Alcohols in Energy Drink by Prominence-i with Differential Refractive Index Detector

Sugars and sugar alcohols display almost no ultraviolet absorption, and are therefore typically detected using a differential refractive index detector or evaporative light scattering detector. By using a ligand exchange column for sugar analysis, it is possible to distinguish among the different isomers based on the position of the hydroxyl group in the chair conformation of glucose and fructose for example. In other words, the hydroxyl group of the sugar and the metal ion of the stationary phase form a complex, making it possible to achieve separation due to the difference in the strength of the complex formation. Also, maintaining a column temperature of 80 °C suppresses sugar anomer separation and peak dispersion, thereby achieving good separation of adjacent peaks.

The new Prominence-i integrated high-performance liquid chromatograph can be connected to the RID-20A differential refractive index detector. The column oven, which can accommodate a 30 cm column and maintain temperature control up to 85 °C, therefore supports applications that require a long column.

In Application News No. 467, we introduced an example of analysis of sugars in juice, in which the Prominence-i was connected to a differential refractive index detector. Here, we introduce an example of simultaneous analysis of sugars and sugar alcohols in an energy drink using the Prominence-i and RID-20A.

■ Analysis of a Standard Mixture of Six Sugars

Sorbitol, xylitol, mannitol and erythritol are a type of sugar alcohol that because of their relative sweetness, are used as sweeteners. When conducting simultaneous analysis of sugars and sugar alcohols, a hydrophilic compound analytical column, such as the SPR-Ca or SPR-Pb, is suitable along with the use of a combination of the size exclusion and ligand exchange modes of analysis. Fig. 1 shows the results of analysis of a standard solution of six sugar alcohol substances (10 g/L each of maltose, glucose, fructose, erythritol, mannitol and sorbitol) using the SPR-Ca column with a 10 µL injection. The analytical conditions are shown in Table 1.

Fig. 2 shows the results of analysis of a standard solution of six sugar substances including sugar alcohols (10 g/L each of maltose, glucose, fructose, mannitol, xylitol, sorbitol) using a 10 µL injection, and Table 2 shows the analytical conditions that were used. The SPR-Pb was used as the analytical column.

Fig. 1 Chromatogram of a Standard Mixture of Six Sugars (10 g/L each, 10 µL Injected)

Peaks
1. maltose
2. glucose
3. fructose
4. erythritol
5. mannitol
6. sorbitol

Fig. 2 Chromatogram of a Standard Mixture of Six Sugars (10 g/L each, 10 µL Injected)

Peaks
1. maltose
2. glucose
3. fructose
4. mannitol
5. xylitol
6. sorbitol

Table 1 Analytical Conditions

Column	: Shim-pack SPR-Ca (250 mm L × 7.8 mm I.D., 8 µm)
Mobile Phase	: Water
Flowrate	: 0.6 mL/min
Column Temp.	: 80 °C
Injection Volume	: 10 µL
Detection	: RID-20A
	Polarity +, Cell temp. 40 °C, Response 1.5 sec

Table 2 Analytical Conditions

Column	: Shim-pack SPR-Pb (250 mm L × 7.8 mm I.D., 8 µm)
Mobile Phase	: Water
Flowrate	: 0.6 mL/min
Column Temp.	: 80 °C
Injection Volume	: 10 µL
Detection	: RID-20A
	Polarity +, Cell temp. 40 °C, Response 1.5 sec
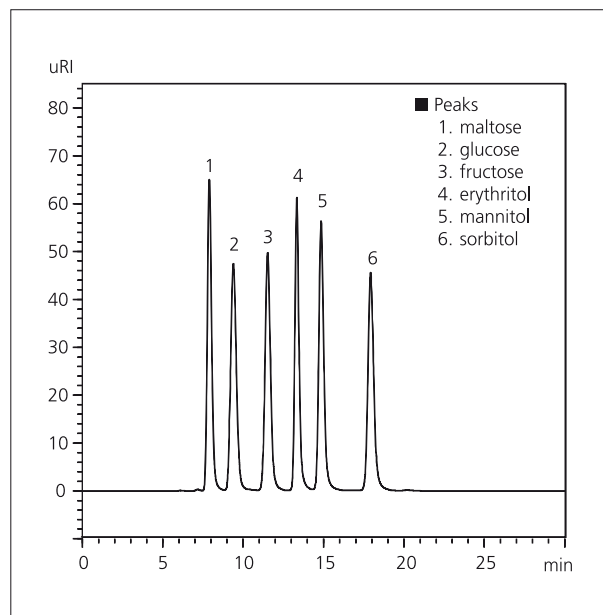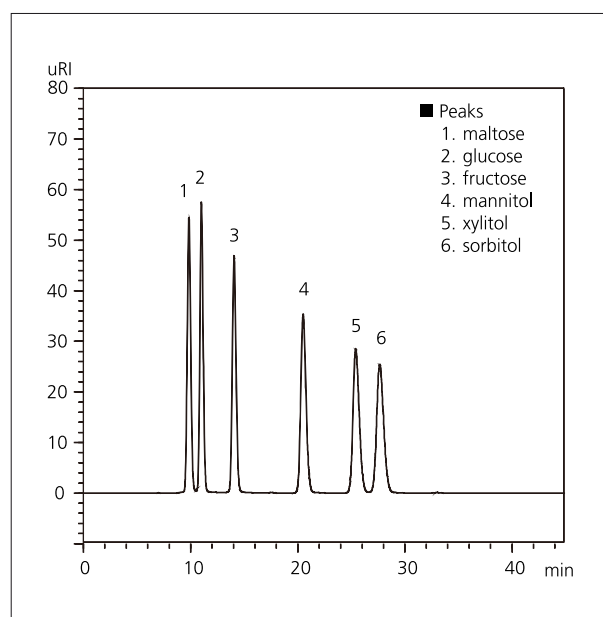
■ Linearity

Fig. 3 shows the calibration curves generated using the analytical conditions of Table 2. When generating the curves for the six components over a concentration range of 0.2 to 10 g/L (using the average of three area values, respectively), excellent linearity with a coefficient of determination greater than $R^2=0.9999$ was obtained for each component.

Table 3 Content of Respective Sugars in Energy Drinks

	Content (g/L)	
	Energy Drink A	Energy Drink B
Glucose	ND	59
Fructose	ND	101
Xylitol	25	ND
Sorbitol	14	ND
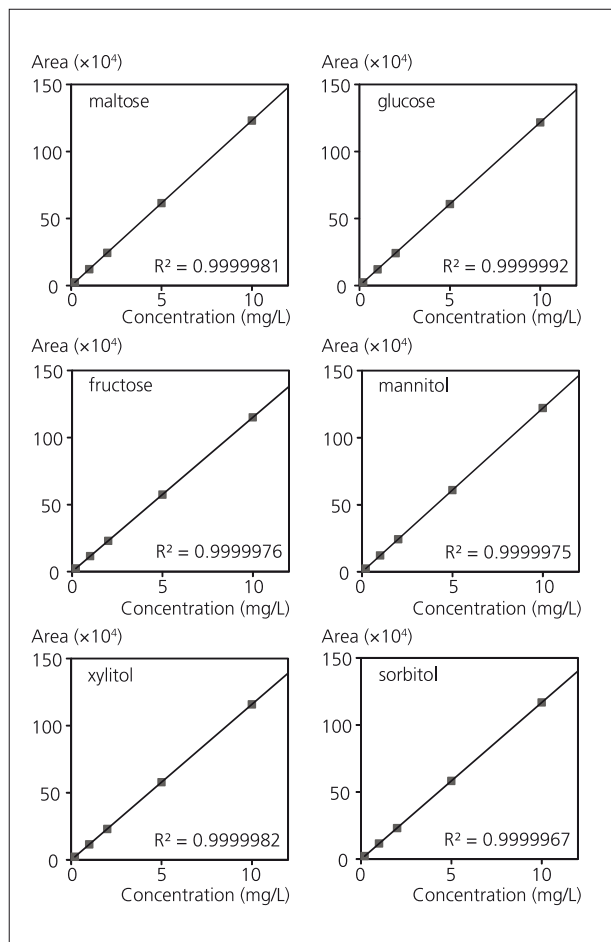
Fig. 3 Calibration Curves of a Standard Mixture of Six Sugars (0.2 – 10 g/L, 10 μL Injected)

Fig. 4 Chromatogram of Energy Drink A (10 μL Injected)

■ Analysis of Energy Drink

Figs. 4 and 5 show the chromatograms obtained from measurement of energy drinks A and B, respectively. Energy drink A was diluted 10:1 with water, and energy B, 20:1 with water, and after each was filtered through a 0.2 μm membrane filter, 10 μL of each sample was injected. The analytical conditions were the same as those of Table 2.

Xylitol and sorbitol were detected in energy drink A, and glucose and fructose were detected in energy drink B. Table 3 shows the quantities of each of these sugars in the respective energy drinks.

Fig. 5 Chromatogram of Energy Drink B (10 μL Injected)

First Edition: Jan. 2015

SHIMADZU

Shimadzu Corporation

www.shimadzu.com/an/

SHIMADZU
Excellence in Science

Application News

No.L437

High Performance Liquid Chromatography

High Speed, High Resolution Analysis (Part 45) Analysis of Pre-Column Derivatized Amino Acids by the Nexera SIL-30AC Autosampler (Part 2)

Application News L432 introduced the analysis of amino acids that are obtained by hydrolysis primarily of proteins. Amino acids were prepared by automated pre-column derivatization using the SIL-30AC. However, for amino acid analysis applications which require the search for functional constituents, etc. in foods, monitoring of even more types of amino acids is becoming necessary.

Here, we introduce an example of the determination of 26 amino acids using a different column size and different mobile phase conditions than were used in L432. The automatic pretreatment feature of the SIL-30AC was utilized for derivatization of the amino acids during analysis, thereby enabling the overall analysis time to be substantially shortened.

■ Simultaneous Determination of 26 Amino Acids

The automatic pretreatment features of the Nexera SIL-30AC autosampler were utilized to conduct automated derivatization of primary amino acids using o-phthalaldehyde (hereafter, OPA) and secondary amino acids, such as proline, etc., using 9-fluorenyl methyl chloro formate (hereafter, FMOC), to produce fluorescent substances within the autosampler. For the

derivatization reagents used in this method and the pretreatment program for the SIL-30AC, refer to the Shimadzu Application News No. L432. Table 1 shows the analytical conditions, and Fig. 1 shows the chromatogram obtained from analysis of a standard mixture of 26 amino acids in solution.

Table 1 Analytical Conditions

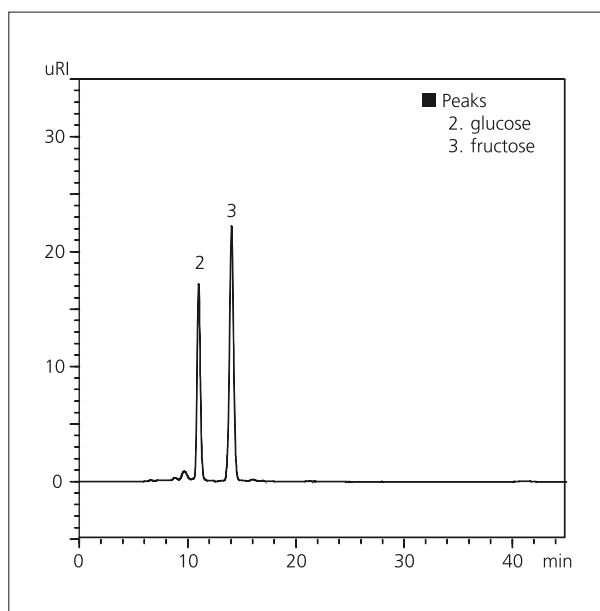|	
Column	: YMC-Triart C18 1.9 μm
	(100 mmL. × 2.0 mmI.D., 1.9 μm, manufactured by YMC Co., Ltd.)
Mobile Phase	: A: 20 mmol/L Phosphate Potussium Buffer (pH 6.5)
	B : 45/40/15 Acetonitrile/Methanol/Water
Time Program	: B Conc.11 % (0.00 - 2.00 min) → 17 % (4.00 min)
	→ 31 % (5.50 min) → 32.5 % (10.00 min)
	→ 46.5 % (12.00 min) → 55 % (15.50 min)
	→ 100 % (15.51 - 19.00 min) → 11 % (19.01 min)
Flow Rate	: 0.4 mL/min
Column Temp.	: 35 °C
Injection Volume	: 1 μL
Detection	: RF-20AXS, Ex. at 350 nm, Em. at 450 nm
	→ Ex. at 266 nm, Em. at 305 nm (14.0 min)
Cell Temp.	: 25 °C
Flow Cell	: Semi-micro cell

■ Peaks
1. Aspartic Acid 2. Glutamic Acid 3. Asparagine 4. Serine 5. Glutamine 6. Histidine 7. Glycine 8. Threonine 9. Citlulline
10. Arginine 11. β-Alanine 12. Alanine 13. Taurine 14. Theanine 15. GABA 16. Tyrosine 17. Cystine 18. Valine
19. Methionine 20. Tryptophan 21. Phenylalanine 22. Isoleucine 23. Leucine 24. Ornithine 25. Lysine 26. Proline
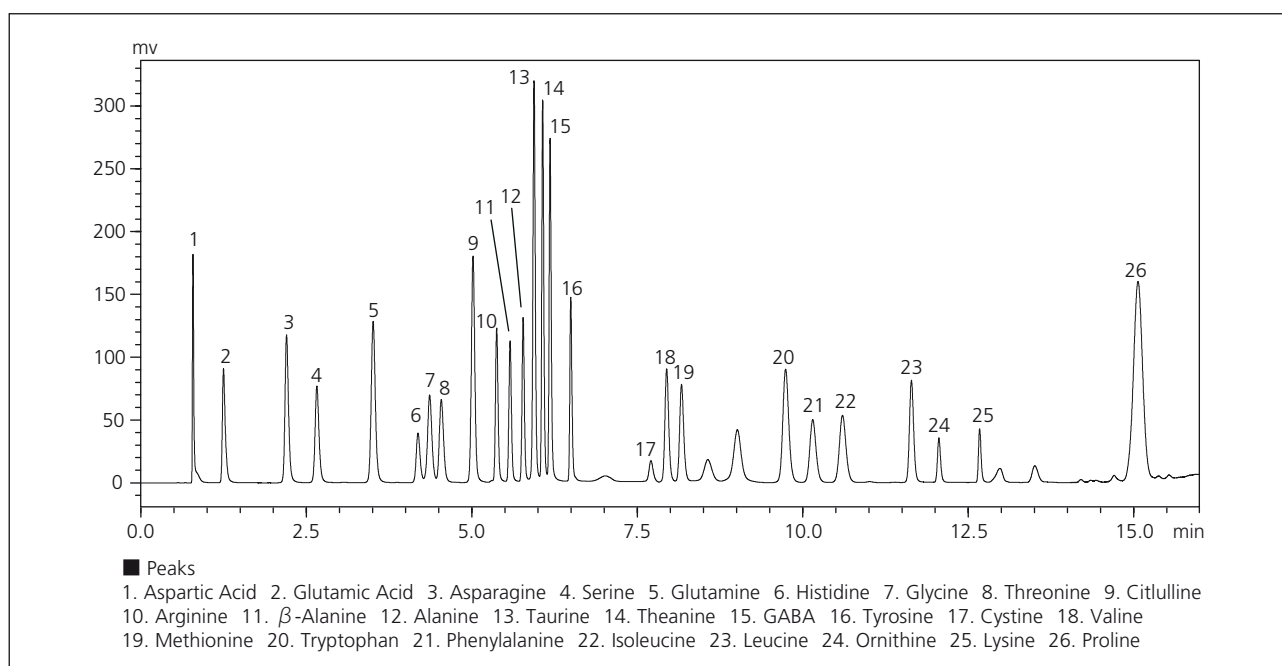
Fig. 1 Chromatogram of Standard Mixture Solution of 26 Amino Acids (10 μmol/L Each)

■ Application of Overlapping Injection Pretreatment Feature

The overlapping injection function of the SIL-30AC allows preparation of the next sample to occur during the current analysis operation, thereby shortening the time necessary for a series of analyses. In the amino acid analysis presented here, the time required to complete an analysis cycle is shortened by conducting sample derivatization (reagent addition and mixing) of the subsequent sample during the current analysis. A derivatized sample is injected into the column, and when the analysis starts, the autosampler begins to prepare the next sample by adding reagent and mixing the contents.

Fig. 2 shows a flow diagram description of the overlapping injection analysis cycle.

■ Analysis of Alcoholic Beverages

Two commercially available alcoholic beverages were analyzed using the automated pre-column derivatization. Fig. 3 shows each of the chromatograms. After diluting each of the samples with 0.1 mol/L HCl,

they were filtered through a 0.2 µm membrane filter, and then derivatized by the SIL-30AC pretreatment procedure. 1 µL of each was injected.
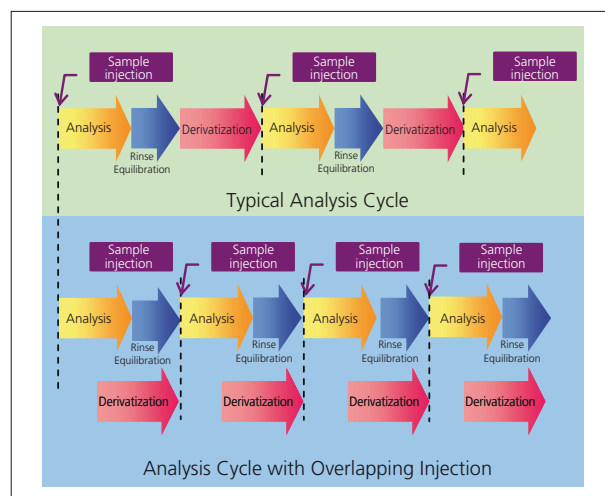
Fig. 2 Automated Derivatization Using Overlapping Injection

■ Peaks
1. Aspartic Acid 2. Glutamic Acid 3. Asparagine 4. Serine 5. Glutamine 6. Histidine 7. Glycine 8. Threonine 9. Citlulline 10. Arginine 11. β-Alanine 12. Alanine 13. GABA 14. Tyrosine 15. Valine 16. Methionine 17. Tryptophan 18. Phenylalanine 19. Isoleucine 20. Leucine 21. Ornithine 22. Lysine 23. Proline
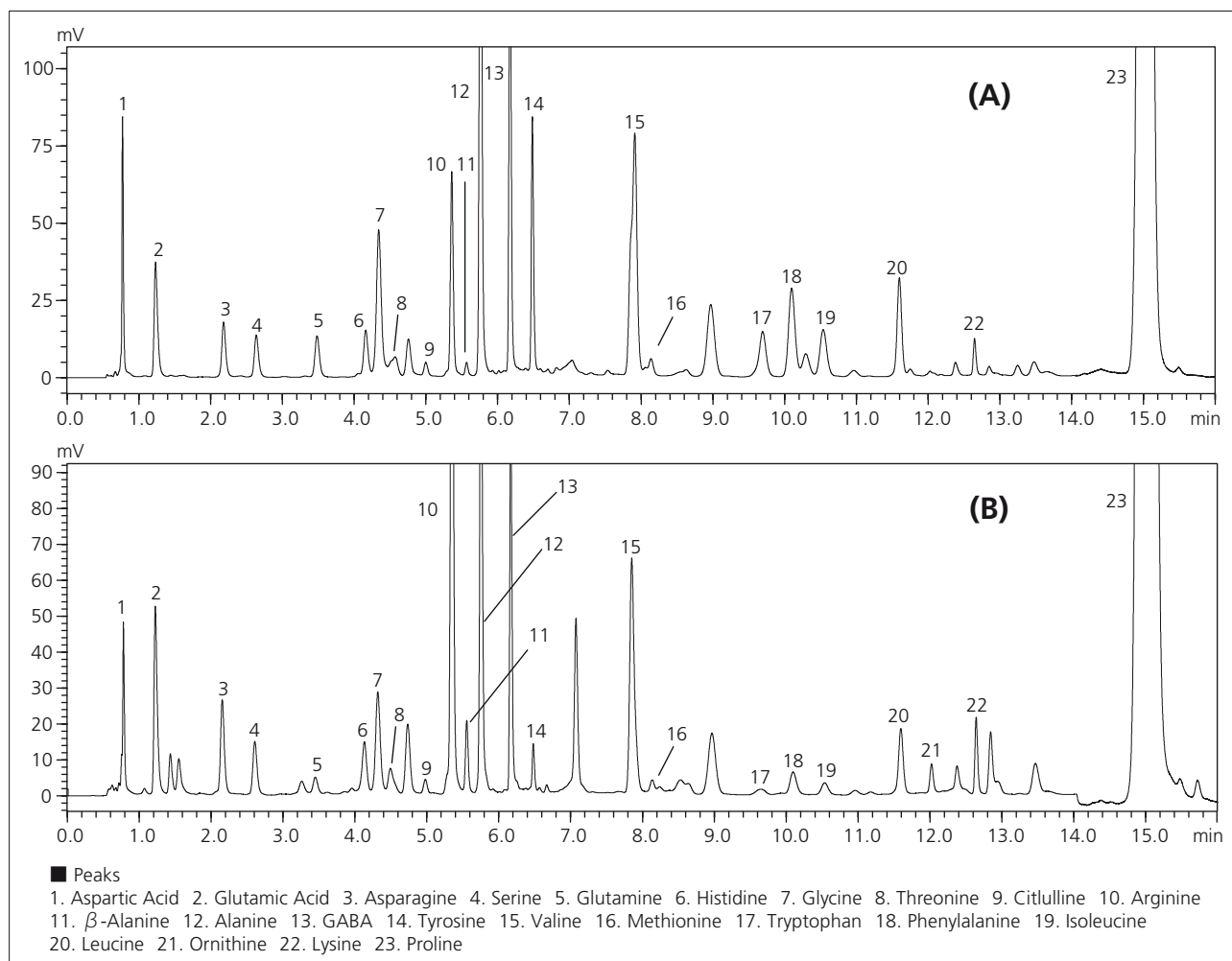
Fig. 3 Chromatograms of Alcoholic Beverages: (A) Beer; (B) White Wine

SHIMADZU

Shimadzu Corporation

www.shimadzu.com/an/

SHIMADZU
Excellence in Science

Application News

No.L484

High Performance Liquid Chromatography

Analysis of Nivalenol and Deoxynivalenol in Wheat Using Prominence-i

Nivalenol and deoxynivalenol (DON, vomitoxin) are types of mycotoxins produced by Fusarium fungi. In Japan, the provisional reference value for deoxynivalenol was set at 1.1 ppm in May, 2002 (Notification No. 0521001 issued by Department of Food Safety, Pharmaceutical and Food Safety Bureau, Ministry of Health, Labour and Welfare of Japan). Previously, in Application News No. L362, the analysis using an ultra high-performance LC system was introduced, but here, referring to the test method for deoxynivalenol specified in the Notification No. 0717001 (issued by Department of Food Safety, Pharmaceutical and Food Safety Bureau, Ministry of Health, Labour and Welfare of Japan, in July 2003), a washing process for the analytical column is included.
The detector component of the new Prominence-i integrated high-performance liquid chromatograph incorporates a temperature control function for both the flow cell component and the optical system. Here, good repeatability was obtained despite the susceptibility of UV detection in the short wavelength region due to environmental temperature fluctuations.

■ Analysis of Standard Mixture

Fig. 1 shows the results of analysis of a standard mixed solution of nivalenol and deoxynivalenol (each at 4.0 ppm) using a 10 µL injection. Table 1 shows the analytical conditions used. The test method specifies the use of isocratic analysis, but a column washing process after elution of the deoxynivalenol was added. As the Prominence-i is equipped with a low-pressure gradient unit as standard, a mobile phase with a high organic solvent ratio can easily be pumped through the system following elution of the target component.
Six repeat analyses of a 0.1 ppm standard solution were conducted, corresponding to about one-tenth the provisional reference value. The relative standard deviation (% RSD) of peak area and retention time obtained for the two substances are shown in Table 2, and the chromatogram is shown in Fig. 2.

Fig. 1 Chromatogram of a Standard Mixture (4.0 ppm each)
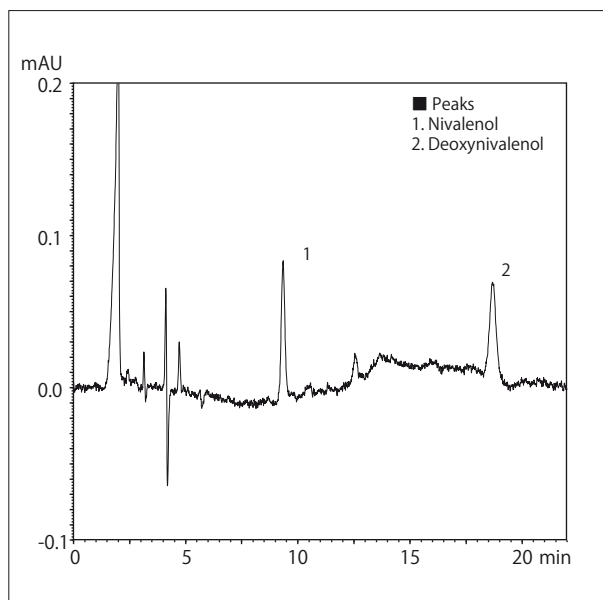
Fig. 2 Chromatogram of a Standard Mixture (0.1 ppm each)

Table 1 Analytical Conditions

Column	: Shim-pack GIS C18 (250 mm L. × 4.6 mm I.D., 5 µm)
Mobile Phase A	: Water / Acetonitrile / Methanol = 90/5/5 (v/v/v)
Mobile Phase B	: Acetonitrile / Methanol = 50/50 (v/v)
Time Program	: B Conc. 0 % (0 - 20 min) → 50 % (20.01 - 25 min) → 0 % (25.01 - 45 min)
Flowrate	: 1.0 mL/min
Column Temp.	: 40 ℃
Injection Volume	: 10 µL
Detection	: UV 220 nm (Cell temp. 45 ℃)

Table 2 Repeatability (0.1 ppm, n=6)

	R.T.%RSD	Area %RSD
Nivalenol	0.09	0.68
Deoxynivalenol	0.06	0.76

■ Calibration Curve Linearity

Fig. 3 shows the calibration curves generated from analyses using the conditions of Table 1. Excellent linearity with a coefficient of determination greater than $R^2=0.9999$ was obtained for both substances over a concentration range of 0.1 to 4 ppm.
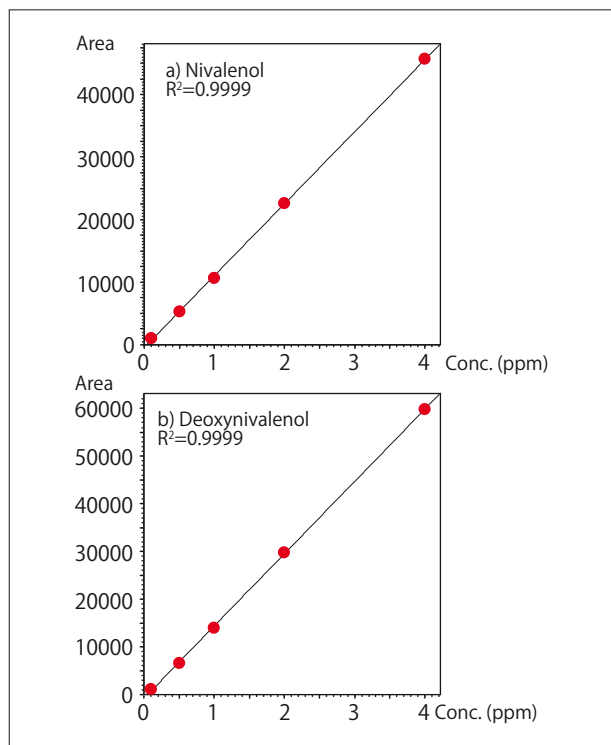
Fig. 3 Linearity of Calibration Curves for a) Nivalenol and b) Deoxynivalenol

Fig. 4 Pretreatment

■ Analysis of Wheat

Fig. 4 shows the pretreatment procedure used for analysis of wheat. Purification of two varieties of wheat was conducted using two types of multi-function columns, the "MultiSep #227" (Romer Labs Inc.) and "Autoprep MF-T" (Showa Denko K.K.).
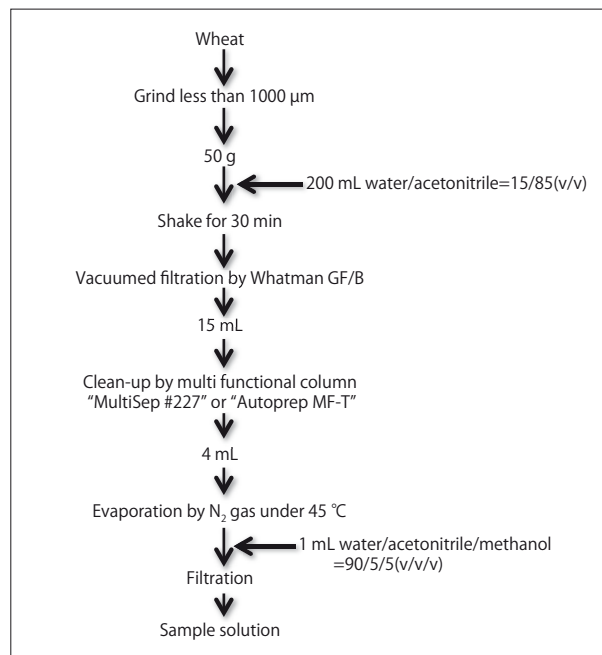
The results are shown in Fig. 5 and Fig. 6, respectively. Here, the pretreated sample solution was spiked with nivalenol and deoxynivalenol to achieve respective concentrations of 1.0 ppm.
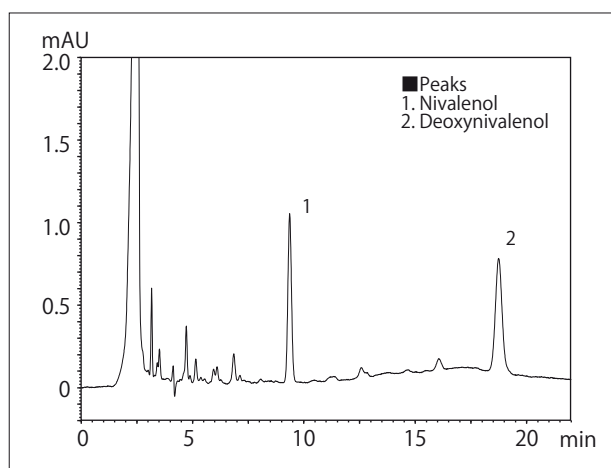
Fig. 5 Chromatogram of Wheat A (Spiked with 1.0 ppm each) (MultiSep #227)
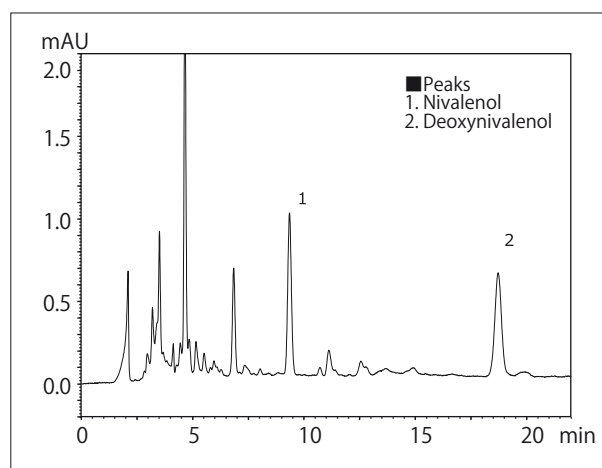
Fig. 6 Chromatogram of Wheat B (Spiked with 1.0 ppm each) (Autoprep MF-T)

SHIMADZU

Shimadzu Corporation

www.shimadzu.com/an/

SHIMADZU
Excellence in Science

Application News

No.L491

High Performance Liquid Chromatography

Comprehensive 2D Separation of Carotenoids in Red Chili Pepper by the Nexera-e System

Carotenoids are naturally occurring organic pigments that are divided into two classes, carotenes, consisting only of carbon and hydrogen, and xanthophylls, which contain oxygen. Carotenoids are rich in double bonds, and therefore have received much attention in recent years as antioxidants, which are known for their disease preventive properties, including lifestyle-related diseases.

The extensive range of carotenoids found in foods makes it difficult to conduct simultaneous separation and quantitation by conventional HPLC. However, the Nexera-e comprehensive two-dimensional LC is particularly suited for such analyses. Here, carotenoids extracted from red chili pepper were subjected to two-dimensional analysis, in which micro-scale separation was conducted in the first stage using normal phase conditions, and separation using reversed phase conditions was tried in the second dimension. For detection, a combination of a photodiode array (PDA) connected to the LCMS-8030 triple quadrupole mass spectrometer was used. Because the separation modes, normal and reversed phases, differ in the first and second dimensions, this might be considered a two-dimensional LC method by which the greatest orthogonality possible is obtained.

■ Comprehensive Separation of Carotenoids Detected by the Photodiode Array Detector

Use of the Nexera-e with a photodiode array detector (PDA) permits the separation of complex coexisting substances and detection at the optimal wavelength in a single analysis. Fig. 1 shows a comprehensive two-dimensional representation of the separation pattern (absorption wavelength = 450 nm) generated using the specialized two-dimensional analysis software, ChromSquare.

By combining the first-dimension cyano column and the second-dimension ODS column, 10 groups of substances, including hydrocarbons, monool esters, diol diesters, diol monoketo diesters, diol diketo diesters, diol mono epoxide monoesters, free monools, diol monoketo monoesters, diol diketo mono esters, and polyoxygenated free xanthophylls were separated according to class based on molecular polarity, and the component separation was verified based on the hydrophobicity of their respective fatty acid residues.

1: Hydrocarbons
2: Monool esters
3: Diol diesters
4: Diol monoketo diesters
5: Diol diketo diesters
6: Diol monoepoxide monoesters
7: Free monools
8: Diol monoketo monoesters
9: Diol diketo monoesters
10: Polyoxygenated free xanthophylls
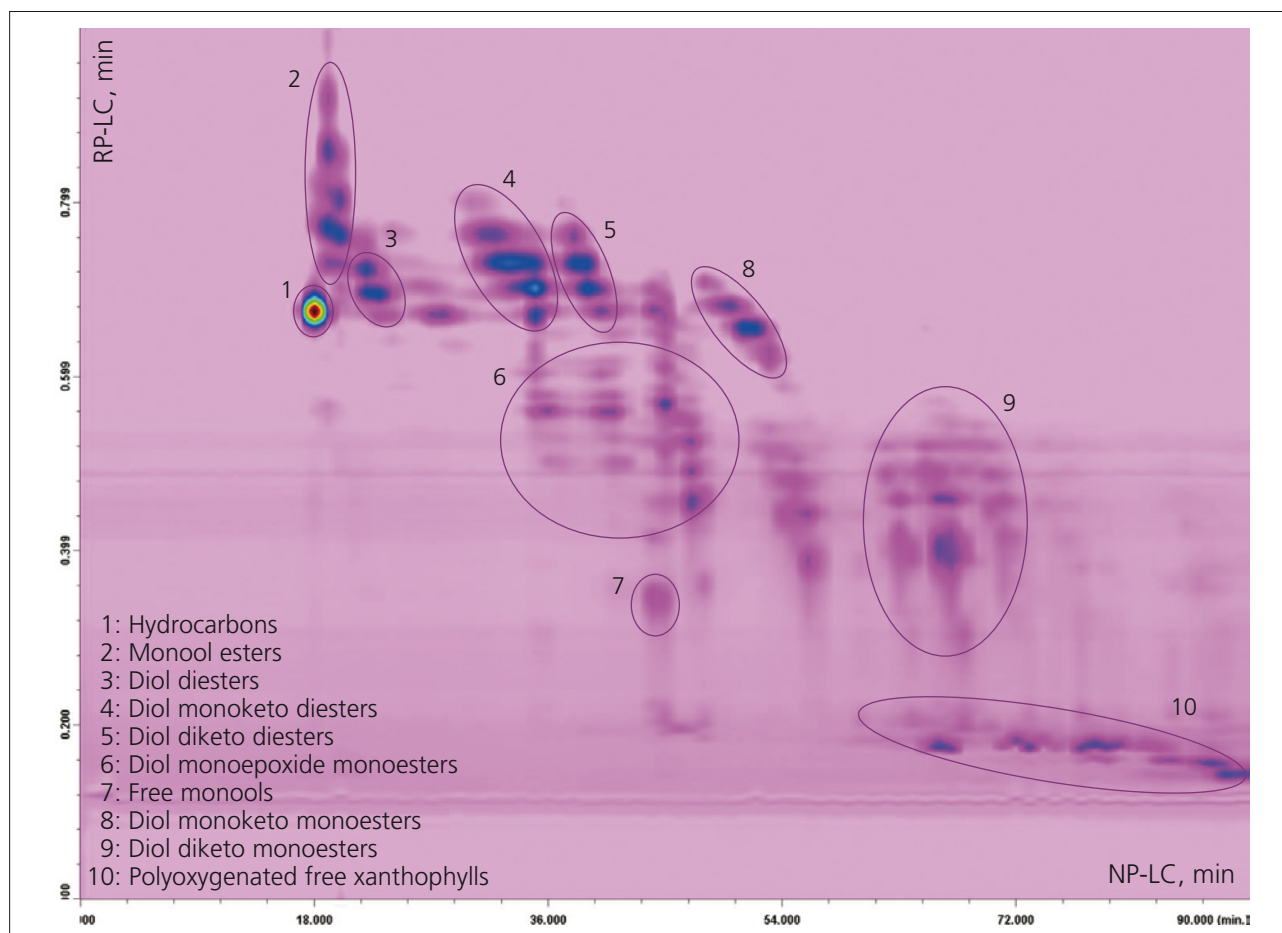
Fig. 1 2D Plot of Carotenoids Using ChromSquare Software

■ Quantitation of *β*-Carotene in Red Chili Pepper by LC/MS/MS

The analytical conditions are shown in Table 1, and the sample pretreatment conditions are shown in Fig. 2. β-carotene, which is a precursor of vitamin A, was detected in the two-dimensional separation of the carotenoids. Quantitation was then conducted using the LCMS-8030 triple quadrupole mass spectrometer. Both high sensitivity and high selectivity can be obtained using MRM analysis, and further, reduced ion suppression can be expected with the two-dimensional separation obtained with the Nexera-e.

Fig. 3 shows the two-dimensional separation data of β-carotene obtained from DUIS-positive mode MRM analysis of the calibration curve, and Fig. 4 shows the linearity of the three values (blobs) in the range of 0.01 to 10 mg/L, which correspond to the peak volumes used for quantitation. The correlation coefficient (r) = 0.998976 indicates results with good linearity. The quantitative result for β-carotene present in red chili pepper was calculated as 1.22 mg/L based on the concentration in the final sample following extraction.

Table 1 Analytical Conditions

1D Colum	: Ascentis Cyano (250 mm L. × 1.0 mm I.D., 5 μm)
Mobile Phase	: A; Hexane
	B; Hexane/Butylacetate/Acetone = 80/15/5 (v/v/v)
Flowrate	: 0.02 mL/min
Time Program	: B Conc. 0 % (0.01 min) → 0 % (5 min) → 100 % (65 min) → 100 % (75 min) → 0 % (76 min)
Column Temp.	: 30 °C
Injection vol.	: 2 μL
Loop vol.	: 20 μL
2D Column	: Ascentis Express C18 (30 mm L. × 4.6 mm I.D., 2.7 μm)
Mobile Phase	: A; acetnitrile
	B; 2-propanol
Flowrate	: 4 mL/min (0.8 mL/min split for MS)
Time Program	: B Conc. 0 % (0.01 min) → 50 % (0.17 - 0.54 min) → 80 % (0.54 - 0.93 min) → 30 % (0.94 min) → STOP (1 min)
Detector	: SPD-M30A Photo diode array detector (standard cell, wave length = 450 nm)
	Shimadzu LCMS-8030 (DUIS positive mode, targeted β-carotene MRM transition: *m/z* 536.40 > 444.30)

Homogenated red chilli pepper
(*Capsicum annuum L.*) 200 g

↓

Add consecutive 300 mL aliquots of methanol
/ethyl acetate/petroleum ether (1:1:1, v/v/v)

↓

Combine extracts and filtrate

↓

Evaporate to dryness under vacuum (30 ˚C)

↓

Dissolved in 3 mL methanol
/tert-butyl methyl ether (1:1, v/v)

↓

Filtrate and inject 2 μL into HPLC

Fig. 2 Sample Preparation

Area = 551615
Concentration = 1.22 mg/L

Fig. 3 2D Plot of *β*-Carotene

Correlation
Coefficient (r) = 0.998976

Conc. (mg/L)
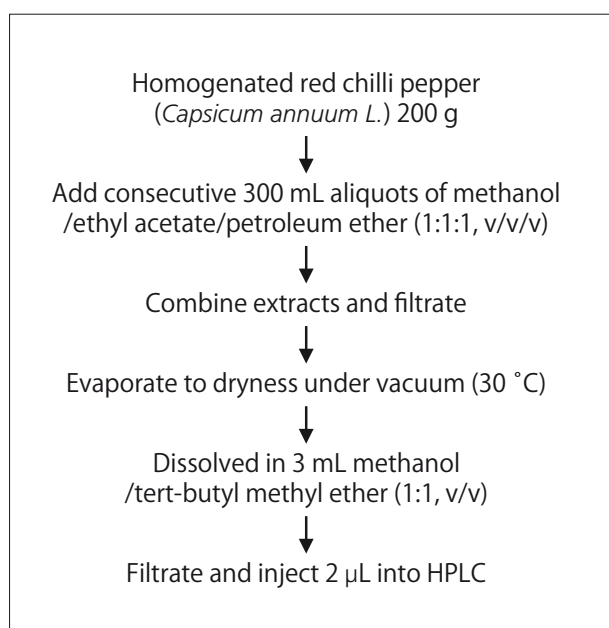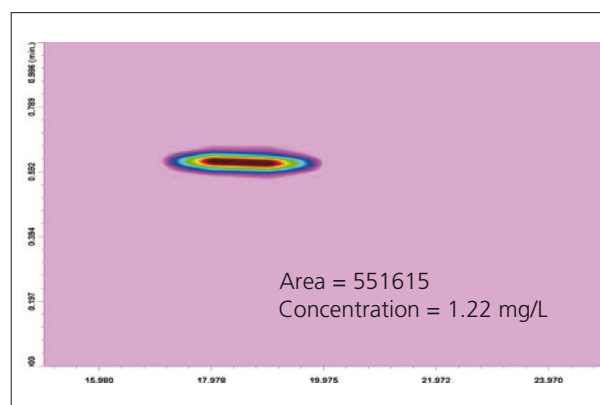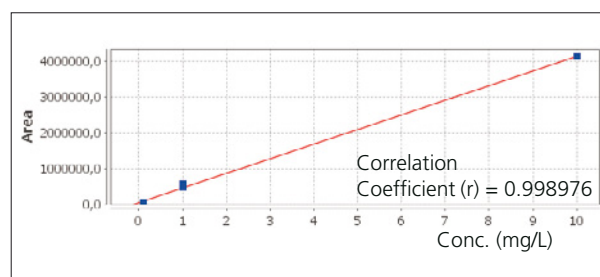
Fig. 4 Linearity of Calibration Curve for *β*-Carotene

SHIMADZU

Shimadzu Corporation

www.shimadzu.com/an/

![SHIMADZU Excellence in Science]

Application News

No.L492

High Performance Liquid Chromatography

Comprehensive 2D Separation of Triglycerides in Vegetable Oil with ELSD/LCMS-IT-TOF Detection

Triglycerides, molecules consisting of a glycerol backbone to which three fatty acids are attached via ester bonds, are considered important functional components in both animal oil and vegetable oil. Triglycerides display low solubility in aqueous solvents, and their separation has typically been conducted by either silver ion-mediated normal phase analysis or reversed phase analysis using an organic solvent. However, as there are numerous molecular species consisting of combinations of fatty acids, mutual separation of the triglycerides in natural fats can be difficult using any single set of separation conditions. The Nexera-e comprehensive two-dimensional liquid chromatograph effectively achieves mutual separation of such complex components.

When conducting comprehensive two-dimensional liquid chromatography, different separation modes are generally selected for the first and second-dimension separations, and depending on the differences in separation selectivity between these dimensions, improved separation is typically seen for components that are difficult to separate in a single, one-dimensional analysis. Here, using borage oil as a sample that contains many triglycerides, micro-scale separation was conducted in the first separation using a silver column (normal phase conditions), and reversed phase separation was conducted in the second dimension by using a two-liquid gradient with non-aqueous organic solvents. Detection was conducted using a combination of an evaporative light scattering detector (ELSD) and an ion trap time-of-flight mass spectrometer (LCMS-IT-TOF). The analytical conditions are shown in Table 1.

■ Comprehensive Separation of Triglycerides in Borage Oil with ELSD Detection

Borage oil is a vegetable oil that is obtained from the seeds of *Borago officinalis*, an annual herb. Rich in triglycerides containing such fatty acid chains as linoleic acid, γ-linolenic acid, oleic acid, and palmitic acid, it offers a variety of health effects associated with these substances, such as moisturizing effect, wrinkle prevention, etc. Compared with other vegetable oils, Borage oil is rich in γ-linolenic acid, which is

said to be effective in maintaining female hormonal balance. Triglycerides in natural fats and oils are generally characterized by the lengths of their alkyl chains and the number and positions of the double bonds in the alkyl chains. Triglycerides having double bonds in particular are said to possess antioxidant action, and there is considerable demand for the separation of these triglycerides depending on the presence or absence of double bonds. It is known that strong interaction is displayed by the formation of a complex comprising the double bond of an alkyl chain with a silver ion. Utilizing this property, an HPLC method in which a stationary phase impregnated with silver is relatively often used to achieve selective retention of compounds containing double bonds. Here, using the Nexera-e to achieve comprehensive separation of multiple components, a silver ion column (normal phase conditions) with strong retention for double bonds was used for the first-dimension separation, an ultra-high-speed reversed phase analytical column was used for the second-dimension separation, and an ELSD was used for detection.

The ELSD converts the target compound to fine particles by evaporating the eluent exiting the column, and by measuring the scattered light, triglycerides, which display almost no UV absorption, are effectively detected. Fig. 1 shows a comprehensive two-dimensional representation of the separation pattern (horizontal axis: separation in the first dimension with a silver ion column × vertical axis: reversed phase separation in the second dimension) generated using the specialized two-dimensional analysis software, ChromSquare. The use of comprehensive two-dimensional separation permitted difficult-to-achieve high separation using a single set of separation conditions, by which thirty-seven of the elution peaks were confirmed.

Table 1 Analytical Conditions

```
[Column1]       : Ag custom column (150 × 1.0 mm; 5.0 µm)
Mobile Phase    : A; 1.5 % v/v of Butyronitrile in n-Hexane
                  B; 2.4 % v/v of Butyronitrile in n-Hexane
Time Program    : B Conc. 0 % (0 min) → 100 % (40 min) → 100 % (150 min)
Flowrate        : 0.007 mL/min (split)
Column Temp.    : 30 °C
Injection Volume : 2 µL
Modulation Time : 1.5 min

[Column2]       : Ascentis Express C18 column
                  (Supelco, 50 × 4.6 mm; 2.7 µm)
Mobile Phase    : A; Acetonitrile
                  B; Isopropanol
Time Program    : B Conc. 30 % (0 min) → 30 % (0.08 min) → 40 % (0.1 min)
                  → 70 % (1.2 min) → 30 % (1.21 min) → 30 % (1.5 min)
Flowrate        : 4 mL/min
Detector        : Shimadzu ELSD LT-II / LCMS-IT-TOF (APCI positive mode)
```
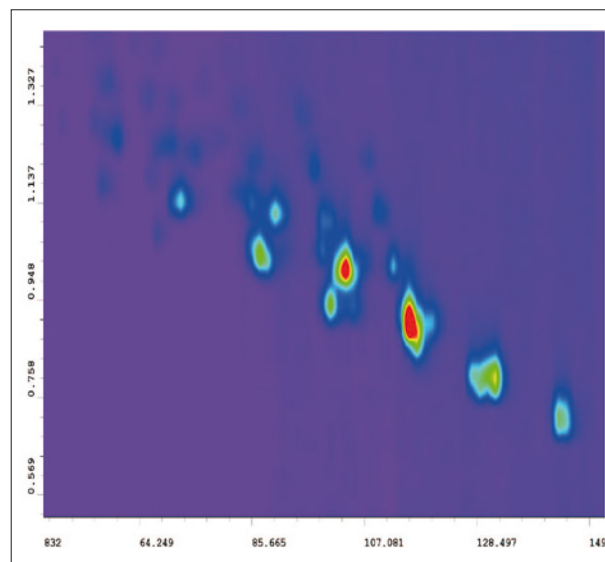

Fig. 1 Comprehensive 2D Plot of Triglycerides in Borage Oil with ELSD Detection

■ Comprehensive Separation of Triglycerides in Borage Oil with LCMS-IT-TOF Detection

As mentioned above, separation in the first dimension in this analysis is conducted based on the presence or absence or the difference in the number of double bonds in the fatty acid side chain. When a silver ion column is used, the greater the number of double bonds in the triglyceride, the stronger the retention will be. However, it is also possible that retention will be affected depending on the positions of the double bonds or the side chain length. In the second-dimension reversed phase separation, two-solution gradient elution is adopted in which, due to the high hydrophobicity of triglycerides, neither water nor buffer solution, etc., is used, but a non-aqueous organic solvent is used for the mobile phase. With this separation mode, elution tends to proceed in the order obtained by subtracting twice the number of double bonds from the total number of triglyceride carbon atoms, which is referred to as the partition number. The top portion of Fig. 2 shows a two-dimensional plot drawn based on the output of the LCMS-IT-TOF mass spectrometer. To facilitate identification of triglycerides using the order of elution described above, a grid is drawn superimposed on the plot. From this plot, it can be seen how separation is conducted according to the difference in the number of double bonds in the first dimension, and the difference in partition number in the second dimension.

Use of the LCMS-IT-TOF as the detector for precise mass measurement in the second dimension permits detailed qualitative analysis of the many components eluted following separation by the Nexera-e. The mass spectra corresponding to the white-circled peaks A, B and C of Fig. 2 are shown in the lower part of Fig. 2. The structural information was obtained from the peak of diglyceride with one side chain detached, and the triglyceride structure were determined as follows:

A   : POP
B   : OOP
C   : PγLnP
Where,
P   : Palmitic acid
O   : Oreic acid
γLn   : γ-Linolenic acid

Since these compounds each have one to three double bonds, they are eluted from the first-dimension column in this order. As lipid-related compounds often display no UV absorption, and gradient elution cannot be applied with differential refractive index detection, a combination of the Nexera-e and ELSD, or a triple quadrupole or LCMS-IT-TOF mass spectrometer can be considered essential for exhaustive analysis in this field.
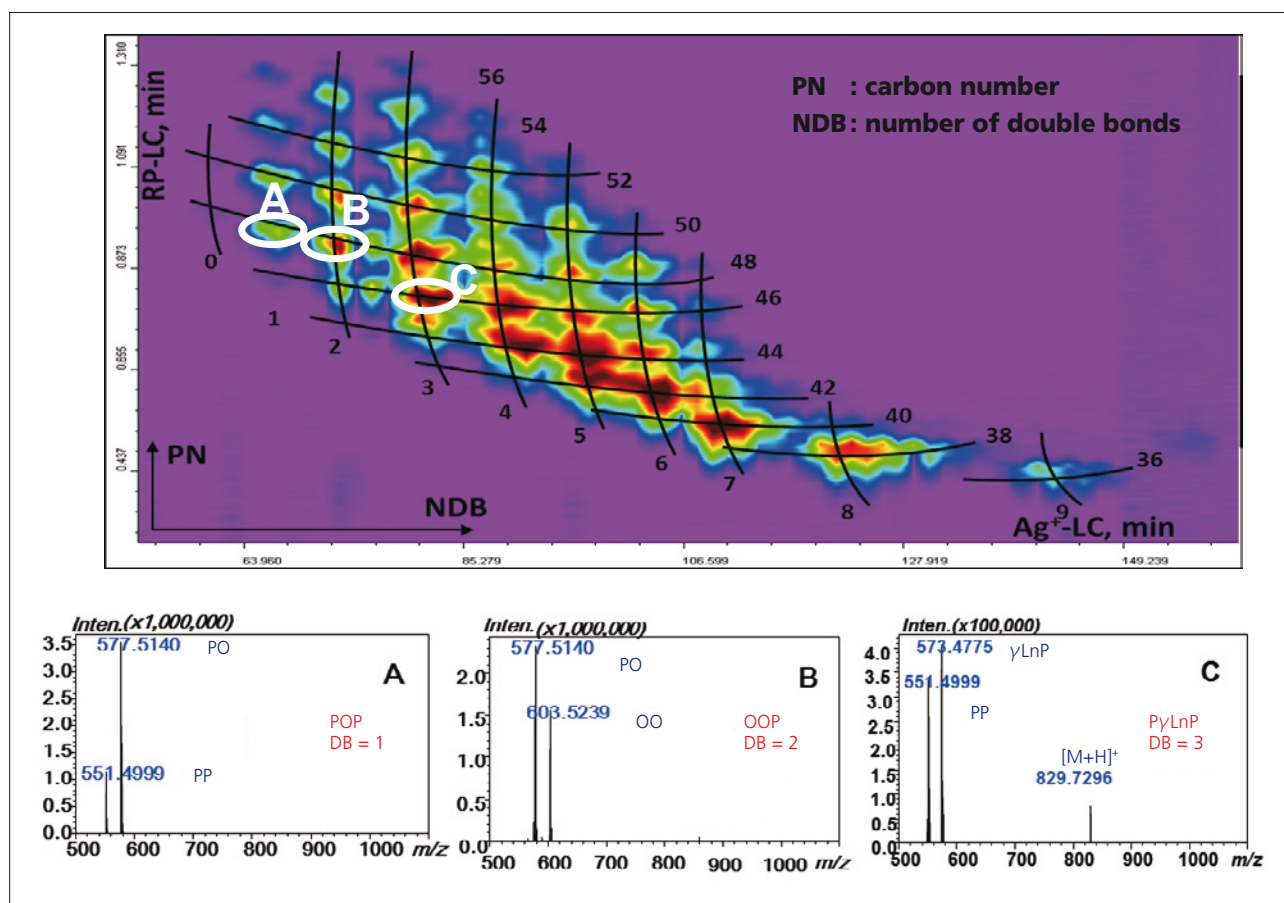

Fig. 2 Comprehensive 2D Plot of Triglycerides in Borage Oil with LCMS-IT-TOF in Addition to the Mass Spectra of Assigned Blobs

Data provided by University of Messina Prof. Luigi Mondello and Chromaleont S.r.l.

SHIMADZU

Shimadzu Corporation

www.shimadzu.com/an/

SHIMADZU
Excellence in Science

Application News

No.L497

Supercritical Fluid Extraction / Chromatography

Using the Nexera UC Online SFE-SFC-MS System to Analyze Residual Pesticides in Agricultural Products

The Nexera UC online SFE-SFC-MS system combines supercritical fluid extraction (SFE) and supercritical fluid chromatography (SFC) in one online system, so that the entire process from extraction of target components to acquisition of data can be performed completely automatically. Furthermore, the system can add polar organic solvents (modifiers) to the supercritical carbon dioxide fluid during SFE and SFC, so that the system can be used to extract and analyze components with a wide range of polarities.

Meanwhile, ever since the positive list system was enacted in 2006 in Japan for residual pesticides in foods, which applies to more than 800 types of pesticides, there has been increasing demand for a system able to simultaneously analyze multiple pesticides with a wide range of properties, including pretreating samples.

This article describes an example of using the Nexera UC online SFE-SFC-MS system to analyze residual pesticides in agricultural products.

■ Online SFE-SFC-MS System

The operating principle of the Nexera UC online SFE-SFC-MS system is shown in Fig. 1. The extraction vessel filled with the sample is placed in the SFE unit and heated to an internal temperature of 40 °C (Fig. 1A). Then supercritical carbon dioxide fluid is pumped into the extraction vessel. After filling the vessel, the flow is stopped to allow static extraction of target components (Fig. 1B). After static extraction, the fluid is pumped through the extraction vessel for dynamic extraction (Fig. 1C). During dynamic extraction, extracted substances flow from the extraction vessel and into the analytical column. However, due to the high level of contaminant components in agricultural products, passing all the extract substances through the analytical column or mass spectrometer could damage the column or contaminate the mass spectrometer. Therefore, the Nexera UC online SFE-SFC-MS system splits the flow to send only a portion of the substances extracted from dynamic extraction through the analytical column. After dynamic extraction, fluid is only sent through the analytical flow line, where the analytical column is used for gradient separation and the mass spectrometer for detecting the target components (Fig. 1D).

■ Sample Preparation

The QuEChERS is a well-known method that prioritizes simplicity and speed and is commonly used to pretreate agricultural products for residual pesticide analysis. However, the method involves many steps, such as adding reagents, solvent extraction, purification by dispersive solid phase extraction, and centrifugal separation. In contrast, the online SFE-SFC-MS system requires only mixing 1 g of agricultural product crushed with a mixer with 1 g of a dehydrating agent* and placing the mixture in the extraction vessel, as shown in Fig. 2. Consequently, the system improves analytical productivity, reduces the environmental impact, and also avoids human errors involved in the pretreatment steps. Using a dedicated rack changer, the system can continuously extract and analyze up to 48 samples at a time.

* "Miyazaki Hydro-Protect" Patent No. 3645552
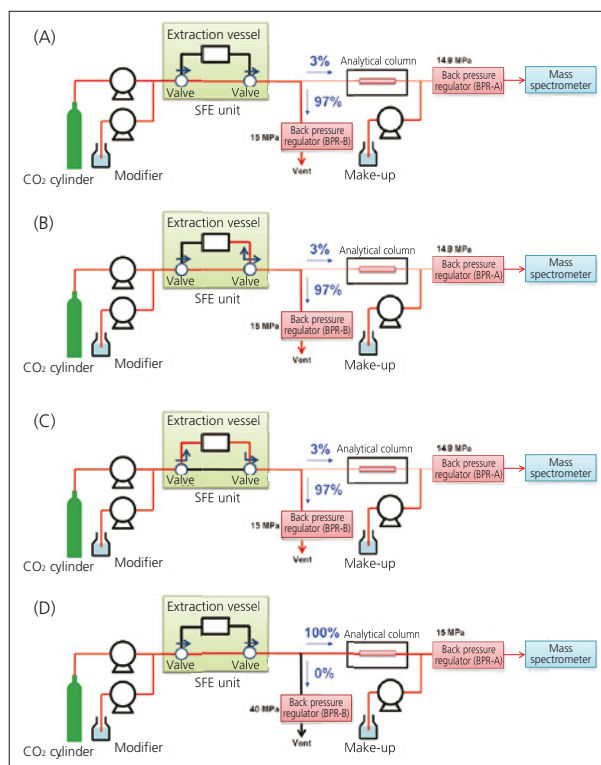
Fig. 1 Analysis Flow by Online SFE-SFC-MS
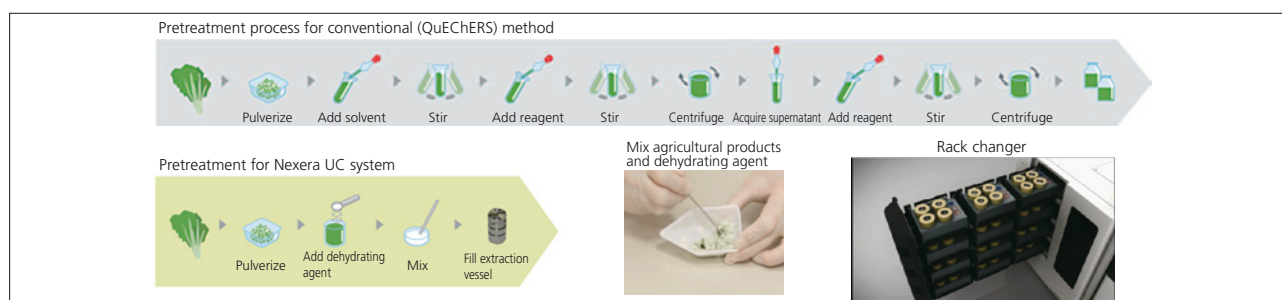
Fig. 2 Sample Preparation

Table 1 Analytical Conditions

[SFE]		[SFC]	
Solvent	: A) Super critical fluid of CO_2 B) 0.1 % Ammmonium formate in methanol	Column	: Shim-pack UC-RP (250 mm L. × 4.6 mm I.D., 5 μm)
Flowrate	: 5 mL/min	Mobile Phase	: A) Super critical fluid of CO_2 B) 0.1 % Ammmonium formate in methanol
Extraction	: 0-3 min. Static mode (B.Conc. 5 %) 3-6 min. Dynamic mode (B.Conc. 5 %)	Time Program	: B.Conc. 0 % (0 min.) → 10 % (11 min.) → 30% (14 min.) → 40 % (14.01-17 min.)
Extraction Vessel Temp.	: 40 °C	Flowrate	: 3 mL/min
BPR Pressure	: A) 14.8 MPa, B) 15 MPa (split rate: 3 %)	Make-up	: 0.1 % Ammmonium formate in methanol (0.1 mL/min.)
Make-up	: 0.1 % Ammmonium formate in methanol (0.4 mL/min.)	Column Temp.	: 40 °C
		BPR Pressure	: A) 15 MPa, B) 40 MPa
		Detector	: LCMS-8050 MRM mode

■ Analysis of Standard Mixture of Pesticides

The standard mixture sample of 510 pesticide components were mixed with a dehydrating agent and analyzed using the analytical conditions indicated in Table 1. Fig. 3 shows the results. Using the system, we were able to accomplish the entire process, from extraction to data acquisition, in about 45 minutes per analysis. For 327 components, we obtained good repeatability for the concentration range from 1 to 100 ng/g (less than 30 %RSD for relative standard deviation for peak area at respective concentrations) and good linearity (contribution ratio of at least R^2 = 0.99). Table 2 also shows how pesticides with a wide range of polarities were analyzed with good repeatability and linearity.
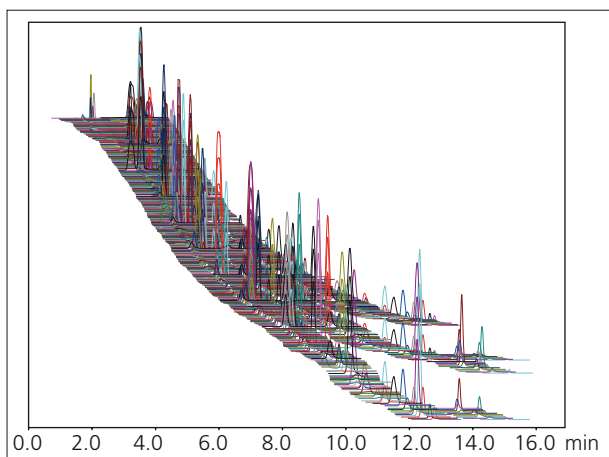
Fig. 3 Mass Chromatogram of Standard Pesticide Mixture Solution

Table 2 Repeatability and Linearity for Representative Pesticides

Compounds	LogPow	Repeatability (%RSD, n=5)	Range (ng/g)	R^2
Ethofenprox	6.9	6.1	1-100	0.9991
Hexaflumuron	5.68	6.8	1-100	0.9992
Benzofenap	4.69	1.4	2-200	0.9990
Mepronil	3.66	4.6	1-100	0.9993
Prometryn	3.34	2.7	1-100	0.9994
Fenamidone	2.8	3.0	2-200	0.9991
Ethylchlozate	2.5	3.0	1-100	0.9996
Imazosulfuron	1.6	6.2	1-100	0.9998
Bensulfuron methyl	0.79	8.1	1-100	0.9996
Primisulfuron methyl	0.2	5.5	1-100	0.9994
Halosulfuron methyl	-0.02	5.5	1-100	0.9996
Azimsulfuron	-1.4	4.2	1-100	0.9998
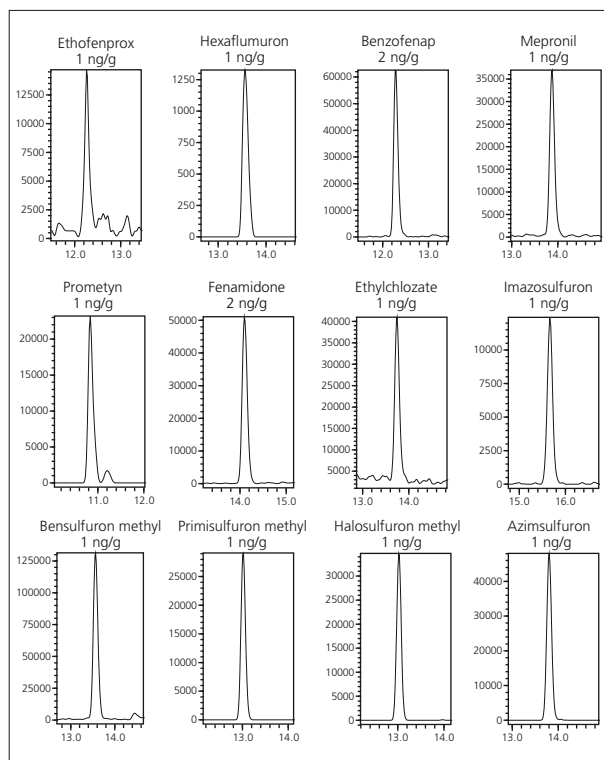
Fig. 4 MRM Chromatograms of Representative Pesticides

■ Analysis of a Tomato

Analysis of 10 ng/g of 510 pesticide components added to a tomato resulted in good repeatability (less than 20 %RSD for the relative standard deviation of the peak area) and a good recovery rate (70 to 120 %) for 248 components. Plots of LogPow and recovery rate results are shown in Fig. 5. It shows that pesticides with a wide range of polarities were analyzed with good recovery.
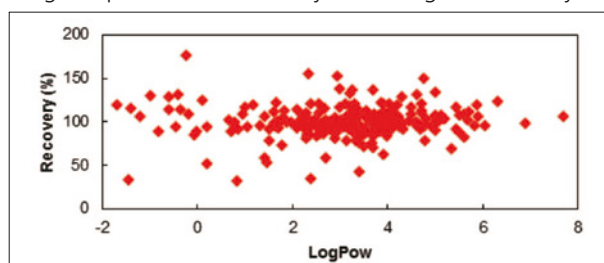
Fig. 5 LogPow vs. Recovery Rate for Tomato Analysis

First Edition: Oct. 2015

SHIMADZU

Shimadzu Corporation

www.shimadzu.com/an/

SHIMADZU
Excellence in Science

Application News

No.L498

High Performance Liquid Chromatography

Analysis of Cyanide Ion and Cyanogen Chloride in Mineral Water by Post-Column Ion Chromatography

On December 22, 2014, the Japan's Ministry of Health, Labour and Welfare (MHLW) issued partial amendment to the standards for ingredients in milk and milk products and the regulatory standards for food products and food additives (MHLW Ordinance No. 141, MHLW Notification No. 482), and specified the corresponding testing methods (Notice No. 1222-4 by Department of Food Safety, Pharmaceutical and Food Safety Bureau, MHLW).

In these standards, the criteria value for cyanogen in mineral water is specified to 0.01 mg/L (combined total of cyanide ions and cyanogen chloride), with post-column ion chromatography specified as the test method.

This example describes using the Shimadzu cyanogen analysis system, compliant with the revised standard for the refreshing drink testing methods, to analyze the cyanide ion and cyanogen chloride levels in mineral water.

■ Analytical Method

The amended regulation specifies separating the cyanide ions and cyanogen chloride with an ion-exclusion column, derivatizing them by 4-pyridinecarboxylic acid-pyrazolone post-column derivatization, and then detecting them at a wavelength of 638 nm. With the post-column method, reactions occur in two stages. The first stage is a chlorination reaction of a chloramine T solution. The second stage is a chromogenic reaction with a 1-phenyl-3-methyl-5-pyrazolone/4-pyridinecarboxylic acid solution.

A flow diagram of the Shimadzu cyanogen analysis system compliant with the amended regulation is shown in Fig. 1.

■ Analysis of Standard Substances

Results from injecting 100 µL of standard cyanide ion and cyanogen chloride solutions (0.01 mg/L each) are shown in Fig. 2. The analytical conditions are shown in Table 1.

1 Pump for Mobile Phase
2,3 Pumps for Reaction Reagents
4 Degasser
5 Autosampler
6 Column
7,8 Reaction Coils
9 Column Oven
10 Reaction Oven
11 UV-VIS Detector
12 Mobile Phase
13,14 Reaction Reagents

Fig. 1 Flow Diagram

Fig. 2 Chromatograms of Standard Cyanide Ion and Cyanogen Chloride Solutions (0.01 mg/L each)

Table 1 Analytical Conditions

<Separation>
Column   : Shimpack-Amino Na (100 mm L.× 6.0 mm I.D.)
Guard Column   : Shimpack CN (G) (10 mm L.× 6.0 mm I.D.)
Mobile Phase   : 10 mmol/L Tartrate (Na) Buffer
Flowrate   : 0.6 mL/min
Column Temp.   : 40 °C

<Post-column Reaction>
First Reaction
  Reagent   : 100 mmol/L Phosphate Buffer
                    containing 3.6 mmol/L Chloramine T
  Flowrate   : 0.5 mL/min
  Reaction Temp. : 100 °C
Second Reaction
  Reagent   : 28.7 mmol/L 1-Phenyl-3-Methyl-5-Pyrazolone
                    + 96.5 mmol/L 4-Pyridimecarboxylate (Na)
  Flowrate   : 0.5 mL/min
  Reaction Temp. : 100 °C
Detection   : SPD-20AV at 638 nm (Lamp: W)

■ Linearity

Calibration curves for the standard cyanide ion and cyanogen chloride solutions are shown in Fig. 3. The calibration curves were prepared for the concentration range specified in the regulation (0.0025 to 0.025 mg/L). The results showed good linearity, with a contribution rate (R^2) over 0.999.

■ Analysis of Mineral Water

Results from injecting 100 µL of three types of mineral water with different mineral content are shown in Figs. 4 to 6. The regulation specifies not adding a phosphate buffer solution to mineral water samples, which is typically done for public drinking water analysis.

Results from injecting 100 µL of mineral water spiked with 1/10 the criteria value for standard cyanogen chloride solutions (0.001 mg/L) are shown in Fig. 7.
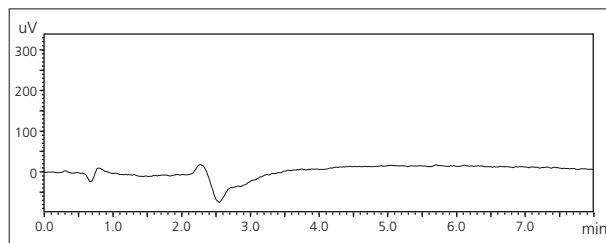
Fig. 4 Chromatogram of Mineral Water A (Hardness 64 mg/L)
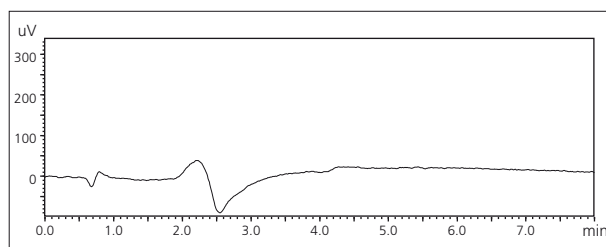
Fig. 5 Chromatogram of Mineral Water B (Hardness 323 mg/L)
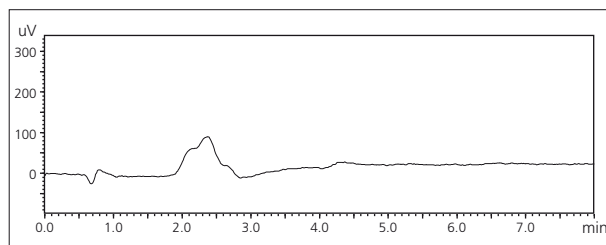
Fig. 6 Chromatogram of Mineral Water C (Hardness 1491 mg/L)

Fig. 3 Linearity of Calibration Curves (Upper: Cyanide Ions; Lower: Cyanogen Chloride)
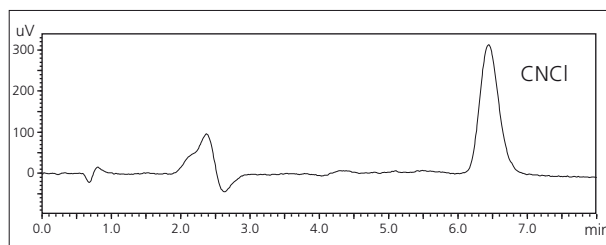
Fig. 7 Chromatogram of Mineral Water C (Spiked with 0.001 mg/L Standard Cyanogen Chloride Solution)

SHIMADZU

Shimadzu Corporation

www.shimadzu.com/an/

SHIMADZU
Excellence in Science

Application News

No.L501

Supercritical Fluid Extraction / Chromatography

Analysis of Vitamin E in a Commercial Supplement by Offline SFE-SFC-PDA

Vitamin E, also called tocopherol, is a fat-soluble vitamin and an important chemical substance that exhibits an antioxidant effect, particularly in the human body. There are four tocopherols (α, β, γ and δ) that differ based on the number and position of methyl groups. The α-tocopherol exhibits the strongest antioxidant activity, and this is the tocopherol form found in most commercial supplements as vitamin E. Since it is highly fat-soluble, a quick and simple extraction method using supercritical fluid is expected to be applicable. In this article, we introduce a procedure for α-tocopherol pretreatment that uses supercritical fluid extraction (SFE).

■ Offline SFE System

While the online SFE-SFC system has already been described in several Application News articles, many have expressed the desire to combine SFE with existing analytical methods other than SFC, and SFE has gained attention for its flexibility in terms of sample handling. The advantages of SFE are as follows.

1. Quick and highly efficient extraction using supercritical fluid that is highly permeable and has a high diffusion rate.
2. Extraction of unstable compounds under mild temperature conditions with light-shielding.
3. Low cost compared to solvent extraction.
4. Complete automation of the extraction procedure.
5. Easy handling of the extraction sample.
6. Compatible with various analysis methods.

Fig. 1 shows a flow diagram for an offline SFE system. A supercritical state is present upstream of the BPR back-pressure control unit. Valves inside the SFE unit are controlled to switch between static extraction via enclosure of supercritical fluid in the vessel and dynamic extraction via passage of supercritical fluid through the vessel, which enables quick and highly efficient extraction of the target compounds.

A HPLC pump with a low-pressure GE valve installed is used in the solvent delivery system, and the extraction conditions can be optimized by changing the type of modifier (maximum of four types, including eluent from the trap column) and the concentration relative to carbon dioxide. Extract is retained in the trap column, and the low-pressure GE valve on the solvent delivery pump is switched to the solvent suitable for elution from the trap column. Then the eluent is collected in test tubes with a fraction collector.

■ SFE Treatment for α-Tocopherol

The commercial supplement used as an actual sample may be present as a paste inside the capsule and may be moisture absorbent. As shown in Fig. 2, we mixed 275 mg of paste supplement with 1 g of Miyazaki Hydro-Protect, which is a dehydrating agent for SFE sold by Shimadzu, and transferred this mixture to the SFE extraction vessel.

275 mg of content of commercial supplement

↓ ← Add 1 g of dehydrating agent MIYAZAKI Hydro-Protect

Mix well

↓

Transfer to 5 mL of vessel
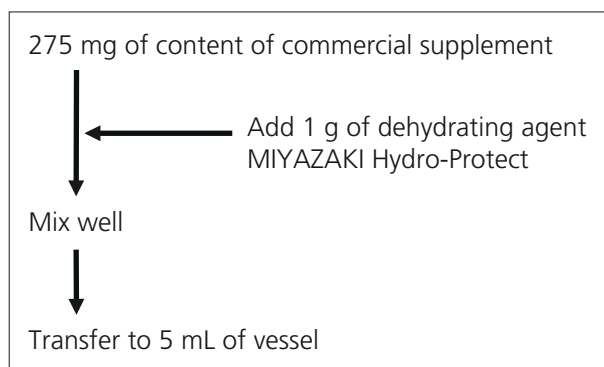
Fig. 2 Preliminary Pretreatment for Supplement Sample Before SFE
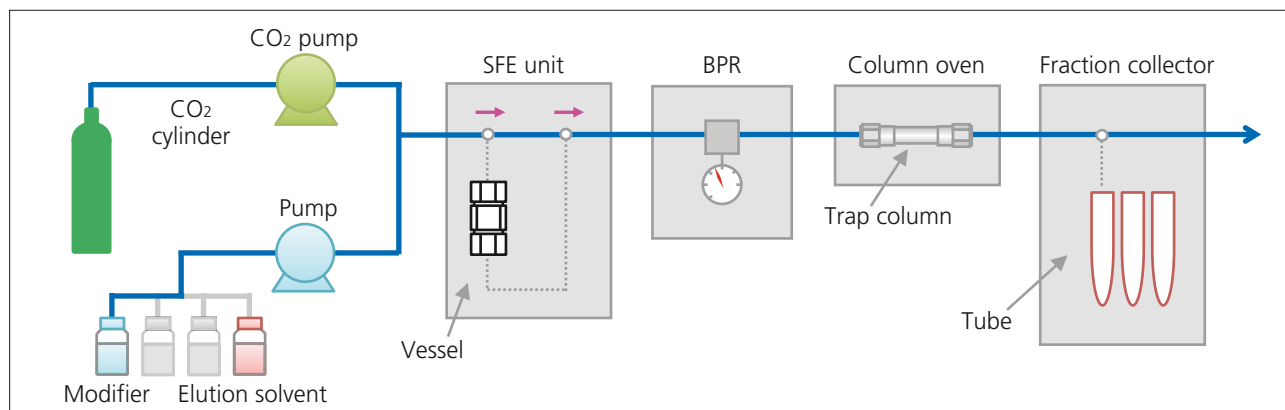
Fig. 1 Flow Diagram of Supercritical Fluid Extraction (SFE) System

The conditions used for SFE are shown in Table 1. We investigated column selection, chose the Shim-pack UCX-SIL analytical column, optimized each analytical condition for online SFE-SFC analysis, then performed analysis using the conditions shown in Table 2.

Table 1 SFE Conditions for α-Tocopherol

Offline SFE:
Extraction Vessel   : 5 mL
Extraction Solvent   : CO_2
Flowrate   : 5 mL/min
Temperature   : 40 ℃
Back Pressure   : 15 MPa
Extraction Time   : 15 min
                         (Static 2 min → Dynamic 3 min) × 3 times

Trap & Pressure Down Conditions
Trap Column   : Shim-pack VP-ODS (50 mm L. × 4.6 mm I.D.)
Temperature   : 60 ℃
Pressure Down Time : 10 min (15 - 25 min)

Recovery Conditions
Elution Solvent   : Hexane
Flowrate   : 2 mL/min
Temperature   : 60 ℃
Fraction Time   : 3.5 min (25 - 28.5 min)

■ **SFE Evaluation of α-Tocopherol in a Commercial Supplement**

For the α-tocopherol extract obtained through offline SFE, we performed SFC under the conditions shown in Table 2 then evaluated the extraction procedure. Extract was mixed with hexane to make up 10 mL before being used for SFC analysis. A representative SFC chromatogram is shown in Fig. 3.

Table 2 SFC Conditions for α-Tocopherol

SFC Conditions:
Column   : Nacalai COSMOSIL Cholester
                  (250 mm L. × 4.6 mm I.D., 5 μm)
Flowrate   : 3 mL/min
Modifier   : IPA
Gradient   : 2 % (0 min) - 20 % (10 min) - 50 % (10 - 12 min)
Temperature   : 40 ℃
Back Pressure   : 15 MPa
Injection Volume : 2 μL
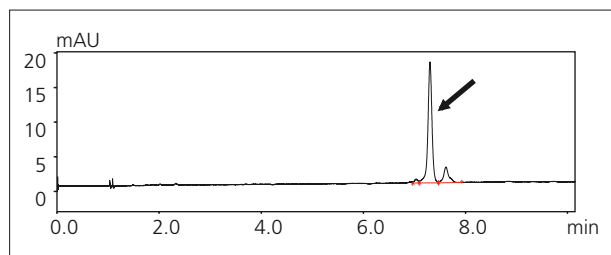
Fig. 3 SFC Analysis of α-Tocopherol Obtained by SFE from a Commercial Supplement

First, we used a standard product to evaluate the suitability of the α-tocopherol SFC conditions used for evaluation of offline SFE. Fig. 4 shows the linearity in the sample concentration range of 0.5 μg/L to 2.0 μg/L, and Table 3 shows the repeatability at a concentration of 1.0 μg/L. Good linearity and sufficient repeatability in terms of retention time, peak area and peak height were obtained.
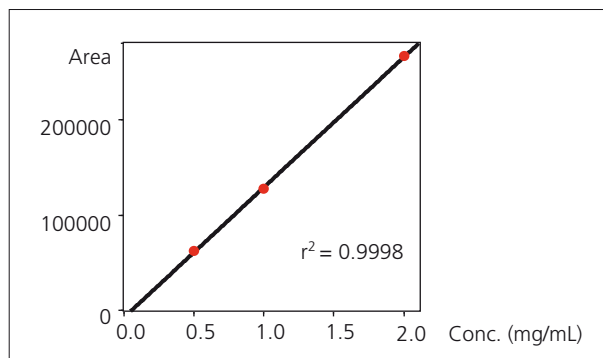
Fig. 4 Linearity for Standard α-Tocopherol Obtained by SFC

Table 3 Repeatability for Standard α-Tocopherol Obtained by SFC (n=6)

No	Retention Time (min)	Area	Height
Average	7.242	127,338	19,682
RSD (%)	0.057	0.573	0.274

Table 4 shows the repeatability of the quantitative α-tocopherol result obtained by repeated SFE treatment, and α-tocopherol recovery relative to the theoretical value (7.4 mg). Fig. 5 shows the overlaid chromatograms for α-tocopherol. Good recovery and repeatability was confirmed after just one extraction, showing that offline SFE is effective for vitamin E compound extraction.

Table 4 Repeatability and Recovery of α-Tocopherol in a Commercial Supplement Using SFE

No	Conc. (mg/mL)	Recovery (%)
1	0.776	104.46
2	0.780	105.00
3	0.772	103.92
4	0.790	106.35
5	0.761	102.44
6	0.758	102.04
Average	0.773	
RSD (%)	1.549	
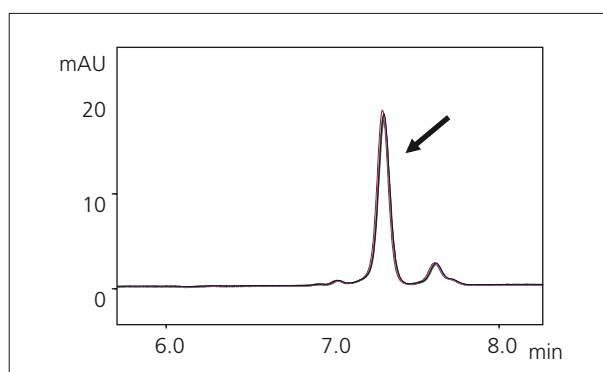
Fig. 5 Overlaid Chromatograms for α-Tocopherol After SFE

First Edition: Jan. 2016

SHIMADZU
Excellence in Science

Application News

No.L502

Supercritical Fluid Extraction / Chromatography

Analysis of Residual Pesticides in Agricultural Products Using Nexera UC Off-Line SFE-GC/MS System

Since enforcement of the positive list system for residual pesticides in foods in 2006 in Japan, over 800 pesticides have been included in the system. Consequently, there is now a strong demand for effective analytical methods encompassing any sample pretreatment steps that are capable of inspecting large numbers of pesticides.

Conventionally, analysis of residual pesticides in foods has involved pesticide extraction by a solvent extraction method before analysis by LC/MS or GC/MS. The problem with solvent extraction methods is that sample pretreatment requires a substantial amount of time and effort, and large quantities of organic solvents are used. Supercritical fluid extraction (SFE) that uses supercritical carbon dioxide as the extraction solvent provides good extraction efficiency, where the solvent is similar to gas in terms of low viscosity and high diffusivity, and similar to fluid in terms of high solubility. This allows for extraction within a short period of time. This extraction method is also less damaging to the environment since it uses a smaller amount of organic solvent compared to conventional solvent extraction methods.

We introduce an example GC/MS analysis of pesticides extracted from an agricultural products using the Nexera UC off-line SFE system.

■ Off-Line SFE System

Fig. 1 shows the principle behind operation of the Nexera UC off-line SFE system. An extraction vessel filled with a sample is placed in the SFE unit, and is heated to 40 °C (Fig. 1 A). The extraction vessel is then filled with supercritical carbon dioxide, and the target components are extracted statically without pumping the liquid (Fig. 1 B). After static extraction, dynamic extraction is performed by pumping supercritical carbon dioxide through the extraction vessel (Fig. 1 C). After trapping the extract material in the trap column, eluate that contains the target components is then collected in the fraction collector (Fig. 1 D).

■ Sample Preparation

The QuEChERS method that prioritizes simplicity and speed is widely used to pretreat agricultural products for residual pesticide analysis. While there is a special kit available for the QuEChERS method, sample preparation for this kit requires a large number of process steps including reagent addition, solvent extraction, purification by dispersive solid phase extraction, and centrifugal separation.

Meanwhile, as shown in Fig. 2, sample preparation for the Nexera UC off-line SFE system only involves mixing 1 g of agricultural product pulverized in a mixer with 1 g of dehydrating agent*, then filling the extraction vessel with this mixture. This not only results in improved productivity and a reduced environmental burden, but also avoids human errors involved in the sample pretreatment process. Using a specially designed rack changer also allows for extraction of a maximum of 48 samples consecutively.

* "Miyazaki Hydro-Protect" Patent No. 3645552
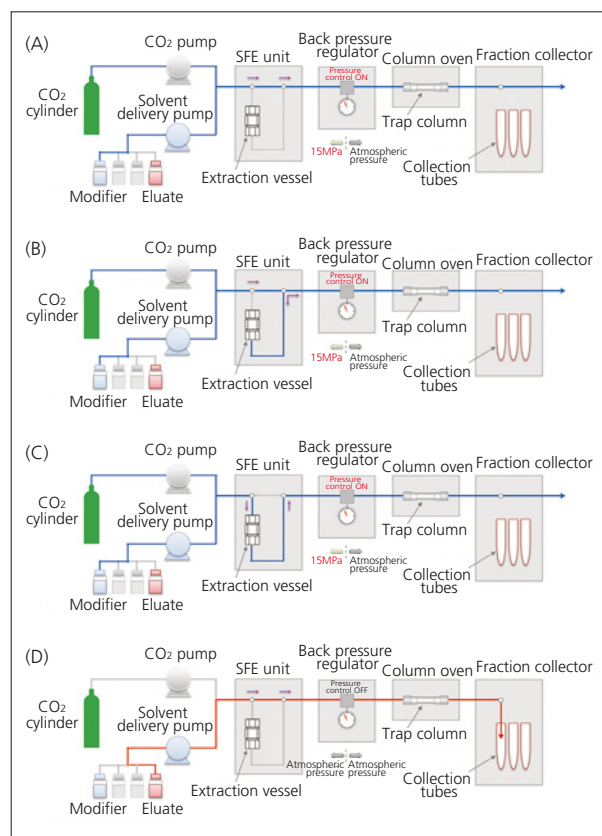
Fig. 1 Flow of Off-Line SFE Extraction
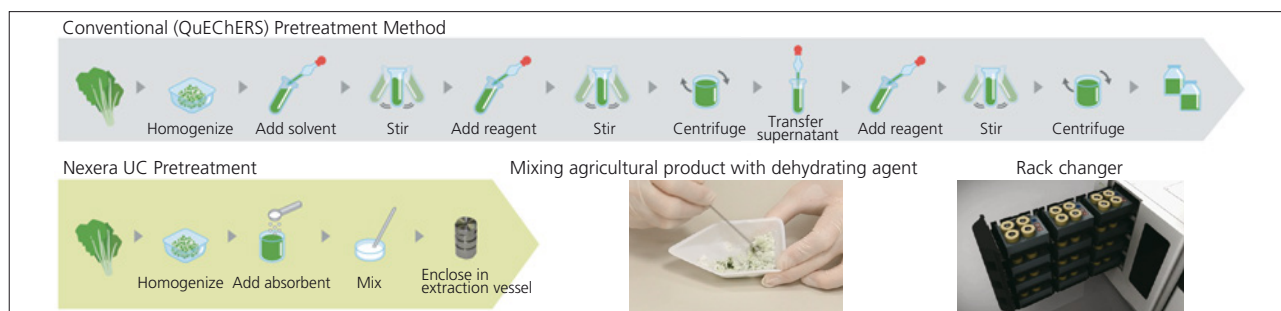
Fig. 2 Sample Preparation

Table 1 Analytical Conditions

[SFE] Nexera UC SFE System	
Extraction	: A) Supercritical fluid of CO_2
Solvent	B) Methanol
Flowrate	: 5 mL/min
Extraction	: 8 min (Static mode → Dynamic mode)
Extraction	
Vessel Temp.	: 40 ℃
BPR Pressure	: 15 MPa
Trap Column	: Shim-pack VP-ODS (50 mm L. × 4.6 mm I.D., 5 μm)
Elution Solvent	: Acetone/Hexane = 50/50 (2 mL/min, 2 min)

[GC-MS] GCMS-TQ8040	
Column	: Rxi®-5Sil MS 30 m × 0.25 mm I.D., df = 0.25 μm
Column Temp.	: 50 ℃ (1 min) → (25 ℃/min) → 125 ℃ → (10 ℃/min) → 300 ℃ (15 min)
Carrier Gas	: He (Constant linear velocity mode)
Linear Velocity	: 47.2 cm/sec
Injection Mode	: Splitless (Sampling time 1.00 min)
High Press Inj.	: 250 kPa (1.5 min)
Injection Volume	: 1 μL
Interface Temp.	: 250 ℃
Ion Source Temp.	: 200 ℃
MS Mode	: MRM
Loop Time	: 0.3 sec

■ Analysis of Brown Rice

A mixed standard solution of pesticides for GC/MS analysis (Hayashi Pure Chemical PL2005 Pesticide GC/MS Mix I-VI, 7) was added to pulverized brown rice to a concentration of 100 ng/g, and SFE was performed using the conditions shown in Table 1. The extraction liquid obtained was made up to 2 mL using eluate, and analyzed by GC/MS. The MRM chromatogram obtained from GC/MS analysis is shown in Fig. 4. Good repeatability (relative standard deviation of quantitation concentration <10 %) and recovery (70-120 %) were obtained for the 301 components. Repeatability and recovery for the 301 pesticides are shown in Table 2. This system uses a very simple pretreatment process, and can perform automated extraction from a single sample in approximately 30 minutes.
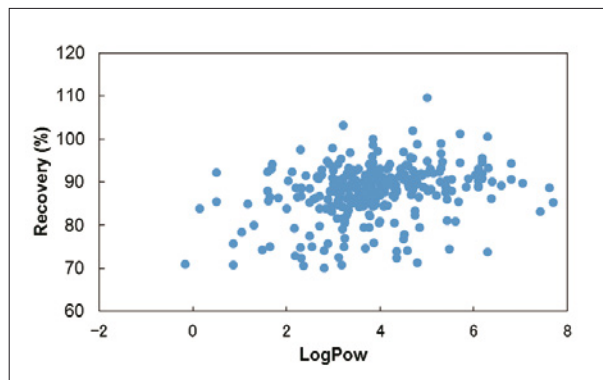
Fig. 3 Recovery in Brown Rice Analysis
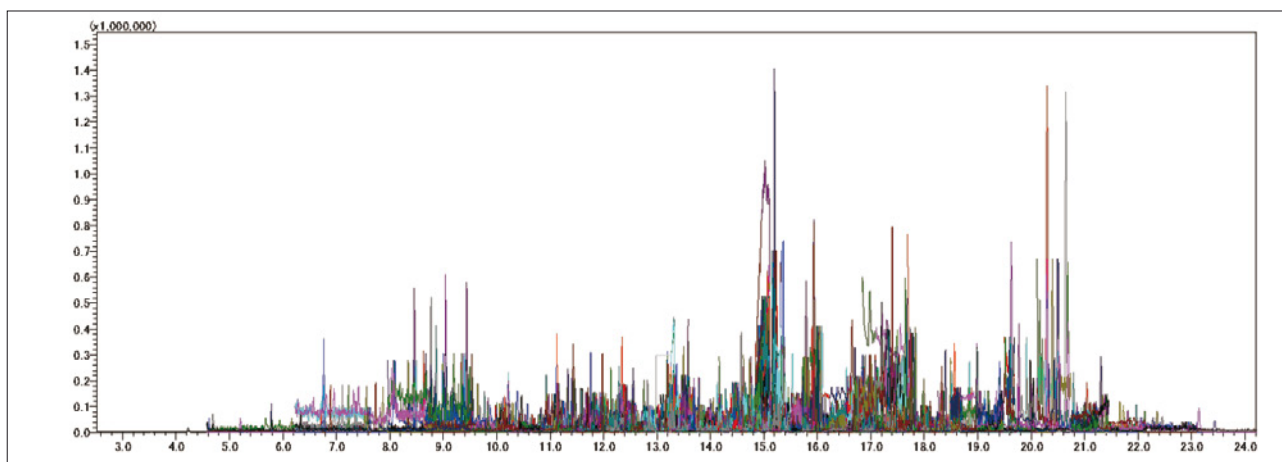
Fig. 4 MRM Chromatogram of Extraction Liquid from Brown Rice

Table 2 Repeatability and Recovery

Compounds	Repeatability (%RSD, n = 6)	Recovery (%)	Compounds	Repeatability (%RSD, n = 6)	Recovery (%)
2-Phenylphenol	3.8	87.0	Azinphos-ethyl	5.3	84.3
Acetochlor	5.9	93.1	Azinphos-methyl	2.7	83.1
Acrinathrin-1	6.8	73.8	Benalaxyl	7.0	84.9
Acrinathrin-2	3.1	100.6	Benfluralin	5.2	90.1
Alachlor	3.6	88.7	Benfuresate	4.1	91.5
Allethrin-3,4	5.9	102.0	Benoxacor	3.2	90.8
Allidochlor	5.3	86.4	beta-BHC	5.3	87.8
alpha-BHC	4.6	88.9	beta-Endosulfan	6.5	90.7
alpha-Endosulfan	9.5	98.7	Bifenox	4.1	84.5
Ametryn	4.1	86.3	Bifenthrin	3.3	89.2
Anilofos	4.7	86.3	Biphenyl	3.5	80.5
Atrazine	4.8	86.7	Bromobutide	4.6	90.4
Azaconazole	5.5	70.5	Bromophos	5.4	90.1
Azamethiphos	9.9	78.4	Bromophos-ethyl	6.0	86.6

Table 2 Repeatability and Recovery (continued)

Compounds	Repeatability (%RSD, n = 6)	Recovery (%)	Compounds	Repeatability (%RSD, n = 6)	Recovery (%)
Bromopropylate	4.1	90.9	Diphenamid	5.7	79.3
Bromuconazole-1	3.7	80.5	Diphenylamine	3.1	91.5
Bromuconazole-2	5.3	77.1	Disulfoton sulfone	5.2	85.0
Bupirimate	7.9	86.8	Ditalimfos	3.2	90.1
Buprofezin	6.6	88.8	Dithiopyr	5.1	90.9
Butachlor	6.4	91.6	Edifenphos	3.5	95.9
Butafenacil	4.4	90.4	Endosulfan sulfate	6.9	95.4
Butamifos	3.8	90.1	EPN	3.8	88.0
Butylate	4.6	84.7	Epoxiconazole	3.7	83.9
Cadusafos	4.1	88.1	EPTC	4.3	81.6
Cafenstrole	5.1	91.1	Esprocarb	2.7	90.6
Captan	9.1	77.6	Ethalfluralin	5.3	93.3
Carbofuran	4.7	83.3	Ethion	3.4	93.1
Carbophenothion	2.9	91.5	Ethofumesate	5.7	91.4
Carfentrazone-ethyl	4.1	96.8	Ethoprophos	4.3	91.0
Chinomethionat	4.2	82.1	Etobenzanid	3.8	86.6
Chlomethoxyfen	5.8	89.8	Etofenprox	3.8	89.7
Chlorbenside	3.9	81.1	Etoxazole	8.2	87.9
Chlorbufam	4.2	84.7	Etridiazole	3.8	85.3
Chlorethoxyfos	4.6	90.3	Etrimfos	2.9	87.9
Chlorfenapyr	7.5	86.5	Famoxadone	5.4	71.2
Chlorfenson	7.7	91.4	Fenamidone	5.7	70.1
Chlorfenvinphos-(E)	4.4	91.2	Fenchlorphos	6.0	92.1
Chlorfenvinphos-(Z)	6.5	88.7	Fenitrothion	6.9	88.7
Chlormephos	3.1	89.6	Fenothiocarb	5.4	88.6
Chlorobenzilate	3.6	92.0	Fenoxanil	6.2	88.2
Chloroneb	6.0	95.0	Fenoxaprop-ethyl	4.1	90.5
Chlorothalonil	5.3	87.7	Fenoxycarb	6.9	84.4
Chlorpropham	4.9	88.5	Fenpropathrin	3.7	91.6
Chlorpyrifos	6.2	90.8	Fenpropimorph	4.7	76.8
Chlorpyrifos-methyl	5.1	90.5	Fenthion	3.6	79.5
Chlorthiophos-2	9.5	88.4	Fenvalerate-1	5.2	88.4
Chlorthiophos-3	2.8	92.8	Fenvalerate-2	4.2	95.0
Chlozolinate	7.8	82.4	Fipronil	8.3	86.7
Cinidon-ethyl	4.3	88.8	Flamprop-methyl	6.6	85.7
Cinmethylin	9.9	94.5	Fluacrypyrim	6.8	97.0
Clomazone	4.2	88.6	Flucythrinate-1	4.0	92.8
Clomeprop	3.3	89.8	Flucythrinate-2	3.7	95.7
Crimidine	6.0	80.0	Flufenpyr-ethyl	1.8	98.0
Cyanofenphos	4.7	91.8	Flumiclorac-pentyl	5.8	91.8
Cyanophos	5.0	91.3	Flumioxazin	9.4	75.0
Cyflufenamid	8.4	89.6	Fluquinconazole	4.3	81.2
Cyfluthrin-1	5.1	95.6	Flusilazole	5.5	86.8
Cyfluthrin-2	3.5	94.6	Fluthiacet-methyl	3.8	79.5
Cyfluthrin-3	4.9	92.0	Flutolanil	9.6	87.8
Cyfluthrin-4	6.0	90.8	Fluvalinate-1	2.6	100.0
Cyhalofop-butyl	4.2	93.4	Fluvalinate-2	2.6	98.6
Cyhalothrin-1	9.1	90.6	Folpet	5.3	87.7
Cyhalothrin-2	4.5	94.4	Fonofos	3.8	91.7
Cypermethrin-1	2.8	99.0	Formothion	5.3	74.4
Cypermethrin-2	3.7	96.6	Fosthiazate-2	9.6	93.2
Cypermethrin-3	3.7	93.2	Furilazole	3.3	92.4
Cypermethrin-4	8.4	93.2	gamma-BHC	4.1	88.7
Cyprodinil	4.0	80.9	Halfenprox	2.3	85.4
delta-BHC	2.2	88.2	Hexaconazole	8.9	85.6
Deltamethrin-2	3.7	103.2	Indanofan	7.9	86.5
Dialifos	3.2	91.4	Indoxacarb	3.7	95.7
Di-allate-1	2.5	91.5	Iprobenfos	4.4	89.5
Di-allate-2	4.7	92.0	Iprodione	2.5	92.7
Diazinon	7.8	90.0	Iprodione metabolite	3.1	106.2
Dichlobenil	4.0	79.8	Isazofos	3.7	94.2
Dichlofenthion	5.2	92.1	Isocarbophos	6.6	84.0
Dichlofluanid	3.3	87.2	Isofenphos	3.2	89.0
Dichlorvos	3.2	83.9	Isofenphos oxon	5.2	84.5
Diclobutrazol	5.2	87.0	Isoprocarb	4.5	86.6
Diclocymet-1	4.3	83.4	Isoprothiolane	7.5	86.1
Diclocymet-2	5.1	82.2	Isoxadifen-ethyl	5.0	90.5
Diclofop-methyl	4.4	91.0	Isoxathion	6.7	93.2
Diethofencarb	4.8	83.8	Kresoxim-methyl	7.0	89.7
Difenoconazole-1	5.5	74.0	Leptophos	3.5	93.3
Difenoconazole-2	5.2	72.4	Malathion	3.2	93.0
Diflufenican	4.4	94.3	MCPB-ethyl	3.5	90.3
Dimepiperate	2.5	87.8	Mecarbam	8.4	97.6
Dimethametryn	6.4	84.8	Mefenacet	4.5	75.1
Dimethenamid	5.4	88.8	Mefenpyr-diethyl	5.0	90.4
Dimethipin	9.9	70.9	Mepronil	4.2	79.5
Dimethylvinphos-(E)	4.5	86.8	Metalaxyl	7.0	86.6
Dimethylvinphos-(Z)	4.9	86.1	Methacrifos	5.9	92.3
Diniconazole	2.3	80.6	Methidathion	4.5	86.0
Dioxabenzofos	4.4	91.5	Methoprene	8.8	109.6
Dioxathion	5.4	88.6	Methoxychlor	3.1	90.6
Dioxathion deg.	4.4	86.1	Metolachlor	2.9	91.1

Table 2 Repeatability and Recovery (continued)

Compounds	Repeatability (%RSD, n = 6)	Recovery (%)	Compounds	Repeatability (%RSD, n = 6)	Recovery (%)
Metominostrobin-(E)	9.6	72.4	Simazine	5.2	74.9
Metribuzin	6.5	75.1	Simeconazole	6.1	79.1
Mevinphos-1	9.9	92.3	Simetryn	5.0	74.1
Mevinphos-2	6.0	85.4	Spirodiclofen	4.6	94.1
Molinate	3.8	86.0	Sulfotep	3.9	92.9
Myclobutanil	5.9	75.7	Sulprofos	4.8	74.5
Naled	6.1	72.8	Swep	5.3	83.6
Nitralin	4.5	94.2	Tebufenpyrad	3.6	88.8
Nitrofen	8.1	88.9	Tebupirimfos	4.6	89.4
Nitrothal-isopropyl	2.4	90.2	Tecnazene	3.1	89.5
Oxabetrinil	3.4	91.7	Tefluthrin	4.5	90.1
Oxadiazon	3.9	94.7	Terbucarb	4.0	87.6
Oxpoconazole	6.4	74.7	Terbufos	3.8	77.9
Oxpoconazole-formyl deg.	9.9	88.9	Terbutryn	4.5	86.0
Oxyfluorfen	8.9	88.3	Tetrachlorvinphos	3.2	93.0
Paclobutrazol	7.5	72.6	Tetraconazole	7.8	84.3
Parathion	6.3	90.1	Tetradifon	5.9	89.5
Parathion-methyl	5.1	90.4	Tetramethrin-1	6.9	93.8
Penconazole	4.7	85.0	Tetramethrin-2	4.3	90.9
Pendimethalin	5.1	86.9	Thenylchlor	3.5	87.3
Pentoxazone	4.2	95.6	Thifluzamide	5.9	84.6
Permethrin-1	4.8	89.0	Thiobencarb	3.5	85.6
Permethrin-2	4.0	88.8	Tolclofos-methyl	3.9	90.6
Phenothrin-1	7.4	93.1	Tolfenpyrad	3.6	81.0
Phenothrin-2	2.5	90.2	Tolylfluanid	5.8	91.1
Phenthoate	2.4	91.7	Triadimefon	3.7	88.3
Phorate	4.1	75.9	Triadimenol-1	6.2	70.8
Phosalone	3.5	88.1	Tri-allate	5.3	91.2
Phosmet	4.2	84.5	Triazophos	4.7	89.9
Phosphamidon-1	8.6	75.8	Tribufos	6.2	90.6
Phosphamidon-2	6.6	70.8	Trichlamide	5.2	85.3
Picolinafen	4.0	90.4	Trifloxystrobin	5.9	90.7
Piperonyl butoxide	3.8	89.2	Trifluralin	3.2	92.5
Piperophos	3.5	88.9	Vinclozolin	4.2	89.6
Pirimiphos-methyl	5.7	90.8	XMC	3.9	86.5
Pretilachlor	5.6	89.8	Xylylcarb	4.5	85.3
Procymidone	7.0	91.6	Zoxamide	3.6	82.6
Profenofos	5.6	94.1			
Prohydrojasmon-1	5.5	87.7			
Prohydrojasmon-2	8.7	88.6			
Prometryn	3.0	86.8			
Propachlor	4.4	88.0			
Propargite-1	9.3	101.3			
Propargite-2	9.5	94.5			
Propazine	4.0	97.1			
Propiconazole-1	6.7	89.4			
Propiconazole-2	3.2	88.3			
Propoxur	5.3	83.9			
Propyzamide	4.2	81.6			
Prothiofos	4.0	85.5			
Pyraclofos	5.1	94.1			
Pyraclostrobin	4.7	93.1			
Pyraflufen-ethyl	4.7	92.7			
Pyrazophos	4.2	92.8			
Pyrazoxyfen	9.4	91.2			
Pyributicarb	3.1	88.1			
Pyridaben	3.1	86.1			
Pyridaphenthion	5.4	84.2			
Pyrifenox-(E)	5.9	85.2			
Pyrifenox-(Z)	7.3	92.9			
Pyrimethanil	6.0	83.9			
Pyrimidifen	4.9	74.2			
Pyriminobac-methyl-(E)	3.9	88.6			
Pyriminobac-methyl-(Z)	5.2	88.6			
Pyriproxyfen	5.7	92.1			
Quinalphos	3.3	93.2			
Quinoxyfen	3.2	87.1			
Quintozene	6.0	90.3			
Quizalofop-ethyl	3.0	86.9			
Resmethrin-1	6.2	88.5			
Resmethrin-2	3.3	86.1			
Silafluofen	3.7	88.6			

SHIMADZU

Shimadzu Corporation

www.shimadzu.com/an/

2. Mass Spectrometry
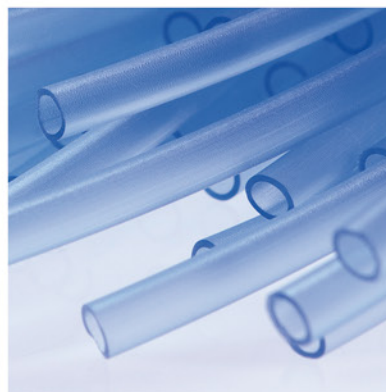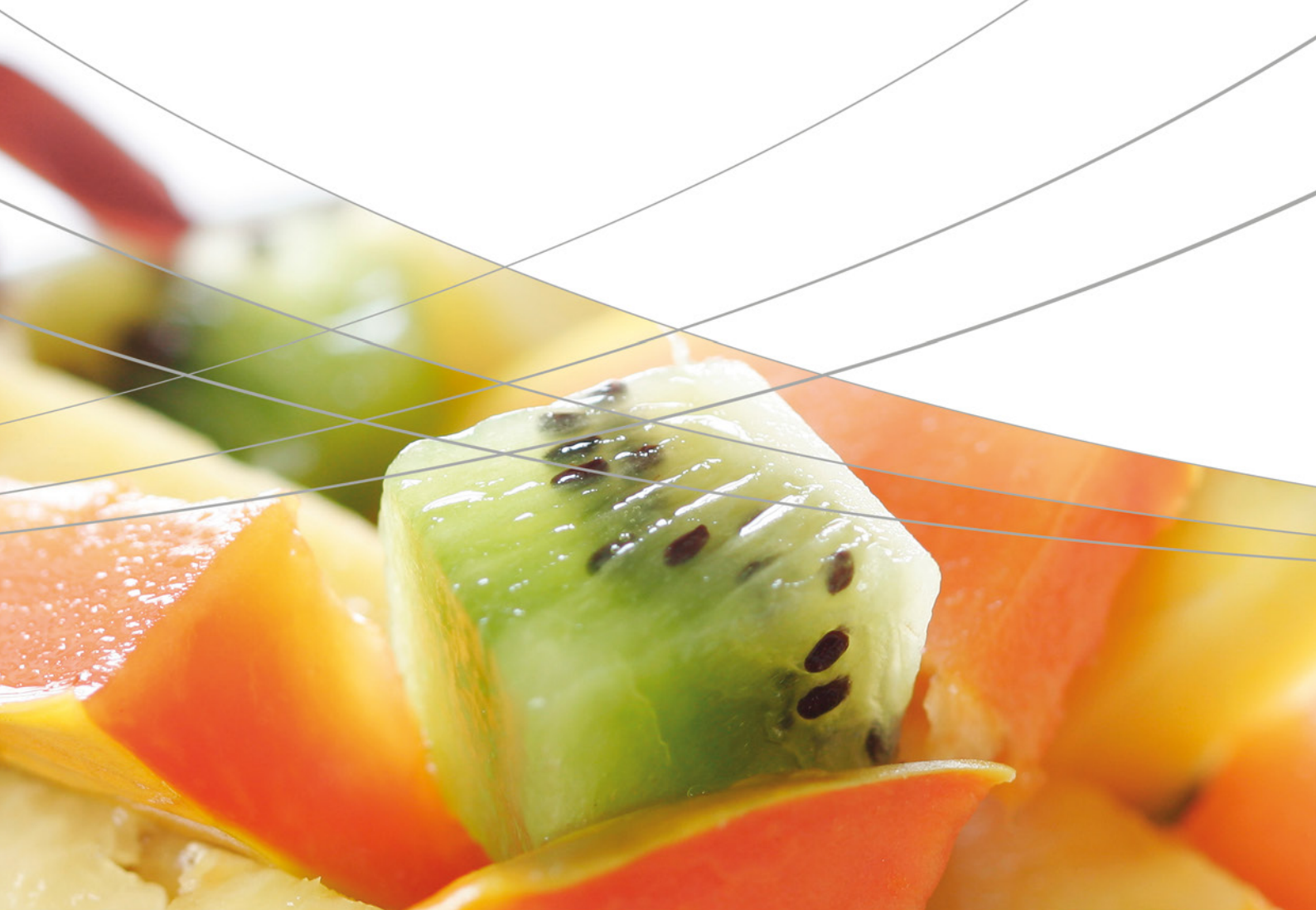
2. Mass Spectrometry

2.1 Gas Chromatography-Mass Spectrometry

Gas Chromatography-Mass Spectrometry (GC-MS) is a hyphenated technique combining the separating power of gas chromatography (GC) with the detection power of mass spectrometry to identify different substances within a sample. Mass spectrometry is a wide-ranging analytical technique which involves the production, subsequent separation and identification of charged species according to their mass to charge (m/z) ratio.

C146-E239	Analysis of MOSH and MOAH using SPE prior to GC×GC-MS analysis
GCMS-1304	Analysis of organophosphorus pesticides in baby foods using a Triple-Quadrupole GC/MS/MS System
No. 68	GC-MS/MS analysis of pesticides in drinking water
No. 72	Scan/MRM analysis of residual pesticides in foods using GC-MS/MS (3)
No. 73	High-sensitivity analysis of 2,4,6-trichloro-anisole in wine using Headspace-Trap GC/MS
No. 93	Easy screening for residual pesticides in processed foods using GC-MS/MS
SCA_280_079	Quantitative analysis of dibenzo-p-dioxins (PCDD) and polychlorinated-p-dibenzofurans (PCDF) in foodstuff and animal feed using the GCMS-TQ8030 tandem mass spectrometer
SCA_280_080	Comprehensive screening of residual 360 pesticides in food using fast GC-MS/MS technology

SHIMADZU
Excellence in Science

Technical Report

Analysis of MOSH and MOAH using SPE prior to GC×GC-MS analysis

Luigi Mondello[1]

Abstract:

The present work is focused on the development/optimization of a comprehensive two-dimensional gas chromatography method, with dual detection [flame ionization (FID) and mass spectrometric], for the simultaneous identification and quantification of mineral-oil contaminants in a variety of food products. The two main classes of contaminants, namely saturated and aromatic hydrocarbons, were previously fractionated on a manually-packed silver silica solid-phase extraction (SPE) cartridge. The presence of a series of unknown compounds was investigated using the mass spectrometric data, and were tentatively-identified as esterified fatty acids, most probably derived from vegetable oil based ink.

Keywords: Food, MOSH, MOAH, GC×GC, Comprehensive GC, Quadrupole mass spectrometer

1. Introduction

Mineral oil products derive from crude petroleum, through distillation processes and various refining steps, and contain proportions of mineral oil saturated hydrocarbons (MOSH, including n-alkanes, isoalkanes and cycloalkanes), and mineral oil aromatic hydrocarbons (MOAH), mainly consisting of alkylated polyaromatic hydrocarbons (PAH)[1].

Mineral oil contamination in foods, deriving from a variety of sources, has been studied for quite a long time[2-4]. One of the major sources of contamination is paperboard packaging, an issue known since 1997[2], even though it has gained great attention only recently[5,6] Such a contamination derives from the printing inks applied directly to the packaging, and/or from the ink used in the newspapers, employed to produce recycled fiber. It has also been demonstrated that mineral oil migrating from paperboard usually contains a large proportion (15–20%) of MOAH[3,4], which are more of a worry from a toxicological viewpoint.

The occurrence and danger of mineral oil products in foods has been discussed widely in recent years[7-10]. The Joint FAO/WHO Expert Committee on Food Additives (JECFA), in 2002, reported a list of admissible daily intake (ADI) values for different white mineral oils[8]; based on such data, an envisioned limit of 0.6 mg kg^{-1} was proposed for MOSH migration (up to C25) in dry foods from paperboard packaging[7]. The European Food Safety Authority (EFSA), published an opinion in June 2012[9], casting doubts on the "JECFA" list, due to the lack of sufficient toxicological information and, as a consequence, the JECFA values were recently withdrawn[10]. Furthermore, even though EFSA emphasized the potential carcinogenic risk of MOAH constituents[9], an official approved evaluation of MOAH is still lacking.

Most of the approaches reported over the last decades have been directed to the analysis of MOSH, exploited as a contamination marker, using both off- and on-line techniques. Off-line methods based on prep LC, or solid-phase extraction (SPE), have been described[11-18]. The lipid fraction can be eliminated either through saponification, followed by silica-gel column chromatography [11,12], or directly through a prep LC silica column[13,14], or an SPE cartridge[15-18]. Several techniques, based on the use of glass SPE, have been described; with regards to packing materials, a variety of solutions have been proposed, such as activated silica gel[16], non-activated silica gel[17], or silver (Ag) silica gel[18].

Considering the application of all methods, it can be affirmed without a doubt, that the most popular technique has been on-line liquid chromatography-gas chromatography (LC-GC), with a silica LC column[6,19-23]. Additionally, and in consideration of the toxicological relevance of MOAH, work has been directed to the clear pre-separation of the MOSH from the MOAH. For example, Biedermann and co-workers exploited the separation efficiency of an LC silica column, in an on-line LC-GC system, to separate the MOAH from the MOSH, and these from the lipidmatrix[20]. It must also be noted that off-line SPE methods, using a Ag silica-gel SPE cartridge, have been developed for MOSH and MOAH determination[24,25].

With regards to detectors, flame ionization (FID) systems have been widely employed for the reliable quantification of the humps of unresolved complex mixtures (UCM), generated in MOSH/MOAH applications; FIDs are useful because they provide virtually the same response *per* mass of hydrocarbons, even though the lack of structural information is certainly a major drawback[23]. In fact, the attainment of profound information on the composition of MOSH and MOAH constituents, can provide

fundamental information on potential toxicity, and on the contamination source. Such an objective was reached by Biedermann and Grob, who used an MS detector, along with the additional information generated by a comprehensive 2D GC (GC×GC) analysis[26]. A pre-separation of the MOSH and MOAH groups was achieved through off-line LC, a process necessary to avoid the overlapping of steranes and hopanes (present in the MOSH fraction), with alkylated (two- and three-ring) aromatics. The GC×GC system was coupled alternatively with an MS system, for qualitative purposes, and with an FID system for quantification, and hence, two applications were required to obtain both information types. A GC×GC-MS method, after an off-line LC pre-separation step, has also been exploited by Mondello and co-workers, to attain a more expanded view on MOSH contamination in homogenized baby foods[27].

The present document describes a GC×GC method, characterized by dual MS/FID detection, for the qualitative and quantitative analysis of MOSH and MOAH in various foods. The pre-separation step was performed by using Ag-SPE.

2. Experimental
2-1. Samples and chemicals

CH_2Cl_2 and *n*-hexane were purchased from Sigma-Aldrich (Milan, Italy), and distilled before use. The C7–C40 standard mixture, the paraffin oil (code 18512), $AgNO_3$, and silica gel 60 (particle size 0.063–0.2 mm, 70–230 mesh) were purchased from Supelco and Sigma-Aldrich (Milan). Glass SPE cartridges (6 mL glass tubes with a frit) were purchased from Macherey-Nagel (Chromabond, Düren, Germany).

2-2. Samples and preparations

Samples of pasta, rice and icing sugar, were purchased in a supermarket. The ground samples were extracted overnight using *n*-hexane, and then purified through Ag-SPE. Briefly, a 1:2 food to solvent ratio was employed to extract MOSH and MOAH from the samples. After, an aliquot of the extract was concentrated prior to SPE clean-up, on a Ag silica gel cartridge. Silver silica gel was prepared by adding a $AgNO_3$ solution (0.75 g/mL in Milli-Q water, Millipore, Bedford, MA, USA) to previously activated (400°C overnight) silica gel, blended for about 30 min, and left to rest for 12 h; finally, the mixture was heated at 75°C overnight to eliminate the remaining water. The SPE cartridge was manually packed with 1 g of Ag silica, prior to sample loading (250 μL). First, the sample was eluted with 1 mL of *n*-hexane, which was discharged; then, the MOSH constituents were eluted with 1.5 mL of *n*-hexane, followed by 0.5 mL of *n*-hexane/dichloromethane (50:50 *v/v*); a 0.5 mL *n*-hexane/dichloromethane fraction followed, which was discharged; finally, the MOAH class was eluted with further 7 mL of *n*-hexane/dichloromethane (50:50 *v/v*).

The eluted fractions were concentrated to a final volume of 100 μL to increase sensitivity, since large volume injection (LVI) was not used.

2-3. GC×GC-MS/FID analysis

GC×GC experiments were performed on a system consisting of a GC-2010 gas chromatograph, and a QP2010 Ultra quadrupole mass spectrometer (Shimadzu, Kyoto, Japan).

The primary column, an SLB-5ms 30 m × 0.25 mm ID × 0.25 μm d_f [silphenylene polymer, virtually equivalent in polarity to poly (5% diphenyl/95% methyl siloxane)], was connected to an uncoated capillary segment (1.0 m × 0.25 mm ID, used to create a double-loop), and to a 1.0 m × 0.10 mm ID × 0.10 μm d_f Supelcowax-10 (polyethylene glycol) segment (Supelco). The second column was connected through a capillary column splitter (SGE) to two uncoated capillaries, with these linked to the FID (0.5 m × 0.1 mm ID) and to the MS (0.25 m × 0.05 mm ID) systems.

2-4. Method parameters

Modulation was performed every 6000 msec, by using a loop-type modulator (under license from Zoex Corporation, Houston, TX, USA). The duration of the hot pulse (350°C) was 375 msec.

GC oven temperature program: 50°C to 280°C (hold 7.5 min) at 4°C/min. Carrier gas, He, was supplied at an initial pressure of 243 kPa (constant linear velocity mode). Injection temperature: 360°C. Injection mode and volume: pulsed injection (300 kPa hold for 1 min) in the split mode (1:10); 6 μL. The FID was operated as follows: H_2 flow: 40.0 mL/min; air flow: 400.0 mL/min; make up (He): 30.0 mL/min.

MS parameters: samples were analyzed in the full scan mode with a scan speed of 20,000 amu/sec and a mass range of 40–510 *m/z*; spectra generation frequency: 33 Hz; interface and ion source temperatures were 250°C and 200°C, respectively. MS ionization mode: electron ionization.

Bidimensional visualization was carried out by using the ChromSquare v. 1.5 software (Shimadzu Europe, Duisburg, Germany). The MS libraries used for spectral matching were NIST05, FFNSC, and FAME library.

3. Results and Discussion
3-1. GC×GC-MS/FID optimization and validation

GC×GC method optimization was achieved by using offset printing ink, which is formed mainly of MOSH (> 90%), and by a minor MOAH fraction. Apart from problems related to co-elution, if the offset ink had been injected neat then the MOSH group would have overloaded the columns and modulator, while the MOAH constituents would have been barely detected; therefore, a pre-separation on the Ag-SPE cartridge was necessary.

Flow division between the FID and MS units was a compromise among different necessities, the main one being the attainment of a satisfactory sensitivity for quantification purposes. Because the detectors employed operate under different pressure conditions, the employment of two branches with equal IDs proved to be a non-ideal choice; the reason was related to the fact that an excessively long "MS" branch was required to generate an adequate flow resistance, to divert the majority of the effluent to the FID. Such a configuration would have led to substantial differences in the second-dimension elution times, between the qualitative and quantitative experiments. A good compromise was found through the use of an MS-linked 0.25 m × 0.05 mm ID branch, and a 0.5 m × 0.1 mm ID FID one.

Such a splitting configuration produced the following flow conditions: about 84% and 16% of the effluent reaching the FID and MS at the initial analysis temperature, respectively. The split ratio changed slightly during the GC run, with about 87% and 13% of the effluent diverted to the FID and MS, at the end. Since the calibration curve was constructed under the same analytical conditions, the quantitative results were not affected.

The GC×GC dual-detection operational conditions were optimized with the aim of maintaining the same chromatography performance, compared to an MS-only system, as shown in Fig. 1. In the MS-only approach, with the same analytical columns, the head pressure (approx. 150 kPa) was selected to generate about 20 cm/sec and 210 cm/sec, in the first and second dimension, respectively. In the dual-detection approach, a 243-kPa pressure produced the same gas velocity in the first dimension (to attain the same elution temperatures), and a slightly lower one in the second (180 cm/sec).
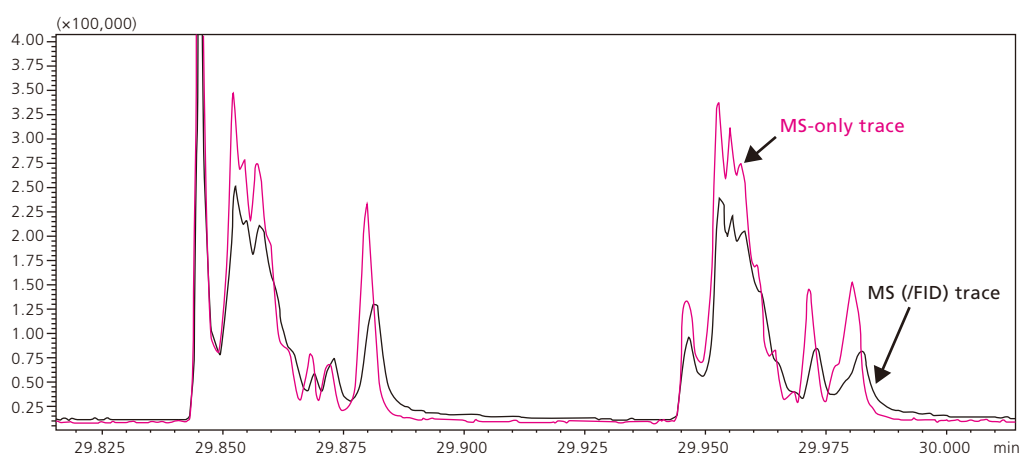
Fig. 1 Comparison of raw TIC chromatogram expansions (printing ink analyses), obtained using a GC×GC-MS and a GC×GC-MS/FID system

A six-point (each point was derived through duplicate applications) calibration curve was constructed through the FID trace, using solutions of paraffin oil in n-hexane, in the 0.35–24 mg/Kg range. The least squares method was exploited to estimate the regression line, while the linearity and the goodness of the curve were evaluated through the regression coefficient (0.9993), and a visual inspection of the residual plot, and were confirmed using Mandel's fitting test ($F_{calc} < F_{tab}$). The significance of the intercept (p = 0.03) was established running a t-test, at the 5% significance level.

Measurement of the limit of quantification (LoQ), in mineral oil analyses, is tightly related to the MW distribution of the contaminants, hence on the hump width. However an approximate estimation of the LoQ was made by considering the standard deviation (n=3), calculated at the lowest calibration point, multiplied by 10. The LoQ was estimated to be approximately 1.2 mg/Kg.

3-2. Food analysis

MOSH and the MOAH fractions, relative to pasta, icing sugar and rice, were quantified up to C25 (as required by the envisioned limit), using the aforementioned method; attention was paid, during integration, to eliminate the natural alkanes from the MOSH compounds, and the "unknown" peaks from the MOAH group. Specifically, for GC×GC-FID quantification, the "polygonal integration function" was applied, which enabled the definition of a polygonal area in which all the integrated peaks are automatically summed, and the data relative to each peak is saved as well. Thus, the undesired peaks can be easily selected, and subtracted from the total area. Quantification information, relative to the three foods, is listed in Table 1.

Table 1 Quantification values relative to the MOSH and the MOAH fractions, in samples of pasta, icing sugar, and rice, using Ag-SPE-GC×GC-MS/FID

Food	MOSH <C25 (mg/Kg)	MOAH< C25 (mg/Kg)
Pasta	3.5	1.6
Icing sugar	8.4	1.3
Rice	33.8	2.2

3-3. GC×GC-MS results for the MOAH fraction

The peaks present in the GC×GC chromatograms, for the three samples, were tentatively-identified on the basis of MS database similarities (≥ 80%) and in accordance with linear retention indices (LRI), contained in the same database. Since a widely-accepted procedure for the calculation of GC×GC LRI values has not been developed, such data were calculated in a one-dimensional mode; furthermore, a rather wide LRI filter window (± 25 units) was applied (to eliminate wrong matches), to compensate for the retention effects of the polar capillary. The tentatively identified compounds, along with experimental and database LRI, are listed in Table 2.

Two compounds were outside the LRI range; specifically, octyldodecanoate and octyltetradecanoate were characterized by a difference of +56 and +57 units, respectively. It noteworthy that, in these cases, the database LRI values (http://webbook.nist.gov/chemistry/), were attained using a methyl silicon capillary column [(Ultra-1) 25 m × 0.32 mm × 0.25 μm], while in the present research a 30 m × 0.25 mm ID × 0.25 μm silphenylene polymer phase was used. Since the similarity matches were satisfactory, and the analyte locations in the 2D chromatogram gave a further idea on the chemical structure, these solutes were given a name.

Figures 2, 3 and 4 show GC×GC-MS chromatograms for the pasta, icing sugar and rice samples, respectively.

Fig. 2 GC×GC-MS chromatogram, relative to the pasta MOAH fraction. Identification as reported in Table 2. FA: fatty acid; DINP: diisopropylnaphthalenes
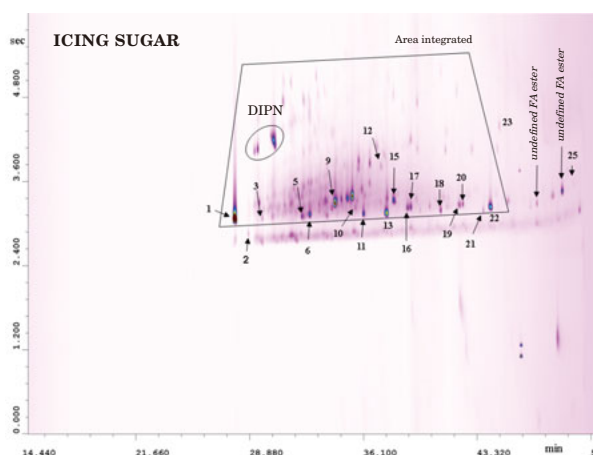
Fig. 3 GC×GC-MS chromatogram, relative to the icing sugar MOAH fraction. Identification as reported in Table 2.
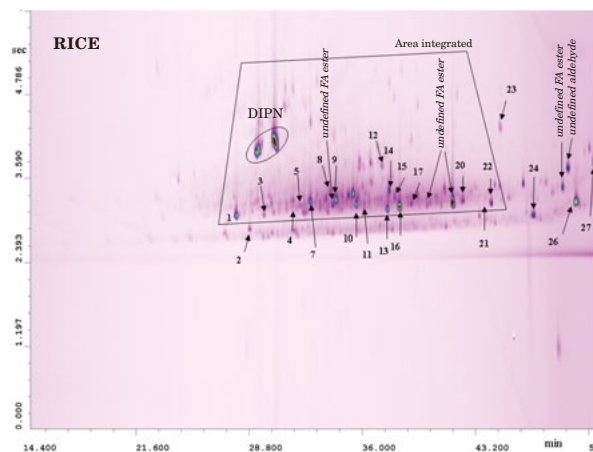
Fig. 4 GC×GC-MS chromatogram, relative to the rice MOAH fraction. Identification as reported in Table 2.

Table 2 Compounds identified in the "MOAH" GC×GC–MS analysis; database-derived (database LRI) and experimental LRI (defined as LRI) values, and spectral similarities (MS%)

	compound	pasta MS%	ice sugar MS%	rice MS%	LRI	database LRI
1	Isopropyldodecanoate	94	93	95	1622	1627
2	Dioctylether	92	93	94	1667	1688
3	2-Ethylhexyl octanoate	87	85	87	1703	1715
4	Ethyltetradecanoate	-	-	82	1798	1795
5	Isopropyltetradecanoate	93	94	93	1821	1828
6	Isoamyldodecanoate	-	92	-	1846	1844
7	6,10,14-Trimethyl-2-pentadecanone	-	-	96	1846	1846
8	2-Heptadecanone	-	-	95	1896	1906
9	Methylhexadecanoate	95	91	93	1929	1925
10	Ethylhexadecanoate	92	83	94	1992	1993
11	Isopropylhexadecanoate	90	90	90	2025	2024
12	Abietatriene	84	81	83	2085	2075
13	Octyldodecanoate	86	84	83	2102	2158
14	2-Nonadecanone	-	-	92	2108	2106
15	Methyloctadecanoate	90	92	90	2130	2124
16	Dodecyloctanoate	95	91	-	2175	2177
17	n-Butylhexadecanoate	92	93	90	2198	2188
18	Octyltetradecanoate	83	85	-	2302	2359
19	Tetradecyloctanoate	84	90	-	2380	2375
20	n-Butyloctadecanoate	84	88	87	2395	2388
21	Pentadecyloctanoate	-	85	84	2477	2475
22	Octylhexadecanoate	83	84	83	2504	2505
23	Di(ethylhexyl) phthalate	95	93	94	2542	2550
24	1-Tetracosanol	-	-	92	2697	2710
25	Squalene	93	93	-	2828	2847
26	1-Hexacosanol	91	-	92	2884	2877
27	Tetradecyltetradecanoate	81	81	89	2968	2950

4

The identification of the specific aromatic compounds, present in the MOAH "cloud", was outside the scope of the investigation; however, even if desired, the identification of such constituents could not have been performed with satisfactory reliability, because of the low amounts of such constituents. However, it was possible to determine the MOAH quantities (FID trace) and patterns, which are highly important to define the contamination source.

A series of peaks, present in the MOAH fraction, were identified as esterified fatty acids. However, their presence did not affect reliable quantification because these compounds were subtracted from the total MOAH area. The esterified fatty acids derived from the paperboard packaging. In fact, in a sample of pasta analyzed prior to box packing, no sign of MOAH contamination was observed.

The possibility to use offset printing ink, based on vegetable oils, has been known for more than fifteen years, though its use has become more frequent since contamination from paperboard packaging has become an issue of worry.

A series of "unknowns" in the GC×GC-MS chromatograms were labeled as "undefined FA esters", since the relative spectra were clearly that of FA esters, although the database searches gave different possible "homologue" matches with good similarities, but not always with a correspondent LRI value. Hence, it was not possible to identify such compounds with sufficient reliability, even though they were marked in the figures, since their chemical nature was evident. It could also not be excluded that such FA esters were not contained in the MS database. For example, in the pasta sample (Fig. 2), only three out of the four main peaks were identified, namely octyldodecanoate, octyltetradecanoate, and octylhexadecanoate. However, it can be deduced from its 2D position that the "undefined FA ester" was most probably octyldecanoate, even though such a compound was not present in the MS databases used. A good "visual" similarity was observed with the spectrum reported in the NIST web site, however no LRI information was found, thus this compound remained unidentified.

It is noteworthy that practically the same compounds were found in all the samples subjected to analyses; however, different quantitative profiles were observed, probably due to a different ink-type and/or to a different contamination source. It can be hypothesized that the vegetable oil offset printing ink was directly used in the pasta packaging (highly contaminated), while it was present, in different amounts, in the recycled fiber used for the packaging of the other two food sample.

Reference

[1] K. Grob, M. Biedermann, A. Caramaschi, B. Pacciarelli, *J. High Resolut. Chromatogr.* 14 (1991) 33–39.

[2] Ch. Droz, K. Grob, *Z. Lebensm. Unters. Forsch.* 205 (1997) 239–241.

[3] M. Biedermann, Y. Uematsu, K. Grob, *Packag. Tech. Sci.* 24 (2011) 61–73.

[4] M. Biedermann, K. Grob, *Eur. Food Res. Technol.* 230 (2010) 785–796.

[5] A. Vollmer, M. Biedermann, F. Grundböck, J. E. Ingenhoff, S. Biedermann-Brem, W. Altkofer, K. Grob, *Eur. Food Res. Technol.* 232 (2011) 175–182.

[6] M. Biedermann, K. Grob, *J. Chromatogr. A* 1255 (2012) 76–99.

[7] German Federal Institute for Risk Assessment (BfR). Stellungnahme Nr. 008/2010 des BfR vom 03, December, 2009.

[8] Joint FAO/WHO Expert Committee of Food Additives (JECFA) 2002, 59th report, 11-20; WHO Technical report Series 913, http://whqlibdoc.who.int/trs/WHO_TRS_913.pdf.

[9] European Food Safety Authority (EFSA), Scientific opinion on Mineral Oil Hydrocarbons in Food, EFSA Journal 10(6) (2012) 2704 1–185.

[10] Summary and conclusion of the 76th Meeting of the Joint FAO/WHO Expert Committee on Food Additives, 29 June 2012.

[11] A. Guinda, A. Lanzòn, T. Albi, *J. Agric. Food Chem.* 44 (1996) 1723–1726.

[12] O. Koprivnjak, G. Procida, L. Favretto, *Food Technolog. Biotechnolog.* 35 (1997) 125–131.

[13] Y. A. Tan, and A. Kuntom. *J. AOAC Int.* 76 (1993) 371–376.

[14] A. S. McGill, C. F. Moffat, P. R. Mackie, P. Cruickshank, *J. Sci. Food Agric.* 61 (1993) 357–363

[15] C. Wagner, H.-P. Neukom, K. Grob, S. Moret, T. Populin, L. S. Conte, *Mitt. Lebensm. Hyg.* 92 (2001) 499–514.

[16] K. Grob, Workshop EU-DG-SANCO and the KLZH, Switzerland (2008).

[17] D. Fiorini, A. Paciaroni, F. Gigli, R. Ballini, *Food Control*, 21 (2010) 1155–1160.

[18] S. Moret, L. Barp, K. Grob, L. S. Conte, *Food Chem.* 129 (2011) 1898–1903.

[19] K. Grob, A. Artho, M. Biedermann, J. Egli, *Food Addit. Contam.* 8 (1991) 437–446.

[20] M. Biedermann, K. Fiselier, K. Gob, *J. Agric. Food Chem.* 57 (2009) 8711–8721.

[21] P. Q. Tranchida, M. Zoccali, G. Purcaro, S. Moret, L. Conte, M. Beccaria, P. Dugo, L. Mondello, *J. Chromatogr. A*, 2011, 1218, 7476–7480.

[22] G. Purcaro, S. Moret, L. S. Conte, *J. Chromatogr. A*, 1255 (2012) 100–111.

[23] M. Biedermann, K. Grob, *J. Chromatogr. A* 1255 (2012) 56–75.

[24] S. Moret, L. Barp, G. Purcaro, L. S. Conte, *J. Chromatogr. A*, 1243 (2012) 1–7.

[25] http://www.bfr.bund.de/cm/349/determination-of-hydrocarbons-from-mineral-oil-or-plastics.pdf, BfR (2012).

[26] M. Biedermann, K. Grob, *J. Sep. Sci.* 32 (2009) 3726–3737.

[27] L. Mondello, M. Zoccali, G. Purcaro, F. A. Franchina, D. Sciarrone, S. Moret, L. Conte, P. Q. Tranchida, *J. Chromatogr. A*, 1259 (2012) 221–226.

Shimadzu GC×GC-QP System
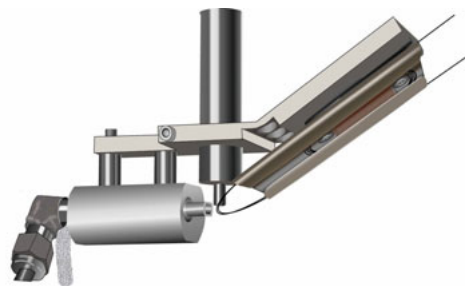
Zoex ZX1 2stage thermal modulator providing excellent modulation.

Shimadzu GCMS-QP2010 Ultra makes possible to obtain the data with high scan speed up to 20,000 u/sec.

The 2-dim chromatogram of fatty acids and scan speed

The high scan speed of GCMS-QP2010 Ultra has the potential of increasing the separation power of the second dimension, that promotes applicability of high sensitive, user friendly and economical quadrupole mass spectrometer to GC×GC-MS analysis.

	50 Hz (20,000 u/sec)	25 Hz (10,000 u/sec)	10 Hz (4,000 u/sec)

GC×GC 2dim Image

TIC

SHIMADZU

Shimadzu Corporation

www.shimadzu.com/an/

Application News

No. GCMS-1304

Analysis of Organophosphorus Pesticides in Baby Foods Using a Triple-Quadrupole GC/MS/MS System

■ **Introduction**

Contamination of food products with pesticides is a growing concern because of recognized adverse health effects, increasing world-wide usage of pesticides, and increasing imports of raw foodstuffs from foreign sources. The concern is particularly acute for baby foods because of the high vulnerability of babies to adverse health effects from synthetic chemicals, particularly pesticides.

Gas chromatography mass spectrometry (GCMS) has been used extensively to quantify trace-level pesticides in food matrices; the most significant challenges have been matrix interference and achievement of meaningful health-based detection limits for the compounds of interest. The QuEChERS (Quick Easy Cheap Effective Rugged and Safe) sample preparation method[1] has helped to overcome some of the problems of matrix interference, and commercialization of QuEChERS kits has promoted

widespread screening of foodstuffs for trace pesticides. But significant interferences still present a formidable problem for analysis of trace-level pesticides in foods, even after QuEChERS extraction and cleanup.

Triple quadrupole GC/MS/MS has emerged as the technique of choice for analysis of trace-level contaminants in complex matrices. Operation of the triple quadrupole GC/MS/MS in the Multiple Reaction Monitoring (MRM) mode provides unmatched sensitivity and selectivity for detection and quantitation of targeted pesticides at low concentrations in the presence of interfering background. This application note presents instrument configuration, operating parameters, and analytical results for analysis of trace levels of 24 organophosphorus (OP) pesticides in four different baby foods using the Shimadzu GCMS-TQ8030 triple quadrupole GC/MS/MS (Figure 1).

■ **Experimental**

The analyses were conducted using a Shimadzu GCMS-TQ8030 triple quadrupole GC/MS/MS. The GCMS-TQ8030 was operated in the multiple reaction monitoring (MRM) mode, using the GC program, optimized MRM transitions, and collision energies detailed in the Shimadzu GC/MS/MS Pesticide Database[2]. The GCMS-TQ8030 allows optimization of the collision energy for each MRM transition, providing

ultimate sensitivity. The Q1 and Q3 resolution can be independently defined for each compound, to deliver individualized selectivity for each pesticide. The instrument configuration and operating conditions, including MRM transitions, optimized collision energies, and retention indices (RI) for the OP pesticides are shown in Table 1.

Figure 1: Shimadzu GCMS-TQ8030 Triple Quadrupole GC/MS/MS

Table 1: Instrument Conditions for Analysis of Pesticides in Baby Food

Gas Chromatograph	GC-2010 Plus
Inlet	250 °C Single taper gooseneck splitless liner with glass wool (Restek 23322.5) Splitless injection, sampling time 1 minute
Column	RXI-5Sil MS 30 m x 0.25 mm x 0.25 µm (Restek 13623) Helium carrier gas Constant linear velocity 47 cm/second
Oven Program	90 °C, hold 1.0 minute 15 °C/minute to 300 °C, hold 5.0 minutes MS interface 250 °C Analysis time 20 minutes
Mass Spectrometer	**GCMS-TQ8030**
Ion Source	200 °C Electron ionization (EI) mode, 70 eV
Operation Mode	Multiple Reaction Monitoring (MRM) Argon gas, 200 kPa Q1 resolution 0.8 u (Unit), Q3 resolution 3.0 u (Low)
Detector	Electron multiplier 1.7 kV

MRM Transition Details							
Compound Name	**Transition 1**	**CE 1**	**Transition 2**	**CE 2**	**Transition 3**	**CE 3**	**Retention Index**
Dichlorvos	185.0>93.0	14	185.0>109.0	14	185.0>63.0	22	1243
Mevinphos	192.0>164.0	4	192.0>127.0	12	192.0>109.0	24	1424
Ethoprophos	200.0>158.0	6	200.0>114.0	14	200.0>97.0	24	1637
Sulfotepp	322.0>202.0	10	322.0>294.0	4	322.0>174.0	18	1673
Monocrotophos	127.1>109.0	12	127.1>95.0	16	127.1>79.0	20	1679
Phorate	260.0>75.0	8	260.0>231.0	4	260.0>47.0	26	1697
Dimethoate	125.0>79.0	8	125.0>47.0	14	125.0>62.0	10	1730
Diazinon	304.1>179.1	10	304.1>162.1	8	304.1>137.1	26	1789
Disulfoton	186.0>97.0	16	186.0>153.0	6	186.0>125.0	10	1813
Methyl parathion	263.0>109.0	14	263.0>136.0	8	263.0>246.0	6	1898
Ronnel	284.9>269.9	21	284.9>239.9	26	284.9>93.0	26	1922
Malathion	173.1>99.0	14	173.1>127.0	6	173.1>145.0	6	1963
Fenthion	278.0>109.0	20	278.0>125.0	20	278.0>169.0	14	1989
Chlorpyrifos	313.9>257.9	14	313.9>285.9	8	313.9>193.9	28	1981
Parathion	291.1>109.0	14	291.1>137.0	6	291.1>81.0	24	1995
Triphenylmethane*	244.1>167.1	10	244.1>243.1	10			2016
Trichloronat	296.9>268.9	17	296.9>222.9	29	296.9>239.9	30	2019
Merphos	209.1>153.0	6	209.1>97.0	8	209.1>57.0	13	2076
Stirofos	328.9>109.0	18	328.9>313.9	17	328.9>79.0	23	2125
Prothiofos	309.0>239.0	21	309.0>281.0	11	309.0>221.0	31	2175
Fensulfothion	293.1>125.0	13	293.1>97.0	23	293.1>109.0	19	2268
Bolstar	322.1>156.1	11	322.1>139.1	13	322.1>97.0	22	2319
Triphenyl phosphate†	326.1>170.1	15	326.1>215.1	20			2407
EPN	169.1>140.9	8	169.1>77.0	22	169.1>158.9	6	2482
Azinphos-methyl	160.1>132.1	6	160.1>77.0	20	160.1>51.0	28	2579
Coumaphos	362.0>109.0	17	362.0>226.0	18	362.0>210.0	20	2731

*Triphenylmethane was the internal standard (IS), spiked at 10 ng/mL

†Triphenyl phosphate was the control standard, spiked at 20 ng/mL

Organic blended peas were used as the test sample matrix; an organic variety was selected so it would be free from pesticide contamination. The sample matrix was extracted and subjected to cleanup using the QuEChERS procedure, and all analytical standards were prepared in the blended peas matrix. A 7-point calibration curve was prepared for the 24 OP-pesticides using the internal standard procedure. The sample preparation did not involve concentrating or diluting the sample, so concentrations expressed in ng/mL (parts-per-billion, ppb) in the calibration standards and extracts are equivalent to ng/g (ppb) in the original sample.

■ **Results and Discussion**

Chromatography

The total ion chromatogram (TIC) acquired in the MRM mode for the OP pesticide mix is shown in Figure 2, and illustrates the chromatographic separation of the OP pesticides. In the MRM mode, the TIC for each analyte is the sum of the signal for each MRM transition for that particular analyte, so the appearance of the chromatogram is slightly different than a typical TIC acquired in the full-scan mode.
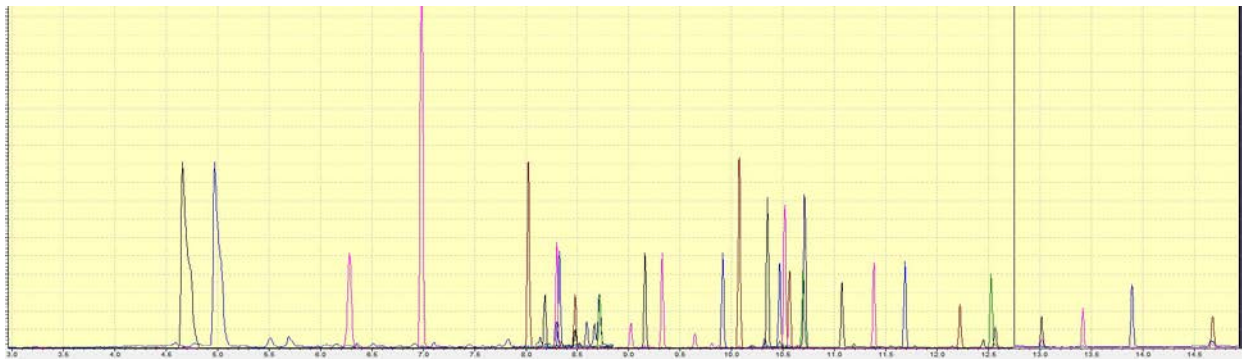
Figure 2: Total Ion Chromatogram of Organophosphorus Pesticide Standard – MRM Mode

The effect of column temperature on chromatographic performance is important for this application. When the QuEChERS procedure is used, the injection solvent is acetonitrile, which is very polar compared to the column phase. When acetonitrile is injected with an initial column temperature of 50-60 °C, severe chromatographic peak splitting occurs, particularly with early-eluting compounds. However, when the initial temperature is increased to 90 °C, chromatographic performance is improved. This effect is illustrated in Figure 3 below. The chromatographic effect with acetonitrile is explained by condensation of solvent droplets on the inside of the chromatographic column at temperatures below the boiling point of acetonitrile (82 °C). The slight peak broadening in the peaks eluting from 4.5-5.0 minutes in the chromatogram shown in Figure 2 is also the result of this chromatographic effect.

Figure 3: Mass Chromatogram for Dichlorovos (m/z 185)

Automatic Adjustment of Retention Times (AART)

Routine maintenance to maintain chromatographic performance frequently involves cutting the chromatographic column, which results in changing method retention times. Dealing with changing retention times can be cumbersome in routine full-scan GCMS analysis, but becomes much more complicated with GC/MS/MS operated in the MRM mode. Not only do the data processing retention times need to be updated, but the MRM data acquisition parameters must also be adjusted to ensure that the specific MRM transitions are applied for the precise retention times of the corresponding analytes.

Method retention times and MRM data acquisition parameters are easily updated using the Shimadzu AART function, based on the fundamental principle of retention index. The retention index is a retention time scale based on the retention times of specific analytes relative to a series of n-alkane hydrocarbons. Retention indices are constant for a given column phase, and are independent of column dimensions or temperature program. When retention indices are known, and retention times of n-alkanes under a given set of conditions are determined, retention times of the specific analytes can be calculated with high accuracy (0.01 min or less). The process is illustrated in Figure 4.
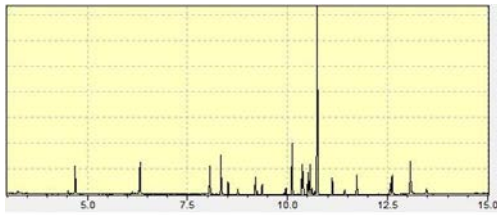
Pesticide standard before cutting column - MRM mode
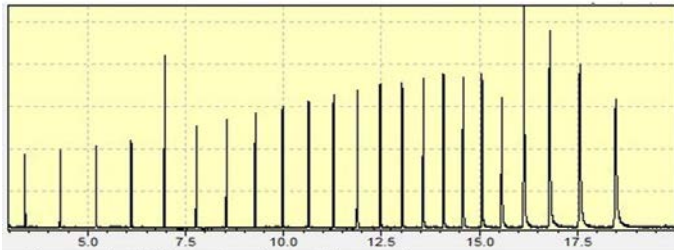
n-Alkane standard before cutting column - full scan mode

AART– Step 1

AART - Step 1
Use method retention times and n-alkane standard retention times from original conditions to calculate retention indices for target compounds on a specific column phase (e.g. RXI-5sil MS).

n-Alkane standard after cutting column - full scan mode

☑ Modify the time of MS Instrument parameters.

AART – Step 2a

AART - Step 2a
After cutting the column, use new n-alkane retention times to update retention times for the method. Instrument data acquisition parameters can also be updated by selecting the checkbox.

AART – Step 2b

AART - Step 2b
Instrument data acquisition parameters are updated when the checkbox is selected in the AART function.
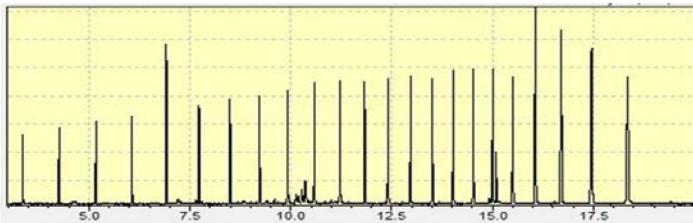
n-Alkane standard after cutting column - full scan mode
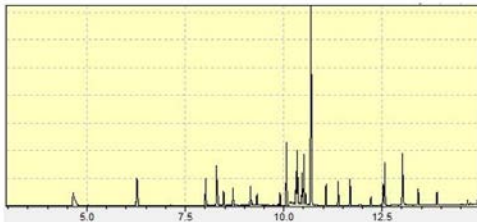
Pesticide standard after cutting column - MRM mode

AART – Step 3

AART - Step 3
Instrument data acquisition parameters and data processing retention times are verified by injection of the pesticide standard in the MRM mode after updating parameters with the AART function.

Figure 4: Illustration of the Automatic Adjustment of Retention Time (AART) Feature

The Shimadzu GC/MS/MS Pesticide Database

The analytical method for detection of the OP pesticides was developed using the Shimadzu GC/MS/MS Pesticide Database for the GCMS-TQ8030. The database includes MRM method parameters that were developed using authentic analytical standards for 430 pesticides (October, 2012). The method information for each of the 430 pesticides includes CAS number, retention index (Rtx-5MS column), and 3 to 5 suggested MRM transitions that can be used for either quantitation or confirmation. Each MRM transition includes an associated collision energy (CE) that has been optimized to provide the greatest sensitivity. Multiple transitions are provided for each pesticide, so the user can choose the ones most appropriate for the matrix being tested.

To use the database, simply select the pesticides of interest by changing the Target/Non-target Flag using the drop-down menu, define the primary quantitation transition (Q) and confirmation transitions (C1 – C4), and use the embedded macro to generate the MRM method. The database includes retention indices (RI) for all 430 pesticides on the Rtx-5MS column, or the user can use the RI determined for alternate columns using the AART function. A portion of the Shimadzu Pesticide Database is shown in Figure 5.

Compound Name (ENG)	Cas#	Ret. Index (Rtx-5MS)		Transition 1	CE1	Transition 2	CE2	Transition 3	CE3
Aldicarb deg.	0 - 00 - 0	901	Q	115.1>100.1	8	115.1>68.0	8	115.1>48.0	12
DCIP	108 - 60 - 1	1061	Q	121.1>45.0	4	121.1>77.0	8	121.1>49.0	24
Aldoxycarb deg.	0 - 00 - 0	1142	Q	80.0>65.0	6	80.0>50.0	4	80.0>48.0	28
Chlofentezine deg.	0 - 00 - 0	1188	Q	137.0>102.0	14	137.0>75.0	26	137.0>51.0	26
Hymexazol	10004 - 44 - 1	1203	Q	99.0>71.0	8	99.0>54.0	26	99.0>58.0	8
Methamidophos	10265 - 92 - 6	1237	Q	141.0>95.0	8	141.0>126.0	4	141.0>79.0	22
Dichlorvos	62 - 73 - 7	1258	Q	185.0>93.0	14	185.0>109.0	14	185.0>63.0	22
Nereistoxin	0 - 00 - 0	1288	Q	149.1>71.1	8	149.1>102.1	6	149.1>84.1	4
Allidochlor	93 - 71 - 0	1302	Q	138.1>96.0	6	138.1>110.1	6	138.1>81.0	6
Dichlobenil	1194 - 65 - 6	1365	Q	170.9>100.0	24	170.9>136.0	14	170.9>110.0	14
EPTC	759 - 94 - 4	1367	Q	189.1>128.1	4	189.1>86.0	12	189.1>160.1	8
Biphenyl	92 - 52 - 4	1399	Q	154.1>128.1	22	154.1>115.1	24	154.1>102.1	28
Butylate	2008 - 41 - 5	1440	Q	174.1>146.1	6	174.1>75.0	4	174.1>89.0	8
Mevinphos	7786 - 34 - 7	1442	Q	192.0>164.0	4	192.0>127.0	12	192.0>109.0	24
Acephate	30560 - 19 - 1	1448	Q	136.0>94.0	14	136.0>119.0	8	136.0>64.0	22
Chlormephos	24934 - 91 - 6	1454	Q	233.9>121.0	12	233.9>154.0	6	233.9>93.0	20
3-Hydroxycarbofuran	16655 - 82 - 6	1471	Q	180.1>137.0	10	180.1>162.1	6	180.1>151.1	8
Nitrapyrin	1929 - 82 - 4	1471	Q	193.9>133.0	16	193.9>157.9	20	193.9>112.0	26
Etridiazole	2593 - 15 - 9	1472	Q	210.9>182.9	10	210.9>139.9	22	210.9>108.0	34
Clothianidin	210880 - 92 - 5	1509	Q	132.0>71.0	14	132.0>45.0	22	132.0>88.0	14
Thiocyclam	31895 - 21 - 3	1515	Q	135.0>71.0	8	135.0>56.0	24		
Methacrifos	62610 - 77 - 9	1516	Q	240.0>208.0	4	240.0>180.0	10	240.0>110.0	20
Chloroneb	2675 - 77 - 6	1526	Q	206.0>191.0	12	206.0>141.0	20	206.0>113.0	24
Tebuthiuron	34014 - 18 - 1	1534	Q	171.1>156.1	10	171.1>129.1	6	171.1>74.0	26
2-Phenylphenol	90 - 43 - 7	1535	Q	170.1>141.1	24	170.1>115.1	28	170.1>155.1	14
Crimidine	535 - 89 - 7	1537	Q	156.1>120.1	8	156.1>66.0	22	156.1>79.0	14
Isoprocarb	2631 - 40 - 5	1554	Q	136.0>121.0	10	136.0>103.0	22	136.0>77.0	26

Figure 5: Shimadzu GC/MS/MS Pesticide Database for the GCMS-TQ8030

Multiple Reaction Monitoring (MRM) Mode

Operation of the GCMS-TQ8030 in the MRM mode provides unmatched sensitivity and selectivity for analysis of trace level contaminants in complex matrices, such as OP pesticides in food extracts. Most co-extracted matrix interferences are virtually eliminated using the MRM mode. The chromatograms in Figure 6A illustrate this point. The chromatograms were generated using Shimadzu's unique Scan/MRM mode, in which full-scan mass spectra and MRM data are simultaneously acquired in the same run. The black trace is the Scan mode of the blended peas sample spiked with 24 OP pesticides at 100 ng/mL. The pink trace is the MRM acquisition of the OP pesticides during the same Scan/MRM analysis. The chromatograms have been normalized to the same intensity scale; the overwhelming intensity of the sample matrix relative to the pesticide spike at 100 ng/mL is apparent in the chromatograms.

Black trace – Scan Mode

Pink trace – MRM Mode
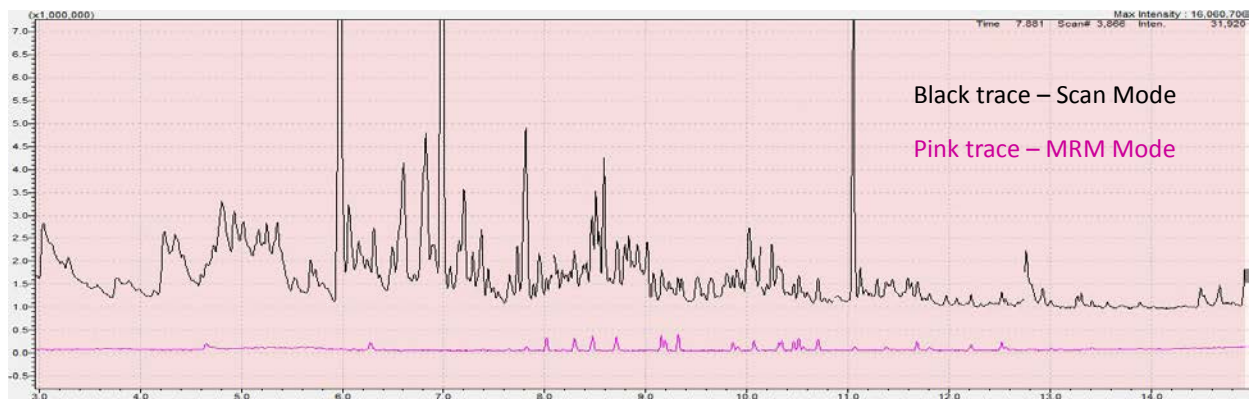
Figure 6A: Blended Pea Extract Spiked at 100 ng/mL and Analyzed in Simultaneous Scan/MRM Mode

The outstanding selectivity of the MRM mode is further illustrated in the chromatograms of three OP pesticides shown in Figure 6B. The top chromatograms represent extracted ion chromatograms (mass chromatograms) from the full scan data, and the bottom chromatograms are the corresponding chromatograms from the MRM mode. Elimination of matrix interference in the MRM mode is evident. The MRM operation mode allows detection and quantitation of trace concentrations of analytes in complex matrices such as food extracts, completely eliminating background interference.
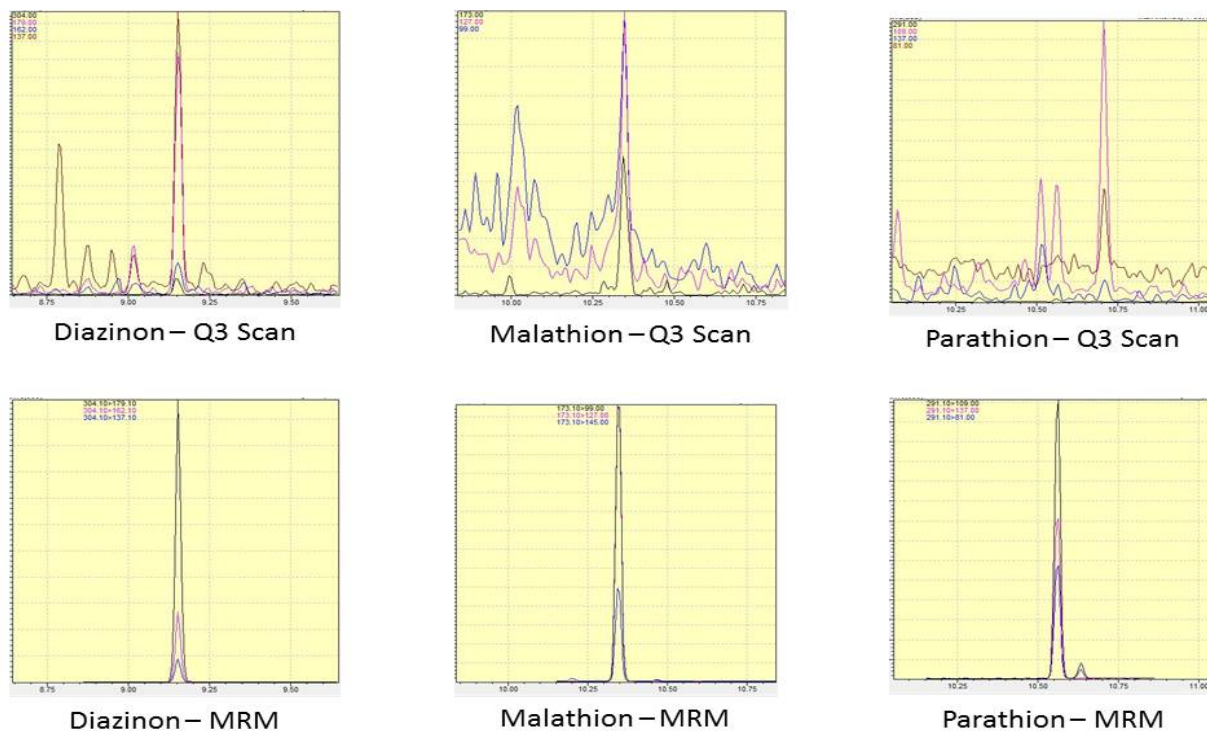
Figure 6B: Extracted Ion Chromatograms (top) and MRM Chromatograms (bottom) for Selected Pesticides in the Spiked Pea Extract Using the Scan/MRM Acquisition Mode

Calibration and Assessment of Precision

Seven calibration standards were prepared in the blended peas matrix over the range of 0.5-200 ng/mL (ppb) and transferred to autosampler vials with limited-volume inserts for analysis; triphenylmethane was used as the the internal standard and was held at a constant concentration of 10 ng/mL. Triphenyl phosphate was used as a control standard, and was held at a constant concentration of 20 ng/mL in all standards and samples. The initial calibration standards were analyzed using the instrument conditions outlined above. The electron multiplier was adjusted to give acceptable response at the lowest calibration level and avoid saturation at the highest calibration level.

Response factors were calculated and relative standard deviation (RSD) determined by the GCMSsolution software. Mean response factors for the initial calibration are presented in Table 2. The precision of the calibration is evaluated using the RSD of the response factors and the correlation coefficient (r) for each of the calibration analytes. The RSD and correlation coefficient values for the multi-point calibration are shown in Table 2.

Eight replicate injections of the 1 ng/mL and 10 ng/mL standards were analyzed to assess the precision of the analytical method and the accuracy of measurement near the low end of the calibration range. The mean concentration and RSD for the replicate analyses are presented in Table 2.

Table 2: 7-Point Calibration and Precision Results for Analysis of Organophosphorus Pesticides by GCMS-TQ8030

Compound Name	Calibration Results			Precision at 1 ng/mL (n = 10)		Precision at 10 ng/mL (n = 10)	
	Mean RRF	RSD (%)	r	Mean Conc.	RSD (%)	Mean Conc.	RSD (%)
Dichlorvos	0.640	22	>.999	0.97	4	10.9	3
Mevinphos	0.485	17	>.999	0.80	8	9.5	4
Ethoprophos	0.724	22	>.999	0.95	5	9.3	3
Sulfotepp	0.371	20	>.999	0.80	7	8.9	2
Monocrotophos	0.754	19	>.999	1.20	13	8.0	6
Phorate	0.325	16	>.999	0.92	9	9.7	2
Dimethoate	0.167	23	>.999	0.77	16	9.3	8
Diazinon	0.446	17	>.999	0.90	9	9.2	2
Disulfoton	0.155	24	0.999	0.87	10	8.8	2
Methyl parathion	0.283	26	0.999	1.02	6	9.2	2
Ronnel	0.950	20	>.999	1.24	17	9.2	3
Malathion	0.630	17	>.999	0.87	9	8.1	1
Fenthion	0.934	21	>.999	0.93	4	8.7	1
Chlorpyrifos	0.525	18	>.999	0.87	4	8.6	2
Parathion	0.103	37	0.997	0.84	12	9.0	3
Trichloronat	1.250	18	>.999	0.91	5	9.2	2
Merphos	0.371	30	0.996	0.79	11	5.8	5
Stirofos	0.804	18	>.999	0.89	5	8.3	2
Prothiofos	0.434	13	>.999	0.94	6	9.2	2
Fensulfothion	0.094	20	0.996	1.03	17	10.6	4
Bolstar	0.320	19	0.997	0.86	11	9.1	2
EPN	0.264	21	0.999	0.93	15	8.7	4
Azinphos-methyl	0.431	16	0.997	0.99	12	8.0	6
Coumaphos	0.198	22	0.997	0.92	10	9.9	3
Triphenyl phosphate*	0.300	3	NA	20.1	3	19.9	1

*The triphenyl phosphate control standard was spiked at 20 ng/mL.

Calibration curves for selected analytes are shown in Figures 7A-7F below. The chromatograms represent the lowest level calibration point (0.5 ppb) for each analyte. All of the chromatographic peaks were easily integrated at the 0.5 ng/mL level.
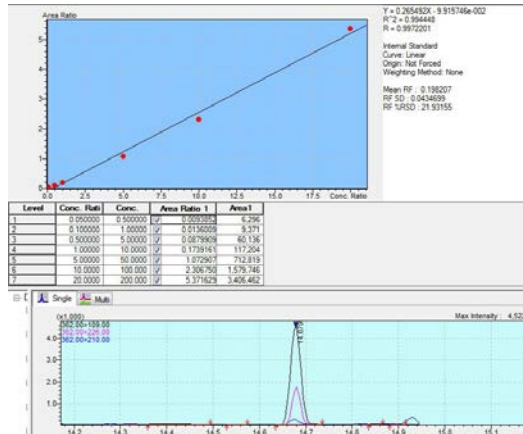
Figure 7A: Coumaphos Calibration
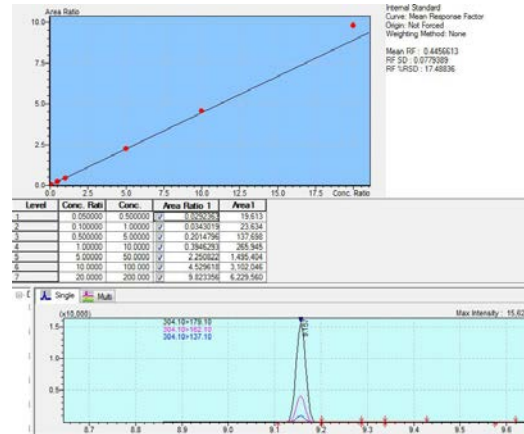
Figure 7B: Diazinon Calibration
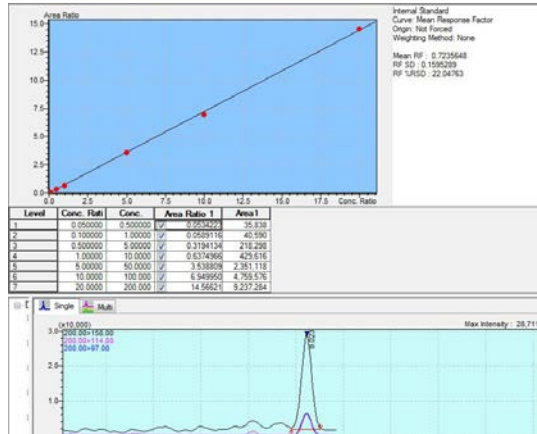
Figure 7C: Ethoprophos Calibration
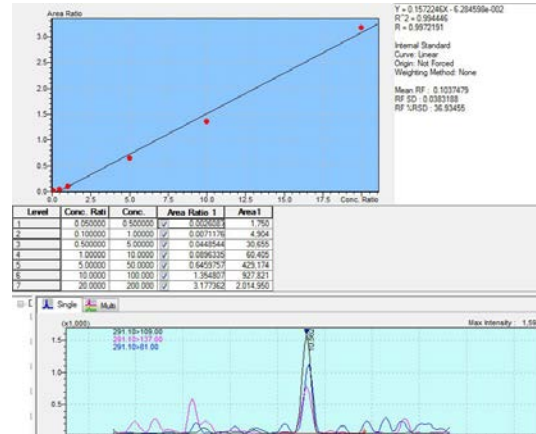
Figure 7D: Parathion Calibration
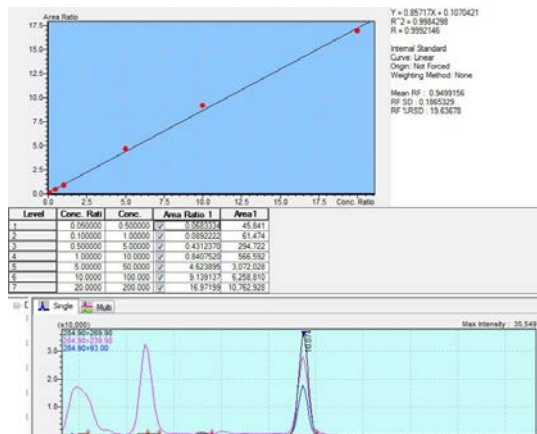
Figure 7E: Ronnel Calibration
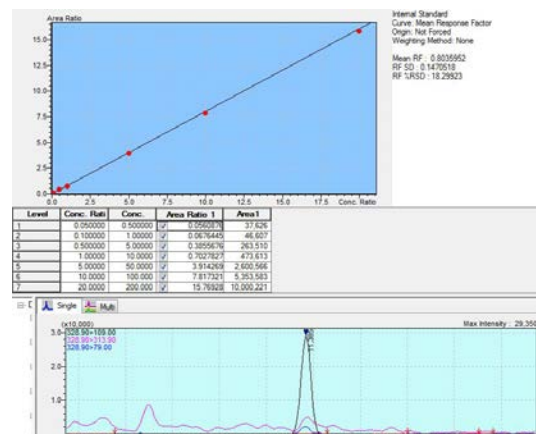
Figure 7F: Stirophos Calibration

Results for Other Sample Matrices

Calibration standards for this study were created by spiking the extract from blended peas which had been prepared using the QuEChERS technique. The calibration was subsequently used to evaluate analytical performance in three additional baby food matrices. The QuEChERs extracts from three baby foods (blended pears, peach oatmeal bar, and chicken broth) were spiked at 10 ng/mL, and were analyzed 10 times each using the MRM method. Results are shown in Table 3. The sample extracts were also analyzed in the Q3 full scan mode to note overall similarities and differences in the gross appearance of the chromatograms. Total ion chromatograms for the analyses of the four QuEChERS extracts are shown in Figures 8A-D. The appearance of the chromatograms between 6 and 9 minutes was remarkably similar; the primary differences are seen in the region after 9 minutes.

Measured concentrations of the OP pesticides in the blended peas ranged between 8.0 and 10.9 ng/mL (10 ng/mL spike), with single-digit precision for all pesticides. Precision at 10 ng/mL was excellent in the other three matrices as well, with RSDs at 11% or better for all compounds, and only three measurements above 9%. Measured concentrations of the OP pesticides in the blended pears and peach oatmeal bar were similar, with recoveries ranging from 77 to 142%. Measured concentrations in the chicken broth, the only animal-based matrix, showed the highest degree of variability, with recoveries from 68 to 217%. Concentration of parathion was high in all three of the additional spiked matrices.

Table 3: Precision Data for Analysis of Organophosphorus Pesticides in Four Different Baby Foods

Compound Name	Chicken Broth		Pears		Peach Oatmeal Bar		Peas	
	Mean (ng/mL)	RSD (%)	Mean (ng/mL)	RSD (%)	Mean (ng/mL)	RSD (%)	Mean (ng/mL)	RSD (%)
Dichlorvos	8.7	3	7.7	3	8.4	2	10.9	3
Mevinphos	8.1	7	7.9	3	8.2	5	9.5	4
Ethoprophos	9.0	3	7.7	2	8.5	4	9.3	3
Sulfotepp	13.8	3	11.5	2	12.0	4	8.9	2
Monocrotophos	8.8	4	9.6	2	8.8	7	8.0	6
Phorate	10.0	3	8.3	4	9.0	5	9.7	2
Dimethoate	11.4	9	10.2	6	14.2	8	9.3	8
Diazinon	8.7	5	8.1	3	9.1	5	9.2	2
Disulfoton	8.9	5	8.0	3	8.7	7	8.8	2
Methyl parathion	9.4	8	9.1	4	9.4	10	9.2	2
Ronnel	8.4	3	7.9	4	8.7	7	9.2	3
Malathion	12.9	5	14.1	2	12.6	6	8.1	1
Fenthion	8.7	5	8.5	1	8.5	8	8.7	1
Chlorpyrifos	8.6	6	8.3	3	13.6	4	8.6	2
Parathion	21.7	6	14.6	3	13.8	8	9.0	3
Trichloronat	10.1	2	8.8	2	8.9	4	9.2	2
Merphos	11.1	4	8.4	2	8.2	5	5.8	5
Stirofos	6.8	4	8.1	2	7.7	7	8.3	2
Prothiofos	10.5	3	9.0	2	9.5	5	9.2	2
Fensulfothion	15.7	11	10.4	5	10.2	10	10.6	4
Bolstar	11.1	6	8.9	4	9.9	7	9.1	2
EPN	15.9	6	12.0	4	13.5	6	8.7	4
Azinphos-methyl	13.8	6	9.3	8	8.1	8	8.0	6
Coumaphos	10.0	8	10.2	3	10.6	10	9.9	3
Triphenyl phosphate	21.7	3	20.8	1	20.3	2	19.9	1
The triphenyl phosphate control standard was spiked at 20 ng/mL. The spike level for all other OP pesticides was 10 ng/mL.								
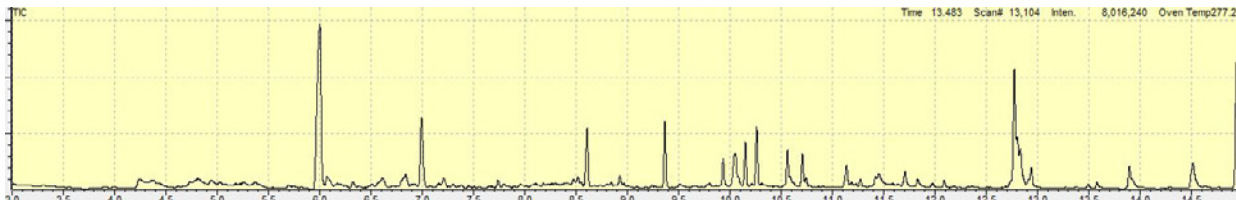
Figure 8A: Total Ion Chromatogram of Chicken Broth QuEChERS Extract (scan mode)
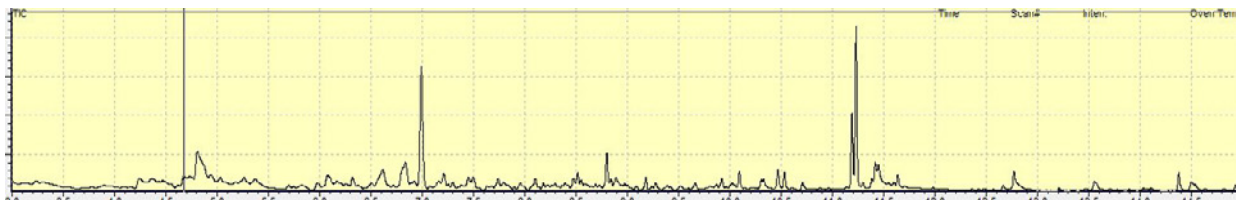
Figure 8B: Total Ion Chromatogram of Pears QuEChERS Extract (scan mode)

Figure 8C: Total Ion Chromatogram of Peach Oatmeal Bar QuEChERS Extract (scan mode)
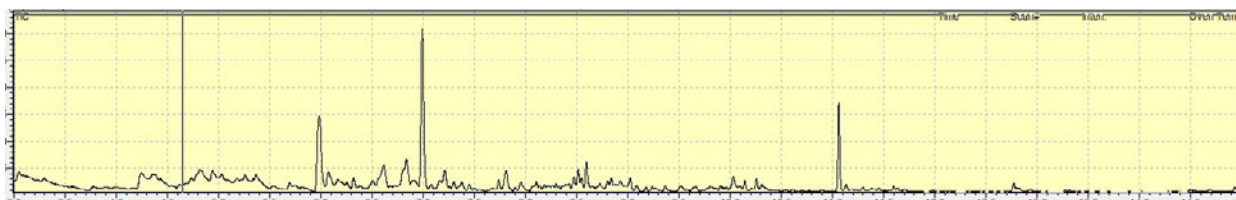
Figure 8D: Total Ion Chromatogram of Peas QuEChERS Extract (scan mode)

■ Conclusion

Detection of the organophosphorus pesticides was demonstrated at low ng/mL (parts-per-billion, ppb) levels in the sample matrix, and linear calibration was demonstrated from 0.5-200 ng/mL. Precision and accuracy were demonstrated by ten replicate analyses of matrix spiked aliquots at 1 and 10 ng/mL.

Calibration was conducted in the blended peas QuEChERS extract, and provided accurate, repeatable results for that sample matrix. Application of the matrix calibration was investigated by analysis of ten replicates of spiked aliquots of three additional baby foods: blended pears, peach oatmeal bar, and chicken broth. Accuracy for the blended peas extract was

80-110 %, and precision was less than 9 % (n = 10) for all compounds. Results for the other sample matrices measured against a calibration in the blended peas extract showed similar precision, but accuracy from 68-217 %.

A Shimadzu GCMS-TQ8030 system operated in the MRM mode was shown to be a rapid, sensitive, and selective technique for analysis of organophosphorus pesticides in baby foods. Reliable, precise measurements were obtained at 1 ng/mL for all 24 OP pesticides. The Shimadzu AART function and GC/MS/MS Pesticide Database simplified development of the MRM method.

■ References

1. AOAC Official Method 2007.01, Pesticide Residues in Foods by Acetonitrile Extraction and Partitioning with Magnesium Sulfate (2007)
2. Shimadzu GCMSMS Pesticide Database (October, 2012)

First Edition: February 2013

SHIMADZU

SHIMADZU Corporation
www.shimadzu.com/an/

SHIMADZU SCIENTIFIC INSTRUMENTS
7102 Riverwood Drive, Columbia, MD 21046, USA
Phone: 800-477-1227/410-381-1227, Fax: 410-381-1222
URL: www.ssi.shimadzu.com

SHIMADZU
Excellence in Science

Application Data Sheet

No.68

GC-MS
Gas Chromatograph Mass Spectrometer

GC-MS/MS Analysis of Pesticides in Drinking Water

According to Japan's list of drinking water quality control substances, pesticides are included as supplemental items subject to analysis. Designed to complement the standards, the Ministry of Health, Labour and Welfare encourages water utilities to monitor pesticide levels and achieve specified targets. Among the 102 listed pesticides, 84 are simultaneously analyzed using solid-phase extraction and GC-MS. In this datasheet, those pesticides were analyzed using GC-MS/MS and Multiple Reaction Monitoring (MRM) mode.

Experimental

Analytical conditions are shown in Table 1.

Table 1: Analytical Conditions

GC-MS	:GCMS-TQ8030
Column	:Rtx-5MS (Length 30 m, 0.25 mm I.D., df=0.25 μm)
Glass liner	:Custom Sky Liner, Splitless Single Taper Gooseneck w/Wool (RESTEK, catalog# 567366)

[GC]
Injection Temp.	:250°C
Column Oven Temp.	:80°C(2 min)→(20°C /min)→180°C →(5°C /min)→280°C(3 min)
Injection Mode	:Splitless (High Pressure Injection 250 kPa, 2.3 min)
Flow Control Mode	:Linear Velocity (44.5 cm/sec)
Injection Volume	:2 μL

[MS]
Interface Temp.	:250 °C
Ion Source Temp.	:230 °C
Data Acquisition Mode	:MRM

MRM Monitoring *m/z*

Compound Name	Quantitative Transition Precursor>Product	CE (V)	Qualitative Transition Precursor>Product	CE (V)	Compound Name	Quantitative Transition Precursor>Product	CE (V)	Qualitative Transition Precursor>Product	CE (V)
Dichlorvos	184.9>109.0	18	184.9>93.0	13	Isofenphos	213.1>185.1	6	213.1>121.1	18
Dichlobenil	170.9>136.0	13	170.9>100.0	23	Captan	149.0>105.1	5	149.0>79.0	19
Etridiazole	210.9>182.9	10	210.9>139.9	20	Dimepiperate	145.1>112.1	9	145.1>69.1	18
Chloroneb	205.9>190.9	12	205.9>140.9	19	Phenthoate	274.0>121.0	11	274.0>125.0	18
Isoprocarb	136.1>121.1	9	136.1>103.1	23	Procymidone	283.1>96.0	10	283.1>68.1	24
Molinate	126.1>55.0	18	126.1>83.1	6	Butamifos oxon	244.0>216.0	7	244.0>136.1	15
Fenobucarb	150.1>121.1	9	150.1>103.1	23	Methidathion	145.0>85.0	8	145.0>58.0	18
Trifluralin	306.1>264.0	7	306.1>206.1	17	9-Bromoanthracene (ISTD)	256.0>177.1	18	256.0>151.1	30
Benfluralin	292.1>264.0	9	292.1>206.1	14	alpha-Endosulfan	240.9>205.9	13	240.9>170.0	26
Pencycuron	180.1>125.0	10	180.1>89.0	29	Butamifos	286.1>202.1	17	286.1>185.0	27
Dimethoate	125.0>79.0	10	125.0>62.0	8	Napropamide	128.1>72.1	7	128.1>100.1	9
Simazine	201.1>173.1	6	201.1>186.1	7	Flutolanil	173.0>145.0	18	173.0>95.0	27
Atrazine	215.2>200.1	8	215.2>173.1	6	Isoxathion oxon	161.1>105.0	11	161.1>77.0	25
Diazinon oxon	273.1>137.1	18	273.1>217.0	10	Isoprothiolane	290.1>204.1	5	290.1>118.0	14
Propyzamide	172.9>144.9	15	172.9>109.0	27	Pretilachlor	238.1>162.2	11	238.1>146.2	10
Pyroquilon	173.1>130.1	20	173.1>144.1	23	Fenthion oxon sulfoxide	262.1>247.1	11	262.1>109.0	22
Diazinon	304.1>179.2	10	304.1>162.1	9	CNP-amino	287.0>108.1	19	287.0>217.0	13
Anthracene-d10 (ISTD)	188.2>160.1	20	188.2>158.1	30	Fenthion oxon sulfone	294.1>104.1	19	294.1>230.2	8
Disulfoton	274.1>88.0	6	274.1>60.0	22	Buprofezin	172.1>57.1	18	172.1>131.1	6
Chlorothalonil	265.9>230.9	19	265.9>169.9	23	Isoxathion	312.9>177.0	7	312.9>130.0	17
Iprobenfos	204.0>91.0	8	204.0>122.0	15	beta-Endosulfan	240.9>205.9	18	240.9>170.0	23
Tolclofos-methyl oxon	249.0>199.0	26	249.0>233.9	15	Fenthion sulfoxide	278.0>109.0	20	278.0>169.1	14
Fenitorothion oxon	244.0>109.0	16	244.0>90.0	18	Fenthion sulfone	310.0>109.0	24	310.0>105.1	16
Bromobutide	232.2>176.1	10	232.2>114.1	9	Mepronil	269.1>119.1	18	269.1>227.1	5
Terbucarb	205.2>177.1	8	205.2>145.1	18	Chlornitrofen	318.9>288.9	12	318.9>238.0	10
Malaoxon	127.1>99.0	7	127.1>109.0	10	Edifenphos	310.0>173.0	13	310.0>109.1	25
Simetryn	213.2>170.1	10	213.2>185.1	7	Propiconazole-1	259.1>69.0	13	259.1>173.0	18
Tolclofos-methyl	265.0>249.9	15	265.0>219.9	23	Endosulfate	271.8>236.8	18	271.8>234.8	19
Alachlor	188.1>160.1	10	188.1>131.1	22	Propiconazole-2	259.0>69.0	11	259.0>172.9	19
Metalaxyl	249.2>190.2	6	249.2>146.1	18	EPN oxon	141.0>77.0	18	141.0>51.0	30
Fenthion oxon	262.0>247.0	8	262.0>109.0	26	Thenylchlor	288.1>141.0	13	288.1>174.1	7
Dithiopyr	354.1>306.0	7	354.1>286.0	17	Pyributicarb	165.1>108.1	10	165.1>93.0	25
Fenitrothion	277.0>260.1	7	277.0>109.0	20	Iprodione	314.0>244.9	11	314.0>56.0	25
Esprocarb	222.1>91.0	19	222.1>162.2	7	Pyridaphenthion	340.0>199.1	8	340.0>109.0	22
Malathion	173.1>127.1	7	173.1>99.0	18	Chrysene-d12 (ISTD)	240.2>236.1	30	240.2>238.2	20
Thiobencarb	257.1>100.1	7	257.1>72.1	23	EPN	157.0>77.0	24	157.0>110.0	14
Chlorpyrifos oxon	298.0>241.8	14	298.0>269.9	6	Piperophos	320.2>122.1	10	320.2>81.0	26
Fenthion	278.1>109.0	18	278.1>169.0	18	Bifenox	341.1>309.9	6	341.1>188.8	19
Chlorpyrifos	314.0>257.9	19	314.0>285.9	7	Anilofos	226.1>184.0	5	226.1>157.0	13
Isofenphos oxon	229.1>201.0	10	229.1>121.1	24	Pyriproxyfen	136.1>96.0	20	136.1>96.0	14
Phthalide	242.8>214.8	18	242.8>178.9	26	Mefenacet	192.0>136.0	17	192.0>109.0	28
Dimethametryn	212.1>122.1	13	212.1>94.0	22	Cafenstrole	188.2>119.1	22	188.2>82.0	20
Pendimethalin	252.1>162.1	11	252.1>191.1	8	Etofenprox	163.1>135.1	10	163.1>107.1	19
Methyldymron	107.1>106.1	13	107.1>77.0	25					

Results

The standard sample mixture of 84 pesticides at the concentration of 5 μg/L was analyzed 5 times. The overlay mass chromatograms from 5 injections and the repeatability are shown in Fig. 1 and Table 2, respectively.

Fenitrothion, *m/z* 277.0>260.1

Captan, *m/z* 149.0>105.1

Isoxathion oxon, *m/z* 161.1>105.0

Fenthion oxon sulfoxide, *m/z* 262.1>247.1

Iprodione, *m/z* 314.0>244.9

Bifenox, *m/z* 341.1>309.9
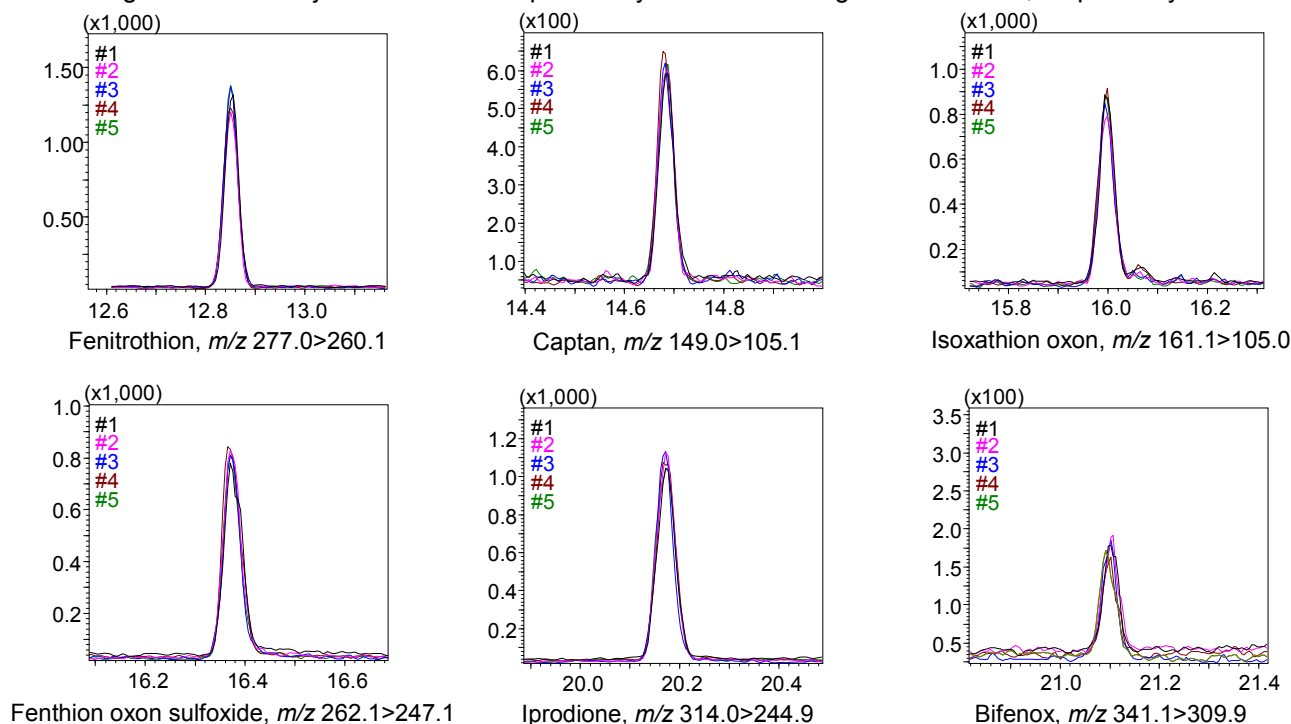
Fig. 1: Overlay mass chromatograms from 5 injections

Table 2: Repeatability (*n*=5, area ratio)

Compound Name	%RSD	Compound Name	%RSD	Compound Name	%RSD
Dichlorvos	1.62	Metalaxyl	3.01	Pretilachlor	7.26
Dichlobenil	0.73	Fenthion oxon	1.88	Fenthion oxon sulfoxide	5.72
Etridiazole	3.38	Dithiopyr	0.66	CNP-amino	1.04
Chloroneb	0.89	Fenitrothion	5.72	Fenthion oxon sulfone	1.19
Isoprocarb	0.47	Esprocarb	1.30	Buprofezin	2.14
Molinate	1.25	Malathion	0.82	Isoxathion	8.25
Fenobucarb	0.65	Thiobencarb	2.83	beta-Endosulfan	5.28
Trifluralin	1.71	Chlorpyrifos oxon	4.14	Fenthion sulfoxide	3.17
Benfluralin	2.09	Fenthion	1.17	Fenthion sulfone	9.61
Pencycuron	0.23	Chlorpyrifos	2.40	Mepronil	3.62
Dimethoate	2.98	Isofenphos oxon	2.03	Chlornitrofen	1.82
Simazine	1.17	Phthalide	1.03	Edifenphos	1.06
Atrazine	3.51	Dimethametryn	1.37	Propiconazole-1	7.70
Diazinon oxon	1.37	Pendimethalin	3.38	Endosulfate	2.98
Propyzamide	1.39	Methyldymron	2.29	Propiconazole-2	5.75
Pyroquilon	1.36	Isofenphos	2.93	EPN oxon	2.31
Diazinon	3.15	Captan	7.46	Thenylchlor	5.43
Disulfoton	3.37	Dimepiperate	3.64	Pyributicarb	0.88
Chlorothalonil	1.57	Phenthoate	2.65	Iprodione	3.03
Iprobenfos	1.29	Procymidone	0.87	Pyridaphenthion	3.78
Tolclofos-methyl oxon	1.56	Butamifos oxon	4.28	EPN	2.85
Fenitorothion oxon	3.75	Methidathion	2.27	Piperophos	5.48
Bromobutide	4.98	alpha-Endosulfan	1.78	Bifenox	7.02
Terbucarb	1.08	Butamifos	5.57	Anilofos	2.48
Malaoxon	2.64	Napropamide	2.38	Pyriproxyfen	2.39
Simetryn	3.14	Flutolanil	1.40	Mefenacet	1.70
Tolclofos-methyl	2.33	Isoxathion oxon	2.71	Cafenstrole	3.14
Alachlor	1.12	Isoprothiolane	4.96	Etofenprox	1.10

First Edition: September, 2012

SHIMADZU
Excellence in Science

Application Data Sheet

No.72

GC-MS
Gas Chromatograph Mass Spectrometer

Scan/MRM Analysis of Residual Pesticides in Foods Using GC-MS/MS (3)

The GCMS-TQ8030 is a triple quadrupole GC-MS/MS system equipped with scan/MRM mode to allow simultaneous scan and MRM data measurements. This data sheet introduces the results of an investigation using the scan/MRM mode, where target pesticides were quantitatively determined using the MRM data, and concentrations of the untargeted pesticides were estimated by applying the scan data to the Compound Composer Database Software Ver.2.

Experimental

For the evaluation, analytical standards (0.001 mg/L to 0.1 mg/L) were used, as well as samples (0.01 mg/L) created by pretreating paprika with the QuEChERS method, and then adding pesticides to the obtained solution. The pesticides specified as targets and their transitions were those recommended in the results of the validity evaluations by the European Reference Laboratory[1]. The analysis conditions are shown in Table 1.

Table 1 Analytical Conditions

GC-MS	:GCMS-TQ8030
Column	:Rxi-5Sil MS (30 m length, 0.25 mm I.D., df=0.25 µm)
Glass Liner	:Sky Liner, Splitless Single Taper Gooseneck w/Wool (Restek Corporation, catalog # 567366)

[GC]

Injection Temp.	:250 °C
Column Oven Temp.	:40 °C (2 min) → (8 °C /min) → 310 °C (5 min)
Injection Mode	:Splitless
Flow Control Mode	:Linear velocity (40.0 cm/sec)
Injection Volume	:1 µL

[MS]

Interface Temp.	:300 °C
Ion source Temp.	:200 °C
Data Acquisition Mode	:Scan/MRM
Event Time	:0.1 sec (Scan), 0.3 sec (MRM)
Scan Mass Range	:m/z 50 – 500
Scan Speed	:5,000 u/sec

MRM Monitoring m/z

Compound Name	Quantitative Transition Precursor>Product	CE (V)	Qualitative Transition Precursor>Product	CE (V)	Precursor>Product	CE (V)	Compound Name	Quantitative Transition Precursor>Product	CE (V)	Qualitative Transition Precursor>Product	CE (V)	Precursor>Product	CE (V)
Diphenylamine	169.10>77.00	26	169.10>115.10	30			Buprofezin	172.10>57.10	18	105.10>104.10	4		
Ethoprophos	200.00>157.90	6	200.00>114.00	14	200.00>97.00	26	Bupirimate	273.10>193.20	8	273.10>108.00	18		
Chlorpropham	213.10>171.10	6	213.10>127.10	18			beta-Endosulfan	240.90>205.90	14	238.90>203.90	14		
Trifluralin	306.10>264.00	8	264.10>206.10	8	264.10>160.10	18	Oxadixyl	163.10>132.10	10	163.10>117.10	24		
Dicloran	206.00>176.00	12	206.00>124.00	26	176.00>148.00	12	Ethion	231.00>174.90	14	231.00>128.90	26		
Propyzamide	172.90>144.90	16	172.90>109.00	26			Triazophos	161.10>134.10	8	161.10>106.10	14		
Chlorothalonil	265.90>230.90	14	265.90>167.90	24	263.90>167.90	24	Endosulfan sulfate	386.90>252.90	10	386.90>216.90	26		
Diazinon	304.10>179.10	12	179.20>137.20	18			Propiconazole-1	259.10>190.90	8	259.10>172.90	18	259.10>69.10	12
Pyrimethanil	199.10>184.10	14	199.10>158.10	14			Propiconazole-2	259.10>190.90	8	259.10>172.90	18	259.10>69.10	12
Tefluthrin	197.10>141.10	26	177.10>127.10	32			Tebuconazole	252.10>127.00	24	250.10>125.10	24		
Pirimicarb	238.20>166.10	10	166.10>96.00	14			Iprodione	314.10>244.90	12	314.10>56.10	24		
Chlorpyrifos-methyl	285.90>270.90	12	285.90>93.00	22			Bromopropylate	340.90>184.90	18	182.90>154.90	16		
Vinclozolin	212.10>172.00	14	212.10>144.90	26	212.10>109.00	30	Bifenthrin	181.10>166.10	16	181.10>165.10	22	181.10>153.10	10
Parathion-methyl	263.10>109.00	18	263.10>81.00	26			Fenpropathrin	265.10>210.10	12	181.10>152.10	24	181.10>127.10	26
Tolclofos-methyl	265.00>249.90	12	265.00>93.00	24			Fenazaquin	160.20>145.10	8	145.20>115.10	24	145.20>91.10	24
Metalaxyl	206.20>162.10	8	206.20>132.10	18			Tebufenpyrad	333.20>276.10	8	333.20>171.00	22		
Fenitrothion	277.10>125.00	18	277.10>109.00	18			Tetradifon	355.90>158.90	12	353.90>159.00	12	228.90>200.90	14
Pirimiphos-methyl	305.10>290.10	12	290.10>125.10	24			Phosalone	182.00>138.00	8	182.00>111.00	18	182.00>102.10	18
Dichlofluanid	332.00>167.10	6	224.00>123.00	12			Pyriproxyfen	136.10>96.00	12	136.10>78.00	24		
Malathion	173.10>117.00	12	173.10>99.00	18			Cyhalothrin	181.10>152.10	24	163.10>127.00	14	163.10>91.00	22
Chlorpyrifos	196.90>168.90	14	196.90>107.00	26			Fenarimol	251.00>139.00	18	139.00>111.00	16		
Fenthion	278.10>125.00	22	278.10>109.00	18			Acrinathrin	289.10>93.10	12	181.10>152.10	24	208.10>181.10	8
Parathion	291.10>109.00	14	291.10>81.00	26			Permethrin-1	183.10>168.10	12	183.10>153.10	18	183.10>115.10	24
Tetraconazole	336.10>218.00	18	336.10>204.00	26			Pyridaben	147.20>132.10	14	147.20>117.10	22		
Pendimethalin	252.20>162.10	12	252.20>161.10	12			Permethrin-2	183.10>168.10	12	183.10>153.10	18	183.10>115.10	24
Cyprodinil	225.20>224.10	6	224.20>208.10	18			Cyfluthrin-1	206.10>151.20	24	163.10>127.10	6	163.10>91.00	14
(E)-Chlorfenvinphos	323.10>266.90	14	267.00>159.00	18			Cyfluthrin-2	206.10>151.20	24	163.10>127.10	6	163.10>91.00	14
Tolylfluanid	137.10>91.00	14	137.10>65.00	26			Cyfluthrin-3	206.10>151.20	24	163.10>127.10	6	163.10>91.00	14
Fipronil	367.00>227.90	26	367.00>212.90	26			Cyfluthrin-4	206.10>151.20	24	163.10>127.10	6	163.10>91.00	14
Captan	79.00>77.00	8	79.00>51.00	22			Cypermethrin-1	181.10>152.10	24	163.10>127.10	6	163.10>91.00	14
(Z)-Chlorfenvinphos	323.10>266.90	14	267.00>159.00	18			Cypermethrin-2	181.10>152.10	24	163.10>127.10	6	163.10>91.00	14
Phenthoate	274.10>125.00	18	274.10>121.10	12			Cypermethrin-3	181.10>152.10	24	163.10>127.10	6	163.10>91.00	14
Folpet	147.10>103.10	10	147.10>76.00	26			Cypermethrin-4	181.10>152.10	24	163.10>127.10	6	163.10>91.00	14
Procymidone	283.10>96.10	12	283.10>67.10	24			Ethofenprox	163.20>135.00	10	163.20>107.10	18		
Methidathion	145.10>85.00	8	145.10>58.00	18			Fenvalerate-1	125.10>99.00	22	125.10>89.00	22		
alpha-Endosulfan	240.90>205.90	14	238.90>203.90	14			tau-Fluvarlinate-1	250.10>200.10	16	250.10>55.00	18		
Mepanipyrim	222.20>220.10	8	222.20>193.10	26			Fenvalerate-2	125.10>99.00	22	125.10>89.00	22		
Profenofos	337.10>266.80	16	207.90>63.00	26			tau-Fluvarlinate-2	250.10>200.10	16	250.10>55.00	18		
Myclobutanil	179.10>152.00	8	179.10>125.00	16			Deltamethrin-1	252.90>93.10	18	181.10>152.10	24		
Flusilazole	233.10>165.10	18	233.10>152.10	18			Deltamethrin-2	252.90>93.10	18	181.10>152.10	24		

Results

An example of the results of the analysis of the analytical standards (0.001 mg/L to 0.1 mg/L) and the pesticide-spiked samples (0.01 mg/L) in scan/MRM mode are shown in Fig. 1. As with Procymidone, shown in Fig. 1, strict quantification of the targeted pesticides could be performed by creating calibration curves from the MRM data. Furthermore, since the scan data was sampled simultaneously, the pesticides could be confirmed from the mass spectrum.

For the untargeted pesticides, data analysis was performed utilizing the Compound Composer Database Software (P/N: 225-13106-92). The simultaneous analysis database software contains information (mass spectra, retention times, and calibration curves) on more than 450 pesticides. As a result, it is possible to identify pesticides from their estimated retention times and mass spectra without using analytical standards, and then calculate semi-quantitative values from the calibration curves. Also in this investigation, it was possible to confirm the detection and semi-quantification of untargeted pesticides such as Quinoxyfen.

Analysis Results for Target Compounds

Procymidone: Quantitative value 0.0098 mg/L

Quantitative determination by creating calibration curves from the MRM data
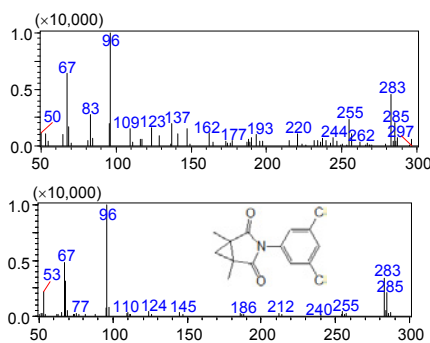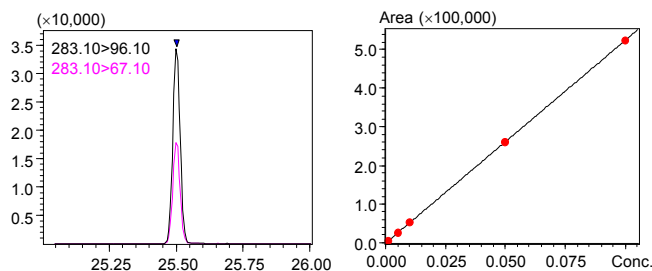
Mass spectral confirmation is possible with the scan data.
(Upper: Sampled mass spectrum; Lower: Mass spectrum in the library)

Measurement Results for Pesticide-Spiked Samples

Scan chromatogram

MRM chromatogram
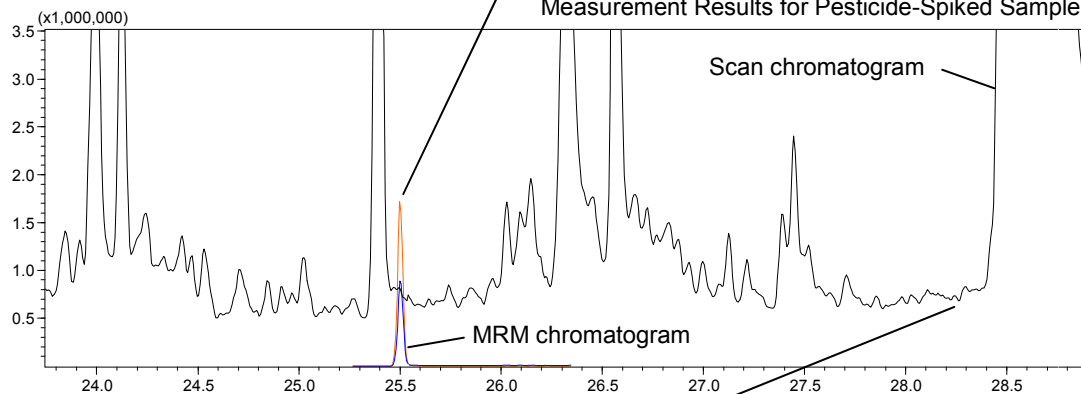
Screening Results for Other Pesticides

Quinoxyfen: Quantitative value 0.0134 mg/L
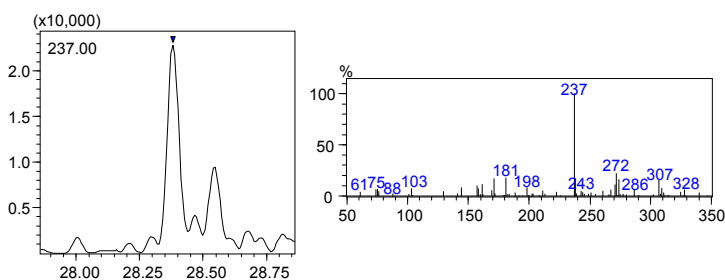
Compound identification and semi-quantitative calculations can be performed utilizing the information contained in the simultaneous analysis database software.
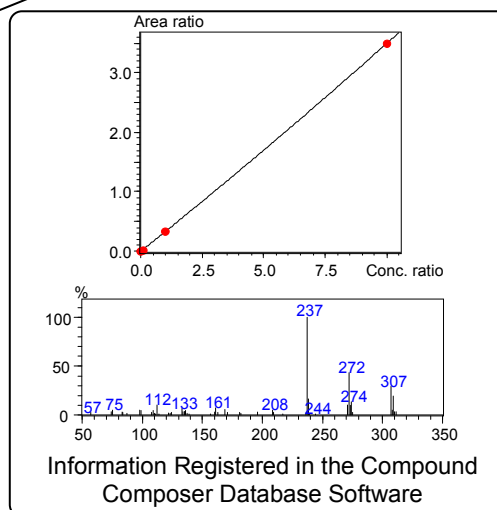
Information Registered in the Compound Composer Database Software

Fig. 1 Scan/MRM Analysis Results

Reference
1) EURL-FV Multiresidue Method using QuEChERS followed by GC-QqQ/MS/MS and LC-QqQ/MS/MS for Fruits and Vegetables (European Reference Laboratory, 2010-M1)

SHIMADZU

Shimadzu Corporation

www.shimadzu.com/an/

SHIMADZU
Excellence in Science

Application Data Sheet

No.73

GCMS
Gas Chromatograph Mass Spectrometer

High-Sensitivity Analysis of 2,4,6-Trichloroanisole in Wine Using Headspace-Trap GC/MS

< Introduction >
2,4,6-trichloroanisole (TCA) emitted from wine corks can taint wine and cause an objectionable odor. Due to the low threshold value for sensing the odor, highly sensitive measurements are required for monitoring. Conventionally, TCA was measured using methods such as purge and trap, which is very effective in concentrating samples, or thermal desorption. The HS-20 headspace sampler includes a trap function that is able to concentrate headspace gases. This Data Sheet describes an example of high-sensitivity measurement of TCA in wine using an HS-trap GC/MS system. The structure of TCA is illustrated in Figure 1 and the mass spectrum is shown in Figure 2.
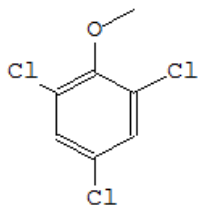
Fig. 1: Structure of TCA
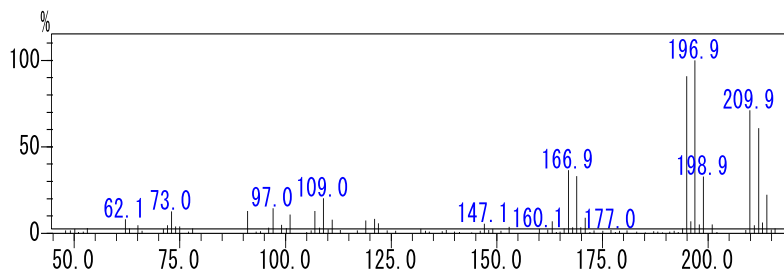
Fig. 2: Mass Spectrum of TCA

■Equipment and Analytical Conditions

Table 1: Analytical Conditions

HS-20

Mode	Trap
Equilibrating time	30 min
Oven temp.	60 °C
Sample line temp.	260 °C
Transfer line temp.	260 °C
Trap equilibrating temp.	80.0 °C
Trap cooling temp.	80.0 °C
Trap desorbing temp.	280.0 °C
Vial pressurizing time	2.0 min
Pressure equilibrating time	0.1min
Load time	0.1 min
Load equilibrating time	0.1 min
Dry purge	5 min
Injection time	20 min
Needle flush	20 min
Injection cycle	3 cycles
Cycle time	50 min
Sample loading volume	5 mL

GCMS-QP2010 Ultra

GC Unit	
Column	Rxi-5ms 0.32 mm I.D. × 60 m L., df=1.0 µm
Column oven temp.	50 °C (1 min) – 10 °C/min – 300 °C (5 min)
Carrier gas control	Constant pressure
Carrier gas pressure	180 kPa
Injection mode	Splitless
Sampling time	3 min
Additional Flow	
APC1	100 kPa
APC3	50 kPa
MS Unit	
Interface temp.	280.0 °C
Ion source temp.	230.0 °C
Solvent elution time	14 min
Measurement start time	15 min
Measurement end time	20 min
Measurement mode	SIM
Selected ions (*m/z*)	211.9, 209.9, 196.9, 194.9
Event time	0.2 sec

■Sensitivity

A wine sample spiked with the equivalent of 1 ng/L TCA was measured by SIM using the HS-trap method (Fig. 3).

The results show how the system was able to analyze low concentrations of TCA with high sensitivity.

A wine sample spiked with the equivalent of 100 ng/L TCA was measured by SIM using the headspace-GC/MS method and HS-trap method, as shown in Figures 4 and 5. A comparison of both shows that the HS-trap method provided about 10 times higher sensitivity.
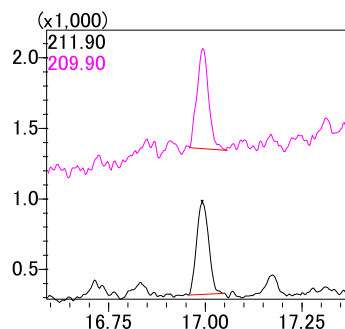
Fig. 3: SIM Chromatogram of TCA in Wine Measured Using HS-Trap (Wine spiked with 1 ng/L TCA)
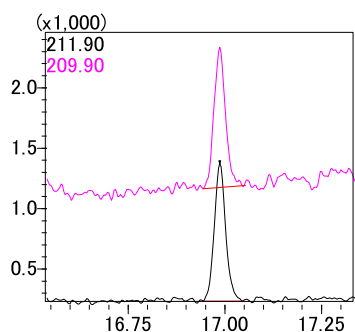
Fig. 4: SIM Chromatogram of TCA in Wine Measured Using Conventional Headspace GC/MS (Wine spiked with 100 ng/L TCA)
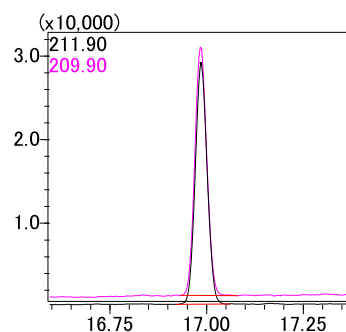
Fig. 5: SIM Chromatogram of TCA in Wine Measured Using HS-Trap (Wine spiked with 100 ng/L TCA)

■Linearity and Repeatability

Linearity was confirmed by adding specific concentrations of trichloroanisole to wine (from 1 to 100 ng/L, as shown in Figure 6). The results showed good linearity.

3 ng/L of trichloroanisole was added to wine to test the repeatability (n = 5) of peak area (Table 2). Results showed good repeatability, with a CV value not exceeding 5 %.
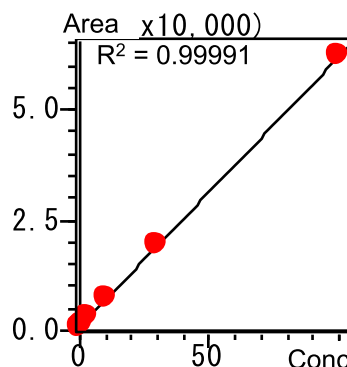
Fig. 6: Linearity of TCA (Wine spiked with 1-100 ng/L TCA)

Table 2: Area Repeatability of TCA (n=5, wine spiked with 3 ng/L TCA)

AREA	1	2	3	4	5	Average	%RSD
TCA m/z 211.9	3,103	3,051	2,925	3,020	2,742	2,968	4.79 %

■Conclusion

This Data Sheet describes an example of high-sensitivity measurement of trichloroanisole in wine using an HS-trap GC/MS system. The results showed that the system was easily able to measure even a few nanograms per liter. This also confirmed that an HS-trap-GC/MS system using the HS-20 headspace sampler is effective in monitoring trichloroanisole in wine.

First Edition: January 2013

SHIMADZU

Shimadzu Corporation

www.shimadzu.com/an/

⊕ SHIMADZU
Excellence in Science

Application Data Sheet

No.93

GC-MS
Gas Chromatograph Mass Spectrometer

Easy Screening for Residual Pesticides in Processed Foods Using GC-MS/MS

The analysis of residual pesticides in processed foods using GC-MS/MS, which provides excellent selectivity and sensitivity, has become a focus of attention.

Before starting GC-MS/MS measurements, it is necessary to optimize MRM transitions (precursor ions & product ions) and collision energies (CE) for each pesticide measured, which is extremely labor intensive. Furthermore, in order to calculate quantitative values, it is necessary to prepare standard samples and create calibration curves.

The Quick-DB database contains the optimal MRM conditions (MRM transitions and CE), mass spectra, retention indices, calibration curves and other information. This enables the semi-quantitative analysis of pesticides without using standard samples. Pesticide surrogates are used as the internal standard substances for calibration curves. Favorable quantitative accuracy is achieved by selecting the surrogates suited to each pesticide.

In analyzing residual pesticides in processed foods, which contain a number of contaminants, separating the pesticides from the contaminants can be impossible, even with GC-MS/MS. In this case, an effective approach to separating and detecting the pesticides is to perform the analysis with two columns respectively, which differ in their separation patterns. The information registered in Quick-DB is also compatible with analysis using two different columns for residual pesticides in processed foods. In addition, if the Twin Line MS system is used, the two columns can be attached to the MS unit simultaneously, so data can be sampled from the different columns smoothly, without compromising the MS vacuum.

This data sheet reports on the results of applying Quick-DB and the Twin Line MS system to the analysis of residual pesticides in curry.

Please also refer to Application Data Sheets No. 91 and No. 92. Application Data Sheet No. 91 introduced an example of easy screening for residual pesticides in foods using GCMS, while No. 92 introduced an example of using two columns with different separation patterns for easy screening of residual pesticides in foods.

Experiment

Using the Restek Q-sepTM, commercially-available retort-pouch curry was pretreated via the QuEChERS method. The sample solution obtained was spiked with 230 standard pesticide samples at a concentration of 10 ng/mL. The pesticide-spiked samples were then subjected to Scan/MRM analysis under the analysis conditions registered in Quick-DB. The analysis conditions are shown in Table 1. The two columns indicated in Table 1 were installed to a single GC-MS with the Twin Line MS system. The retention times for the pesticide components were estimated based on the analysis results for the n-alkane standard sample.

Table 1 Analysis Conditions

GC-MS:	GCMS-TQ8030 (Twin Line MS System)
Column 1:	Rxi-5Sil MS (30 m L., 0.25 mm I.D., df=0.25 µm) (Restek Corporation, P/N: 13623)
Column 2:	Rtx-200MS (30 m L., 0.25 mm I.D., df=0.25 µm) (Restek Corporation, P/N: 15623)
Glass Insert:	Sky Liner, Splitless Single Taper Gooseneck w/Wool (Restek Corporation, P/N: 567366)

[GC]
Vaporization Chamber Temperature: 250 °C
Column Oven Temperature: 60 °C (1 min) → (25 °C /min) → 160 °C → (4 °C /min) → 240 °C → (10 °C /min) → 290 °C (11 min)
Injection Mode: Splitless
High Pressure Injection: 250 kPa (1.5 min)
Carrier Gas Control: Linear velocity (40.0 cm/sec)
Injection Quantity: 2 µL

[MS]
Interface Temp.: 300 °C
Ion Source Temp.: 200 °C
Solvent Elution Time: 1.5 min
Measurement Mode: FAAST (Scan/MRM simultaneous measurement)
Scan Mass Range: m/z 50 to 330
Scan Event Time: 0.15 sec
Scan Speed 5,000 u/sec

Analysis Results

The liquid food extract spiked with pesticides was analyzed, and data processing was performed with Quick-DB. The analysis results are shown in Fig. 1. When semi-quantitative analysis was performed using the calibration curves registered in Quick-DB, favorable semi-quantitative values were obtained, close to the additive concentration of 10 ng/mL for many of the components.

To evaluate the quantitative accuracy for this analysis method, ratios were calculated for the semi-quantitative values with respect to the additive concentration. Then the pesticides were classified into those with a ratio under 50 %, 50 % to 200 %, and over 200 %, to find the distribution. The results are shown in Fig. 2. A significant 83 % of components had a semi-quantitative value 50 % to 200 % that of the concentration of the standard pesticide samples added. From this, it is evident that semi-quantitative analysis can be performed with high accuracy.
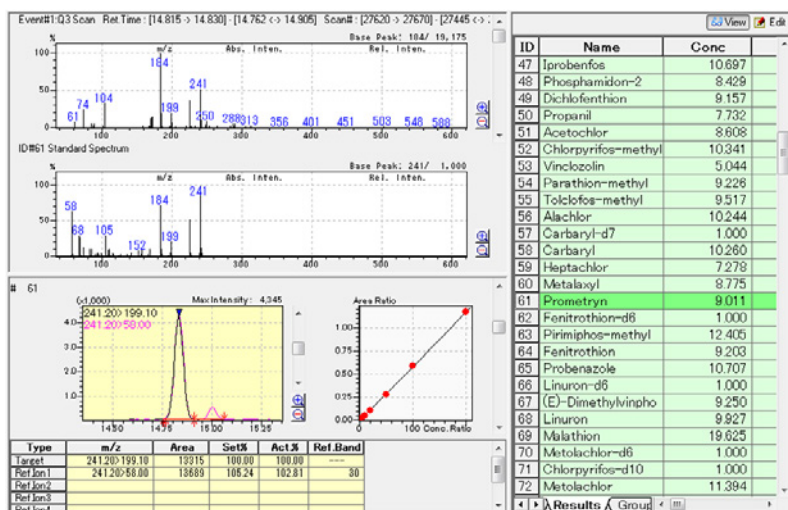
As a result of calculation of the semi-quantitative values using the calibration curves preregistered in Quick-DB, favorable quantitative values were obtained.
(*The concentration of the internal standard is indicated as 1 ng/mL.)

Fig. 1 Analysis Results for the Pesticide-Spiked Samples (10 ng/mL concentration)

6%
(14 compounds)

11%
(24 compounds)

83%
(192 compounds)

■ <50% ■ 50-200% ■ 200%<
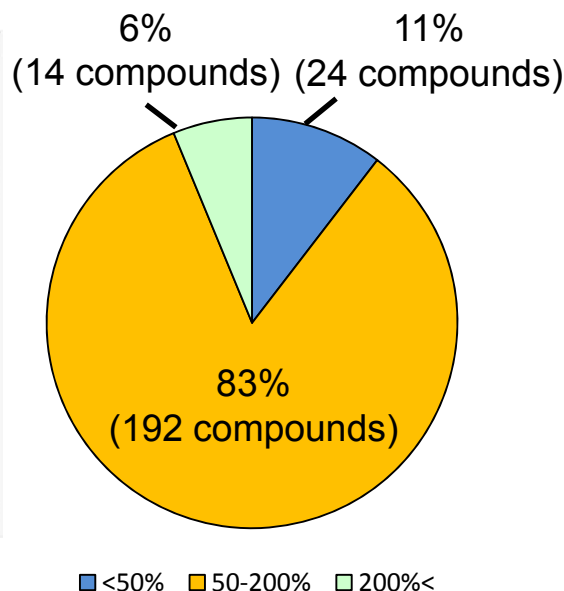
Fig. 2 Percentage Distribution of Semi-Quantitative Values with Respect to the Additive Concentration

In the analysis of residual pesticides in foods, when pesticide peaks are detected, it is necessary to check whether contaminants have been misidentified as pesticides, and whether contaminant overlap has inflated the size of the quantitative values. One confirmation method is to analyze the samples with columns with different separation patterns, and then check that essentially the same quantitative values are obtained for the pesticides detected in the respective columns. As an example, Fig. 3 shows the analysis results for dimethoate. With the Rxi-5Sil MS, there was an impact from contaminants, but with the Rts-200MS, there was not. Semi-quantitative value obtained from the calibration curves registered in Quick-DB was favorable, 9.6 ng/mL, for the use of the Rtx-200MS column. In this way, even for pesticides of which separation from contaminants is difficult, separation is possible if using columns with different separation patterns, enabling highly reliable semi-quantitative analysis.
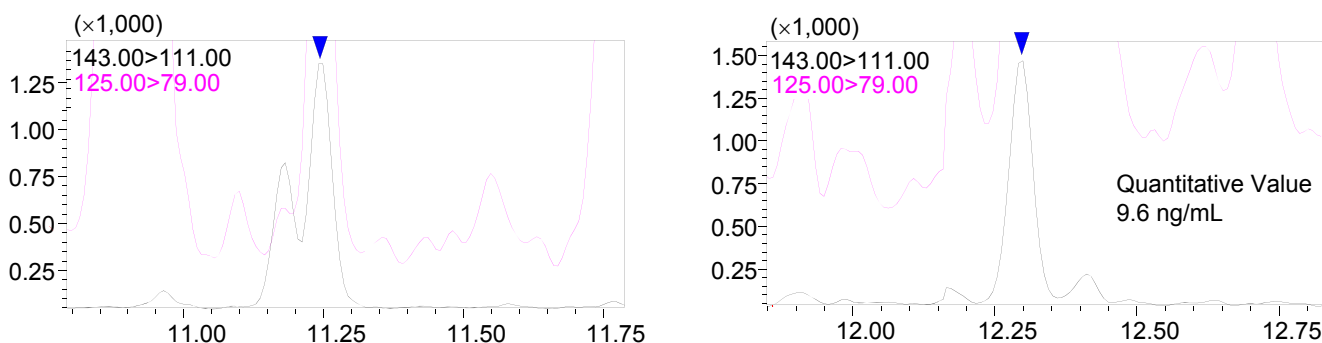
Fig. 3 Chromatograms for Liquid Curry Extract, Spiked with Dimethoate (10 ng/mL Concentration)
(Left: Rxi-5Sil MS; Right: Rtx-200MS)

High-accuracy semi-quantitative analysis was achieved quickly and easily, by attaching two columns to the GCMS-TQ8030 utilizing the Twin Line MS system, and then screening for residual pesticides in processed foods using Quick-DB.

⊕ SHIMADZU

Shimadzu Corporation

www.shimadzu.com/an/

Quantitative Analysis of Dibenzo-p-dioxins (PCDD) and Polychlorinated-p-Dibenzofurans (PCDF) in Foodstuff and animal Feed using the GCMS-TQ8030 tandem mass spectrometer

Hans-Ulrich Baier (Shimadzu Europa GmbH)

Introduction

Contaminations of food and feed with persistent organic pollutants (POP) are determined routinely by various analytical technologies. Dioxins and dioxin like substances belong to this category. They are regarded to have high degree of toxicity to humans. The majority of dioxin contamination of humans is done via the food chain. Dioxins are introduced via several ways into the food products. As an example eggs can be contaminated via the feed of hens. The current methods to determine the amount of dioxins and dioxin like substances is described in American and European legislations [1,2]. In the past mainly gas chromatography coupled to high resolution mass spectrometry with isotopic dilution has been used as analytical method for analyzing and quantifying dioxins. Since June 2014 the EU regulation also allows gas chromatography coupled to tandem quadrupole mass spectrometry (GCMSMS) as a confirmatory method. Dioxins as referred to in this regulation cover a group of 75 polychlorinated dibenzo-para-dioxin (PCDD) congeners and 135 polychlorinated dibenzofuran (PCDF) congeners, of which 17 are of toxicological concern. Polychlorinated biphenyls (PCBs) are a group of 209 different congeners which can be divided into two groups according to their toxicological properties: 12 congeners exhibit toxicological properties similar to dioxins and are therefore often termed dioxin-like PCBs (DL-PCBs). The other PCBs do not exhibit dioxin-like toxicity and have a different toxicological profile.

There have been several publications where the suitability of GCMS [3] or GCMSMS [4] has been tested in the past. Based on those data the new EU regulation included GCMSMS as an alternative for quantitative confirmation of dioxins and PCBs. In this application more than 50 samples of different matrices were split and analysed by the Shimadzu GCMS-TQ8030 triple quadrupole mass spectrometer and the Waters Autospec GCHRMS.

Experimental

Calibration standards of polychlorinated dibenzo-p-dioxins and polychlorinated dibenzo-p-furans with appropriate ^{13}C isotope labelled internal standards were supplied by Greyhound chromatography (Wellington). ^{13}C labelled internal standards were spiked before sample preparation and used for quantification. Additionally, ^{13}C labelled recovery standards were added before instrumental analysis.

The schematic diagram of sample preparation is shown in figure 1.

For this application samples prepared and measured with HRMS were also analysed with the Shimadzu GCMS-TQ8030 tandem mass spectrometer1). The chromatographic column was a 5% phenyl with 60 m, 0.25 mm, 0.1 µm film MS column. Injection volume was 2 µl into the SPL-2010 in splitless mode. Each compound was measured with 2 MSMS transitions.

The mass spectrometer time settings are shown in table 1. Table 2 shows the target compounds and their internal standards which were measured together with one quantifier and one qualifier MSMS transition.

	start T	end T		Event Time (s)	MRM (Quant)	CE	MRM(Qual)	CE
13C TCDF ISTD	20	28	MRM	0,01	315.95>251.95	33	317.95>253.95	33
TCDD-2378	20	28	MRM	0,3	319.90>256.90	24	321.90>258.90	24
13C TCDD-2378 ISTD	20	28	MRM	0,01	331.90>268.00	24	333.90>270.00	24
13C TCDD-1234 ISTD	20	28	MRM	0,01	331.90>268.00	24	333.90>270.00	24
TCDF	20	28	MRM	0,3	303.90>240.95	33	305.90>242.95	33
PeCDF-23478	28	35	MRM	0,3	339.90>276.90	35	337.90>274.90	35
13C PeCDF-23478 ISTD	28	35	MRM	0,01	351.90>287.90	35	349.90>285.90	35
PeCDD	28	35	MRM	0,3	355.90>292.90	25	353.90>290.90	25
13C PeCDD ISTD	28	35	MRM	0,01	365.90>301.90	25	367.90>303.90	25
HxCDF	35	38	MRM	0,2	373.80>310.90	35	375.80>312.90	35
13C HxCDF ISTD	35	38	MRM	0,01	385.80>321.90	35	387.80>323.90	35
HxCDD	35	38	MRM	0,2	389.80>326.90	25	391.80>328.80	25
13C HxCDD ISTD	35	38	MRM	0,01	399.90>335.90	25	401.80>337.90	25
HpCDD	38	40	MRM	0,2	423.80>360.80	25	425.80>362.80	25
13C HpCDD ISTD	38	40	MRM	0,01	435.80>371.80	25	437.80>373.80	25
HpCDF	38	40	MRM	0,2	407.80>344.80	36	409.80>346.80	36
13C HpCDF ISTD	38	40	MRM	0,01	419.80>355.90	36	421.80>357.90	36
OCDF	40	43	MRM	0,2	441.80>378.80	35	443.80>380.80	35
13C OCDF ISTD	40	43	MRM	0,01	453.80>389.80	35	455.80>391.80	35
OCDD	40	43	MRM	0,2	457.70>394.70	26	459.70>396.70	26
13C OCDD ISTD	40	43	MRM	0,01	469.80>405.80	26	471.80>407.80	26

Table 1: MRM table with measuring window (start T, end T), event time in seconds and transitions with collision energy CE. Total number of time segments is 5. The MS resolution was set to Q1: high/unit (depending on peak) and Q3: low
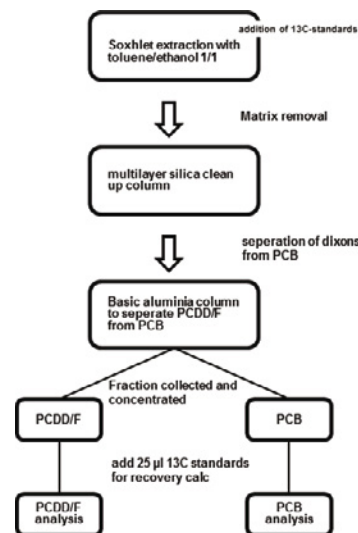
Figure 1: flow diagram of real world sample preparation

The other instrument parameters were: Splitless injection into a splitless liner (Shimadzu) at an injector temperature of 280 °C. GC oven temperature started at 130 °C for 1 min, 20 °C/min to 190 °C, 8 min, 2 °C/min to 220 °C, 3 min, 6 °C/min to 244 °C. The pneumatics were operated in the constant linear velocity mode at 34.7 cm/sec. Interface and ion source temperature were at 280 °C and 230 °C, respectively.

Results

In figure 2 the results recorded with a standard are shown. The target compounds are shown together with the calibration curves. The concentrations are: Tetra: 0.1 pg/µl, Penta, Hexa, Hepta: 0.2 pg/µl, Octa: 0.5 pg/µl.
The compounds with retention times and quantifier/qualifier transitions are shown in table 2.
The calibration ranges used were 0.1 pg/µl – 10 pg/µl for Tetra and Penta, 0.2 pg/µl – 20 pg/µl for Hexa and Hepta, 0.5 pg/µl – 50 pg/µl for OCDD and OCDF with R^2 > 0.999.
Eight replicates were done on the lowest standard. The RSD% was below 3%. The instrument detection limit is calculated from the following formula:

IDL = $t_{\alpha n}$ n · RSDx (amount standard)/100%

$t_{\alpha n}$ = 2.998 (student t table, α = 0.01
(99% confident level)

The IDL calculated by that formula is 16.78 fg (Tetra, Penta).
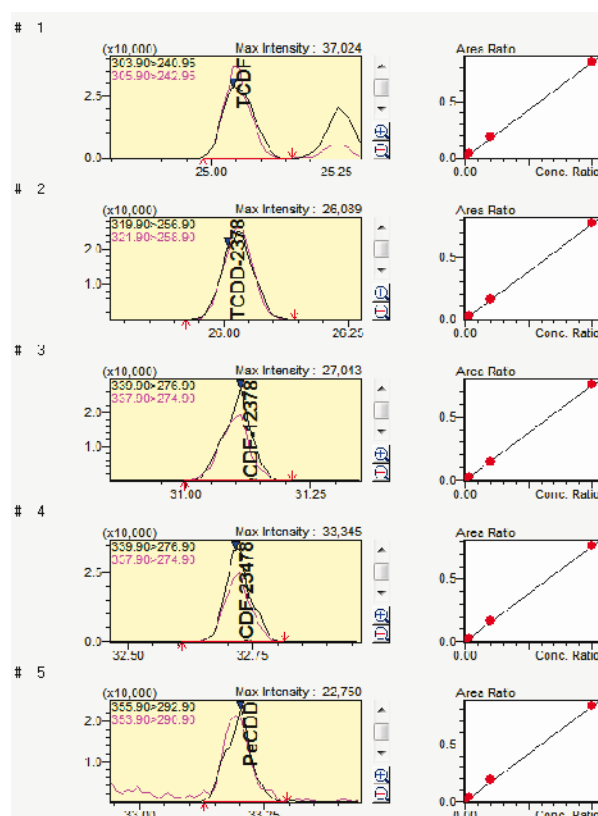
Figure 2: Native PCDD and PCDF congeners recorded with the lowest standard. Within the window of Compound No 17 partial signal from ^{13}C-OCDF is observed next to the target (see also report from standard supplier Wellington)

Table 2: Compound table list with internal standards.
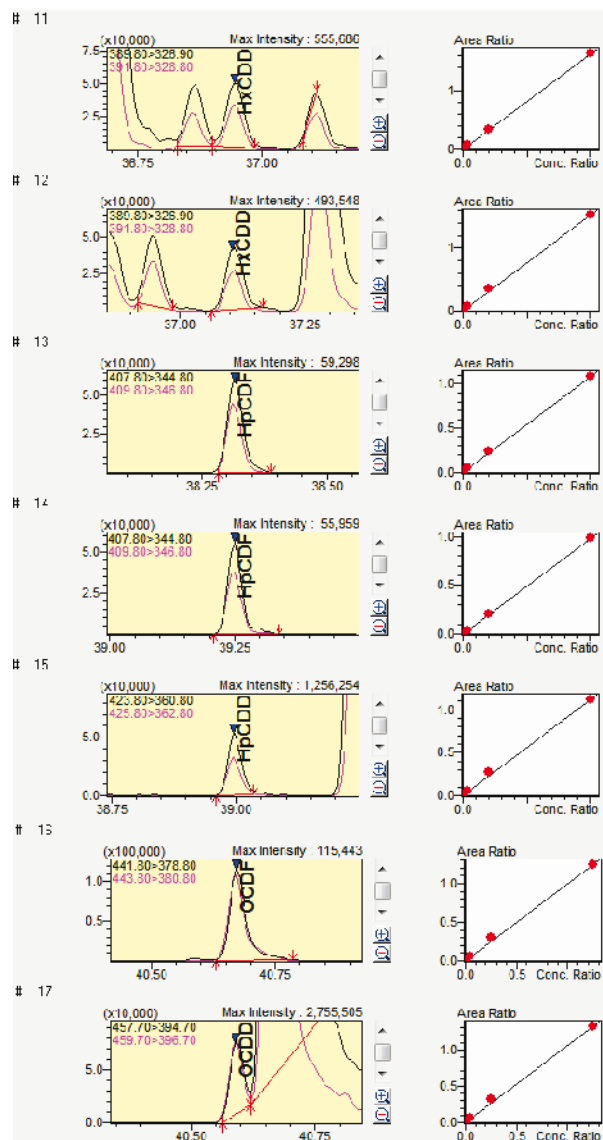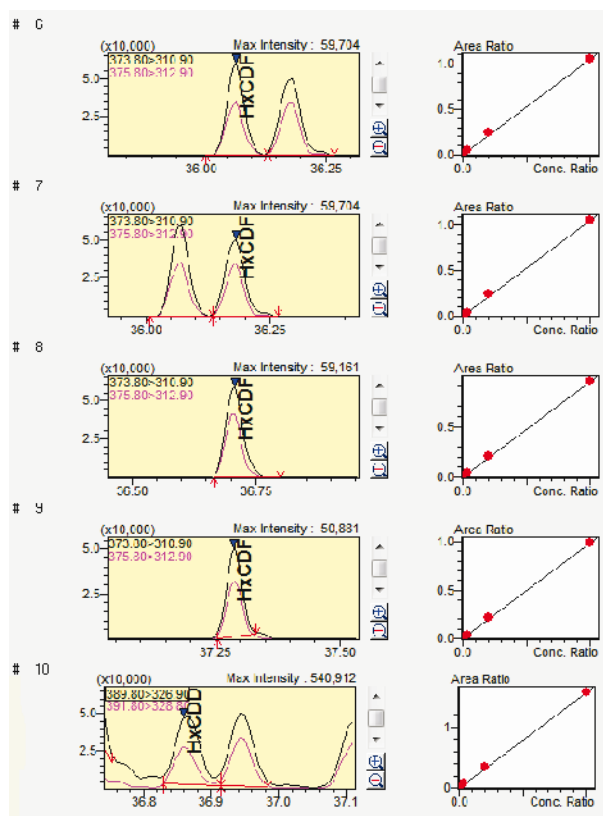
Compound	Ret.-Time	Quantifier	Qualifier
1. 2378-TCDF	25.048	303.90>240.95	305.90>242.95
2. 2378-TCDD	26.023	319.90>256.90	321.90>258.90
3. 12378-PeCDF	31.099	339.90>276.90	337.90>274.90
4. 23478-PeCDF	32.715	339.90>276.90	337.90>274.90
5. 12378-PeCDD	33.192	355.90>292.90	353.90>290.90
6. 123478-HxCDF	36.064	373.80>310.90	375.80>312.90
7. 123678-HxCDF	36.176	373.80>310.90	375.80>312.90
8. 234678-HxCDF	36.704	373.80>310.90	375.80>312.90
9. 123789-HxCDF	37.286	373.80>310.90	375.80>312.90
10. 123478-HxCDD	36.862	389.80>326.90	391.80>328.80
11. 123678-HxCDD	36.942	389.80>326.90	391.80>328.80
12. 123789-HxCDD	37.106	389.80>326.90	391.80>328.80
13. 1234678-HpCDF	38.312	407.80>344.80	409.80>346.80
14. 1234789-HpCDF	39.247	407.80>344.80	409.80>346.80
15. 1234678-HpCDD	38.994	423.80>360.80	425.80>362.80
16. OCDF	40.671	441.80>378.80	443.80>380.80
17. OCDD	40.591	457.70>394.70	459.70>396.70
18. 13C-2378-TCDF	25.027	315.95>251.95	317.95>253.95

Compound	Ret.-Time	Quantifier	Qualifier
19. 13C-1234-TCDD	25.245	331.90>268.00	333.90>270.00
20. 13C-2378-TCDD	25.994	331.90>268.00	333.90>270.00
21. 13C-12378-PeCDF	31.073	351.90>287.90	349.90>285.90
22. 13C-23478-PeCDF	32.703	351.90>287.90	349.90>285.90
23. 13C-12378-PeCDD	33.179	365.90>301.90	367.90>303.90
24. 13C-123478-HxCDF	36.055	385.80>321.90	387.80>323.90
25. 13C-123678-HxCDF	36.169	385.80>321.90	387.80>323.90
26. 13C-234678-HxCDF	36.692	385.80>321.90	387.80>323.90
27. 13C-123789-HxCDF	37.28	385.80>321.90	387.80>323.90
28. 13C-123478-HxCDD	36.856	399.90>335.90	401.80>337.90
29. 13C-123678-HxCDD	36.935	399.90>335.90	401.80>337.90
30. 13C-123789-HxCDD	37.099	399.90>335.90	401.80>337.90
31. 13C-1234678-HpCDF	38.308	419.80>355.90	421.80>357.90
32. 13C-1234789-HpCDF	39.242	419.80>355.90	421.80>357.90
33. 13C-1234678-HpCDD	38.99	435.80>371.80	437.80>373.80
34. 13C-OCDD	40.587	469.80>405.80	471.80>407.80
35. 13C-OCDF	40.667	453.80>389.80	455.80>391.80

Real world samples

In figure 3 the results recorded with a fish oil sample are shown.

The concentrations calculated were TCDF 0.089, PeCDF 0.049, HxCDF 0.0714, 0.012, HpCDD 0.03, OCDF 0.024, OCDD 0.16 pg/2 µl.
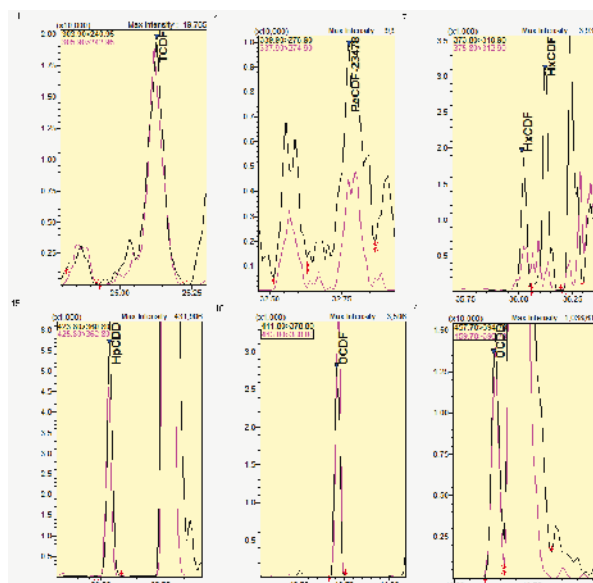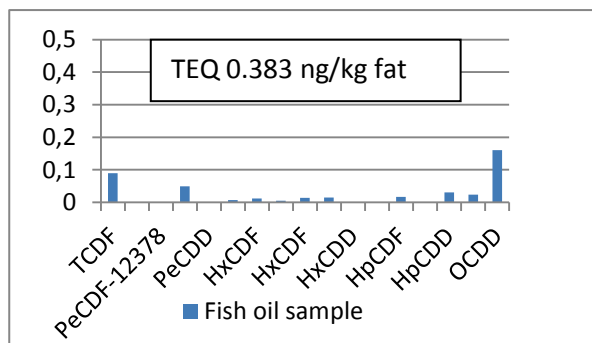
Figure 3: Results for detected compounds in a fish oil sample. Left: Concentration calculated for each congener. Right: peaks from the quantitation window

Each congener shows different toxicity which is expressed by the Toxic Equivalent Factor (TEF). This means that the analytical results relating to all the individual dioxin and dioxin-like PCB congeners of toxicological concern are expressed in terms of a quantity, namely the toxic equivalent (TEQ).

The Toxic Equivalent Factors are according to WHO from 2005 and are for the dibenzo-p-dioxins and furans: 2378-TCDD 1, 12378-Pe CDD 1, 123478-HxCDD 0.1, 123678-HxCDD 0.1, 123789-HxCDD 0.1, 1234678-HpCDD 0.01, CDD 0.0003 and 2378-TCDF 0.1, 12378-Pe CDF 0.03, 123478-HxCDF 0.1, 123678-HxCDF 0.1, 123789-HxCDF 0.1, 1234678-HpCDF 0.001, 1234789-HpCDD 0.01, and OCDF 0.0003. The main contribution to the TEQ value of 0.383 ng/kg fat in figure 3 comes from TCDF (TEQ is calculated by multiplication of the concentration).

Comparison of results with HRMS

A total number of more than 50 samples were measured with both technologies. In figure 4, a component based comparison is shown for an animal feed and fish sample. The TEQ values calculated from these samples were for the animal feed sample 0.0899 ng/kg (GCHRMS) and 0.0895 ng/kg (GCMSMS) and for the fish sample 0.307 ng/kg (GCHRMS) and 0.324 ng/kg (GCMSMS).
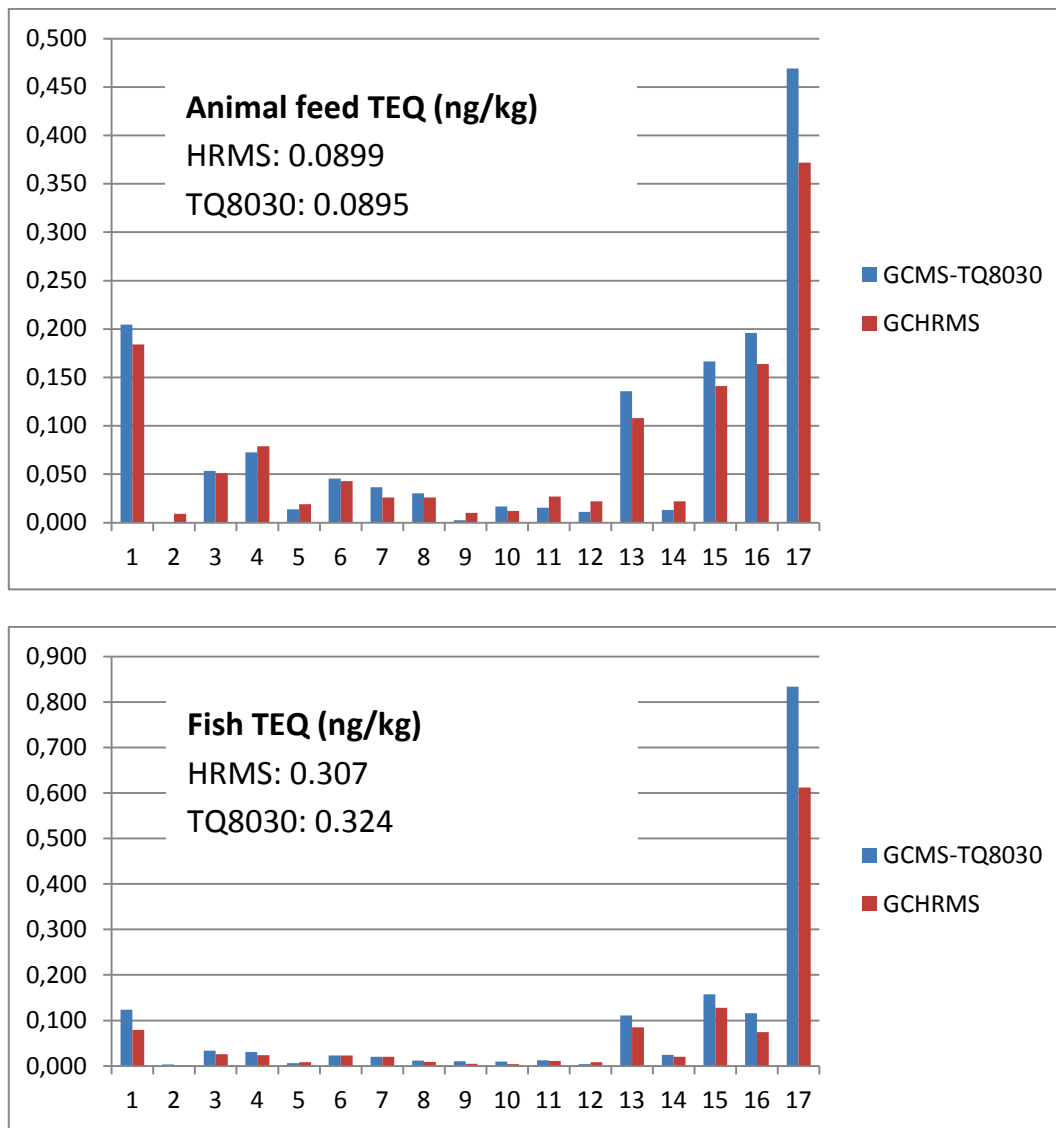
Figure 4: Comparison of concentrations (pg/µl) of individual PCDD and PCDF congeners determined with an animal feed (top) and fish sample (bottom). The x-axis numbers refer to the compounds listed in table 2.
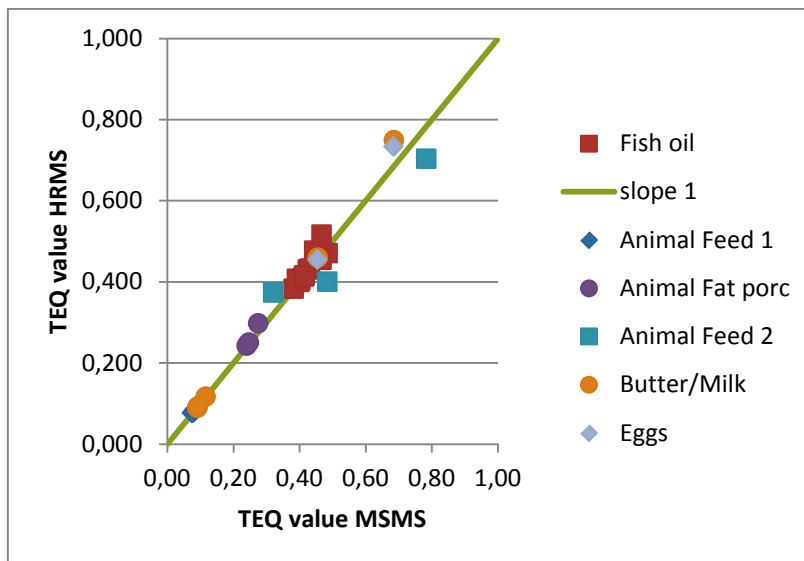
Figure 5: TEQ values (upper bound) in ng/kg calculated from GCHRMS and GCMSMS for various matrices

Then the method was applied to more than 50 samples. In figure 5 TEQ values calculated from GCHRMS and GCMSMS data are plotted against each other for various matrices. In addition the ideal curve with slope 1 is shown as well. To have a better indication on the statistics, figure 6 shows the percentage deviation of 14 fish oil samples with TEQ values (upper bound) of 0.383 to 0.477 ng/kg fat.
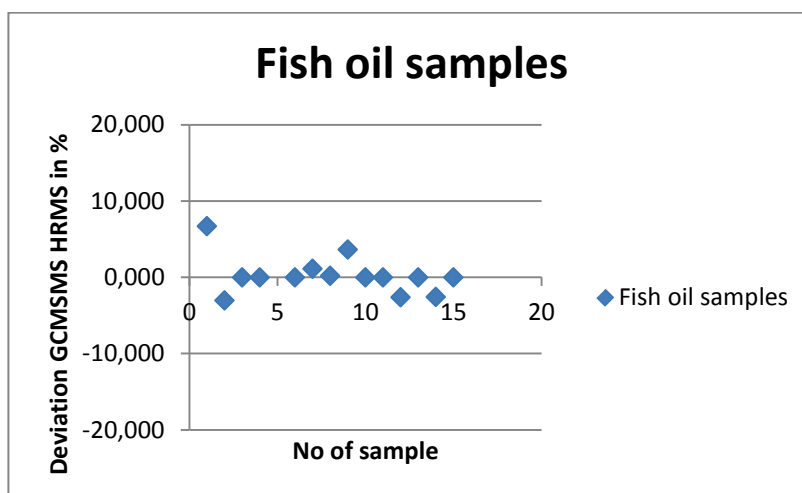
Figure 6: 14 samples (fish oil) are plotted to show the percentage deviation of the results obtained with GCMSMS relative to the ones obtained with GCHRMS.

Discussion

The TEQ values derived from the GCMSMS methods shown above, indicate a very good correlation with the established HRGCMS methods. For the matrix fish, the deviation is less than 10% at TEQ levels of about 0.45 ng/kg fat. Those values are below the regulatory levels which are 1.75 ng/kg (marine oil, fish oil). The highest TEQ value observed was about 10 ng/kg. The recovery of the compounds was calculated for every sample from the recovery internal standards and the results were between 60 and 100%.

Conclusions

The data shown in this application news indicate that the GCMS-TQ8030 proves sufficient accuracy for quantitative screening of dioxins in food and feed samples.

The maximum deviation of TEQ values calculated from GCMSMS data compared to the one from HRMS were below 10% for many matrices measured, even for low TEQ values below 0.5 ng/kg.

[1] Sample preparation and measurement were performed at SGS Antwerp: HRMS: Waters Autospec, MSMS: Shimadzu GCMS-TQ8030

References

[1]   Commission Regulation (EC) No 882/2012 of 28 March 2012 amending Regulation (EC) No 152/2009 of (OJ L 91, 29.3.2012, p. 8–22)

[2]   Commission Regulation (EU) No 589/2014 of 03 June 2014 repealing Regulation (EU) No 252/2012

[3]   M. Geissler, S. Schröder Lab&more 2/11, p20

[4]   A. Kotz et al, Organohalogen Compounds Vol. 74, 156-159 (2012)

SHIMADZU

Application News

No. SCA_280_080

Comprehensive screening of residual 360 pesticides in food using fast GC-MS/MS technology

Introduction

Contamination of food products with pesticides is a growing concern because of recognized adverse effects on health, increasing world-wide usage of pesticides and higher imports of raw foodstuffs from foreign sources. Consequently, the number of samples as well as pesticides monitored has become significantly higher in the last decade. To handle this high sample load, a Quick, Easy and Cheap cleanup procedure called QuEChERS was established [1].

Unfortunately, samples prepared by this method contain large matrix signals which popularized the use of highly selective tandem MS. Along with matrix interference, the analysis time is a crucial point when handling a high sample load. The usage of narrow bore capillary columns has been shown to be a powerful tool for drastically reducing analysis time while maintaining chromatographic resolution in different GCMS applications [2].

Combining the speed of fast GC and the selectivity of tandem MS is a powerful tool to increase laboratory efficiency and reduce working costs. As fast GC reduces the peak width at half height (FWHM) down to about 1 s, the detector must be able to follow sharp increases of signals. Fast MRM (Multiple Reaction Monitoring) switching modes with no interfering cross talks are therefore needed. The potential of this approach is demonstrated by analyzing 360 pesticides in apple QuEChERS extract in less than 10 minutes.

Experimental

QuEChERS apple extract was used as test sample matrix. A 6-point calibration curve (0.5 ppb to 100 ppb) was created by spiking the blank sample matrix with 360 pesticides using TPP as internal standard. A Shimadzu GCMS-TQ8040 triple quadrupole system equipped with the GL Sciences' Optic-4 multi-mode inlet was used for sample measurement. MRMs and collision energies (CE) were taken from Shimadzu´s SmartDB for pesticides. SmartMRM was utilized for the measurement time optimization. All compounds were measured with one quantifier and one qualifier. See detailed summary of analytical conditions below.

GC-MS:	GCMS-TQ8040
Injector:	Optic-4, IP deactivated liner with lass insert
Column:	BPX 5 MS, 20 m x 0.18 mm i.D., 0.18 µm film thickness (SGE)
Software:	GCMSSolution 4.2 with SmartMRM and MRM Optimization Tool

Injector:		MS	
Injection Mode:	Splitless (1.3 min)	Ion Source Temp.:	200 °C
Injection Volume:	1 µl	Interface Temp.:	300 °C
PTV-Program:	70 °C, 15 °C/s to 280 °C, 1.2 min, 15 °C/s to 320 °C, 6 min	Emission current:	100 µA
		Ionization Method:	EI, 70 eV
GC:		Acquisition Mode:	MRM
Column Oven Temp.:	80 °C, 1 min, 35 °C/min to 210 °C, 25 °C/min to 320 °C, 2 min	Mass Resolution:	Q1 0.8 Da, Q3 3.0 Da (FWHM)
		Loop time:	0.18 sec
Linear Velocity:	40 cm/s	Processing time:	±0.1 min

Results

Figure 1 shows the full chromatogram of the 360 pesticides measured. It can be seen that all compounds eluted in less than 10 minutes. Moreover, a strong tendency towards co-elutions was evident. To follow such a high information density, the use of a highly selective detector such as a triple quad MS is inevitable.
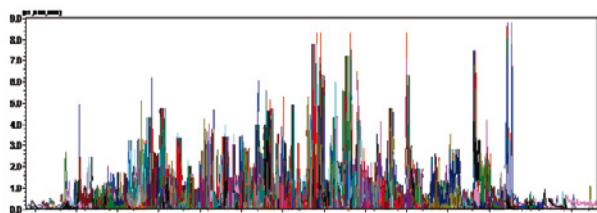
Figure 1: Chromatogram 360 Pesticides In Apple Matrix

Results shown in figure 1 were obtained using a 5 ms 20 m, 0.18 mm, 0.18 µm fast GC column. It is noteworthy that there are columns available, which have lower dimensions and offer even faster chromatographic results. Using fast GC columns, two contradictory effects have to be taken into account when choosing ideal measurement conditions. On the one hand the lower inner diameter and higher possible

heating rates enable sharpened peaks and consequently higher S/N ratios. On the other hand the sample capacity decreases by lowering the column dimensions, which results in lower absolute sample amounts and minimization of sensitivity [3]. Therefore, the used intermediate column is a good compromise to decrease analysis time while maintaining high sensitivity.

Matrix calibration curves (0.5 ppb – 100 ppb) were measured for all 360 pesticides. The linear correlation factor was higher than 0.9980 for every compound. Nearly all components were detectable at the lowest concentration of 0.5 ppb. Figure 2 shows peak profiles and calibration curves for some typical pesticides. As already indicated by the correlation factor, linearity was very good for all compounds.

Peak widths at half maximum (FHMW) are easily decreased below 1 sec using fast GC separation. This decline was also found for the peaks shown in figure 2. Furthermore, it is known that for a good reproducibility at least 10 data points per peak are needed [4]. To enable this number of data points a loop time
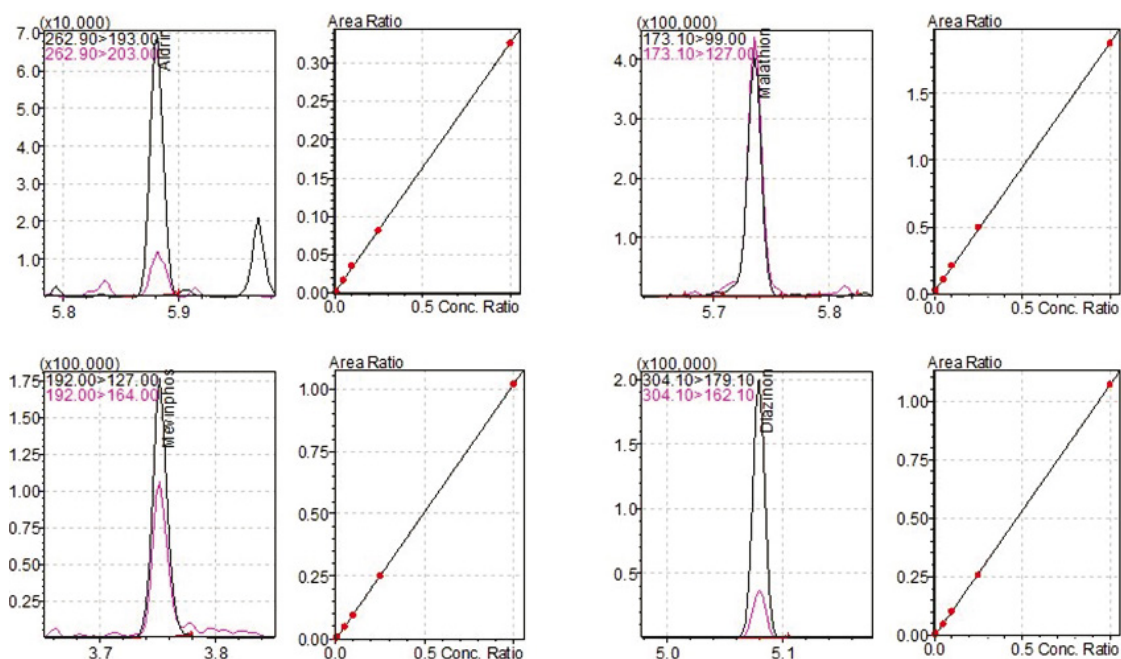
Figure 2: Calibration Curve (0.5 ppb –100 ppb) and Peak Profile at 5 ppb

of 0.18 s was chosen. As in some parts of the chromatogram up to 30 compounds eluted in the same processing window and for each compound two transitions (1 Quantifier and 1 Quantifier) were needed, the total number of transitions reached up to 60 per data point. Consequently, the lowest dwell time per MRM was in some cases 3 msec. At these short dwell times, precision and speed of the instrument become very important in order to obtain good reproducibility for all transitions measured. Figure 3 shows superimpositions and RSD-values of three different peaks measured with a data point dwell time of less than 3 ms. It is evident that RSDs for these peaks are below 10%. This high degree of precision was found for most of the compounds.

Trifloxystrobin, %RSD = 7.6   Isazofos, %RSD = 6.4
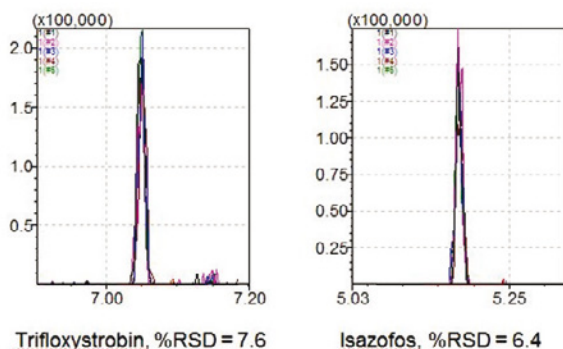
Conclusion

The actual study shows the successful combination of fast GC and tandem mass spectrometry. It was possible to determine 360 pesticides spiked in a QuEChERS apple extract with excellent calibration curve linearity and good reproducibility in less than 10 minutes. The shown application can help to increase routine laboratory efficiency.

Literature

[1] QuEChERS, European Standard, EN 15662,

[2] Baier, H.-U. In Practical Gas Chromatography: A Comprehensive Reference; Dettmer-Wilde, K.; Engewald, W., Eds.; 2014; Chapter 12; to be published,

[3] Mondello, L. et al., Journal of Chromatography A, 2004, 1035, 237-247,

[4] Mastovska, K., Lehotay, S. J.; Journal of Chromatography A, 2003, 1000, 153–180.

SHIMADZU

Shimadzu Europa GmbH

www.shimadzu.eu

2. Mass Spectrometry

2.2 Liquid Chromatography-Mass Spectrometry

Liquid Chromatography-Mass Spectrometry (LC-MS) is an analytical chemistry technique that combines the physical separation capabilities of liquid chromatography with the mass analysis capabilities of mass spectrometry (MS). It is a powerful technique that brings together very high sensitivity and high selectivity. Its application is oriented towards the separation, general detection and potential identification of chemicals of particular masses in the presence of other chemicals (e.g. complex mixtures). It is widespread in many application fields such as food safety.

AD-0051	Quantitative analysis of carbohydrates in food samples using APCI-LC/MS with post-column reagent addition and ligand exchange chromatography
C99	Quantitative analysis of veterinary drugs using the Shimadzu LCMS-8050 Triple Quadrupole Mass Spectrometer
SCA_210_013	Highly sensitive and rapid simultaneous method for 45 mycotoxines in baby food samples by HPLC-MS/MS using fast polarity switching
SCA_210_014	Simultaneous quantitative analysis of 20 amino acids in food samples without derivatization using LC-MS/MS
SCA_210_015	Determination of industrial dyes in food by LCMS-IT-TOF
SCA_210_016	Micro flow UHPLC-MS/MS in pesticide analysis of infant foods
Technical report	Multi-residue analysis of 210 pesticides in food samples by Triple Quadrupole UHPLC-MS/MS
C89	Analysis of 9 haloacetic acids in tap water using the LCMS-8040 Triple Quadrupole Mass Spectrometer
C95	Analysis of haloacetic acids in drinking water using Triple Quadrupole LC/MS/MS (LCMS-8050)
C96	Analysis of phenols in drinking water using Triple Quadrupole LC/MS/MS (LCMS-8040)
C104	Analysis of diarrhetic shellfish toxin using Triple Quadrupole LC/MS/MS (LCMS-8050)
C105	Analysis of sulfamic acid in fertilizers using LC/MS (LCMS-2020)
C108	Application of direct analysis in real time (part 1) rapid analysis of fatty acids and amino acids in food using LCMS-2020
C109	Application of direct analysis in real time (part 2) rapid analysis of triglycerides and fatty acids in food oil using LCMS-2020
C110	Application of direct analysis in real time (part 3) rapid analysis of fatty acids in rice bran using LCMS-2020
C111	Direct analysis of volatile compounds in real time using DART-MS (Part 1) analysis of flavor release from chocolate-like food
C112	Direct analysis of volatile compounds in real time using DART-MS (Part 2) analysis of volatile compounds in spices, herb tea, and flavored oils
C117	Direct determination of trace hormones in drinking water by large volume injection using the LCMS-8050 Triple Quadrupole Mass Spectrometer
C119	Analysis of cartap, pyraclonil, and ferimzone in drinking water using a Triple Quadrupole LC/MS/MS system
C120	Analysis of glufosinate, glyphosate, and AMPA in drinking water using a Triple Quadrupole LC/MS/MS system
No. 36	Analysis of pesticides in drinking water using Triple Quadrupole LC/MS/MS (LCMS-8040)
No. 39	Quantitative analysis of pyrethroids in soil using Triple Quadrupole LC-MS/MS
No. 43	High speed analysis of haloacetic acids in tap water using Triple Quadrupole LC-MS/MS

Application News

LCMS-2020

No. AD-0051

Quantitative Analysis of Carbohydrates in Food Samples Using APCI-LC/MS with Post-column Reagent Addition and Ligand Exchange Chromatography

Sensitive LC/MS methods for quantification of carbohydrates are in demand increasingly in foods, nutrition and biochemistry fields. The conventional analytical methods based on GC/MS or HPLC with ELSD, UV or fluorescence detection were used normally for few sugars or carbohydrates and derivatization of the compounds prior to analysis was needed mostly. It is desired to use LC/MS method without derivatization for quantitative determination of more carbohydrates. It is well known that ionization of carbohydrates by atmospheric pressure ionization (API) is difficult. Therefore, post-column addition of reagent such as chloroform is required [1, 2]. However, the high content of chloroform in the mobile phase may cause strong ion suppression and contamination to the interface and ion optics of LC/MS. Here, we report a new LC/MS method using a reduced content of chloroform by post-column addition in mobile phase and ligand exchange chromatography for analysis of twelve carbohydrates.

❏ Experimental

A single quadrupole LCMS-2020 (Shimadzu Corporation) was employed in this work. The LC and MS conditions are shown in Table 1. Twelve carbohydrates (see table 2) used as standards were obtained in powders from Sigma Aldrich, AnalaR Normapur, Wako Chemicals, Fluka, Merck and TCI. A mixed stock solution of the 12 carbohydrates was prepared with pure water as the solvent. The mixed standard solution was diluted into a calibrant series ranging from 0.1 mg/L to 400 mg/L.

Table 1: LC and MS Conditions for Carbohydrates Analysis

LC Conditions:

Column	Shim-pack SCR-101 P (7.9 x 300 mm)
Flow Rate	0.60 mL/min
Elution Mode	Isocratic elution
Mobile Phase	Water
Post Column solvent	Methanol:Chloroform, 95:5 (0.1 mL/min)
Oven Temp	80 °C
Injection Volume	10 µL

MS Conditions (Shimadzu LCMS-2020):

Interface	APCI
MS Mode	Negative Mode (SIM)
Interface Temp.	450 °C
Block Temp.	200 °C
DL Temperature	250 °C
Nebulizing Gas Flow	Nitrogen, 2.5 L/min
Drying Gas Flow	Nitrogen, 5.0 L/min

❏ Results and Discussion

Method Development

Figure 1 shows the SIM chromatograms of the 12 carbohydrates using LCMS-2020. The LC separation of the compounds was carried out by ligand exchange chromatography using a Shim-pack SCR-101P column (7.9mmID x 300mmL) with pure water as the mobile phase (0.60 mL/min, isocratic mode). Chloroform reagent of 5% in MeOH was pumped at 0.1 mL/min into APCI interface through a post-column addition flow line to promote ionization of the carbohydrates to form [M+Cl]⁻ ions in negative mode.

One of the advantages of LC/MS method is the capability of separation of co-eluting compounds with different molecular masses. In this analysis, there were two pairs of co-eluting compounds: galactose and rhamnose (RT at 14.78 min and 14.81 min); myo Inisitol and glycerol (RT at 19.42 min and 19.47 min). Having different m/z of [M+Cl]⁻, for example, galactose with m/z of 215.1 and rhamnose with m/z of 199.1, they could be detected separately in SIM mode.

The calibration curves of the 12 carbohydrates were set up using mixed standard samples with concentrations from 0.1 or 0.5 mg/L to 400 mg/L. Linear calibration curves were obtained for all compounds (r2 > 0.999) (shown in Figure 2). The limits of detection (LODs) of these compounds in neat solutions were at 0.05~1 mg/L depending on compounds.

The repeatability of the method was evaluated and the RSD (%, n=6) of peak area obtained for 10 mg/L concentration were found below 5.0% except for ribose (6.9%) (See Table 2).
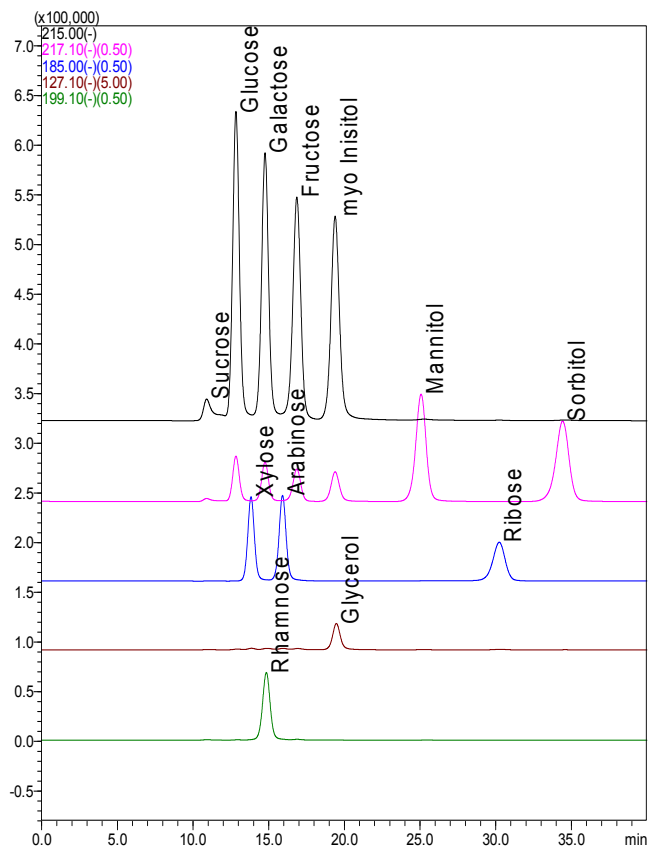
Fig 1: SIM chromatograms of 12 carbohydrates by LC/MS.
        Concentration: 100 mg/L.

Analysis of Food and Beverage Samples

The LC/MS method established was applied to a variety of liquid samples including beverage and food (Japanese "Sake", soya sauces and soft drink). The liquid samples investigated were diluted 1000 times in water and were filtered with 2 µm filters before injection. The SIM chromatograms of some food and beverage samples are shown in Figure 3. The results of identification about the types of sugars and sugar alcohols as well as their quantification results were in accordance with the contents available on the product labels (Table 3).

Table 3: Results of carbohydrates in samples tested (g/L)

Carbohydrate	Sample		
	Sake	Soya sauce	Soft drink
Sucrose	-	27.09	-
Glucose	26.49	3.52	40.99
Galactose	-	2.25	-
Fructose	-	1.51	59.2
myo Inisitol	-	0.87	-
Glycerol	-	19.76	-
Mannitol	-	0.34	-

Table 2: Calibration curve and repeatability of the method for quantitative analysis of 12 carbohydrates

Carbohydrate	MW	[M+Cl]⁻	RT (min)	Calibration Conc. range / mg/L	r² value	%RSD Peak Area
Sucrose	342.3	$[M-C_6H_{10}O_5+Cl]^-$ 215.1	10.74	0.5 - 100	0.9998	4.7
Glucose	180.16	215.1	12.82	0.1 - 400	0.9999	1.6
Xylose	150.13	185.1	13.84	0.1 - 400	0.9998	3.2
Galactose	180.16	215.1	14.78	0.1 - 400	0.9998	1.5
Rhamnose	164.17	199.1	14.81	0.1 - 400	0.9993	4.2
Arabinose	150.13	185.1	15.94	0.1 - 400	0.9997	4.1
Fructose	180.16	215.1	16.86	0.1 - 400	0.9996	4.1
myo Inisitol	180.16	215.1	19.42	0.1 - 400	0.9994	2.5
Glycerol	92.09	127.1	19.47	0.1 - 400	0.9995	3.1
Mannitol	182.17	217.1	25.07	0.1 - 400	0.9997	3.2
Ribose	150.13	185.2	30.19	0.1 - 400	0.9994	6.9
Sorbitol	182.17	217.1	34.40	0.1 - 400	0.9995	2.8
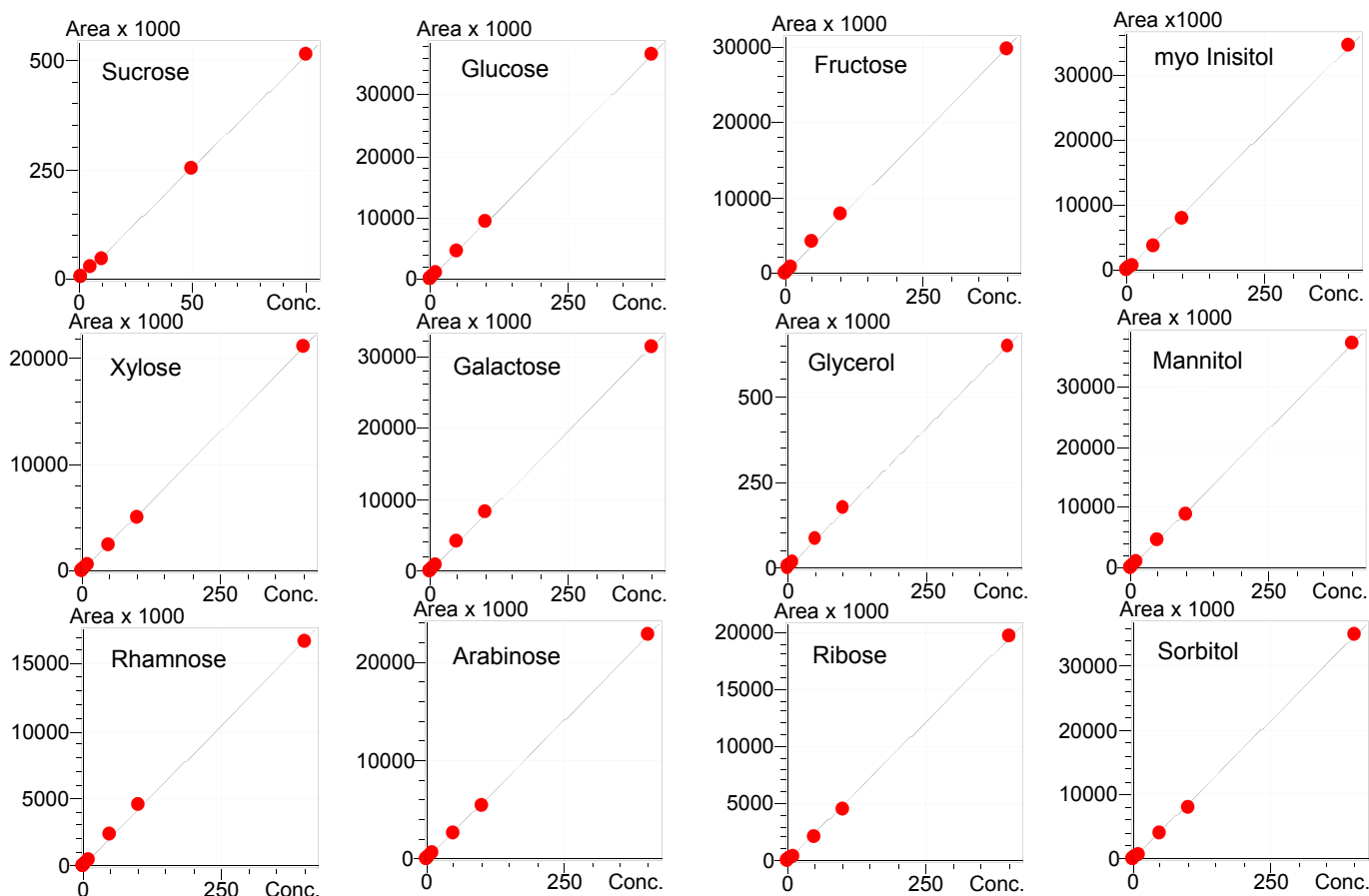
Fig 2: Calibration curves of 12 carbohydrate standards, peak area ~ concentration (mg/L)
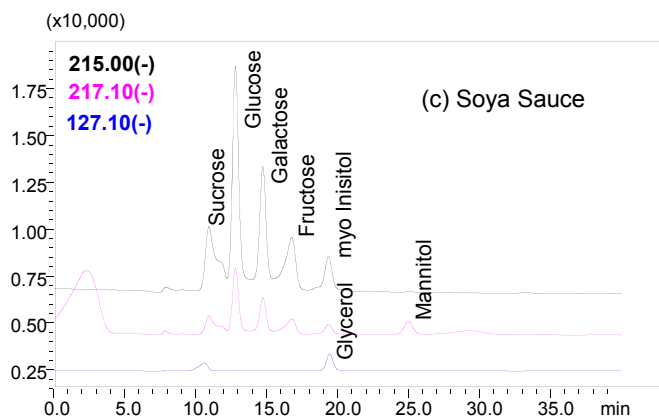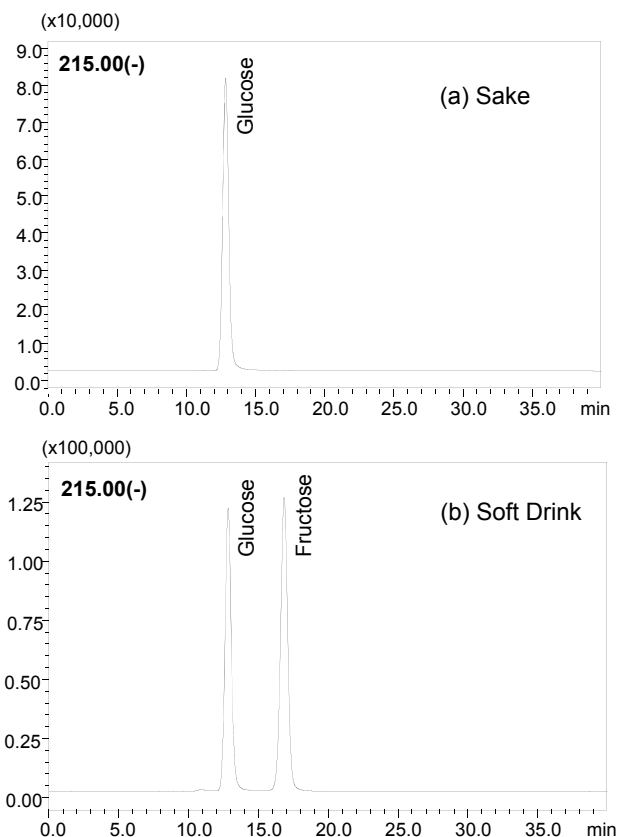
Fig 3: Food and beverage sample at 1000x dilution,
(a) Sake, (b) Soft drink and (c) Soya sauce

❑ Conclusions

A new APCI-Ligand Exchange Chromatography/MS method was developed for quantitative analysis of twelve carbohydrates. The results showed that as low as 0.7% of chloroform as post-column addition reagent was sufficient for effective ionization of the twelve carbohydrates studied to achieve desired sensitivity of 0.05~1 mg/L.

❑ References

[1] Application News No. C74, Shimadzu,
http://www.shimadzu.com/appli/index.html
[2] Kato, Y. Numajiri, Y., J. Chromatography 562, 81-97(1991).

SHIMADZU
Excellence in Science

SHIMADZU
Excellence in Science

Application News

No. C99

Liquid Chromatography Mass Spectrometry

Quantitative Analysis of Veterinary Drugs Using the Shimadzu LCMS-8050 Triple Quadrupole Mass Spectrometer

Foods in which chemical residues, like pesticides, feed additives, and veterinary drugs found in excess of maximum residue levels have been banned from sale in many countries around the world. Compounds that are subject to residue standards vary widely and the list is expected to grow. Because of this, there is a need for a

highly sensitive and rapid analytical technique to analyze as many of these compounds as possible in a single run. This Application News introduces an example of the high-sensitivity analysis of 89 veterinary drugs in a crude extract of livestock and fishery products.

■ Sample Preparation

The typical samples used in the analysis of veterinary drugs contain large amounts of lipids because they are commonly meat and fish samples. Sample preparation is extremely important to ensure excellent sensitivity and repeatability. To avoid the typical time-consuming and laborious solid phase extraction sample preparation procedure, the QuEChERS method, which is typically used for the preparation of vegetables, was selected to simplify sample preparation.

The QuEChERS method normally consists of two steps, the first is an acetonitrile extraction and the second a cleanup step, but this time only the acetonitrile extraction step was used.

* QuEChERS Extraction Salts kit: Restek Q-sep™ AOAC2007.01

(1) Homogenize 100 g sample (chicken, pork, salmon, shrimp) in food processor
(2) Weigh out 10 g homogenized sample, transfer to 50 mL test tube
(3) Add 5 mL water, shake gently by hand
(4) Add acetonitrile containing 1 % acetic acid and QuEChERS salts*, shake by hand (1 min)
(5) Centrifuge separation (3 min)
(6) Collect acetonitrile layer and filter
(7) LC/MS/MS analysis
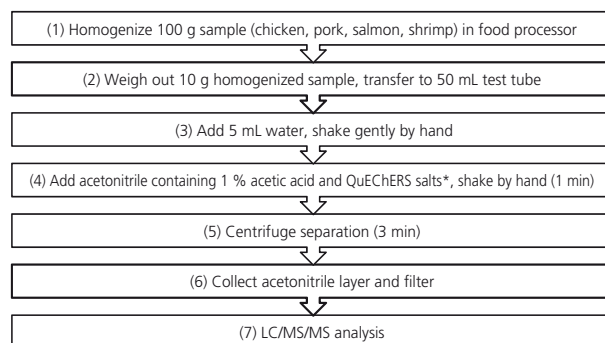
Fig. 1 Sample Preparation Procedure

■ Improved Peak Shape Using Sample / Water Co-Injection

When conducting reversed phase chromatography, the peaks of polar compounds may split or collapse depending on the relationship between the sample solvent and mobile phase. In cases where the sample solvent is rich in organic solvent, the elution strength must be lowered (by substitution or dilution) with the addition of water. As the pretreated sample solvent in this analysis consists of 100 % acetonitrile, injection in that state into the LC/MS will result in split peaks for some of the substances (Fig. 2 left).

To eliminate as much of the time and effort typically associated with sample preparation, the pretreatment features of the autosampler (SIL-30A) were utilized to conduct co-injection of sample and water, which resulted in improved peak shapes.

Draw Sample   Draw Air   Draw Water   Inject

Diaveridine

7:261.15>123.10 (+)   7:261.15>123.10 (+)

2.0 2.5 3.0 3.5   2.0 2.5 3.0 3.5

Difloxacin

26:400.10>356.20 (+)   26:400.10>356.20 (+)

2.5 3.0 3.5 4.0   2.5 3.0 3.5 4.0

Sample 2 µL   Sample 2 µL
                       + Water 10 µL

Note: Sample solvent: **100 % Acetonitrile**

Fig. 2 Comparison of Peak Shape

■ MRM Analysis of Matrix Standards

Fig. 3 shows the MRM chromatogram of the matrix standard solution consisting of the sample solution with added standard solution (data obtained using pork extract solution). Table 1 shows the lower limits of quantitation for the standard solution without added matrix and with added matrix, respectively. In a crude extract obtained by acetonitrile extraction alone, sensitivity was comparable to that obtained for most of

the compounds using only standard solution. Although there were several compounds for which the lower limit of quantitation was different in the standard solution than the matrix-added solution, rather than attributing this to matrix effects, it is thought to be caused by elevated background due to ions derived from contaminating components (Refer to Fig. 5).
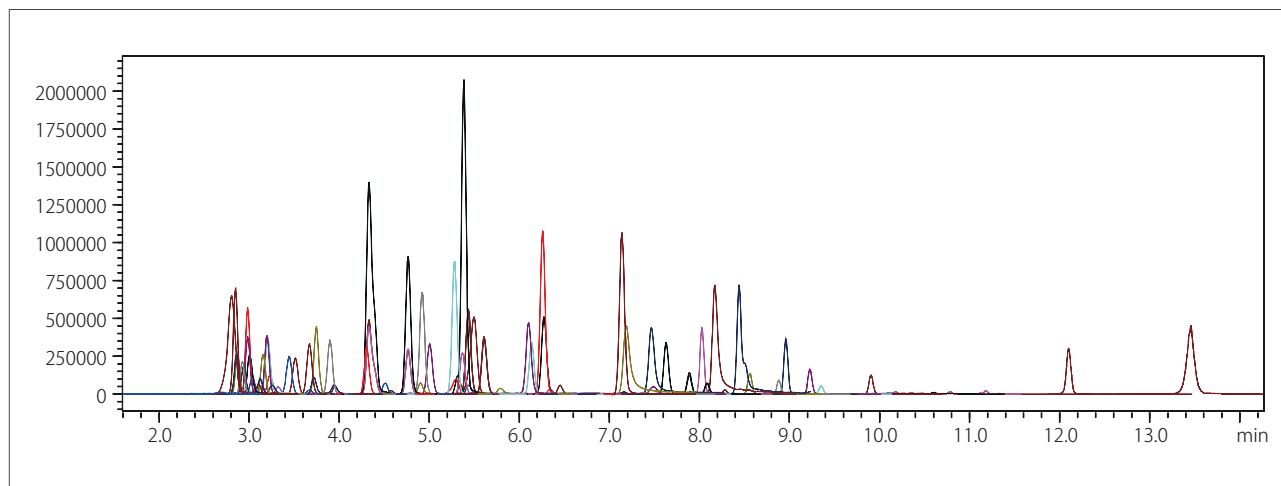
Fig. 3 MRM Chromatograms of 89 Veterinary Drugs (10 μg/L pork extract solution with added standard solution)

Table 1 LOQs of Veterinary Drugs in Neat Standards and Matrix Standards and Calibration Range of Veterinary Drugs in Matrix Standards

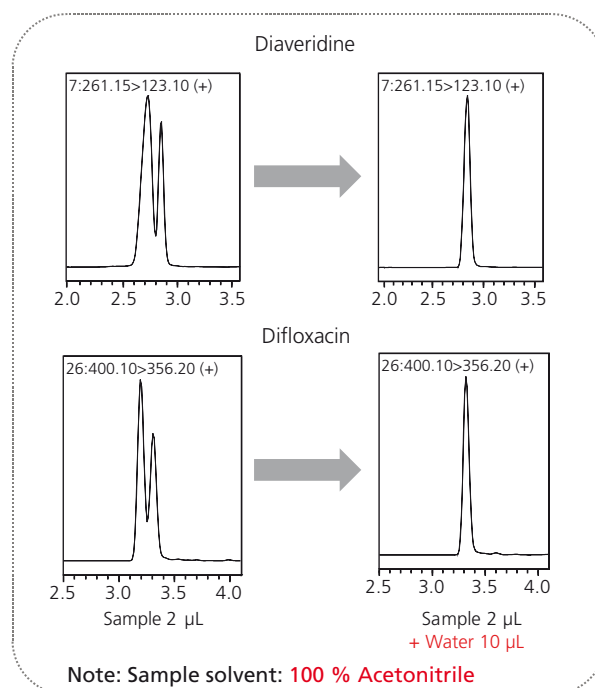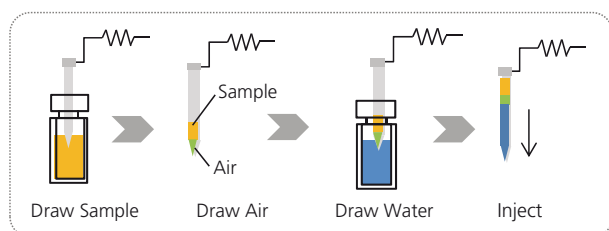|	Std. Solution	Matrix-Added Std. Solution			Std. Solution	Matrix-Added Std. Solution	
	Min. Conc.	Min. Conc.	Max. Conc.		Min. Conc.	Min. Conc.	Max. Conc.
Gentamicin	0.5	1	50	Sulfachloropyridazine	0.02	0.02	20
Sulfanilamide	1	1	50	Sulfadimethoxine	0.02	0.02	10
Levamisole	0.05	0.05	50	Tylosin	0.05	0.05	50
Lincomycin	0.01	0.01	10	Sulfamethoxazole	0.02	0.1	10
5-Propylsulfonyl-1-benzimidazole-2-amine	0.05	0.05	10	Sulfaethoxypyridazine	0.02	0.02	10
				Tiamulin	0.01	0.01	50
Diaveridine	0.01	0.01	10	Florfenicol	0.5	10	50
Trimethoprim	0.02	0.02	20	2Acetylamino 5nitrothiazole	0.05	0.05	50
Marbofloxacin	0.01	0.01	50	Sulfatroxazole	0.01	0.01	5
Sulfisomidine	0.02	0.02	20	Leucomycin	0.01	0.01	50
Norfloxacin	0.5	0.5	50	Sulfisoxazole	0.01	0.05	50
Ormetoprim	0.02	0.02	10	Oxolinic acid	0.01	0.1	50
Thiabendazole	0.01	0.01	10	Chloramphenicol	0.5	1	50
Ciprofloxacin	0.05	0.5	10	Clorsulon	0.5	1	50
Neospiramycin I	0.01	0.05	10	Sulfabenzamide	0.01	0.01	10
Danofloxacin	0.1	0.1	10	Ethopabate	0.01	0.01	10
Enrofloxacin	0.05	0.1	50	Sulfadoxine	0.02	0.02	20
Oxytetracycline	0.01	0.1	50	Sulfaquinoxaline	0.02	0.02	10
Xylazine	0.01	0.01	10	Prednisolone	0.1	0.05	20
Orbifloxacin	0.05	0.05	50	Ofloxacin	0.5	0.5	50
Sulfacetamide	1	1	50	Flubendazole	0.01	0.01	50
Clenbuterol	0.01	0.01	10	Methylprednisolone	0.5	0.5	50
Tetracycline	0.05	0.01	50	Nalidixic acid	0.01	0.01	50
Spiramycin I	0.01	0.01	50	Dexamethasone	0.5	0.5	50
Sarafloxacin	0.5	0.5	50	Flumequine	0.01	0.01	50
Difloxacin	0.05	0.1	50	Benzylpenicillin	0.5	0.5	50
Sulfadiazine	0.02	0.1	20	Sulfanitran	0.2	0.2	50
Sulfathiazole	0.02	0.1	20	Sulfabromomethazine	0.01	0.01	50
Sulfapyridine	0.02	0.1	20	betaTrenbolone	0.02	0.1	50
Carbadox	0.05	0.05	10	Emamectin B1a	0.01	0.01	50
Pyrimethamine	0.02	0.02	20	alphaTrenbolone	0.02	0.1	50
Sulfamerazine	0.02	0.02	20	Piromidic acid	0.01	0.05	50
Chlortetracycline	0.1	0.1	50	Zeranol	1	0.1	50
Tilmicosin	0.1	0.1	50	Ketoprofen	0.01	0.05	50
Thiamphenicol	1	1	50	Testosterone	0.01	0.05	10
Sulfadimidine	0.02	0.02	20	Famphur	0.05	0.05	50
Sulfametoxydiazine	0.01	0.02	10	Fenobucarb (BPMC)	0.01	0.01	50
Sulfamethoxypyridazine	0.02	0.02	20	Clostebol	0.05	0.05	50
Sulfisozole	0.01	0.01	50	Dichlofenac	0.01	0.01	50
Trichlorfon (DEP)	0.05	0.05	50	Melengestrol Acetate	0.05	0.05	50
Sulfamonomethoxine	0.02	0.02	20	Temephos (Abate)	0.01	0.5	50
Furazolidone	1	1	50	Allethrin	0.1	1	50
Difurazone	0.05	0.05	50	Closantel	0.01	0.01	10
Erythromycin A	0.01	0.01	50	Monensin	0.01	0.01	10
Cefazolin	0.5	0.5	50				

(Unit: μg/L)
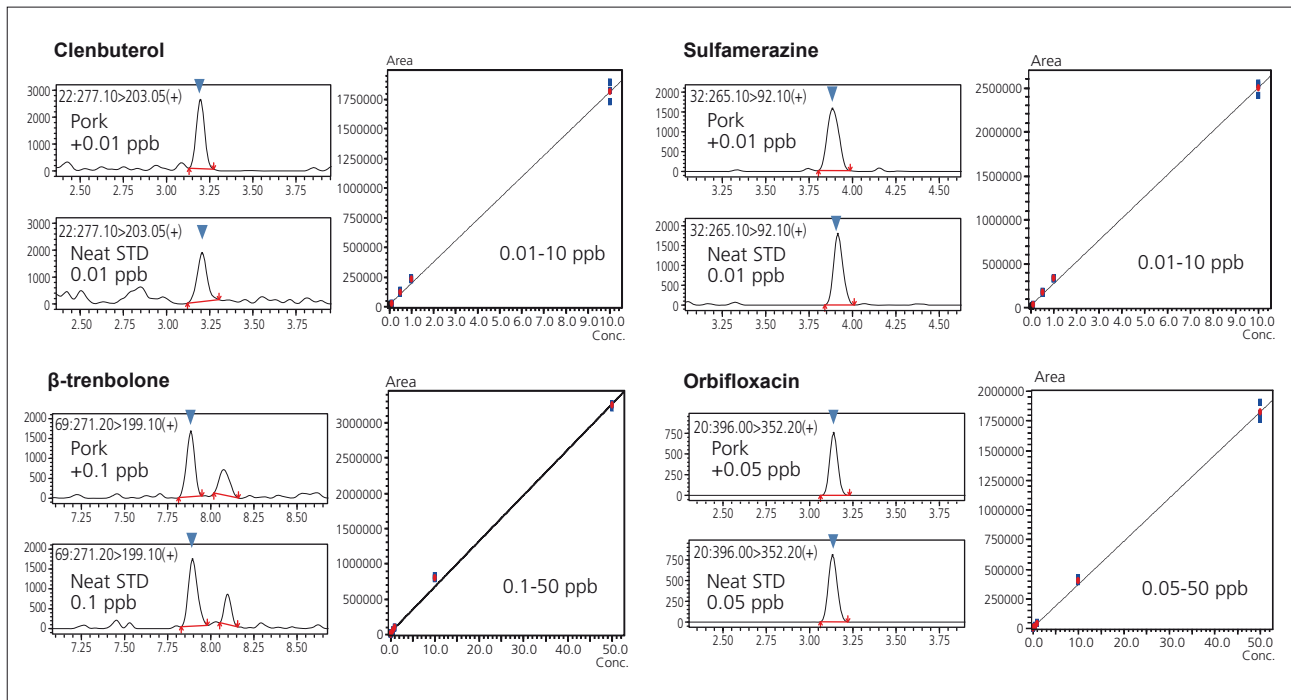
Fig. 4 MRM Chromatograms in the Vicinity of the LOQ and Calibration Curves of Typical Compounds

■ **Recoveries of Veterinary Drugs in Crude Extracts from Livestock and Fishery Products (Matrix Effect Verification)**

We examined whether or not the matrix affected measurement of actual samples. This time, four types of food product samples were used, including shrimp, chicken meat, pork, and salmon. Standard solution was added to the acetonitrile extraction solution of each of these to obtain a final concentration of 10 µg/L, after which the rates of recovery were determined. The results indicated that 90 % of the compounds were recovered at rates of 70 to 120 % and measurement was accomplished without any adverse matrix effects even though the crude extract solution was subjected only to acetonitrile extraction.
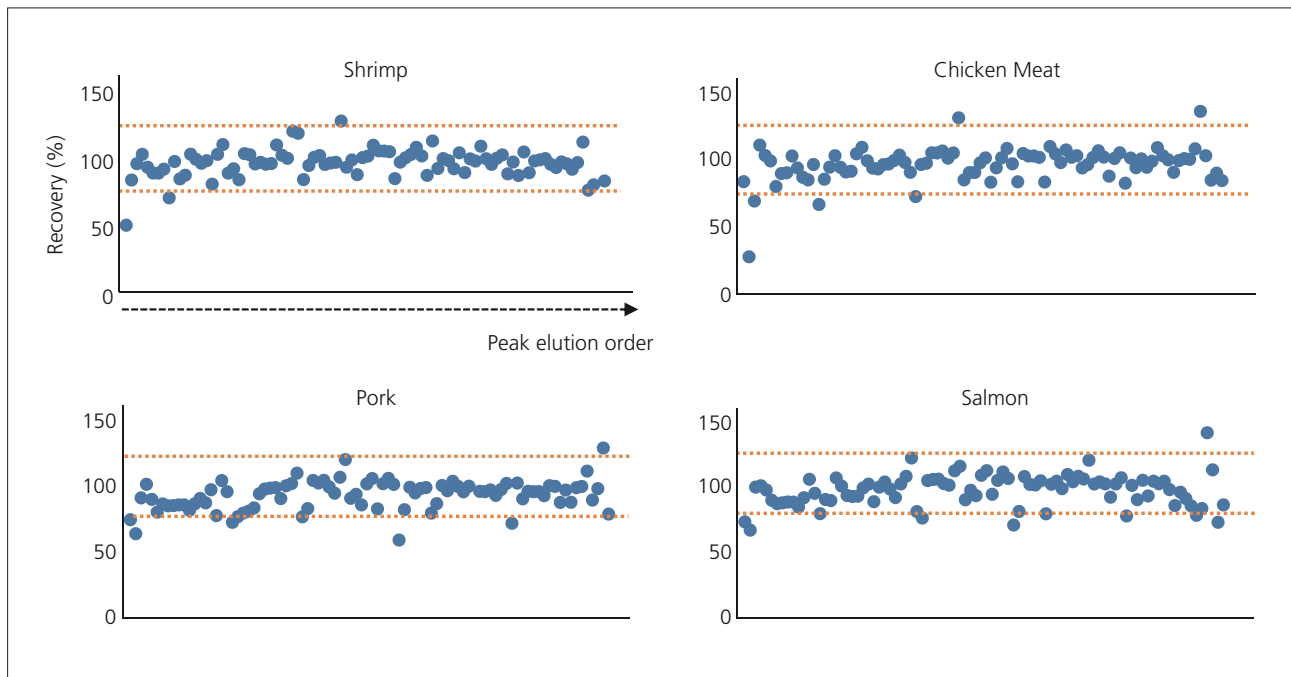
Fig. 5 Recoveries of Veterinary Drugs in Each of the Matrices

■ Acetonitrile Extraction Efficiency Using QuEChERS Method

To check the efficiency of acetonitrile extraction by the QuEChERS method, standard solution was added at stage (2) of Fig. 1 to obtain a concentration of 10 µg/L, and the recoveries were determined. Good recoveries of approximately 80 % were obtained in cases both with and without the addition of matrix. However, relatively poor recoveries were seen for highly polar compounds such as tetracycline and quinolone. For these compounds, it is necessary to examine the use of a separate extraction solvent and extraction reagent.

Table 2 Recoveries (Pre-Spike)

Recovery	Without Matrix	With Matrix (Pork)	Compounds with Poor Recovery
< 50 %	17 (19 %)	13 (15 %)	Tetracyclines Quinolones
50 % - 70 %	1 (1 %)	8 (9 %)	
> 70 %	71 (80 %)	68 (76 %)	

■ Robustness

We checked the long-term stability of the instrument using a solution of pork crude extract (spiked with 10 µg/L standard solution). Even after continuous measurement of an extremely complex matrix over a period of 3 days, we were able to obtain stable data.

Compounds	%RSD (%) (n=220)
Sulfaquinoxaline	1.5
Sulfamethoxazole	2.8
Ketoprofen	2.3
β - trenbolone	3.2
Teststerone	3.5
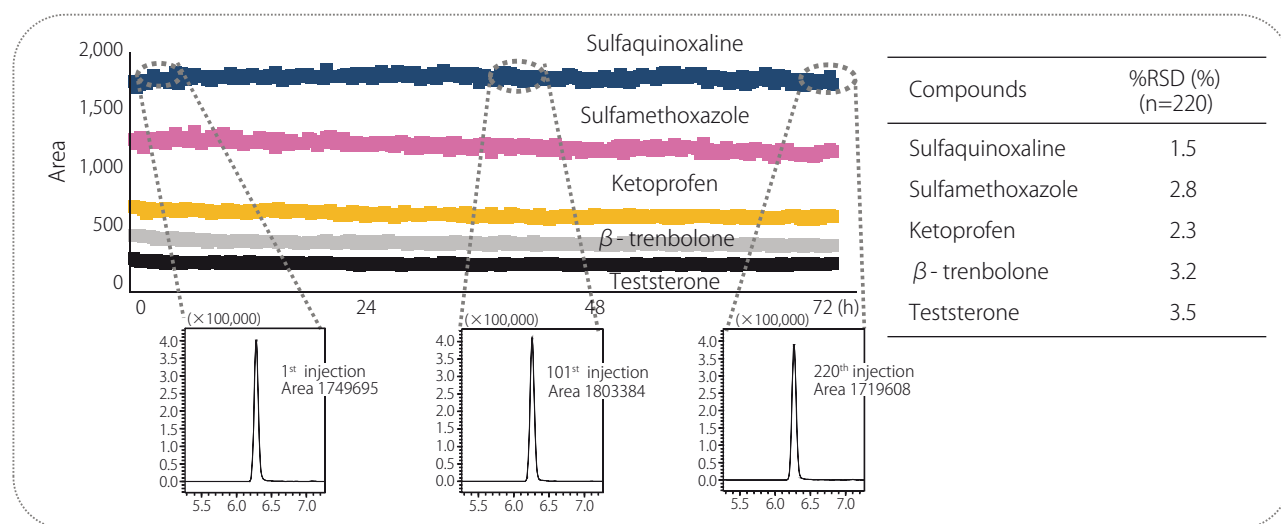
Fig. 6 Area Plot and %RSD of Typical Compounds with Continuous Analysis

Table 3 Analytical Conditions

Column	: Shim-pack XR-ODS II (75 mm × 2.0 mm I.D., 2.2 µm)
Mobile Phase A	: 0.1 % Formic Acid - Water
Mobile Phase B	: Acetonitrile
Time Program	: 1 %B (0 min) → 15 %B (1 min) → 40 %B (6 min) → 100 %B (10-13 min) → 1 %B (13.01-16 min)
Flowrate	: 0.2 mL/min.
Injection Volume	: 2 µL (2 µL sample solution + 10 µL water)
Oven Temperature	: 40 °C
Ionization Mode	: ESI (Positive / Negative)
Probe Voltage	: +2.0 kV / -1.0 kV
Neburizing Gas Flow	: 3.0 L/min.
Drying Gas Flow	: 10.0 L/min.
Heating Gas Flow	: 10.0 L/min.
Interface Temperature	: 400 °C
DL Temperature	: 200 °C
Block Heater Temperature	: 400 °C

SHIMADZU

Shimadzu Corporation

www.shimadzu.com/an/

Application News

No. SCA_210_013

Highly sensitive and rapid simultaneous method for 45 mycotoxines in baby food samples by HPLC-MS/MS using fast polarity switching

1. Introduction

Mycotoxins are toxic metabolites produced by fungal molds on food crops. For consumer food safety, quality control of food and beverages has to assay such contaminants. Depending on the potency of the mycotoxin and the use of the food, the maximum allowed level is defined by legislation. Baby food is particularly critical. For example, European Commission has fixed the maximum level of Aflatoxin B1 and M1 to 0.1 and 0.025 µg/kg, respectively, in baby food or milk.
Therefore, a sensitive method to assay mycotoxins in complex matrices is mandatory. In order to ensure productivity of laboratory performing such assays, a unique rapid method able to measure as much mycotoxins as possible independently of the sample origin is also needed.
In this study, we tested three kind of samples: baby milk powder, milk thickening cereals (flour, rice and tapioca) and a vegetable puree mixed with cereals.

2. Materials and Methods

2-1. Sample preparation
Sample preparation was performed by homogenization followed by solid phase extraction using specific cartridges (Isolute® Myco, Biotage, Sweden) covering a large spectrum of mycotoxins.
Sample (5 g) was mixed with 20 mL of water/acetonitrile (1/1 v/v), sonicated for 5 min and agitated for 30 min at room temperature. After centrifugation at 3000 g for 10 min, the supernatant was diluted with water (1/4 v/v). Columns (60 mg/3 mL) were conditioned with 2 mL of acetonitrile then 2 mL of water. 3 mL of the diluted supernatant were loaded at the lowest possible flow rate. Then column was washed with 3 mL of water followed by 3 mL of water/acetonitrile (9/1 v/v). After drying, compounds were successively eluted with 2 mL of acetonitrile with 0.1% of formic acid and 2 mL of methanol.
The eluate was evaporated under nitrogen flow at 35 ºC until complete drying (Turbovap, Biotage, Sweden).
The sample was reconstituted in 150 µL of a mixture of water/methanol/acetonitrile 80/10/10 v/v with 0.1% of formic acid.

2-2. LC-MS/MS analysis
Extracts were analysed on a Nexera X2 (Shimadzu, Japan) UHPLC system coupled to a triple quadrupole mass spectrometer (LCMS-8050, Shimadzu, Japan). Analysis was carried out using selected reaction monitoring acquiring 2 transitions for each compound.

Table 1 – LC conditions

Analytical column	Shimadzu GLC Mastro™ C18 150x2.1 mm 3 µm
Mobile phase	A = Water 2mM ammonium acetate and 0.5% acetic acid B = Methanol/Isopropanol 1/1 + 2mM ammonium acetate and 0.5% acetic acid
Gradient	2%B (0.0 min), 10%B (0.01 min), 55%B (3.0 min), 80%B (7.0 -8.0 min), 2%B (8.01 min), Stop (11.0 min)
Column temperature	50 °C
Injection volume	10 µL
Flow rate	0.4 mL/min

Table 2 – MS/MS conditions

| Ionization mode	Heated ESI (+/-)
Temperatures	HESI: 400 ºC Desolvation line: 250 ºC Heat block: 300 ºC
Gas flows	Nebulizing gas (N2): 2 L/min Heating gas (Air): 15 L/min Drying gas (N2): 5 L/min
CID gas pressure	270 kPa (Ar)
Polarity switching time	5 ms
Pause time	1 ms
Dwell time	6 to 62 ms depending on the number of concomitant transitions to ensure a minimum of 30 points per peak in a maximum loop time of 200 ms (including pause time and polarity switching)

Table 3 – MRM transitions

Name	Ret. Time (min)	MRM Quan	MRM Qual
15-acetyldeoxynivalenol (15ADON) [M+H]+	3.37	339 > 297.1	339 > 261
3-acetyldeoxynivalenol (3ADON) [M+H]+	3.37	339 > 231.1	339 > 231.1
Aflatoxine B1 (AFB1) [M+H]+	3.78	312.6 > 284.9	312.6 > 240.9
Aflatoxine B2 (AFB2) [M+H]+	3.57	315.1 > 259	315.1 > 286.9
Aflatoxine G1 (AFG1) [M+H]+	3.46	329.1 > 242.9	329.1 > 199.9
Aflatoxine G2 (AFG2) [M+H]+	3.26	330.9 > 244.9	330.9 > 313.1
Aflatoxine M1 (AFM1) [M+H]+	3.30	329.1 > 273	329.1 > 229
Altemariol [M-H]-	4.78	257 > 214.9	257 > 213.1
Altemariol monomethylether [M-H]-	5.81	271.1 > 255.9	271.1 > 228
Beauvericin (BEA) [M+H]+	8.03	784 > 244.1	784 > 262
Citrinin (CIT) [M+H]+	4.16	251.3 > 233.1	251.3 > 205.1
D5-OTA (ISTD)	5.22	409.2 > 239.1	N/A
Deepoxy-Deoxynivaletenol (DOM-1) [M-H]-	3.02	279.2 > 249.3	279.2 > 178.4
Deoxynivaletenol (DON) [M-CH3COO]-	2.61	355.3 > 295.2	355.3 > 265.1
Deoxynivaletenol 3-Glucoside (D3G) [M-CH3COO]-	2.45	517.5 > 457.1	517.5 > 427.1
Deoxynivaletenol 3-Glucoside (D3G) [M-CH3COO]-	2.45	517.5 > 457.1	517.5 > 427.1
Diacetoxyscirpenol (DAS) [M+NH4]+	1.2	384 > 283.3	384 > 343
Enniatin A (ENN A) [M+H]+	8.51	699.2 > 682.2	699.2 > 210
Enniatin A1 (ENN A1) [M+H]+	8.22	685.3 > 668.3	685.3 > 210.1
Enniatin B (ENN B) [M+H]+	7.57	657 > 640.4	657 > 195.9
Enniatin B1 (ENN B1) [M+H]+	7.92	671.2 > 654.2	671.2 > 196
Fumagillin (FUM) [M+H]+	6.16	459.2 > 131.1	459.2 > 338.7
Fumonisine B1 (FB1) [M+H]+	4.10	722.1 > 334.2	722.1 > 352.2
Fumonisine B2 (FB2) [M+H]+	4.71	706.2 > 336.3	706.2 > 318.1
Fumonisine B3	4.38	706.2 > 336.2	706.2 > 688.1
Fusarenone-X (FUS-X) [M+H]+	2.84	355.1 > 247	355.1 > 175
HT2 Toxin [M+NA]+	4.58	446.9 > 344.9	446.9 > 285
Moniliformin (MON) [M-H]-	1.16	97.2 > 40.9	N/A
Neosolaniol (NEO) [M+NH4]+	2.90	400.2 > 215	400.2 > 185
Nivalenol (NIV) [M+CH3COO]-	2.41	371.2 > 280.9	371.2 > 311.1
Ochtratoxin A (OTA) [M+H]+	5.53	404.2 > 239	404.2 > 358.1
Ochtratoxin B (OTB) [M+H]+	4.83	370.2 > 205.1	370.2 > 187
Patulin (PAT) [M-H]-	2.35	153 > 81.2	153 > 53
Sterigmatocystin [M+H]+	5.60	325.3 > 310	325.3 > 281.1
T2 Tetraol [M+CH3COO]-	1.64	356.8 > 297.1	356.8 > 59.1
T2 Toxin [M+NH4]+	4.94	484.2 > 215	484.2 > 305
Tentoxin [M-H]-	4.77	413.1 > 140.9	413.1 > 271.1
Tenuazonic acid (TEN) [M-H]-	4.51	196.1 > 138.8	196.1 > 112
Wortmannin (M-H)	3.95	426.9 > 384	426.9 > 282.1
Zearalanol (alpha) (ZANOL) [M-H]-	5.17	321.3 > 277.2	321.3 > 303.2
Zearalanol (beta) (ZANOL) [M-H]-	4.85	321.3 > 277.2	321.3 > 303.1
Zearalanone (ZOAN) [M-H]-	5.43	319 > 275.1	319 > 301.1
Zearalenol (alpha) (ZENOL) [M-H]-	5.25	319.2 > 275.2	319.2 > 160.1
Zearalenol (beta) (ZENOL) [M-H]-	4.94	319.2 > 275.2	319.2 > 160.1
Zearalenone (ZON) [M-H]-	5.52	316.8 > 174.9	316.8 > 131.1

3. Results and discussion

3-1. Method development
LC conditions were transferred from a previously described method (Tamura et al., Poster TP-739, 61st ASMS). In particularly, the column was chosen to provide very good peak shape for chelating compounds like fumonisins thanks to its inner PEEK lining. Small adjustments in the mobile phase and in the gradient program were made to handle more mycotoxins, especially the isobaric ones. These modifications are reported in the Table 1.
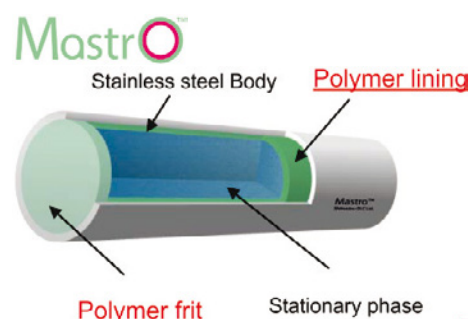
Figure 1 – Structure of the Mastro™ column

Also, autosampler rinsing conditions were kept to ensure carry-over minimisation of some difficult compounds.
Electrospray parameters (gas flows and temperatures) were cautiously optimized to find the optimal combination for the most critical mycotoxins (aflatoxins). Since these parameters act in a synergistic way, a factorial design experiment is needed to find it. Manually testing all combinations in the chromatographic conditions is very time consuming. Therefore, new assistant software (Interface Setting Support) was used to generate all possible combinations and generate a rational batch analysis. Optimal combination was found in chromatographic conditions. The difference observed between optimum and default or worst parameters was of 200 and 350%, respectively.
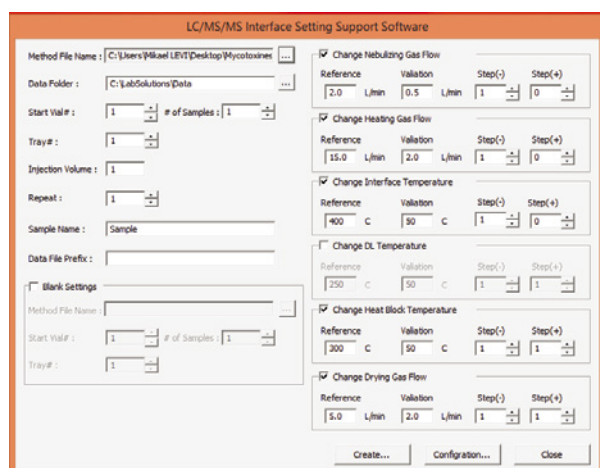
Figure 2 – Parameters selection view in the Interface Setting Support Software

3-3 Results

Extraction and ionisation recovery for aflatoxins was measured in the three matrices by comparing peak areas of the raw sample extract to extract spiked at 50 ppb after or before extraction and to standard solution. Results in table 4 showed that the total recovery was quite acceptable to ensure accurate quantification. Results from other matrices were not significantly different.

Table 4 – Extraction and ionisation recoveries in puree

	AFB1	AFB2	AFG1	AFG2	AFM1
Extraction recovery	101%	109%	104%	114%	118%
Ionisation recovery	49%	90%	96%	106%	91%
Total recovery	49%	98%	100%	121%	108%

Repeatability was evaluated at low level for aflatoxins. Figure 3 show an overlaid chromatogram (n=4) for aflatoxins.
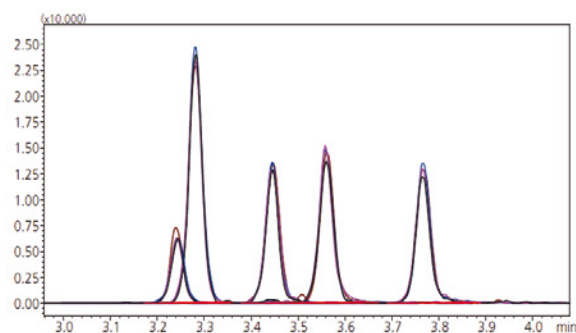
Figure 3 – Chromatogram of Aflatoxines at 0.1 ppb in milk thickening cereals
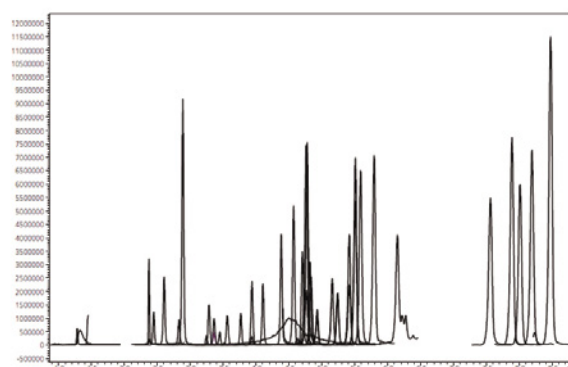
Figure 4 – Chromatogram of the 45 mycotoxins in standard at 50 ppb (2 ppb for aflatoxins and ochratoxines)

4. Conclusion

- A very sensitive method for multiple mycotoxines was set up to ensure low LOQ in baby food sample

- Thanks to high speed polarity switching, a high number of mycotoxines can be assayed using the same method in a short time

- The extraction method demonstrate good recoveries to ensure accurate quantification

SHIMADZU

Shimadzu Europa GmbH
www.shimadzu.eu

Simultaneous quantitative analysis of 20 amino acids in food samples without derivatization using LC-MS/MS

Keiko Matsumoto; Jun Watanabe (Shimadzu Corporation, Kyoto, Japan) Itaru Yazawa (Imtakt Corporation, Kyoto, Japan)

1. Introduction

In order to detect many kinds of amino acids with high selectivity in food samples, the LC/MS analysis have been used widely. Amino acids are high polar compounds, so they are hard to be retained to reverse-phased columns such as ODS (typical method in LC/MS analysis). It needs their derivartization or addition of ion pair reagent in mobile phase to retain them. For easier analysis of amino acids, it is expected to develop the method without using reagents mentioned above.

This time, we tried to develop a simultaneous high sensitive analysis method of 20 amino acids by LC/MS/MS with mix-mode column (ion exchange, normal-phase) and the typical volatile mobile phase suitable for LC/MS analysis.

2. Methods and Materials

Amino acid standard reagents and food samples were purchased from the market. Standards of 20 kinds of amino acids were optimized on each compound-dependent parameter and MRM transition.

As an LC-MS/MS system, HPLC was coupled to triple quadrupole mass spectrometer (Nexera with LCMS-8050, Shimadzu Corporation, Kyoto, Japan). Sample was eluted with a binary gradient system and LC-MS/MS with electrospray ionization was operated in multi-reaction-monitoring (MRM) mode

> **High Speed Mass Spectrometer**
>
> **UF-MRM**
> High-Speed MRM at 555 ch/sec
>
> **UF-Switching**
> High-Speed Polarity Switching 5 msec

Figure 1 - LCMS-8050 triple quadrupole mass spectrometer

3. Result

3-1. Method development

First, MRM method of 20 amino acids was optimized. As a result, all compounds were able to be detected highly sensitive and were detected in positive MRM transitions. As the setting temperature of ESI heating gas was found to have an effect on the sensitivity of amino acids, it was also optimized. Even though amino acids were not derivatized and ion-pairing reagent wasn't used, 20 amino acids were retained by using a mixed-mode stationary phase and separated excellently on the below-mentioned condition.

HPLC conditions (Nexera system)

Column: Intrada Amino Acid (3.0 mm, I.D. 50 mm, 3 μm, Imtakt Corporation, Kyoto, Japan)

In this study, two conditions of mobile phase were investigated. It was found that 20 amino acids were separated with higher resolution in case 2.

Mobile phase:

Case 1

A: Acetonitrile/Formic acid = 100/0.1
B: 100 mM Ammonium formate

Time program: B conc. 14% (0-3 min) - 100% (10 min) - 14% (10.01-15 min)

Case 2 (High Resolution condition)

A: Acetonitrile/Tetrahydrofuran 25 mM Ammonium formate/Formic acid = 9/75/16/0.3
B: 100 mM Ammonium formate/Acetonitrile = 80/20

Time program: B conc. 0 % (0-2 min) -5 % (3 min) – 30 % (6.5 min) – 100 % (12 min) – 0 % (12.01 – 17 min)

Flow rate   0.6 mL/min,
Injection volume: 2 μL
Column temperature: 40 °C

MS conditions (LCMS-8050)
Ionization: ESI, positive MRM mode
MRM transitions are shown in Table 1

Case 1
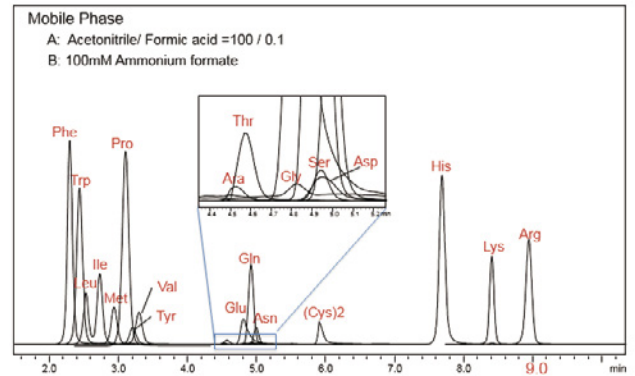
Figure 2 - Mass Chromatograms of 20 Amino acids
(concentration of each compound: 10 nmol/mL)

Case 2 (High Resolution condition)
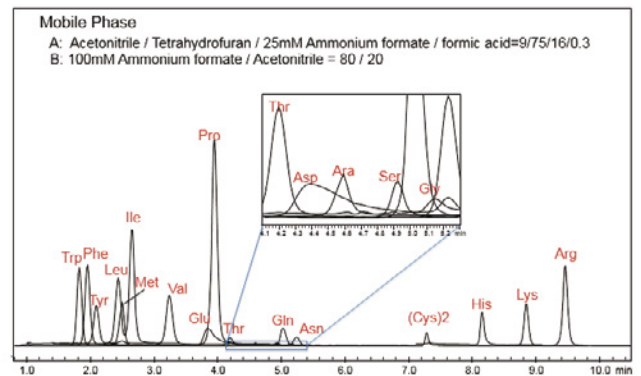
Figure 3 - Mass Chromatograms of 20 Amino acids
(concentration each compound: 10 nmol/mL)

As the mobile phase condition of case 1 is simpler and the result of case 1 was sufficiently well, case 1 analytical condition were used for quantitative analysis. The dilution series of these compounds were analyzed. All amino acids were detected with good linearity and repeatability (Table1).

Table1 Linearity and Repeatability of 20 amino acids

	MRM Transition	Linearity		Repeatability*
		Range (nmol/mL)	Coefficient (r2)	%RSD
Trp	205.10>188.10	0.01-100	0.9950	1.4
Phe	166.10>120.10	0.01-100	0.9971	1.2
Tyr	182.10>136.00	0.05-100	0.9900	1.7
Met	150.10>56.10	0.05-200	0.9963	0.1
Lue,Lle	132.10>86.15	0.01-100	0.9955	0.7
Val	118.10>72.05	0.05-100	0.9991	1.9
Glu	148.10>84.10	0.05-10	0.9965	4.5
Pro	116.10>70.10	0.01-50	0.9933	1.5
Asp	134.20>74.10	0.5-500	0.9953	1.4
Thr	120.10>74.00	0.1-50	0.9923	4.5
Ala	90.10>44.10	0.5-500	0.9989	16.2
Ser	106.10>60.20	0.5-500	0.9988	6.5
Gln	147.10>84.10	0.05-1	0.9959	3.9
Gly	76.20>29.90	5-200	0.9974	11.0
Asn	133.10>74.05	0.05-20	0.9939	6.1
(Cys)2	241.00>151.95	0.05-20	0.9909	2.3
His	156.10>110.10	0.05-200	0.9983	1.7
Lys	147.10>84.10	0.05-5	0.9908	0.9
Arg	175.10>70.10	0.01-100	0.9956	0.5

*@ 0.5nmol/mL : except for Gly, 5nmol/mL : for Gly

3-2. The analysis of 20 amino acids in food samples

The analysis of the amino acids contained in sports beverage on the market was carried out. In the case of sports beverage, all amino acids written in the package were detected.
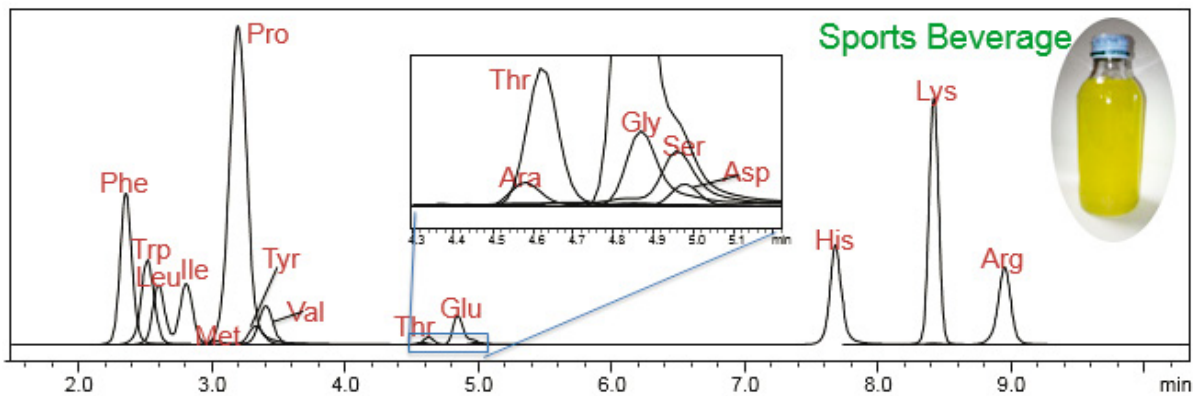
Figure 4 - Mass Chromatograms of Sports Beverages (100 fold dilution with 0.1 N HCl)

Furthermore, Japanese Sake, Beer and sweet cooking rice wine (Mirin) were analyzed using this method. Japanese Sake and Beer were diluted with 0.1N HCl. Sweet cooking rice wine was diluted in the same way after a deproteini- zing preparation. These were filtered through a 0.2 µm filter and then analyzed. MRM chromatograms of each food samples are shown in Figure 5, 6, 7. Amino acids of each sample were detected with high sensitivity.
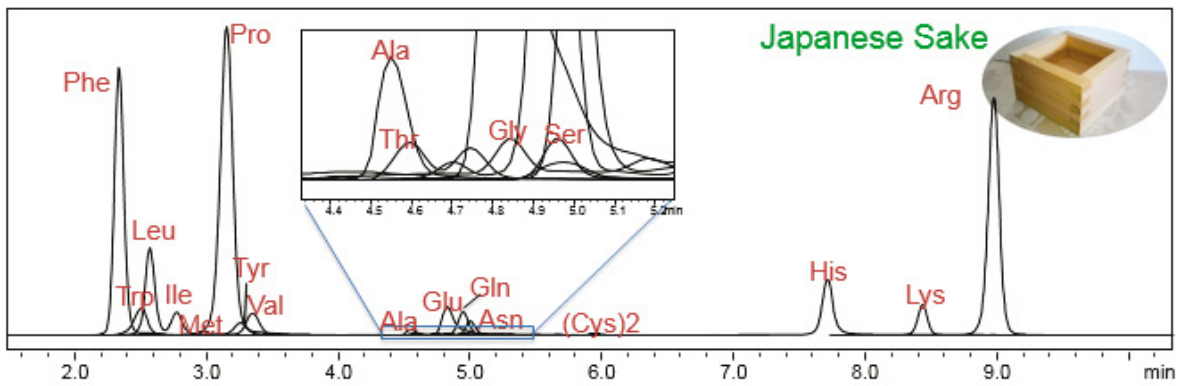
Figure 5 - Mass Chromatograms of Japanese Sake (100 fold dilution with 0.1 N HCl)
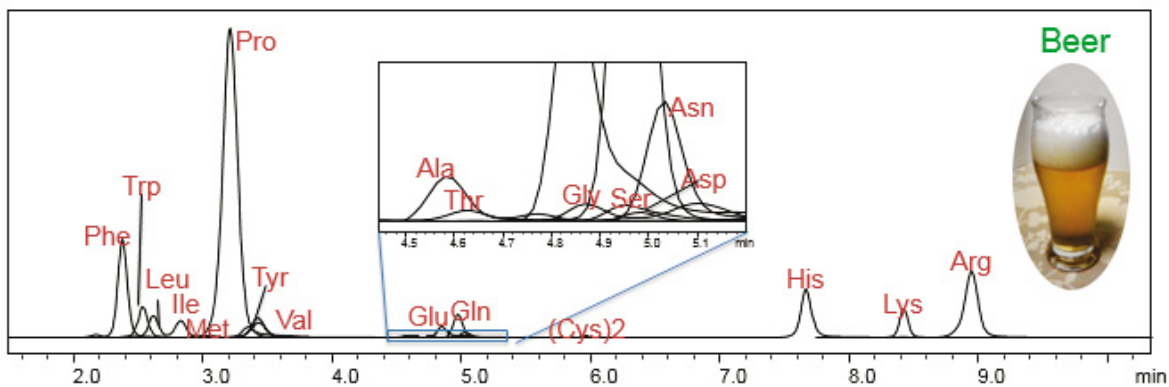
Figure 6 - Mass Chromatograms of Beer (10 fold dilution with 0.1 N HCl)
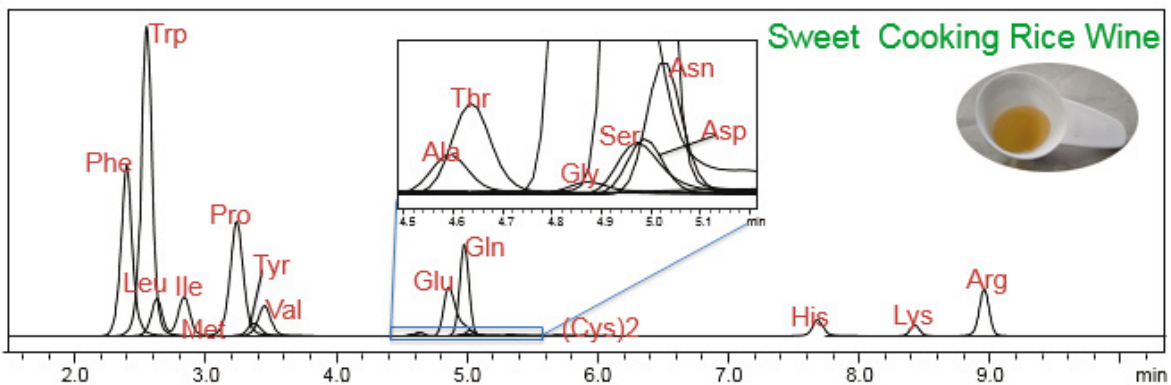
Figure 7 - Mass Chromatograms of Sweet Cooking Rice Wine (100 fold dilution with 0.1 N HCl)

4. Conclusions

- 20 amino acids could be separated without derivatization using a typical volatile mobile phase suitable for LC/MS analysis and detected with high sensitivity.
- This method was able to be applied to the analysis of amino acids in various food samples.

No. SCA_210_015 | Determination of Industrial Dyes in Food by LCMS-IT-TOF

Xiaozhen Chen, Liying Huang, Jin Wang, Hui Cao (Zhejiang Institute of Quality Inspection Science);
Luying Zhou, Jinting Yao, Hengtao Dong, Hongyuan Hao, Taku Tsukamoto, Taohong Huang, Shin-ichi Kawano,
Yuki Hashi (Shimadzu Global COE, Shimadzu (China) Co., Ltd.)

1. Introduction

Industrial dyes is a class of dyes which has been widely used in the production of textile, fur and leather, wood and china, while using them as food additive is forbidden because of potential toxic effects. Industrial dyes illegally added in food were reported frequently, therefore departments like China FDA focused on the determination of industrial dyes in food, and they needed to develop a quick, high sensitivity and high accuracy qualitative and quantitative method. The food samples were extracted by a mixed organic solution, cleaned up on a SPE column, then the extracts were analyzed by LCMS-IT-TOF. In this study, 10 basic industrial dyes and 9 acidic industrial dyes in food were analyzed. External standard method was used for quantitative analysis, and MS^n (n>2) results were used for qualitative analysis.

2. Experimental

Sample pretreatment method:

Basic industrial dyes - The food sample was extracted with acetonitrile, and then skimmed with acetonitrile and hexane. Finally the sample was purified by Oasis WCX column.
Acidic industrial dyes - The food sample was extracted with a mixed solution (methanol/water = 80/20, V/V), and then skimmed with acetonitrile . In the end, the sample was purified by Oasis WAX column. After above three steps, the final extract was injected and detected with LCMS-IT-TOF.

UHPLC/MS parameters:

The analysis was performed on a Prominence UFLC (Shimadzu, Kyoto, Japan) equipped with LC-20AD pumps, a CTO-20A column oven, a SIL-20A autosampler, a DGU-20A$_5$ degasser, a CBM-20A communication bus module and an LCMS-IT-TOF mass spectrometer.

Analytical conditions for UHPLC

Column	:	Shim-pack XR-ODSII (100 mmL. x 2.0 mmi.d., 2.2 µm)
Flow rate	:	0.2 mL/min
Column oven	:	30 ºC
Elution mode	:	Gradient elution
Mobile phase	:	For basic dyes: A: 5 mmol/L ammonium acetate, B: 0.1% formic acid in acetonitrile For acidic dyes: A: 10 mmol/L ammonium acetate, B: methanol

Analytical conditions for MS

Ionization	:	ESI
Polarity	:	basic dyes; positive acidic dyes; negative
Mass range	:	basic dyes *m/z* 250-510 acidic dyes *m/z* 210-700
Nebulizer gas	:	N$_2$ 1.50 L/min;
Drying gas	:	N$_2$ 10 L/min;
CDL temperature	:	200 ºC
Heat block temperature	:	200 °C
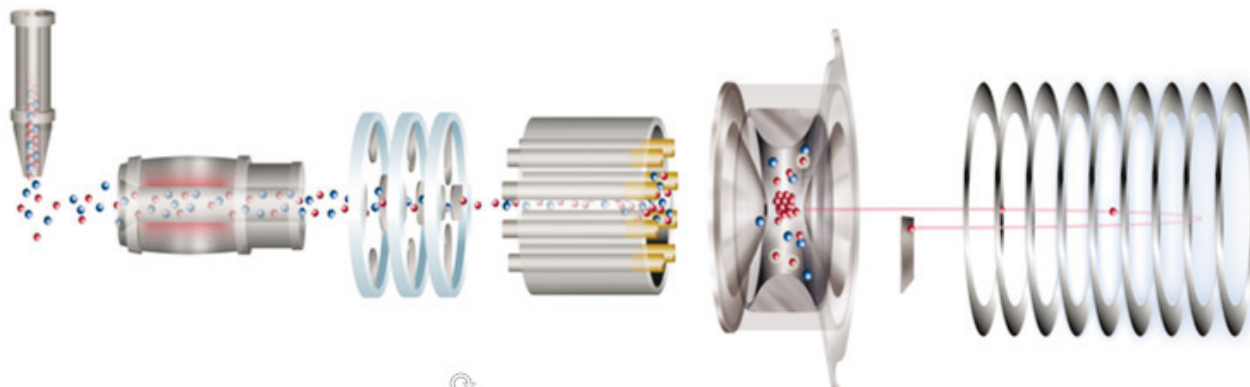
Figure 1 - Schematic diagram of the LCMS-IT-TOF

3. Results and Discussion
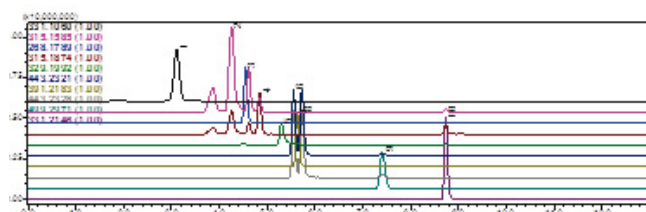
Figure 2 Mass chromatograms of 10 basic dyes
(1. Rhodamine 110, 2. Basic red 2, 3. Auramine O, 4. Astrazon Orange G, 5. Malachite Green, 6. Rhodamine B, 7. Astrazon Orange R, 8. Rhodamine 6G, 9. Butyl Rhodamine B, 10. Leucomalachite Green)
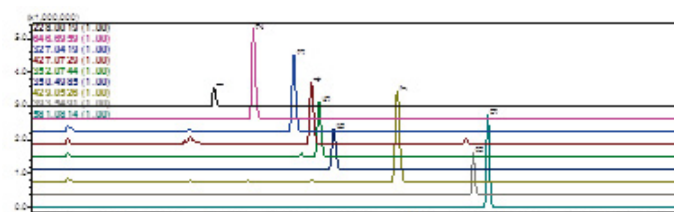
Figure 3 Mass chromatograms of 9 acidic dyes
(1. Azorubin, 2. Acid Red 87, 3. Orange 2, 4. Acid Yellow A4-R, 5. Acid Yellow 36, 6. Tracid Brilliant Red B, 7. Orange 3, 8. Tracid Brilliant Red10B, 9. Acid Orange 67)

No.	Basic Dyes	R.T. (min)	m/z	Linear Equation	Linear Range (μg/L)	Correlation coefficient (r)	RSD/% (n=7)
1	Rhodamine 110	3.034	331.1060	Y = 726481.7X + 3355202	1-100	0.9944	5.0
2	Basic red 2	4.147	315.1585	Y = 939612.0X + 6832046	1-100	0.9924	2.9
3	Auramine O	4.55	268.1789	Y = 478763.8X + 2212455	1-100	0.9954	4.4
4	Astrazon Orange G	4.867	315.1874	Y = 416215.4X + 1143541	1-100	0.9988	3.8
5	Malachite Green	5.386	329.1992	Y = 351826.8X + 408018.1	1-100	0.9989	4.1
6	Rhodamine B	5.669	443.2321	Y = 519311.1X + 3287386	1-100	0.9935	3.1
7	Astrazon Orange R	5.76	391.2183	Y = 432170.3X + 2682160	1-100	0.9931	2.5
8	Rhodamine 6G	5.801	443.2328	Y = 551295.2X + 3627538	1-100	0.9932	2.9
9	Butyl Rhodamine B	8.069	499.2971	Y = 608686.3X + 3178368	1-100	0.9944	8.5
10	Leucomalachite Green	8.827	331.2146	Y = 570237.4X + 4472225	1-100	0.9915	4.6

Table 1 Quantitative result of basic dyes

No.	Acidic Dyes	Matrix	R.T. (min)	m/z	Linear Equation	Linear Range (mg/L)	correlation coefficient (r)	RSD/% (n=7)
1	Acid Red 87	Condiment	5.755	646.6959	Y = 18712.66X - 2188798	0.1-4	0.9960	4.4
2	Acid Yellow 36	Condiment	7.465	352.0744	Y = 120547.8X - 205766.1	0.01-0.4	0.9996	1.9
3	Orange 2	Condiment	6.810	327.0419	Y = 151089.4X + 147236.4	0.01-0.4	0.9997	1.6
4	Azorubin	Condiment	4.740	228.0019	Y = 1680.244X - 94578.77	0.2-8	0.9996	3.8
5	Orange 3	Condiment	9.500	429.0526	Y = 2059937X + 1033213	0.001-0.04	0.9989	2.2
6	Acid Orange 67	Condiment	11.900	581.0814	Y= 69577.60X + 759077.10	0.02-0.8	0.9972	4.7
7	Tracid Brilliant Red 10B	Condiment	11.515	393.5491	Y = 18895.15X - 1572,776	0.05-2	0.9919	3.3
8	Acid Yellow A4-R	Condiment	7.275	427.0729	Y = 117428.3X - 167170.2	0.01-0.4	0.9996	2.1
9	Tracid Brilliant Red B	Condiment	7.830	350.4985	Y = 12013.91X - 1654,808	0.1-4	0.9969	2.0

Table 2 Quantitative result of acidic dyes
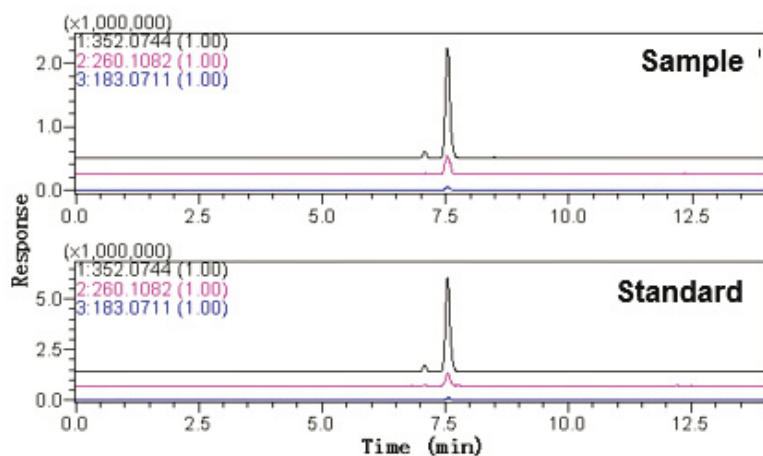
Figure 4 - Mass chromatograms of Yellow 36 in red pepper
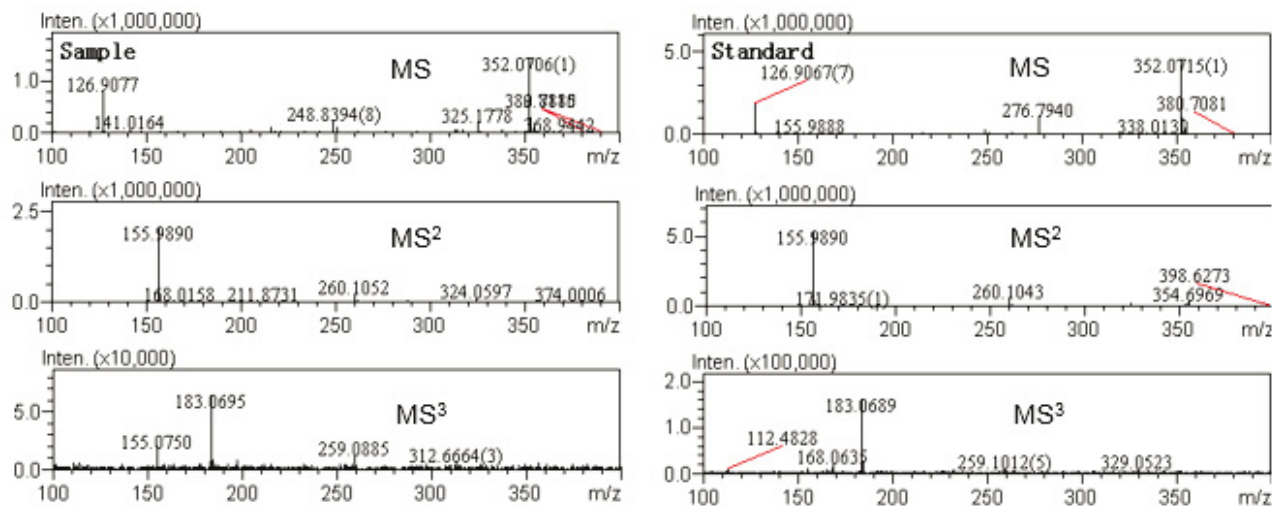
Figure 5 - MS^3 spectrum of Acid Yellow 36
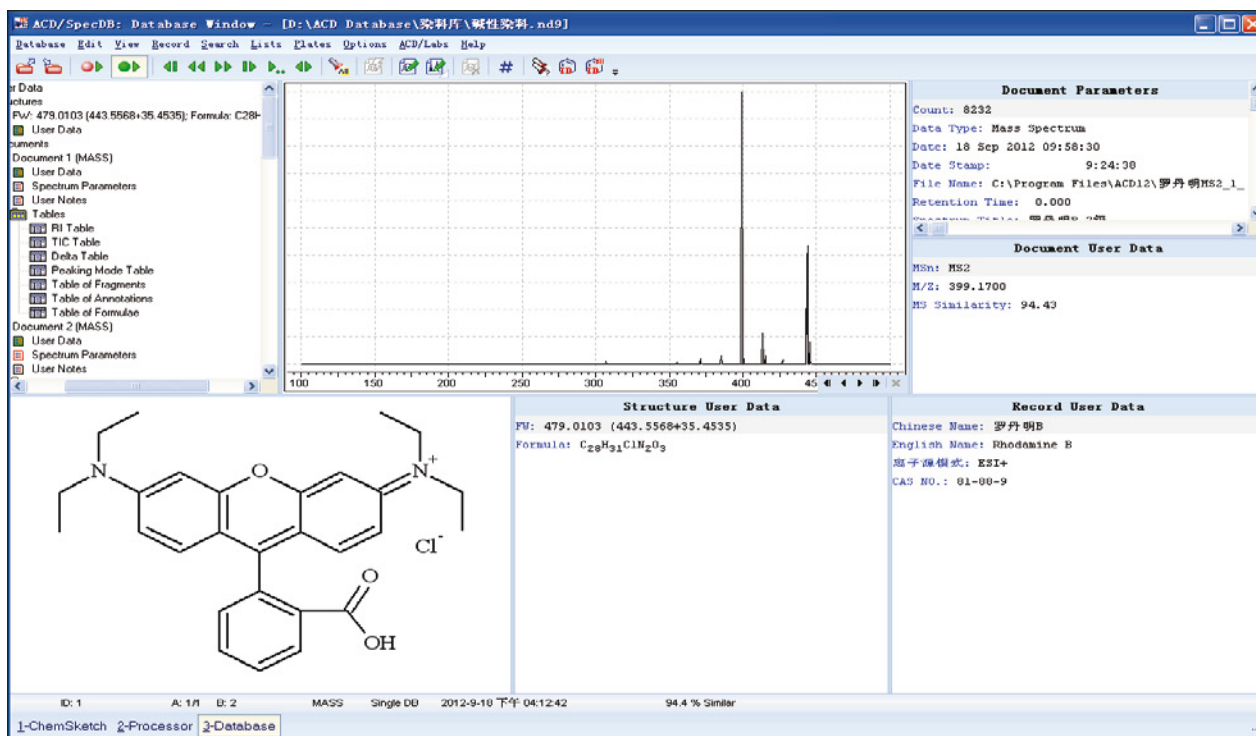
Figure 6 - ACD MS Manager database

4. Conclusions

10 basic industrial dyes and 9 acidic industrial dyes in food were determined by LCMS-IT-TOF, and quantified by external standard method. The developed methods show a good linearity range, and in the certain concentration ranges with their correlation coefficients (r) more than 0.99. For basic industrial dyes analysis, the relative standard deviations (n=7) were less than 9%. The levels (2, 10 and 25 µg/kg) were ranged from 65.3% to 119.2%. For acidic industrial dyes analysis, average recoveries of acid dyes in the spiked samples at three different levels varied from 64.8% to 106.0% with the relative standard deviations (n=5) better than 6.7%.In general, the methods established in our study were simple, rapid, and highly sensitive. They were suitable for the simultaneous determination of basic dyes or acidic dyes residue in food. An MS[n] database (ACD MS Manager database) for these industrial dyes had been created, which provided a quick and easy way for accurate qualitative analysis and screening of industrial dyes in food.

SHIMADZU

Shimadzu Europa GmbH

www.shimadzu.eu

Micro Flow UHPLC-MS/MS in Pesticide Analysis of Infant Foods

David R. Baker, Neil Loftus (Shimadzu, Manchester, UK); Simon Hird (Food and Environment Research Agency, York; UK)

1. Introduction

Food safety with regards to infant food is of the upmost importance; however, it is also recognised as a challenging matrix to analyse due to the low maximum residue limit (MRL) of 0.01 mg/kg required by European Directive 2006/141/EC for all pesticides. Furthermore, the European Directive prohibits the use of certain very toxic pesticides in the production of infant foods and establishes even lower MRLs for a few other very toxic pesticides. Additionally, the analysis of infant food is complicated by their wide range of fat content.

LC-MS/MS has been widely used for the quantitation of pesticides in infant food. The analytical methods typically use conventional LC flow rates (approximately 0.5 mL/min). Micro flow LC uses significantly lower flow rates (10 to 100 µL/min). With the same sample amount and identical LC peak width, the reduction in LC flow rate can result in an improved detection limit for concentration-dependent detection techniques such as electrospray ionization (ESI) mass spectrometry. Here, we utilise the improved response from micro flow LC to achieve the required low limits of detection for over one hundred pesticides in infant food. Initial validation results are presented for the micro flow LC method, in addition to robustness data.

2. Materials and Methods

2-1. Sample preparation

Samples were extracted using QuEChERS (quick, easy, cheap. effective, rugged and safe) methods developed by the Food and Environment Research Agency, UK. Sample extracts in acetonitrile were spiked with 130 pesticides. Sample extracts were diluted five times with water before LCMS injection.

2-2. LC-MS/MS analysis

UHPLC	Nexera UHPLC system
Flow rate	90µL/min
Mobile phase	A= Water (95%) and methanol (5%) with 5mM ammonium formate B= Methanol with 5mM ammonium formate
Gradient	0% B - 100% B (12 min), 100% B (14 min), 10% B (17 min)
Analytical column	ACQUITY UPLC HSS T3; 1 mm X 100 mm, 1.8 µm
Column temperature	35ºC
Injection volume:	5µL
MS	LCMS-8040 triple quadrupole mass spectrometer
Ionisation	Electrospray, positive and negative mode
SRM	130 pesticides (260 SRMs) Pause 1 msec./Dwell 3 msec.
Desolvation line	200ºC
Drying/Nebulising gas	15L/min, 2L/min
Heating block	400ºC

3. Results and discussion

3-1. Micro flow LC method
Micro flow LC was utilised for the analysis of 130 pesticides using a 90 µL/min flow rate and a 1.0 mm I.D. analytical column. The flow rate was reduced from conventional flow rates (approximately 500 µL/min) in order to increase analyte response and reduce costly

solvent consumption. All 130 pesticides were eluted within 12.7 minutes with a typical peak width of 7 seconds. An example chromatogram is displayed in Figure 1. A high speed data acquisition mass

spectrometer was utilised to acquire reliable data with a 1 msec pause and 3 msec dwell time, which allowed the acquisition of a large number of overlapping MRM transitions.
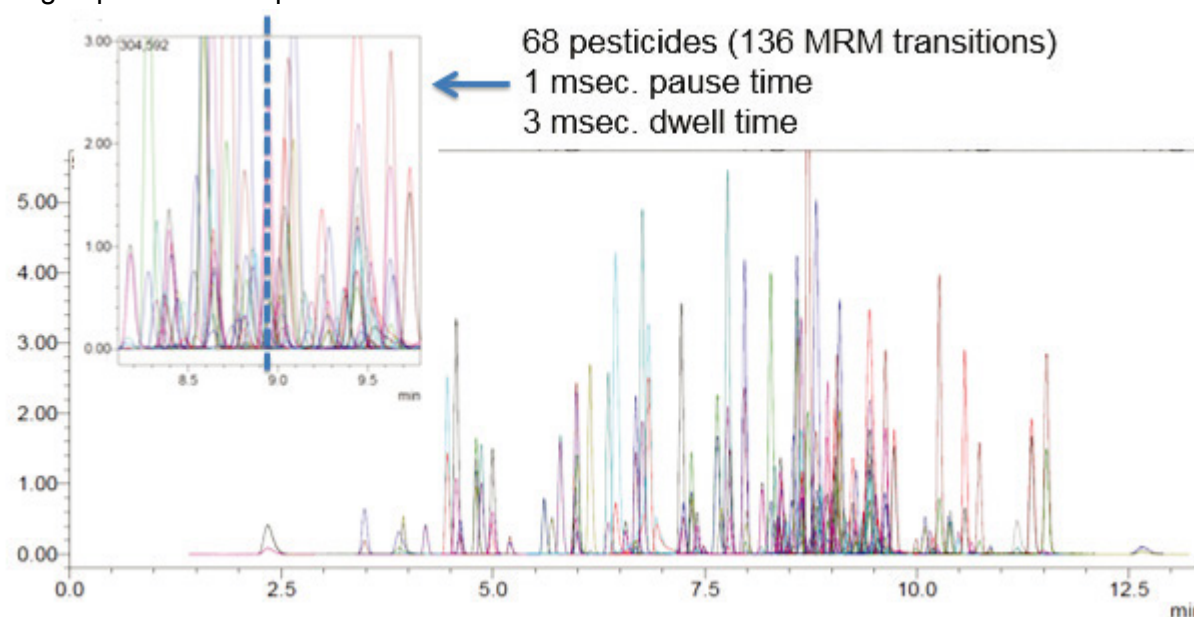
Figure 1 – Micro flow LC analysis of 130 pesticides in infant food (0.05 mg/kg)

3-2. Linearity

Calibration curves were prepared in the range 0.5xRL (reporting limit) to 20xRL. For the vast majority of pesticides this was in the range 0.005 - 0.2 mg/kg (0.5 – 200 ppb). The developed method achieved the necessary sensitivity to detect all 130 pesticides at the lowest required level. Figure 2 displays calibration curves for nine example pesticides including the first eluting analyte (methamidophos) and latest eluting analyte (fenbutatin). All analytes displayed linearity with R^2 > 0.996, with typical R^2 of 0.9990.

3-3. Intra- and inter-day precision

To assess the intra-day and inter-day variability of the LC-MS/MS method, QC samples were prepared in infant food at low (0.01 mg/kg) and high (0.2 mg/kg) concentrations. Intra- (n=6) and inter-day (n=3 over 3 days) precision were determined as %RSD of peaks areas. Table 2 lists precision data for compounds over the run time, including the first eluting analyte (methamidophos) and latest eluting analyte (fenbutatin). Intra-day precision was typically less than 4%, while inter-day precision was typically less than 7%.
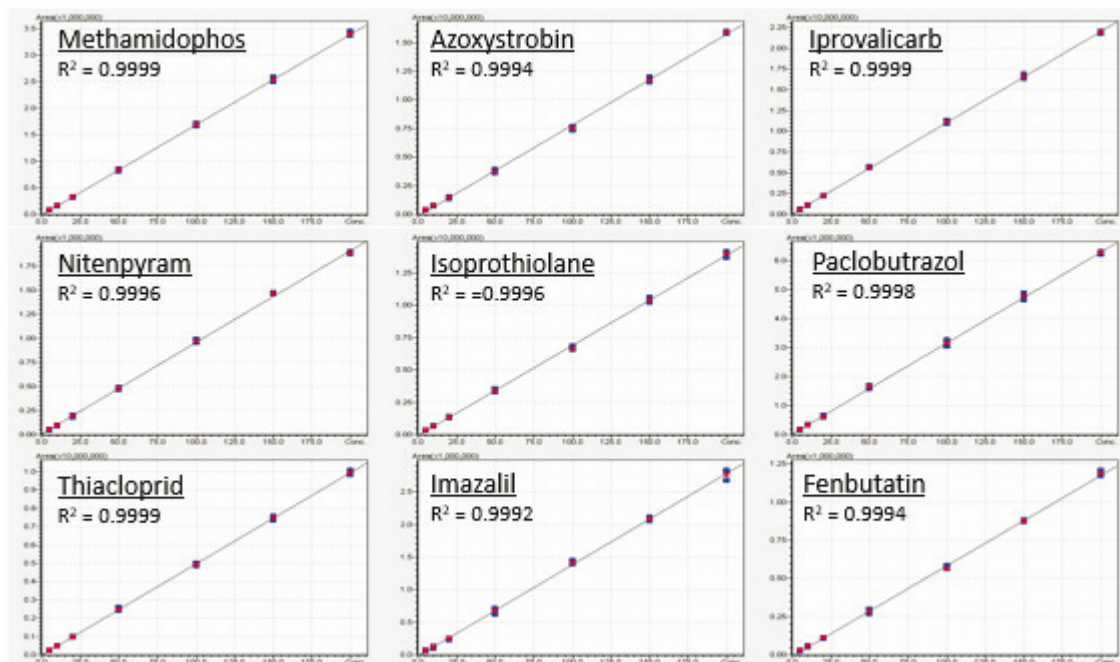
Figure 2 – Calibration curves (weighting 1/x), 0.005 – 0.2 mg/kg (0.5 – 200 ppb) of nine pesticides in infant food

Compound	Retention time	Intra-day (%RSD)		Inter-day (%RSD)	
		Low	High	Low	High
Methamidophos	2.3	2.14	3.53	2.80	4.50
Acephate	3.4	1.56	2.55	3.54	3.85
Aldicarb sulfoxide	4.2	1.31	0.70	4.84	3.91
Methomyl	4.8	2.02	2.03	3.61	4.86
Imidacloprid	5.6	2.05	0.64	3.46	4.59
Carbendazim	6.5	1.70	0.72	2.69	3.80
Carbaryl	7.4	3.41	0.93	5.38	4.77
Fosthiazate	7.6	1.21	1.19	2.55	4.50
Azoxystrobin	8.2	1.90	1.78	2.78	4.30
Dimethomorph	8.5	3.05	2.28	5.03	4.95
Triazophos	8.7	1.45	1.19	3.47	4.78
Iprovalicarb	8.8	2.40	1.71	3.08	4.47
Cyazofamid	8.9	2.60	2.16	2.89	5.74
Penconazole	9.3	1.58	1.61	4.55	4.15
Hexaconazole	9.4	2.37	1.77	4.16	4.35
Pencycuron	9.6	2.59	2.27	2.69	4.43
Pyriproxyfen	10.2	1.02	1.02	1.32	5.39
Fenpyroximate	10.7	2.96	1.29	12.8	2.97
Etofenprox	11.4	2.55	1.00	2.03	4.72
Fenbutatin	12.6	2.40	2.90	2.72	4.51

Table 2 – Intra- and inter-day precision of selected pesticides over the run time

3-4. System robustness

To the investigate the robustness of the micro flow system infant food extract was repeatedly injected over 48 hours. In total, 162 injections were performed with infant food extract at 0.02 mg/kg. The stability of the system was assessed in terms of peak area stability (Figure 4) and retention time stability. The data showed excellent stability with peak area deviation typically 3-5% and retention time stability typically less than 0.12 %RSD.
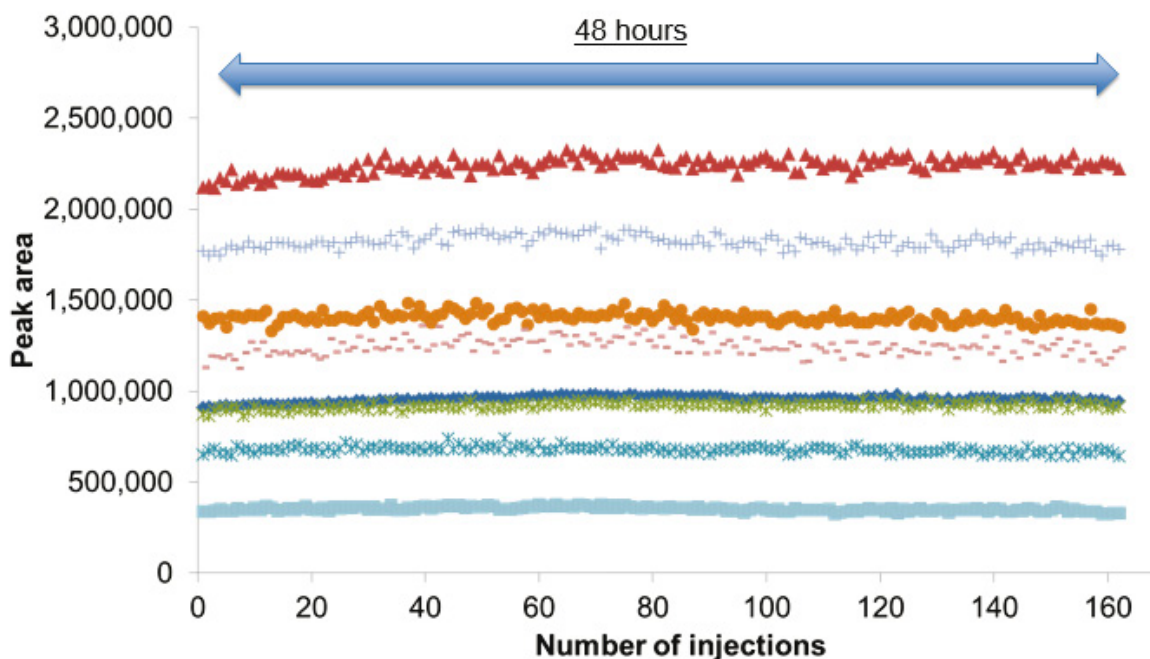
Figure 4 – Peak area stability (%RSD) of pesticides in infant food extract over 48 hours of repeat injections

4. Conclusion

- The developed micro flow LC methodology achieved the required MRL of 0.01 mg/kg for all 130 pesticides with all compounds eluted within 12.7 minutes.
- Initial validation data displayed excellent linearity for all compounds, low intra- and inter-day precision, no observed carryover, and good peak area and retention time stability over 48 hours.
- Precise data was acquired with the use of low pause and dwell times (1 msec pause and 3 msec dwell times)

- Micro flow analysis was successfully carried out a UHPLC system capable of both conventional higher flow rates and lower micro flow rates.
- Micro flow LC is a possible alternative to conventional flow LC if extra sensitivity is needed or reduction in solvent consumption is required.

Multi-Residue Analysis of 210 Pesticides in Food Samples by Triple Quadrupole UHPLC-MS/MS

David R. Baker[1], Chris Titman[1], Alan J. Barnes[1], Neil J. Loftus[1], Alexander Mastoroudes[2], Simon Hird[3]

[1]Shimadzu Corporation, Manchester, UK
[2]Kings College London, London, UK
[3]Food and Environment Research Agency, York, UK

Abstract

Pesticides and their metabolites are of great concern to society as they are harmful to human health, pollute natural resources and disturb the equilibrium of the ecosystem. Consequently, stricter food safety regulations are being enforced around the world, placing pesticide analysis laboratories under increasing pressure to expand the list of targeted pesticides, detect analytes at lower levels and with greater precision, reduce analysis turnaround times, and all the while maintaining or reducing costs. In this study a method was successfully developed for the quantitation of 210 commonly analysed pesticides in food samples using the Nexera UHPLC and LCMS-8040. Initial validation was performed to demonstrate instrument capabilities. Limits of detection (LOD) for 90 % of compounds were less than 0.001 mg kg^{-1} (1 ppb) and all compounds were less than 0.01 mg kg^{-1} (10 ppb) for both the quantifying and qualifying transitions using only a 2 µL injection. Repeatability at the 0.01 mg kg^{-1} reporting level was typically less than 5 %RSD for compounds and correlation coefficients were typically greater than 0.997 in a variety of studied food extracts. Consequently, the LCMS-8040 is ideally suited for routine monitoring of pesticides below the 0.01 mg kg^{-1} default level set by EU and Japanese legislation.

Keywords: **Pesticides; Multi-residue analysis; LCMS-8040; Food safety; Fruit; Vegetables**

1. Introduction

Pesticide residues in food continue to be the target of studies due to the uncertainty concerning adverse effects that those residues may have on human health after a lengthy exposure at low levels. More than 1000 active ingredients have been utilised and are formulated in thousands of different commercial products. They include a variety of compounds, mainly insecticides, herbicides and fungicides, as well as their metabolites, with very different physico-chemical characteristics and large differences in polarity, volatility and persistence.[1] Consequently, in order to ensure food safety for consumers and to facilitate international trade, regulatory bodies around the world have established maximum residue levels (MRLs) for pesticide residues in food commodities; that is, the maximum amount of pesticide residue and its toxic metabolites that might be expected on a commodity if good agricultural practice was adhered to during the use of the pesticide.[2]

In the European Union regulation 396/2005/EC was implemented in 2008 harmonising pesticide MRLS in all member states for 435 pesticide active substances in 378 commodities.[3] This EU regulation covers pesticides both currently and formerly used in agriculture in or outside the EU. For pesticide and food commodity combinations not listed in the regulation a default MRL of 0.01 mg kg^{-1} applies (Art 18(1b) of European Union Regulation No 396/2005).[3] In general, MRLs in the European Food regulation are in the range 0.01 - 10 mg kg^{-1} depending on the pesticide-commodity combination, with the lowest levels set for banned pesticides. For vegetables, fruits and cereals intended for the production of baby foods, Directive 2006/141/EC requires that baby food contains no detectable levels of pesticide residues defined as < 0.01 mg kg^{-1} and prohibits the use of certain very toxic

pesticides in the production of infant foods and establishes even lower MRLs for a few other very toxic pesticides.[4] Regulatory bodies around the world, as in the EU, have produced similar guidelines. In the US, tolerances for more than 450 pesticides and other ingredients are stated in the electronic Code of Federal Regulations (US Environmental Protection Agency Office of Pesticide Programs) and are enforced by the US FDA.[5] Japan's positive list system for agricultural chemical residues in foods, introduced in 2006, contains MRLs for over 400 pesticides in various commodities.[6] China published national standard GB 2763-2005 in 2005 and more recently GB 28260-2011 which was introduced in 2012 and specifies 181 MRLS for 85 pesticides in food.[7,8]

Consequently, pesticide analysis laboratories are under increasing pressure to expand the list of targeted pesticides, detect analytes at lower levels and with greater precision, reduce analysis turnaround times and reduce usage of hazardous solvents while maintaining or reducing costs. Pesticide residues were traditionally analysed mainly by GC-based multi-residue methods often with MS detection. However, many modern

(semi)polar compounds and/or ionic compounds could not be analysed in this way due to poor thermal stability or volatility without the need for derivatisation.[9] Recent improvements in liquid chromatography - tandem mass spectrometry, combined with the discussed pitfalls of GCMS, have meant LCMSMS has become a vital technique. LC-tripe quadruple mass spectrometry enables highly selective and sensitive analysis and is well suited to the multi-class analysis of large numbers of pesticides at trace levels.

In this work, we discuss the development of a multi-residue pesticide method for 210 pesticides using the Nexera UHPLC and LCMS-8040 triple quadruple. Pesticides were matrix-matched in food matrix (lettuce, pear and dried fruit) following QuEChERS sample preparation. The method was evaluated in matrix to ensure that the necessary reporting limits were obtained according to the various regulatory guidelines around the world with acceptable precision, in addition to ensuring chromatographic resolution of pesticide isomers with identical SRM transitions.

2. Experimental

A stock of pesticides was obtained from the Food and Environment Agency, UK, at a concentration of 0.01 mg kg^{-1} (for each pesticide) in acetone:acetonitrile 1:1. Linearity was investigated over a nine-point calibration with samples ranging from 0.5 µg kg^{-1} - 0.2 mg kg^{-1} (0.5 – 200 ppb) analysed in duplicate; calibration samples were injected once in increasing order and once in decreasing order. Linearity was assessed with four calibration curves prepared by serial dilution of: (1) acetonitrile, (2) dried fruit extract, (3) lettuce extract and, (4) pear extract. Instrumental area repeatability was determined by replicate (n=6) injection of pear matrix at 0.01 mg kg^{-1}. LC-MS mobile phase solvents and additives were all of LC–MS quality and purchased from Sigma–Aldrich.

Food extracts were supplied by the Food and Environment Agency, UK, following established QuEChERS protocols. QuEChERS is acronym for Quick Easy Cheap Effective Rugged Safe and is a widely used sample preparation technique for the extraction of pesticides from food. Food samples included dried fruit, lettuce and pear, with the final extracts prepared in 100% acetonitrile.

LC Parameters

UHPLC:	Nexera UHPLC system
Column:	Shim-pack XR-ODS III (150 x 2 mm, 2.2 µm particle size)
Column temp.:	40 ^{o}C
Mobile phase:	A = Water with 5 mM ammonium formate and 0.01 % formic acid B = Methanol with 5 mM ammonium formate and 0.01 % formic acid
Gradient:	Time (min) A% B% 0 5 95 16 0 100 18 0 100 18.1 5 95 20 5 95
Flow rate:	0.4 mL min^{-1}
Injection volume:	32 µL (stacked injection: 2µL sample + 30µL water)
Needle wash:	1000 µL Methanol

MS Parameters

MS:	LCMS-8040 triple quadrupole mass spectrometer
Ionisation:	ESI - Positive and negative (15 msec. polarity switch)
SRM:	Dwell time 5 msec. Pause time 1 msec.
Desolvation line:	250 ^{o}C
Heating block:	400 ^{o}C
Drying gas:	15 L min^{-1}
Nebulising gas:	2 L min^{-1}
SRM optimisation:	1:1 water:methanol with 10mM ammonium acetate Flow rate: 0.5mL min^{-1} Flow injection analysis (No column fitted) 0.2 µL (0.01 mg kg^{-1} pesticide standard solution)
Mobile phase screening:	Carrier 1:1 water:methanol Flow rate: 0.3mL min^{-1} Flow injection analysis (No column fitted) 5µL injection (0.01 mg kg^{-1} pesticide standard solution) 1µL air gap (see text for mobile phase compositions)

Pesticide limits of detection were calculated based on the method described by the US-EPA in Title 40 Code of Federal Regulation Part 136,[10] using a standard deviation of 7 replicates in pear matrix at a concentration value that corresponds to an instrument signal to noise ratio in the range of 2.5 to 5 and a Student's t 99% confidence interval:

$$MDL = St(n - 1, 1 - \alpha = 0.99) \ x \ s.d.$$

Where, t(n-1,1-α=0.99) = Student's t value for the 99% confidence level with n-1 degrees of freedom (t = 3.14 for 7 replicates), n = number of replicates, and s.d. = standard deviation of the replicate analyses.

3. Results and discussion

3.1 SRM optimisation

Target precursor and product ions were selected based on recommendations from the Food and Environment Agency, UK, and data from the EURL DataPool.[11] Typically the protonated or deprotonated molecule was used for the precursor ion. In order to try to prevent interference of SRM transitions from matrix, product ions greater than m/z 100 were selected where possible as they are typically more diagnostic.[12] Analyte specific MS parameters (Q1 pre-bias (V), Q3 pre-bias (V) and collision energy) were optimised using automated flow injection analysis. Briefly, this involves placing pesticide standards into the auto-sampler, from where they are then rapidly injected into the MS with a different parameter optimised on each injection. Each compound was optimised in only a few minutes using the automated software provided in LabSolutions. This allowed large numbers of compounds to be optimised overnight; this is in stark contrast to traditional time-consuming infusion in order to optimise parameters. The compounds studied and their associated transitions are shown in Table 1.

Table 1 - *Studied compounds and their chemical formulas, CAS numbers, SRMs, retention times, limits of detection and R^2*

Compound	Formula	CAS	Transition 1	Transition 2	Pear extract				
					RT (min.)	Transition 1 LOD (ppb)	Transition 2 LOD (ppb)	%RSD (10ppb)	R^2
Avermectin B1a	C48H72O14	71751-41-2	891 > 305	891 > 567	16.4	0.35	0.56	5.0	0.9975
Acephate	C4H10NO3PS	30560-19-1	184 > 143	184 > 49	3.0	0.17	0.31	1.0	0.9999
Acetamiprid	C10H11ClN4	135410-20-7	223 > 126	223 > 99	7.2	0.50	1.00	1.1	0.9979
Acrinathrin	C26H21F6NO5	101007-06-1	559 > 208	559 > 181	16.1	1.32	2.36	4.4	0.9990
Alachlor	C14H20ClNO2	15972-60-8	270 > 238	270 > 162	13.4	0.09	0.26	1.5	0.9995
Aldicarb	C7H14N2O2S	116-06-3	208 > 116	208 > 89	8.5	0.05	0.10	1.7	0.9998
Aldicarb sulfone	C7H14N2O4S	1646-88-4	240 > 223	240 > 86	4.3	0.17	0.13	1.8	0.9999
Aldicarb sulfoxide	C7H14N2O3S	1646-87-3	207 > 89	207 > 132	3.9	0.22	0.36	2.3	1.0000
Amidosulfuron	C9H15N5O7S2	120923-37-7	370 > 261	370 > 139	9.3	0.14	0.22	2.8	0.9984
Asulam	C8H10N2O4S	3337-71-1	231 > 156	231 > 92	3.4	0.72	2.03	3.8	0.9979
Atrazine	C8H14ClN5	1912-24-9	216 > 174	216 > 104	11.1	0.10	0.22	2.4	0.9989
Azinphos-methyl	C10H12N3O3PS2	86-50-0	318 > 132	318 > 77	11.8	0.50	0.50	2.7	0.9903
Azoxystrobin	C22H17N3O5	131860-33-8	404 > 372	404 > 344	12.1	0.03	0.30	2.1	0.9989
Bendiocarb	C11H13NO4	22781-23-3	224 > 109	224 > 167	9.8	0.10	0.09	1.5	0.9996
Benthiavalicarb-isopropyl	C18H24FN3O3S	177406-68-7	382 > 180	382 > 116	12.7	0.12	0.41	0.9	0.9997
Bispyribac sodium	C19H17N4NaO8	125401-92-5	453 > 297	453 > 179	12.1	1.41	5.43	7.4	0.9954
Boscalid	C18H12Cl2N2O	188425-85-6	343 > 307	343 > 140	12.5	0.81	1.19	4.6	0.9968
Bromoxynil*	C7H3Br2NO	1689-84-5	274 > 79	276 > 81	9.9	2.24	2.61	4.5	0.9968
Bromuconazole	C13H12BrCl2N3O	116255-48-2	376 > 159	376 > 70	13.0	0.72	1.79	2.9	0.9994
Butachlor	C17H26ClNO2	23184-66-9	312 > 238	312 > 57	15.3	0.29	0.39	1.6	0.9998
Butocarboxim	C7H14N2O2 S	34681-10-2	208 > 75	208 > 191	8.4	0.13	0.87	3.1	0.9999
Butocarboxim sulfone	C7H14N2O4S	34681-23-7	223 > 106	223 > 166	4.1	2.63	3.23	9.7	0.9949
Butocarboxim sulfoxide	C7H14N2O3S	34681-24-8	207 > 88	207 > 75	3.7	0.22	0.21	1.9	0.9999
Carbaryl	C12H11NO2	63-25-2	202 > 145	202 > 127	10.3	0.13	0.22	2.4	0.9988
Carbendazim	C9H9N3O2	10605-21-7	192 > 160	192 > 132	7.1	0.50	1.00	1.1	0.9996
Carbofuran	C12H15NO3	1563-66-2	222 > 165	222 > 123	11.1	0.12	0.18	0.7	0.9993
Carboxin	C12H13NO2S	5234-68-4	236 > 143	236 > 87	10.2	0.09	0.25	0.9	0.9991
Chlorantraniliprole*	C18H14BrCl2N5O2	500008-45-7	482 > 284	482 > 177	11.8	0.50	1.00	2.3	0.9979
Chlorfenvinfos	C12H14Cl3O4P	470-90-6	361 > 155	361 > 99	14.0	0.28	0.49	2.3	0.9966
Chloridazon	C10H8ClN3O	1698-60-8	222 > 92	222 > 104	7.2	0.20	0.18	3.2	0.9990
Chlorotoluron	C10H13ClN2O	15545-48-9	213 > 72	213 > 46	10.8	0.05	0.13	1.3	0.9967
Chromafenozide	C24H30N2O3	143807-66-3	395 > 175	395 > 91	13.0	0.05	0.60	1.0	0.9977
Clethodim	C17H26ClNO3S	99129-21-2	360 > 164	360 > 268	14.7	0.08	0.45	0.7	0.9970
Clofentezine	C14H8Cl2N4	74115-24-5	303 > 138	303 > 102	14.4	4.03	5.76	9.5	0.9967
Clothianidin	C6H8ClN5O2S	210880-92-5	250 > 132	250 > 169	6.5	0.25	0.12	1.6	0.9978
Cyazofamid	C13H13ClN4O2S	120116-88-3	325 > 108	325 > 261	13.3	0.39	3.74	2.4	0.9964
Cycloxydim	C17H27NO3S	101205-02-1	326 > 280	326 > 180	14.8	0.33	0.73	1.0	0.9989
Cyflufenamid	C20H17F5N2O2	180409-60-3	413 > 295	413 > 241	14.2	0.27	0.29	2.9	0.9982
Cymoxanil	C7H10N4O3	57966-95-7	199 > 128	199 > 111	7.7	2.99	3.52	5.5	0.9960
Cyproconazole	C15H18ClN3O	113096-99-4	292 > 70	292 > 125	12.8	0.41	0.60	3.5	0.9988
Cyprodinil	C14H15N3	121552-61-2	226 > 93	226 > 108	13.9	0.89	0.91	1.3	0.9990
Cyromazine	C6H10N6	66215-27-8	167 > 85	167 > 125	2.2	2.57	4.79	7.4	0.9994
Demeton-S-methyl sulfoxide	C6H15O4PS2	301-12-2	247 > 169	247 > 109	5.0	0.01	0.03	1.2	0.9999
Demeton-S-methyl sulfone	C6H15O5PS2	17040-19-6	263 > 169	263 > 109	5.3	0.03	0.10	3.1	0.9999
Desmedipham	C16H16N2O4	13684-56-5	318 > 182	318 > 136	11.6	0.08	0.33	0.5	0.9971
Diclobutrazol	C15H19Cl2N3O	75736-33-3	328 > 70	330 > 70	13.8	0.17	0.20	2.7	0.9988

Table 1 – Continued...

Compound	Formula	CAS	Transition 1	Transition 2	Pear extract				
					RT (min.)	Transition 1 LOD (ppb)	Transition 2 LOD (ppb)	%RSD (10ppb)	R^2
Diethofencarb	C14H21NO4	87130-20-9	268 > 226	268 > 124	12.2	0.06	0.12	2.2	0.9996
Difenoconazole	C19H17Cl2N3O3	119446-68-3	406 > 251	406 > 188	14.5	0.18	0.53	2.6	0.9994
Diflubenzuron	C14H9ClF2N2O2	35367-38-5	311 > 158	311 > 141	13.5	2.21	7.48	9.2	0.9936
Dimethoate	C5H12NO3PS2	60-51-5	230 > 125	230 > 199	7.0	0.05	0.07	1.6	0.9997
Dimethomorph	C21H22ClNO4	110488-70-5	388 > 301	388 > 165	12.7	0.29	0.41	2.5	0.9991
Dimoxystrobin	C19H22N2O3	149961-52-4	327 > 205	327 > 116	13.7	0.12	0.14	0.5	0.9997
Dinotefuran	C7H14N4O3	165252-70-0	203 > 129	203 > 157	3.9	0.10	0.22	2.9	0.9994
Disulfoton sulfoxide	C8H19O3PS3	2497-07-6	291 > 213	291 > 97	10.8	0.05	0.15	2.6	0.9980
Diuron	C9H10Cl2N2O	330-54-1	233 > 72	235 > 72	11.4	0.09	0.26	0.6	0.9971
DMPF	C10H14N2	33089-74-6	163 > 107	163 > 122	4.8	1.00	2.00	2.5	0.9910
Dodine	C15H33N3O2	2439-10-3	228 > 71	228 > 60	13.5	0.30	0.54	1.7	0.9946
Epoxiconazole	C17H13ClFN3O	135319-73-2	330 > 121	330 > 101	13.3	0.12	0.37	2.5	0.9998
Ethiofencarb	C11H15NO2S	29973-13-5	226 > 107	226 > 169	10.6	0.18	0.59	0.7	0.9994
Ethiofencarb sulfone	C11H15NO2S2	53380-23-7	275 > 107	275 > 201	6.2	0.02	0.16	0.9	0.9999
Ethiofencarb sulfoxide	C11H15NO3S	53380-22-6	242 > 107	242 > 185	6.5	0.02	0.02	0.9	0.9999
Ethirimol	C11H19N3O	23947-60-6	210 > 140	210 > 98	10.8	0.14	0.24	1.8	0.9977
Etofenprox	C25H28O3	80844-07-1	394 > 177	394 > 359	16.9	0.03	0.06	3.1	0.9983
Fenamidone	C17H17N3OS	161326-34-7	312 > 92	312 > 236	12.4	0.06	0.18	1.9	0.9988
Fenamiphos	C13H22NO3PS	22224-92-6	304 > 217	304 > 202	13.5	0.05	0.28	1.9	0.9970
Fenamiphos sulfone	C13H22NO5PS	31972-44-8	336 > 266	336 > 188	10.2	0.31	0.25	4.3	0.9961
Fenamiphos sulfoxide	C13H22NO4PS	31972-43-7	320 > 108	320 > 171	10.0	0.18	0.52	3.3	0.9976
Fenbuconazole	C19H17ClN4	114369-43-6	337 > 125	337 > 70	13.4	0.23	0.40	5.0	0.9964
Fenhexamid	C14H17Cl2NO2	126833-17-8	302 > 97	302 > 55	13.1	0.75	0.95	0.9	0.9944
Fenoxycarb	C17H19NO4	79127-80-3	302 > 88	302 > 116	13.6	0.10	0.20	2.4	0.9989
Fenpropimorph	C20H33NO	67564-91-4	304 > 147	304 > 117	14.1	0.05	0.13	1.6	0.9995
Fenpyroximate	C24H27N3O4	111812-58-9	422 > 366	422 > 215	15.9	0.02	0.17	1.2	0.9997
Fenthion sulfoxide	C10H15O4PS2	3761-41-9	295 > 109	295 > 280	10.1	0.18	0.27	1.5	0.9985
Fenthion sulfone	C10H15O5PS2	3761-42-0	311 > 109	311 > 125	10.4	3.75	3.61	9.8	0.9974
Fipronil*	C12H4Cl2F6N4OS	120068-37-3	435 > 330	435 > 250	13.5	0.11	0.35	4.1	0.9998
Fluazifop acid*	C15H12F3NO4	69335-91-7	328 > 282	328 > 91	11.8	0.55	3.61	7.1	0.9983
Fluazinam*	C13H4Cl2F6N4O4	79622-59-6	463 > 416	463 > 398	15.2	0.20	0.27	2.7	0.9994
Fludioxonil*	C12H6F2N2O2	131341-86-1	247 > 126	247 > 180	12.4	1.00	1.00	4.2	0.9974
Flufenacet	C14H13F4N3O2S	142459-58-3	364 > 152	364 > 194	13.2	0.04	0.06	1.6	0.9986
Flufenoxuron	C21H11ClF6N2O3	101463-69-8	489 > 158	489 > 141	15.7	0.24	0.63	8.2	0.9989
Fluometuron	C10H11F3N2O	2164-17-2	233 > 72	233 > 46	10.6	0.12	0.14	1.3	0.9996
Fluopicolide	C14H8Cl3F3N2O	239110-15-7	383 > 173	383 > 145	12.7	0.05	0.17	2.1	0.9967
Fluoxastrobin	C21H16ClFN4O5	361377-29-9	459 > 427	459 > 188	13.1	0.19	0.22	1.7	0.9987
Fluroxypyr*	C7H5Cl2FN2O3	69377-81-7	253 > 195	255 > 197	7.8	1.13	1.75	5.7	0.9993
Flutriafol	C16H13F2N3O	76674-21-0	302 > 70	302 > 123	11.1	0.29	0.43	3.2	0.9984
Fosthiazate	C9H18NO3PS2	98886-44-3	284 > 104	284 > 228	10.7	0.05	0.12	2.7	0.9985
Furathiocarb	C18H26N2O5S	65907-30-4	383 > 195	383 > 252	15.1	0.07	0.13	1.8	1.0000
Halofenozide	C18H19ClN2O2	112226-61-6	331 > 105	331 > 275	12.3	0.05	0.05	1.7	0.9947
Halosulfuron-methyl*	C13H15ClN6O7S	100784-20-1	435 > 182	437 > 182	11.5	0.30	0.96	3.1	0.9968
Haloxyfop acid*	C15H11ClF3NO4	69806-34-4	360 > 288	362 > 290	13.3	6.20	6.86	13.4	0.9999
Heptenophos	C9H12ClO4P	23560-59-0	251 > 127	251 > 89	11.4	0.15	1.36	4.7	0.9982
Hexythiazox	C17H21ClN2O2S	78587-05-0	353 > 228	353 > 168	15.6	2.25	1.02	4.5	0.9956

Table 1 – Continued...

Compound	Formula	CAS	Transition 1	Transition 2	Pear extract				
					RT (min.)	Transition 1 LOD (ppb)	Transition 2 LOD (ppb)	%RSD (10ppb)	R^2
Imazalil	C14H14Cl2N2O	35554-44-0	297 > 159	297 > 69	11.8	0.30	0.48	3.5	0.9988
Imidacloprid	C9H10ClN5O2	138261-41-3	256 > 209	256 > 175	6.4	0.50	0.50	1.9	0.9966
Indoxacarb	C22H17ClF3N3O7	144171-61-9	528 > 203	528 > 150	14.5	0.40	0.37	3.9	0.9964
Ioxynil*	C7H3I2NO	1689-83-4	370 > 127	370 > 215	11.0	0.12	1.00	3.6	0.9961
Iprovalicarb	C18H28N2O3	140923-17-7	321 > 119	321 > 203	13.1	0.06	0.23	2.5	0.9981
Isazofos	C9H17ClN3O3PS	42509-80-8	314 > 120	314 > 162	12.9	0.04	0.13	2.2	0.9994
Isocarbofos	C11H16NO4PS	24353-61-5	307 > 231	307 > 121	11.4	0.07	0.12	2.7	0.9991
Isofenphos	C15H24NO4PS	25311-71-1	346 > 245	346 > 217	14.3	0.17	0.13	1.7	0.9991
Isofenphos-methyl	C14H22NO4PS	99675-03-3	332 > 231	332 > 273	13.8	0.03	0.13	1.2	0.9996
Isoprocarb	C11H15NO2	2631-40-5	194 > 95	194 > 137	11.1	0.20	0.49	1.9	0.9990
Isoprothiolane	C12H18O4S2	50512-35-1	291 > 189	291 > 231	12.6	0.10	0.09	0.9	0.9994
Isoproturon	C12H18N2O	34123-59-6	207 > 72	207 > 46	11.3	0.10	0.11	1.7	0.9996
Isoxaben	C18H24N2O4	82558-50-7	333 > 165	333 > 150	12.6	0.02	0.06	0.9	0.9989
Kresoxim-methyl	C18H19NO4	143390-89-0	314 > 116	314 > 206	13.8	0.15	0.18	3.3	0.9991
Lenacil	C13H18N2O2	2164-08-1	235 > 153	235 > 136	11.2	0.18	0.64	2.2	0.9987
Linuron	C9H10Cl2N2O2	330-55-2	249 > 160	249 > 182	12.2	3.15	3.20	3.7	0.9979
Lufenuron*	C17H8Cl2F8N2O3	103055-07-8	509 > 339	509 > 175	15.2	0.35	2.39	3.8	0.9918
Malathion	C10H19O6PS2	121-75-5	348 > 127	348 > 331.2	12.6	0.04	0.31	1.0	0.9989
Mandipropamid	C23H22ClNO4	374726-62-2	412 > 328	412 > 356	12.5	0.11	0.45	4.2	0.9991
Mecarbam	C10H20NO5PS2	2595-54-2	330 > 227	330 > 97	13.2	0.15	0.30	2.0	0.9992
Mepanipyrim	C14H13N3	110235-47-7	224 > 106	224 > 77	13.1	0.19	0.39	3.6	0.9993
Mepronil	C17H19NO2	55814-41-0	270 > 119	270 > 91	12.7	0.05	0.07	1.1	0.9972
Mesosulfuron-methyl	C17H21N5O9S2	208465-21-8	504 > 182	504 > 83	10.9	0.27	0.96	3.4	0.9996
Metaflumizone	C24H16F6N4O2	139968-49-3	507 > 178	507 > 287	15.1	2.63	3.42	6.6	0.9986
Metalaxyl	C15H21NO4	57837-19-1	280 > 220	280 > 192	11.3	0.04	0.06	1.9	0.9998
Metamitron	C10H10N4O	41394-05-2	203 > 175	203 > 104	7.0	0.21	0.44	2.3	0.9990
Metconazole	C17H22ClN3O	125116-23-6	320 > 70	322 > 125	14.2	0.10	0.30	3.6	0.9976
Methabenzthiazuron	C10H11N3OS	18691-97-9	222 > 165	222 > 150	11.1	0.11	0.19	0.9	0.9989
Methamidophos	C2H8NO2PS	10265-92-6	142 > 94	142 > 125	2.3	0.06	0.69	1.3	0.9991
Methiocarb	C11H15NO2S	2032-65-7	226 > 121	226 > 169	12.3	0.10	0.28	2.9	0.9948
Methiocarb sulfoxide	C11H15NO3S	2635-10-1	242 > 122	242 > 170	6.9	0.04	0.15	1.5	0.9996
Methomyl	C5H10N2O2S	16752-77-5	163 > 88	163 > 106	5.0	0.10	0.10	0.8	0.9996
Methoxyfenozide	C22H28N2O3	161050-58-4	369 > 149	369 > 313	12.7	0.50	1.00	1.7	0.9980
Metobromuron	C9H11BrN2O2	3060-89-7	259 > 148	259 > 91	10.9	0.35	0.63	3.2	0.9987
Metolachlor	C15H22ClNO2	51218-45-2	284 > 252	284 > 176	13.4	0.06	0.31	1.5	0.9962
Metolcarb	C9H11NO2	1129-41-5	166 > 109	166 > 94	9.1	0.12	0.29	2.4	0.9996
Metosulam	C14H13Cl2N5O4S	139528-85-1	418 > 175	418 > 140	10.1	0.24	0.23	2.2	0.9968
Metoxuron	C10H13ClN2O2	19937-59-8	229 > 72	229 > 156	8.7	0.04	0.30	1.4	0.9997
Metrafenone	C19H21BrO5	220899-03-6	409 > 209	409 > 227	14.4	0.09	0.10	1.3	0.9993
Metsulfuron-methyl	C14H15N5O6S	74223-64-6	382 > 167	382 > 77	9.2	0.19	0.97	1.2	0.9982
Mevinphos	C7H13O6P	7786-34-7	225 > 127	225 > 193	7.1	0.05	0.16	2.5	0.9998
Molinate	C9H17NOS	2212-67-1	188 > 126	188 > 55	12.9	2.08	1.25	3.1	0.9956
Monocrotophos	C7H14NO5P	6923-22-4	224 > 193	224 > 127	5.6	0.72	1.35	4.8	0.9991
Monuron	C9H11ClN2O	150-68-5	199 > 72	199 > 46	9.4	0.13	0.21	1.6	0.9995
Myclobutanil	C15H17ClN4	88671-89-0	289 > 70	289 > 125	12.8	0.23	0.44	2.6	0.9990
Neoquassin	C22H30O6	76-77-7	391 > 373	391 > 207	10.2	0.29	1.63	2.3	0.9970

Table 1 – Continued...

Compound	Formula	CAS	Transition 1	Transition 2	Pear extract				
					RT (min.)	Transition 1 LOD (ppb)	Transition 2 LOD (ppb)	%RSD (10ppb)	R^2
Nitenpyram	C11H15ClN4O2	120738-89-8	271 > 126	271 > 225	4.7	0.15	0.29	2.6	1.0000
Nuarimol	C17H12ClFN2O	63284-71-9	315 > 252	315 > 81	12.2	0.75	2.66	2.8	0.9990
Omethoate	C5H12NO4PS	1113-02-6	214 > 125	214 > 183	3.6	0.16	0.18	1.6	0.9998
Oxadixyl	C14H18N2O4	77732-09-3	296 > 279	296 > 219	9.0	0.25	0.26	1.7	0.9999
Oxamyl	C7H13N3O3S	23135-22-0	237 > 72	237 > 90	4.6	0.03	0.10	1.5	0.9999
Paclobutrazol	C30H40Cl2N6O2	76738-62-0	294 > 70	294 > 125	12.6	0.18	2.74	2.4	0.9982
Penconazole	C13H15Cl2N3	66246-88-6	284 > 70	284 > 159	13.9	0.17	0.20	2.6	0.9992
Pencycuron	C19H21ClN2O	66063-05-6	329 > 125	329 > 218	14.4	0.03	0.39	1.5	0.9992
Phenmedipham	C16H16N2O4	13684-63-4	318 > 168	318 > 136	11.8	0.36	0.32	1.0	0.9949
Phenthoate	C12H17O4PS2	2597-03-7	321 > 79	321 > 247	13.7	0.32	0.55	2.3	0.9993
Phorate sulfone	C7H17O5PS2	2588-04-7	293 > 171	293 > 97	11.0	0.51	0.26	3.4	0.9964
Phorate sulfoxide	C7H17O4PS2	2588-05-8	277 > 97	277 > 199	10.8	0.26	0.13	0.9	0.9979
Phosphamidon	C10H19ClNO5P	297-99-4	300 > 174	300 > 127	9.3	0.10	0.19	1.0	0.9998
Phoxim	C12H15N2O3PS	14816-18-3	299 > 77	299 > 129	14.1	0.25	0.30	2.0	0.9992
Picolinafen	C19H12F4N2O2	137641-05-5	377 > 238	377 > 145	15.2	0.26	1.38	5.4	0.9999
Picoxystrobin	C18H16F3NO4	117428-22-5	368 > 145	368 > 205	13.5	0.12	0.17	1.3	0.9994
Pirimicarb	C11H18N4O2	23103-98-2	239 > 72	239 > 182	10.8	0.05	0.10	2.1	0.9996
Pirimicarb-desmethyl	C10H16N4O2	152-16-9	225 > 72	225 > 168	8.5	0.04	0.04	1.7	0.9996
Prochloraz	C15H16Cl3N3O2	67747-09-5	376 > 308	376 > 70	14.3	0.10	0.19	2.8	0.9987
Profenofos	C11H15BrClO3PS	41198-08-7	375 > 305	375 > 347	15.0	0.30	0.38	2.6	0.9997
Promecarb	C12H17NO2	2631-37-0	208 > 109	208 > 151	12.5	0.44	0.42	3.1	0.9993
Prometryn	C10H19N5S	7287-19-6	242 > 158	242 > 200	13.1	0.07	0.08	1.6	0.9998
Propamocarb free base	C9H20N2O2	24579-73-5	189 > 102	189 > 74	3.1	0.23	0.22	1.4	0.9984
Propaquizafop	C22H22ClN3O5	111479-05-1	444 > 100	44 > 371	15.2	0.15	0.85	1.2	0.9990
Propiconazole	C15H17Cl2N3O2	60207-90-1	342 > 159	342 > 69	14.0	0.23	0.60	3.6	0.9998
Propoxur	C11H15NO3	114-26-1	210 > 111	210 > 168	9.7	0.07	0.08	2.6	0.9998
Propyzamide	C12H11Cl2NO	23950-58-5	256 > 190	258 > 192	12.7	1.83	1.94	6.0	0.9915
Prosulfuron	C15H16F3N5O4S	94125-34-5	420 > 141	420 > 167	11.7	0.43	0.82	2.0	0.9940
Prothioconazole	C14H15Cl2N3OS	178928-70-6	312 > 70	314 > 70	13.4	0.16	0.50	2.3	0.9952
Pymetrozine	C10H11N5O	123312-89-0	218 > 105	218 > 79	5.0	0.05	0.39	2.9	0.9994
Pyraclostrobin	C19H18ClN3O4	175013-18-0	388 > 194	388 > 163	14.2	0.50	1.00	1.9	0.9996
Pyrethrin I	C21H28O3	121-21-1	329 > 161	329 > 105	15.9	0.25	1.20	2.3	0.9998
Pyrethrin II	C22H28O5	121-29-9	373 > 161	373 > 133	14.6	0.70	2.27	4.2	0.9992
Pyrimethanil	C12H13N3	53112-28-0	200 > 107	200 > 82	12.3	0.10	0.50	0.9	0.9999
Pyriproxyfen	C20H19NO3	95737-68-1	322 > 96	322 > 185	15.5	0.07	0.10	0.6	0.9999
Quassia	C22H28O6	76-78-8	389 > 223	389 > 163	9.1	0.57	0.80	2.7	0.9968
Quinmerac	C11H8ClNO2	90717-03-6	222 > 204	222 > 141	6.8	0.09	0.45	1.8	0.9966
Quinoxyfen	C15H8Cl2FNO	124495-18-7	308 > 197	308 > 162	15.6	0.18	0.23	3.2	0.9998
Rimsulfuron	C14H17N5O7S2	122931-48-0	432 > 182	432 > 325	10.0	0.31	0.64	2.8	0.9989
Rotenone	C23H22O6	83-79-4	395 > 213	395 > 192	13.5	0.44	0.52	3.5	0.9976
Spinosyn A	C41H65NO10	131929-60-7	733 > 142	733 > 98	14.1	0.03	0.19	1.6	0.9997
Spinosyn D	C42H67NO10	131929-63-0	747 > 142	747 > 98	14.6	0.20	0.97	3.3	1.0000
Spiromesifen	C23H30O4	283594-90-1	388 > 273	388 > 371	15.6	0.05	0.34	2.3	0.9998
Spiroxamine	C18H35NO2	118134-30-8	298 > 144	298 > 100	11.7	0.08	0.18	2.1	0.9999
Sulcotrione	C14H13ClO5S	99105-77-8	329 > 139	329 > 69	7.5	0.70	5.00	4.3	0.9969
Tebuconazole	C16H22ClN3O	107534-96-3	308 > 70	310 > 70	13.9	0.10	0.34	2.1	0.9993

Table 1 – Continued...

Compound	Formula	CAS	Transition 1	Transition 2	Pear extract				
					RT (min.)	Transition 1 LOD (ppb)	Transition 2 LOD (ppb)	%RSD (10ppb)	R^2
Tebufenozide	C22H28N2O2	112410-23-8	353 > 133	353 > 297	13.5	0.04	0.10	1.5	0.9980
Tebufenpyrad	C18H24ClN3O	119168-77-3	334 > 117	334 > 147	15.2	0.30	0.28	0.9	0.9998
Teflubenzuron*	C14H6Cl2F4N2O2	83121-18-0	379 > 339	379 > 359	15.3	0.29	0.40	3.6	0.9973
Terbufos sulfone	C9H21O4PS3	56070-16-7	321 > 97	321 > 171	12.1	0.55	0.52	3.8	0.9956
Terbufos sulfoxide	C9H21O3PS3	10548-10-4	305 > 187	305 > 97	12.1	0.09	0.09	1.3	0.9989
Tetraconazole	C13H11Cl2F4N3O	112281-77-3	372 > 159	372 > 70	13.2	0.29	0.55	2.6	0.9950
Thiabendazole	C10H7N3S	148-79-8	202 > 175	202 > 131	8.2	2.50	2.50	1.5	0.9987
Thiacloprid	C10H9ClN4S	111988-49-9	253 > 126	253 > 90	7.9	0.10	0.50	1.0	0.9991
Thiamethoxam	C8H10ClN5O3S	153719-23-4	292 > 211	292 > 181	5.3	0.04	0.08	2.4	0.9995
Thiodicarb	C10H18N4O4S3	59669-26-0	355 > 88	355 > 108	10.6	0.08	0.18	1.1	0.9991
Thiophanate-methyl	C12H14N4O4S2	23564-05-8	343 > 151	343 > 311	9.7	0.25	0.62	1.1	0.9967
Tolfenpyrad	C21H22ClN3O2	129558-76-5	384 > 197	384 > 91	15.3	0.28	0.73	3.0	0.9983
Triadimefon	C14H16ClN3O2	43121-43-3	294 > 69	294 > 197	12.8	0.24	0.31	2.6	0.9985
Triadimenol	C14H18ClN3O2	55219-65-3	296 > 70	298 > 70	13.1	0.24	0.54	3.7	0.9982
Triasulfuron	C14H16ClN5O5S	82097-50-5	402 > 141	402 > 167	9.6	0.42	0.36	1.5	0.9993
Triazamate acid*	C11H18N4O3S	112143-82-5	287 > 198	287 > 170	10.1	0.09	0.26	4.4	0.9996
Triazophos	C12H16N3O3PS	24017-47-8	314 > 162	314 > 119	12.9	0.02	0.12	1.5	0.9992
Triclopyr*	C7H4Cl3NO3	55336-06-3	256 > 198	254 > 196	11.1	1.95	1.81	8.9	0.9969
Tricyclazole	C9H7N3S	41814-78-2	190 > 136	190 > 163	8.3	0.10	0.20	2.3	0.9993
Trifloxystrobin	C20H19F3N2O4	141517-21-7	409 > 186	409 > 145	14.6	0.02	0.05	1.2	0.9994
Triflumizole	C15H15ClF3N3O	68694-11-1	346 > 278	346 > 43	14.8	0.09	0.09	1.3	0.9996
Triflumuron*	C15H10ClF3N2O3	64628-44-0	357 > 154	357 > 176	14.2	1.76	3.12	4.6	0.9991
Triforine	C10H14Cl6N4O2	26644-46-2	435 > 390	437 > 392	11.7	0.92	3.53	4.8	0.9963
Triticonazole	C17H20ClN3O	131983-72-7	318 > 70	320 > 70	13.2	0.40	0.41	1.9	0.9993
Zoxamide	C14H16Cl3NO2	156052-68-5	336 > 187	336 > 159	14.0	0.09	0.29	1.3	0.9951
2,4-D*	C8H6Cl2O3	94-75-7	219 > 161	219 > 125	10.3	1.09	5.00	9.7	0.9980

* Negative electrospray ionisation

3.2 Rapid screening of different mobile phase compositions on signal response

The signal intensity in LCMS can be strongly influenced by the mobile phase composition. In order to optimise the signal intensity, pesticides were added into vials containing different mobile phase compositions and injected into the interface with no column installed. The Nexera auto-sampler was setup to inject an air gap both before and after the injected sample in order to prevent the sample mixing with carrier mobile phase. This approach enables a large number of potential mobile phase compositions to be screened in a short automated period of time and without the need to manually change mobile phases. Ten different mobile phase compositions were tested, including: ammonium acetate, ammonium formate, formic acid, acetic acid, and ammonium formate with formic acid in water:methanol or acetonitrile 1:1. A total of 23 different pesticides were assessed, selected to include a range of different polarities and both positively and negatively ionised compounds. The different mobile phases tested and their peak area response, relative to the highest peak area response obtained for that compound, are shown in Table 2.

As expected with multi residue methods, there was not one optimum mobile phase for all pesticides. Overall, the lowest signal was achieved for mobile phases containing water:methanol only, and the mobile phase containing water:acetonitrile 10 mM ammonium acetate. Negatively ionised compounds (fludioxinil and ioxynil) provided superior responses in water:methanol 10mM ammonium acetate, while the addition of either formic acid or acetic acid decreased response. The highest signals were typically found in 10 mM ammonium formate, 10mM ammonium acetate, and 10 mM ammonium formate with 0.1 % formic acid. The effect of methanol and acetonitrile in the mobile phase was also investigated. Comparison of 10mM ammonium formate in methanol and acetonitrile showed that intensities were typically lower with the use of acetonitrile. Similarly the use of ammonium acetate in methanol and acetonitrile presented the same trend. The same observation with regards to methanol and acetonitrile for pesticide analysis have been reported by others.[13]

Table 2 - Results of rapid mobile phase screening using flow injection analysis for 23 pesticides. All peaks areas were normalised against the maximum peak area achieved for that compound. Accordingly, 100 % indicates the highest peak area achieved and is highlighted.

Compound	H2O:MeOH	H2O:MeOH 0.05% Formic acid	H2O:MeOH 0.1% Formic acid	H2O:MeOH 0.2% Formic acid	H2O:MeOH 5mM Ammonium acetate	H2O:MeOH 10mM Ammonium acetate	H2O:MeOH 20mM Ammonium acetate	H2O:MeOH 50mM Ammonium acetate	H2O:MeCN 10mM Ammonium acetate	H2O:MeOH 10mM Ammonium formate	H2O:MeCN 10mM Ammonium formate	H2O:MeOH 0.1% Acetic acid	H2O:MeOH 0.1% Formic acid 50mM ammonium formate
Atrazine	52	**100**	99	88	52	71	66	62	48	80	50	52	87
Azinphos-methyl	14	32	32	27	75	98	87	59	26	**100**	26	30	96
Azoxystrobin	27	30	29	25	69	87	77	58	65	**100**	82	29	99
Carbendazim	66	**100**	91	92	37	42	38	32	26	71	36	64	81
Chlorantraniliprole	**100**	46	52	41	69	81	92	69	27	91	60	94	56
Cyprodinil	66	94	88	86	55	63	57	41	51	**100**	82	67	78
Difenoconazole	27	85	90	72	70	**100**	92	73	59	99	62	61	90
Fludioxinil	69	42	38	37	74	**100**	95	84	60	94	81	55	76
Imazalil	85	69	62	63	66	78	73	62	51	**100**	68	58	74
Ioxynil	**100**	47	41	43	41	60	60	51	34	62	53	55	53
Isoproturon	28	34	34	30	74	93	84	75	78	**100**	90	30	98
Metalaxyl	30	31	31	25	68	92	81	76	79	**100**	87	31	92
Myclobutanil	15	71	75	57	65	**100**	91	73	23	86	25	58	84
Pirimicarb	82	85	76	78	66	90	80	68	68	**100**	80	66	78
Pirimicarb-desmethyl	72	90	81	83	64	85	74	67	64	**100**	82	70	86
Prochloraz	38	**100**	94	89	47	65	56	45	45	61	46	64	64
Pyraclostrobin	33	32	30	27	62	78	70	55	61	**100**	82	26	93
Pyrimethanil	54	**100**	92	91	54	65	54	31	48	92	74	62	76
Tebufenozide	28	40	40	36	70	88	78	65	73	96	84	33	**100**
Thiabendazole	96	**100**	91	89	58	69	61	48	37	99	60	67	84
Thiacloprid	16	28	28	25	53	59	45	32	34	86	49	18	**100**
Thiophanate methyl	24	21	24	17	62	77	62	44	34	98	43	31	**100**
Triadimenol	17	96	**100**	81	56	88	86	74	44	79	46	66	74
Minimum	14	21	24	17	37	42	38	31	23	61	25	18	53
Maximum	100	100	100	92	75	100	95	84	79	100	90	94	100
Average	**50**	**64**	**62**	**57**	**61**	**80**	**72**	**58**	**49**	**91**	**63**	**52**	**83**

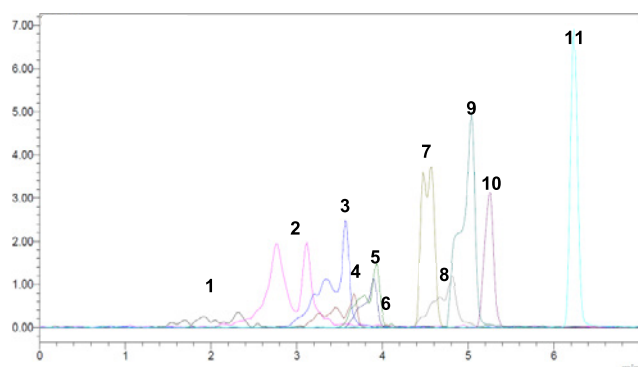## 3.3 Performance Optimising Injection Sequence (POISe)

In reversed phase UHPLC, early eluting compounds typically display the greatest peak distortion. Peak distortion is a particular problem is pesticide analysis as samples are typically extracted by QuEChERS, with samples diluted in 100% acetonitrile (a strong eluting solvent). To solve this issue, laboratories may decide to dilute the acetonitrile extracts in water before LCMS injection. However, doing so adds an additional sample preparation step and dilution in water can also negatively affect the stability of some analytes.[14]

To minimise peak dispersion with the injection of acetonitrile extracts, one potential solution is the use of a band compression technique.[15] Band compression is achieved by injecting a band of weak eluting solvent onto the column after the analytes. As the analyte and the weak eluting solvent bands travel towards the column, minute mixing occurs. Therefore, the analytes are dissolved in a weak eluting solvent when they reach the column leading to isocratic band compression.

The performance optimising injection sequence (POISe) was evaluated by injecting between 5 – 40 µL of water following a 3 µL injection of pear extract in 100% acetonitrile. This was achieved using the Nexera auto-sampler (SIL-30AC) pre-treatment program to perform this function.

Figure 1 shows the injection of pear extract *with* and *without* the performance optimising injection sequence. Using POISe, band dispersion was minimised considerably for early eluting pesticides, with peak widths reduced by 5-69%. The optimum amount of water to inject following the sample was found to be 30 µL. Increasing this volume to 40 µL did not provide any significant improvements. Early eluting compounds are affected by the injection of a weak eluting solvent band to a much larger extent in comparison to analytes with higher retention factors. This improvement is due to the reduction in the sample solvent elution strength, which has a large impact on the early eluting compounds. Whereas, analytes with higher retention factors will experience some degree of band compression in the mobile phase already. Table 3 lists the peak width for 11 early eluting compounds. Compounds are arranged in retention time order to show the improvement using the POISe on early eluting analytes**.**

(A) 3 µL pear extract injection *without* the POISe

(B) 3 µL pear extract injection *with* the POISe (30 µL water)
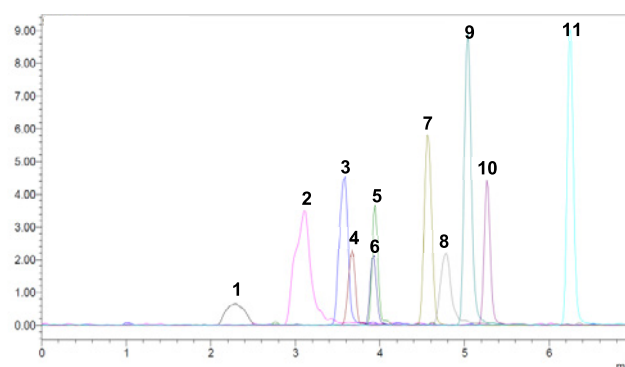
Figure 1 – Pear extract (0.050 mg kg^{-1}) injected without (A) and with (B) the performance optimising injection sequence

Table 3 – Peak widths obtained with and without the performance optimising injection sequence

No.	Compound	Peak width (min.)		Peak width change (%)
		Without POISe	*With POISe*	
1	Methamidophos	1.193	0.466	**-60.9**
2	Propamocarb	0.937	0.473	**-49.5**
3	Omethoate	0.773	0.247	**-68.0**
4	Butocarboxim sulfoxide	0.664	0.205	**-69.1**
5	Aldicarb sulfoxide	0.545	0.195	**-64.2**
6	Dinotefuran	0.460	0.247	**-46.3**
7	Oxamyl	0.317	0.248	**-21.8**
8	DMPF	0.309	0.254	**-17.8**
9	Demeton-S-methyl sulfoxide	0.418	0.271	**-35.2**
10	Demeton-S-methyl sulphone	0.277	0.248	**-10.5**
11	Ethiofencarb sulphone	0.233	0.220	**-5.6**

3.4 UHPLC gradient optimisation

Based on the results of the mobile phase screening investigation (section 3.2) the three superior compositions were tested: 1) 10 mM ammonium formate, 2) 10 mM ammonium acetate and 3) 10 mM ammonium formate with 0.1 % formic acid. Separation was achieved using a Shim-Pack XR-ODS III, 2.0 x 150 mm, 2.2 µm particle size. Ammonium formate was found to be the most effective compromise for all 210 compounds in terms of signal to noise ratios and peak shapes.

However two problems with ammonium formate were observed; early elution of asulam and poor peak shape of propamocarb. Consequently, 0.01 % formic acid was tested and found to increase the retention of asulam, and improve the peak shape of propamocarb. The addition of acid was found to shorten the retention time of cyromazine (RT 2.2 min.), yet this retention time was still in excess of 2 column volumes as required in quality control procedures for pesticide residues analysis in food and feed.[13]

A number of pesticide isomers have identical transitions and consequently must be separated chromatographically. Employing a 16 minute gradient resulted in resolution greater than 1 between all necessary pesticides including: butocarboxim sulphoxide / aldicarb sulphoxide, ethiofencarb sulphone / methiocarb sulphone, diuron / fluometronsulam and desmedipham / phenmedipham. Figure 2 highlights the excellent peak shapes achieved on the Nexera UHPLC.

3.5 Final method performance

In order to assess the performance of the LCMS-8040 for real samples, limits of detection, linearity and repeatability were determined in food extracts. Linearity was assessed from 0.5 – 200 ppb in four types of sample: (1) acetonitrile, (2) dried fruit extract, (3) lettuce extract and, (4) pear extract. All 210 pesticides achieved excellent correlation coefficients greater than 0.99 in all four types of matrix with typical values greater than 0.997. Correlation coefficients are listed in Table 1 for all pesticides in pear extract, and the calibration curves of eight selected pesticides shown in Figure 3.

Pesticide limits of detection were calculated based on the method described by the US-EPA (see experimental section). Limits of detection were assessed for both the quantifying transition and the qualifying transition and are listed in Table 1. All of the studied pesticides presented LODs less than the 0.01 mg kg^{-1} reporting level for both transition 1 and 2.

A limit of detection less than 0.001 mg kg^{-1} (1ppb) was achieved for the quantifying transition and less than 0.002 mg kg^{-1} (2 ppb) for the qualifying transition for 90 % of compounds: thereby highlighting the excellent sensitivity of the LCMS-8040 for pesticide analysis. Furthermore, these limits of detection were achieved with an injection volume of only 2 µL. Therefore, detection limits could be reduced even further with larger injection volumes. An injection volume of 2 µL was used in the study to allow the injection of 100 % acetonitrile extracts without detriment to early eluting peak shapes.

Repeatability was assessed at the 0.01 mg kg^{-1} reporting level as peak area %RSD for six replicate injections in pear extracts. Repeatability less than 5 %RSD was achieved for 92 % of the 210 pesticides studied. All of the studied compounds presented repeatability less than 10 %RSD, with exception of haloxyfop acid (13.4 %).
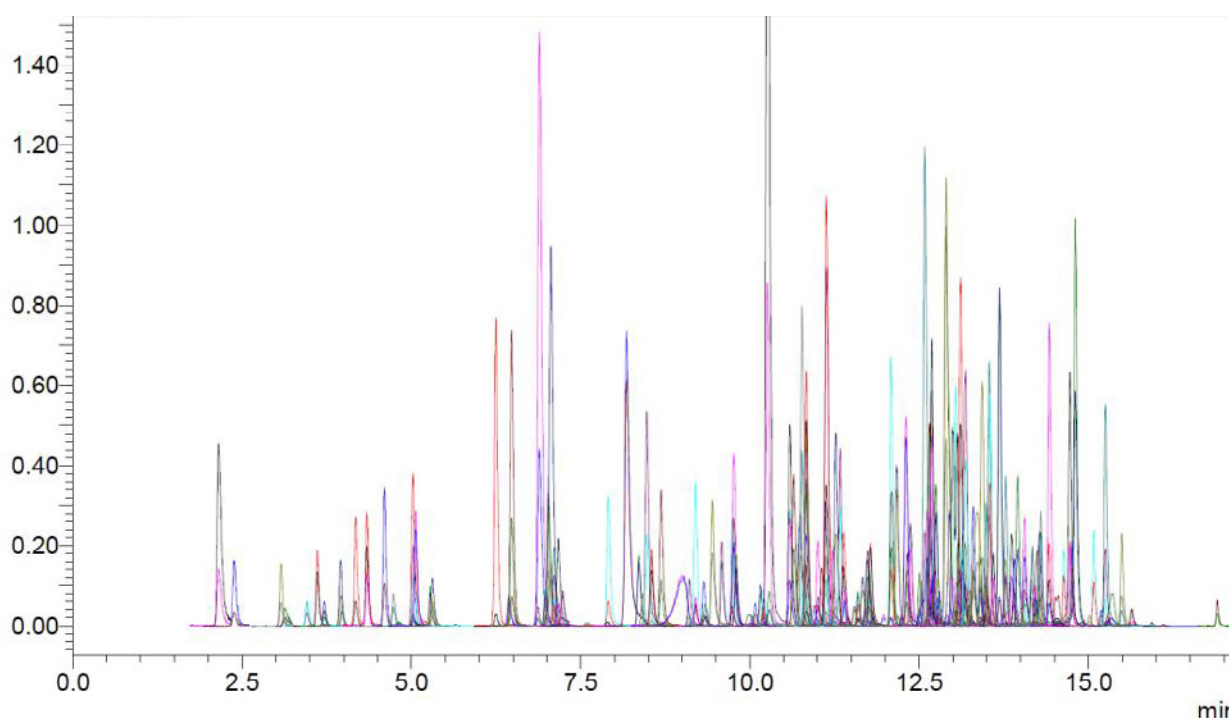
Figure 2 – *Extracted ion chromatogram of 210 pesticides using the Shimadzu Nexera UHPLC and the Shimadzu LCMS-8040; 2 µL injection of a 0.05 mg kg^{-1} standard solution.*
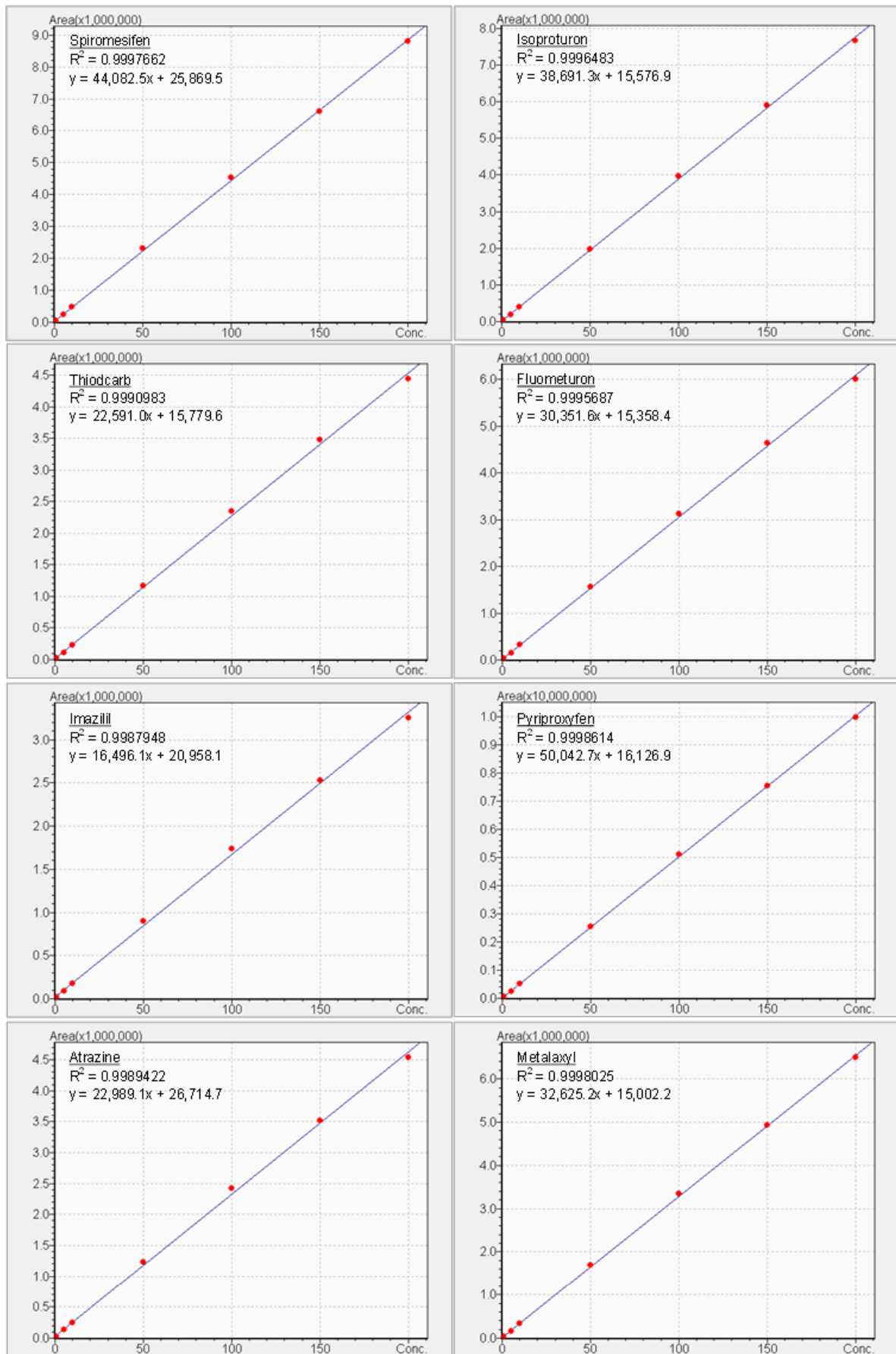
Figure 3 – *Calibration curves,* 0.5 μg kg^{-1} - 0.2 mg kg^{-1} (0.5 – 200 ppb), *of eight pesticides in pear matrix*

4. Conclusion

The results of the developed methodology show that the Shimadzu LCMS-8040 triple quadrupole can achieve excellent sensitivity, linearity and repeatability in food extracts for over 200 commonly analysed pesticides. Limits of detection were less than 0.01 mg kg^{-1} (10 ppb) for both the quantifying and qualifying transitions for all compounds studied, while for 90% of compounds was less than 0.001 mg kg^{-1} (1ppb) (quantifying transition) and 0.002 mg kg^{-1} (2 ppb) (qualifying transition); therefore providing excellent response, especially given that the injection volume was only 2µL. The sensitivity of the LCMS-8040 was able to meet the 0.01 mg kg^{-1} (10 ppb) requirements of regulatory guidelines such as those established by the EU and Japan. Repeatability at the 0.01 mg kg^{-1} reporting level was less than 5% for nearly all compounds and correlation coefficients greater than 0.99 for all compounds in a variety of food samples. Consequently the LCMS-8040 is ideally suited for routine monitoring of pesticides in regulatory laboratories.

Acknowledgements

5. References

1. H. V. Botitsi, S. D. Garbis, A. Economou and D. F. Tsipi, Mass Spectrometry Reviews 2011, 30, 907-939.

2. C. Solera, J. Mañesa and Y. Picó, Critical Reviews in Analytical Chemistry 2008, 38, 93-117.

3. Commission Regulation (EC). 2005. No 396/2005 of the European Parliament and of the Council, maximum residue levels of pesticides in or on food and feed of plant and animal origin. Official Journal of the European Union, L 70: 1-16

4. Commission Directive 2006/141/EC of 22 December 2006 on infant formulae and follow-on formulae and amending Directive 1999/21/EC. Official Journal of the European Union L401: 1-33.

5. US Environmental Protection Agency, Electronic code of federal regulation: Title 40: Part 180 - tolerances and exemptions for pesticide chemical residues in food. http://www.ecfr.gov/cgi-bin/text-idx?c=ecfr&tpl=/ecfrbrowse/Title40/40cfr180_main_02.tpl

6. Japanese Ministry of Health, Labour and Welfare, Department of Food Safety. 2006. Director Notice about Analytical Methods for Residual Compositional Substances of Agricultural Chemicals, Feed Additives, and Veterinary Drugs in Food (Syoku-An No. 0124001 January 24, 2005; amendments May 26, 2006).

7. Republic of China National Standard GB 2763-2005. 2005. Maximum residue limits for pesticides in food, Ministry of Health of the People's Republic of China and Ministry of Agriculture of the People's Republic of China.

8. Republic of China National Standard GB 28260-2011. 2011. Maximum residue limits for 85 pesticides in food, Ministry of Health of the People's Republic of China and Ministry of Agriculture of the People's Republic of China

9. L. Alder, K. Greulich, G. Kempe and B. Vieth, Mass Spectrometry Reviews 2006, 25, 838-865

10. US Environmental Protection Agency, Procedure 40 CFR, Part 136, Appendix B.

11. EURL datapool, EU Reference Laboratories, http://www.eurl-pesticides-datapool.eu

12. European Commission, SANCO. 2011. Method validation and quality control procedures for pesticide residues analysis in food and feed, Document SANCO/12495/2011

13. C. Jansson, T. Pihlström, B.-G. Österdahl and K. E. Markides, Journal of Chromatography A 2004, 1023, 93-104.

14. K. Maštovská and S. J. Lehotay, Journal of Chromatography A 2004, 1040, 259-272

15. A. C. Sanchez, J. A. Anspach and T. Farkas, Journal of Chromatography A 2012, 1228, 338-348

SHIMADZU
Excellence in Science

Application News

No.C89

LC/MS
Liquid Chromatography Mass Spectrometry

Analysis of 9 Haloacetic Acids in Tap Water Using the LCMS-8040 Triple Quadrupole Mass Spectrometer

Haloacetic acids are produced as byproducts of chlorination during water treatment purification processes. Three haloacetic acids are subject to tap water quality standards with established limits, monochloroacetic acid (MCAA: 0.02 mg/L), dichloroacetic acid (DCAA: 0.04 mg/L), and trichloroacetic acid (TCAA: 0.2 mg/L).

Historically, methods for determination of haloacetic acids required solvent extraction and methylation with diazomethane followed by GC/MS analysis. However, Japan's Ministry of Health, Labor and Welfare Notification No. 66, 2012, recently specified LC/MS (/MS) as a new, alternative analytical method for haloacetic acids. Since LC/MS (/MS) analysis permits direct sample injection without the necessity for solvent extraction and derivatization as required by the GC/MS method, a significant improvement in laboratory efficiency can be expected.[1,2]

In accordance with the method specified for LC/MS (/MS) analysis, simultaneous determination of the three specified targets in a water quality standard, together with six bromine-containing haloacetic acids, was conducted for a total of nine substances. The instrument used for analysis was the LCMS-8040 triple quadrupole mass spectrometer.

Fig. 1 shows an MRM chromatogram of a 0.001 mg/L standard solution. Calibration curve correlation coefficients (R) and peak area repeatability (%RSD, n=3) for each component are shown in Table 1. Excellent linearity was obtained for each component, and peak area repeatability at 0.001 mg/L was less than 5 %.

Quantitation of tap water and spiked tap water samples was conducted for each of the haloacetic acids. Although the test method specifies that cleanup of the test water sample be conducted if necessary when the sample contains high concentrations of anions, excellent recoveries from 90 to 110 % were obtained using direct analysis of the tap water without significant interference from contaminants (Table 2).

139.00>35.00(-)@1*20.0
172.90>82.90(-)@2
182.90>78.90(-)@3*4.00
218.90>128.90(-)@4*1.50
262.80>172.80(-)@5*0.60
206.90>116.90(-)@6*0.40
252.80>162.90(-)@7*0.60
296.80>206.80(-)@8*1.25
340.70>250.80(-)@9*2.50

Monochloroacetic acid (MCAA)   : *m/z* 139.0>35.0,   Monobromoacetic acid (MBAA)   : *m/z* 182.9>78.9,
Dichloroacetic acid (DCAA)   : *m/z* 172.9>82.9,   Bromochloroacetic acid (BCAA)   : *m/z* 218.9>128.9,
Dibromoacetic acid (DBAA)   : *m/z* 262.8>172.8,   Trichloroacetic acid (TCAA)   : *m/z* 206.9>116.9,
Bromodichloroacetic acid (BDCAA) : *m/z* 252.8>162.9,   Chlorodibromoacetic acid (CDBAA) : *m/z* 296.8>206.8,
Tribromoacetic acid (TBAA)   : *m/z* 340.7>250.8

Fig. 1 MRM Chromatograms of 9 Haloacetic Acids in a Standard Solution Mixture (0.001 mg/L)

Table 1 Calibration Curve Linearity and Peak Area Repeatability

	Correlation Coefficient R 0.001–0.2 mg/L	Area %RSD 0.001 mg/L
MCAA	0.9956	2.6
MBAA	0.9988	0.3
DCAA	0.9950	2.7
BCAA	0.9960	1.9
DBAA	0.9965	0.8
TCAA	0.9987	0.7
BDCAA	0.9991	1.2
CDBAA	0.9983	3.3
TBAA	0.9956	0.9

Table 2 Tap Water Quantitation and Spike Recovery Results

	Tap Water Sample Concentration mg/L	Recovery % (Spiked at 0.001 mg/L)
MCAA	N.D.	92
MBAA	N.D.	102
DCAA	Tr.	109
BCAA	N.D.	104
DBAA	Tr.	99
TCAA	0.0031	105
BDCAA	00.0017	103
CDBAA	0.00034	105
TBAA	Tr.	98

N.D.: Not Detected, Tr.: Trace Level
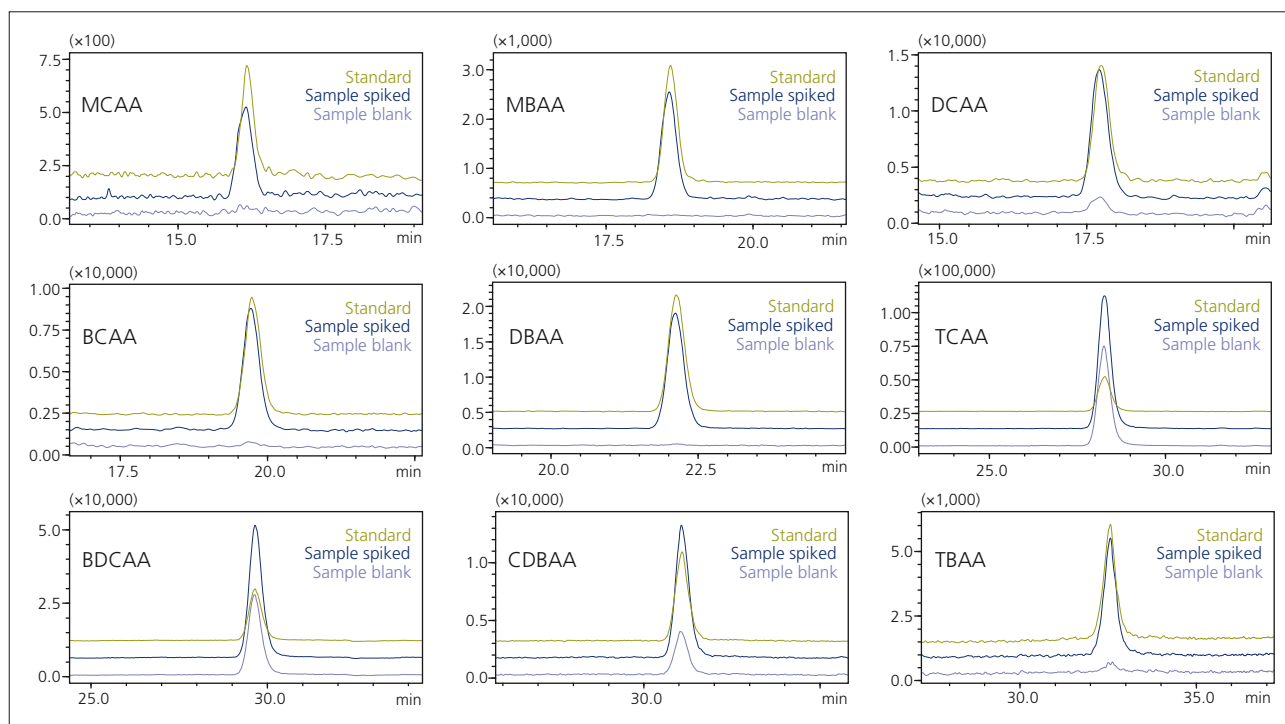
Fig. 2 MRM Chromatograms of Haloacetic Acid Standard Solution (0.001 mg/L), Tap Water Blank, and Haloacetic Acid-Spiked Sample (0.001 mg/L each)

Table 3 Analytical Conditions

Column	: CAPCELL PAK MGⅢ (150 mm L. × 4.6 mm I.D., 3 µm)
Mobile Phases	: A: 0.2 % Formic acid-water, B: Methanol
Time Program	: 5 %B (0 min)→100 %B (38 min) →5 %B (38.01-50 min)
Flowrate	: 0.2 mL/min
Injection Volume	: 50 µL
Column Temperature	: 30 °C
Probe Voltage	: -3.5 kV (ESI-negative mode)
DL Temperature	: 150 °C
Block Heater Temperature	: 400 °C
Nebulizing Gas Flow	: 1.5 L/min
Drying Gas Flow	: 15 L/min
DL Voltage/Q-array Voltage	: Using default values
MRM Transition	: MCAA m/z 139.0>35.0, MBAA m/z 182.9>78.9, DCAA m/z 172.9>82.9, BCAA m/z 218.9>128.9, DBAA m/z 262.8>172.8, TCAA m/z 206.9>116.9, BDCAA m/z 252.8>162.9, CDBAA m/z 296.8>206.8, TBAA m/z 340.7>250.8

[References]
1) Maiko Tahara, Naoki Sugimoto, Reiji Kubota, Tetsuji Nishimura: Establishment of Direct Quantitation Method of Haloacetic Acids in Tap Water Using Liquid Chromatograph/Mass Spectrometer, Journal of the Japan Water Works Association, 907, 18-22 (2010).
2) Maiko Tahara, Reiji Kubota, Norihiro Kobayashi, Taku Tsukamoto, Naoki Sugimoto, Tetsuji Nishimura: Verification of Quantitative Accuracy of the LC/MS/MS and LC/MS Analysis of Haloacetic Acids in Tap Water in the Presence of Anions, Journal of the Japan Water Works Association, 931, 20-27 (2012).

SHIMADZU

Shimadzu Corporation

www.shimadzu.com/an/

![SHIMADZU Excellence in Science]

Application News

No.C95

Liquid Chromatography Mass Spectrometry

Analysis of Haloacetic Acids in Drinking Water Using Triple Quadrupole LC/MS/MS (LCMS-8050)

Haloacetic acids (HAAs), by-products of water disinfection, are formed from naturally occurring organic and inorganic materials in water which react with the disinfectants chlorine and chloramine. The Japanese Ministry of Health, Labour and Welfare has established criterion values for three of these substances, monochloroacetic acid (MCAA: 0.02 mg/L), dichloroacetic acid (DCAA: 0.04 mg/L), and trichloroacetic acid (TCAA: 0.2 mg/L). The official analytical method for measuring these haloacetic acids utilizes solvent extraction and diazomethane derivatization prior to GC/MS quantitation.

In April, 2012, this method was amended to include LC/MS/MS as an additional method for measuring haloacetic acids. These LC/MS methods, which permit analysis of HAAs directly from water samples, offer greater sample throughput by eliminating the solvent extraction and derivatization steps required when using GC/MS. This Application News introduces the use of the LCMS-8050 triple quadrupole mass spectrometer for analysis of these HAAs in accordance with the official LC/MS methodology requirements.

In this high speed method, MCAA, DCAA, and TCAA are eluted at 3.1, 3.4, and 5.2 minutes, respectively. Fig. 1 shows an MRM chromatogram of these HAAs each at a concentration of 0.001 mg/L. The calibration curve in Fig. 2 demonstrates linearity from 0.001 to 0.1 mg/L for each substance, and peak area repeatability at 0.001 mg/L (less than 1/10 the criterion value) (n=5), which was less than 3 % (%RSD).
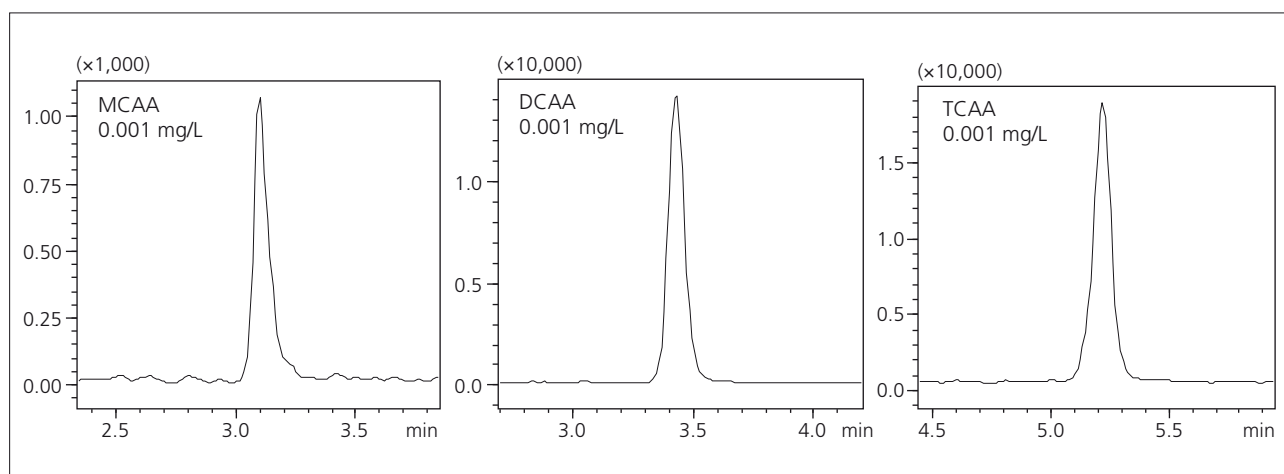
Fig. 1 MRM Chromatograms of MCAA, DCAA and TCAA (0.001 mg/L)
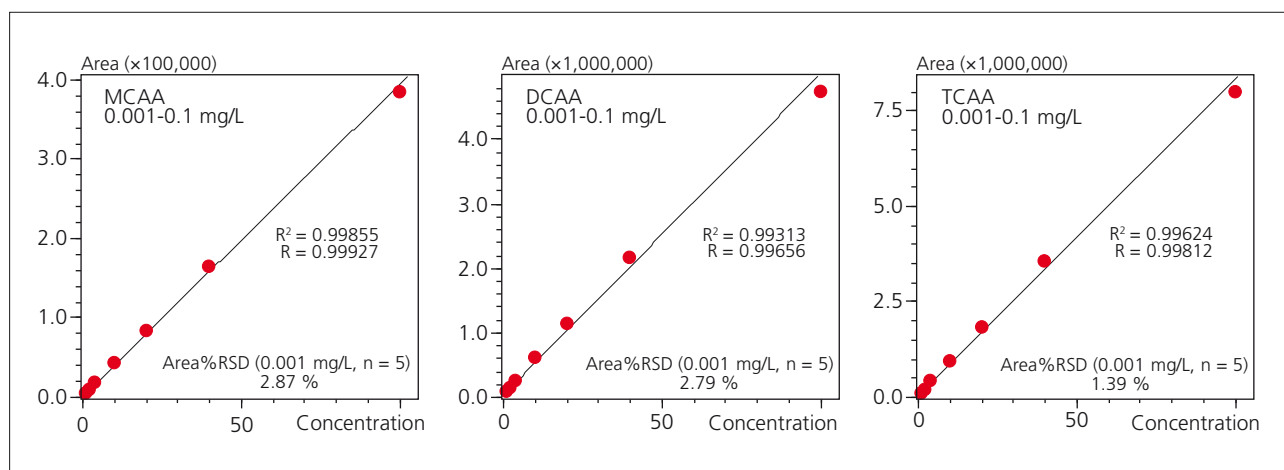
Fig. 2 Calibration Curve Linearity and Peak Area Repeatability

Quantitation and spike and recovery testing of haloacetic acids in tap water were conducted. To reduce residual chlorine in the tap water, sodium ascorbate was added at a ratio of 2 mg/100 mL. Fig. 3 shows MRM chromatograms obtained from tap water spiked with the three HAAs, each at 0.001 mg/L. The recovery rate was determined using the average area value obtained in five repeat measurements. The official method specifies that anions present at high concentrations in the test water must be reduced "as needed." However, during these analyses, no anion contamination-related interference was observed.
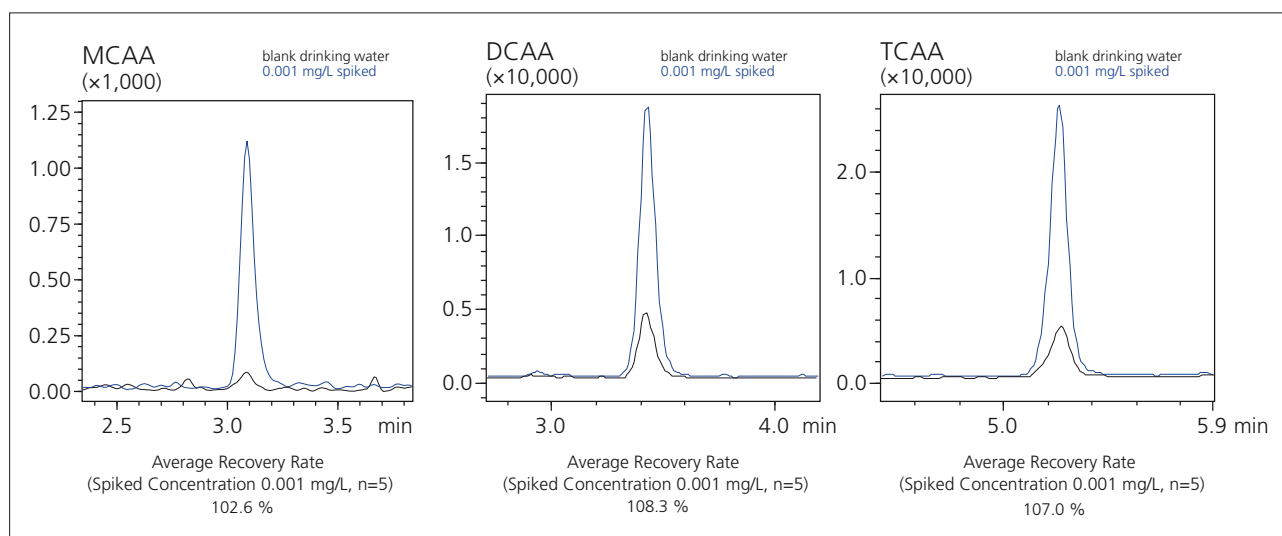
Fig. 3 MRM Chromatograms of Drinking Water Blank and Spiked with MCAA, DCAA and TCAA Respectively (0.001 mg/L)

The spike and recovery testing was conducted using tap water samples collected from four different regions (Samples 1 to 4). The results indicated no dependence on the water sampling region, with recoveries ranging from 90 to 110 % from each collection location (see Table 1). Further, the concentrations of haloacetic acids detected were all below the criterion value.

Table 1 Quantitation and Recovery Results for Tap Water Samples

	Sample 1		Sample 2		Sample 3		Sample 4	
	Sample Conc. (mg/L)	Recovery (%)	Sample Conc. (mg/L)	Recovery (%)	Sample Conc. (mg/L)	Recovery (%)	Sample Conc. (mg/L)	Recovery (%)
MCAA	Tr.	102.6	0.00076	103.6	0.00069	94.9	0.00034	100.4
DCAA	Tr.	108.3	0.01151	101.7	0.00742	102.9	0.00635	92.3
TCAA	Tr.	107.1	0.00861	107.2	0.00622	104.5	0.00452	102.9

Table 2 Analytical Conditions

Column	: CAPCELL PAK MGIII (150 mm L. × 3 mm I.D., 3 μm)
Mobile Phases	: A 0.2 % Formic acid-water
	: B 0.2 % Formic acid-methanol
Flowrate	: 0.5 mL/min
Column Temperature	: 50 ℃
Injection Volume	: 25 μL
Probe Voltage	: -3.5 kV (ESI-negative mode)
DL Temperature	: 150 ℃
Block Heater Temperature	: 100 ℃
Interface Temperature	: 100 ℃
Nebulizing Gas Flow	: 3 L/min
Drying Gas Flow	: 5 L/min
Heating Gas Flow	: 15 L/min
MRM Transition	: MCAA; m/z 93.00 > 35.00
	DCAA; m/z 126.90 > 82.90
	TCAA; m/z 161.10 > 116.90

Shimadzu Corporation

www.shimadzu.com/an/

![SHIMADZU Excellence in Science]

Application News

No.C96

Liquid Chromatography Mass Spectrometry

Analysis of Phenols in Drinking Water Using Triple Quadrupole LC/MS/MS (LCMS-8040)

Phenols can be formed as wastewater purification and disinfectant by-products, and Japan's Ministry of Health, Labour and Welfare have designated six phenols, including phenol, 2-chlorophenol, 4-chlorophenol, 2,4-dichlorophenol, 2,6-dichlorophenol, and 2,4,6-trichlorophenol as subject to water quality standards requirements. The method designated (by the ministry notification) for analysis of these six phenol components is solid-phase extraction – derivatization – GC/MS.

Here, we introduce an example of phenol analysis by UHPLC/MS/MS. Unlike the use of GC/MS for this analysis, LC/MS/MS does not require derivatization, and therefore simplifies the analysis process[1), 2)].

■ UHPLC/MS/MS Analysis

Sample pretreatment was conducted using the same solid phase extraction procedure as that designated in the notification (solid-phase extraction – derivatization – GC/MS) (Fig. 2). For the solid phase column, an N-containing poly (styrene-divinylbenzene-methacrylic acid) copolymer was used.

Fig. 1 shows the results obtained from measurement of a standard solution containing 0.4 µg/L of each of the six analytical target substances. Since the test water sample concentration is increased 50-fold using solid phase extraction, the equivalent concentration in the test water becomes 0.008 µg/L. Table 1 shows the linearity of the calibration curves over a concentration range equivalent to 0.008 to 1 µg/L in the test water sample, and the repeatability using a concentration of 0.008 µg/L. Excellent linearity and repeatability were obtained with respect to all of the components.
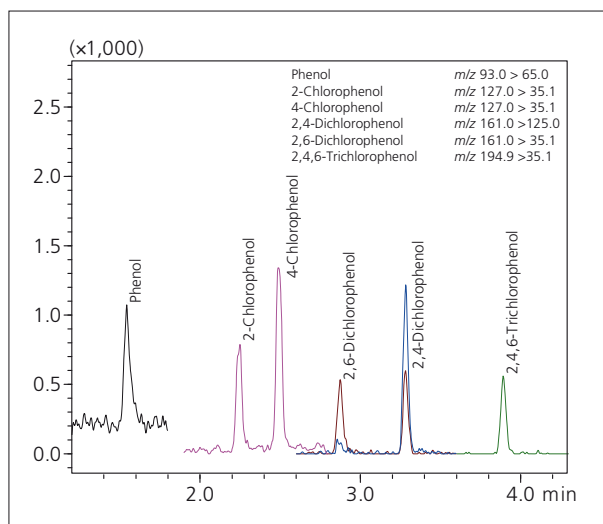
Fig. 1 Mass Chromatograms (MRM) of Phenols

Phenol	m/z 93.0 > 65.0
2-Chlorophenol	m/z 127.0 > 35.1
4-Chlorophenol	m/z 127.0 > 35.1
2,4-Dichlorophenol	m/z 161.0 >125.0
2,6-Dichlorophenol	m/z 161.0 > 35.1
2,4,6-Trichlorophenol	m/z 194.9 >35.1

Fig. 2 Pretreatment Flow

Step	Description
Sample, 500 mL	Adjusted to pH 2 with hydrochloric acid
InertSep PLS-3 230 mg	Conditioning Methanol, 5 mL Distilled water, 5 mL
Washing	Distilled water, 5 mL
Dewatering	Drying gas flow, 10 min
Elution	Methanol, 2 mL
Adjust volume	Adjust to 10 mL using water
Analysis	

Table 1 Calibration Curves and Repeatability

	Injection Sample Concentration (µg/L)	Test Water Sample Concentration (µg/L)	Coefficient of Determination R²	Area Repeatability %RSD (Calibration point minimum concentration)
Phenol	0.4 – 50	0.008 – 1	0.99938	7.4
2-Chlorophenol	0.4 – 50	0.008 – 1	0.99967	4.5
4-Chlorophenol	0.4 – 50	0.008 – 1	0.99960	5.0
2,4-Dichlorophenol	0.4 – 50	0.008 – 1	0.99966	3.9
2,6-Dichlorophenol	0.4 – 50	0.008 – 1	0.99960	7.0
2,4,6-Trichlorophenol	0.4 – 50	0.008 – 1	0.99960	7.8

■ Spike and Recovery Test for Drinking Water

Using this analytical method, we conducted spike and recovery testing of the phenols in tap water. Fig. 3 shows mass chromatograms (MRM) of a blank tap water sample subjected to pretreatment, and a test water sample spiked with six different phenol compounds, each at a concentration equivalent to 0.08 µg/L in the test sample. These spike concentrations were approximately equivalent to 1/10 the reference values of the phenols (in terms of the amount of phenol, 0.005 mg/L or less). Regarding the tap water samples analyzed here, there was no indication of significant interference due to contaminating components (Fig. 3). In addition, good recoveries were obtained, ranging between and 90 to 110 % (Table 2).
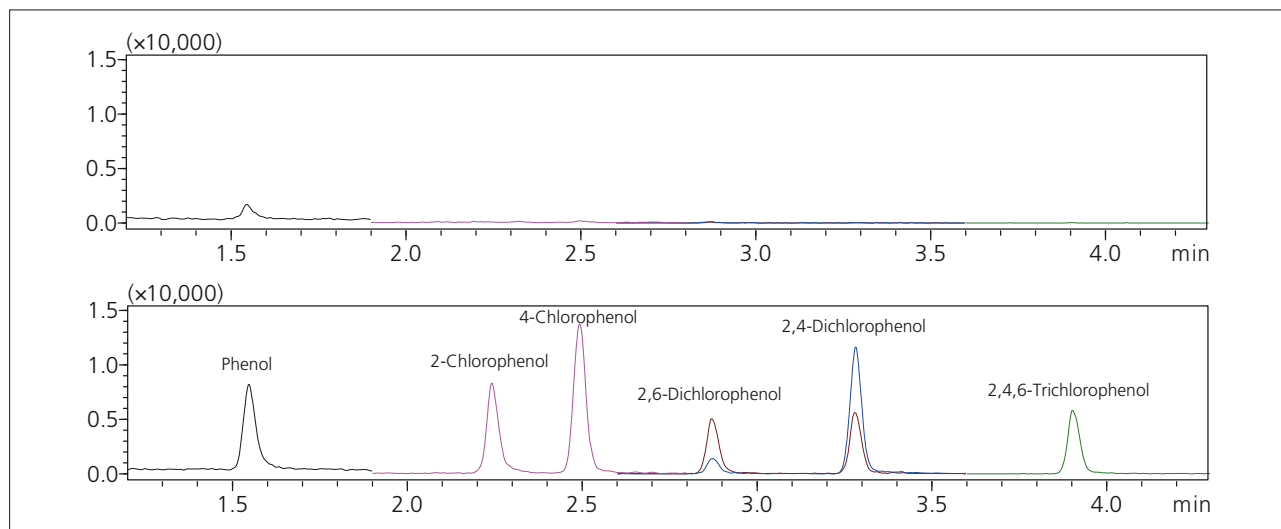
Fig. 3 Mass Chromatograms (MRM) of Drinking Water (Upper: Blank, Lower: 0.08 µg/L spiked)

Table 2 Results of Spike and Recovery Test (n=5)

	Recovery % (Corresponding to 0.08 µg/L)	Recovery % (Corresponding to 0.4 µg/L)
Phenol	103.7	99.6
2-Chlorophenol	104.8	100.1
4-Chlorophenol	104.1	100.2
2,4-Dichlorophenol	104.6	100.4
2,6-Dichlorophenol	102.0	100.3
2,4,6-Trichlorophenol	105.6	99.3

Table 3 Analytical Conditions

Column	: InertSustain C18 HP (100 mm L. × 2.1 mm I.D., 3 µm)
Mobile Phases	: A) Water
	: B) Methanol
Flowrate	: 0.5 mL/min
Time Program	: B conc. 40 % (0 min) – 95 % (4.8 – 5.4 min) – 40 % (5.41 – 7.5 min)
Column Temperature	: 40 °C
Injection Volume	: 50 µL
Probe Voltage	: -3.5 kV (APCI-negative mode)
DL Temperature	: 200 °C
Block Heater Temperature	: 200 °C
Interface Temperature	: 350 °C
Nebulizing Gas Flow	: 3 L/min (Air)
Drying Gas Flow	: 5 L/min (N$_2$)
MRM Transition	: Phenol: m/z 93.0 > 65.0, 2-Chlorophenol: m/z 127.0 > 35.1, 4-Chlorophenol: m/z 127.0 > 35.1, 2,4-Dichlorophenol: m/z 161.0 > 125.0, 2,6-Dichlorophenol: m/z 161.0 > 35.1, 2,4,6-Trichlorophenol: m/z 194.9 > 35.1

[References]
1) Reiji Kubota, Norihiro Kobayashi, Maiko Tahara, Naoki Sugimoto, Yoshiaki Ikarashi: Investigation of the Analytical Method for Phenols and Chlorophenols in Tap Water by Solid-Phase Extraction - LC/MS; The 22nd Annual Conference and Symposium of Japan Society for Environmental Chemistry (JEC), p.586-587 (2013)
2) Reiji Kubota, Norihiro Kobayashi, Kaori Saito, Nobuhiro Saito, Toshiya Suzuki, Yuki Kosugi, Minako Tanaka, Taku Tsukamoto, Hiroshi Hayashida, Tatsuya Hirabayashi, Isoaki Yamamoto, Yoshiaki Ikarashi: Validity Assessment of Phenols Investigation Method by Solid-Phase Extraction - LC/MS; The 23rd Annual Conference and Symposium of Japan Society for Environmental Chemistry (JEC), p.126-127 (2014)

First Edition: Sep. 2014

SHIMADZU

Shimadzu Corporation

www.shimadzu.com/an/

![SHIMADZU — Excellence in Science]

Application News

Liquid Chromatography Mass Spectrometry

Analysis of Diarrhetic Shellfish Toxin Using Triple Quadrupole LC/MS/MS (LCMS-8050)

No.C104

The Japanese Ministry of Health, Labour and Welfare (JMHLW) specified in July, 1980 that the mouse bioassy (MBA) be used as the official method for diarrhetic shellfish toxin, and that the permissible exposure limit be 0.05 MU per gram of edible shellfish*⁾. Shellfish in which the toxin exceeds this limit are prohibited from being sold at market according to the Japanese Food Sanitation Law Article 6, Item 2.

Due to significant technological advances since 1980, the sensitivity and accuracy obtained using the MBA method are significantly inferior compared to the high-precision, high-sensitivity possible using liquid chromatography mass spectrometry analytical instrumentation, which is currently used for this application. A complete transition to instrumental analysis for lipophilic marine biotoxins is scheduled to be implemented by January 2015 throughout the EU.

Based on this international trend, the JMHLW is currently considering migration to an instrumental analysis assay and setting new reference values to be used with instrumental analysis, in addition to the introduction of the Codex standard for okadaic acids (OA, Reference 1).

Table 1 CODEX Standard 292-2008

	Reference Value
OA Acids (OA and DTX group)	**Permissible ingestion limit of 0.16 mg OA per kg of edible shellfish**

Fig. 1 shows examples of LC/MS/MS high-sensitivity analysis of okadaic acid (OA), dinophysistoxin 1 (DTX1) and pectenotoxins (PTX1, 2, 6) and yessotoxin 1 (YTX1). Thus, it is possible to conduct high-sensitivity, high-separation analysis of each component.

Fig. 2 and Fig. 3 show MRM chromatograms of standard samples of OA and DTX1, respectively.

* The amount of toxin resulting in the death of two out of three mice following intraperitoneal administration of the equivalent of 20 g per edible shellfish.
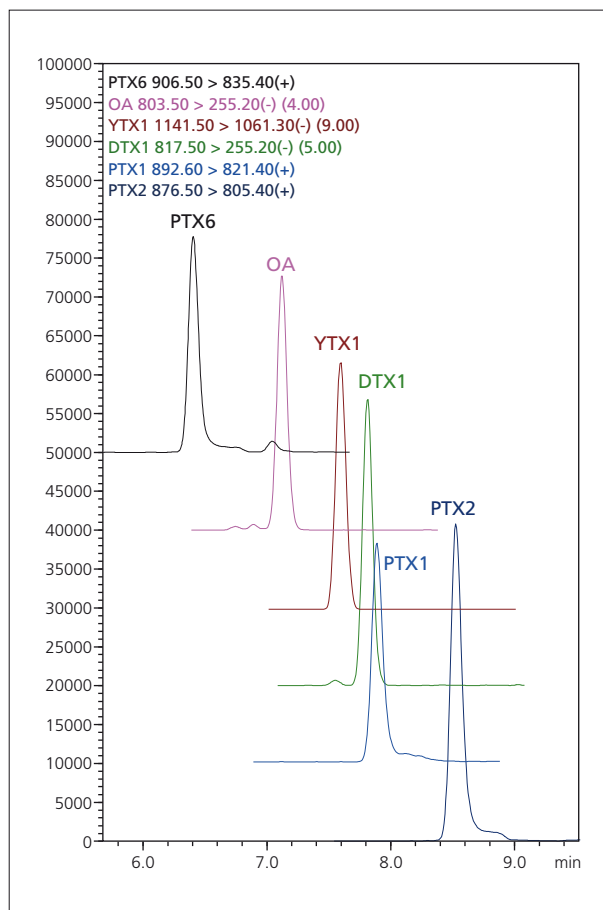
Fig. 1 MRM Chromatograms of Diarrhetic Shellfish Toxin (1 ng/mL)
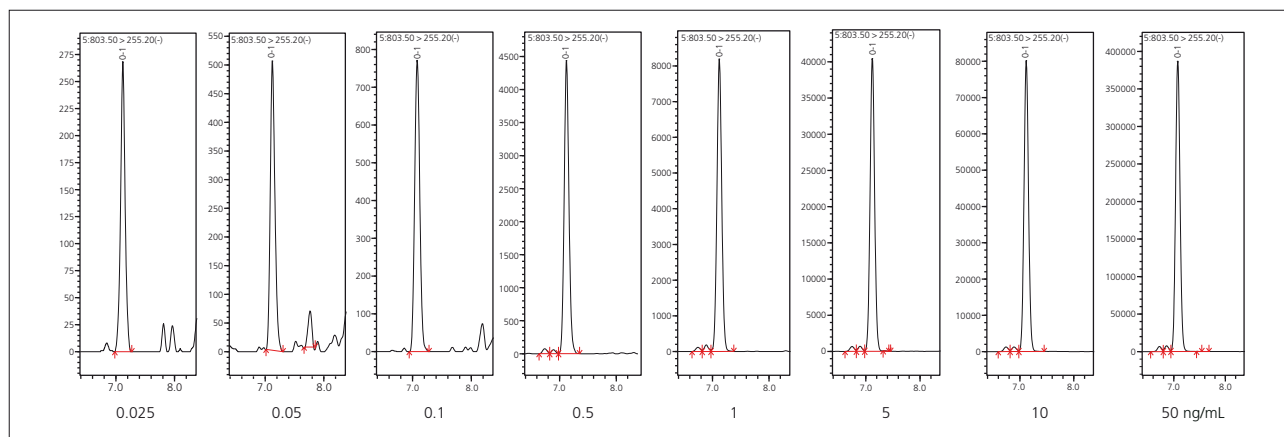
Fig. 2 MRM Chromatograms of Okadaic Acid (OA)
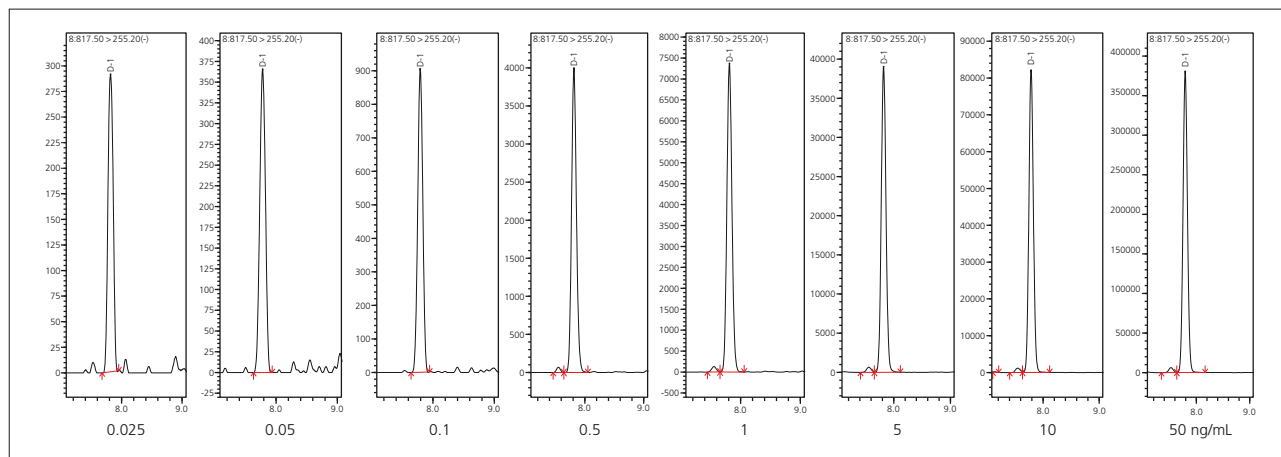
Fig. 3 MRM Chromatograms of Dinophysistoxin 1 (DTX1)

In addition, the calibration curves of OA and DTX1 are shown in Fig. 4. In both cases, the coefficient of determination R^2 was greater than 0.9999, indicating excellent linearity. Comparable linearity was also obtained for the other four substances.

Thus, instrumental analysis of shellfish by LC/MS/MS offers high sensitivity and accuracy, making it a highly effective analytical method. For this reason it is attracting attention as an alternative to the traditional MBA method.
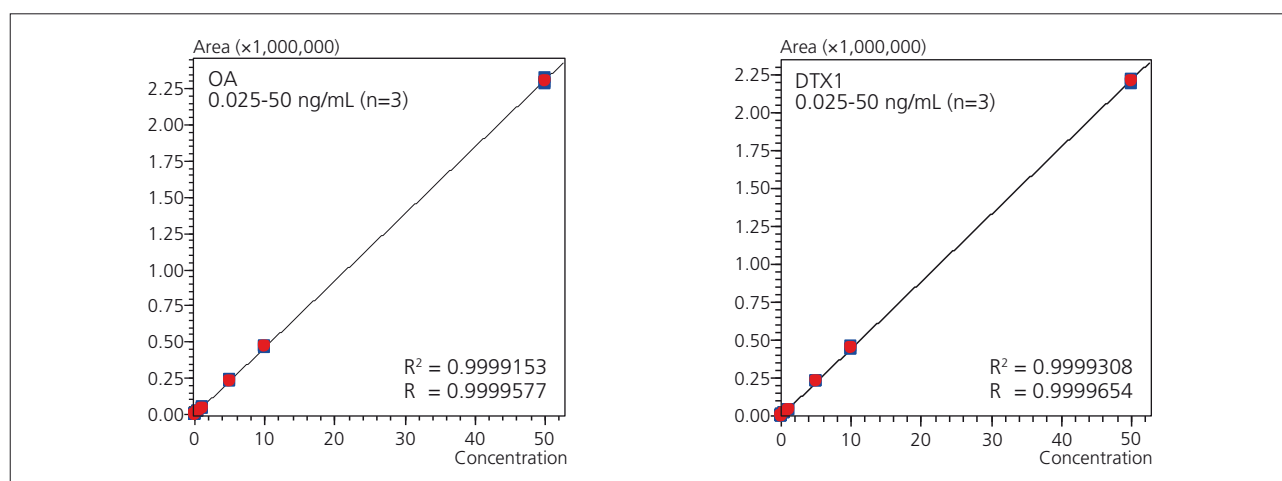
Fig. 4 Calibration Curves of OA and DTX1

Table 2 Analytical Conditions

Column	: InertSustain C8 (50 mm L. × 2.1 mm I.D., 3 μm)
Mobile Phases	: A 2 mmol/L Ammonium Formate – Water (pH adjusted to 8.5 with ammonia water)
	: B Methanol
Time Program	: 20 %B (0 min) – 100 %B (10 min) – 20 %B (10.01 min) – STOP (15 min)
Flowrate	: 0.2 mL/min
Column Temperature	: 40 ℃
Injection Volume	: 10 μL
Probe Voltage	: +4.0 kV/-3.0 kV (ESI-positive / negative mode)
DL Temperature	: 200 ℃
Block Heater Temperature	: 400 ℃
Interface Temperature	: 350 ℃
Nebulizing Gas Flow	: 3 L/min
Drying Gas Flow	: 10 L/min
Heating Gas Flow	: 10 L/min
MRM Transition	: (+) PTX6 906.50 > 835.40, PTX1 892.60 > 821.40, PTX2 876.50 > 805.40
	: (-) OA 803.50 > 255.20, YTX1 1141.50 > 1061.30, DTX1 817.50 > 255.20

The diarrhetic shellfish toxin standards were provided courtesy of Dr. Toshiyuki Suzuki of the Japanese National Research Institute of Fisheries Science.

Reference 1: July, 2014, Food Safety Commission of Japan "Natural Poison Evaluation Report – Okadaic Acid Group Among Bivalves"
        http://www.fsc.go.jp/fsciis/evaluationDocument/list?itemCategory=009

SHIMADZU

Shimadzu Corporation

www.shimadzu.com/an/

SHIMADZU
Excellence in Science

Application News

No.C105

Liquid Chromatography Mass Spectrometry

Analysis of Sulfamic Acid in Fertilizers Using LC/MS (LCMS-2020)

Sulfamic acid, due to its plant growth inhibiting effects, is subject to maximum limits in fertilizers as specified in the official standard[1] for ordinary fertilizers according to the Japanese Fertilizers Regulation Act. According to the Testing Methods for Fertilizers[2] supervised by Japan's Food and Agricultural Materials Inspection Center (FAMIC), the ion chromatography (IC) method is specified as the test method for sulfamic acid in ammonium sulfate. It has been reported, however, that when applying this IC method with byproduct compound fertilizer (fertilizer produced by concentrating and drying liquid byproducts obtained from fermentation plants involved in amino acid production, etc.) samples that contain large amounts of organic matter, it is difficult to separate the sulfamic acid peaks from contaminant peaks generated from sample matrix.[3]

In this application, we investigated the analytical conditions for LC/MS that would permit acquisition of mass information and provide high selectivity in order to eliminate the effects of contaminating components. The LCMS-2020 single quadrupole mass spectrometer was used for the analysis.

Good quantitative results were obtained, confirming the applicability of this method using byproduct compound fertilizer as the actual sample.

■ Analysis of Standard Solution

Table 1 shows the analytical conditions, and Fig. 1 shows chromatogram obtained using a standard solution (0.1 mg/L aqueous solution) of sulfamic acid.

As retention of a zwitterionic compound such as sulfamic acid is difficult using reversed phase conditions, we adopted conditions using a HILIC column. Isocratic analysis was conducted using a mobile phase consisting of acetonitrile / ammonium formate + formic acid (pH 3.2).

Applying the LC/MS method (ESI-Negative), we conducted selected ion monitoring (SIM) analysis using the deprotonated molecule at *m/z* 95.9. Fig. 2 shows the calibration curve. Excellent linearity was obtained over the entire concentration range of 0.001 to 0.1 mg/L, with a correlation coefficient greater than 0.999.
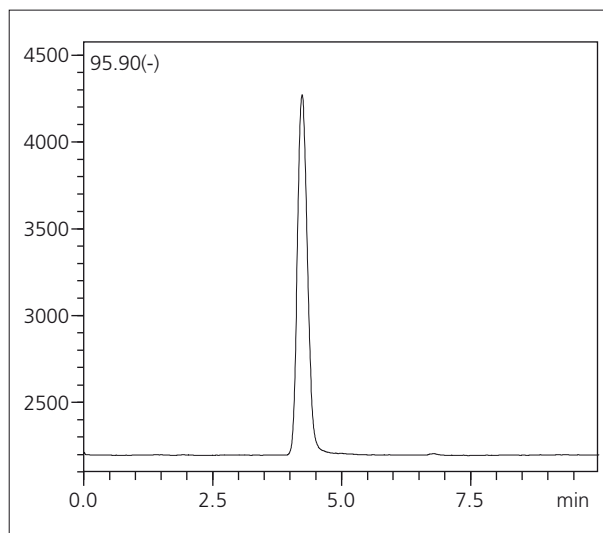
Fig. 1 Mass Chromatogram (SIM) of Sulfamic Acid (0.1 mg/L)

$R = 0.9991732$
$R^2 = 0.9983472$

Area % RSD (0.001 mg/L, n=5) 2.72 %
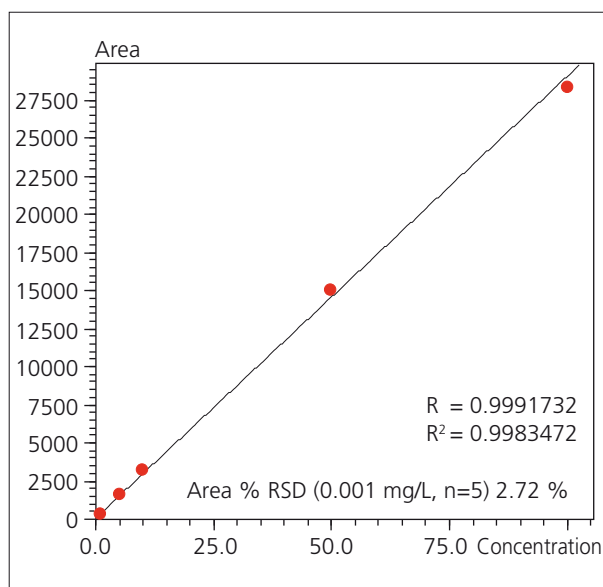
Fig. 2 Calibration Curve (0.001 – 0.1 mg/L)

Table 1 Analytical Conditions

Column	: Phenomenex Luna HILIC 20A (100 mm L. × 2.0 mm I.D., 5 µm)
Mobile Phases	: Acetonitrile/100 mmol/L Ammonium Formate+ Formic Acid (pH 3.2) = 90:10, v/v
Flowrate	: 0.2 mL/min
Column Temperature	: 40 ℃
Injection Volume	: 1 µL
Probe Voltage	: -3.5 kV (ESI-negative mode)
DL Temperature	: 250 ℃
Block Heater Temperature	: 400 ℃
Nebulizing Gas Flow	: 1.5 L/min
Drying Gas Flow	: 15 L/min
Monitoring Ion (SIM)	: *m/z* 95.9

■ Analysis of Sulfamic Acid in Fertilizers

We verified the applicability of the LC/MS method using a byproduct compound fertilizer as an actual sample. The permissible content level of sulfamic acid is set based on the total amount of the principal component in each type of fertilizer. Here, taking the lower limit of quantitation of sulfamic acid in fertilizer as 1/5 the value of the minimum concentration permissible (sulfamic acid concentration 0.005 % per principal component 1 %), we conducted spike and recovery testing using a spike quantity equivalent to the lower limit of quantitation.

Fig. 3 shows the sample pretreatment procedure. The extraction method conforms to the Testing Methods for Fertilizers (2013) supervised by FAMIC. After weighing out 1 g of byproduct compound fertilizer, extraction was conducted using 100 mL of water, and after further diluting this 100 to 1 with water, the mixture was filtered to complete preparation of the fertilizer measurement solution.

As the total quantity of the principal component represented 5 % of the fertilizer content, the concentration of sulfamic acid corresponding to the lower limit of quantitation is calculated as 50 mg/kg of fertilizer. In the spike and recovery test, 0.5 mL of 100 mg/L standard sample was added to the fertilizer, and after letting the mixture stand for 30 minutes, a measurement solution was prepared using the same procedure. The concentration of sulfamic acid in the measurement solution is therefore 0.005 mg/L.

Representative chromatograms are shown in Fig. 4 including chromatograms of the standard sample (0.005 mg/L), the sample spiked with sulfamic acid, and the byproduct compound fertilizer measurement solution. Table 2 shows the analytical results. Sulfamic acid was not detected in the byproduct compound fertilizer, nor were there any noticeable peaks associated with contaminant components.

In the spike and recovery test, excellent results were obtained in continuous analysis (n=5), with an average recovery rate of 101 %. The LC/MS method investigated here in the analysis of highly contaminated byproduct compound fertilizer was demonstrated to permit quantitation by simply adding a dilution step following extraction, as opposed to the IC method which requires tedious processing to address the issue of high-contaminant content.
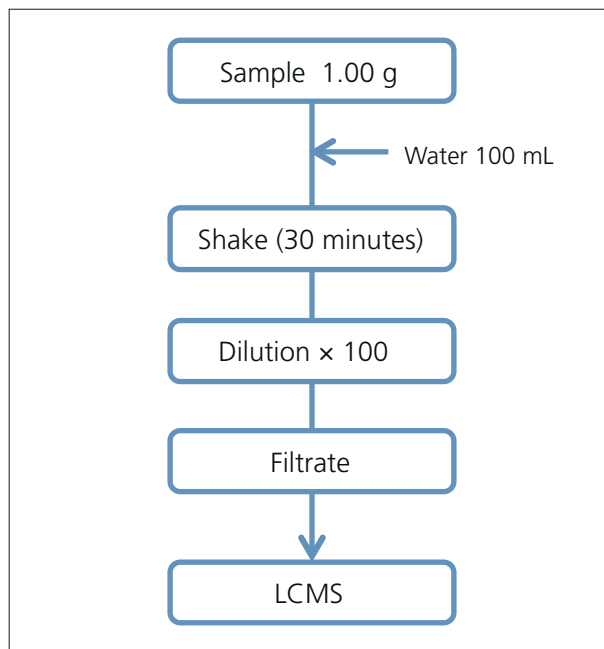
Fig. 3 Preparation Flow
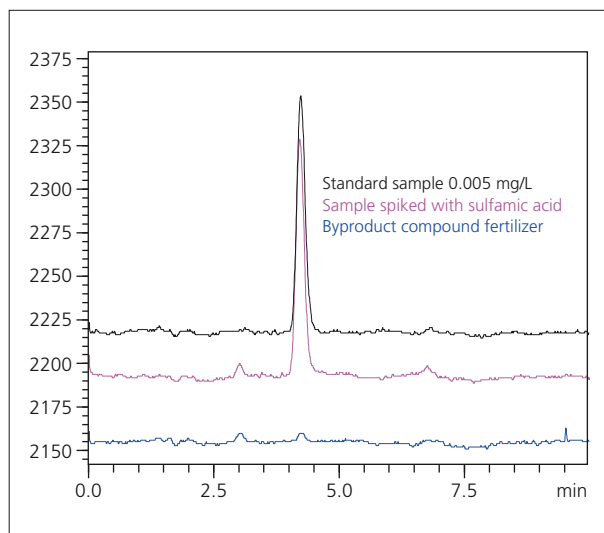
Fig. 4 SIM Chromatograms of STD and Fertilizer Sample

Table 2 Repeatability of Peak Area and Retention Time in Spike and Recovery Test

	R.t (min)	Peak Area	Recovery (%)
1st	4.217	1564	103
2nd	4.252	1561	102
3rd	4.229	1508	99
4th	4.224	1511	99
5th	4.219	1534	100
Ave	4.228	1535	101
%RSD	0.336	1.735	

[References]
1) Notification Regarding Determination of the Official Standard for Ordinary Fertilizer Based on the Fertilizers Regulation Act, February 22, 1986, the Japan's Ministry of Agriculture, Forestry and Fisheries Notification No. 284, Final Revision December 5, 2013 the Ministry of Agriculture, Forestry and Fisheries Notification No. 2939 (2013)
2) Food and Agricultural Materials Inspection Center (FAMIC): Testing Methods for Fertilizers
< http://www.famic.go.jp/ffis/fert/sub9.html >
3) Hiroi T., Shirai Y.: Simultaneous Determination of Sulfamic Acid and Ammonium Thiocyanate in Ammonium Sulfate by Nonsuppressed Ion Chromatography, Research Report of Fertilizer, 5, 1 – 12 (2012)

SHIMADZU

Shimadzu Corporation

www.shimadzu.com/an/

SHIMADZU
Excellence in Science

Application News

Liquid Chromatography Mass Spectrometry

Application of Direct Analysis in Real Time (Part 1) Rapid Analysis of Fatty Acids and Amino Acids in Food Using LCMS-2020

No.C108

DART (Direct Analysis in Real Time) is a method which permits direct ionization of the sample, and when used in combination with a mass spectrometer, analysis of the target compound can be conducted quickly without the need for pretreatment. Furthermore, analysis is possible regardless of the sample form, be it gas, liquid or solid, providing that the sample can be ionized via exposure to the gas emitted from the DART ion source. Typically, a cumbersome pretreatment process, such as extraction, is required for analysis of a specific component in a solid food. However, due to the considerable time and effort associated with this process, there is demand for a method which permits convenient screening analysis. We believe that DART is suitable for such a purpose.

Here, we introduce an example of direct analysis of free fatty acids and amino acids in solid dried bonito samples without conducting sample pretreatment. Normally, such an analysis requires considerable time and effort for sample pretreatment.

Katsuobushi (dried bonito), which was included on the Representative List of the Intangible Cultural Heritage in 2013 as an essential Japanese food item, is manufactured using processes including thorough boiling, roasting, drying and preservation using mold. The mold, in this case, is intentionally used to impart a mellow flavor. Bonito is referred to as "arabushi" when in the state prior to molding, and "hongarebushi" after molding. Here, we conducted characterization analysis of the product in these two states.

■ Analytical Conditions Used for Katsuobushi

The two kinds of katsuobushi (Fig. 1), arabushi and hongarebushi, were sliced to divide them into internal and surface parts. The sliced pieces of dried bonito were then held up to DART with pincers, and measured by DART.

The DART SVP ion source (IonSense, Inc., MA, USA), was used in combination with the LCMS-2020 single quadrupole mass spectrometer (Fig. 2). The LCMS-2020, with its maximum 15,000 u/sec high-speed scanning and 15 msec ultra-high-speed polarity switching, permits one-second multiple scanning over the range of m/z 50 to 1500 using dual, positive – negative polarity. These features made it possible to simultaneously detect a spectrum of amino acids (positive ion detection) and fatty acids (negative ion detection). And, since analysis could be carried out by simply exposing the sample to the gas, measurement time was kept to about ten seconds per sample, thereby achieving high-throughput analysis.

Fig. 1 Katsuobushi Samples (A: Arabushi, B: Hongarebushi)
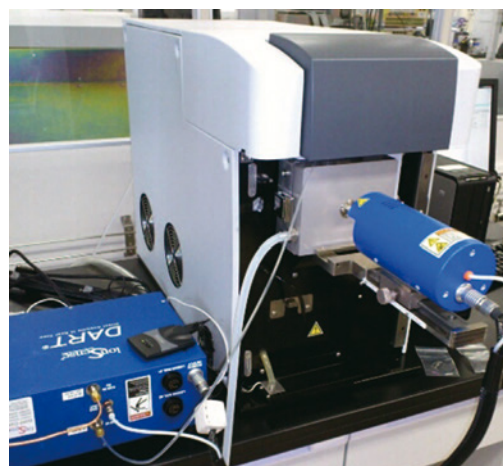
Fig. 2 DART-SVP Ion Source Coupled with LCMS-2020 Single Quadrupole Mass Spectrometer

■ Analysis of Fatty Acids in Katsuobushi

Typically, fatty acids in food are analyzed by GC or GC/MS following preparation which includes extraction from the sample and methyl esterification. This sample preparation process is quite time-consuming, but the analytical method presented here requires only that the sample be exposed to the gas, without any pretreatment, thereby dramatically shortening the analysis time.

The free fatty acids, including palmitic acid, oleic acid, and stearic acid, were detected in both the arabushi and hongarebushi types of katsuobushi (Fig. 3).

Table 1 Analytical Conditions

DART Heater Temperature	: 100, 200, 300, 400, 500 ℃
Scan type	: m/z 50 - 1500 (Positive / Negative)
Neburizing Gas Flow	: 1.5 L/min.
Drying Gas Flow	: 5.0 L/min.
DL Temperature	: 250 ℃
Block Heater Temperature	: 400 ℃

Traditional Method

Extraction of fatty acids from sample → Methyl esterification → GC, GC/MS analysis → Analysis, results verification

Instant Analysis Method (DART-MS)

Sample exposed to direct analysis → Analysis, results verification

(Analysis time greatly shortened)

In addition, the distinctive free fatty acids of fish, namely docosahexaenoic acid (DHA) and eicosapentaenoic acid (EPA), were also easily detected.
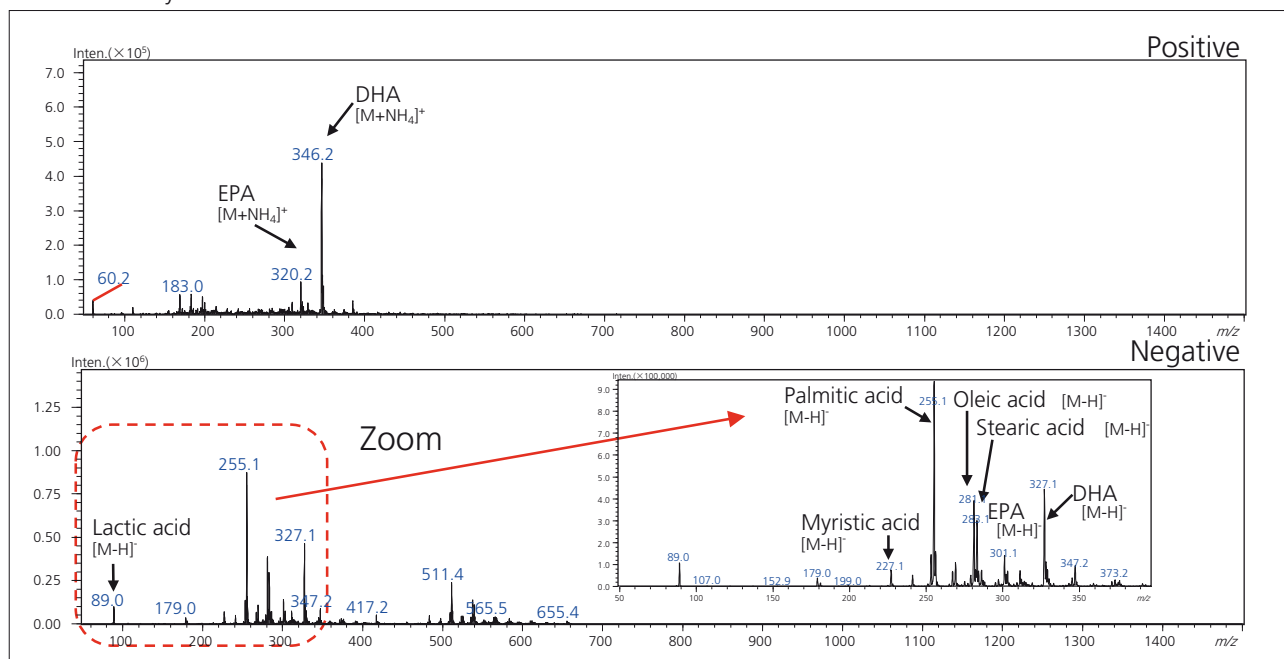
Fig. 3 Mass Spectra Obtained from Surface of Hongarebushi; DART Heater Temperature: 200 °C

■ Analysis of Amino Acids in Katsuobushi

Although GC-GC/MS or LC-LC/MS can be used for analysis of amino acids in foods following pretreatment which includes extraction and derivatization, DART-MS was similarly applied to this analysis using direct detection without pretreatment.

The peak of the amino acid histidine, characteristic of pelagic and migratory fish, and those of the dipeptides carnosine and anserine, commonly contained in highly migratory species, were confirmed from the positive mass spectrum.
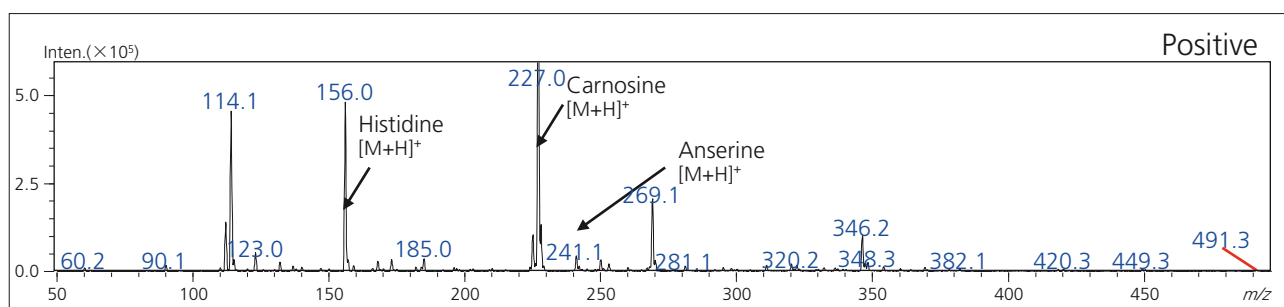
Fig. 4 Mass Spectrum from Internal Surface of Hongarebushi; Heater Temp: 400 °C

■ Katsuobushi Differences According to Type and Sample Site

To verify differences in fatty acid detection between arabushi and hongarebushi, or between their surfaces and internally, the signal intensities of four typical fatty acids were compared. The results are shown in Table 2. Regardless of the fatty acid, the quantity was greatest on the surface of the hongarebushi type. Since the hongarebushi is the bonito in which the molding process was applied, it is believed that the mold may be associated with the increase in free fatty acid content.

Table 2 Fatty Acids Detected from Each Katsuobushi

Fatty Acid \ Katsuobushi Site/Type	Hongarebushi Surface	Hongarebushi Internal	Arabushi Surface	Arabushi Internal
Palmitic acid	+++	++	++	+
Oleic acid	+++	++	++	+
EPA	+++	+	+	−
DHA	+++	++	++	−

(**+**: Abundant, **−**: Scarce)

*DART is a product of IonSense Inc. (http://www.ionsense.com/).

SHIMADZU

Shimadzu Corporation

www.shimadzu.com/an/

SHIMADZU
Excellence in Science

Application News

Liquid Chromatography Mass Spectrometry

No.C109

Application of Direct Analysis in Real Time (Part 2) Rapid Analysis of Triglycerides and Fatty Acids in Food Oil Using LCMS-2020

DART (Direct Analysis in Real Time), when used with a mass spectrometer, permits quick analysis of analyte compounds without the need for sample pretreatment. Application News C108 introduced an analysis of free fatty acids and amino acids in food products using the LCMS-2020 equipped with DART as the ion source.

Fatty acids present in foods are often bound to triglycerides, and when people ingest these triglycerides, not only do they serve as a source of energy, people acquire the physiological functions of the various fatty acids. Therefore, there is interest in research associated with triglyceride molecular species. Generally, LC and GC are used for triglyceride analysis, but these methods are known to have such drawbacks as complicated sample preparation, long analysis time and carryover.

Here, using the same system as that used for the previous Application News, No. C108, we introduce an example of analysis of lipids in food containing triglycerides, without conducting any sample preparation.

■ DART-MS Analytical Conditions

The analytical system used consisted of the DART SVP ion source (IonSense, Inc., MA, USA), and the LCMS-2020 single quadrupole mass spectrometer. The LCMS-2020, with its maximum 15,000 u/sec high-speed scanning and 15 msec ultra-high-speed polarity switching, permits one-second multiple scanning over the range of m/z 50 to 1500 using dual, positive – negative polarity. These features made it possible to simultaneously detect a spectrum of triglycerides (positive ion detection) and fatty acids (negative ion detection). And, since analysis can be conducted by simply exposing the sample to the gas discharged from the DART ion source, measurement time was kept to about ten seconds per sample, thereby achieving high-throughput analysis.

Table 1 Analytical Conditions

DART Heater Temperature	: 400 ℃
Scan Type	: m/z 50-1500 (Positive / Negative)
Neburizing Gas Flow	: 1.5 L/min.
Drying Gas Flow	: 5.0 L/min.
DL Temperature	: 250 ℃
Block Heater Temperature	: 400 ℃

■ Analysis of Triglycerides and Fatty Acids in Various Food Oils

The mass spectra of food product oils and fats (shortening and lard) with known fatty acid composition are shown in Fig. 1 and Fig. 2, respectively. The monoglycerides, diglycerides and triglycerides were detected in the positive ion mass spectra of both samples. As for the negative ions, linoleic acid and oleic acid were primarily detected in the shortening, while oleic acid was primarily detected in the lard.

Fig. 1 Mass Spectra for Shortening

Fig. 2 Mass Spectra for Lard

Shown below are expanded views of the MS spectra of the negative ions in shortening and lard, respectively, over the range of *m/z* 200 to 320 (Fig. 3, Fig. 4). The intensity of the peak originating from palmitic acid is weak in the shortening, while oleic acid and linoleic acid are detected with strong intensity. On the other hand, the peaks of oleic acid and palmitic acid in the lard indicate they were detected with strong intensity.

Fig. 3 Negative Mass Spectrum for Shortening (*m/z* 200-320)

Fig. 4 Negative Mass Spectrum for Lard (*m/z* 200-320)

An expanded view of the mass spectrum of positive ions in the range of *m/z* 800 to 920 is shown below. (The triglyceride fatty acids in the figure are displayed only in the combined state.) In the case of shortening, peaks derived from the triglycerides comprising oleic acid or linoleic acid are clearly detected, such as triolein (OOO), in which all three fatty acids consist of oleic acid, indicating that the result is related to the free fatty acid composition. From the mass spectra for lard, on the other hand, peaks derived from the triglycerides comprising oleic acid and palmitic acid are detected.

Fig. 5 Positive Mass Spectrum for Shortening (*m/z* 800-920)

*DART is a product of IonSense Inc. (http://www.ionsense.com/).

Fig. 6 Positive Mass Spectrum for Lard (*m/z* 800-920)

The same trend is seen with the monoglycerides and diglycerides peaks. The positive MS spectra for lard from *m/z* 300 to 380 and *m/z* 540 to 620 are shown in enlarged views (Fig. 7, Fig. 8). The peaks derived from the monoglyceride and diglyceride oleic and palmitic acids are seen.

Fig. 7 Positive Mass Spectrum for Lard (*m/z* 300-380)

Fig. 8 Positive Mass Spectrum for Lard (*m/z* 540-620)

First Edition: Sep. 2015

SHIMADZU

Shimadzu Corporation

www.shimadzu.com/an/

SHIMADZU
Excellence in Science

Application News

No.C110

Liquid Chromatography Mass Spectrometry

Application of Direct Analysis in Real Time (Part 3) Rapid Analysis of Fatty Acids in Rice Bran Using LCMS-2020

The DART (direct analysis in real time) method can be used to directly ionize samples. Application News No. C109 describes an example of rapidly analyzing the lipids in foods without pretreatment.

This article describes an example of analyzing the lipids in rice bran, which is known to involve an extremely tedious and time-consuming pretreatment process. Rice bran contains about 18 to 20 % oil, which is used as rice oil. A key characteristic of rice oil is its stability with respect to oxidation, due to its low content of linolenic acid, which is a polyunsaturated fatty acid. The rice germ portion of rice bran, which is known for its high nutritional value, contains high levels of rice oil. However, extracting it requires using hexane or other organic solvents and is time-consuming. Therefore, we evaluated the use of the DART method to analyze the lipids by simply exposing the rice bran to direct analysis, without involving solvent extraction or any other pretreatment process.

■ **Analytical Conditions for Rice Bran**

A rice bran containing known fatty acids, mostly listed in Table 1, was used for measurements.

Fig. 1 Rice Bran Used for Measurements

Table 1 Primary Fatty Acids in the Rice Bran Used for Analysis

Myristic acid	0.3 %
Linolenic acid	1.1 %
Palmitic acid	17 %
Linoleic acid	33.4 %
Oleic acid	44 %
Stearic acid	1.7 %

A DART-SVP ion source (from IonSense Inc., in MA, USA) and an LCMS-2020 single quadrupole mass spectrometer were used for analysis. Due to its ultra fast scan speed capability up to 15000 u/sec and ultra fast polarity switching time of 15 msec, the LCMS-2020 is able to perform multiple scans within the 50 to 1500 m/z range using both positive and negative polarity modes, all within one second. Using this functionality, we were able to simultaneously detect spectra for both triglycerides (detected using the positive ion mode) and fatty acids (detected using the negative ion mode).

Table 2 Analytical Conditions

DART Heater Temperature	: 200, 300, 400 °C
Scan Type	: m/z 50 – 1500 (Positive / Negative)
Neburizing Gas Flow	: 1.5 L/min.
Drying Gas Flow	: 5.0 L/min.
DL Temperature	: 250 °C
Block Heater Temperature	: 400 °C

■ **Analysis of Lipids in Rice Bran**

A mass spectrum of rice bran is shown in Fig. 2. At a DART heater temperature of 200 ˚C, peaks were detected for linoleic acid and other fatty acid in the negative mode mass spectrum. An enlargement of the m/z range from 170 to 320 is shown in Fig. 3. It shows that oleic acid, linoleic acid, and then palmitic acid are detected based on prominent peaks. A peak for a sugar is also shown at m/z 269.
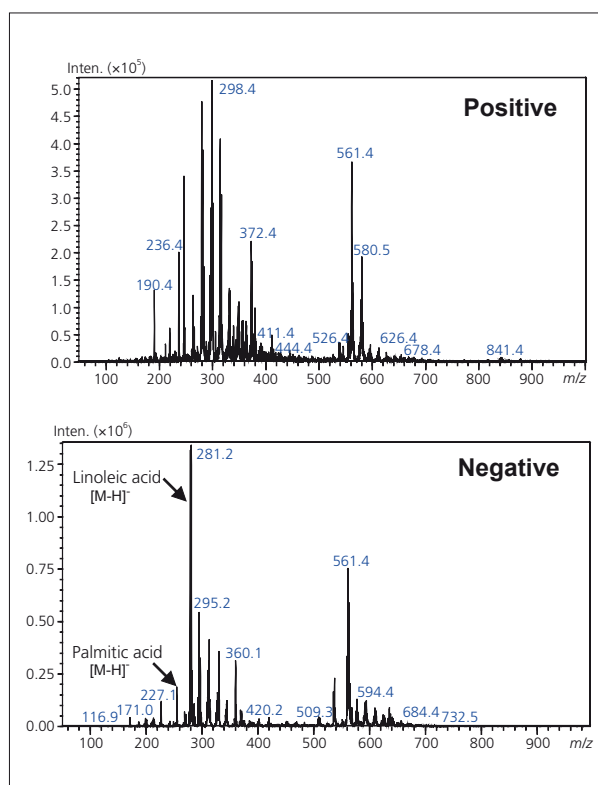
Fig. 2 Mass Spectra of Rice Bran (200 ˚C DART heating temperature)
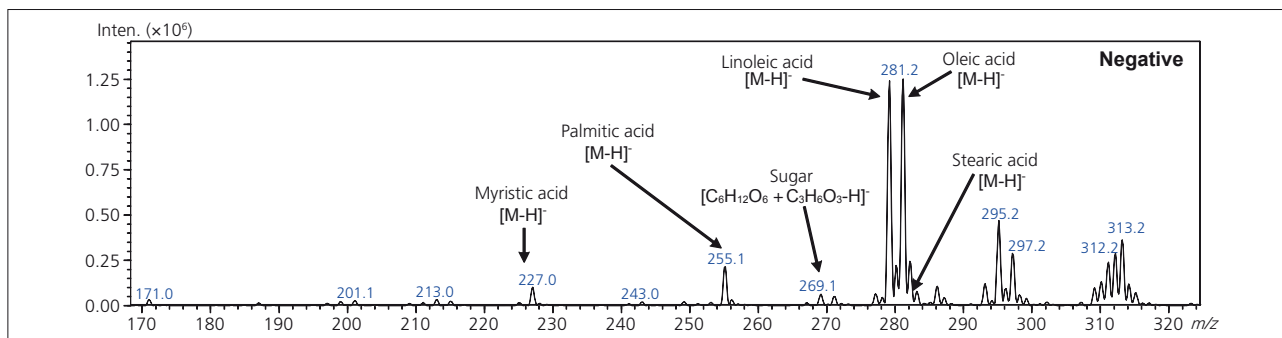
Fig. 3 Mass Spectra of Rice Bran (200 ˚C DART heating temperature)

MS spectra for a heating temperature of 400 ˚C are shown in Fig. 4. This shows peaks for lipid such as diglycerides, that were not visible in the positive-mode MS spectra for a 200 ˚C heating temperature. (The triglyceride fatty acids in the figure are displayed only in the combined state.) Enlarged views of the positive-mode results between *m/z* 540 and 650 and between 800 and 920 are shown. They show diglycerides and triglycerides, including oleic acid and linoleic acid. These spectra also show correlation with the signal intensity ratio of fatty acids detected by negative mode shown in Fig. 3.
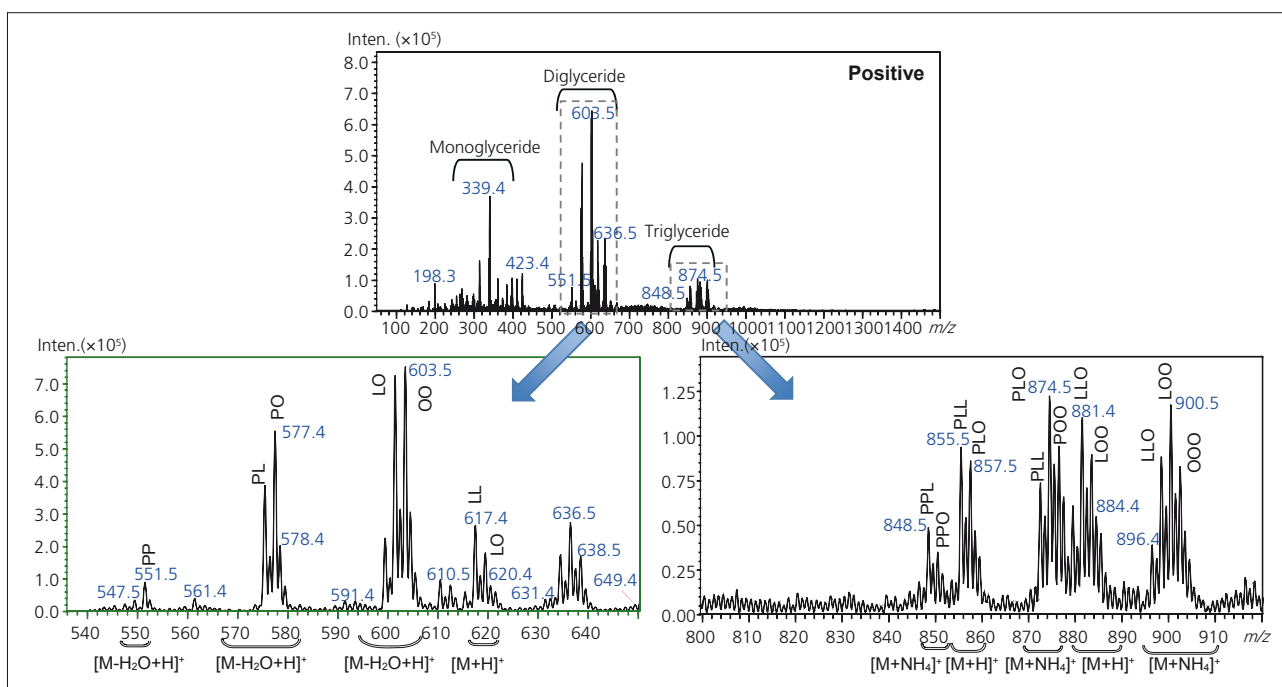
Fig. 4 Mass Spectra of Rice Bran (400 ˚C heating temperature)

To evaluate the optimal heating temperature and reproducibility for fatty acids, sugars, and lipids, samples were measured consecutively at three different heating temperatures. Extracted ion chromatograms of linoleic acid, monosaccharide, and triglyceride (LOO) are shown in Fig. 5. This confirmed that fatty acids are detected more favorably at a lower temperature, between 200 and 300 ˚C, and sugars and triglycerides are detected more favorably at a higher temperature of 400 ˚C or higher. Reproducibility of signal intensity was also achieved.
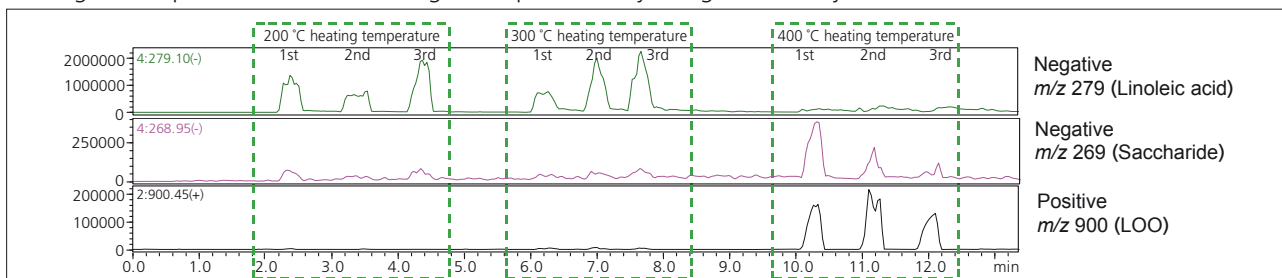
Fig. 5 Extracted Ion Chromatogram (DART heating temperature between 200 and 400 ˚C)

First Edition: Oct. 2015

SHIMADZU

Shimadzu Corporation

www.shimadzu.com/an/

SHIMADZU
Excellence in Science

Application News

No.C111

Liquid Chromatography Mass Spectrometry

Direct Analysis of Volatile Compounds in Real Time Using DART-MS (Part 1)
Analysis of Flavor Release from Chocolate-like Food

The release of flavor when food is masticated has attracted interest in the determining the compounds that affect how good something tastes or smells, which are being studied using a variety of evaluation methods. Attempts have been made to continuously measure the volatile compounds that pass through the nose during mastication. However, these involve humans as the testing medium and present various problems, such as the difficulty in repeating tests multiple times and the long data collection intervals. The DART (direct analysis in real time) system, which is able to directly ionize samples, could be used to rapidly analyze such volatile compounds if the compounds could be introduced into the ion source efficiently. This Application News describes an example of continuously measuring the volatile compounds emitted as a chocolate-like model food melts.

■ Analytical Conditions for Analyzing Chocolate-like Food

An LCMS-8030 system was used as the mass spectrometer. A DART-SVP (from IonSense Inc., in MA, U.S.) was used as the ion source, and a Volatimeship device (from Bio Chromato Inc. in Kanagawa, Japan) was inserted between the ion source and the mass spectrometer (Fig. 1) for efficiently analyzing the volatile compounds emitted from the model food.
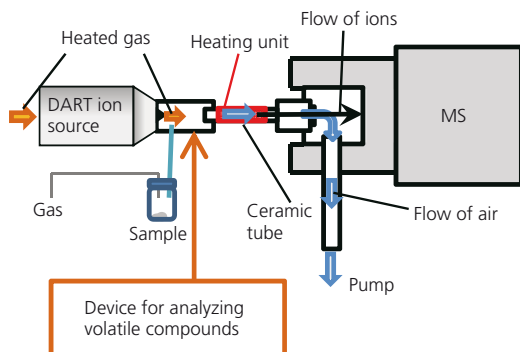
Fig. 1 Measurement System

The model food was prepared by adding different concentrations of two volatile compounds (L-carvone and D-limonene) to a solid fat base used to represent the chocolate (Table 1).

0.02 g of each sample and 1 mL of ultrapure water were placed in vials and loaded in the measurement system. Then the vials were heated by inserting the bottom of the vials in a water bath. Then the volatile compounds evolved in the headspace were measured. For the purpose of confirming the release of flavor as the sample fat melted, analysis was performed until the water temperature reached equilibrium inside the vials (about 2 minutes).

In addition to full scans in positive and negative modes, multiple MRM channels were used to identify carvone and limonene with high reliability. Due to both the ultra fast scanning (15,000 u/sec) and ultra fast polarity switching (15 msec) capabilities of the LCMS-8030, positive and negative scanning and multichannel simultaneous MRM analysis were accomplished in less than a second per data point (Table 2).
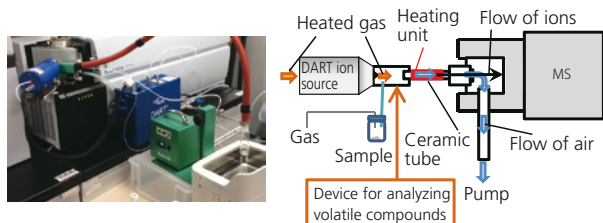
Table 1 Composition of Two Volatile Compounds in Chocolate-like Food

Sample No.	Carvone (%)	Limonene (%)
①	0.1	0
②	0.1	0.01
③	0.1	0.03
④	0.1	0.05
⑤	0	0.1

Table 2 Analytical Conditions

DART Heater Temperature	: 300 °C
Scan Type	: Q3 scan m/z 50 – 1500 (Positive / Negative)
MRM Transition	: Carvone 151 > 109 and 5ch (Positive)
	Limonene 137 > 81 and 12ch (Positive)
Drying Gas Flow	: 5. 0 L/min.
DL Temperature	: 250 °C
Block Heater Temperature	: 400 °C
Water Bath Temperature	: 65-70 °C

■ Analysis of Volatile Compounds in Chocolate-like Food

A total ion current chromatogram (TICC) of samples (1) to (5) is shown in Fig. 2. For each sample, a peak begins to rise immediately after loading the sample vial (labeled "Load sample" in Fig. 2). One minute after loading the vials, immediately after starting to heat the vials in a water bath, an increase in an even larger peak is shown. Presumably, this is due to the heat promoting the volatilization of volatile components.
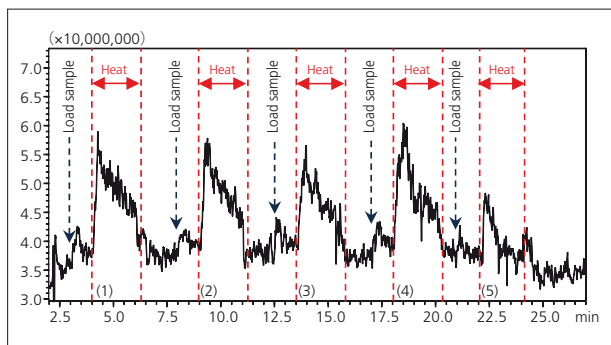
Fig. 2 Total Ion Current Chromatogram of Chocolate-like Food

The MRM mode was used for analyzing samples to detect limonene and carvone with high sensitivity and high selectivity and also to avoid affects from contaminant compounds. MRM chromatograms for representative limonene and carvone transitions during the analysis of samples (1) to (5) are shown in Fig. 3.

As shown in Table 1, identical carvone concentrations were added to samples (1) to (4) and none to sample (5). Consequently, the resulting MRM chromatograms for samples (1) to (4) include similarly strong peaks for the carvone transition at Q1/Q3 = 151/109, whereas that peak was not detected for sample (5). In the case of limonene, increasing concentrations levels were added to samples (1) to (5). Consequently, the resulting MRM chromatograms show corresponding increasing signal intensity from the limonene transition in samples (1) to (5), which indicates a correlation between the concentration added and the signal intensity.
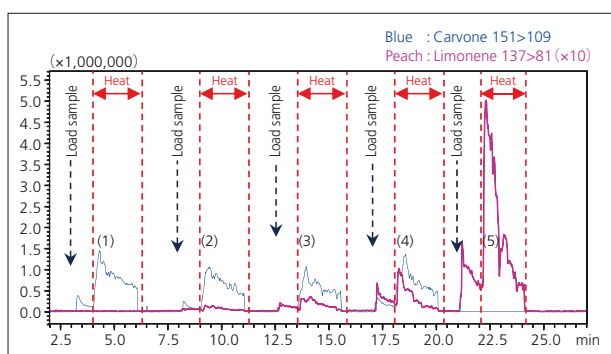
Fig. 3 MRM Chromatogram of Chocolate-like Food

To confirm the change in temperature inside the vials containing samples, water was placed in a vial instead of a sample and the water temperature was measured as a function of time. Those results, shown in Fig 4, confirm that the temperature increased to 50 °C in about 20 seconds after applying heat.

An enlargement of the MRM chromatogram for sample (4) from zero to 20 seconds after heating is shown in Fig. 5. This confirms that the ion intensity from the carvone transition increased immediately after heating. This behavior is almost the same as the water temperature behavior in Fig. 4. In contrast, the signal intensity increase from the limonene transition occurs later than for carvone and then decreased after reaching its maximum intensity, about 15 seconds after heating.
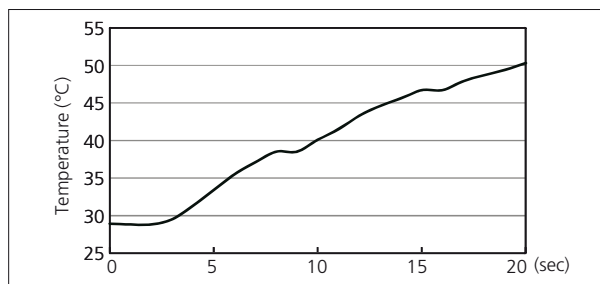
Fig. 4 Water Temperature Inside Vial
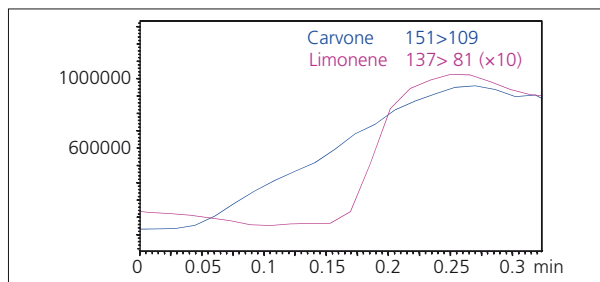
Fig. 5 MRM Chromatogram of Sample (4)

Each sample was measured three times in a row. The corresponding MRM chromatograms for samples (3) and (4) are shown in Fig. 6. This confirms the reproducibility of the behavior shown in Fig. 5.
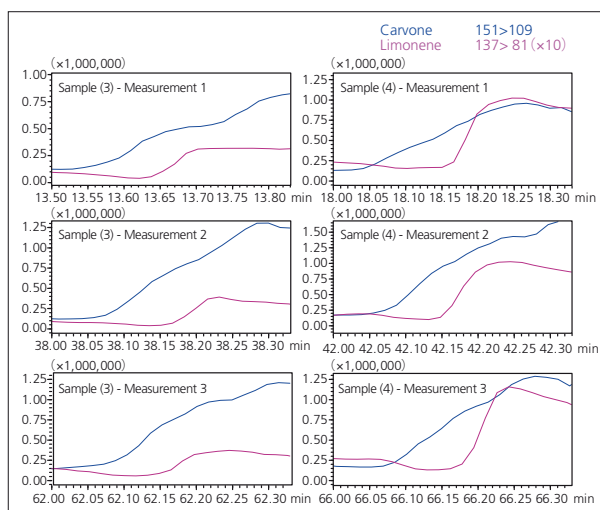
Fig. 6 MRM Chromatograms of Samples (3) and (4) (n = 3)

Thanks to the short data acquisition time of less than one second per sample, it was possible to clearly show differences in behavior of volatile compounds during a short period. This suggests the system's potential for measuring flavor-release phenomena.

Data was provided and analyzed with the generous cooperation from Mr. Takehito Sagawa at S&B Foods.

[References]
Takehito Sagawa et al., Continuous Analysis of Volatile Compounds from Foods During Flavor Release Using Direct Analysis in Real Time Mass Spectrometry, Journal of the Japanese Society for Food Science and Technology, 62 (7), 335-340, 2015

DART is a product of IonSense Inc. (http://www.ionsense.com/).

SHIMADZU

Shimadzu Corporation

www.shimadzu.com/an/

SHIMADZU
Excellence in Science

Application News

No.C112

Liquid Chromatography Mass Spectrometry

Direct Analysis of Volatile Compounds in Real Time Using DART-MS (Part 2)
Analysis of Volatile Compounds in Spices, Herb Tea, and Flavored Oils

When food is cooked, it emits a variety of aromas that can stimulate appetite. To study the science of such food aromas, there has been interest in analyzing the volatile compounds of such aromas. Because the volatile compound profile varies extremely quickly immediately after cooking food, samples must be collected in a timely manner and efficiently introduced into the analytical instrument.

Application News No. C111 described an example of continuous measurements of flavor compounds released when a chocolate-like model food melts, using the DART (direct analysis in real time) method, capable of ionizing samples directly, in combination with a Volatimeship volatile compound measurement device and an LCMS-8030 mass spectrometer system.

This article describes an example of using the same system to continuously measure the flavor compounds released from spices, herb tea, and flavored oils that provide a pleasant cooling sensation.

■ DART-MS Analytical Conditions

An LCMS-8030 was used as the mass spectrometer. A DART-SVP (from IonSense Inc., in MA, U.S.) was used as the ion source, and a Volatimeship device (from Bio Chromato Inc. in Kanagawa, Japan) was inserted between the ion source and the mass spectrometer (Fig. 1) for efficiently analyzing the volatile components emitted from the food sample.

Due to both the ultra fast scanning (15,000 u/sec) and ultra fast polarity switching (15 msec) capabilities of the LCMS-8030, multichannel scanning and multichannel simultaneous MRM analyses were accomplished in less than a second per data point (Table 1).

Two kinds of spices (clove and allspice), herb tea made from fresh spearmint leaves, and two kinds of flavored oils were used for measurements.

The spices and flavored oils were placed directly in vials, sealed, and loaded in the measurement system. The vials were heated by inserting the bottom of the vials in a water bath. Then the Volatimeship device was used to inject the volatile compounds from the headspace into the ion source for measurement.

Raw leaves of the herb tea were placed in a vial with boiling water and sealed. After 1 to 3 minutes of steeping, the bottom of the vial was heated in a water bath, in the same manner as for the spices. Then the volatile compounds in the headspace were measured.

■ Analysis of Volatile Compounds in Spices

The positive mass spectra from analyzing the clove and allspice are shown in Fig. 2.

By connecting the Volatimeship device to the DART-MS system for analysis, the volatile compounds in the spices were able to be analyzed in real time and with high sensitivity, without having to collect the volatile compounds first. The volatile compounds were identified from the detected signals based on standard sample spectral patterns for the volatile compounds. From the clove, signals for compounds presumed to be 1,8-cineole, eugenol, eugenol acetate, and caryophyllene were detected. From the allspice, compounds presumed to be 1,8-cineole, eugenol, methyl eugenol and caryophyllene were detected.

Fig. 1 Measurement System

Table 1 Analytical Conditions

DART Heater Temperature	: 300 °C
Scan Type	: Q3 scan m/z 50 – 1500 (Positive / Negative)
MRM Transition	: Carvone 151 > 109 and 5ch (Positive)
	Limonene 137 > 81 and 12ch (Positive)
Drying Gas Flow	: 5. 0 L/min.
DL Temperature	: 250 °C
Block Heater Temperature	: 400 °C
Water Bath Temperature	: 65-70 °C
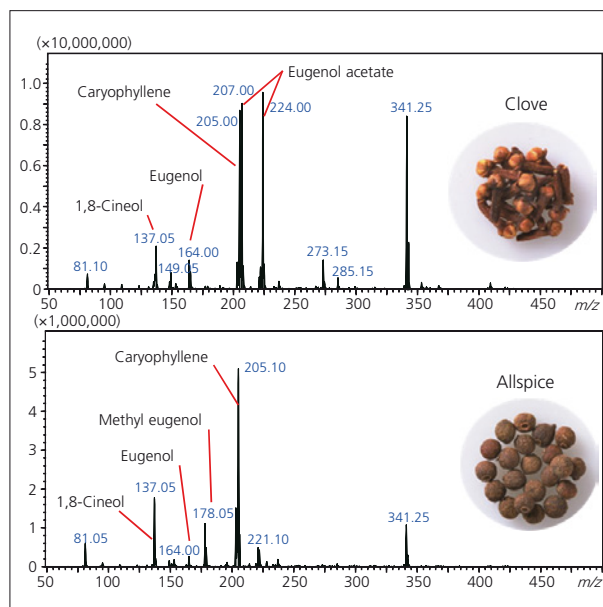
Fig. 2 Mass Spectra (positive) of Two Kinds of Spices

■ Analysis of Volatile Compounds in Herb Tea

Analysis was performed to simulate the change in volatile compounds as they escape a teapot when the lid is removed after steeping the herb tea in the teapot for a given time. Measurement targeted the compounds that typify spearmint, namely a mild sweet fragrance (carvone) and a ground tangerine peel fragrance (limonene). MRM transitions optimized for standard samples of carvone and limonene were used for detection. After steeping the herb tea for 3 minutes, it was heated in a water bath for 2 minutes and measured by MRM. The results are shown in Fig. 3. The ion intensity increased for both carvone and limonene immediately after starting the measurement. The ion intensity for carvone showed no major changes until the measurement was finished, whereas the ion intensity for limonene dropped sharply about 20 seconds after starting the measurement, after which it remained constant. The results confirmed that the composition of the herb tea fragrance changed with time.
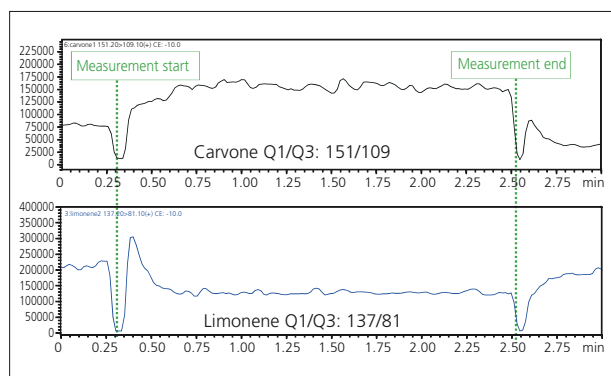
Fig. 3 MRM Chromatograms of Herb Tea (steeped for 3 min)

MRM chromatograms for two types of volatile compounds (carvone and limonene) emitted from herb tea steeped 1, 2, or 3 minutes are shown in Fig. 4 (the portion up to 10 seconds after starting heating is shown enlarged).

All herb tea steeping times produced similar results of the ion intensity for limonene sharply increasing and then decreasing, whereas the carvone ion intensity increased and then remained constant. However, the results showed that the longer the steeping time, the higher carvone ratio with respect to limonene. This showed that the fragrance of herb tea changed depending on the length of steeping time.
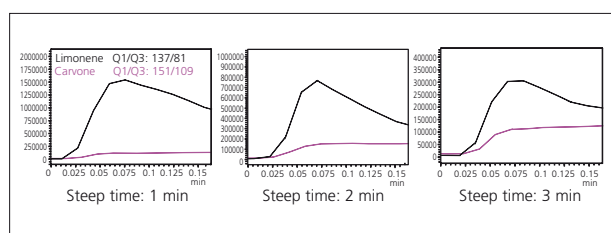
Fig. 4 MRM Chromatograms of Herb Tea (steeped for 1, 2, or 3 min)

■ Analysis of Volatile Compounds in Flavored Oils

Differences in the aroma that depend on the base material that includes volatile compounds were investigated. Fig. 5 shows MRM chromatograms obtained when a spearmint essential oil and a flavored oil with a medium-chain triglyceride (MCT) base material, both containing roughly equal amounts of carvone, were heated in a water bath.

The carvone MRM signal intensity from the essential oil gradually increase, whereas it dramatically increases about 3 seconds after starting the analysis for the MCT-based flavored product. The analytical data confirms that even if samples contain the same volatile compounds, differences in the base material potentially can affect how the product smells.
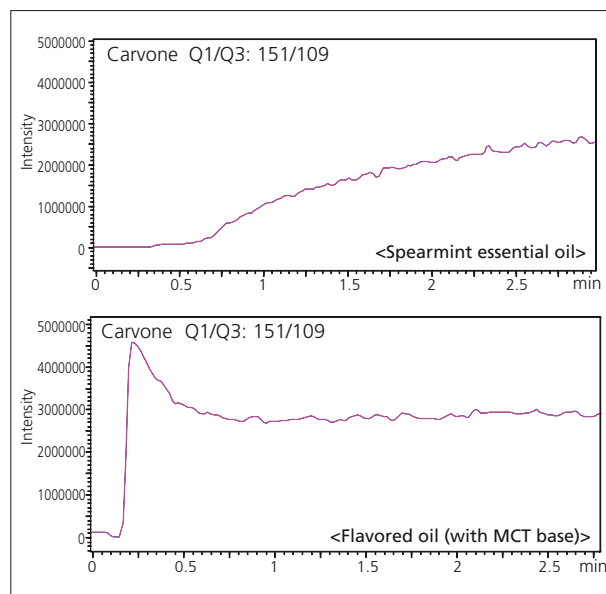
Fig. 5 MRM Chromatogram of Flavored Oils

Data was provided and analyzed with the generous cooperation from Mr. Takehito Sagawa at S&B Foods.

[References]
Takehito Sagawa et al., Continuous Analysis of Volatile Compounds from Foods During Flavor Release Using Direct Analysis in Real Time Mass Spectrometry, Journal of the Japanese Society for Food Science and Technology, 62 (7), 335-340, 2015

DART is a product of IonSense Inc.
 (http://www.ionsense.com/).

First Edition: Oct. 2015

SHIMADZU

Shimadzu Corporation

www.shimadzu.com/an/

SHIMADZU
Excellence in Science

Application News

LCMS

No. C117

Liquid Chromatography Mass Spectrometry

Direct Determination of Trace Hormones in Drinking Water by Large Volume Injection using the LCMS-8050 Triple Quadrupole Mass Spectrometer

David R. Baker, Neil Loftus
Shimadzu Corporation, Manchester, UK

■ **Abstract**

Endocrine disrupting compounds enter the aquatic environment primarily through the discharge of treated and raw sewage and are detrimental to aquatic organisms even at sub-nanogram per litre levels. In the majority of North American and European cities wastewater treatment plant effluent is indirectly re-used, through discharge into rivers which are also a source of drinking water. Consequently, there is the possibility that trace amounts may enter into drinking water even after special treatment processes. Several hormones (estrone, estriol, 17-β-estradiol, equilin, androstenedione, testosterone and 17-α-ethynylestradiol) are routinely monitored by the US EPA in drinking water as part of the Unregulated Contaminant Monitoring program (UCMR3). In this study, the LCMS-8050 triple quadrupole mass spectrometer was used for the highly selective and sensitive detection of hormones in water to meet the requirements of UCMR3. This direct high volume injection method of analysis avoids the disadvantages associated with extracting samples using SPE as is commonly performed. Ammonium fluoride as an aqueous mobile phase additive was found to significantly improve response for all studied hormones in comparison to ammonium hydroxide. The excellent sensitivity of the final method provided detection limits ranging from 0.005 ng/L (testosterone) to 0.330 ng/L (17-α-ethynylestradiol).

Keywords: Hormones, Steroids, LCMS-8050, Drinking Water, UCMR3, Estrone, Estriol, 17-β-estradiol, Equilin, Androstenedione, Testosterone, 17-α-Ethynylestradiol, Ammonium Fluoride

■ **Introduction**

There is growing concern over the exposure of fish, wildlife and humans to the aquatic environment contaminated with trace levels of hormones due to their endocrine disruption potential.[1,2] Endocrine disrupting compounds may interfere with the body's endocrine system and produce adverse developmental, reproductive, neurological, and immune effects.[3] These compounds include naturally occurring steroid hormones such as estrone (E1), 17-β-estradiol (E2), and estriol (E3) and synthetically prepared ones such as 17-α-ethynylestradiol (EE2).

There are a variety of ways hormones enter the aquatic environment. Primarily this is due to the discharge of treated and untreated sewage water into receiving waters.[4] During wastewater treatment these hormones are susceptible to removal by biodegradation or sorption to sewage sludge, where secondary treatment can reduce concentrations consistently by over 85%,[5] however nanogram per litre concentrations of individual compounds may still be present in effluents.[4] Further routes include runoff into receiving waters from cattle given certain growth promoters, and from sludge and manure applied to agricultural fields.

In the majority of North American and European cities wastewater treatment plant effluent is indirectly re-used, through discharge into rivers which are also a source of drinking water.[6] Consequently, there is the possibility that trace amounts may penetrate into drinking water even after special treatment processes.[2] Several hormones are routinely monitored by the US EPA in drinking water as part of the Unregulated Contaminant Monitoring program (UCMR3).[7] These hormones include estrone, estriol, 17-β-estradiol, equilin, androstenedione, testosterone and 17-α-ethynylestradiol. The European Union has identified a list of priority substances, which includes estradiol and 17-α-ethynylestradiol (Directive 2013/39/EU amending Directives 2000/60/EC and 2008/105/EC).[8] Both regulations require highly sensitive and selective methods with ng/L or pg/L reporting levels. Previously published methods typically use solid phase extraction as a concentration step to achieve the regulatory reporting limits[2]. However, this approach adds an additional expense and complexity.

This technical report describes an optimized approach to the direct analysis of hormones in water regulated by EPA Method 539 and UCMR3. The integration of a high volume injection cycle with a highly robust and sensitive MS/MS detection system has resulted in an effective solution for routine hormone analysis in drinking water without the need for extensive sample preparation using conventional SPE methods.

■ Experimental

Table 1. Acquisition parameters for the analysis of steroids in drinking water using a large volume injection mode.

Liquid chromatography			Mass spectrometry	
UPLC	Nexera LC system		LC/MS/MS	LCMS-8050
Analytical column	Shim-pack XR-ODS III column (150 x 2 mm, 2.2 µm particle size).		Ionisation mode	Heated electrospray
Column temperature	45°C		Polarity switching time	5 ms
Column fitted between the mixer and autosampler	Kinetex XB-C18 column (50 x 2.1, 1.7 µm particle size)		Pause time	1 ms
Injection cycle	3 x 400 µL injections (500 µL loop fitted) Total injection volume 1200 µL		Dwell times	10-100ms
Flow rate	0.3mL/minute		Interface temperature	400°C
Solvent A	0.15mM ammonium fluoride		Heating block	400°C
Solvent B	Methanol		Desolvation line	200°C
Binary Gradient	Time (mins)	%B	Heating gas	10 L/min
	0	10	Drying gas	5 L/min
	0.3	10	Nebulising gas	2.8 L/min
	1	45		
	15	100		
	17	100		
	17.1	10		
	22	Stop		
Needle wash	500 µL Methanol / acetonitrile / 2-propanol / Water (1:1:1:1) 0.1 % formic acid			

Table 2. MRM transitions for the target compounds

Compound	Formula	CAS	Retention Time	Polarity	SRM Transitions	Q1 (V)	CE	Q3 (V)	MS1 Res.	MS2 Res.
Estriol	$C_{18}H_{24}O_3$	50-27-1	8.9	Negative	289 > 97	11	36	17	Unit	Unit
					289 > 109	11	42	27	Unit	Unit
Equilin	$C_{18}H_{20}O_2$	474-86-2	12.0	Negative	267 > 143	19	34	27	Unit	Unit
					267 > 223	19	33	24	Unit	Unit
17-α-Ethynylestradiol	$C_{20}H_{24}O_2$	57-63-6	12.1	Negative	269 > 145	11	44	26	Unit	Unit
					269 > 143	11	54	29	Unit	Unit
17-β-Estradiol	$C_{18}H_{24}O_2$	50-28-2	12.1	Negative	287 > 97	10	40	27	Unit	Unit
					287 > 109	10	40	19	Unit	Unit
Estrone	$C_{18}H_{22}O_2$	53-16-7	12.2	Negative	287 > 171	20	38	29	Unit	Unit
					287 > 145	20	55	27	Unit	Unit
Androstenedione	$C_{19}H_{26}O_2$	63-05-8	12.2	Positive	271 > 145	-14	-23	-18	Unit	Unit
					271 > 183	-14	-24	-11	Unit	Unit
Testosterone	$C_{19}H_{28}O_2$	58-22-0	12.7	Positive	295 > 145	-30	-22	-18	Unit	Unit
					295 > 143	-30	-24	-21	Unit	Unit

Estrone (E1)

17-β-estradiol

Estriol (E3)

17-α-ethynylestradiol (EE)

Testosterone

Androstenedione

Equilin
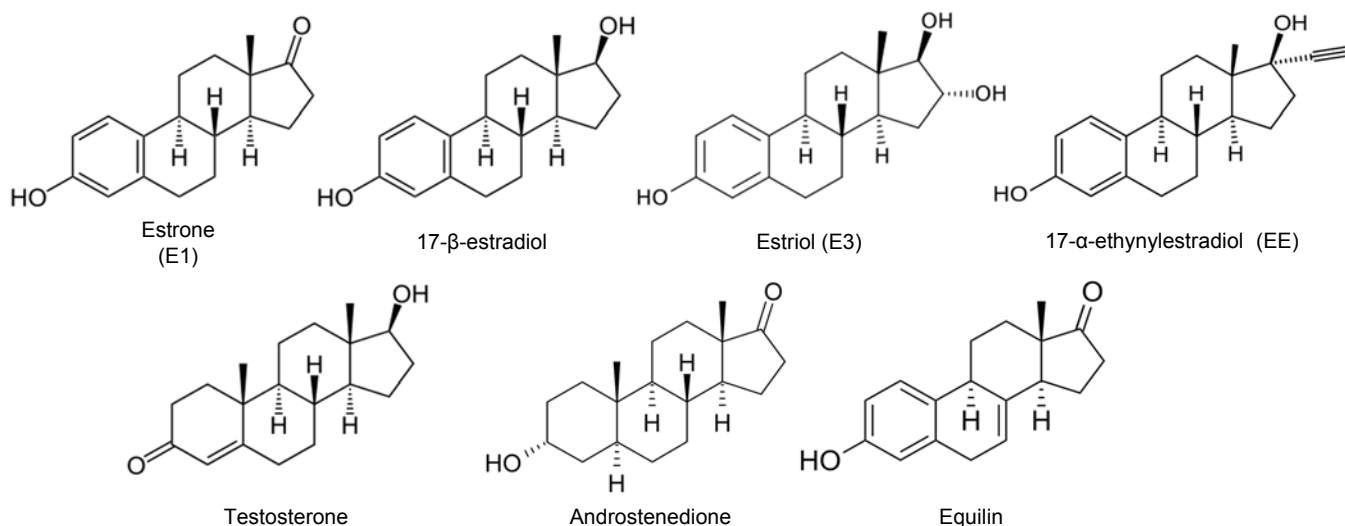
Figure1. Endocrine disruptor structures.

■ Results and Discussion

Method development

Previously published methods for the analysis of endocrine disruptors have used ammonium hydroxide as the mobile modifier and it is the currently recommended approach in EPA method 539.[9]

In this study ammonium fluoride was tested at different concentrations (0.1, 0.2, 0.3 and 0.5mM) in the aqueous phase, with methanol used as the organic phase. Improved response was observed for all hormones using ammonium fluoride, in comparison to ammonium hydroxide, as is shown in Figure 2. The optimum concentration was determined to be 0.15mM which is consistent with the results of others.[10] Ammonium fluoride (approx. pH 6) offers further benefits in comparison to ammonium hydroxide (approx. pH 9.5) as the lower pH means that analytical columns, other than those stable at high pH, can be employed.

Methanol was used as the organic solvent although acetonitrile resulted in a marginal improvement in signal to noise for compounds responding in negative ion but this advantage was countered by a marked reduction in the positive ion response.

As the panel of target compounds resulted in an optimal response in both positive and negative ion detection, a rapid polarity switching method was used in routine analysis without compromising data quality or response (Figure 3).

Key points in enhancing EPA method 539

0.15mM ammonium fluoride generated higher sensitivity compared to ammonium hydroxide. Heated electrospray further enhanced sensitivity and a 5 ms polarity switching optimized the hormone panel detection.
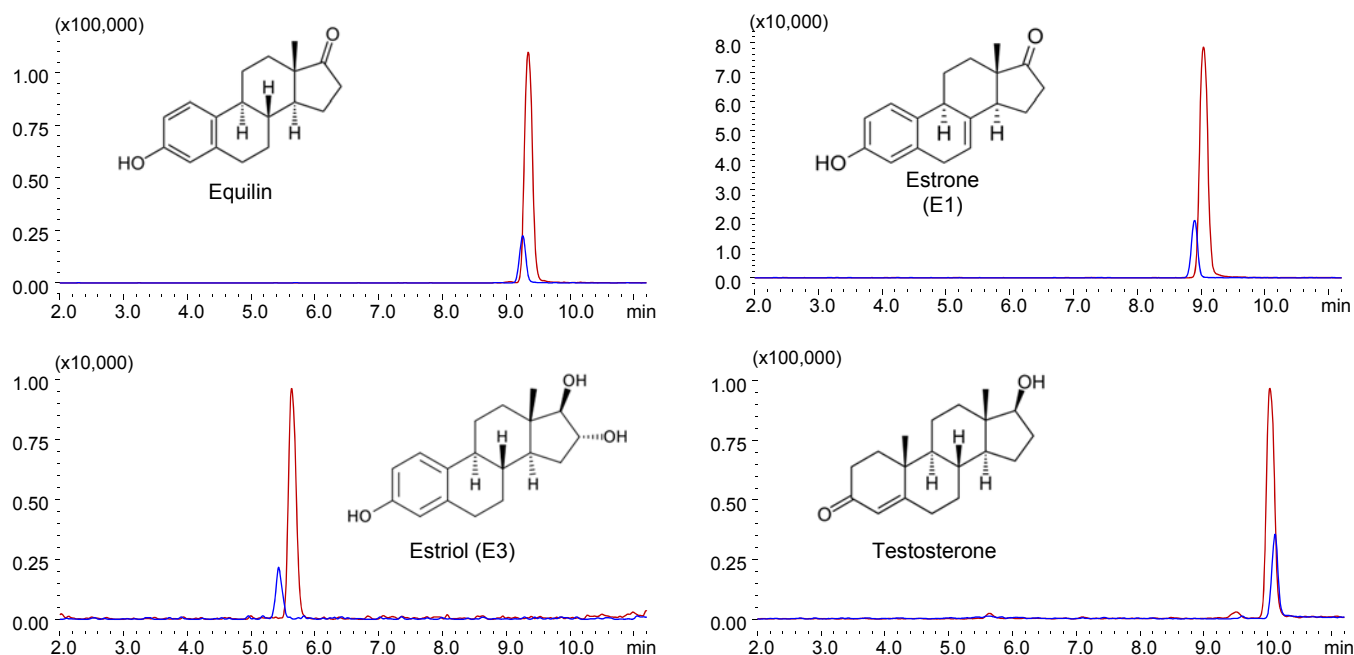
Figure 2. A comparison between the response generated using ammonium hydroxide (blue trace) and ammonium fluoride (red trace). Ammonium fluoride delivers an increase signal to noise for all compounds (for example, equilin x4.0, estrone x4.8, estriol x4.5 and testosterone x2.8).
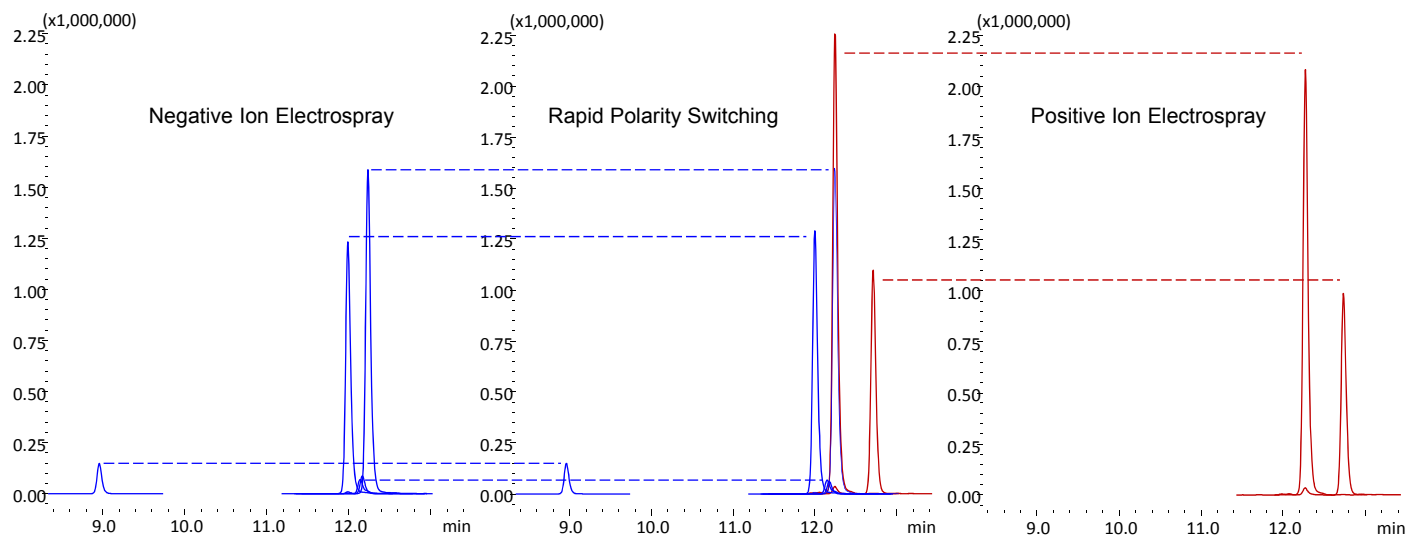
Figure 3. Rapid positive/negative switching using a 5ms switching time results in the highest data quality for all target hormone compounds in a single analysis.

Table 3. Concentration of each compound in the calibration series in drinking water.

Compound	Level 1 (ng/L)	Level 2 (ng/L)	Level 3 (ng/L)	Level 4 (ng/L)	Level 5 (ng/L)	Level 6 (ng/L)	Level 7 (ng/L)	Level 8 (ng/L)
Equilin	2	4	8	20	40	80	200	400
Estrone	1	2	4	10	20	40	100	200
17-α-Ethynylestradiol	0.45	0.9	1.8	4.5	9	18	45	90
Estriol	0.4	0.8	1.6	4	8	16	40	80
17-β-Estradiol	0.2	0.4	0.8	2	4	8	20	40
Androstenedione	0.15	0.3	0.6	1.5	3	6	15	30
Testosterone	0.05	0.1	0.2	0.5	1	2	5	10

Equilin;
16 points used, 8 calibration levels
Y = (30635.5)X + (-3866.97)
R² = 0.9998
Fit; linear, 1/C weighting
Zero not forced
%RSD=3.27

Estradiol;
16 points used, 8 calibration levels
Y = (18276.4)X + (-422.911)
R² = 0.9998
Fit; linear, 1/C weighting
Zero not forced
%RSD=5.72

Androstenedione;
16 points used, 8 calibration levels
Y = (1.07781e+006)X + (-42036.8)
R² = 0.9997
Fit; linear, 1/C weighting
Zero not forced
%RSD=6.01

Testosterone;
16 points used, 8 calibration levels
Y = (1.06473e+006)X + (6811.35)
R² = 0.9994
Fit; linear, 1/C weighting
Zero not forced
%RSD=8.49

Figure 4. Calibration curves for equilin (2-400ng/L), estradiol (0.2-40ng/L), androstenedione (0.15-30ng/L) and testosterone (0.05-10ng/L) spiked into drinking water.

Linearity was investigated over an eight point calibration curve in drinking water, analysed in duplicate, covering two and a half orders of magnitude. Concentrations of each compound at each level are listed above in Table 3. Peak area repeatability (n=7) was assessed at low (level 2) and high (level 5) concentrations. The robustness study was performed using drinking water spiked at level 5.

Hormone limits of detection were calculated based on the method described by the the EPA Method 539,[9] using a standard deviation of 7 replicates at a concentration value that corresponds to an instrument signal to noise ratio in the range of 2.5 to 5 and a Student's t 99% confidence interval.

$$DL = t\ (n\text{ - }1,\ 1 - \alpha = 0.99)\ x\ s.d.$$

Parameter	Description
DL	Detection Limit
t(n-1,1-α=0.99)	Student's t value for the 99% confidence level with n-1 degrees of freedom (t = 3.14 for 7 replicates),
n	number of replicates
s.d	standard deviation of the replicate analyses

■ Method validation

Quantitative Method Validation

In order to test the performance of the developed method, limits of detection, linearity, repeatability (low and high concentrations), and longer term robustness were assessed.

Linearity was assessed from 0.5 x the required reporting level to 100 x times the reporting level. The concentration for each compound in spiked drinking water is listed in Table 3.

Table 4. Detection Limit (DL) is defined as the minimum concentration of an analyte that can be identified, measured, and reported with 99% confidence that the analyte concentration is greater than zero.

Compound	DL (ng/L)	DL (fg on column)
17-α-Ethynylestradiol	0.330	396
Equilin	0.073	88
17-β-Estradiol	0.052	62
Estriol	0.035	42
Estrone	0.031	38
Androstenedione	0.012	14
Testosterone	0.005	6

All seven hormones achieved excellent correlation coefficients $R^2>0.999$ using a weighted (1/C) least squares regression analysis. Calibration curves for equilin, estradiol, androstenedione and testosterone are shown in Figure 4. Hormone limits of detection were calculated based on the method described by the EPA Method 539 and are listed in Table 4. Using the developed method on the LCMS-8050 detection limits ranged from 0.0058 ng/L for testosterone to 0.33 ng/L for 17-α-ethynylestradiol. Figure 5 shows the chromatograms at the lowest calibration standard (level 1).
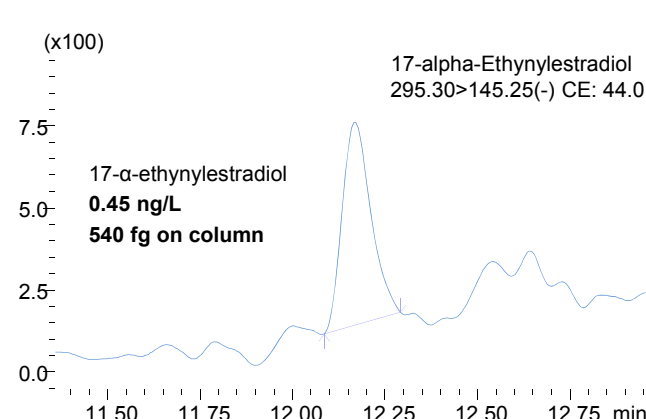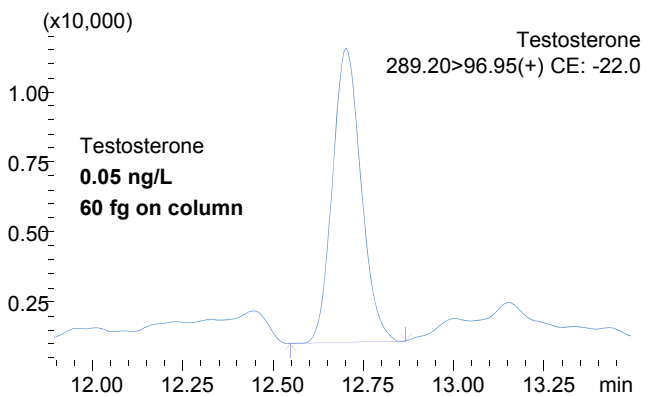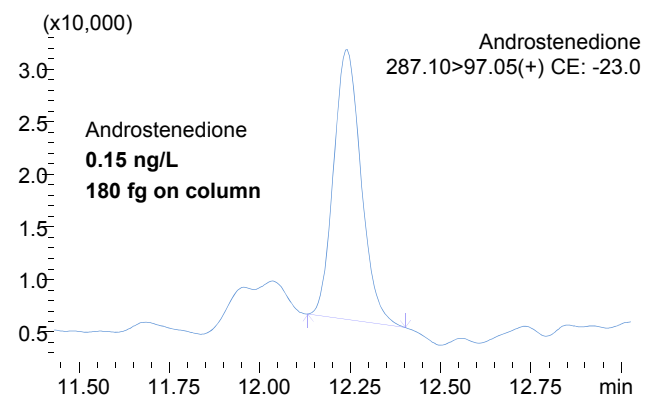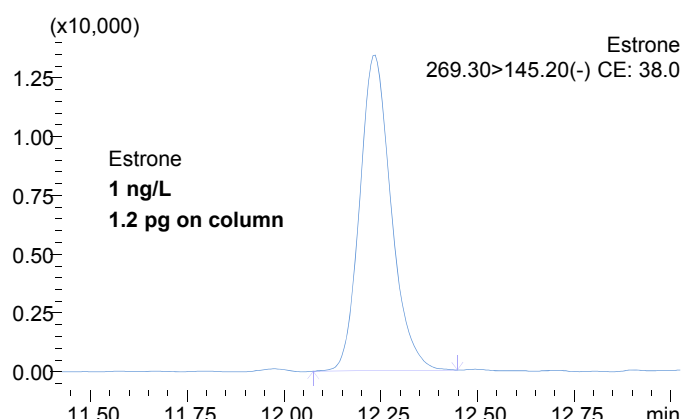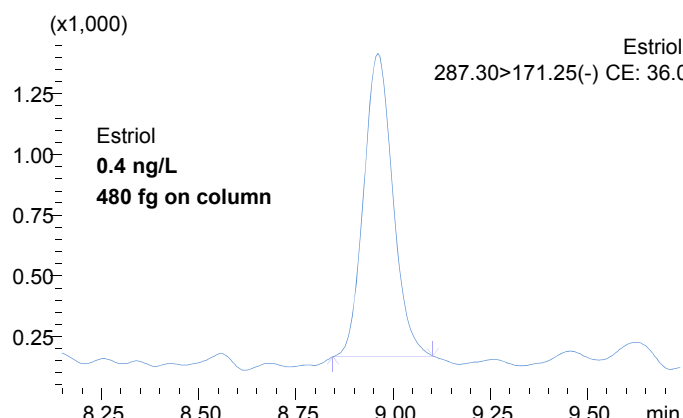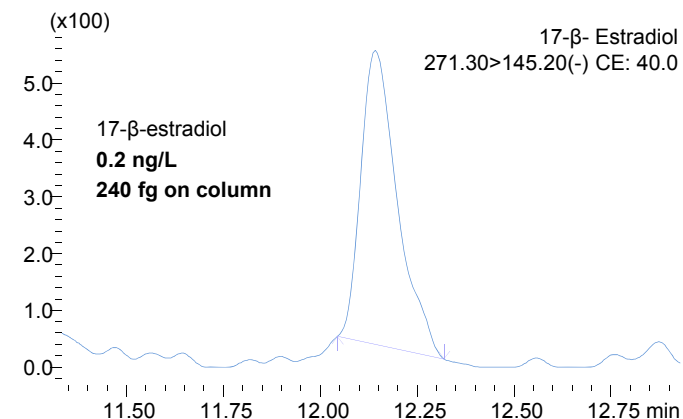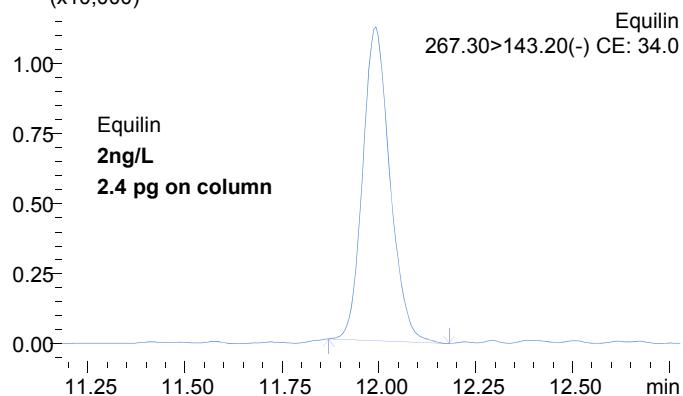
Figure 5. MRM chromatograms of target hormones at the lowest calibration standard (level 1) using an injection volume of 1200uL.

■ Reproducibility

Peak area reproducibility (n=8) was assessed at the reporting level corresponding to 'low concentration' (level 2) and a 'high concentration' (level 5). At the low concentration repeatability was < 4.3 %RSD, with the exception of 17-α-ethynylestradiol (12.2 %RSD). At the high concentration repeatability was < 3.9 %RSD for all compounds. Table 5 lists the repeatability results.

To assess the robustness of system, repeat injections were performed over a 62 hour period using drinking water spiked at level 5.

Results for the three compounds with the lowest peak area are displayed in Figure 6. These results show that even over a much extended time period deviation of less than 5 %RSD was achieved for the three compounds.

Table 5. Peak area repeatability (n=7) at low and high concentrations

Compound	Low (level 2) %RSD	High (level 5) %RSD
17-α-Ethynylestradiol	12.2	2.4
Androstenedione	2.2	2.9
17-β-Estradiol	4.3	3.9
Equilin	3.5	2.7
Estriol	3.4	1.5
Estrone	4.2	1.7
Testosterone	2.8	3.5
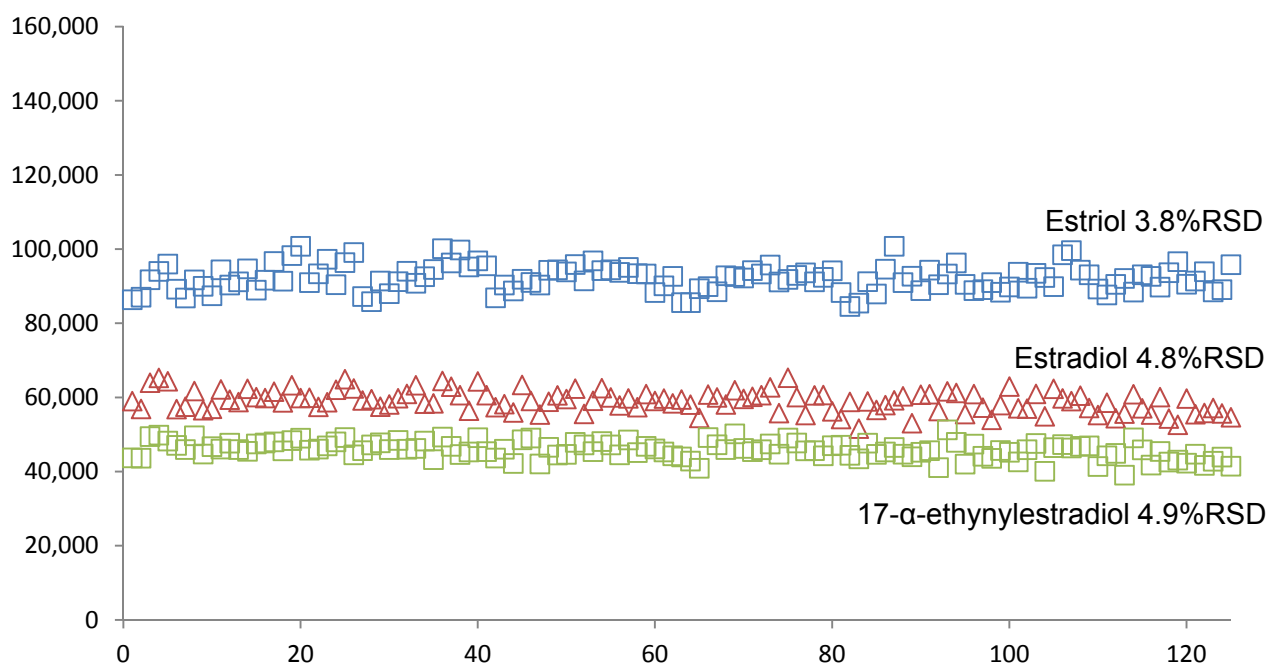
Figure 6. Peak area response for three hormones over 62 hours. The legend displays the %RSD for each compound.

■ Conclusion

A fast, selective and highly sensitive method has been developed for the measurement of hormones in drinking water. By integrating a direct high volume injection cycle with a fully optimised LC/MS/MS method, the LCMS-8050 delivers precise and accurate detection limits regulated by EPA method 539 and is in accordance with UCMR3.

The LCMS-8050 triple quadrupole mass spectrometer method delivered high sensitivity with detection limits ranging from 0.005 ng/L (testosterone) to 0.330 ng/L (17-α-ethynylestradiol). Correlation coefficients for all compounds were greater than 0.999 and peak area repeatability was determined to be typically less than 5%RSD at 'low' (corresponding to the reporting level) and 'high' concentrations.

■ References

1. Bermudez, D.S.; Gray, L.E.; Wilson, V.S. . Modelling defined mixtures of environmental oestrogens found in domestic animal and sewage treatment effluents using an in vitro oestrogen-mediated transcriptional activation assay (T47D-KBluc). Int J Androl. 2012, 35 (3), pp 397-406.

2. Briciu, R.D.; Kot-Wasik A.; Namiesnik, J. Analytical challenges and recent advances in the determination of estrogens in water environments. J Chromatogr. Sci. 2009, 47 (2), pp127-139

3. National Institute of Environmental Health Sciences (NIEHS), Endocrine Disruptors. http://www.niehs.nih.gov/health/topics/agents/endocrine/. Accessed November 17, 2014

4. Griffith, D.R.; Kido-Soule, M.C.; Matsufuji, H.; Eglinton, T.I.; Kujawinski, E.B.; Gschwend, P. M. Measuring Free, Conjugated, and Halogenated Estrogens in Secondary Treated Wastewater Effluent. Environ. Sci. Technol., 2014, 48 (5), pp 2569–2578

5. Johnson, A.C.; Sumpter, J.P. Removal of Endocrine-Disrupting Chemicals in Activated Sludge Treatment Works. Environ. Sci. Technol. 2001, 35 (24), pp 4697–4703.

6. Falconer, I.R. Are Endocrine Disrupting Compounds a Health Risk in Drinking Water? Int. J. Environ. Res. Public Health. 2006, 3 (2), pp 180-184

7. United States Environmental Protection Agency (US EPA), Methods and Contaminants for the Unregulated Contaminant Monitoring Rule 3 (UCMR 3). http://water.epa.gov/lawsregs/rulesregs/sdwa/ucmr/ucmr3/methods.cfm. Accessed Oct. 7 2014

8. European Union. Directive 2013/39/EU of the European Parliament and of the Council of 12 August 2013 amending Directives 2000/60/EC and 2008/105/EC as regards priority substances in the field of water policy. 2013, L 226/1

9. United States Environmental Protection Agency. Method 539: Determination of hormones in drinking water by solid phase extraction (SPE) and liquid chromatography electrospray ionization tandem mass spectrometry (LC-ESI-MS/MS). 2010, EPA Document No. 815-B-10-001.

10. Fiers, T.; Casetta, B.; Bernaert, B.; Vandersypt, E.; Debock, M.; Kaufman, J.M. Development of a highly sensitive method for the quantification of estrone and estradiol in serum by liquid chromatography tandem mass spectrometry without derivatization. J Chromatogr B Analyt Technol Biomed Life Sci. 2012, 15 (893-894), pp 57-62

SHIMADZU

Shimadzu Corporation

www.shimadzu.com/an/

SHIMADZU
Excellence in Science

Application News

No. C119

Liquid Chromatography Mass Spectrometry

Analysis of Cartap, Pyraclonil, and Ferimzone in Drinking Water Using a Triple Quadrupole LC/MS/MS System

Cartap, pyraclonil, and ferimzone are widely used agricultural insecticides, with pyraclonil and ferimzone intended for use in flooded rice fields. These pesticides are designated for monitoring based on target values for drinking water quality control. Though target values were specified, no method for inspecting them has been specified so far.

However, in March 2015, the Japan's Ministry of Health, Labour and Welfare, Health Service Bureau, Water Supply Division issued a notification (No. 0325 Item 3 - 6) specifying the use of LC/MS/MS for water quality control inspections of cartap, pyraclonil, and ferimzone, for which an inspection method was not previously specified.

This article describes an example of inspecting samples for these three components by simultaneous analysis using a liquid chromatograph-mass spectrometer system, as specified in Appendix Method 20-2. Cartap decomposes to nereistoxin in water, so the Cartap is measured as nereistoxin. Ferimzone includes type E and Z isomers, the concentrations of which are totaled to determine the Ferimzone concentration.

■ Analyzing a Standard Mixture Solution of Nereistoxin (Cartap), Pyraclonil, and Ferimzone

A standard solution with 1/100 the target concentration of nereistoxin, pyraclonil, and ferimzone respectively was measured, with the resulting MRM chromatogram shown in Fig. 1.

Fig. 2 shows calibration curves for a concentration range that includes 1/100 of each target concentration value, as well as indicating the repeatability at the lowest calibration point concentration. The results showed good linearity and repeatability for all substances.
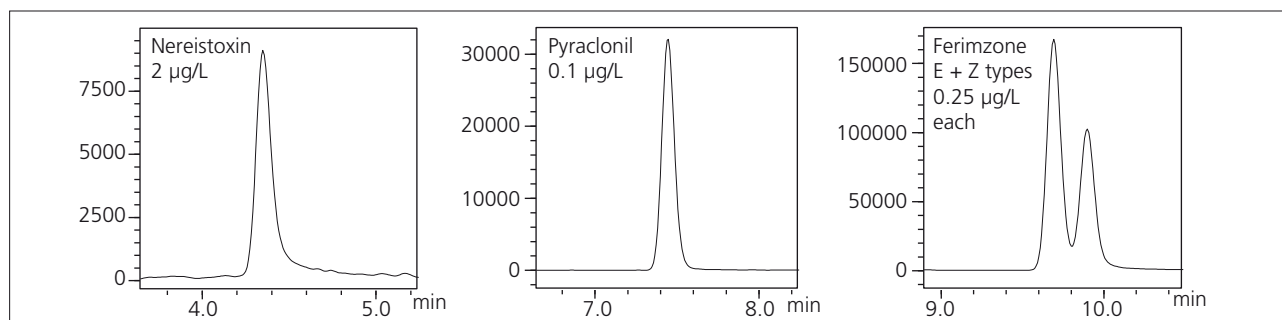
Fig. 1 MRM Chromatograms for Each Substance in a Standard Mixture Solution of Nereistoxin (Cartap), Pyraclonil, and Ferimzone

	Injected Sample Concentration	Contribution Ratio R^2	Area Value %RSD (n = 5)
Nereistoxin (Cartap)	1 – 50 μg/L	0.999	2.9 % (1 μg/L)
Pyraclonil	0.05 – 2.5 μg/L	0.999	2.4 % (0.05 μg/L)
Ferimzone (E)	0.125 – 6.25 μg/L	0.999	0.7 % (0.125 μg/L)
Ferimzone (Z)	0.125 – 6.25 μg/L	0.999	1.0 % (0.125 μg/L)
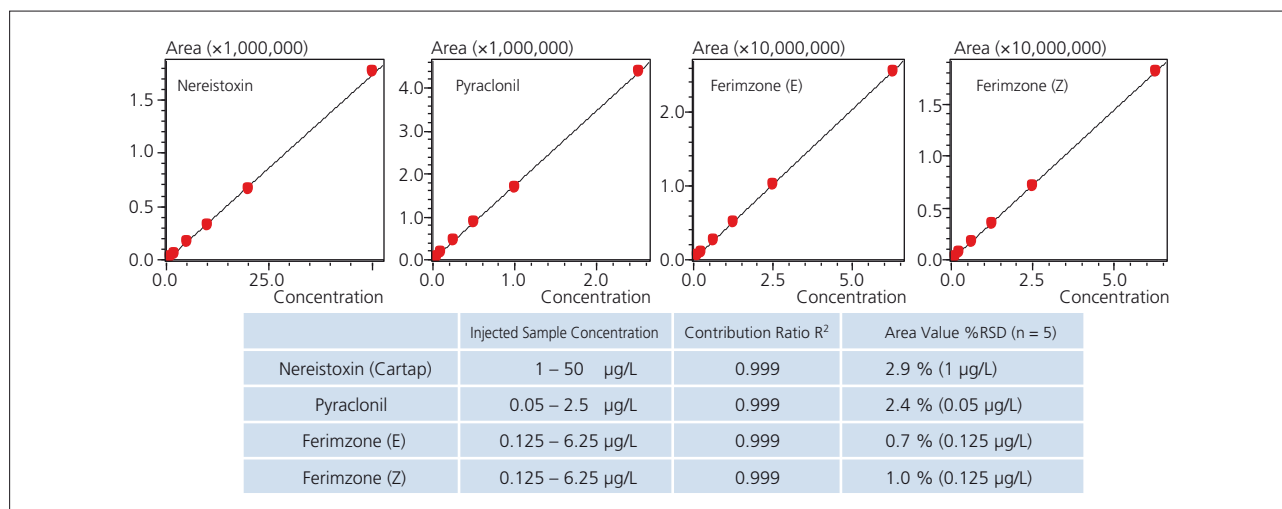
Fig. 2 Contribution Ratio and Area Repeatability

■ Spike and Recovery Test Using Drinking Water

Drinking water was spiked with nereistoxin, pyraclonil, and ferimzone to test the recovery rate. The public drinking water was treated to remove residual chlorine using sodium thiosulfate, rather than sodium ascorbate. (20 mg was added per liter of drinking water.)

Fig. 3 shows MRM chromatograms of blank pretreated drinking water and pretreated drinking water spiked with 1/100 the target value of each substance (2 µg/L nereistoxin, 0.1 µg/L pyraclonil, and 0.125 µg/L each of ferimzone types E and Z).

The recovery rate was calculated from the average of area values measured from five repetitions.

Good results were obtained for each substance, with 102 % recovery for nereistoxin, 95 % for ferimzone E, 100 % for ferimzone Z, and 95 % for pyraclonil.

Analytical conditions for these measurements are listed in Table 2.
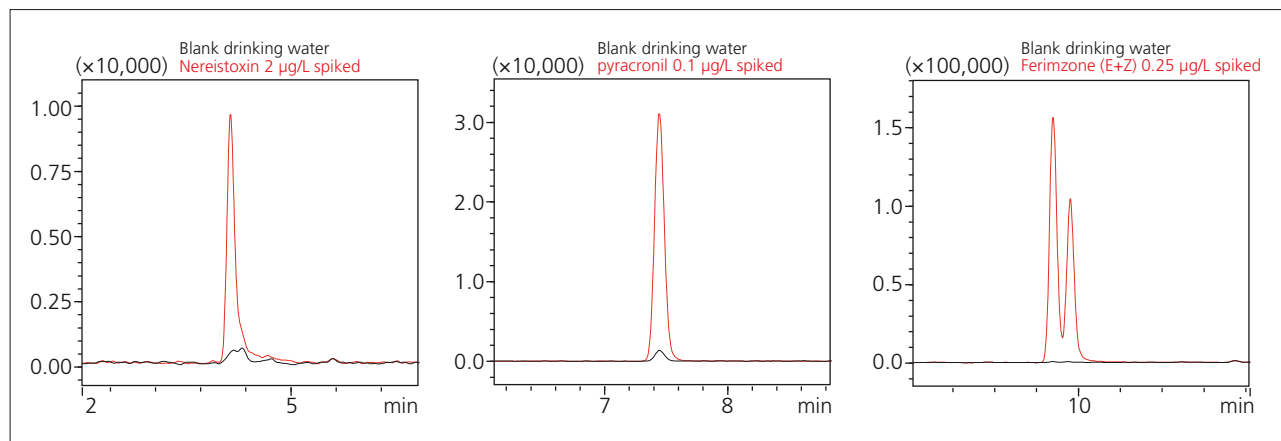
Fig. 3 MRM Chromatograms for Blank Drinking Water and Drinking Water Spiked with Nereistoxin, Pyraclonil, and Ferimzone

Table 1 Spike and Recovery Test Results (n = 5)

	Spike Concentration	Recovery Rate (%)
Nereistoxin (Cartap)	2 µg/L	102
Pyraclonil	0.1 µg/L	95
Ferimzone (E)	0.125 µg/L	95
Ferimzone (Z)	0.125 µg/L	100

Table 2 Analytical Conditions

Column	: L-Column2 ODS (75 mm L. × 2.1 mm I.D., 2 µm, CERI)
Mobile Phases	: A 5 mmol/L Ammonium acetate-Water
	B 5 mmol/L Ammonium acetate-Methanol
Flowrate	: 0.2 mL/min
Time Program	: B. Conc 5 % (0 min) → 45 % (2 min) → 75 % (12 - 13.5 min → 5 % (13.51 - 20 min)
Column Temperature	: 40 ˚C
Injection Volume	: 10 µL
Probe Voltage	: 4 kV (ESI-Positive)
DL Temperature	: 200 ˚C
Block Heater Temperature	: 400 ˚C
Interface Temperature	: 200 ˚C
Nebulizing Gas Flow	: 2 L/min
Drying Gas Flow	: 10 L/min
Heating Gas Flow	: 10 L/min
MRM Transition	: Nereistoxin (Cartap) m/z 150 > 105
	Pyraclonil m/z 315 > 169
	Ferimzone m/z 255 > 91

SHIMADZU

Shimadzu Corporation

www.shimadzu.com/an/

SHIMADZU
Excellence in Science

Application News

No.C120

Liquid Chromatography Mass Spectrometry

Analysis of Glufosinate, Glyphosate, and AMPA in Drinking Water Using a Triple Quadrupole LC/MS/MS System

Glufosinate is a popular amino acid-based herbicide and glyphosate a popular foliage treatment herbicide. Glyphosate metabolizes in soil or water to form aminomethylphosphonic acid (AMPA).
In March 2015, the Japan's Ministry of Health, Labour and Welfare, Health Service Bureau, Water Supply Division issued a notification (No. 0325 Item 3 - 6) specifying the use of LC/MS/MS for water quality control inspections of glufosinate, since it is one of the pesticides designated for monitoring based on the specified target values for drinking water quality control, but no method for inspecting them has been specified so far.

■ Sample Pretreatment

Method 22 involves first derivatizing samples with 9-fluorenylmethyl chloroformate (Fmoc-Cl) under basic conditions and then concentrating the samples with solid phase extraction. The structural formulas of derivatized glufosinate, glyphosate, and AMPA are shown in Fig. 1.
A flowchart of the pretreatment process is shown in Fig. 2.

The Appendix Method 22 specified for glyphosate inspection by simultaneous analysis using a "derivatization - solid phase extraction - liquid chromatograph-mass spectrometer" system, can analyze both glyphosate and AMPA at the same time, which were previously inspected using separate methods (Appendix Methods 12 and 15) involving high-performance liquid chromatography.
In this example, Appendix Method 22 is used to analyze glufosinate, glyphosate, and AMPA. In addition, by using the LCMS-8050, samples can be analyzed directly without the pretreatment process of concentrating samples by solid phase extraction.

Fig. 1 Structure of Each Fmoc Derivative

20 mL sample	Add 0.2 mg sodium ascorbate
Derivatization	Sodium borate solution 2 mL Fmoc solution*1 50 ℃ (20 min) 1.2 mL 2 % phosphoric acid
Inert Sep C18 200 mg	Conditioning 3 mL acetonitrile 3 mL purified water
Rinse	1 mL aqueous solution of 5 mM ammonium acetate
Elution	1.5 mL eluate*2
Fill to volume	Add eluate to make 2 mL
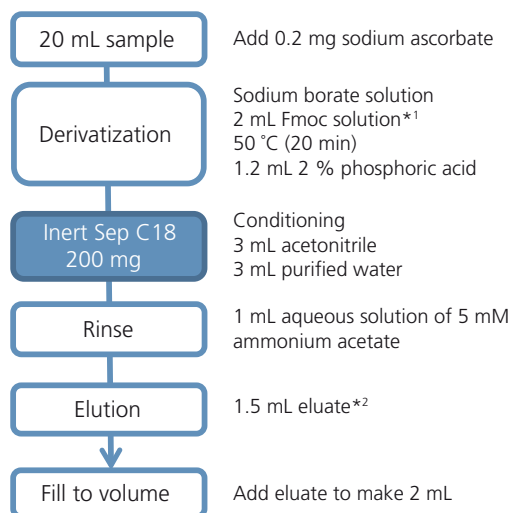
*1 Fmoc 1 mg/mL acetonitrile solution
*2 Acetonitrile / 5 mmol/L ammonium acetate = 40/60

Fig. 2 Pretreatment Process

■ Analyzing Glufosinate, Glyphosate, AMPA Standard Solutions (with Solid Phase Extraction)

After derivatizing the glufosinate, glyphosate, and AMPA standard mixture solution (with 0.1 μg/L each), the solution was concentrated by ten times with solid phase extraction, and measured. The resulting MRM chromatograms are shown in Fig. 3. Analytical conditions are indicated in Table 2.
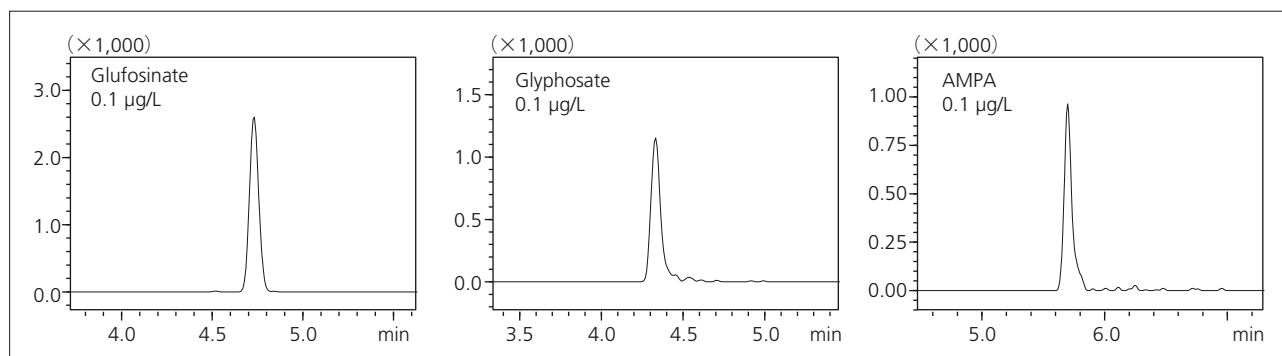
Fig. 3 MRM Chromatograms of Glufosinate, Glyphosate, AMPA Standard Solutions (with Solid Phase Extraction)

■ Analyzing Glufosinate, Glyphosate, AMPA Standard Solutions by Derivatization and Direct Analysis

The glufosinate, glyphosate, and AMPA standard mixture solutions (0.1 µg/L) were also analyzed without pretreatment by solid phase extraction, after only derivatization. The resulting MRM chromatograms and area value %RSD (n = 5) are shown in Fig. 4. Even for concentrations lower than 1/100 of the target value, results easily satisfied the criteria of less than 30 %RSD and even if the sample concentration step is skipped, high-sensitivity analysis is possible using the LCMS-8050.
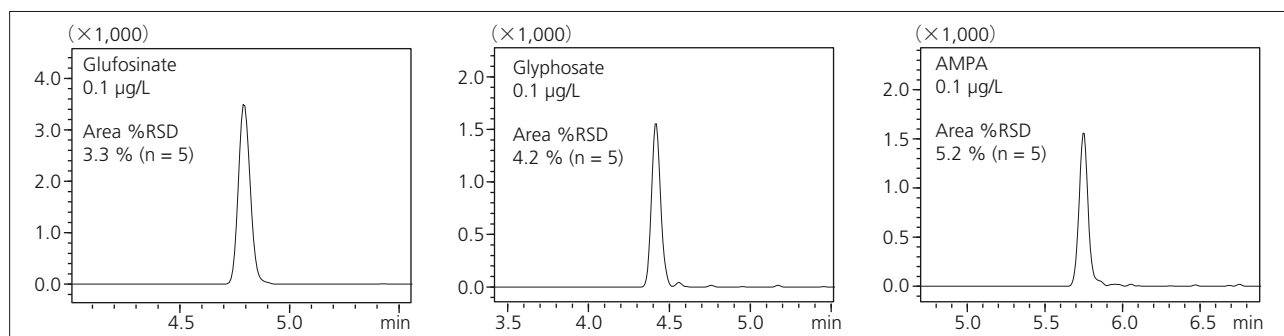
Fig. 4 MRM Chromatograms of Glufosinate, Glyphosate, AMPA Standard Solutions (Without Solid Phase Extraction)

■ Spike and Recovery Test Using Drinking Water (Derivatization - Direct Analysis)

Glufosinate, glyphosate, and AMPA were added to actual public drinking water and the recovery rate was evaluated by analyzing samples with only derivatization, without solid phase extraction pretreatment. MRM chromatograms for the blank drinking water, and water spiked respectively with 0.2 µg/L glufosinate, glyphosate, and AMPA are shown in Fig. 5. The corresponding recovery rates are indicated in Table 1. Good recovery rates (accuracy) were obtained within 70 to 120 %.

Table 1 Spike and Recovery Test Results (n = 5)

	Recovery Rate (%)	
	0.2 µg/L Added	2 µg/L Added
Glufosinate	96	99
Glyphosate	88	77
AMPA	96	104
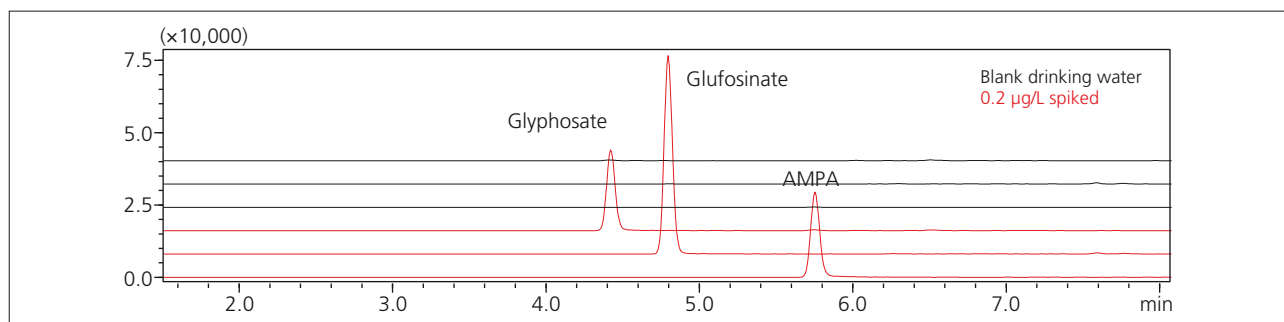
Fig. 5 MRM Chromatograms for Drinking Water (Blank) and Water Spiked with Glufosinate, Glyphosate, and AMPA (Without Solid Phase Extraction)

Table 2 Analytical Conditions

Column	: Mastro C18 (100 mm L. × 2.1 mm I.D., 3 µm, Shimadzu GLC)
Mobile Phases	: A 5 mmol/L Ammonium acetate-Water
	B Acetonitrile
Flowrate	: 0.25 mL/min
Time Program	: B.conc 5 % (0 min) → 50 % (7 min) → 95 % (7.01 - 11 min) → 5 % (11.01 - 13 min)
Column Temperature	: 40 ˚C
Injection Volume	: 2 µL (With solid phase extraction), 20 µL (Without solid phase extraction)
Probe Voltage	: - 3 kV (ESI - Negative)
DL Temperature	: 150 ˚C
Block Heater Temperature	: 400 ˚C
Interface Temperature	: 300 ˚C
Nebulizing Gas Flow	: 2 L/min
Drying Gas Flow	: 10 L/min
Heating Gas Flow	: 10 L/min
MRM Transition	: Glyphosate m/z 390 > 168 Glyphosinate m/z 402 > 180
	AMPA m/z 332 > 110

SHIMADZU

Shimadzu Corporation

www.shimadzu.com/an/

SHIMADZU
Excellence in Science

Application Data Sheet

No.36

LC-MS
Liquid Chromatograph Mass Spectrometer

Analysis of Pesticides in Drinking Water Using Triple Quadrupole LC/MS/MS (LCMS-8040)

With respect to agricultural chemicals in drinking water in Japan, 102 substances have been determined as water quality control targets under Japan 's Ministry of Health, Labour and Welfare' s Water Supply Act. However, revisions were recently made, and on March 28, 2013, notification of new categories, target values, and investigation methods was released. This data sheet presents an example of the simultaneous analysis of 48 compounds newly added by this notification.

41 of the 48 compounds added are measured in positive ion mode, and 7 are measured in negative ion mode. The LCMS-8040 triple quadrupole mass spectrometer was used for analysis. It features an ultrafast polarity switching time of 15 msec, enabling the acquisition of favorable data even from a single simultaneous analysis of multiple compounds with intermingled positive/negative ionization modes.

HPLC Conditions (Prominence UFLC)

Analytical column:	Shim-pack FC-ODS (2.0 mm I.D. × 75 mm L., 3 µm)
Mobile phase A:	5 mM aqueous ammonium acetate solution
Mobile phase B:	5 mM methanol ammonium acetate solution
Time program:	5 % B (0 min) – 40 % B (4 min) – 75 % B (39 min) – 100 % B (44–50 min) – 5 % B (50–60 min)
Flow rate:	0.15 mL/min
Injection volume:	100 µL
Column temperature:	30 °C

MS Conditions (LCMS-8040)

Ionization method:	ESI Positive/Negative
Probe voltage:	4.5 kV (ESI+), -3.5 kV (ESI-)
Nebulizer gas flow rate:	3 L/min
Drying gas flow rate:	15 L/min
DL temperature:	250 °C
Heat block temperature:	400 °C

Additional 48 Compounds

<Positive mode>
1. Dinotefuran
2. Nitenpyram
3. Pymetrozine
4. Thiamethoxam
5. Monocrotophos
6. Trinexapac-ethyl
7. Imidacloprid
8. Clothianidin
9. Acetamiprid
10. Thiacloprid
11. Cyanazine
12. Metribuzin
13. Bromacil
14. Fluazifop-P
15. Furametpyr
16. Metominostrobin
17. Pyriminobac-methyl (E), (Z)
18. Ametryn
19. Linuron
20. Boscalid
21. Cyproconazole (1), (2)
22. Cumyluron
23. Prometryn
24. Chromafenozide
25. Simeconazole
26. Tetraconazole
27. Diclomezine
28. Naproanilide
29. Tetrachlorvinphos (CVMP)
30. Tebufenozide
31. Tebuconazole
32. Fentrazamide
33. Cyprodinil
34. Etobenzanid
35. Oxadiargyl
36. Pirimiphos-methyl
37. Difenoconazole (1), (2)
38. Benzofenap
39. Oxaziclomefone
40. Quizalofop-ethyl
41. Clomeprop

<Negative mode>
42. Dichlorprop
43. Propanil
44. Inabenfide
45. Tiadinil
46. Flusulfamide
47. Thifluzamide
48. Fluazinam

Listed in RT order

(×1,000,000)

MRM Chromatogram for the 48 Newly Added Compounds

■ List of Compound Names

No.	Compounds	Polarity	RT (min)	m/z	No.	Compounds	Polarity	RT (min)	m/z
1	Dinotefuran	ESI(+)	5.1	203 > 129	25	Simeconazole	ESI(+)	31.5	294 > 70
2	Nitenpyram	ESI(+)	5.6	271 > 126	26	Tetraconazole	ESI(+)	32.2	372 > 159
3	Pymetrozine	ESI(+)	6.1	218 > 105	27	Diclomezine	ESI(+)	31.9	255 > 159
4	Thiamethoxam	ESI(+)	6.2	292 > 211	28	Naproanilide	ESI(+)	33.6	292 > 171
5	Monocrotophos	ESI(+)	6.5	224 > 193	29	Tetrachlorvinphos (CVMP)	ESI(+)	34.1	367 > 127
6	Trinexapac-ethyl	ESI(+)	7.0	253 > 69	30	Tebufenozide	ESI(+)	34.2	353 > 133
7	Imidacloprid	ESI(+)	7.1	256 > 175	31	Tebuconazole	ESI(+)	35.5	308 > 70
8	Clothianidin	ESI(+)	7.2	250 > 169	32	Fentrazamide	ESI(+)	35.9	350 > 83
9	Acetamiprid	ESI(+)	7.9	223 > 126	33	Cyprodinil	ESI(+)	36.5	226 > 93
10	Thiacloprid	ESI(+)	8.9	253 > 126	34	Etobenzanid	ESI(+)	36.9	340 > 179
11	Cyanazine	ESI(+)	11.8	241 > 214	35	Oxadiargyl	ESI(+)	37.8	358 > 341
12	Metribuzin	ESI(+)	12.8	215 > 49	36	Pirimiphos-methyl	ESI(+)	38.3	306 > 108
13	Bromacil	ESI(+)	13.1	261 > 205	37	Difenoconazole (1)	ESI(+)	39.7	406 > 251
14	Fluazifop-P	ESI(+)	15.5	328 > 282		Difenoconazole (2)	ESI(+)	40.1	406 > 251
15	Furametpyr	ESI(+)	19.0	334 > 157	38	Benzofenap	ESI(+)	42.0	431 > 105
16	Metominostrobin	ESI(+)	22.2	285 > 196	39	Oxaziclomefone	ESI(+)	42.6	376 > 190
17	Pyriminobac-methyl (E)	ESI(+)	24.1	362 > 330	40	Quizalofop-ethyl	ESI(+)	42.7	373 > 299
	Pyriminobac-methyl (Z)	ESI(+)	27.5	362 > 330	41	Clomeprop	ESI(+)	43.2	324 > 120
18	Ametryn	ESI(+)	25.2	228 > 186	42	Dichlorprop	ESI(-)	13.0	233 > 161
19	Linuron	ESI(+)	25.3	249 > 160	43	Propanil	ESI(-)	25.5	216 > 160
20	Boscalid	ESI(+)	27.0	343 > 307	44	Inabenfide	ESI(-)	16.1	337 > 122
21	Cyproconazole (1)	ESI(+)	28.2	292 > 70	45	Tiadinil	ESI(-)	29.0	266 > 71
	Cyproconazole (2)	ESI(+)	30.0	292 > 70	46	Flusulfamide	ESI(-)	31.7	413 > 171
22	Cumyluron	ESI(+)	29.7	303 > 185	47	Thifluzamide	ESI(-)	33.0	527 > 125
23	Prometryn	ESI(+)	30.6	242 > 158	48	Fluazinam	ESI(-)	42.3	463 > 416
24	Chromafenozide	ESI(+)	31.0	395 > 175					

SHIMADZU

Shimadzu Corporation

www.shimadzu.com/an/

SHIMADZU
Excellence in Science

Application Data Sheet

No.39

LC-MS
Liquid Chromatograph Mass Spectrometer

Quantitative Analysis of Pyrethroids in Soil Using Triple Quadrupole LC-MS/MS

Pyrethroids are insecticides used worldwide for both household and farming applications. Pyrethroids have limited water solubility and are easily adsorbed in soil. Recently, it has been reported that pyrethroids remain in the soil and sediment in farming and urban regions for long periods. Although pyrethroids are not particularly harmful for humans, they are very toxic for insects and water creatures and their influence on the ecosystem is a big concern. There is a demand for new methodology that enables measurement of pyrethroids in soil and sediment with high sensitivity and throughput.

Traditionally, pyrethroids are measured by Gas Chromatography with or without mass spectrometry. Here, we report a method using LC-MS/MS to show that LC-MS/MS can measure these compounds traditionally analyzed by GC. This report illustrates a simultaneous analysis of 15 pyrethroids using the Shimadzu UFMS Triple Quadrupole LCMS-8050 with ultrafast polarity switching. The polarity switching speed of the LCMS-8050 is just 5 milliseconds under any conditions.

Combined with the Nexera X2, the LCMS-8050 provides much faster run times without sacrificing the quality of results.
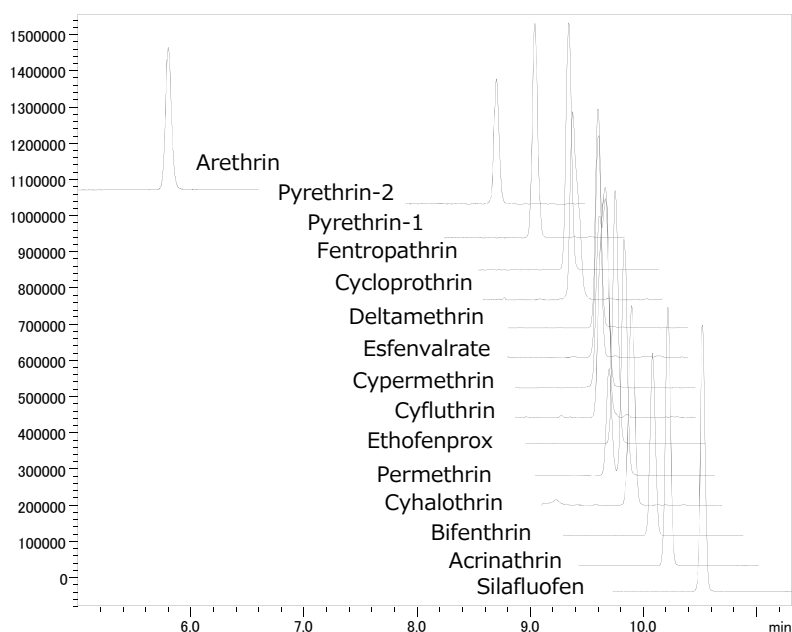
Figure 1: Representative MRM chromatograms of 15 pyrethroids

■ Compounds List

Compounds	Polarity	Precursor (*m/z*)	Product (*m/z*)
Amethrin	+	228.00	186.10
Pyrethrin-1	+	329.20	161.10
Pyrethrin-2	+	373.20	161.20
Fenpropathrin	+	367.20	125.20
Cycloprothrin	+	498.90	181.10
Deltamethrin	+	522.80	280.90
Esfenvalrate	+	437.10	167.30
Cypermethrin	+	433.10	191.10
Cyfluthrin	+	450.90	191.00
Ethofenprox	+	394.20	177.30
trans-Permethrin	+	408.10	183.30
cis-Permethrin	+	408.10	183.30
Cyhalothrin	+	467.10	225.10
Bifenthrin	+	440.00	181.20
Acrinathrin	-	540.10	372.20
Silafluofen	+	426.20	287.10

HPLC conditions (Nexera X2)

Column	: Phenomenex Kinetex 2.6u PFP 100A
Mobile phase A	: 5 mM Ammonium acetate water
Mobile phase B	: Methanol
Time program	: 40%B (0min) – 100%B(10-12min) – 70%B (12.01-15min)
Flow rate	: 0.2 mL / min.
Injection volume	: 1 µL
Oven temperature	: 40 ℃

MS conditions (LCMS-8050)

Ionization	: ESI (Positive / Negative)
Probe voltage	: ＋4.5 kV / -3.5 kV
Nebulizing gas flow	: 3.0 L / min.
Drying gas flow	: 15.0 L / min.
Heating gas flow	: 15.0 L / min.
Interface temperature	: 100 ℃
DL temperature	: 100 ℃
Heat block temperature	: 400 ℃

Table 1: Calibration range and linearity for 15 pyrethroids

Compounds	Range (µg/L)	r²
Amethrin	0.01 - 100	0.9992
Pyrethrin-1	0.5 - 500	0.9996
Pyrethrin-2	0.5 - 500	0.9997
Fenpropathrin	0.02 - 100	0.9993
Cycloprothrin	0.5 - 100	0.9991
Deltamethrin	0.05 - 100	0.9992
Esfenvalrate	0.5 - 100	0.9990
Cypermethrin	0.05 - 100	0.9986
Cyfluthrin	0.5 - 100	0.9976
Ethofenprox	0.01 - 100	0.9993
trans-Permethrin	0.02 - 100	0.9996
cis-Permethrin	0.02 - 100	0.9994
Cyhalothrin	0.1 - 100	0.9993
Bifenthrin	0.02 - 100	0.9995
Acrinathrin	0.1 - 100	0.9994
Silafluofen	0.01 - 100	0.9999
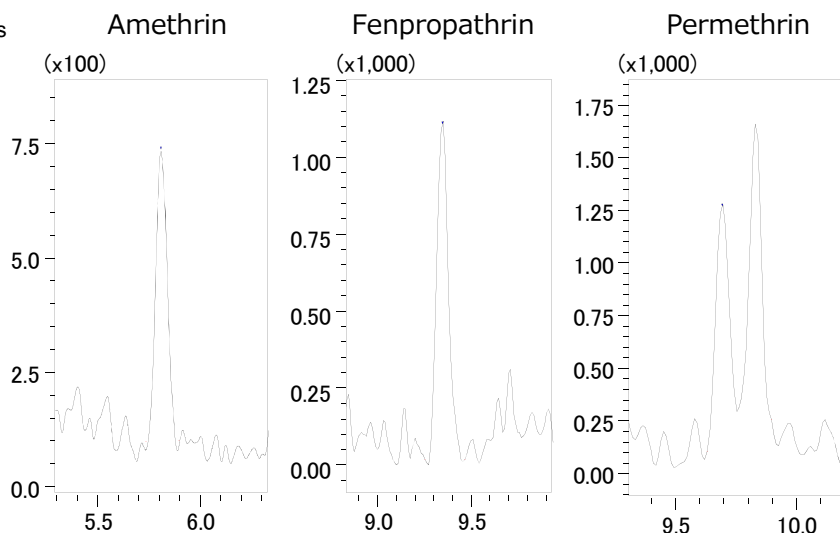
Figure 2: Chromatograms at the lowest calibration level
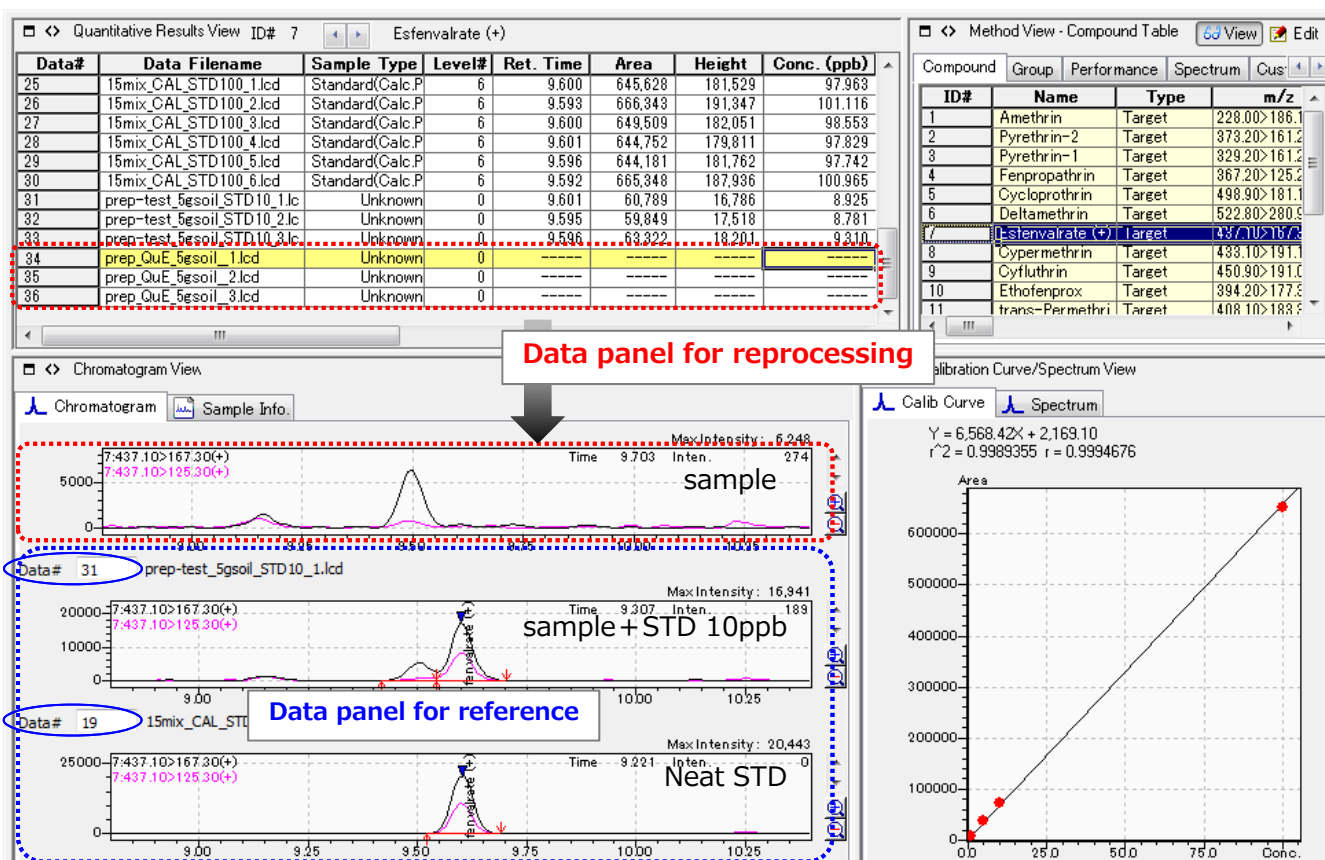
Figure 3: Quant Browser

The figure above is a screen shot of LabSolutions Quant Browser loaded with the data from a set of soil extracts, matrix matched calibration curve and neat standards. QuEChERS was used for sample clean-up for soil samples. Recoveries were excellent, ranging from 70 to 100%. In residual pesticide analysis, sample matrix is very complex. So, it is important to identify the analyte accurately and to carry out peak integration appropriately.

LabSolutions Quant Browser makes intuitive and "at-a-glance" data reprocessing possible with multiple data files. Figure 3 illustrates the quantitative results of Esfenvalerate. Esfenvalerate was not detected in real-world samples, but its possible isomer was detected at RT 9.5 minutes. Reviewing multiple results, such as sample, matrix matched standard and neat standard results, in a single panel saves data reprocessing time.

SHIMADZU

Shimadzu Corporation

www.shimadzu.com/an/

SHIMADZU
Excellence in Science

Application Data Sheet

No.43

LC-MS
Liquid Chromatograph Mass Spectrometer

High Speed Analysis of Haloacetic Acids in Tap Water Using Triple Quadrupole LC-MS/MS

Haloacetic acids (HAAs), by-products of water disinfection, are formed from naturally-occurring organic and inorganic materials in water which react with the disinfectants chlorine and chloramine. Certain haloacetic acids have been shown to cause adverse reproductive or developmental effects in laboratory animals. Three HAAs regulated by numerous government bodies such as the US EPA include chloroacetic acid (CAA), dichloroacetic acid (DCAA) and trichloroacetic acid (TCAA). A Liquid Chromatography Mass Spectrometry (LC-MS/MS) method for measuring HAAs capable of direct injection of water samples has been developed to replace previously used methods requiring tert-butyl-methyl ether liquid extraction and diazomethane derivitization prior to GC analysis, thus reducing the effort required for sample preparation. Reduced sample preparation times combined with rapid UHPLC chromatography increase the productivity of water control laboratories. This data sheet illustrates results from a high speed method acquired using a LCMS-8050 triple quadrupole mass spectrometer coupled with a Nexera X2 UHPLC.

■ Comparison of Sensitivity and Reproducibility between Standard and High Speed Methods

In the high speed method, CAA, DCAA, and TCAA eluted at 3.1, 3.4, and 5.2 minutes, shortening the run time by 25 minutes relative to the standard method (Figure 1). Figure 2 illustrates each HAA MRM chromatogram and area reproducibility at 0.001 mg/L. Each HAA demonstrates excellent reproducibility and sensitivity at this concentration.
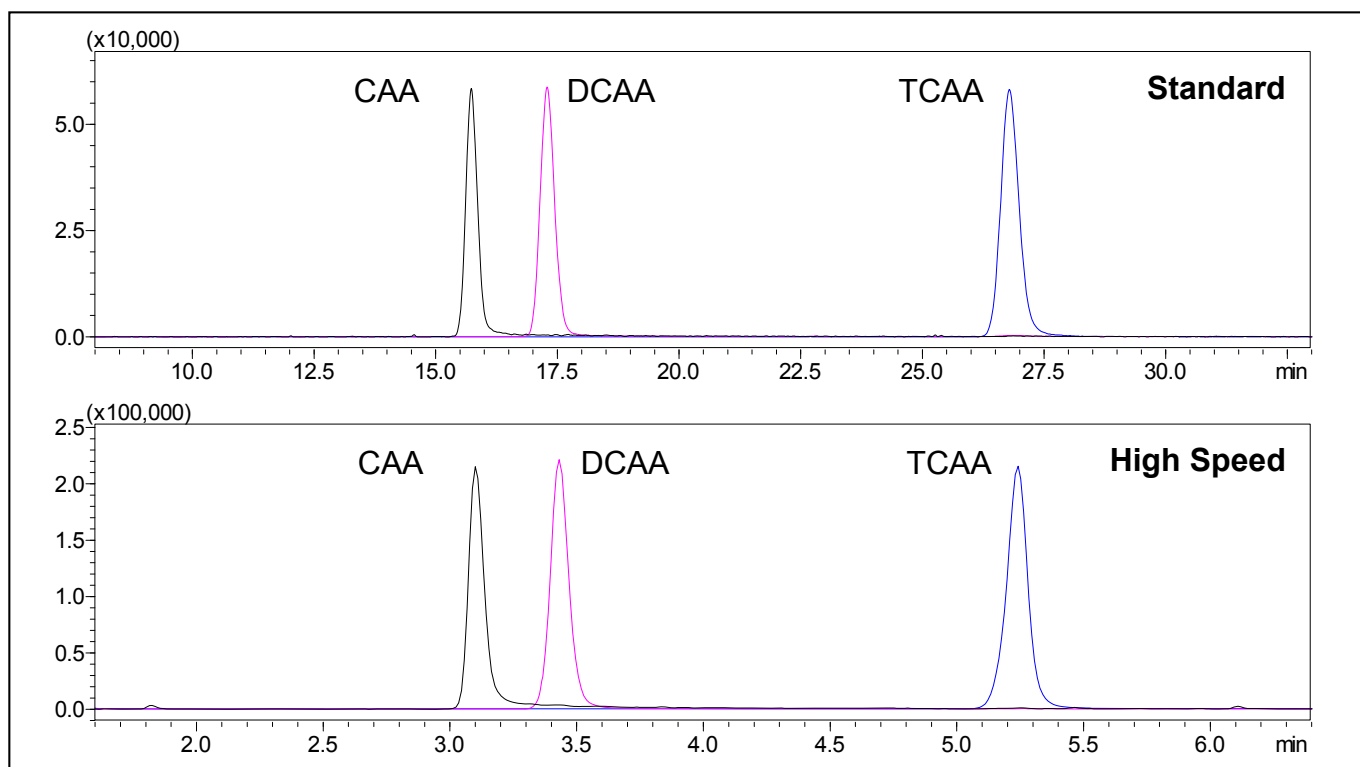
Fig. 1 MRM Chromatograms of Haloacetic Acids
(Top: Standard Analytical Method, Bottom: High Speed Analytical Method)
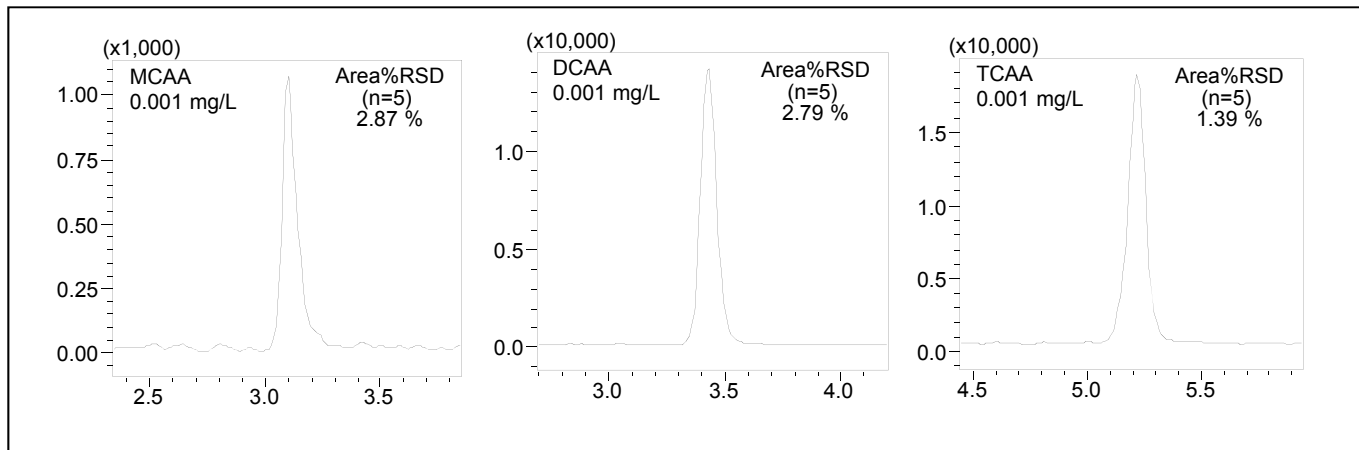
Fig. 2 MRM Chromatograms of CAA, DCAA and TCAA in neat solution at 0.001 mg/L. Reproducibility at 0.001 mg/L, n=5.
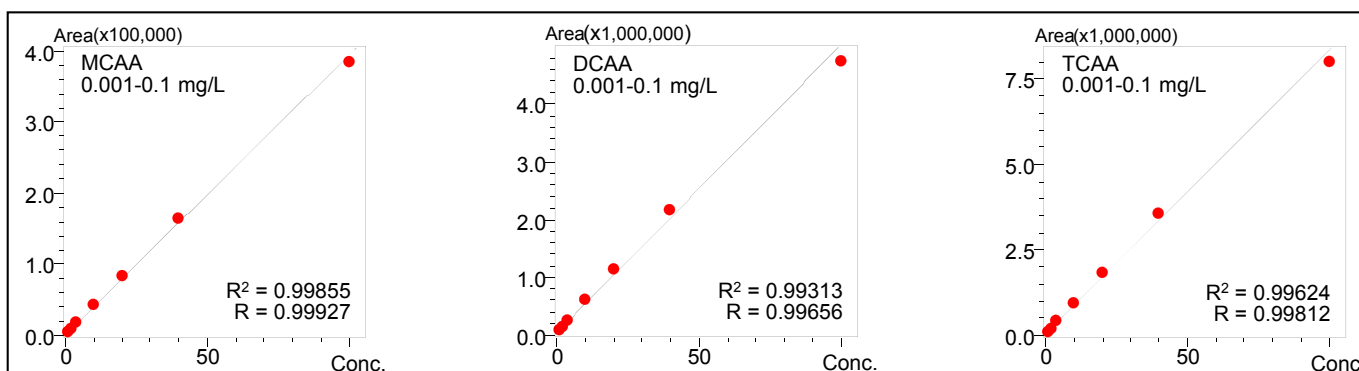
Fig. 3 Linearity of Peak Area of CAA, DCAA and TCAA

Table 1 Analytical Conditions

Column	: CAPCELL PAK MGIII (150 mm X 3 mm, 3 μm)
Mobile Phases	: A 0.2 % Formic acid-water
	: B 0.2 % Formic acid-methanol
Flow Rate	: 0.5 mL/min
Column Temperature	: 50 ℃
Injection Volume	: 25 μL
Probe Voltage	: -3.5 kV (ESI-negative mode)
DL Temperature	: 150 ℃
Block Heater Temperature	: 100 ℃
Interface Temperature	: 100 ℃
Nebulizing Gas Flow	: 3 L/min
Drying Gas Flow	: 5 L/min
Heating Gas Flow	: 15 L/min
MRM Transition	: CAA; *m/z* 93.00>35.00, DCAA; *m/z* 126.90>82.90, TCAA; *m/z* 161.10>116.90

■ Recovery Test on Tap Water

A recovery test on tap water from four locations was conducted using this high speed method. Figure 4 demonstrates the quality of chromatograms produced when these three HAAs were spiked at 0.001 mg/L into each of the four tap water samples with no further sample preparation. Regardless of tap water location (Figure 5), excellent recoveries ranging from 90 to 110% were obtained for each sample. (Table 2)

Table 2 Quantitative Results and Recovery Tests of Tap Water

	Sample 1		Sample 2		Sample 3		Sample 4	
	Tap water conc. (mg/L)	Recovery (%)	Tap water conc. (mg/L)	Recovery (%)	Tap water conc. (mg/L)	Recovery (%)	Tap water conc. (mg/L)	Recovery (%)
CAA	Tr.	102.6	0.00076	103.6	0.00069	94.9	0.00034	100.4
DCAA	Tr.	108.3	0.01151	101.7	0.00742	102.9	0.00635	92.3
TCAA	Tr.	107.1	0.00861	107.2	0.00622	104.5	0.00452	102.9
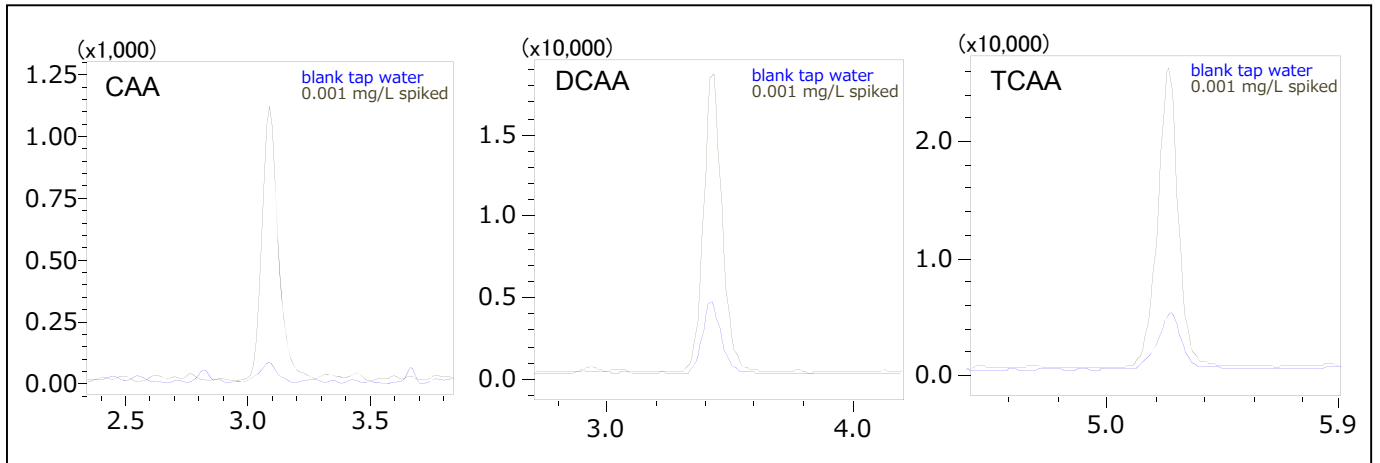
Fig. 4 MRM Chromatograms of Blank Tap Water (Blue) and CAA, DCAA and TCAA Spiked on Blank Tap Water (Sample 1: 0.001 mg/L each)
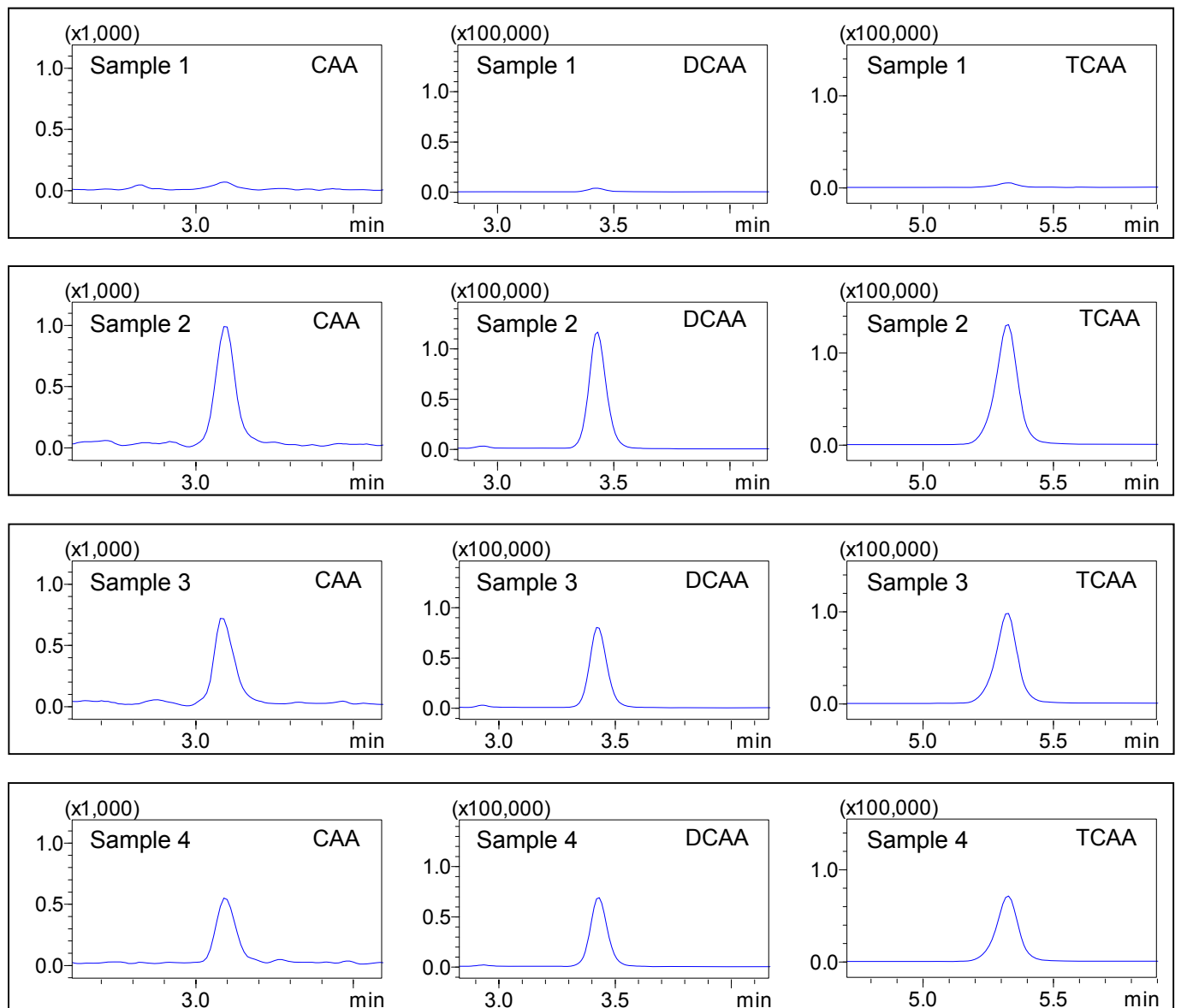
Fig. 5 MRM Chromatograms of Tap Water (Sample 1 to 4)

■Intuitive Data Processing with LabSolutions Quant Browser

In a busy water control laboratory, it is important to not only increase the speed of measurement but also the throughput of data processing. Quant Browser provides an intuitive, quantitative data processing environment allowing multi-chromatogram visualization of different data files synchronized to analyze a compound of interest.

When measuring analytes from any matrix, there is a possibility of interferences, therefore, the results can be easily reviewed and confirmed by comparing the sample and standard data within a single chromatogram panel.

Figure 6 provides a Quant Browser screen capture displaying a CAA chromatogram from tap water (upper) and from standard solution (lower). With only a glance, it is clear there is no interference in the tap water chromatogram.
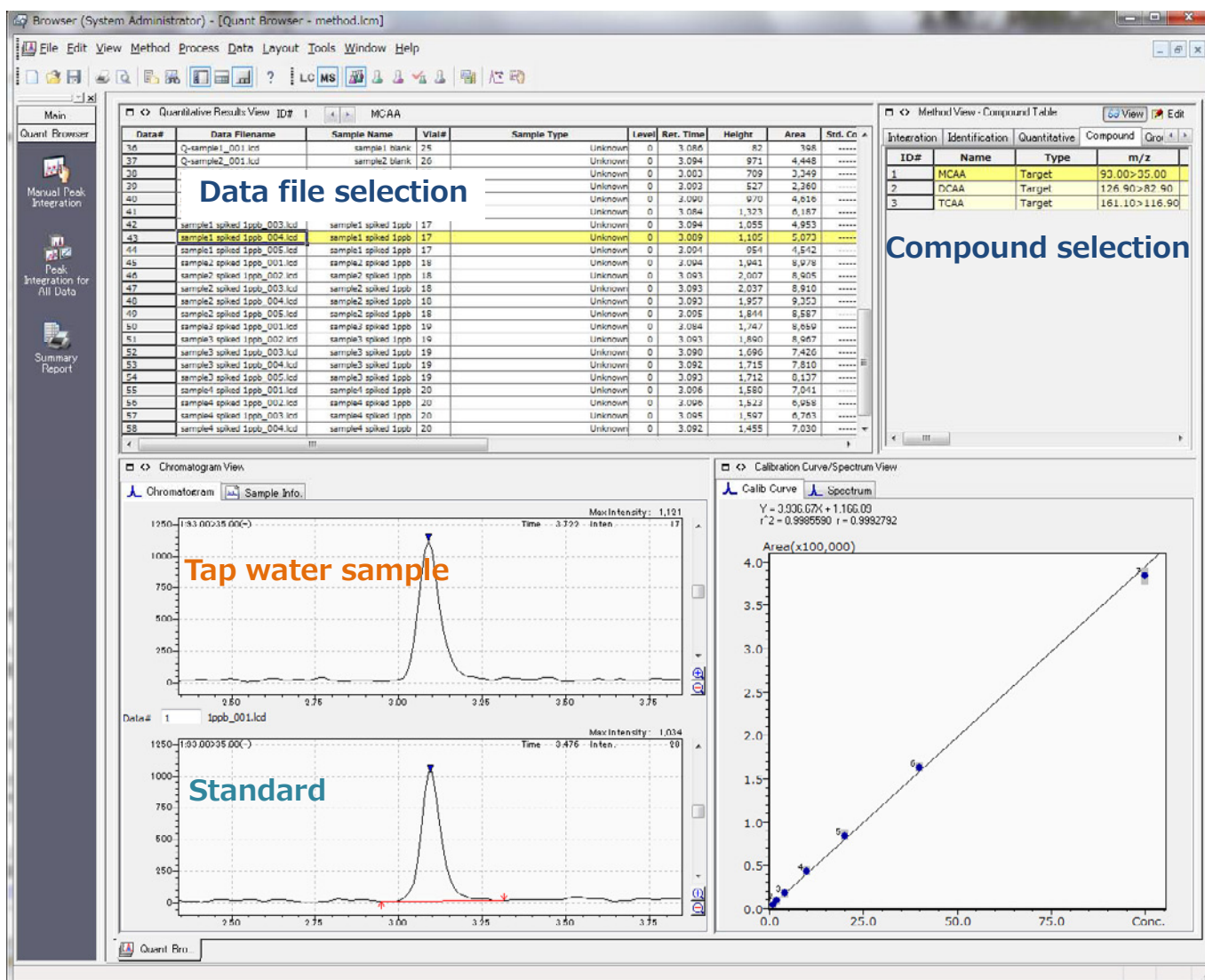
Fig. 6 Multiple Quantitative Data Processing with Quant Browser in LabSolutions

SHIMADZU

Shimadzu Corporation

www.shimadzu.com/an/
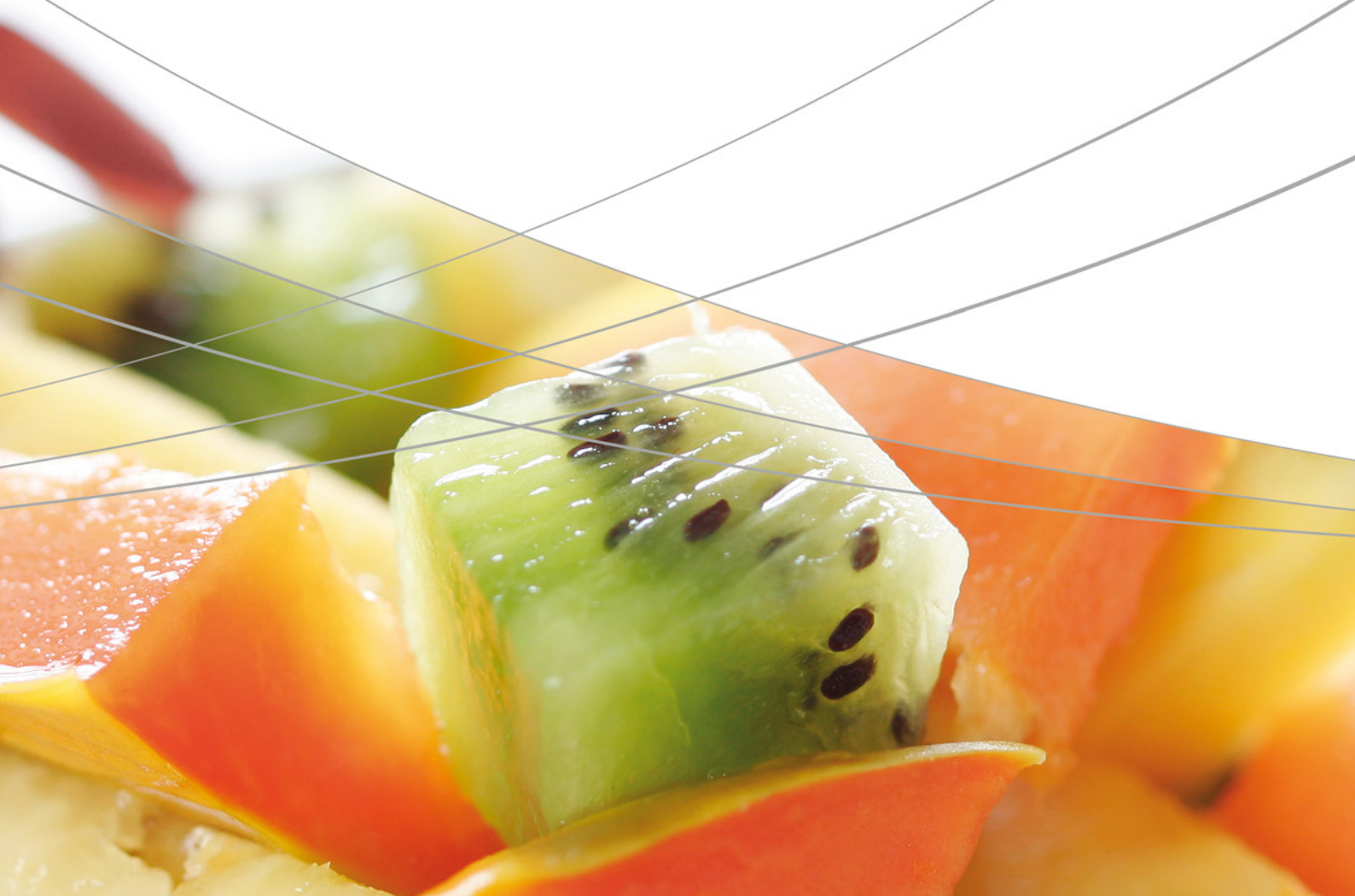
3. Spectroscopy

3. Spectroscopy

3.1   Atomic Spectroscopy

3.1.1 Atomic Absorption Spectroscopy

AAS quantitates concentrations of elements in a vapor, when a ground state atom absorbs light energy of a specific wavelength and is elevated to an excited state. The amount of light energy absorbed at this wavelength is increased when the number of atoms of the selected element in the light path increases. The relationship between the amount of light absorbed and the concentration of the element present in known standard solutions can be used to determine unknown sample concentrations by measuring the amount of light they are absorbing.

A469A	Measurement of cadmium (Cd) and lead (Pb) in food additives by electrothermal atomic absorption spectrometry (ETAAS)
SCA-120-025	Analysis of Na, K, Ca and Mg in mineral water using microsampling method
SCA-120-026	Analysis of Cu and Zn in red wine using atomic absorption spectrometry
SCA-120-027	Determination of antimony in soft drinks
SCA-120-029	Determination of thallium in the food chain using AA-7000
A487	Direct determination of Pb in edible oils by GF-AAS
A495	Measurement of arsenic and selenium in white rice and river water by hydride generation-atomic absorption spectrometry
SCA-120-034	Analysis of Cu and Zn in beer using atomic absorption spectrometry
AA-004	Analysis of "The Big Four" heavy metals in hops by electrothermal atomization and cold vapor

3.1.2 Energy Dispersive X-Ray Fluorescence EDX

XRF allows analysis of element composition of samples in a wide variety of applications. This technique provides non-destructive and fast measurements of liquid and solid samples and is best suited for analyzing the elemental range from sodium/ carbon to uranium, which covers the majority of the metallic elements.

X246	EDXRF analysis of arsenic and lead in dietary supplement
X247	Qualitative and quantitative analysis of seafood by EDXRF

3.1.3 Inductively Coupled Plasma Optical Emission Spectroscopy

Inductively Coupled Plasma Optical Emission Spectroscopy (ICP-OES) is the measurement of light emitted by all elements present in a sample introduced into an ICP source. The emission intensities measured are then compared with the intensities of standard samples of known concentration to obtain the elemental concentrations in the unknown samples. The argon plasma is generated by an RF field and ionized argon gas. The advantage of the plasma in comparison to other energy sources is the high temperature of 10,000 ˚K, enabling complete atomization of the elements in a sample while minimizing interferences.

J103	Simultaneous analysis of trace and major elements in rice by ICPE-9820
SCA-115-017	Determination of trace elements in natural water using ICP-OES
SCA-115-023	Determination of heavy metals in wine using simultaneous ICP-OES
J104	Analysis of multiple elements in drinking water by ICPE-9820
J109	Content analysis of toxic elements in soil by ICPE-9800 Series
J116	Analysis of nutritional and harmful elements in powdered milk by ICPE-9820 / HVG-1

![SHIMADZU Excellence in Science]

Application News

Spectrophotometric Analysis

Measurement of Cadmium (Cd) and Lead (Pb) in Food Additives by Electrothermal Atomic Absorption Spectrometry (ETAAS)

No.A469A

■ Introduction

A food additive is defined in Japan's Food Sanitation Act as "an item to be used for the purpose of storage or processing of food, which is added to, mixed with, or diffused into food in any manner."
Food additives are used for a variety of purposes, as, for example, preservatives, sweeteners, coloring agents, and stabilizers. Test methods and component standards have been established for many of these, and have been published as a food additives compendium titled "Japan's Specifications and Standards for Food Additives." One of the purity test items is heavy metal testing (in terms of lead content), for which the eighth edition of the compendium adopts a colorimetric method using Nessler cylinders. However, in the ninth edition, a different test method is under review, in which the element lead is handled individually.
Here, we introduce an example of analysis of cadmium (Cd) and lead (Pb) in α-cyclodextrin (cyclic oligosaccharide), a substance used in functional foods, pharmaceuticals, cosmetics, etc. The analysis was conducted by electrothermal atomic absorption spectrometry (ETAAS) using the AA-7000 atomic absorption spectrophotometer.

■ Sample Preparation

Sample digestion was conducted using the ETHOS One microwave sample preparation system (Milestone Srl). Compared to pretreatment using dry ashing or an open system such as wet digestion, microwave digestion permits quick digestion of the sample, making it unlikely that contamination or volatilization of the measurement element will occur. The digestion process flow is shown in Fig. 1.
For validity assessment of the pretreatment and measurement, the same process was conducted on a sample spiked with standard solution prior to digestion. Preparation was conducted so that the spiked solid concentrations were 0.05 µg/g of Cd and 0.5 µg/g of Pb.

Transfer 0.5 g sample to digestion container.
↓
Add small amount of distilled water and 8 mL nitric acid, then mix.
↓
Seal container, set in ETHOS One, digest for approx. 1 hour.
↓
After cooling, transfer to a vessel, add distilled water to a volume of 50 mL.
↓
Measure the sample by electrothermal atomic absorption spectrometry.
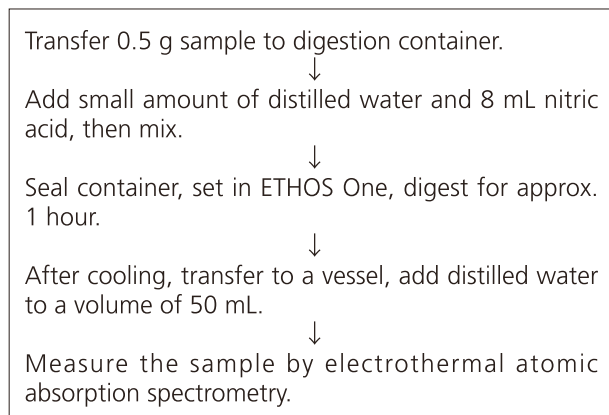
Fig. 1 Flowchart of Sample Decomposition

■ Analysis Method and Conditions

The standard solutions for atomic absorption analysis were prepared by diluting a 1000 mg/L standard solution to obtain 1 µg/L of cadmium and 10 µg/L of lead, respectively. The calibration curves were generated using an autosampler to adjust the injection volumes of standard solution in a stepwise manner. In addition, 5 µL of a palladium nitrate solution (50 mg/L palladium content) was added as a matrix modifier to all of the samples. The main conditions that were used for the spectrometer and atomization are shown in Tables 1 and 2.

Table 1 Optics Parameters

	Cd	Pb
Analytical wavelength	228.8 nm	283.3 nm
Slit width	0.7 nm	
Ignition mode	BGC-D2	

Table 2 Atomizing Conditions

	Cd	Pb
Ashing temperature	700 ℃	800 ℃
Atomizing temperature	2200 ℃	
Standard solution concentration (ppb)	0.2, 0.5, 1.0	2.5, 5, 10
Tube type	Platform	
Sample injection volume	20 µL	
Matrix modifier	5 µL of 50 ppm palladium nitrate	None

With the microwave digestion method, since much of the acid that is added remains, it is not uncommon for the acid concentration in the sample solution to be more than 10 %. High acid concentration is a factor that can lead to a decrease in repeatability and sensitivity. The platform tube used for this measurement (see Fig. 2) is resistant to the effects of acidity and coexisting substances in the matrix because the sample is injected into a plate having a recess (platform) that is mounted in the tube and then uniformly heated by radiant heat from the outer wall. Fig. 3 shows the changes in absorbance of a lead standard solution caused by varying the nitric acid concentration. A fairly constant absorbance was found to be obtained up to a nitric acid concentration of 20 %.
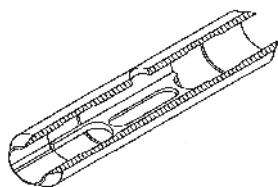
Fig. 2 Sectional View of Platform Tube
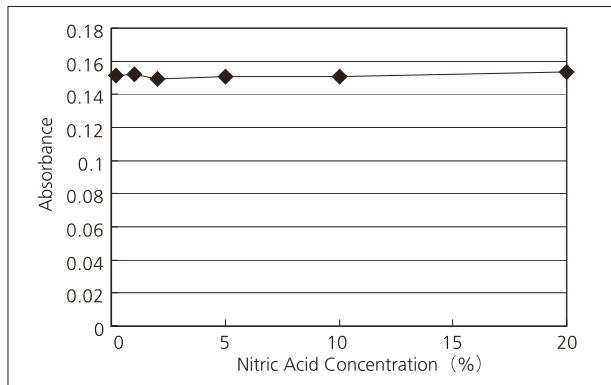
Fig. 3 Sensitivity Variation of Pb 10 µg/L Standard Solution Due to Changes in Nitric Acid Concentration When Using a Platform Tube

Fig. 4 Calibration Curve of Cd

Fig. 5 Calibration Curve of Pb

■ **Results and Conclusion**

The sample measurement results are shown in Table 3. Neither of the elements was detected in the sample. Calculation of the lower limit of quantitation as a concentration in a solid at an absorbance of 0.01 Abs yielded 0.003 µg/g for cadmium and 0.07 µg/g for lead. Good values were obtained in spike and recovery testing, and high-sensitivity analysis of heavy metals was possible using electrothermal atomic absorption spectrometry with a platform tube, without adverse effects from the acid concentration. The calibration curves are shown in Figs. 4 and 5, respectively, and the peak profiles are shown in Fig. 6.

The AA-7000 Series features a lineup that includes not only dedicated instruments for the flame method and electrothermal method, but also a dual-use instrument that offers automatic switching of the atomization method, thereby supporting a wide range of application requirements.

Regarding the α-cyclodextrin that was measured in this application, the eighth edition of the Specifications and Standards for Food Additives specifies a separate reference value for lead (1 µg/g or less). For pretreatment, after ashing 10 g of sample, nitric acid is added to bring the solution to a volume of 10 mL, and flame atomic absorption is specified as the measurement method. When the AA-7000 flame method is used to analyze the sample prepared in this manner, the expected detection limit of lead in a solid sample is about 0.2 µg/g.
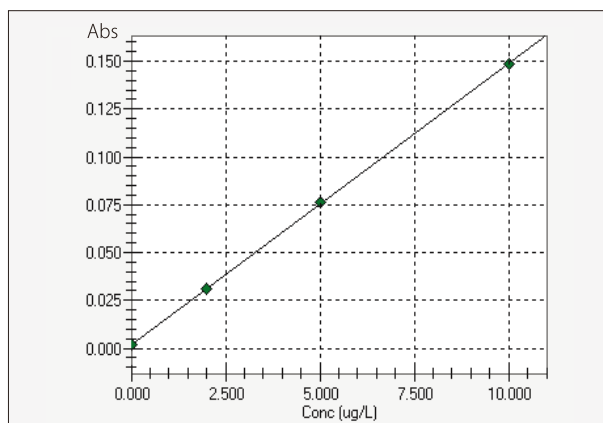
Fig. 6 Peak Profiles

Table 3 Measurement Results of Cd and Pb in α-Cyclodextrin

Element	Cd	Pb
Measured value	＜0.003 µg/g	＜0.07 µg/g
Spike and recovery rate	105 %	99 %

SHIMADZU

Shimadzu Corporation

www.shimadzu.com/an/

Spectroscopy – AAS

Analysis of Na, K, Ca and Mg in mineral water using Microsampling method

The AA-7000 in combination with the ASC-7000 sample preparation station allows the automated flame micro sampling method (Figure 1). In this method, the flame atomic absorption analysis is conducted with small sample volumes (2 – 90 µL), while in the conventional flame method (hereafter "flame continuous method"), the sample is continuously aspirated with a flow rate of approximately 8 ml/min and larger sample volumes are needed for aspiration.

The flame micro sampling method has several advantages over the flame continuous method: analysis is possible with a small amount of sample, and when the autosampler is used, automatic dilution of the sample and automatic addition of buffer solutions are possible in order to compensate interferences. Moreover, since only a small amount of sample is introduced, the flame micro sampling method is effective for analysis of high matrix samples which may cause clogging of the burner in the flame continuous method. So the method is the right choice for determination of alkaline and alkaline earth elements in mineral water.

Sodium, Potassium, Calcium, and Magnesium belong to the essential mineral substances in the human organism. These elements take influence in the generation of enzymes and hormones, control the osmotic pressure in tissues and body fluids and are important for the exchange procedures in the cell membranes.[1] The recommended daily amounts (Na: 550, K: 2000, Ca: 800-1000, Mg: 350 mg/L [1]) are possible to be partly covered by consumption of mineral waters. But the composition of mineral waters according to the essential elements has a wide variety, and depending on the origin the composition might be quite different.
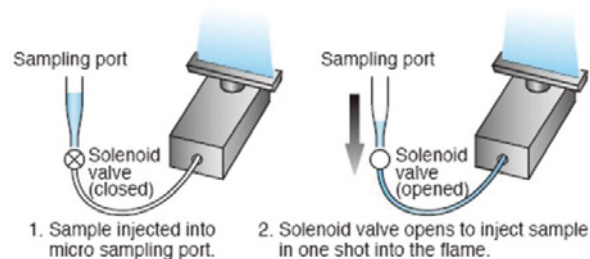
Figure 1: Microsampling method

■ Method

The control of Na, K, Ca and Mg in a variety of mineral waters has been performed according to the actual DIN/EN regulations[2], with the Shimadzu atomic absorption spectrophotometer AA-7000 in a fully automatic multi element sequence.

The blank, standards and the water samples are all placed in the autosampler and then will be mixed automatically with the corresponding reagents which have to be added according to the DIN/ EN method. In case of Sodium and Potassium 40 µl of CsCl-solution (12,65 g CsCl + 50 ml HCl (d=1,16) filled up to 500 ml volume with H_2O) will be added for a 400 µl mixing volume of standard and sample solution which is homogenized before injection to the flame. In case of Calcium and Magnesium a La_2O_3-solution (5,875 g La_2O_3 + 50 ml HCl (d=1,12) filled up to 250 ml volume with H_2O) has been used.

The instrumental parameters and measuring conditions are listed in Table 1 below. These conditions are automatically set for each element including optimized burner high and gas flow rates.

■ **Results and Conclusion**

Under these conditions, a series of more than 20 drinking water and mineral water samples has been analyzed. A reference material (NIST SRM 1640) was measured along with this series as a laboratory control sample. The excellent recoveries are listed in Table 2.

Elem.	Certified [mg/L]	Result [mg/L]	Recovery [%]
Ca	0.7045 $\pm$ 0.089	6.980	99.08
K	0.994 $\pm$ 0.027	1.015	102.11
Mg	5.819 $\pm$ 0.056	5.850	100.53
Na	29.35 $\pm$ 0.31	29.19	99.42

Table 2: Comparison of the certified and measured concentrations of NIST SRM 1640 control sample
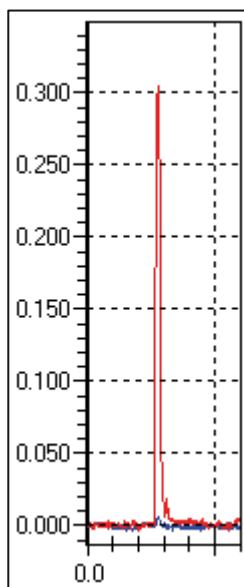
Figure 2: Potassium peak profile (50 µL injection)

Figure 1: Potassium calibration curve

Instrument	AA 7000 with autosampler ASC 7000 incl. Microsampling Kit			
Measurement element	Na	K	Ca	Mg
Wavelength	589,0 nm	766,5 nm	422,7 nm	285,2 nm
Slit width	0,2 nm	0,7 nm	0,7 nm	0,7 nm
Lamp current	8/600 mA	8/600 mA	10 mA	8 mA
Backgroundcorrection	SR	SR	D_2	D_2
Flame type	Air-C_2H_2	Air-C_2H_2	Air-C_2H_2	Air-C_2H_2
Gas flow rate	1,8 l/min	2,0 l/min	2,0 l/min	1,8 l/min
Sampling time	20 sec	20 sec	20 sec	20 sec
Interference buffer	CsCl-solution	CsCl-solution	La_2O_3-solution	La_2O_3-solution
Calibration range [mg/L]	0,1 – 1,0	0,1 – 1,0	0,25 – 5,0	0,025 – 0,5

Table 1: Instrument and Analytical Conditions

[1] Mineralstoffe und Spurenelemente, Verlag Bertelsmann Stiftung, 1991
[2] Deutsche Einheitsverfahren (DEV) zur Wasser-, Abwasser- und Schlamm-untersuchung, Verlag Chemie, Weinheim; DIN 38406-E14 (Natrium), DIN 38406-E13 (Kalium), DIN EN ISO 7980-E3-1 (Calcium, Magnesium)

Application News

No. SCA-120-026

Analysis of Cu and Zn in Red Wine Using Atomic Absorption Spectrometry

Wine is one of the oldest cultural products in human history. Wines have been cultivated for over 8000 years. The oldest known archaeological evidence of winemaking is an 8000-year old wine- and fruit press found near Damascus. Awareness of the medicinal effects of wine also date back to this time. Hippocrates (460 – 377 B.C.) recommended wine diluted with water as a remedy against headaches and digestive disorders.

Figure 1: Grapes – the source of red wine

■ Spectroscopic methods: quality assurance

A meticulous quality control procedure is essential, and during each stage of the production process spectroscopic methods such as AAS-, ICP-, FTIR-, and UV-VIS spectroscopy are applied for quality assurance or for product characterisation. For the quantitative determination of copper and zink, the atomic absorption spectrometry is the method of choice, since the sensitivity of AA-7000F in flame atomization allows a fast and precise analytical procedure.

■ Quality Standards

The quality standards are fixed in the national wine regulations such as the German "Weinverordnung" (Bundesgesetzblatt Teil 1 Nr. 32) from 22nd May 2002, and the European Union's new wine regulations from 2009, which includes the classification of wines from different locations but also the production process, alcohol concentrations and the maximum allowable concentrations of the elements as listed in table 1.

Element	Max. Concentration [mg/L]
Al	8.00
As	0.10
B	80
Cd	0.01
Cu	2.00
Pb	0.25
Sn	1.00
Zn	5.00

Table 1: Maximum allowable concentration of elements in wine

■ Experimental work

The control of copper and zinc is a typical application for the Shimadzu flame atomic absorption spectrophotometer AA- 7000F in a fully automatic multi element sequence in combination with the ASC-7000.

Copper in concentrations of higher than 1 mg/L has a strong influence on the quality of the wine. It can cause a metallic bitter taste, and also generates turbidity. Higher copper concentrations are mainly generated from the bordeaux mixture, consisting of

copper sulphate and hydrated lime, which is used as a fungicide in the vineyards. It was invented in the Bordeaux region of France, where it is known locally as Bouillie Bordelaise. This fungicide has been used for over a century and is still used, although the copper will be accumulated in the ground.

The blank, standards and the wine samples are all placed in the autosampler and then will be automatically aspirated to the flame. The advantage of ASC-7000 is the improved rinsing mechanism shown in figure 2, the "overflow method" which is minimizing the carry over effects when analyzing high concentration samples. The blank and standard samples have been adjusted to the matrix of the wine samples using 10% ethanol.

The instrumental parameters and measuring conditions are listed in Table 2. These conditions are automatically set for each element including optimized burner height and gas flow rates.
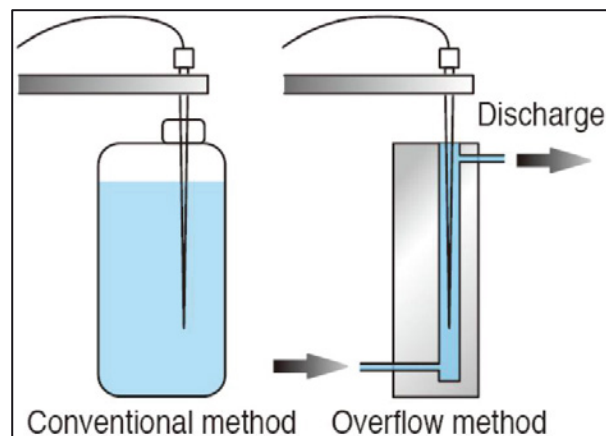
Figure 2: Rinsing method of ASC-7000

Instrument	AA-7000 with ASC-7000	
Element	Cu	Zn
Wavelength	324,8 nm	213,9 nm
Slit width	0,7 nm	0,7 nm
Lamp current	6 mA	4/ 100 mA
Background-correction	D2	SR
Flame type	Air-C2H2	Air-C2H2
Gas flow rate	1,8 l/min	2,0 l/min
Integration time	3 sec	3 sec
Calibration range [mg/L]	0,5 - 4,0	0,1 - 1,0

Table 2: Instrument and Analytical Conditions

■ **Conclusion**

For the determination of copper and zinc AA-7000F is the "state of the art" tool for the daily routine in quality control of wine samples. Furthermore the AA-7000 is able in combination with GFA-7000 to achieve calibration ranges as low as 1 to 10 ppb.
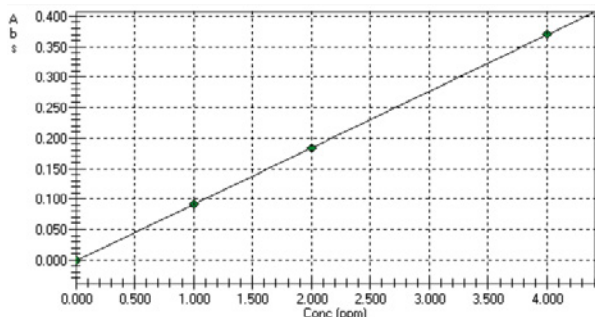
Figure 3: Copper calibration curve
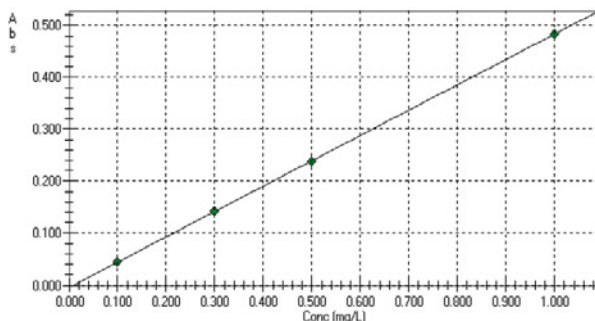
Figure 4: Zinc calibration curve

SHIMADZU

Application News

Determination of Antimony in Soft Drinks

No. SCA-120-027

In the last few years some studies prove an increased concentration level of antimony (Sb) in several mineral waters, softdrinks, and fruit beverages.[1] This is an alarming aspect because almost all Sb-compounds are somehow toxic and harmful to the environment. It is assumed that the Sb in the beverages originates from their packing material polyethylene terephthalate bottles (PET), because antimony trioxide (Sb_2O_3) is used as a catalyst in the PET-production process. Whereat the drinking water used for the beverages are subjected to the European drinking water directive (Sb-limit value = 5 µg/L)[2] it is of equally interest to analyze the stored and ready-to-drink beverages.

This application segment describes how to analyse antimony in soft drinks, esp. in cola. The research is done with the AA-7000G **A**tomic **A**bsorption Spectrophotometer with the high sensitivity graphite furnace GFA-7000 and the sample preparation station ASC-7000 as shown in figure 1.

Keywords such as system plus method parameters and use of modifier outline user expectations in this application segment.

■ Sb in bottle material

All the bottles of the soft drinks were examined concerning their content of Sb. Here the EDX-720-HS can with direct measurement of the solid samples. All the PET-material (bottles) in this research includes 200-300 mg/kg antimony.

Figure 1: AA-7000G with GFA-7000 and ASC-7000

■ Standard system Configuration

– AA-7000G with GFA-7000
– ASC-7000
– Teflon-tube pipette (for many samples)
– Omega platform tube

The omega platform tube (figure 2) is used because it has a more reproducible heating performance compared with conventional graphite tubes. The sample can be well placed on the inner concentric platform. The outer graphite tube is electrothermic heated and the omega platform underlies the uprisen thermal radiation of the outer tube.

Figure 2: Design of the omega platform tube

■ Matrix Modifier

Because the antimony is highly volatile and the present sample matrix is very heavy (e.g. high content of sugar in soft drinks), the measurement is not trivial. The first step to get better results is already done by using the omega platform tube. The second step is the use of a Modifier. Here the addition of 5 ng palladium and 3 ng magnesium (absolute) to each measurement (table 1) was very helpful to separate and ash the matrix without an early volatilization of the antimony.

Chemical	Amount (for 25 mL)
Pd-modifier (10g/L)	6,25 mL
Mg(NO$_3$)$_2$·6H2O	395 mg
Deionised water	Up to the 25mL mark

Table 1: Composition of PdMg-Modifier

■ Method parameters

Choose the 217.6 nm line to analyse Sb in Soft drinks like cola. The corresponding temperature program is listed in table 2. Because of the platform tube and the modifier, here are higher temperatures used than in the normal temperature program. This is necessary because of the indirect platform heating plus the heavy matrix. The high temperatures are possible because of the modifier.

	Temp. [°C]	Time [sec.]	Heat Mode
1	150	20	RAMP
2	250	10	RAMP
3	1000	15	RAMP
4	1000	10	STEP
5	1000	3	STEP
6	2500	3	STEP
7	2600	2	STEP

Table 2: Temperature program

Method parameters	
Slit width	0.7 nm
Lamp current	
Backgroundcorr.	D2
Calibration range	5 – 20 µg/L

Table 3: Method parameters

The samples are measured in standard addition mode. In table 4 there is the volume scheme for one sample. The matrix of Sb-standards differs clearly in comparison to the sample. Thus, the standard addition mode should be used to get more secured results.

	MSA-1	MSA-2	MSA-3
1. Water	10	10	10
2. Sb 40 µg/L	10	5	0
3. Sample	0	5	10
4. Modifier	2	2	2

Table 4: Standard addition volumes

■ Results and Conclusion

Shimadzu's AA 7000G incl. GFA 7000 and ASC 7000 is an ideal tool for analysis of antimony in soft drinks. With the described parameters it was possible to examine cola of different brands. The determined Sb-amounts are listed in table 5. For each sample antimony was detected.

	c(Sb) [µg/L]
Cola 1	2.0 ± 0.1
Cola 2	2.0 ± 0.2
Cola 3	2.2 ± 0.2
Cola 4	5.4 ± 0.4

Table 5: Result overview

[1] Claus Hansen (2010) Elevated antimony concentrations in commercial juices. J. Environ. Monit. 12, page 822-824

[2] COUNCIL DIRECTIVE 98/83/EC (03.11.1998) on the quality of water intended for human consumption

Spectroscopy – AAS

Determination of Thallium in the Food Chain using AA-7000

Thallium, as well as the equally toxic elements lead and cadmium, belongs to the group of heavy metals. Thallium is prevalent in nature, for instance in potassium-containing clays and soils. Thallium is used in the manufacture of optic glasses for fax machines and photocopiers, just to mention an industrial application. The element is present in very small amounts in foods, drinking water and in air. Increased thallium concentrations are most notably measured near cement plants and smelters.

■ **Limited Concentrations in Water**

Humans primarily absorb thallium through food. Particularly in vegetables, relatively high amounts of thallium can be detected. The average daily amount of thallium absorbed has been estimated at 2 - 5 µg per day. Thallium concentrations of up to 15 µg per liter have been detected in natural mineral waters. There are no limit values for thallium in the European Drinking Water Ordinance of 2006 [1]. The US EPA refers to a maximum value of 2 µg/L in its Drinking Water Standard based on a water consumption of 2 liters per day.

■ **Quantitative Determination with AA-7000**

Quantitative determination of the element thallium in aqueous samples has been carried out using Shimadzu's AA-7000 atomic absorption spectrometer (Figure 1), which is equipped as standard with deuterium and high-speed self-reversal background compensation.

Figure 1: AA-7000G with GFA-7000 and ASC-7000

For electrothermal atomization, the high sensitivity GFA-7000 graphite furnace with digital control was used. For experimental investigations, standard solutions, diluted measuring solutions as well as reference standard solutions were used. The Thallium determination was carried out in the concentration range of 1 to 10 µg/L in accordance with *DIN 38406-26:1997-07,* German standard methods for the examination of water, waste water and sludge- Cations (group E)- Part 26: Determination of thallium by atomic absorption spectrometry (AAS) using electrothermal atomisation(E 26). Atomization was carried out at 2,700°C on a pyrolytically coated graphite tube with Omega platform (Figure 2) while adding 5µL rhodium modifier.

Figure 2: Design of the omega platform tube

■ Method parameters

The 276.8 nm line has been selected to analyse Thallium in natural mineral water samples. The optimized temperature program is listed in table 1. Because of the Omega platform tube and the Rhodium modifier, it was possible to maximize the element absorption signal (red) while minimizing the background (blue). The peak profiles are displayed in Figure 3.
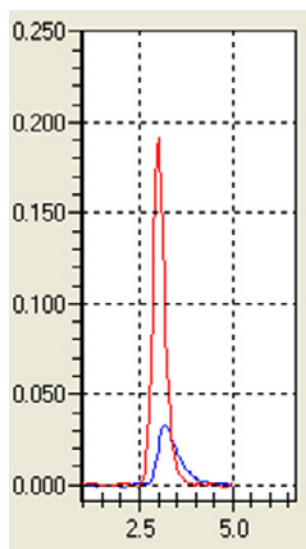
Figure 3: Peak profiles for Thallium (10µg/L)

	Temp. [°C]	Time [sec.]	Heat Mode
1	150	20	RAMP
3	1000	15	RAMP
4	1000	10	STEP
5	1000	3	STEP
6	2700	3	STEP
7	2900	2	STEP

Table 1: Temperature program

Method parameters	
Slit width	0.7 nm
Lamp current	6 mA
Backgroundcorrection	D_2
Calibration range	5 – 20 µg/L

Table 2: Method parameters
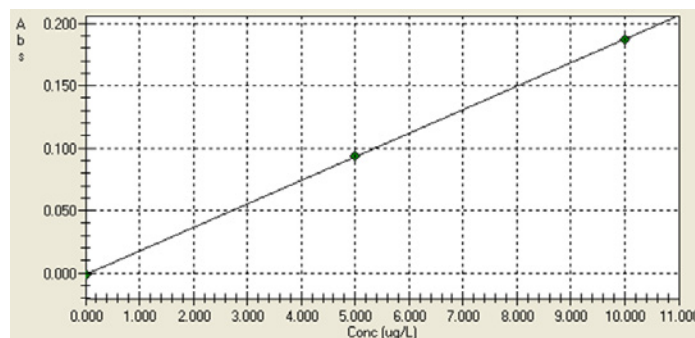
Figure 3: Calibration Curve for Thallium

■ Reliable determination of toxic heavy metals

Under these conditions, aqueous samples can be analyzed without interferences. The ASC-7000 sample preparation station enables fully automated processing of 60 samples within one analytical run. The quality assurance criteria of the WizAArd software allow the use of laboratory control samples and automated calculation of the recovery rates. The AA-7000 in combination with the GFA-7000 is a suitable monitoring system for reliable determination of toxic heavy metals such as thallium in drinking water and mineral water.

■ Standard system Configuration

– AA-7000G with GFA-7000
– ASC-7000
– Omega platform tube

■ References

[1] Federal Institute for Risk Assessment (BfR) (2006), Thallium in natural mineral waters

SHIMADZU
Excellence in Science

Application News

Spectrophotometric Analysis

Direct Determination of Pb in Edible Oils by GF-AAS

No.A487

■ Introduction

Edible oils, probably the most widely used cooking ingredient in the world, are produced from a wide variety of basic ingredients, including fruits (olives, coconuts, palm, etc.), nuts (walnuts, macadamia nuts, almonds, etc.), seeds (sesame, sunflower, etc.), and a variety of plants (soy, canola, capsicum (peppers)). These oils are not only used for frying and baking, but are also consumed as food, serving as dressings and toppings, etc. Thus, with this wide consumption of edible oils, it is important to not only ensure their safety and non-toxicity, but that they satisfy quality specifications.

Here, using the Shimadzu AA-7000 atomic absorption spectrophotometer and the GFA-7000 graphite furnace atomizer, we introduce an example of direct quantitation of lead in edible cooking oil in accordance with AOAC Official Method 994.02, Lead in Edible Oils and Fats – Direct Graphite Furnace Atomic Absorption Spectrophotometric Method.

The GFA-7000 graphite furnace atomizer supports heating at temperatures from ambient to 3000 °C, and the high-sensitivity optical sensor and digital temperature control system provide accurate temperature control over the entire temperature range from drying to atomization. In addition, the dual electronic flowrate control system permits independent setting of the argon gas flowrate to 0.01 L/min, thus providing high-accuracy measurement with high sensitivity.

Table 1 Optics Parameters

Lamp current (mA)	10
Measurement wavelength (nm)	283.3
Slit width (nm)	0.7
BGC mode	BGC-D2

■ Sample

Sesame oil (one type)

■ Sample Preparation

First, a matrix modifier solution was prepared by dissolving 2 g of lecithin in cyclohexane modifier (2 % w/v solution of lecithin). The measurement sample consisted of a mixture of 5 g of sesame oil and 5 g of 2 % w/v lecithin solution. For measurement validation, a spike and recovery test sample was prepared by adding 50 ppb of lead to the equivalent of a sample solution.

Table 2 Temperature Program

Pb	Temperature (°C)	Time (Sec)	Heating Mode	Sensitivity	Gas Type	Gas Flowrate
1	120	10	RAMP		#1	0.30
2	120	20	STEP		#1	0.30
3	800	60	RAMP		#1	0.30
4	800	20	STEP		#1	0.30
5	800	3	STEP		#1	0.00
6	1800	5	STEP		#1	0.00
7	2500	1	RAMP		#1	0.05
8	2500	3	STEP		#1	0.05

Atomization Stage No. 6

■ Instrument and Analytical Conditions

For the measurement, the Shimadzu AA-7000 atomic absorption spectrophotometer and GFA-7000 graphite furnace atomizer were used together with the ASC-7000 autosampler. The optics parameters that were used are shown in Table 1, and the temperature program, in Table 2.

When analyzing samples containing large amounts of organic solvents and organic compounds, accurate control of temperature and gas flowrate from drying to atomization is important to ensure the vaporization, decomposition and elimination of solvents and organic compounds.

■ Analysis

Lead standard solutions of 20, 50, and 100 ppb were prepared by appropriately diluting a commercially available oil mixture standard solution (CONOSTAN®S-21) with blank oil. Preparation was conducted on a weight basis (wt%) using commercially available salad oil as blank oil for dilution.

Mixtures consisting of 5 g of each of the standard solutions and 5 g of 2 % w/v of lecithin solution were used as standard solutions. Using a platform graphite tube for measurement, the sample injection volume was 10 μL.

■ **Analytical Results**

Fig. 1 shows the calibration curve obtained using this method, and Fig. 2 shows the peak profiles for the respective standard solutions. Table 3 shows the measurement results and spike and recovery results for sesame oil. Excellent spike and recovery results were obtained with nearly 100 % recovery. Fig. 3 shows the peak profile obtained in the measurement of sesame oil.

Abs=0.0023487Conc-0.00019383
r=0.9998
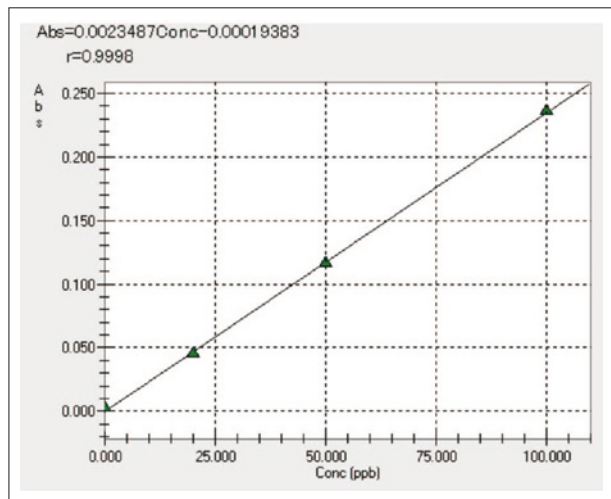
Fig. 1 Calibration Curve for Pb in Edible Oil
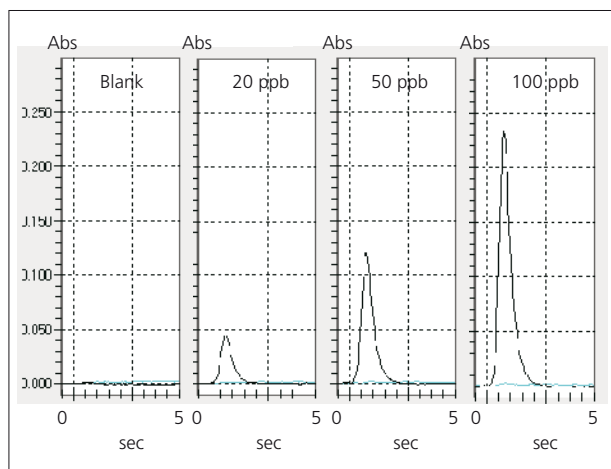
Fig. 2 Peak Profile of Pb in Standard Solution

Table 3 Measurement Results for Pb in Sesame Oil

Element	Sesame Oil	50 ppb Spike and Recovery Test Solution	Recovery (%)
Pb	< 4 ppb*	50 ppb	100 %

* Absorbance 0.01 or less
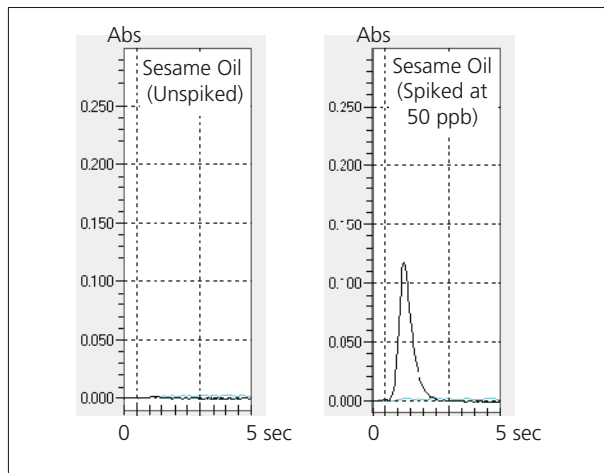
Fig. 3 Peak Profile of Pb in Sesame Oil

■ **Summary**

In this Application News, we conducted direct analysis of lead in edible oils using the AA-7000 and ASC-7000 autosampler together with the GFA-7000 graphite furnace atomizer in accordance with AOAC Official Method 994.02. Excellent sensitivity and recovery were obtained over the specified concentration range (18 µg/kg (ppb) or greater).

■ **References**

1) AOAC Official Method 994.02, Lead in Edible Oils and Fats, Direct Graphite Furnace Atomic Absorption Spectrophotometric Method

2) Application News No.AA-003 "AOAC 994.02: Determination of Pb in Edible Oils and Fats by GF-AAS" SHIMADZU SCIENTIFIC INSTRUMENTS (SSI)

SHIMADZU

Shimadzu Corporation

www.shimadzu.com/an/

Application News

No.A495

Spectrophotometric Analysis

Measurement of Arsenic and Selenium in White Rice and River Water by Hydride Generation-Atomic Absorption Spectrometry (HG-AAS) with Electric Cell Heating

■ Introduction

The hydride generation method is known as a technique for high-sensitivity measurement of elements such as arsenic (As) and selenium (Se), based on the fact that at ambient temperature such elements react with newly generated active hydrogen to generate hydrogen gas compounds. Because it is not easy affected by alkaline metals, alkaline earth metals, and other elements coexisting in samples, it is often used for high-sensitivity measurement of As, Se, and other elements in the environment, foods, and other samples, not only in atomic absorption spectrometry, but also in ICP atomic emission spectrometry, ICP mass spectrometry, and other methods.

The method commonly used for atomic absorption spectrometry involves sending the hydrogen compound gas (AsH_3 and H_2Se) generated in a hydride vapor generator into a quartz absorption cell and atomizing the elements by thermal decomposition. Then either a flame or electric heating (furnace) is used to heat the absorption cell.

Electric heating avoids the need for gas supplies required for the flame method (acetylene and air) and offers about 1.5 times higher sensitivity than the flame method for As and Se measurements.

In this example, hydride generation-atomic absorption spectrometry (HG-AAS) with an electric cell heater for heating the absorption cell was used to measure arsenic and selenium in certified white rice reference material (NMIJ CRM 7502-a) and certified river water reference materials (JSAC 0301 with nothing added and JSAC 0302 with As and Se added).

■ Pretreatment

(1) White Rice

About 1 g of the sample was weighed into a beaker, moistened with a small amount of water, 10 mL of nitric acid was added, and then the sample was thermally decomposed on a hot plate. After the vigorous reaction was finished, 5 mL of nitric acid and 1 mL of perchloric acid were added and thermal decomposition was further continued. After white smoke appeared, the sample was heated to almost dryness and allowed to cool. Then 5 mL of hydrochloric acid (1 + 1) was added to dissolve soluble salts. The result was transferred to a separate container and pure water was added to make 25 mL of the sample stock solution.

Then 10 mL of this sample stock solution was prereduced to create 20 mL of the measurement sample. Arsenic was prereduced by adding hydrochloric acid, potassium iodide and ascorbic acid and selenium by adding hydrochloric acid to make 20 mL of the measurement solutions.

(2) River Water

10 mL was prereduced to create 20 mL of the measurement sample, in the same manner as for the white rice.

■ System Configuration and Measurement Conditions

The system was configured from an AA-7000 atomic absorption spectrophotometer connected to an HVG-1 hydride vapor generator and SARF-16C atomic muffle furnace (electric cell heater). The cell heater is shown in Fig. 1.

Major measurement conditions are indicated in Table 1.

Heating furnace

Temperature controller
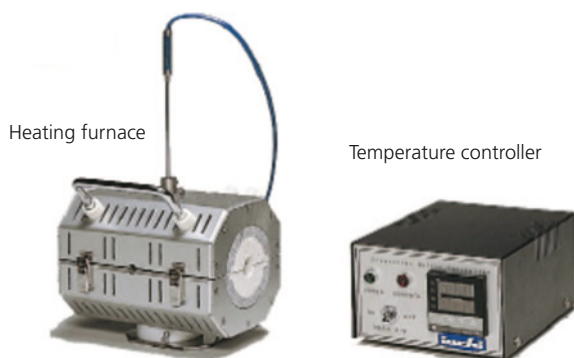
Fig. 1 SARF-16C Atomic Muffle Furnace (Electric Cell Heater)

Table 1 Measurement Conditions

	As	Se
Analytical wavelength	193.7 nm	196.0 nm
Slit width	0.7 nm	
Background correction	Deuterium lamp method (D2 method)	
Absorption cell heating system	Electric heating (800 °C)*	
Carrier gas	Ar (about 0.1 L/min)	
Integration time (number of times repeated)	5 sec (n = 5)	
Reagent concentration	$NaBH_4$ 0.4 % (NaOH 0.4 %)	
	5 mol/L hydrochloric acid	
Sample delivery rate	4 mL/min (0 to 7 mL/min variable)	
Reagent delivery rate	1.5 mL/min (0 to 2.5 mL/min variable)	

* The electric cell heater cannot be installed as a dual-purpose (flame and furnace) unit for the AA-7000 system.

■ Analytical Results
Calibration Curve and Sensitivity

Calibration curves for As and Se are shown in Figs. 2 and 3, respectively. As a guideline for the lower limit of detection, a 1 % absorption value (0.0043 Abs) was achieved at a concentration of 0.05 ppb for As and 0.09 ppb for Se in the measurement solution.

Abs=0.082764Conc+0.0051532
r=0.9995
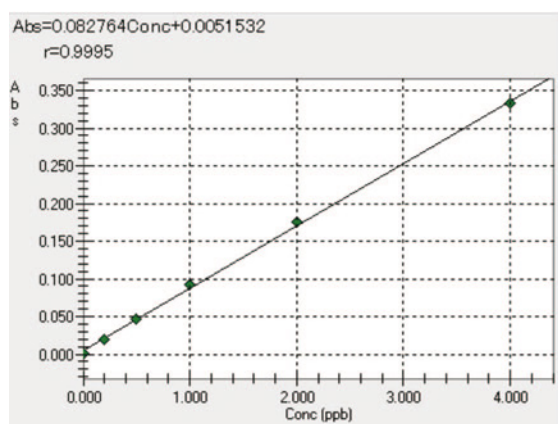
Operation	Sample ID	Concentration Setting (ppb)	Absorbance	%RSD
STD-AV	Blank	0.0000	0.0010	134.72
STD-AV	0.2ppb	0.2000	0.0196	2.65
STD-AV	0.5ppb	0.5000	0.0470	2.39
STD-AV	1ppb	1.0000	0.0929	1.87
STD-AV	2ppb	2.0000	0.1747	1.23
STD-AV	4ppb	4.0000	0.3330	1.79

Fig. 2 Calibration Curve for As

Abs=0.046703Conc+0.0015978
r=0.9999
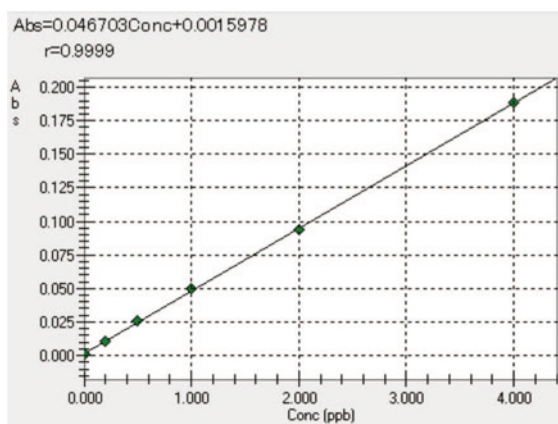
Operation	Sample ID	Concentration Setting (ppb)	Absorbance	%RSD
STD-AV	Blank	0.0000	0.0011	78.53
STD-AV	0.2ppb	0.2000	0.0103	17.81
STD-AV	0.5ppb	0.5000	0.0257	4.26
STD-AV	1ppb	1.0000	0.0495	3.12
STD-AV	2ppb	2.0000	0.0941	1.30
STD-AV	4ppb	4.0000	0.1885	2.12

Fig. 3 Calibration Curve for Se

Analytical Results

Measurement results for white rice are indicated in Table 2 and for river water in Table 3. Results from both samples closely matched respective certified values.

Table 2 Measurement Results of As and Se in White Rice

White Rice (NMIJ CRM 7502-a)

Element	As	Se
Certified Value (mg/kg)	0.109	–
Measured Value (mg/kg)	0.101	0.010
%RSD (n = 5)	1.7 %	8.5 %

Table 3 Measurement Results of As and Se in River Water

River Water (JSAC 0301-3 unspiked)

Element	As	Se
Certified Value (μg/L)	0.20	(0.08)*
Measured Value (μg/L)	0.21	< 0.2
%RSD (n = 5)	7.4 %	–

* Reference value

River Water (JSAC 0302-3 spiked)

Element	As	Se
Certified Value (μg/L)	5.2	5.0
Measured Value (μg/L)	5.1	5.3
%RSD (n = 5)	1.5 %	1.0 %

■ Conclusion

This example shows how an AA-7000 system with electrically heated hydride generation can be used to analyze the arsenic and selenium in food and environmental water with high sensitivity, without the need for gas supplies (acetylene and air) required by flame methods.

SHIMADZU

Shimadzu Corporation

www.shimadzu.com/an/

Application News

Spectroscopy – AAS

Analysis of Cu and Zn in Beer Using Atomic Absorption Spectrometry

No. SCA-120-034

Beer is the most popular alcoholic beverage in Europe. In Germany, beer enjoys a particularly high status due to the German Beer Purity Law of 1516 ("Reinheitsgebot"), which defines the ingredients of beer to be hop, malt, yeast and water. This makes the German Beer Purity Law the oldest food law in the world, which is still valid today and makes beer, in addition to drinking water, one of the most researched food products with the highest standards regarding quality, freshness, appearance and flavor.

Figure 1: Beer - most popular drink in Europe

■ Analytical methods: quality assurance

A meticulous quality control procedure is essential, and during each stage of the production process analytical methods such as spectroscopy, chromatography and mass spectrometry are applied for quality assurance or for product characterisation. For the quantitative determination of copper and zinc, the atomic absorption spectrometry is the method of choice, since the sensitivity of

AA-7000F in flame atomization allows a fast and precise analytical procedure.

■ Quality Standards

The quality standards for beer analysis are described in the European Brewery Convention (EBC), which includes the determination of elements like copper, zinc, sodium, potassium, calcium and more, anions such as nitrate and sulfite as well as organic components such as ethanol, glycerine and others [1].

Even though the most abundant constituent of beer is water, it is important to control all other constituents, which are dissolved in it. The determination of copper is important as high concentrations are disadvantageous on the colloidal stability and the taste of the beer. Same with zinc, which is an essential trace element for yeast influencing metabolic processes such as protein synthesis and nucleic acid metabolism. Typical concentration levels of copper and zinc in beer are 0.2 mg/L [2].

■ Experimental work

The determination of copper and zinc concentrations is a typical application for the Shimadzu flame atomic absorption spectrophotometer AA- 7000F in a fully automatic multi element sequence in combination with the ASC-7000.
A typical measuring procedure according to EBC is the method of standard addition. This requires the preparation of standard solutions containing the same amount of beer, but

different amounts of copper standard, for example, five standard solutions with 0.0, 0.1, 0.2, 0.4, and 0.6 mg/L. The flasks are all filled up to the mark and mixed well. The idea of this procedure is that the total concentration of the analyte is the combination of the unknown (beer) and the standard, and that the total concentration varies linearly. If the signal response is linear in this concentration range, then a calibration curve similar to what is shown in figure 2 is generated.

The blank, standards and the beer samples are all placed in the autosampler and then will be automatically aspirated to the flame. The advantage of ASC-7000 is the improved rinsing mechanism shown in figure 3, the "overflow method" which is minimizing the carry over effects when analyzing high concentration samples. The instrumental parameters and measuring conditions are listed in Table 1. These conditions are automatically set for each element including optimized burner height and gas flow rates. The preparation for zinc is done in the same way as copper using the standard addition method with concentrations of 0.0, 0.2, 0.4, and 0.8 mg/L.
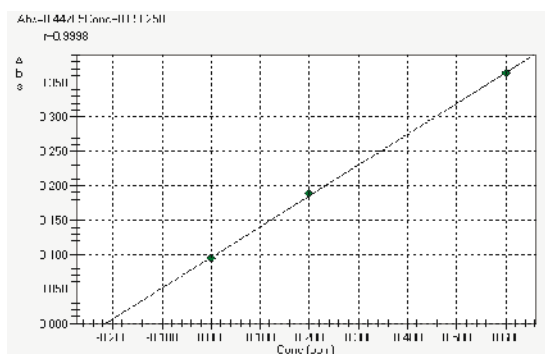
Figure 2: Copper calibration (standard addition)
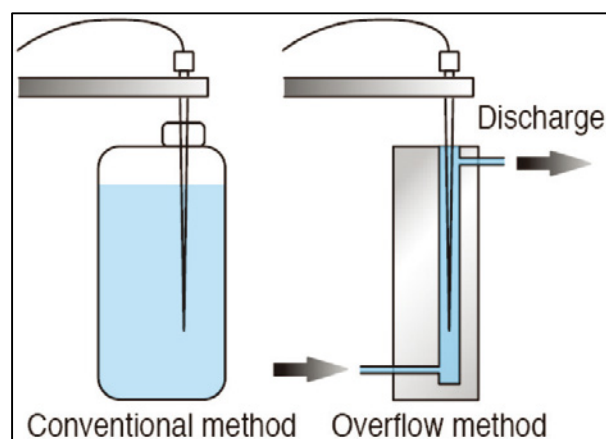
Figure 3: Rinsing method of ASC-7000

Instrument	AA-7000 with ASC-7000	
Element	Cu	Zn
Wavelength	324.8 nm	213.9 nm
Slit width	0.7 nm	0.7 nm
Lamp current	6 mA	4/ 100 mA
Background-correction	D2	SR
Flame type	Air-C2H2	Air-C2H2
Gas flow rate	1.8 l/min	2.0 l/min
Integration time	3 sec	3 sec
Calibration range [mg/L]	0.1 - 0.6	0.1 - 0.8

Table 1: Instrument and Analytical Conditions

■ **Conclusion**

For the determination of copper and zinc in beer samples the AA- 7000F atomic absorption spectrometer is an ideal tool for quality control. Furthermore, the AA-7000 is able in combination with GFA-7000 to *achieve calibration ranges as low as 1 to 10 µg/L for toxic ingredients such as lead, cadmium and arsenic [3].

■ **References**

[1] Pfenninger, H.: Brautechnische Analysenmethoden (1996)

[2] Hough, J.S. et al.: Malting and brewing science (1982)

[3] Davis, D.: Shimadzu Application AA-004 (2015)

Spectrophotometric Analysis

Analysis of "The Big Four" Heavy Metals in Hops by Electrothermal Atomization and Cold Vapor

Dan Davis, Keith Long, Justin Masone

■ Introduction

Plants concentrate metals by absorbing them from the soil in which they are grown. Some metals are beneficial and essential for life whereas other metals are highly toxic and have negative effects with even the lowest of levels. Because of their toxicity, quantification of these elements is needed.

This application news will investigate the preparation and analysis for heavy metals in Cascade Hops using Electrothermal Atomization and Cold Vapor techniques.

Spike and Recovery tests are performed at or below the analysis target levels to ensure accuracy and sensitivity of the technique.

Element	Analysis Target PPM	As Prepped (50x dil.) PPB
Lead	1.20	24
Cadmium	0.82	16
Mercury	0.40	8.0
Arsenic	2.00	40

Table 1: Metals Analysis Target

■ Sample Preparation

Cascade Hops were purchased pre-dried and ground. 0.5 grams of Hops were added to a closed vessel digester, and 4 mL of Nitric Acid, 2 mL of 30% H_2O_2, and 1 mL of DI H_2O were added. The sample was ramped to 900 watts over 15 minutes and held for another 20 minutes at that power. The sample was then allowed to cool and brought to 25 mL total volume with DI H_2O.

2 mL of the solution was reserved for analysis of Cd, As and Pb by Electrothermal atomization.

20 mL of sample was reserved for Hg analysis by Cold Vapor; 10 mL of untreated sample, and 10 mL of sample spiked to 1 ppb Hg.

0.5 grams Cascade Hops

    4 mL Nitric Acid Added

    2 mL H2O2 (30%) Added

    1 mL H2O Added

Ramp 900 Watts   15 min.

Hold 900 Watts   20 min.

    DI H2O Added

25 mL Total Volume DI H2O
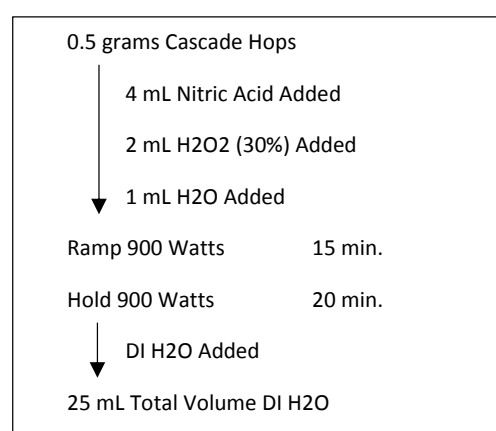
Fig. 1: Digestion/Preparation Procedure

■ Analytical Method and Conditions

Measurement was conducted using the calibration curve method. The main measurement parameters of the instrument are shown in Table 2.

	As	Pb	Cd	Hg
WaveLength nm	194	283	228	254
Slit Width nm	0.7			
Ignition mode	BG-D2			
Atomization	Electrothermal			Cold Vapor

Table 2: Measurement Conditions

The standard solutions were prepared by diluting commercially available standard solutions for atomic absorption measurement. 100 mL of calibration solution was prepared at 20 ppb As, Pb, 10 ppb Hg and 1 ppb Cd stabilized with 1% nitric acid. Reserve 50 mL for Calibration solution 1. Bring 50 mL of Calibration solution 1 to 100 mL. Reserve 50 mL for Calibration solution 2. Calibration solution 3 was adjusted to

account for the lower target levels in Table 1. A similar dilution as the previous scheme could be used.

Calibration Solution	1	2	3	Units
As	20	10	4.0	ppb
Cd	1.0	0.5		ppb
Hg	10	5.0	1.0	ppb
Pb	20	10	5.0	ppb

Table 3: Calibration Solutions

■ Results and Conclusion

Figures 2, 3, 4 and 5 show the generated calibration curves for each of the analytes. All calibration curves achieved a good linear coefficient of 0.999 or better, showing the instrument is capable of measuring the specified target range shown in Table 1 and Table 3.
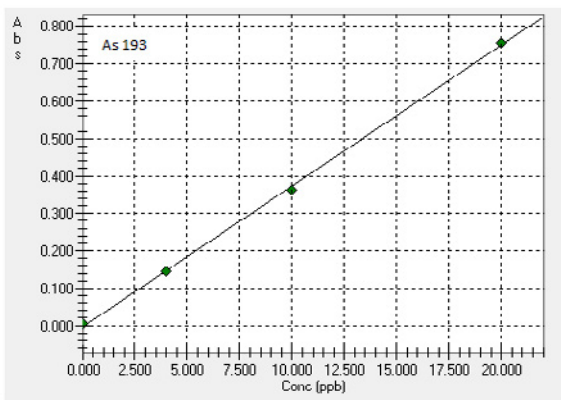
Fig. 2: As Calibration Curve
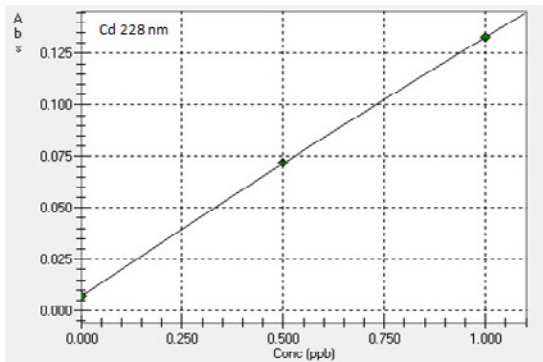
Fig. 3: Cd Calibration Curve
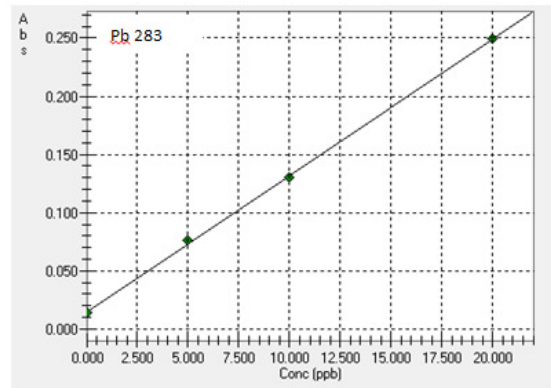
Fig. 4: Pb Calibration Curve
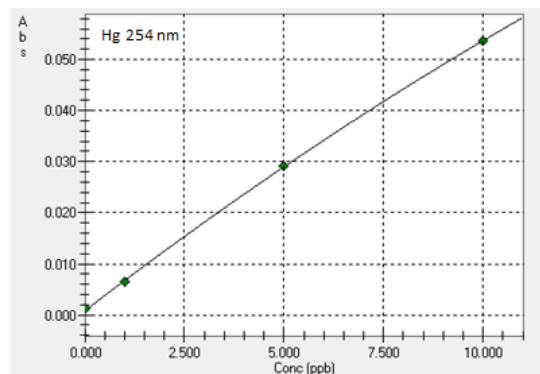
Fig. 5: Hg Calibration Curve

Figures 6 and 7 shows the signals of each analyte of the unknown samples and that of the spikes for As, Cd, Hg and Pb. There is good signal distinction at each of the target analysis levels indicated in Table 1.
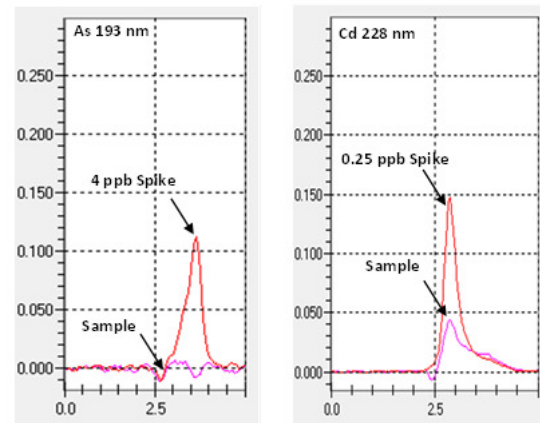
Fig. 6: As & Cd Sample & Spike
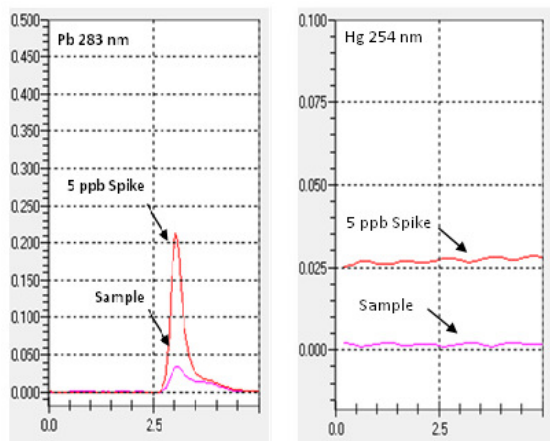
Fig. 7: Pb & Hg Sample & Spike

Element	Sample PPB	Spike PPB	Spike Result PPB	Recovery %
Lead	0.85	5.00	5.98	102.6
Cadmium	0.20	0.25	0.47	109.8
Total Mercury	0.09	5.00	4.96	97.4
Total Arsenic	0.53	4.00	4.71	104.5

Table 4: Results of Sample and Spikes

The results in Table 4 show that all of the elements were within the target analysis and the sample spikes achieved recoveries of 90%-110% of their theoretical values. The recoveries show that the system is capable achieving good sensitivity and accuracy at the desired elemental concentration levels.

ICPE-9800
Emission Spectrometer

AA-7000
Atomic Absorption

First Edition: June 2015

SHIMADZU

Application News

X-ray Analysis

EDXRF Analysis of Arsenic and Lead in Dietary Supplement

No.X246

In recent years, dietary supplements have become widely available in convenience stores and supermarkets. They are defined as food products that promote and maintain health and are used to improve disease prevention and enhance immunity. They are available in various types and forms, including tablet and powdered supplements, and processed herbal products, etc. Among these are products that are subject to safety standards that address the presence and concentrations of heavy metals, etc.[1]

Analysis of toxic heavy metals such as As and Pb is typically conducted using an emission spectrophotometer (ICP) or atomic absorption spectrophotometer (AA), however, these require time-consuming preparation procedures. For analyte quantities ranging from a few to tens of ppm, measurement can be conducted using an X-ray fluorescence spectrometer, which permits very easy sample preparation.

Using an energy dispersive X-ray fluorescence spectrometer, we conducted quantitative analysis of As and Pb in a dietary supplement (herbal medicine), and evaluated their lower limit of detection and quantitation, respectively.

1) Example: Japan Health and Nutrition Food Association (JHNFA)

■ Standard Samples

Seven standard samples were prepared by mixing herbal powder with a standard solution used for atomic absorption analysis. The elements and standard values are shown in Table 1, and the preparation procedure is shown in Fig. 1.

Table 1 Standard Values

No.	As	Pb
(1)	50	0
(2)	30	5
(3)	20	10
(4)	10	20
(5)	5	30
(6)	0	50
(7)	0	0

Unit: ppm

Fig. 1 Preparation Procedure

Grind and homogenize in mortar (Fig. 2)
↓
Weigh out herbal powder of 2.000 g
↓
Add 1,000 ppm standard solution dropwise
Example) To No. (6), 50 ppm, 50 μL (Fig. 3)
↓
Dry for 30 min at room temperature
↓
Mix using mortar
↓
Pressing. Total pressure 50 kN, 30 sec (Fig. 4)
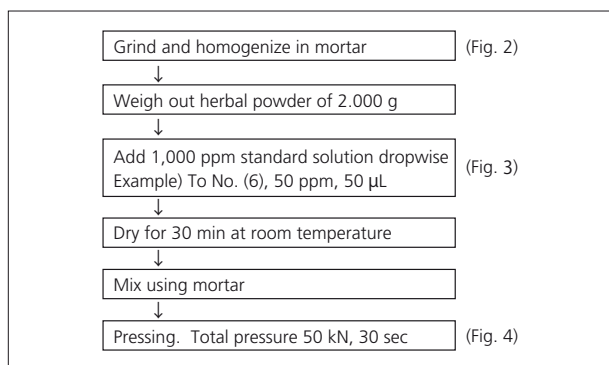
Fig. 2 Homogenization by Pulverizing

Fig. 3 Blend in Standard Solution

Fig. 4 Formed Briquette

■ Calibration Curves

The calibration curves for As (Kα line) and Pb (Lβ line) are shown in Fig. 5 and 6, respectively. Correction by the dj method was conducted for As, which is overlapped by Pb. We also generated those calibration curves with the internal standard which line is the RhKα C scattering (Compton) (figure not shown). Table 2 shows the accuracy of the respective calibration curves with and without internal standard correction. Accuracy refers to the variation of the calibration point using a numerical value indicated as 1 σ.

Pb Overlap Correction Coefficient $I_{Pb} = 0.521578$
Standard Value

Fig. 5 Calibration Curves

Standard Value
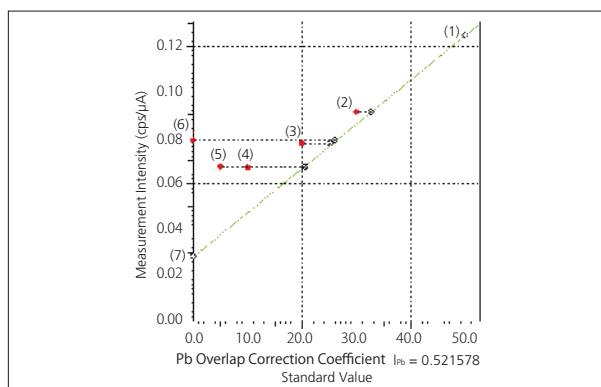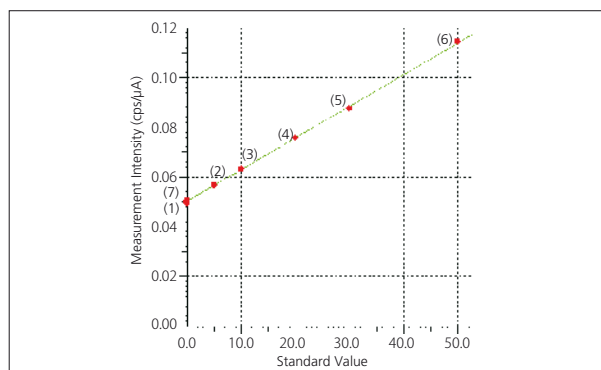
Fig. 6 Calibration Curve for Pb

Table 2 Accuracy of Calibration Curve

Internal Standard Correction	Without		With	
Internal Standard Line	–		RhKαC	
Element	As	Pb	As	Pb
Analytical line	Kα	Lβ1	Kα	Lβ1
Accuracy (1 σ)	0.23	0.42	0.60	0.83

Unit: ppm

■ Profile

Fig. 7 shows the profile overlap of standard sample No. (4) (As: 10 ppm, Pb: 20 ppm) and No. (7) (Blank). Since the AsKα line and PbLα line are adjacent, one or a combination of the following processing methods is selected.
A) Intensity peak separation
B) Intensity overlap correction
C) Overlap correction of the dj method on Calibration curve
Here, we applied method C) only.
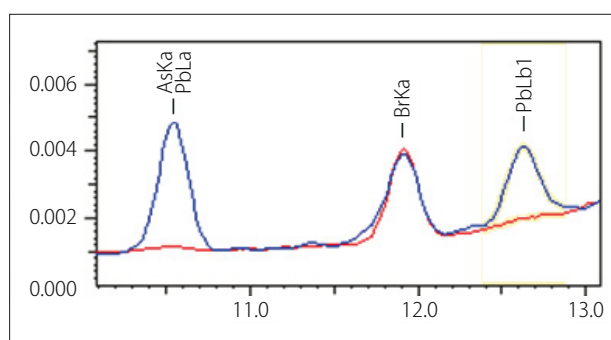
Fig. 7 Qualitative Profile Overlap of As and Pb
Blue: No. (4); Red: No. (7) (Blank)

■ Lower Limits of Detection and Quantitation

Ten times repeatability test of the No. (7) Blank were conducted, and the lower limit of detection (3σ) and lower limit of quantitation (10σ) were determined.
Table 3 shows the results obtained using 2 different sample preparation methods, pressing and simple compression. In the case of simple manual compression, quantitation was conducted using an internal standard calibration curve to correct for flatness and density effects. The powder preparation procedure used is shown in Fig. 8.

Table 3 Lower Limits of Detection and Quantitation for As and Pb

Preparation Method	Pressing		Powder, Sample Container	
Internal Standard Correction	Without		With	
Element	As	Pb	As	Pb
Average Value	(-0.08)	0.35	0.32	(-0.18)
Standard Deviation	0.18	0.26	0.18	0.26
Lower Limit of Detection (3σ)	0.53	0.77	0.55	0.78
Lower Limit of Quantitation (10σ)	1.8	2.6	1.8	2.6

Unit: ppm

Sample container covered with 5 µm polypropylene film
↓
Sample depth of at least 5 mm
↓
Use rod to compress and remove air layer
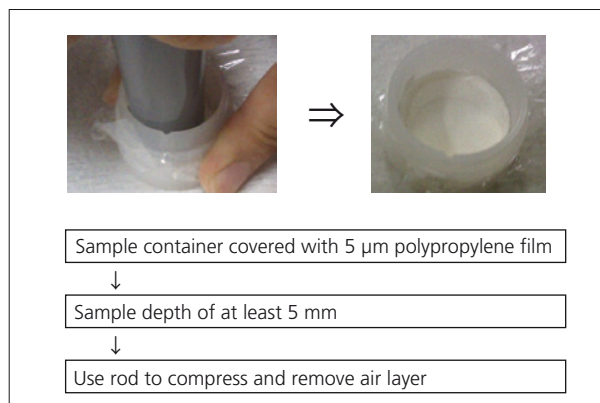
Fig. 8 Simple Powder Compression by Hand

■ Conclusion

Table 2, which shows the accuracy of the calibration curves, indicates that without conducting internal standard correction, accuracy improved 2.6 times for As, and 2.0 times for Pb. The cause is thought to be that the fluctuation of the RhKαC is added to the fluctuations in the respective intensities of AsKα and PbLβ1 .
On the other hand, both for As and Pb, Table 3 indicates that the lower limit of detection and lower limit of quantitation are the same for both formed briquette samples and manually compressed samples. The reason for this lack of any substantial difference is thought to be due to a zero net intensity for the blank.
Therefore, since either method is valid for measuring dietary supplements, using the pressing sample preparation method without the use of an internal standard or the easy compression (powder) sample preparation method with an internal standard is suitable.

■ Analytical Conditions

Table 4 Analytical Conditions

Instrument	: EDX-720 (EDX-GP)
X-Ray Tube	: Rh target
Tube Voltage	: 50 kV
Tube Current	: (Auto sensitivity control) µA
Filter	: #3 (EDX-720)
	#4 (EDX-GP)
Atmosphere	: Air
Measurement Diameter	: 10 mm
Measurement Time	: 1200 sec
Dead Time	: Max 40 %

SHIMADZU

Shimadzu Corporation

www.shimadzu.com/an/

SHIMADZU
Excellence in Science

Application News

No.**X247**

X-ray Analysis

Qualitative and Quantitative Analysis of Seafood by EDXRF

X-ray fluorescence analysis, in addition to its effectiveness in analysis of inorganic materials such as metals and ceramics, is also effective for the detection and quantitative analysis of minerals and heavy metals in foods. Not only can samples be analyzed directly without conducting time-consuming pretreatment, sensitive and accurate measurement is also possible using simple preparation measures, such as pressure forming. Quantitative analysis by XRF does not necessarily require a standard sample, as approximate quantitative results can easily be obtained even when the principal components are organic matter. Here we introduce these preparation methods and our investigation of their respective differences in quantitation values and detection limits.

Furthermore, we also examined the differences attributable to instrument model, as well as the use of iodine and cesium.

(Regarding the analysis of radioactive elements, we cannot guarantee that the detector or electronic equipment will not be susceptible to adverse effects. Thus, in this investigation, we used stable isotopes.)

■ Standard Samples

NMIJ certified reference material (powder)
(1) CRM 7405-a No. 99 (Powdered hijiki seaweed)
     Trace Elements and Arsenic Compounds in Seaweed (Hijiki)
(2) CRM 7403-a No. 52 (Powdered swordfish)
     Trace Elements Arsenobetaine and Methylmercury in Swordfish Tissue
NMIJ: National Metrology Institute of Japan, National Institute of Advanced Industrial Science and Technology

Fig. 1 Standard Samples (NMIJ)
(1) Seaweed; (2) Swordfish Tissue

■ Sample Preparation

Samples were prepared in two different ways, as described below.
(1) Pressure Forming (Fig. 2)
     The sample is pressed into a 25 mmϕ vinyl chloride ring, and pressure forming is conducted using 50 kN for 20 seconds.

(2) Easy Press (Fig. 3)
   1) 4 µm thick PROLENE[*1] film is spread over the surface of the sample cup, and the layer of powdered sample is then placed over the film at a thickness greater than 5 mm.
   2) A small hole is then made in the film to allow the escape of air from the sample cup.

Fig. 2 Machine-Formed Briquette of Swordfish Tissue

Fig. 3 Seaweed Hand-Pressed (Easy Press) into Cup

■ Qualitative and Quantitative Analysis

The qualitative and quantitative analysis results for powdered seaweed and powdered swordfish tissue are shown in Fig. 4, Table 1, and Fig. 5, Table 2, respectively. The principle components are assumed to be organic material overall and are represented with the chemical composition CH_2O[*2], and the balance (remaining content) was quantified by the FP method.

The error (quantitative value versus standard value) is determined using a quick and easy quantitative method, in which it is:
1) within about 30 % for non-sodium elements present at greater than 0.1 %
2) within about 50 % for sodium present at less than 1 %
3) within about twice the value for trace elements present at less than 0.1 %

Regarding the differences due to the sample preparation method, it is clear from Fig. 4 and Fig. 5 that since pressure forming resulted in better sensitivity for Na – Ca, this method is effective when the detection of light elements is important.

*1 PROLENE is a registered trademark of Johnson & Johnson.
*2 CH_2O in the FP method is equivalent to the composition expressed by the formula $C_6H_{12}O_6$.

■ **Seaweed (Hijiki)**
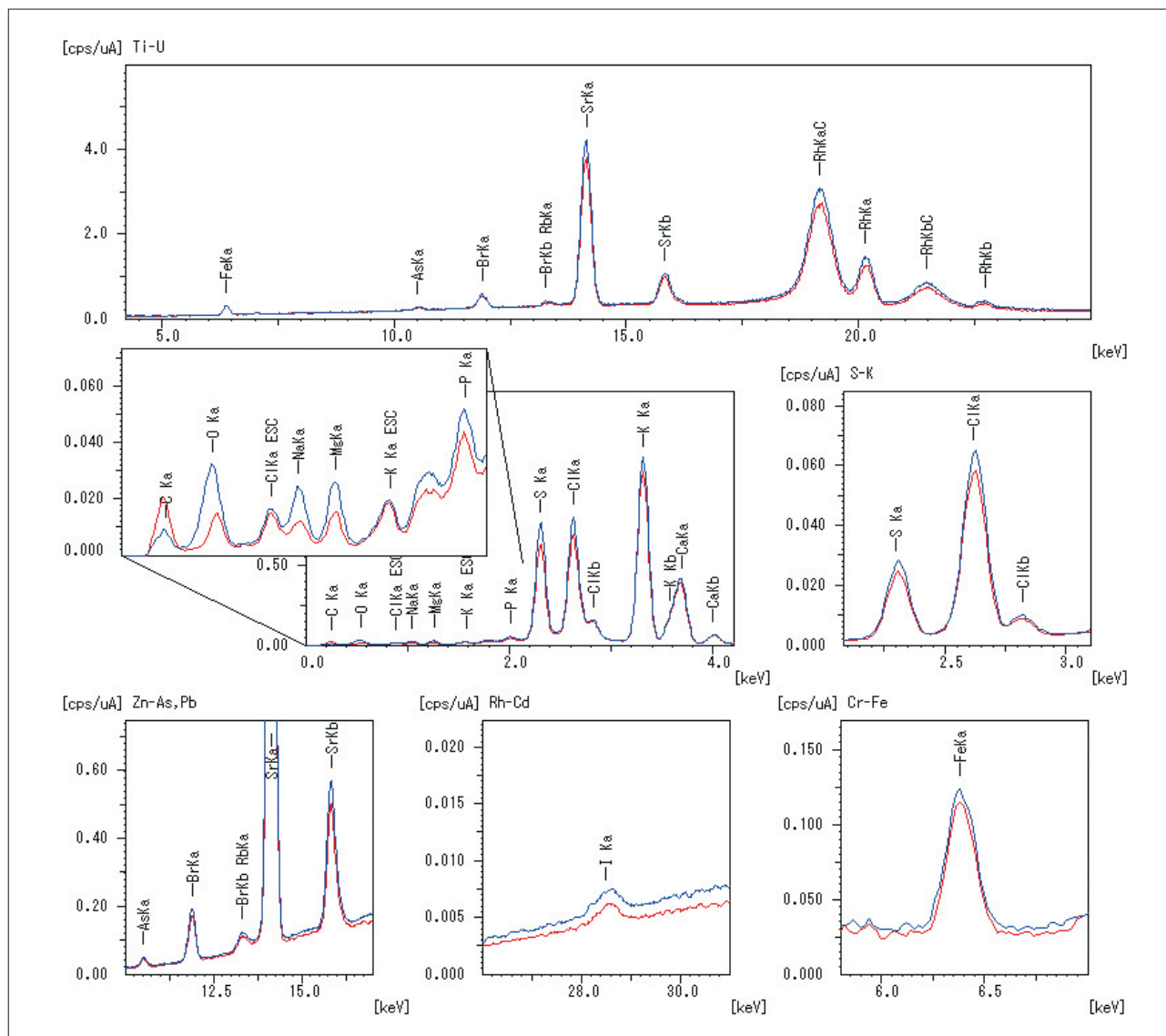
Fig. 4 Qualitative Results for Seaweed Blue: Briquette Red: Easy Press

Table 1 Quantitative Results for Seaweed by FP Method

Element	Standard Value [mass%, (ppm)][*3]	Quantitative Value [mass%, (ppm)]	
		Briquette	Easy Press
11 Na	1.62	1.59	2.05
12 Mg	0.679	0.54	0.54
15 P	0.101	0.091	0.085
16 S	–	1.40	1.31
17 Cl	–	2.03	1.93
19 K	4.75	4.60	4.33
20 Ca	1.52	1.28	1.26
26 Fe	311　[ppm]	315　[ppm]	287　[ppm]
33 As	35.8 [ppm]	27.5　[ppm]	24.4　[ppm]
35 Br	–	116　[ppm]	100　[ppm]
37 Rb	–	21.5　[ppm]	18.5　[ppm]
38 Sr	0.147	0.12	0.10
53 I	–	75.5　[ppm]	77.9　[ppm]
Balance CH_2O ($C_6H_{12}O_6$)	–	88.30	88.35

*3 g/kg expresses 1/10 mass%, and mg/kg expresses ppm.

■ **Swordfish Tissue**
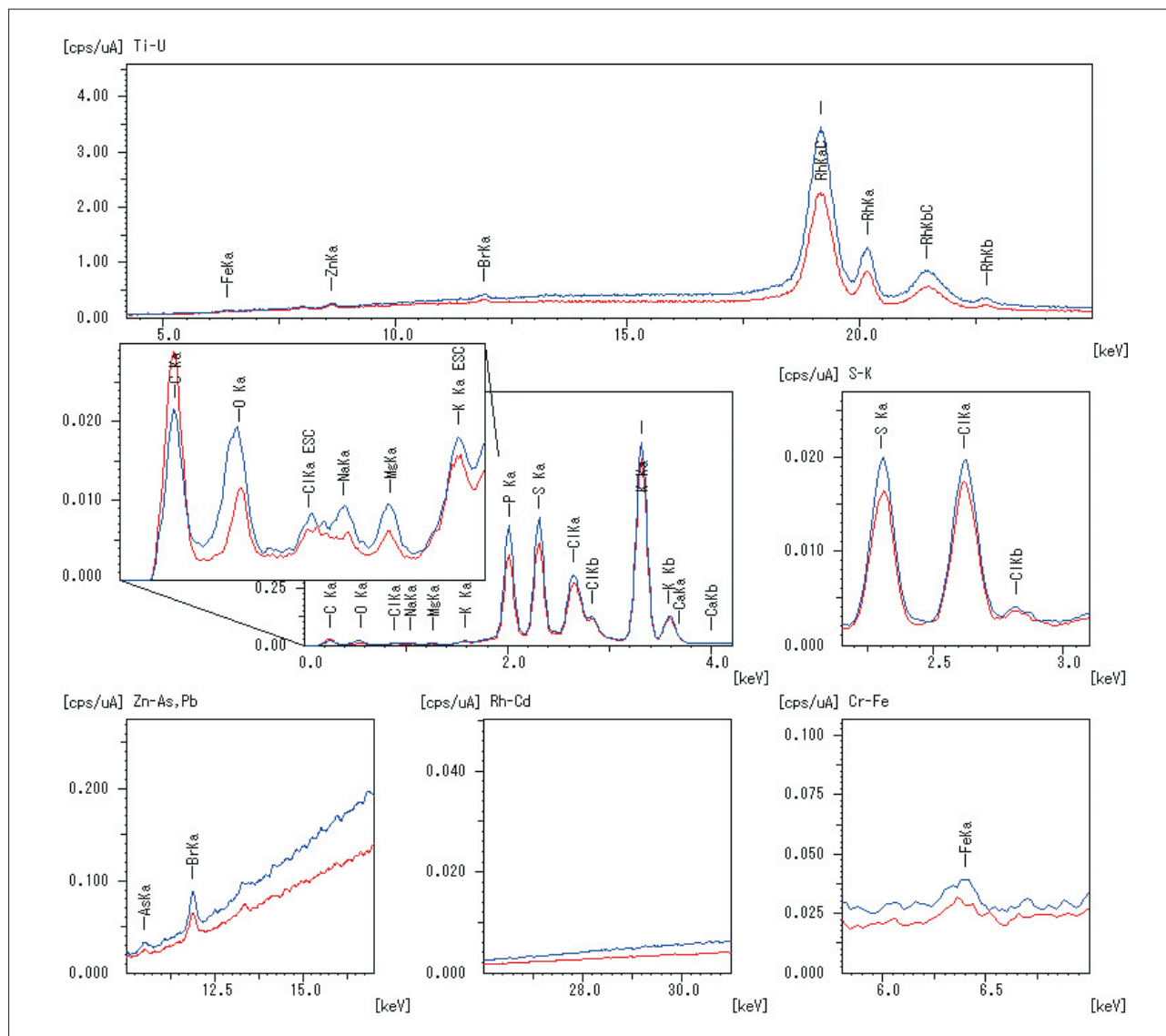
Fig. 5 Qualitative Results for Swordfish Tissue Blue: Briquette Red: Easy Press

Table 2 Quantitative Results for Swordfish Tissue by FP Method

Element	Standard Value [mass%, (ppm)][*3]	Quantitative Value [mass%, (ppm)]	
		Briquette	Easy Press
11 Na	0.357	0.47	0.54
12 Mg	0.158	0.14	0.14
15 P	1.45	1.62	1.50
16 S	–	0.95	0.88
17 Cl	–	0.52	0.49
19 K	2.63	2.97	2.76
20 Ca	0.0189	0.035	Not detected
26 Fe	13.1 [ppm]	26.9 [ppm]	22.0 [ppm]
30 Zn	33.6 [ppm]	31.6 [ppm]	19.1 [ppm]
33 As	6.62 [ppm]	6.7 [ppm]	4.0 [ppm]
35 Br	–	21.2 [ppm]	14.9 [ppm]
Balance CH_2O ($C_6H_{12}O_6$)	–	93.28	93.69

*3 g/kg expresses 1/10 mass%, and mg/kg expresses ppm.

Qualitative Analysis of Iodine and Cesium

Powdered swordfish was spiked with I (iodine) and Cs (cesium), and the results of qualitative analysis of this sample using the 2 instruments, EDX-720 and EDX-800HS, were compared. The sample was homogenized by mixing, and then pressure-formed into a briquette. The overlaid qualitative analysis results are shown in

Fig. 6. The L spectral lines of elements with close atomic numbers are adjacent to one another, but since the K spectral lines separate, when such elements are coexistent, it is effective to conduct measurement using the K spectral line.
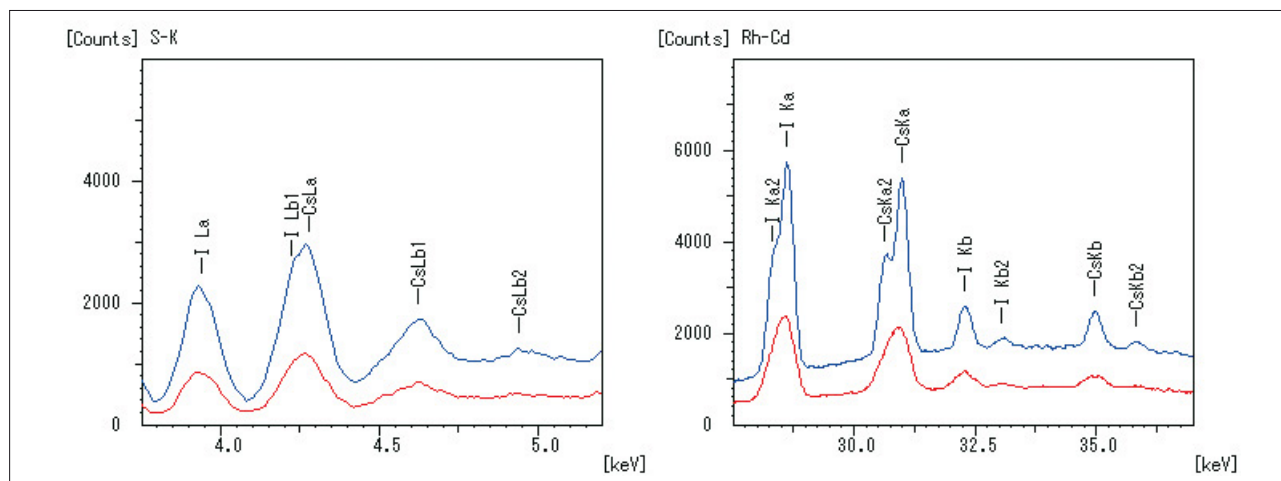
Fig. 6 Powdered Swordfish Spiked with I (1,000 ppm) and Cs (1,500 ppm) Blue: EDX-720 Red: EDX-800HS

Theoretical Lower Limits of Detection (L.L.D.)

(1) Comparison of the Lower Limits of Detection According to Sample Preparation Method
Table 3 shows the values for hijiki calculated from the qualitative and quantitative analysis results.

Table 3 L.L.D. - Comparison of Sample Preparation ([ppm], 300 sec)

Element	Briquette	Easy Press
$_{11}$Na	503	1,008
$_{12}$Mg	208	349
$_{15}$P	54	66
$_{16}$S	(31)	(32)
$_{17}$Cl	(89)	(90)
$_{19}$K	53	57
$_{20}$Ca	47	48
$_{26}$Fe	17	17
$_{33}$As	4.3	4.4
$_{35}$Br	(3.0)	(2.8)
$_{37}$Rb	(3.0)	(2.9)
$_{38}$Sr	3.9	4.1
$_{53}$I	(14)	(13)

Analysis line spectrum: Kα (Values in parentheses are reference values based on quantitated values)

(2) Comparison of the Lower Limits of Detection According to Instrument Used
1) Table 4 shows the values calculated from the qualitative analysis results (Fig. 6).

Table 4 L.L.D. - Comparison of Two Instruments ([ppm], 300 sec)

Element	Spectral Line	EDX-800HS	EDX-720
$_{53}$I	I Kα	11	6.0
$_{53}$Cs	CsKα	23	15

2) Relationship Between Concentration and Radioactivity
Taking for example the radioactivity of Cs (^{137}Cs), the level of radioactivity at the detection limit is calculated as follows. Assuming 1 g sample at 10 ppm (10 μg), approximately 32 MBq (32 million becquerel)
$(= 7.29 \times 10^{-10} \cdot W \times 10^{-6} \cdot m \div 136.9 \cdot 6.02 \times 10^{23})$

^{137}Cs decay constant	: 7.29×10^{-10} [1/s]
Concentration	: W [ppm]
Sample weight	: m [g]
Atomic weight	: 136.9 [g/mol]
Avogadro's number	: 6.02×10^{23} [particles/mol]

(Ref: 10 Bq/kg ≈ 0.003 ppt)

Analytical Conditions

	EDX-800HS (C–U)	EDX-720 (Na–U)
Instrument	: EDX-800HS (C–U)	EDX-720 (Na–U)
X-ray Tube	: Rh target	Rh target
Filter	: Without (C, O, Na, Mg, P, S, K, Ca), Al (Cl, Cs), Ti (Fe), Ni (Zn, As, Br, Sr, Rb), Mo (I, Cs)	#1 (I, Cs L-line) #5 (I, Cs K-line)
Tube Voltage	: 15 [kV] (C–Ca), 50 [kV] (Ti–U)	15 [kV] (L-line), 50 [kV] (K-line)
Tube Current	: Auto	Auto
Atmosphere	: Vacuum	Vacuum
Measurement Diameter	: 10 [mmφ]	10 [mmφ]
Measurement Time	: 300 [sec] × 5 ch	300 [sec] × 2 ch
Dead Time	: Max 25 [%]	Max 40 [%]

First Edition: Sep, 2012

SHIMADZU

Shimadzu Corporation

www.shimadzu.com/an/

SHIMADZU
Excellence in Science

Application News

No.J103

Inductively Coupled Plasma Atomic Emission Spectrometry

Simultaneous Analysis of Trace and Major Elements in Rice by ICPE-9820

■ Introduction

Among the world's three major crops, rice, corn, and wheat, rice is the staple food crop of the people of Asia. Brown rice refers to the grain that remains after the outer shell is removed from the rice fruit. Also, once the germ and rice bran are removed by milling the surface of the brown rice, the remaining grain is referred to as white rice. As brown rice contains a good balance of nutrients, including proteins and lipids, minerals, vitamins, and dietary fiber, this grain is gaining widespread recognition as a health food in recent years. Aside from the benefits of nourishment however, health problems associated with rice have occurred due to contamination from polluted water and other farmland contaminants. In particular, cadmium (Cd) consumed over a long period of time can result in kidney failure, and is therefore strictly regulated so as to contain less than 0.4 mg/kg by international standards (CODEX).

Brown rice contains potassium (K) and phosphorus (P) as major elements, at about %. However, to conduct simultaneous analysis of its principle beneficial elements together with toxic trace elements such as cadmium (Cd), an instrument having a wide dynamic range is required.

Here, using the Shimadzu ICPE-9820 multi-type ICP atomic emission spectrometer, we conducted simultaneous analysis of the elements present in brown rice samples. The ICPE-9820, with its dual plasma axial (AX) / radial axis (RD) viewing, permits the simultaneous analysis of elements present at high- to trace-level concentrations.

■ Sample

Brown rice powder standard samples NIES No. 10-a, -b, and -c

■ Sample Preparation

After weighing out 0.4 g of sample into a digestion vessel, 4.5 mL nitric acid and 0.5 mL hydrochloric acid were added, and the sample was set aside for about one hour for pre-reaction processing. The decomposition vessel was then sealed, and digestion was conducted using a microwave sample preparation system. After cooling, the digest solution volume was adjusted to 20 mL using distilled water, and this was used as the sample solution.

■ Instrument and Analytical Conditions

The ICPE-9820 was used for the analysis. The analytical conditions are shown in Table 1. The ICPE-9820 features auto-switching between radial view (RD) measurement for high-concentration elements and the axial view (AX) for high sensitivity measurement. Fig. 1 shows calibration curves for K (maximum concentration 200 mg/L) using the axial view and radial view, respectively. Better linearity was obtained with the

radial view than with the axial view for K at a high-concentration. On the other hand, for Cd at a trace level concentration, high sensitivity measurement can be conducted using the axial view. Thus, by conducting measurement utilizing automatic switching of the two views, high-concentration components and trace components can be measured simultaneously using the same solution.

Table 1 Analytical Conditions

Instrument	: ICPE-9820
Radio frequency power	: 1.2 kW
Plasma gas Flowrate	: 10 L/min
Auxiliary gas Flowrate	: 0.6 L/min
Carrier gas Flowrate	: 0.7 L/min
Sample introduction	: Nebulizer 10
Misting chamber	: Cyclone chamber
Plasma torch	: Mini Torch
Observation	: Axial (AX) / Radial (RD)
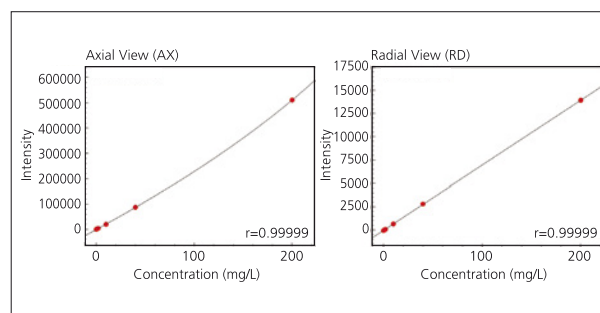
Fig. 1 Calibration Curves of K766.490 nm by Axial View and Radial View (Maximum Concentration 200 mg/L)

■ Analysis

Quantitative analysis was conducted by the calibration curve method.

[Reference]
1) CODEX GENERAL STANDARD FOR CONTAMINANTS AND TOXINS IN FOODS (CODEX STAN 193-1995, Rev. 3-2007)

■ Analytical Results

Table 2 shows the analytical results. Fig. 2 and 3 show the spectral profile and calibration curve, respectively, for Cd.

Analysis of the brown rice standard substances conducted here indicated 3 levels of Cd contamination. However, all were present at trace levels, below the regulatory limit of 0.4 mg/kg, indicating good results. Further, excellent results were also obtained for many of the elements other than Cd, with values closely matching the certified values.

■ Conclusion

Using the ICPE-9820, Cd can be analyzed at trace levels with high sensitivity, while high-concentration principle component elements (K, P, etc.) present in the same solution can be analyzed at the same time.

Table 2 Analytical Results for Brown Rice (Unit: µg/g)

Element	NIES No.10-a		NIES No.10-b		NIES No.10-c	
	Quantitation Value	Certified Value	Quantitation Value	Certified Value	Quantitation Value	Certified Value
Al	3.1	(3)	2.1	(2)	1.7	(1.5)
Ca	96	93 ± 3	79	78 ± 3	96	95 ± 2
Cd	0.02	0.023 ± 0.003	0.31	0.32 ± 0.02	1.80	1.82 ± 0.06
Cu	3.6	3.5 ± 0.3	3.4	3.3 ± 0.2	4.3	4.1 ± 0.3
Cr	0.08	(0.07)	0.20	(0.22)	0.10	(0.08)
Fe	12.2	12.7 ± 0.7	12.8	13.4 ± 0.9	10.9	11.4 ± 0.8
K	2750	2800 ± 80	2520	2450 ± 100	2780	2750 ± 100
Mn	33.8	34.7 ± 1.8	30.8	31.5 ± 1.6	39.4	40.1 ± 2.0
Mo	0.37	0.35 ± 0.05	0.45	0.42 ± 0.05	1.63	1.6 ± 0.1
P	3430	3400 ± 70	3180	3150 ± 60	3380	3350 ± 80
Pb	1.1	-	1.2	-	1.2	-
Zn	24.8	25.2 ± 0.8	22.0	22.3 ± 0.9	22.8	23.1 ± 0.8

Values in parentheses are reference values.
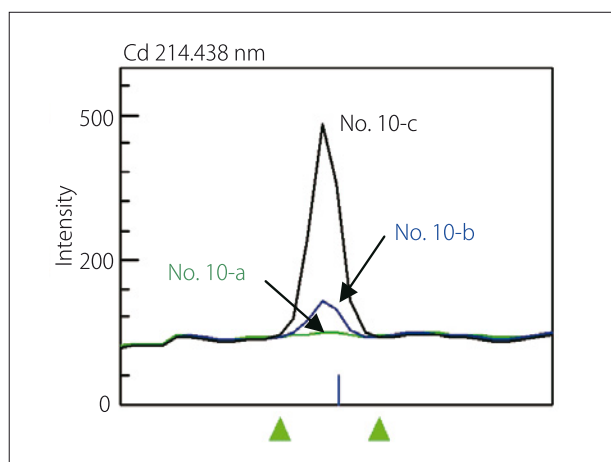
Fig. 2 Spectral Profile of Cd
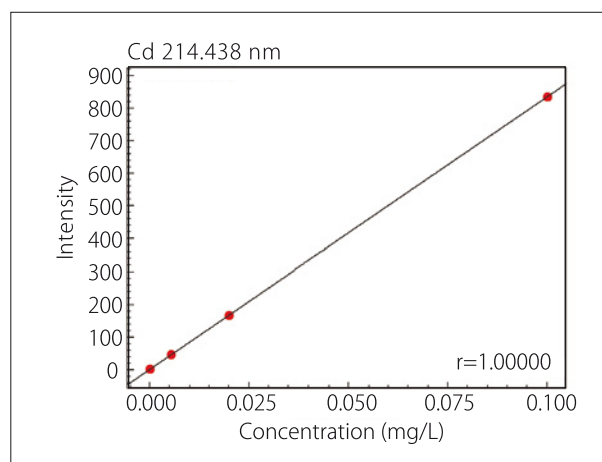
Fig. 3 Calibration Curve of Cd

Shimadzu Corporation

www.shimadzu.com/an/

Determination of Trace Elements in Natural Water using ICP-OES

Multi-element analysis of aqueous solutions in compliance with the German Drinking Water regulation and the German Water Discharge Law is one of the main application areas of the ICPE-9000 (**I**nductively **C**oupled **P**lasma **E**mission spectrometer). The performance data and system characteristics of this instrument are tailored specifically to the requirements of water analysis. Keywords such as sample throughput, operating costs and performance outline user expectations in this application segment.

Figure 1: ICPE-9000

■ High sample throughput

The ICPE-9000 is suitable for axial and radial plasma observation. Its high-performance Echelle optics enable the effective use of the entire 1024 x 1024 pixel CCD detector area. In this way, a resolution of better than 0.005nm is attained. The extremely sensitive detector with antiblooming function reliably acquires signal intensities, even at long exposure times. All samples can therefore be determined accurately within one single analysis sequence – even those samples with very different element concentrations. The unique "reprocessing" function of the ICPEsolution software enables the determination of additional elements or changing the concentration range for alternate wavelengths without the need for new measurements. Time-consuming dilution of samples is finally a thing of the past.

■ Low argon consumption

The vacuum optics combined with mini torch technology considerably reduces the argon gas consumption, which usually constitutes a major part of the operating costs. The innovative mini torch actually reduces the argon gas consumption by half that of conventional torches and allows a plasma gas flow of only 10L/min without loss in sensitivity. In addition, time-consuming purging of the optics with ultra-pure gas is no longer necessary. The system is ready for operation and stable within the shortest possible time. Equipped with the optional autosampler ASC-6100, the ICPE-9000 can be fully automated for high sample throughput operation. The system status including information about temperature, vacuum and gas settings is monitored continuously and can be retrieved at any time.

■ Analysis of natural water

An extensive program of accessories is available for sample introduction. Aqueous samples, for example drinking water, are introduced into the cyclone spray chamber via a coaxial nebulizer and transferred subsequently into the mini torch via the carrier gas flow of 0.7 mL/min. The system parameters are shown in Table 1.

Under these conditions, a series of more than 20 drinking water and mineral water samples has been analyzed for main and trace elements. A reference material (NIST SRM 1640) was measured along with the series as a control sample. The excellent recoveries are shown in Table 2.

Instrument	ICPE-9000
RF generator power	1.2 kW
Cooling gas	10 L/min
Plasma gas	0.6 L/min
Carrier gas	0.7 L/min
Plasma torch	Mini torch
Observation	Axial

Table 1: System parameters
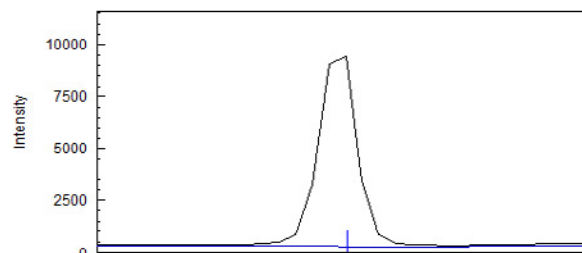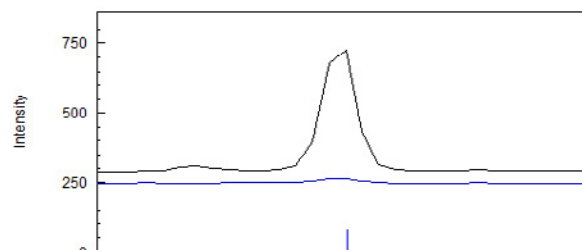
Figure 2: Peak profiles for Mn and Fe

Element	Certified [µg/L]			Measured [µg/L]	Recovery [%]
Al	52	±	1.5	52	100
Ag	7.62	±	0.25	7.60	99.73
As	26.67	±	0.41	26.4	98.99
B	301.1	±	6.1	286	94.99
Ba	148.0	±	2.2	147	99.32
Be	34.94	±	0.41	34.8	99.60
Ca	7054	±	89	7040	99.80
Cd	22.792	±	0.96	21.7	95.21
Co	20.28	±	0.31	20.1	99.11
Cr	38.6	±	1.6	38.2	98.96
Cu	85.2	±	1.2	85.0	99.77
Fe	34.3	±	1.6	33.9	98.83
K	994	±	27	1010	101.61
Li	50.7	±	1.4	50.8	100.20
Mg	5819	±	56	5820	100.02
Mn	121.5	±	1.1	121	99.59
Mo	46.75	±	0.26	46.3	99.04
Ni	27.4	±	0.8	26.5	96.72
Pb	27.89	±	0.14	26.9	96.42
Sb	13.79	±	12.5	13.7	99.35
Se	21.96	±	0.51	21.1	96.08
Si	4073	±	120	4080	100.17

Table 2: Certified and measured concentrations of the NIST SRM 1640

■ Standard system Configuration

ICPE-9000 incl. radial view unit

Mini torch

Cyclone spray chamber

Coaxial nebulizer with sampling rate of 1 mL/min

ASC-6100

SHIMADZU

Spectroscopy – ICP-OES

Determination of Heavy Metals in Wine using simultaneous ICP-OES

Figure 1: Grapes – the source of wine

Element	Max. concentration [mg/L
Aluminum	8.00
Arsenic	0.10
Boron	80.0
Cadmium	0.01
Copper	2.00
Lead	0.25
Tin	1.00
Zinc	5.00

Table 1: Maximum allowable concentrations of elements in wine

Food and drinks are always a hot topic of discussion and in the focus of "state of the art" analytical techniques. Food scandals all around the world from eggs to horsemeat, tainted wine, oil, and milk force the European Community to establish an integrated approach to food control. The target is a high level of food safety, animal health, animal welfare and plant health within the European Union through so-called "farm-to-table" measures and monitoring, ensuring the effective functioning of the European market.

■ Wine Quality

The quality standards for wine analysis are defined in national wine regulations such as the "German Weinverordnung" (Bundes-gesetzblatt Teil 1 Nr. 32) from 22nd May 2002, with the latest revision in 2012. It includes the classification of wines from different locations, as well as the production process, alcohol concentrations and the maximum allowable concentrations of the elements listed in Table

■ Quantitative Analysis

For quantitative determination of the elements in the required concentration range, ICP is the most preferable tool for quality control because of a high sensitivity, a wide dynamic range and a high sample throughput. Figure 2 shows the new simultaneous ICPE-9820 with CCD (charge-coupled device) detector, which has been used for all determinations. This system configuration is equipped with a unique optical system which sets new standards with respect to performance and speed and can be optimized for any type of complex samples such as wine analysis.

The vacuum system allows precise analysis of elements in the lower UV range under extremely stable conditions. The use of a mini torch allows a cooling gas flow rate of only 10 L/min. The system setup for determination of low concentration heavy metals in wine has been optimized using the dual view option in order to analyze low level elements at the same time with high matrix elements. The

Figure 2: ICPE-9820

wine samples have been diluted 4 times, and aspirated in the same way as aqueous solutions in the cyclone chamber. The standard solutions have been prepared including ethanol in order to match the matrix with an ethanol concentration of 3.5 % after dilution, for direct aspiration into the mini torch. Table 2 shows a summary of the system parameters.

Parameter	Setting
RF generator power	1.2 kW
Cooling gas	10 l/min
Plasma gas	0.6 l/min
Carrier gas	0.7 l/min
Nebulizer	Coaxial
Plasma observation	Axial/Radial
Sensitivity	Wide Range
Exposure time	15 sec.

Table 2: Analytical conditions for wine analysis

The concentration of copper in wine is limited to a maximum concentration level of 2 mg/L. In case of higher copper concentrations the wine may have a metallic, bitter taste and the fermentation process will also be influenced by higher copper concentrations. Copper in wine originates from the Bordeaux mixture fungicide, which is a mixture of copper (II) sulfate ($CuSO_4$) and calcium hydroxide ($Ca(OH)_2$) solution used in vineyards to protect against downy mildew and other fungi. Since the Bordeaux mixture is applied in large quantities, the copper accumulates in the soil and becomes a pollutant. This is why the Bordeaux mixture will most probably be banned in the European community as of 2016. The calibration curve in figure 3 shows the standards with concentrations starting at 250 µg/L up to the maximum concentration of 1000 µg/L. The limit of detection is calculated with < 0.02 µg/L (3 s). Furthermore the determination of arsenic and lead is important, as these elements still can be found in the environment generated from lead arsenate ($PbHAsO_4$) which has been used as an inorganic insecticide until 1988, after which it was officially banned.
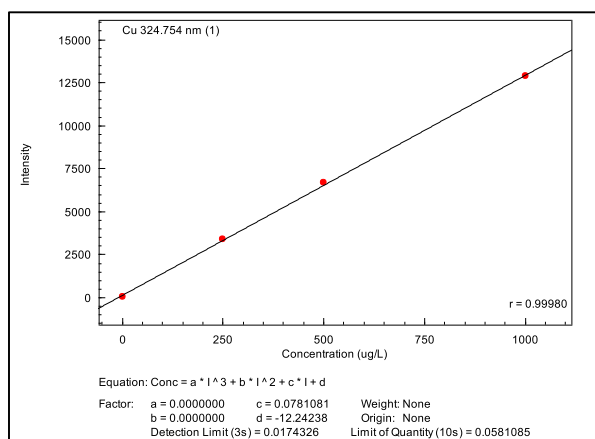
Figure 3: Copper Calibration

■ **Conclusion**

For the element analysis, ICP-OES Spectrometry using a simultaneous instrument is the "state of the art" tool for the daily routine in quality control of wine samples. The ICPE-9820 in dual view configuration is flexible enough to achieve calibration ranges in axial view in ppb level concentrations and at the same time high concentration levels of Boron, Potassium, Sodium and others in ppm scale in radial observation as well.

Application News

No.J104

Inductively Coupled Plasma Atomic Emission Spectrometry

Analysis of Multiple Elements in Drinking Water by ICPE-9820

■ Introduction

The amount of water typically consumed by an adult is said to be about two liters per day, and nearly all of this is tap water or mineral water, generally referred to as "drinking water." Conducting safety inspections are the responsibility of each country according to their respective regulations. Typically, there are many target elements included in the test, such as sodium (Na), calcium (Ca), etc. which are present at the mg/L level or greater, and toxic trace elements such as lead (Pb) and cadmium (Cd), which are normally present at the µg/L level or less.

Here, using the Shimadzu ICPE-9820 multi-type ICP atomic emission spectrometer and an ultrasonic nebulizer, we conducted analysis of river water, typically the source of tap water.

The ICPE-9820, with its auto-switching of axial/radial viewing which permits total overall measurement from trace to high concentrations, in addition to the newest CCD detector which allows acquisition of all elements over the entire wavelength region, greatly improves analysis throughput for multiple elements and multiple samples. Moreover, as a system designed to reduce running costs, it increases lab productivity.

■ Sample

The river water certified reference materials JSAC 0301-1 (unspiked), 0302 (spiked) (Japan Society for Analytical Chemistry certification) were used as the samples.

■ Sample Preparation

5 mL of nitric acid was added to 50 mL of test water, and the mixture was then heated to complete dissolution. After cooling, the internal standard element Y (yttrium) was added to obtain a concentration of 0.5 mg/L, and the test solution volume was adjusted to 50 mL.

■ Instrument and Analytical Conditions

For measurement, the Shimadzu ICPE-9820 multi-type ICP atomic emission spectrometer and UAG-1 ultrasonic nebulizer were used. The measurement conditions are shown in Table 1.

Table 1 Analytical Conditions

Instrument	: ICPE-9820
Radio frequency power	: 1.2 kW
	1.0 kW (UAG-1)
Plasma gas Flowrate	: 10 L/min
Auxiliary gas Flowrate	: 0.6 L/min
Carrier gas Flowrate	: 0.7 L/min
Sample introduction	: Nebulizer 10
	Ultrasonic Nebulizer (UAG-1)
Misting chamber	: Cyclone chamber
Plasma torch	: Mini Torch
Observation	: Axial (AX) / Radial (RD)

With its echelle spectrometer and CCD detector, ICPE-9820 permits simultaneous analysis of all elements, at all wavelengths, and high-throughput analysis is possible even when there are many target elements and samples.

Also, thanks to the automatic switching between axial viewing (AX) for high sensitivity, and radial viewing (RD) for high-concentration analysis, simultaneous analysis of both trace- and high-concentration elements is possible using the same solution, without conducting dilution.

Example) In the measurement of high-concentration Na using the axial view, the sample must be diluted because a linear calibration curve cannot be obtained. On the other hand, using the radial view, good linearity can be obtained up to the high-concentration region, permitting analysis to be conducted without dilution. Fig. 1 shows the calibration curve for Na (maximum 200 mg/L = water quality standard value for drinking water).
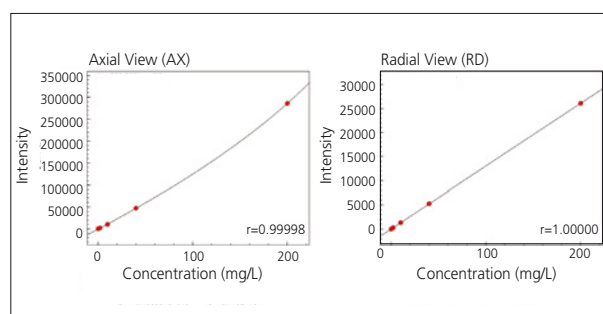
Fig. 1 Calibration Curves for Na 588.592 nm Using Axial View and Radial View (Maximum Concentration 200 mg/L)

In addition, the mini-torch which limits Ar gas consumption, the Eco mode which keeps standby gas and electrical power consumption to a minimum, in addition to the use of a vacuum-type spectrometer which eliminates the need for purge gas, all serve to significantly reduce running costs compared to existing ICP instruments.

■ Analysis

We conducted quantitative analysis using the calibration curve – internal standard method. For measurement of B, K, Na, Ca, and Mg, the Nebulizer 10 was used, and for sample introduction of other trace elements, the ultrasonic nebulizer UAG-1 was used.

[References]
1) National Primary Drinking Water Regulations: US-EPA (2012)
2) Guidelines for Drinking-Water Quality – 4th ed. ©WHO2011

■ Analytical Results

Table 2 shows the analytical results. In addition, the drinking water maximum limit (MCL) according to the US-EPA, and the drinking water guideline values according to WHO are also shown. Fig. 2 shows the spectral profiles of Cd, Cr, and Pb. As for the quantitation values, good results matching the guaranteed values were obtained, even at trace concentrations. Regarding the detection limits, all of the elements were detected at less than 1/10 the limit values and guideline values, indicating excellent sensitivity.

■ Conclusion

The ICPE-9820 can be used for accurate, low-cost measurement of the many elements in drinking water, from those present at trace levels to those at high concentrations.

Table 2 Analytical Results for River Water

Element	EPA Drinking Water Maximum Limit	WHO Drinking Water Guideline Value	Detection Limit	Introduction Method	Sample: JSAC0301-1		Sample: JSAC0302	
					Quantitation Value	Certified Value	Quantitation Value	Certified Value
Unit (µg/L)								
Al	200		0.1	UAG	19.8	19.0 ± 0.9	66.3	67 ± 1
B		2400	0.2	STD	8.8	8.6 ± 0.3	59.6	59 ± 1
Ba	2000	700	0.002	UAG	0.62	0.60 ± 0.02	0.60	0.60 ± 0.01
Be	4		0.004	UAG	<		0.98	0.99 ± 0.04
Cd	5	3	0.02	UAG	<	0.002 ± 0.0007	1.02	1.01 ± 0.01
Cr^{6+}	100	50	0.04	UAG	0.2	0.15 ± 0.01	10.2	10.1 ± 0.2
Cu	1300	2000	0.1	UAG	0.6	0.57 ± 0.07	10.4	10.3 ± 0.2
Fe	300		0.02	UAG	4.9	4.7 ± 0.3	56.3	56 ± 1
Mn	50*		0.006	UAG	0.12	0.125 ± 0.007	5.1	5.0 ± 0.1
Mo		70	0.1	UAG	0.4	0.38 ± 0.01	0.4	0.38 ± 0.01
Ni		20	0.05	UAG	<		10.1	9.9 ± 0.2
Pb	15	10	0.3	UAG	<	0.005 (Reference value)	10.2	10.1 ± 0.2
Zn	5000*		0.04	UAG	0.2	0.19 ± 0.03	10.1	10.2 ± 0.3
Unit (mg/L)								
K			0.001	STD	0.56	0.57 ± 0.02	0.58	0.57 ± 0.01
Na			0.0005	STD	4.35	4.4 ± 0.1	4.35	4.33 ± 0.07
Mg			0.00001	STD	2.82	2.85 ± 0.04	2.84	2.83 ± 0.03
Ca	250*		0.00001	STD	12.2	12.0 ± 0.2	12.3	12.2 ± 0.2

Cr^{6+}: Measured as total chromium
EPA Drinking Water Standard: EPA Maximum Contaminant Levels of Drinking Water Contaminant
*: National Secondary Drinking Water Regulations
WHO Drinking Water Guidelines: Guidelines for Drinking-Water Quality - 4th ed. ©WHO 2011
Detection Limit: 10 repeat measurements of calibration curve blank are conducted, and 3 times the concentration of the standard deviation is obtained.
<: Below the detection limit
UAG: Ultrasonic nebulizer (UAG-1), STD: Nebulizer 10
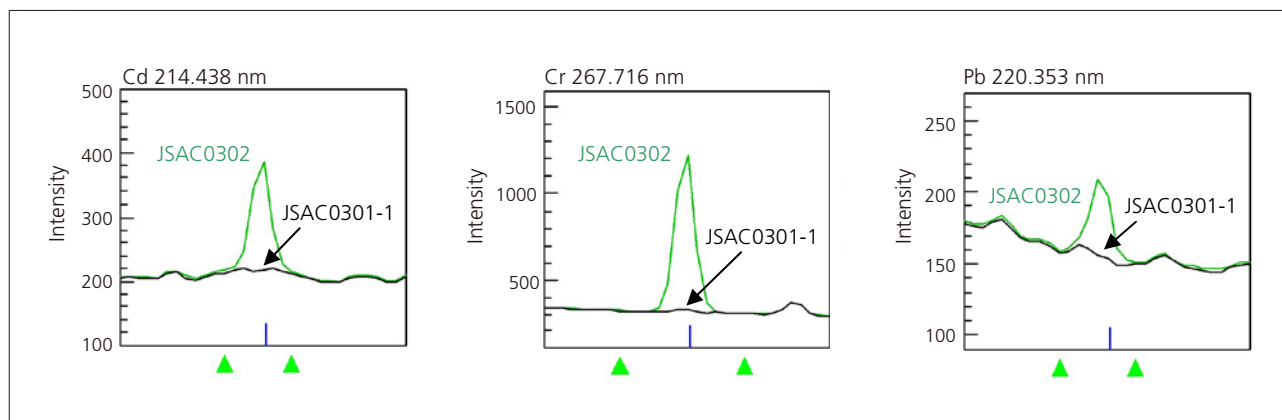
Fig. 2 Spectral Profiles of River Water

First Edition: Sep. 2014

SHIMADZU

Shimadzu Corporation

www.shimadzu.com/an/

![SHIMADZU logo] **SHIMADZU**
Excellence in Science

Application News

No.J109

Inductively Coupled Plasma Atomic Emission Spectrometry

Content Analysis of Toxic Elements in Soil by ICPE-9800 Series

■ Introduction

Contaminated soil not only leads to contamination of untreated drinking water through permeation into river water and rainwater, it adversely affects health when the soil itself is directly ingested as a child puts the ground into a stoma into a play etc. Therefore, assessment of soil toxicity using a defined method is required. In Japan, the Soil Contamination Countermeasures Law specifies content standards and related inspection methods (measurement method according to soil content investigation). Table 1 shows the established standard values for soil content. The testing method consists of elution tests based on the assumption that when soil is ingested, harmful elements contained in the soil will be absorbed in the body. The apparatus used for the analysis is required to accurately measure those elements at trace concentrations equivalent to or lower than the reference values.

Here, using the Shimadzu ICPE-9800 series multi-type ICP atomic emission spectrometer, we conducted content analysis of soil. The ICPE-9800 series, with its mini-torch plasma and spectrometer capable of simultaneous analysis of all elements at all wavelengths, can be used to conduct high-throughput, low-cost analysis with high sensitivity and high precision.

Table 1 Soil Concentration Standard Values (Unit: mg/kg)

Element	As	B	Cd	Cr^{6+}	Hg	Pb	Se
Soil Concentration Standard Value	150	4000	150	250	15	150	150

■ Sample

For analysis, we used a sample consisting of a standard substance with certified content (1 mol/L hydrochloric acid content survey method), as specified in the Ministry of the Environment Notification No. 19.
 - Soil certified reference material (brown forest soil) JSAC0402, 0403 (The Japan Society for Analytical Chemistry)

■ Sample Preparation

Sample preparation was conducted according to the Test Solution Preparation Method of Soil Content Survey (Ministry of the Environment Notification No. 19), in conjunction with the total digestion method using a microwave sample preparation system.

- Test Solution Preparation Method for Soil Content Survey (Ministry of the Environment Notification No. 19, March 6, 2003)

Elution was performed using 200 mL of 1 mol/L hydrochloric acid per 6 g of soil sample, and Yb (Ytterbium) and In (Indium) were added as internal standard elements to the obtained eluate, which was then filtered through a 0.45 μm membrane filter. The obtained filtrate was used as the analytical sample.

- Total content digestion method (Digestion using microwave sample preparation system)

Nitric acid and hydrofluoric acid were added to 0.2 g of sample, and digestion was conducted using a microwave sample preparation system. After transferring the digest solution to a fluorine resin beaker, the mixture was heated to near dryness (about 200 °C) on a hot plate. Dilute nitric acid and dilute hydrochloric acid were added to dissolve the contents. Yb and In were added as internal standard elements, and the volume was adjusted to 20 mL using distilled water. This solution served as the analytical sample.

■ Instrument and Analytical Conditions

Measurement was conducted using the Shimadzu ICPE-9800 series ICP atomic emission spectrometer. The analytical conditions are shown in Table 2.

The ICPE-9800 series, with a newly designed CCD which permits simultaneous measurement of all elements at all wavelengths, is built for high-throughput measurement, even when there are large numbers of samples and target elements. Further, the mini torch which suppresses the plasma gas flowrate, the Eco mode which suppresses gas and power consumption during wait periods, and use of a vacuum spectrometer which does not require purge gas, all serve to greatly reduce running costs as compared with conventional ICP instruments.

Table 2 Analytical Conditions

Instrument	: ICPE-9800 series
Radio frequency power	: 1.2 kW
Plasma gas Flowrate	: 10 L/min
Auxiliary gas Flowrate	: 0.6 L/min
Carrier gas Flowrate	: 0.7 L/min
Sample introduction	: Nebulizer 10
Misting chamber	: Cyclone chamber
Plasma torch	: Mini Torch
Observation	: Axial (AX)
Measurement time	: 2.5 min/sample (Including rinse time)

■ Analysis

Here, using the internal standard method – calibration curve method, we conducted quantitative analysis of a standard containing seven elements. As internal standard elements, we used Yb and In, which are few concentration in soil.

■ Analytical Results

Soil samples contain high concentrations of co-existing elements, such as Fe, Al, and Si, etc., and therefore may be the source of spectral interference with respect to trace elements in the matrix. For example, as can be seen in Fig. 1, the spectrum of Fe interferes with that of Cd at 214.438 nm. Correction between elements in which this type of interference (overlapping) occurs refers to the software feature which permits subtraction of the coexisting element spectrum. Table 3 shows the effectiveness of interference element correction (IEC), whereby the accuracy is significantly improved.

The results of the soil content analysis are shown in Table 4. The lower limit of determination is now less than 1/10 that of the reference values for all elements. Good results matching the certified value were also obtained for elements in the low-concentration region below the reference value.

■ Conclusion

The ICPE-9800 series permits quick and accurate measurement of trace elements in the soil, at lower cost.

[References]
1) Soil Contamination Countermeasures Law Enforcement Regulations (Ministry of the Environment Ordinance No. 29, December 26, 2002)
2) Determination of Measurement Methods According to Soil Content Investigation (Ministry of the Environment Notification No. 19, March 6, 2003)
3) JIS K0102-2013 (Testing Method for Industrial Wastewater)
4) US EPA SW-846 Method 3052 (Microwave Assisted Acid Digestion of Siliceous and Organically Based Matrices)

Table 3 Effectiveness of interference element correction (IEC) for Cd at 214.438 nm

JSAC0402 (Total content digestion method)	Cd (mg/kg)	Co-Existing Element (Fe) (%)
Certified value	18.5 ± 1.1	4.2 (Reference value)
Quantitation value (with IEC)	18.4	
Quantitation value (without IEC)	19.9	
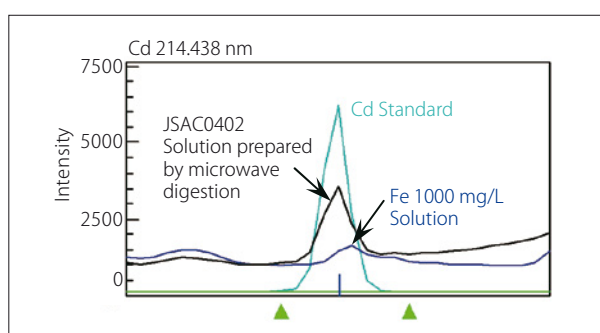
Fig. 1 Spectral Interference of Cd 214.438 nm

Table 4 Results of Soil Content Analysis (Unit: mg/kg)

		Pretreatment	Public Method (Ministry of the Environment Ordinance No. 19)				Total Content Digestion Method			
	Sample Name		JSAC0402		JSAC0403		JSAC0402		JSAC0403	
Element	Concentration Standard	Detection Limit	Quantitation Value	Certified Value	Quantitation Value	Certified Value	Quantitation Value	Certified Value	Quantitation Value	Certified Value
As	150	0.2	11	10.3 ± 0.9	115	111 ± 7	42	41.6 ± 3.2	195	199 ± 15
B	4000	0.02	15.8	15.6 ± 0.9	157.7	157 ± 3		115 ± 15		269 ± 46
Cd	150	0.007	17.1	17.3 ± 0.4	178.2	178 ± 5	18.4	18.5 ± 1.1	182.2	183 ± 7
Cr^{6+}	250	0.02	7.4		64.8		91	90.5 ± 6.9	250.4	257 ± 9
Hg	15	0.1	0.6	0.6 ± 0.1	6.7	7 ± 1		1.3 ± 0.1		11.1 ± 1
Pb	150	0.1	32	32.3 ± 0.8	193	197 ± 4	44	45.2 ± 7.1	216	224 ± 13
Se	150	0.2	3	2.7 ± 0.6	64	63.5 ± 6.4	18	17 ± 1.7	163	169 ± 13

Content reference value : Soil content reference value according to the Soil Contamination Countermeasures Law
Detection limit : 3 times the concentration of the standard deviation obtained from 10 measurements of a calibration curve blank × Dilution factor (200/6)
Cr^{6+} : The content standard is Cr^{6+}, but the analytical value is the total Cr value.

SHIMADZU

Shimadzu Corporation

www.shimadzu.com/an/

SHIMADZU
Excellence in Science

Application News

No.J116

Inductively Coupled Plasma Atomic Emission Spectrometry

Analysis of Nutritional and Harmful Elements in Powdered Milk by ICPE-9820 / HVG-1

■ Introduction

Minerals required for infant growth are well balanced in powdered infant formula. According to Japan's Health Promotion Law, a specific formulation of essential minerals, including calcium (Ca), iron (Fe) and copper (Cu), etc., has been established for infant formula as a special-use food, and is required to be displayed on the product label.[1]

However, the potential adverse effects of certain harmful elements such as arsenic (As) on infant growth and development is of utmost concern, accentuating the importance of strict safety management in the production of infant formula from the raw material stage to the finished product.

Here, using the Shimadzu ICPE-9820 simultaneous ICP atomic emission spectrometer, we conducted simultaneous analysis of elements in powdered milk (NMIJ-certified reference material). In addition, high-sensitivity analysis using an HVG-1 hydride vapor generator was conducted for the detection and quantification of the minute levels of arsenic in the sample.

The ICPE-9820 permits analysis using both high-sensitivity axial (AX) direction observation and high-concentration radial (RD) observation, thereby allowing simultaneous analysis of elements present at concentrations ranging from very low to high levels. As for detection of arsenic, the HVG-1 permits detection of As at the several tens ng/L trace level.

■ Sample

NMIJ-certified reference material; Trace Elements in Milk Powder (NMIJ CRM 7512-a: No. MI-040)

■ Sample Preparation

(1) Acid Digestion

Sample decomposition was conducted using a microwave sample digestion system. Each sample was weighed out to approximately 0.5 g, and digestion was conducted by adding 5 mL nitric acid, 2 mL hydrochloric acid and 1 mL hydrogen peroxide. Table 1 shows the sample digestion conditions. Following sample digestion, 0.5 mL of perchloric acid was added, and after conducting digestion again using the same digestion conditions, the total volume was adjusted to 20 mL using purified water. At this time, yttrium (Y) and indium (In) were added as internal standard elements to the measurement solution to obtain concentrations of 0.5 mg/L for Y, and 5.0 mg/L for In.

Table 1 Digestion Conditions Using Microwave Digestion System

STEP	Temperature (°C)	Time (Minutes)	Power (W)
1	50	2	1000
2	30	3	0
3	180	25	1000
4	150	1	0
5	180	4	1000
6	180	15	1000

(2) Pretreatment for High-Sensitivity Analysis of As Using HVG-1

After conducting digestion as described in step (1), the sample was heated (180 °C) to near-dryness on a hot plate. Then, 3 mL hydrochloric acid, 2 mL potassium iodide (200 g/L) and 0.4 mL ascorbic acid (100 g/L)

were added, and the mixture was left standing for 60 minutes. The total volume was then adjusted to 20 mL using purified water.

In addition, as reagents for operation of the HVG-1, 6 M hydrochloric acid solution and sodium borohydride solution were prepared.

(3) Validation

For validation of the analytical values, a spike and recovery test sample spiked with the standard solution containing the trace-level analyte elements (As, Cd, Cr, Pb) was prepared prior to digestion.

■ Instrument and Analytical Conditions

Measurement was conducted using the Shimadzu ICPE-9820 simultaneous ICP atomic emission spectrometer and the HVG-1 hydride vapor generator. The typical measurement conditions are shown in Table 2, and the measurement conditions using the HVG-1 are shown in Table 3.

Constituents present at high and trace level concentrations were measured using radial (RD) and high-sensitivity axial (AX) observation, respectively. This all-at-once analysis of both high-concentration components and trace components is possible due to the automatic switching between the radial and axial observation directions featured in the ICPE-9820.

The HVG-1 permits analysis of As with sensitivity that is several hundred times higher than that possible using typical measurement. Moreover, the proprietary design of the gas-liquid separator permits acquisition with stable analytical results over an extended period of time.

Table 2 Analytical Conditions

Instrument	: ICPE-9820
Radio Frequency Power	: 1.20 kW
Plasma Gas Flowrate	: 10.0 L/min
Auxiliary Gas Flowrate	: 0.60 L/min
Carrier Gas Flowrate	: 0.70 L/min
Sample Introduction	: Nebulizer 10
Misting Chamber	: Cyclone chamber
Plasma Torch	: Mini torch
Observation	: Axial (AX) / Radial (RD)

Table 3 Analytical Conditions (HVG-1)

Instrument	: ICPE-9820, HVG-1
Radio Frequency Power	: 1.20 kW
Plasma Gas Flowrate	: 10.0 L/min
Auxiliary Gas Flowrate	: 0.60 L/min
Carrier Gas Flowrate	: 0.80 L/min
Plasma Torch	: Mini torch

■ Analysis

The calibration curve method (internal standard method) was used to conduct simultaneous analysis of the minerals and harmful elements in powdered milk.

[Reference]
1) Allowable Standard for Component Composition and Display of Breast Milk and Infant Formula (published by Japan's Ministry of Health, Labour and Welfare)

■ Analytical Results

The analytical results are shown in Table 4. The results for the mineral elements were within the certification range, and good spike and recovery test results were obtained for the trace level toxic elements.

Table 5 shows the analysis result and spike and recovery test result for As using the HVG-1. The As detection limit in aqueous solution was 0.04 µg/L, and in powder, 2 µg/L. As for the spike and recovery test, excellent result of 99 % was obtained.

Fig. 1 shows the results of continuous analysis of a standard solution of As over a 4-hour period. The relative standard deviation (RSD) was 1.6 %, demonstrating stable results over an extended period.

■ Conclusion

These results demonstrate that the ICPE-9820 can be used for simultaneous analysis of the elements in powdered milk, from the minerals present at high concentrations to the toxic substances present at trace levels. Further, in combination with the HVG-1, measurement of As at trace levels is also possible.

Table 4 Analytical Results for Powdered Milk (NMIJ CRM 7512-a)

Element	Unit	Analytical Value in Powder	NMIJ-Certified Value	Expanded Uncertainty	Detection Limit in Powder (DL: 3σ)	Analytical Value in Measurement Solution mg/L	Spike Concentration mg/L	Spike and Recovery %	Detection Limit in Measurement Solution (DL: 3σ) mg/L
Ca	g/kg	8.63	8.65	0.38	0.0000002	211	-	-	0.000005
Fe		0.100	0.104	0.007	0.000006	2.45	-	-	0.0001
K		8.66	8.41	0.33	0.00002	215	-	-	0.0004
Mg		0.838	0.819	0.024	0.0000002	20.5	-	-	0.000005
Na		1.78	1.87	0.09	0.00001	50.2	-	-	0.0003
P		5.52	5.62	0.23	0.0002	135	-	-	0.005
Cu	mg/kg	4.70	4.66	0.23	0.02	0.115	-	-	0.0005
Mn		0.957	0.931	0.032	0.002	0.023	-	-	0.00005
Mo		0.229	0.223	0.012	0.02	0.006	-	-	0.0006
Sr		5.89	5.88	0.20	0.0008	0.144	-	-	0.00002
Zn		40.9	41.3	1.4	0.01	1.00	-	-	0.0003
Cd	µg/kg	<DL	-	-	10	<DL	0.5	98	0.0002
Cr		<DL	-	-	15	<DL	0.5	100	0.0004
Pb		<DL	-	-	97	<DL	0.5	100	0.002

<DL: Below detection limit (3σ) (concentration in measurement solution)

Spike and Recover Rate (%) = (Analytical value of spike-and-recovery test solution – Analytical Value) / Spike Concentration × 100

Table 5 Results of Analysis of As in Powdered Milk Using HVG-1 and Results of Spike and Recovery Test

Element	Unit	Analytical Value in Powder	NMIJ Reference Value	Detection Limit in Powder (DL: 3σ)	Analytical Value in Measurement Solution µg/L	Spike Concentration µg/L	Spike and Recovery %	Detection Limit in Measurement Solution (DL: 3σ) µg/L
As	µg/kg	(2.5)	2.1	2	(0.06)	4	99	0.04

Reference values in ( ) indicate value greater than detection limit, and value less than the lower limit of quantitation.
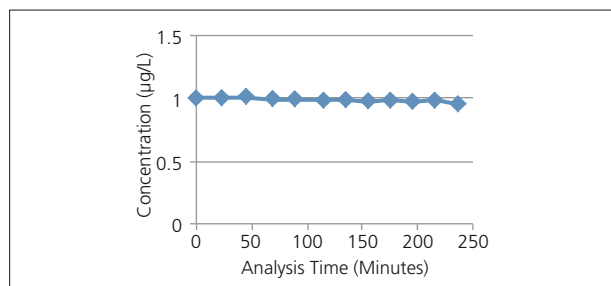
Fig. 1 Long Term Stability of As Value Using HVG-1

Continuous measurement of As 1 µg/L solution (10 % HCl-based) measured continuously every 20 minutes for four hours.
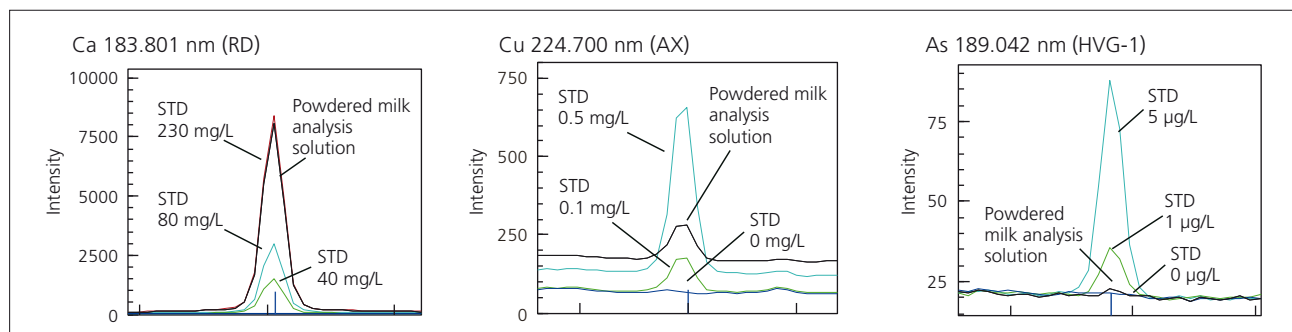
Fig. 2 Spectral Profiles of Ca , Cu, and As

SHIMADZU

Shimadzu Corporation

www.shimadzu.com/an/

3. Spectroscopy

3.2 Molecular Spectroscopy

3.2.1 Ultraviolet Visible Spectroscopy and Near Infrared

Analysis of metals, ions, colors and molecules
The ultraviolet and visible range of the light spectrum is sensitive on color determination and carbon hydrogen bonding determination. Color reactions, DNA and protein methods are easily to solve in low concentrations.

A447	Spectroscopic measurement and multivariate analysis for classification of beer types
A463	Reflectance measurements of an apple and pear, and prediction of elapsed days by multivariate analysis
A473	Evaluation of light-shielding effect of milk cartons using a UV-VIS-NIR spectrophotometer
A477	Color measurement of food – color measurement in sugar and juice
A480	Quantitative analysis of fat in mayonnaise by reflectance spectroscopy and multivariate analysis
SCA-100-017	Wine bottle measurement with UV-2600 and MPC-2600 quality control of color
A492	Simple quantitative analysis of concentrated suspension drink by spectroscopic analysis
UV-012	Maple syrup color analysis using the Shimadzu UV-2600 UV-Vis spectrophotometer

3.2.2 Fourier Transform Infrared Spectroscopy

Quantification and identification of substances
The infrared spectroscopy can analyze all materials which react with heat. The physical vibration correlated to this heat is a identification tool for each material.

A451	Analysis of contaminant adhering to frozen pizza
SCA-110-087	Analysis of bread with FTIR-ATR technique – view to the water content in different appearances of bread
SCA-110-089	Packing made from food analysis of polymer chips with infrared spectros-copy
SCA-110-090	Coffee bean measurement under the pressure of the "Quest™" with infrared spectroscopy
SCA-110-091	Tea bags in the focus of identification single reflection ATR measurements with infrared spectroscopy
FTIR-1403	Quantification and identification of various sugars in maple syrup by MID FTIR spectroscopy
FTIR-1401	Quantification of natural sugars in baby food products by MID FTIR spectroscopy

SHIMADZU
Excellence in Science

Application News

No.A447

Spectrophotometric Analysis

Spectroscopic Measurement and Multivariate Analysis for Classification of Beer Types

Beer is an alcoholic beverage that is quite popular, and consumed in large quantities. Furthermore, the market is now bustling with beverages such as non-alcoholic beer and low-malt beer with beer-like flavors. Beer, low-malt beer, and non-alcoholic beer can all be considered types of beer. A great many varieties of these have been produced and marketed with modifications to the ingredients to adjust such characteristics as alcohol and calorie content. From the standpoint of spectrometric analysis—assuming that the absorption spectra should reflect specific characteristics depending on the types and quantities of ingredients in different beers—we were very interested to see the kinds of differences that would occur upon actual examination.

Here, we introduce the results of our investigation into the differences in absorption spectra obtained from measurement of a variety of beers using the UV-3600 Ultraviolet-Visible Near-Infrared Spectrophotometer. Also presented here is our attempt to classify different types of beer using multivariate analysis.

■ Samples and Measurement Results

The absorption spectra of 14 types of commercially available beers (4 types of beer, 6 types of low-malt beer, 4 types of non-alcoholic beer) were measured using the UV-3600. Degassing was conducted using ultrasonic irradiation for 3 minutes, and measurement was conducted using a 2 mm optical path length quartz cell and a blank sample consisting of air. The measurement results are shown in Fig. 1, and the analytical conditions in Table 1. In addition, expanded spectra of the ultraviolet region (230 – 400 nm) and the near-infrared region (1400 – 1500 nm and 1650 – 1750 nm) are shown in Figs. 2 through 4, respectively. The large peak in the vicinity of 1450 nm in Fig. 3 is due mainly to the absorption of water, while the peak in the vicinity of 1695 nm in Fig. 4 is attributed mainly to ethanol absorption. For reference, the absorption spectra of water and ethanol (99.5 %) are shown in Fig. 5. It is clear that the peak indicated by the arrow near 1450 nm corresponds to the peaks in Fig. 3, and that the peak indicated by the arrow near 1695 nm corresponds to the peaks in Fig. 4.

Due to the apparent signal saturation in the ultraviolet region of this data, the absorption spectra were measured in the ultraviolet region (230 – 400 nm) once again after diluting all of the samples 5-fold with distilled water. Those results are shown in Fig. 6. The peaks that can be seen in the 230 – 300 nm region are believed to be due mainly to absorption of the protein contained in beers.

The alcohol content in the samples is, for beer: 5 %; low-malt beer: 3 – 5.5 %; non-alcoholic beer: 0 %. The protein content per 100 mL is, for beer: 0.2 – 0.4 g; and for low-malt and non-alcoholic beer: 0 – 0.3 g.

The alcohol content for each sample is indicated on their product labels as some "value" or "range" within the above-mentioned ranges.

The degrees of absorption in the ultraviolet and near-infrared regions in these data approximately reflect the given content values for protein and alcohol, respectively.
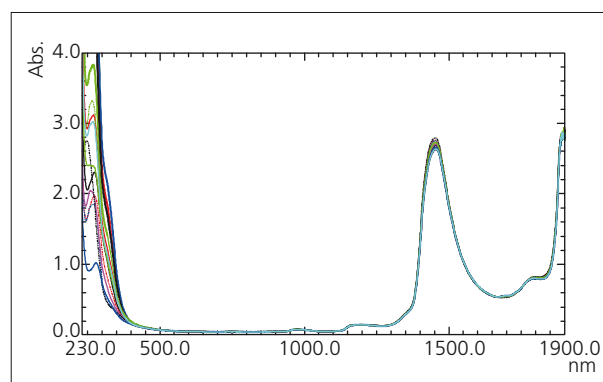
Fig. 1 Absorption Spectra of Beers, Low-Malt Beers, and Non-Alcoholic Beers
(Thick Line: Beers; Thin Line: Low-Malt Beer; Dotted Line: Non-Alcoholic Beers)

Table 1 Analytical Conditions

Instrument	: Shimadzu UV-3600 Ultraviolet-Visible Near-Infrared Spectrophotometer
Measurement wavelength range	: 230 nm – 1900 nm
Scan speed	: Medium
Sampling pitch	: 1.0 nm
Photometric value	: Absorbance
Slit width	: 3 nm
Detector switching wavelengths	: 870 nm, 1650 nm
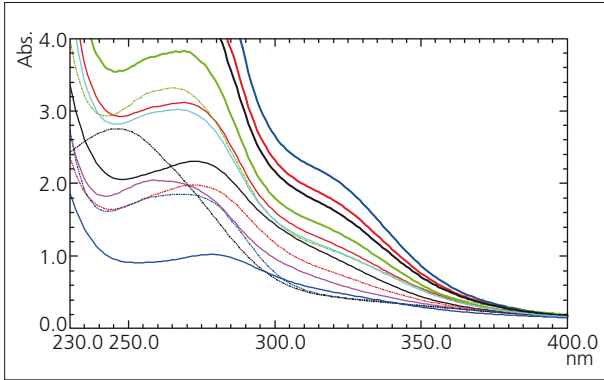
Fig. 2 Expanded Spectra of Fig. 1 (230 – 400 nm)
(Thick Line: Beers; Thin Line: Low-Malt Beers;
Dotted Line: Non-Alcoholic Beers)
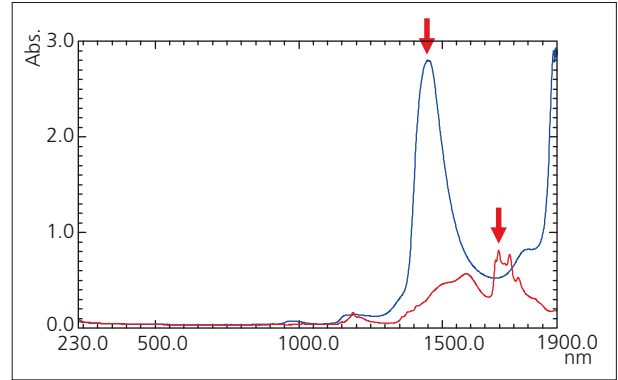
Fig. 5 Absorption Spectra of Water and Ethanol
(Blue Line: Water; Red Line: Ethanol)
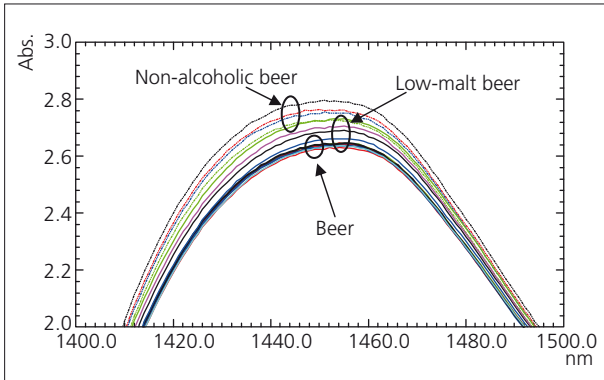
Fig. 3 Expanded Spectra of Fig. 1 (1400 – 1500 nm)
(Thick Line: Beers; Thin Line: Low-Malt Beers;
Dotted Line: Non-Alcoholic Beers)
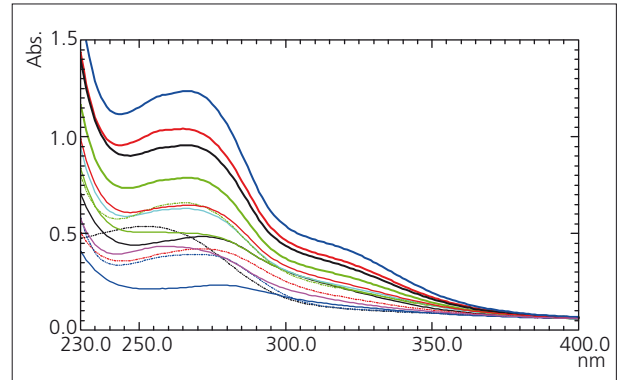
Fig. 6 Absorption Spectra of Samples Diluted 1:5
(Thick Line: Beers; Thin Line: Low-Malt Beers;
Dotted Line: Non-Alcoholic Beers)
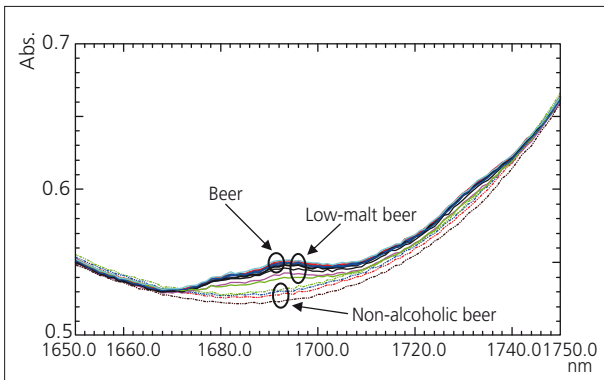
Fig. 4 Expanded Spectra of Fig. 1 (1650 – 1750 nm)
(Thick Line: Beers; Thin Line: Low-Malt Beers;
Dotted Line: Non-Alcoholic Beers)

■ **Classification of Beer Types by Multivariate Analysis**

We attempted to classify the beers using multivariate analysis. Using the 5-fold dilution absorbance data (230 – 400 nm) and the undiluted sample absorbance data (401 – 1870 nm), we conducted principal component analysis (PCA)[1]. The obtained score plot[2] is shown in Fig. 7. "A" corresponds to beer, "B" to low-malt beer, and "C" to non-alcoholic beer. The samples of A, B, and C are clearly grouped accordingly. The closer the points are to each other on the score plot, the greater the corresponding samples should resemble one another. Accordingly, A1 and A3, and C1 and C2 should be similar to each other, and in fact, as can be seen from their respective ultraviolet spectra shown in Fig. 8, they are similar.

Looking at the loading plot[3] shown in Fig. 9 reveals the characteristics of the various groups. As shown in Fig. 9, loading vector components[3] corresponding to the data components of the ultraviolet region are plotted to the right (or upper right) of the center. This indicates that the further to the right a sample is plotted in Fig. 7, the greater its ultraviolet absorption will be. The beer samples A1 – A4, which are actually distributed in that direction, display high ultraviolet absorbance as shown in Fig. 6. Also, in the loading plot of Fig. 9 there are many loading vector components plotted in the upper left quadrant from 1400 – 1480 nm, which corresponds to the absorption of water. This means that the further to the upper left a sample is plotted on the score plot, the closer that sample is to pure water, and the lower the alcohol content. The non-alcoholic beer samples C1 – C4, which are actually distributed in that direction, display high absorbance in the vicinity of 1450 nm, the wavelength associated with water absorption, as shown in Fig. 3.

From the above, it is clear that the further to the right the samples are plotted on the score plot, the greater their ultraviolet absorbance values will be. Correspondingly, the further to the upper left the samples are plotted, the lower their alcohol content will be. Put another way, the further to the right a sample is plotted on the score plot, the greater the amount of organic matter (e.g., protein) it will contain; the further to the upper left a sample is plotted, the lower its alcohol content will be. As for the low-malt beers B1 – B6, their positions in the lower left region are probably due to the fact that their absorbance values are not that high in the ultraviolet region (comparable to those of non-alcoholic beer), while several of them have alcohol content comparable to that of beer.
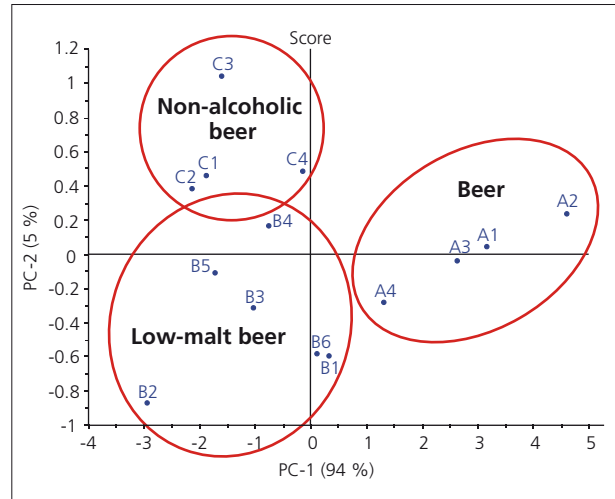
Fig. 7 Score Plot
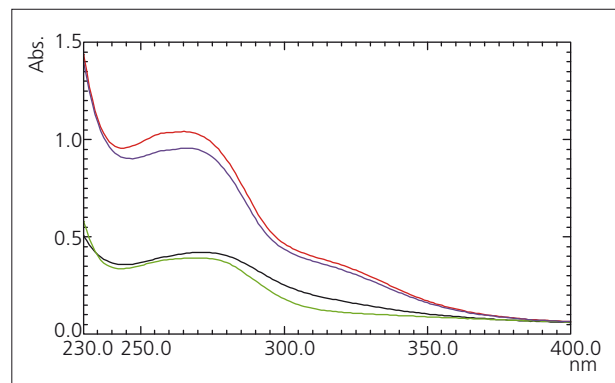
Fig. 8 Absorption Spectra of A1 and A3, C1 and C2
(Red Line: A1; Blue Line: A3; Black Line: C1; Green Line: C2)
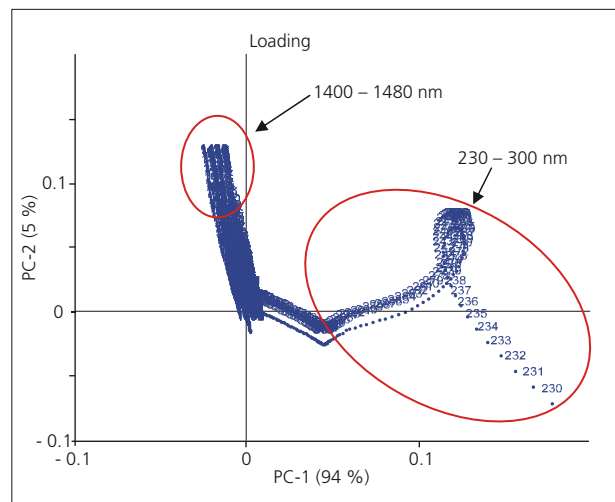
Fig. 9 Loading Plot

■ **Summary**

We were able to confirm the possibility in this investigation of determining the differences in alcohol and protein content in beers by examining their absorption spectra. Further, by applying multivariate analysis to the acquired measurement data, we were able to classify the groups according to the type of beer, and thereby gain an understanding of their characteristics. Comparative investigation of many products is required in the research and development of food products, but an understanding of the degree of similarity among samples is possible using principal component analysis (PCA). The results obtained in this study suggest that a combination of spectral analysis and multivariate analysis can be effective in the development of food products, including beer.

1) The Unscrambler®, a multivariate analysis software application, was used for conducting analysis. The Unscrambler is a trademark or registered trademark of CAMO.
   Regarding the present analysis, principal component analysis was conducted using mean centering of the acquired data.
2) A score plot involves the projection of each sample point expressed in multidimensional space on two loading vectors, expressed as a two-dimensional graph.
   For a description of "loading vector," refer to the following Note 3.
3) A loading plot refers to the plotting via two-dimensional coordinates of substances corresponding to the loading vectors of the first principal component and second principal component (or another combination of principal components). Here, the loading vector refers to the vector obtained by performing eigenvalue calculation for data matrix.

SHIMADZU

Shimadzu Corporation

www.shimadzu.com/an/

SHIMADZU
Excellence in Science

Application News

No.A463

Spectrophotometric Analysis

Reflectance Measurements of an Apple and Pear, and Prediction of Elapsed Days by Multivariate Analysis

Fruit gradually undergoes change with the passage of time after harvesting. Examination of how the physical properties of fruit change over time is important, but if testing requires cutting out a portion of the fruit sample, the number of samples tested would most likely be greatly reduced. Non-destructive fruit properties inspection testing is commonly conducted using a spectrophotometer, and testing of sweetness and acidity by this means is well known.

This type of testing is valuable not only for understanding the physical properties, but for quality management as well. Ripeness, in particular, can be judged based on the number of days that have elapsed from the time of harvesting from the tree. Fruit ripeness is known to be associated with the change in chlorophyll content.[1], [2] Here, we conducted a simulation experiment in which we investigated the time-course changes in purchased fruit samples over a period of days, focusing on changes in the absorption peak of chlorophyll. The results of measurement of apple and pear samples using a UV-VIS-NIR spectrophotometer revealed a correlation between the reflectance spectra of the samples and the number of days elapsed from the time they were obtained. Applying multivariate analysis, we used a prediction formula to calculate and predict the number of elapsed days from the time the samples were obtained. Good results were obtained with the apple sample, as reported in this paper.

■ Measurement Method

We measured the total light reflectance in an apple and a pear using the SolidSpec-3700DUV UV-VIS-NIR spectrophotometer equipped with an integrating sphere. The purchased apple was of the "Fuji" variety, and the pear was the "Nansui" variety. Reflectance measurements were conducted using fluoro-resin Spectralon® standard target plates from Labsphere Inc. (USA). Three measurements were taken for each of the 2 samples at each measurement session, and the samples were positioned at nearly the same position, respectively, for each measurement session over the course of the experiment. After purchasing the samples, time-course measurements were taken at day 0 (purchase date), day 7, 14, 21, 28, and day 35, all the while keeping the samples at room temperature. The experiment was conducted during the autumn, from October to November.

Fig. 1 and Fig. 2 show the apple and pear, respectively, mounted in the integrating sphere, and Table 1 shows the measurement conditions. The SolidSpec-3700DUV has a large sample chamber, and is equipped with an integrating sphere as standard, permitting measurement of large samples like apples and pears. Below, the results of analysis of the apple are presented first, and the results obtained with the pear are discussed later.
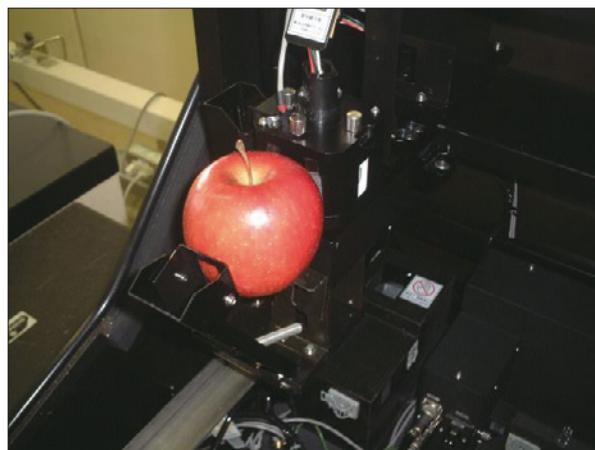
Fig. 1 Apple Mounted in Integrating Sphere
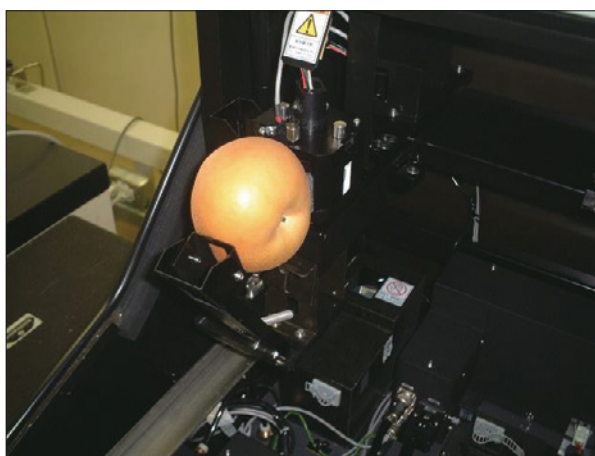
Fig. 2 Pear Mounted in Integrating Sphere

Table 1 Analytical Conditions

Instrument	: SolidSpec-3700DUV UV-VIS-NIR spectrophotometer
Measurement wavelength range	: 200 nm - 2700 nm
Scan speed	: Medium
Sampling pitch	: 1.0 nm
Photometric value	: Reflectance
Slit width	: (20) nm
Detector switching wavelengths	: 870 nm, 1650 nm

■ Measurement Results for the Apple and Prediction of Elapsed Days by Multivariate Analysis

The results for the apple are shown in Fig. 3. It is clear from this figure that there is a large spectral change in the visible region, but almost no change in the infrared region. Fig. 4 presents an expanded view of the visible region in which there is a large spectral change. The downward peak in the vicinity of 680 nm is due to the absorption of chlorophyll.[1], [2] This peak clearly became smaller as the number of elapsed days increased.

Using the data in the region of this peak, it is possible to make predictions about the number of elapsed days the apple was left standing. Therefore, we tried calculating this number of elapsed days using a prediction formula based on quantitative methods of multivariate analysis. We used two types of multivariate analysis, the PLS (Partial Least Squares) method and the multiple linear regression method, and then compared the prediction accuracy between the two. For the PLS method, we utilized data centering.

Of the data obtained from the three repeat measurements, we used those of the first and second analyses to generate a calibration model. The third data points were used as verification data for evaluating the prediction accuracy of the calibration model. Using the PLS method, we created a calibration model using all of the spectral data within the range of 450 nm to 750 nm, and using the multiple linear regression method, we created a calibration model using the spectral data associated with three wavelengths, 540 nm, 664 nm and 676 nm. Fig. 5 shows the data within the selected wavelength range using the PLS method as a blue line, and the wavelength positions of the data using multiple linear regression as red arrow marks.

Each of the generated calibration models was used to predict the elapsed number of days associated with the verification data (data obtained from the third measurement). The results are shown in Table 2. Good results were obtained using both methods, with the data matching within ±3 days of the actual elapsed number of days. The calculations were conducted using the Unscrambler® multivariate analysis software, a product of CAMO. Regarding this analysis, principal component analysis was conducted using mean-centering. Multiple regression calculations were conducted using the "regression analysis" function of the Microsoft Excel® spreadsheet software.

Fig. 4 **Expanded Spectra of Fig. 3 (450 nm - 800 nm)**
(Red: 0 Days, Blue: 7 Days, Green: 14 Days, Black: 21 Days, Purple: 28 Days, Light Blue: 35 Days)

Table 2 Prediction Results for Verification Data

Actual Elapsed Days	Prediction Results with PLS Method Verification Data	Prediction Results with Multiple Linear Regression Verification Data
0	-0.66	2.56
7	7.33	6.10
14	15.26	12.77
21	21.72	21.02
28	30.32	27.54
35	35.19	33.92
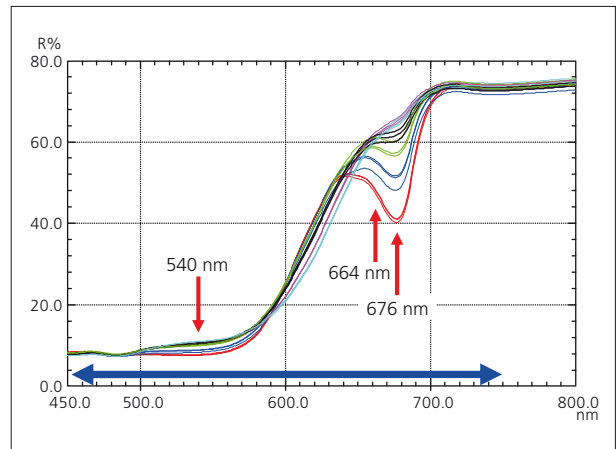
Fig. 5 **Data Used for Partial Least Squares (PLS) and Multiple Linear Regression**
(Blue Line Range: PLS, Red Arrow: Multiple Linear Regression)
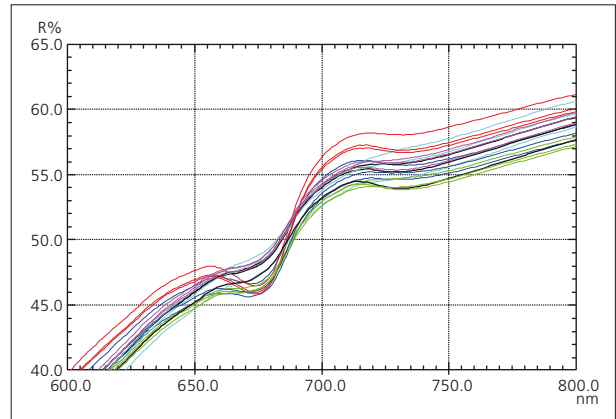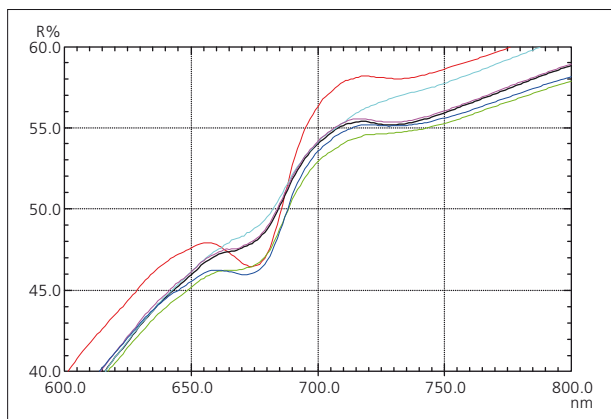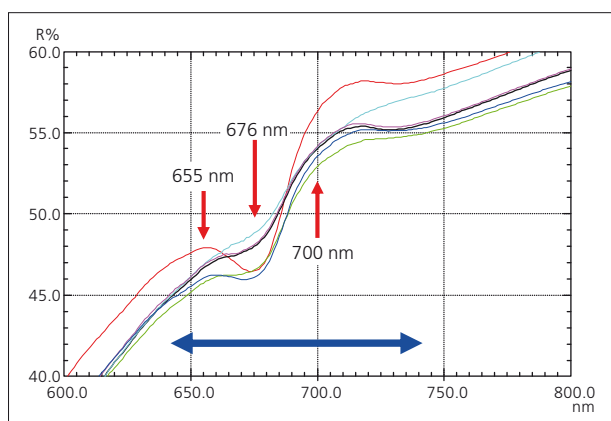(Red: 0 Days, Blue: 7 Days, Green: 14 Days, Black: 21 Days, Purple: 28 Days, Light Blue: 35 Days)

Fig. 3 **Reflectance Spectra of an Apple**
(Red: 0 Days, Blue: 7 Days, Green: 14 Days, Black: 21 Days, Purple: 28 Days, Light Blue: 35 Days)

■ **Measurement Results for the Pear and Prediction of Elapsed Days by Multivariate Analysis**

We conducted measurements for the pear just as we did for the apple. The measurement results for the pear are shown in Fig. 6. The regions from 500 nm to 1000 nm and 1000 nm to 1800 nm are expanded in Fig. 7 and Fig. 8, respectively. The weak absorption peak of chlorophyll can be seen in the vicinity of 680 nm in Fig. 7. Looking at Fig. 8, a big difference is noticeable between the spectrum at Day 0 and those of all the other elapsed days, but this is presumed to be due to a change in the hardness of the pear.[2]

Fig. 9 shows the expanded region of the chlorophyll absorption peak of Fig. 6, and Fig. 10 shows only the first measured spectrum of those in Fig. 9. From Fig. 9 and Fig. 10, it is clear that while the absorption peak of chlorophyll is extremely weak compared to that of the apple, the spectrum changes in a way that is correlated with the elapsed number of days. The greater the elapse of time, the smaller becomes the spectral "constriction" corresponding to absorption.

Using the data in the vicinity of this chlorophyll absorption region, as in the case of the apple, we created calibration models by the PLS and multiple linear regression methods, respectively. Data associated with the 640 - 740 nm wavelength range was used for the PLS method, and those associated with 655 nm, 676 nm and 700 nm were used for the multiple linear regression method. Fig. 11 shows the data within the wavelength range using the PLS method as a blue line, and the wavelength positions of the data using multiple linear regression as red arrow markings.

Using each of the generated calibration models, we predicted the number of elapsed days for the verification sample (data associated with the third sample measurement). Those results are shown in Table 3. The calculated prediction of 35 days differed significantly from the actual number of days in both the multiple linear regression method and the PLS method. Thus, the good result obtained with the apple was not obtained with the pear. It is believed that this might be due to the low absorption of chlorophyll in the nansui pear used here, possibly introducing a degree of error.
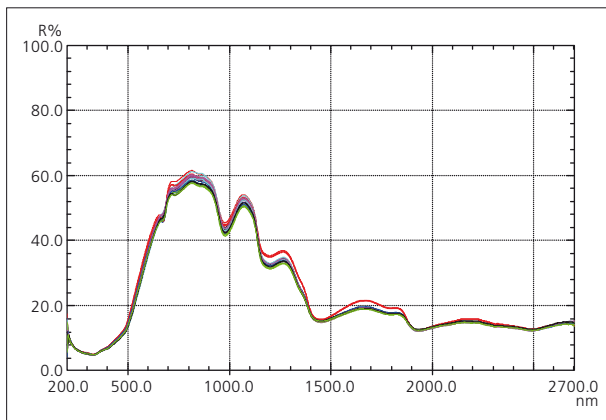
Fig. 6 Reflectance Spectra of a Pear
(Red: 0 Days, Blue: 7 Days, Green: 14 Days, Black: 21 Days, Purple: 28 Days, Light Blue: 35 Days)
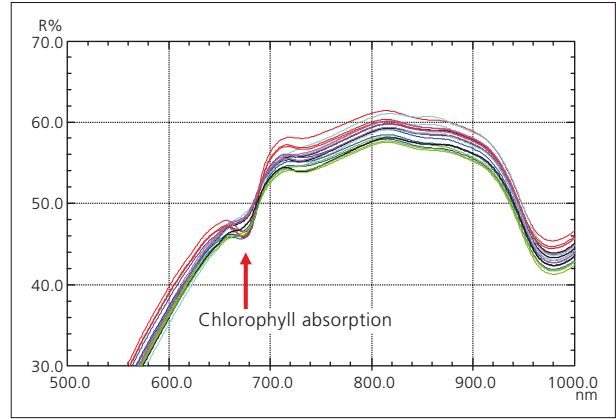
Fig. 7 Expanded Spectra of Fig. 6 (500 nm - 1000 nm)
(Red: 0 Days, Blue: 7 Days, Green: 14 Days, Black: 21 Days, Purple: 28 Days, Light Blue: 35 Days)
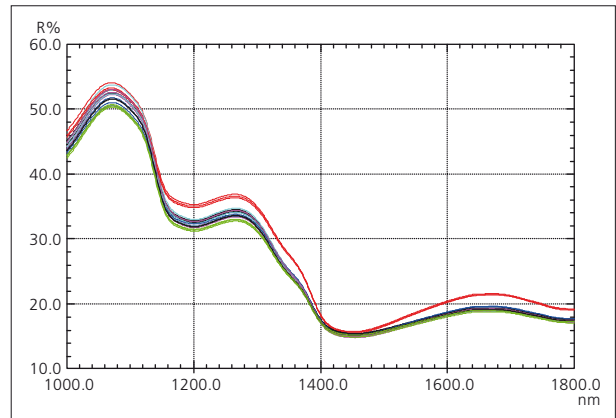
Fig. 8 Expanded Spectra of Fig. 6 (1000 nm - 1800 nm)
(Red: 0 Days, Blue: 7 Days, Green: 14 Days, Black: 21 Days, Purple: 28 Days, Light Blue: 35 Days)

Fig. 9 Expanded Spectra of Fig. 6 (600 nm - 800 nm)
(Red: 0 Days, Blue: 7 Days, Green: 14 Days, Black: 21 Days, Purple: 28 Days, Light Blue: 35 Days)

**Fig. 10 First Spectra Measured for Each Elapsed Day in Fig. 9
(Red: 0 Days, Blue: 7 Days, Green: 14 Days, Black: 21 Days,
Purple: 28 Days, Light Blue: 35 Days)**

**Fig. 11 Data used for Partial Least Squares (PLS) and Multiple
Linear Regression
(Red: 0 Days, Blue: 7 Days, Green: 14 Days, Black: 21 Days,
Purple: 28 Days, Light Blue: 35 Days)**

Table 3 Prediction Results for Verification Data

Actual Elapsed Days	Prediction Results with PLS Method Verification Data	Prediction Results with Multiple Linear Regression Verification Data
0	-1.49	-1.54
7	5.55	6.17
14	12.65	13.51
21	21.07	21.54
28	28.99	28.16
35	23.42	25.15

■ **Conclusion**

By applying multivariate analysis to the reflectance data of samples measured at 7 day intervals, we were able to predict the number of elapsed days within ±3 days during the course of 35 days. In the case of the pear, however, the prediction accuracy was poor compared to that for the apple, and this was thought to be due to the low absorption of chlorophyll. These results may also be subject to variation due to such factors as sample type, number of measurement samples, as well as the season when measurement is conducted. It is also necessary to consider that the results will depend on when the sample is harvested from the tree. However, because there is a definite correlation between the number of days that elapsed from the date of purchase and the absorption of chlorophyll, the present study suggests that this method can be applied to predict the number elapsed days from the date of harvest. It is believed that the combination of spectroscopy and multivariate analysis is effective for studying the maturity and degradation of chlorophyll-containing fruit.

[References]
1) Takefumi Kudo, Hiroshi Murotani, Masahiro Hazima, Souta Suzuki, Moriaki Wakaki: "Dependence of Maturity on Surface Color of Pear," Proceedings of the Faculty of Engineering of Tokai University, Vol. 46 No.2 p.29-34 (2006)
2) Yasuyuki Sagara: "Food Preference Measurement, Evaluation and Advanced Technologies - Food Sensitivity Engineering Proposal," Journal of Food Science and Technology Vol. 41, Supplement No. 6

First Edition: May. 2013

SHIMADZU

Shimadzu Corporation

www.shimadzu.com/an/

SHIMADZU
Excellence in Science

Application News

No.**A473**

Spectrophotometric Analysis

Evaluation of Light-Shielding Effect of Milk Cartons Using a UV-VIS-NIR Spectrophotometer

Foods that are on display in shops are exposed to various types of light, including ultraviolet, visible, and near-infrared light, all of which can pass through packaging materials and containers. Such exposure of these foods and beverages to light can cause protein oxidation, vitamin destruction, fading, and other adverse effects in the foods. Consequently, examination of the light-shielding effect (transmittance) of food containers is very important. Previously, transmittance in various types of PET bottles was measured in Application News No. A461. Those results indicated differences in transmittance among the bottles in the near-infrared and ultraviolet regions.

Here, we examined the transmission characteristics of paper-based milk cartons using the UV-3600 ultraviolet-visible-near-infrared spectrophotometer. The results of measurements conducted on the 3 types of milk cartons indicated differences in transmittance depending on the carton sample. Further, differences in transmittance were also found within each of the respective samples, depending on the measurement site. This paper introduces those results.

■ **Total Light Transmittance Measurement of Milk Cartons**

After mounting the integrating sphere accessory in the UV-3600, measurement of the total light transmittance was conducted for the three types of milk cartons, A, B, and C. Fig. 1 shows a diagram of the principle of total light transmittance measurement. First, baseline correction is conducted in the absence of a sample. Then, by conducting measurement with a sample mounted in the integrating sphere accessory, the total light transmittance consisting of the combined linear and diffuse transmittance can be obtained. Using this method makes it possible to capture all of the transmitted light including not only the linearly transmitted light, but the diffusely transmitted light as well. This total light transmittance measurement

technique is often used when measuring the transmittance of samples having some degree of turbidity (cloudiness), such as films, plastics, and paper. Here, the sample consisted of a milk carton that had been washed out with water, and then allowed to dry naturally. Three pieces, each a few centimeters in size, were cut from the same sample carton, and measurements were conducted at three differently colored sites on each sample. Fig. 2 shows a photograph of a milk carton sample mounted in the integrating sphere accessory, and Table 1 shows the analytical conditions used.
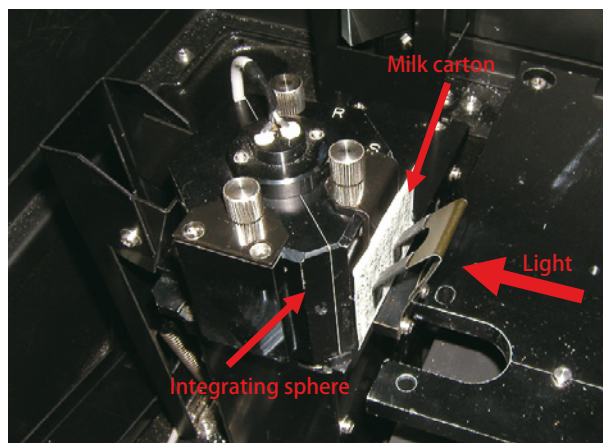
Fig. 2 Photograph of a Sample Set in an Integrating Sphere

Table 1 Analytical Conditions

Instruments	: UV-3600 UV-VIS-NIR spectrophotometer MPC-3100 large sample compartment (with built-in integrating sphere)
Measurement Wavelength Range	: 200 nm to 2300 nm
Scan Speed	: Medium
Sampling Pitch	: 1.0 nm
Measurement Value	: Transmittance
Slit Width	: (20) nm
Detector Switching Wavelength	: 870 nm
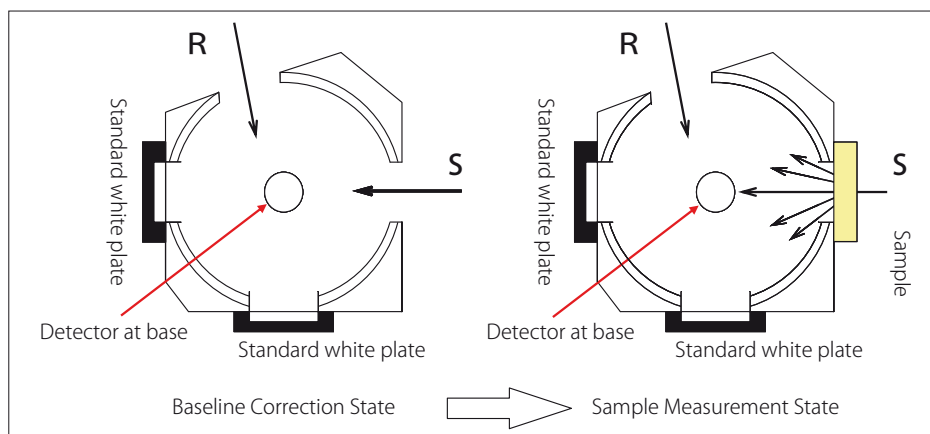
Fig. 1 Total Light Transmittance Measurement

■ Results

The measurement results for each of the milk cartons A to C are shown in Figures 3 to 5. The differences in print color are reflected in the transmittance spectra obtained from measurement at three sites in the same sample, respectively, in Fig. 3 and Fig. 4. For example, in milk carton B of Fig. 4, measurements were conducted at sites that were printed with reddish, whitish, and mixed black and white colors, respectively. The measurement results are shown using a red, blue and black trace, respectively, for each of the spectra. The shape of the red-trace spectrum is different from that of the others, but this is thought to be due to absorption of green light and blue light in the region of 400 to 600 nm, causing a decrease in transmitted light in that region. Further, comparing this to the green- and black-trace spectra, the black trace shows lower transmittance. At the site printed with the mixed black and white color system corresponding to the black-trace spectrum, it is believed that the overall low transmittance is due to the ease with which a black surface absorbs light.

From the results of Figures 3 and 4, it is clear that even in the same milk carton, the transmittance varies depending on the printed color at the measurement site. As for the data associated with milk carton C shown in Fig. 5, the transmittance for all three color regions was about 0 %. This was undoubtedly due to the aluminum film affixed to the inner surface of milk carton C, preventing the transmission of nearly all light, from the ultraviolet to near-infrared region.
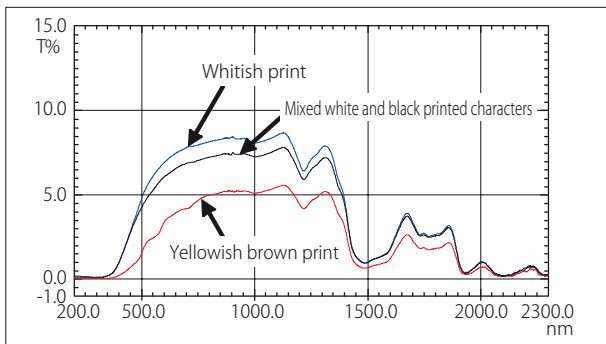
Fig. 3 Transmittance Spectra of Three Positions in Sample A
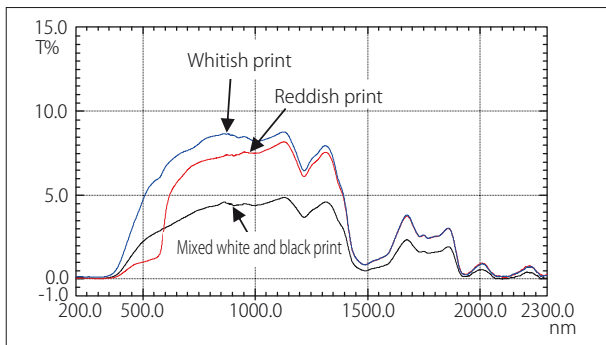
Fig. 4 Transmittance Spectra of Three Positions in Sample B
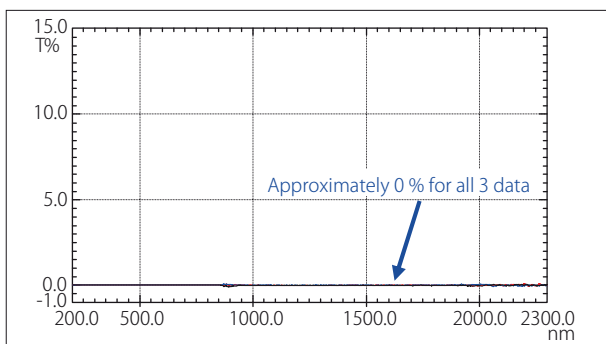
Fig. 5 Transmittance Spectra of Three Positions in Sample C

■ Comparison of Milk Carton and PET Bottle

We compared the transmittance spectra of the PET bottles measured previously in Application News No. A461 with those of the milk cartons measured here. The results are shown in Fig. 6. The blue-trace spectrum of Fig. 3 represents that of the milk carton, and the PET bottle spectrum is that of sample A in the above-mentioned Application News.

From Fig. 6, it is clear that the transmittance in the milk carton is very low over the entire measurement range as compared with that of the PET bottles. The ultraviolet region from 200 to 380 nm is shown in Fig. 7. While transmission of ultraviolet radiation occurs above 320 nm in the case of the PET bottle, almost no ultraviolet radiation is transmitted with the milk carton. Thus, it is clear that the light-shielding effect of the paper-based container is superior to that of the PET bottle.
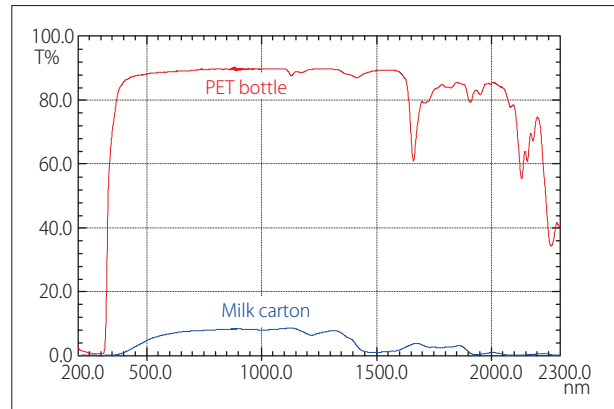
Fig. 6 Transmittance Spectra of PET Bottle and Milk Carton
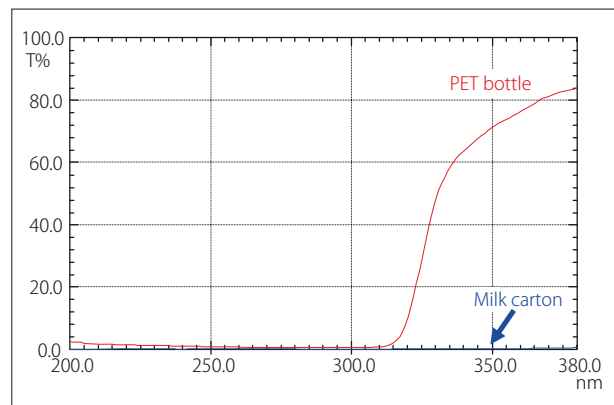
Fig. 7 Expanded Spectra of Fig. 6 (Ultraviolet Region)

■ Conclusion

The results of measurement of the three types of milk cartons conducted here indicated that the light transmission characteristics vary depending on the milk carton. Even measurements taken using the same milk carton showed differences in transmittance depending on the printed color. This suggests that light-shielding performance can be changed through the selective use of the colors printed on the carton. Also, affixing aluminum film to the inner surface achieves nearly complete shielding in the ultraviolet to near-infrared regions. Such use of aluminum film could be an effective means of protecting foods that are especially susceptible to light. It was also found that the light-shielding effect of milk cartons is higher than that of PET bottles. From these results, it is believed that transmittance measurement using a spectrophotometer is effective for assessment of light shielding in food containers.

SHIMADZU

Shimadzu Corporation

www.shimadzu.com/an/

SHIMADZU
Excellence in Science

Application News

No.A477

Spectrophotometric Analysis

Color Measurement of Food
— Color Measurement in Sugar and Juice —

Foods come in a wide variety of colors, providing visual enjoyment in our lives. These colors also play a role in enhancing or reducing our appetite, and are an important factor in visually determining food quality. Color is a sensory-related phenomenon, but by conducting measurement of food samples using a spectrophotometer to express the color as an objective numerical value, it is possible to compare color quantitatively among multiple samples.

Here, we conducted measurement of sugar and juice samples to determine their color values. For sugar, we used castor or "superfine" sugar, soft brown sugar and brown sugar, etc. as samples, and conducted measurement using a powdered sample holder to compare the color among the samples. For juice, we measured the difference in color between vegetable juice and fruit juice using a screw-cap vial to conduct the measurements and investigate the differences in color.

Fig. 1 Sugars (A – F)

■ Measurement of Sugars

We prepared measurement samples for each of 6 types of sugar to be analyzed. Table 1 lists the 6 prepared samples designated using the letters A – F. The sugar varieties used for measurement are shown in the photograph of Fig. 1. It is clear from the photographs that except for A, all of the sugars are yellowish. Fig. 2 shows the powder sample holder used for the measurements. At the left is the sample cell with a built-in glass window plate, and at right is the holder used for mounting the window plate-mounted sample cell in the integrating sphere. The window plate-mounted cell packed with sample B is shown in the photograph of Fig. 3. Samples that do not easily harden into a clump may spill out of the integrating sphere sample dish, but this sample loss can be prevented by using a window plate-mounted cell.
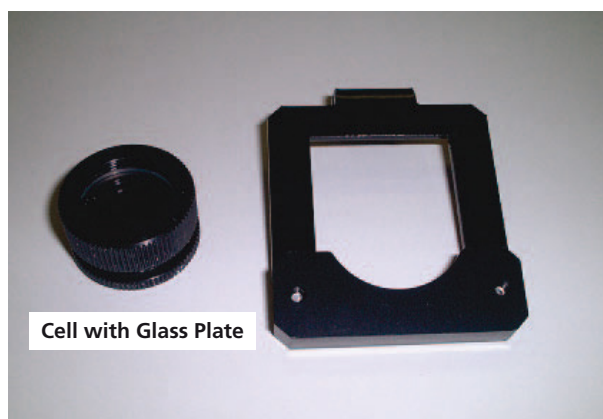
Cell with Glass Plate

Fig. 2 Holder for Powder Sample

Table 1 Six Measured Sugars

Sample	Sugar Name
A	Castor sugar
B	Table sugar
C	Table sugar
D	Soft brown sugar
E	Processed brown sugar
F	Processed brown sugar

Fig. 3 Sample B Set in Cell with Glass Plate

■ Measurement Results for Sugars

The sample was placed in the integrating sphere as shown in Fig. 4, and the total light reflectance was measured in the visual region of 380 nm to 780 nm. Each sample type was measured twice, replacing the sample in the cell for each measurement. In addition, baseline correction was conducted using a cell filled with barium sulfate as a reflectance standard.

The measurement results and measurement conditions are shown in Fig. 5 and Table 2, respectively. The reflectance of Sample A showed almost no change over the measurement range, confirming its achromaticity. The samples other than A showed relatively low reflectance in the blue region below 500 nm, and relatively high reflectance in the green and red regions above 500 nm, indicating that they belong to the yellow color system, consisting of a mixture of these green and red colors.
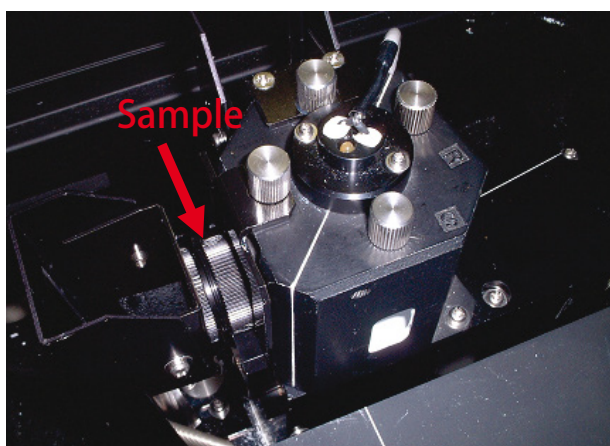
Fig. 4 Sample Set in Integrating Sphere
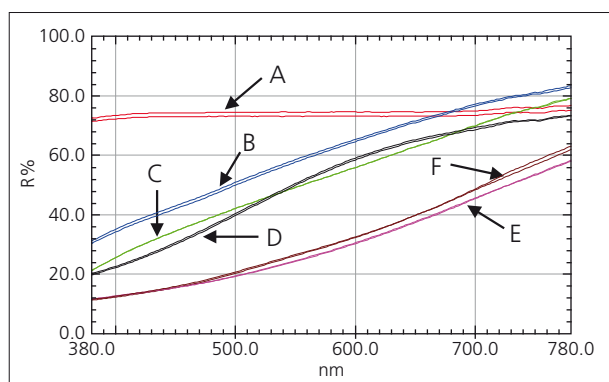
Fig. 5 Total Luminous Reflectance Spectra of Samples
Red: A, Blue: B, Green: C, Black: D, Purple: E, Brown: F

Table 2 Analytical Conditions

Instrument	: UV-3600 Ultraviolet-Visible-Near-Infrared Spectrophotometer MPC-3100 Large-Sample Compartment (with built-in integrating sphere)
Measurement wavelength range	: 380 nm – 780 nm
Scan speed	: Medium
Sampling pitch	: 2.0 nm
Photometric value	: Reflectance
Slit width	: 8 nm

■ Sugar Color Calculation

Using color measurement software, we calculated the color values of the L*a*b* color system based on the measurement results shown in Fig. 5. Those results are shown in Table 3. The calculations were conducted based on Illuminant D65 and a 10-degree field of view. The values of Table 3 are expressed in the L*a*b* color space diagram of Fig. 6, and Fig. 7 shows an expanded view of the region in the vicinity of the plotted points on the a*b* graph (horizontal axis: a* values, vertical axis: b* values) on the right side of Fig. 6.

In the L*a*b* color space diagram, the L values are plotted on the histogram on the left, and the a* and b* values are plotted on the graph plot on the right. In the L* graph, the higher the sample position in the graph, the brighter the color. As can be seen in Fig. 6 and Table 3, sample A is relatively brighter, and E and F are darker. In the a*b* graph on the right, it can be seen that the nearer the sample is to the center of the circle, the duller the color, and the further outside of the circle, the brighter the sample color. The radial direction of the a*b* graph represents the hue, the direction to the right while facing the circle represents reddish, the upward direction represents yellowish, the direction to the left represents greenish, and the downward direction represents bluish. From Fig. 6 and Fig. 7, it is clear that except for A, the samples are reddish yellow.

Thus, it is possible to determine the relative differences in color among samples by displaying the colors in a 2-dimensional chromaticity diagram.

Table 3 L*a*b* Values (D65 lamp, 10-degree field of view)

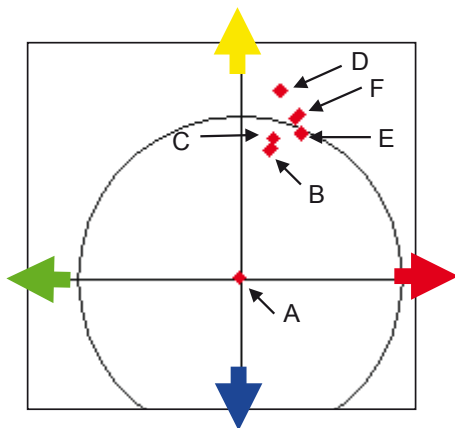| Data Name	L*	a*	b*
A-1	89.15	-0.06	0.22
A-2	88.48	-0.04	0.14
B-1	80.93	3.62	15.72
B-2	80.46	3.76	16.07
C-1	75.55	4.06	17.23
C-2	75.56	4.09	17.20
D-1	75.75	5.01	23.28
D-2	76.12	4.93	23.11
E-1	57.12	7.59	18.03
E-2	56.92	7.58	17.67
F-1	58.84	6.86	19.85
F-2	58.54	7.16	20.17
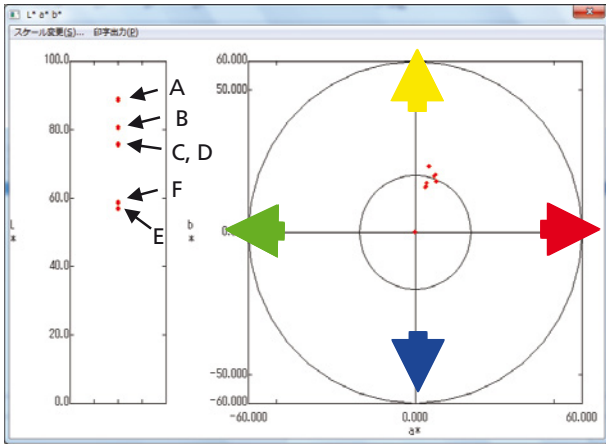
Fig. 6 L*a*b* Color Space

Fig. 7 Expanded a*b* Graph of Fig. 6

■ Measurement of Juices

We prepared 5 types of juices, including 1 type of tomato juice, 3 types of vegetable juice, and 1 type of carrot juice. Table 4 lists the 5 types of juice samples using alphabetical designations. The samples are shown in the photograph of Fig. 8. The samples were transferred to screw-cap vials, which were placed in the integrating sphere for measurement as shown in Fig. 9. Total reflectance measurement was conducted twice for each sample, using a different vial for each measurement. A positioning jig was used to secure the samples to ensure that they were all measured in exactly the same position. The measurement range used was the visible region of 380 nm – 780 nm, and disposable screw-cap vials were used. In addition, we used as a reference plate for reflectance measurement a Spectralon® fluorine-based resin white plate obtained from Labsphere, Inc. (United States).

Table 4 Five Measured Juices

Sample	Juice Type
A	Tomato juice
B	Vegetable juice
C	Vegetable juice
D	Vegetable juice
E	Carrot juice
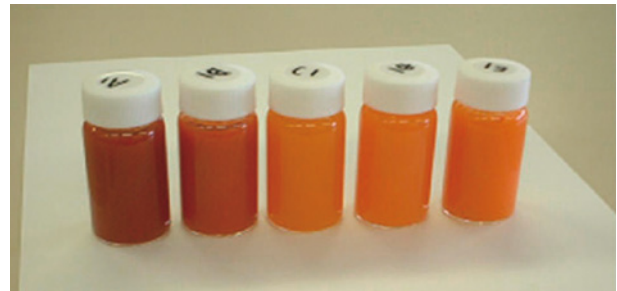
Fig. 8 Samples in Screw-Cap Vials (A – E from left to right)
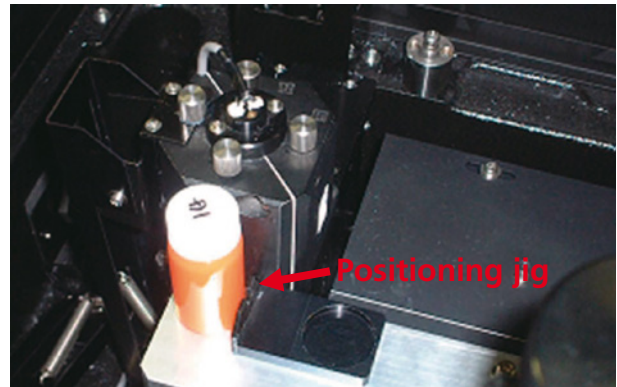
Fig. 9 Sample Set in Integrating Sphere

■ Measurement Results for Juices

The juice measurement results are shown in Fig. 10, and the analytical conditions are the same as those shown in Table 2.

As can be seen in Fig. 8, samples A and B are more reddish in color, while C, D and E are closer to orange. Fig. 10 reflects those results, in which A and B reflect a lot of light in the red region above 600 nm, while C, D and E reflect some light in the green region in addition to light in the red region. The orange color results from the mixing of those colors.
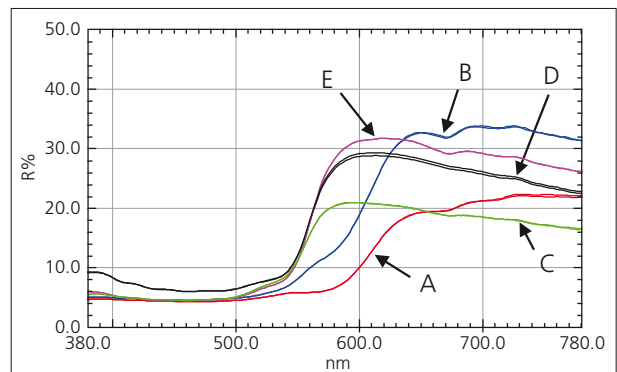
Fig. 10 Total Luminous Reflectance Spectra of Samples
Red: A, Blue: B, Green: C, Black: D, Purple: E

■ Juice Color Calculation

We calculated the L*a*b* color system values based on the measurement results shown in Fig. 10. Those results are shown in Table 5. The calculations were conducted based on illumination C and a 2-degree field of view.

The values of Table 5 are expressed in the L*a*b* color space diagram of Fig. 11, and Fig. 12 shows an expanded view of the region in the vicinity of the plotted points on the a*b* graph on the right side of Fig. 11. It is clear from Fig. 11 and Table 5 that samples D and E are relatively bright, and that A is dark. It is also clear from Fig. 12 that sample A is closer to red, while C closer to yellow. Also, with respect to color saturation (vividness), sample A is relatively dull in color, while E has a vivid color.
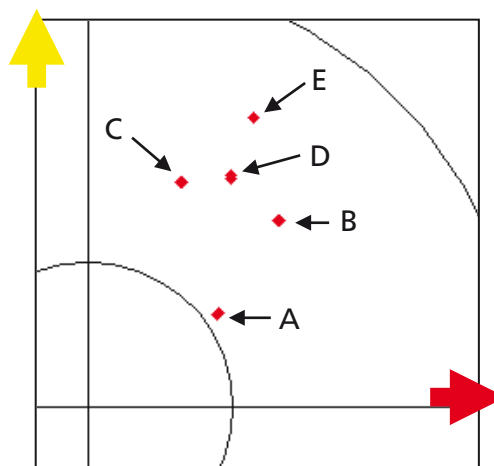
Fig. 12 Expanded a*b* Graph of Fig. 11

Table 5 L*a*b* Values (C lamp, 2-degree field of view)

Data Name	L*	a*	b*
A1	32.46	17.85	12.82
A2	32.44	17.95	12.86
B1	40.67	26.27	25.69
B2	40.66	26.16	25.62
C1	43.79	12.90	30.94
C2	43.87	12.88	30.86
D1	48.80	19.78	31.85
D2	48.51	19.58	31.45
E1	48.94	22.82	39.91
E2	48.95	22.78	39.91

■ Conclusion

For this Application News, we conducted color measurement for various types of sugars and juices, and compared their colors. The sugars were measured using a powder sample holder, and the juices were measured using screw-cap vials. Reflectance data were acquired in both cases. We were able to express the color differences among samples by obtaining the color values using color measurement software which permitted the results to be plotted on a two-dimensional color space. These expressions can provide useful information for conducting comparative research of product colors.

Thus, by combining the use of an ultraviolet-visible spectrophotometer with color measurement software, it becomes possible to visually and quantitatively grasp the colors of various types of samples.

Fig. 11 L*a*b* Color Space

SHIMADZU

Shimadzu Corporation

www.shimadzu.com/an/

SHIMADZU
Excellence in Science
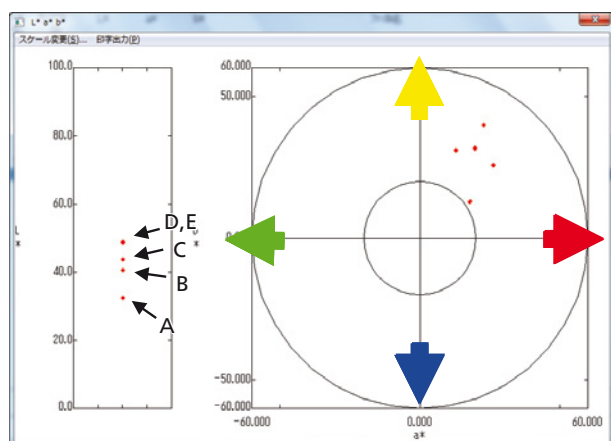
Application News

No.A480

Spectrophotometric Analysis

Quantitative Analysis of Fat in Mayonnaise by Reflectance Spectroscopy and Multivariate Analysis

Mayonnaise is one of various seasonings that are used on a daily basis. Reflecting the health consciousness that is prevalent in recent years, fat content-adjusted mayonnaise products have been sold in great quantities. Accordingly, it is important that the fat content listed on the label reflect the fat content determined through accurate measurement. Fat content in mayonnaise is typically determined using the Soxhlet extraction method. However, the process involving the repeated evaporation of solvent required to extract the target substance is quite time consuming.

We therefore investigated a simple method based on reflectance measurement for this fat quantitation. Combining reflectance measurement using a screw-cap vial with multivariate analysis, we demonstrated the ease with which fat quantitation can be accomplished. Multivariate analysis was conducted using both multiple regression and the PLS method, and the quantitative accuracy was compared between the two methods. Both methods were found to provide good results. Furthermore, good quantitative accuracy using both the multiple regression and the PLS method were obtained even when the original mayonnaise containers were used "as is." Here, we introduce the results of this investigation.

Fig. 1 Sample Set in an Integrating Sphere

■ Total Luminous Reflectance Measurement of Mayonnaise

The measurement samples included eight types of mayonnaise containing different levels of fat content. Table 1 shows the fat content of each sample as indicated on labels affixed to mayonnaise containers. The samples are indicated using the letters A – H, based on descending order of the indicated fat content.

For this investigation, measurements were conducted after a jig for securing all the samples in the same position was attached to the integrating sphere. After transferring a sample into a glass screw-cap vial, and setting the vial in the integrating sphere as shown in Fig. 1, each sample type was measured twice, replacing the vial for the same sample between the two measurements. Disposable screw-top vials were used for measurement. Thus, a total of 16 data points (8×2=16) were obtained. In addition, we used as a reference plate for reflectance measurement a Spectralon® fluorine-based resin white plate obtained from Labsphere Inc. (United States).

The measurement conditions and measurement results are shown in Table 2 and Fig. 2, respectively. The vertical axis of Fig. 2 expresses the absorbance-related $\log_{10}$ (R_0/R) value. Here, R_0 is reflection intensity of the standard white plate, and R is the reflection intensity of the sample. The "Abs." of Fig. 2 represents $\log_{10}$ (R_0/R). As is evident from Fig. 2, the results from each set of two measurements are practically overlapped, indicating that switching of the screw-top vials had little effect on the results.

Fig. 3 shows an expanded view of Fig. 2 in the range of 1000 nm – 1500 nm. The region in which fat absorption occurs (in the vicinity of 1210 nm) is circled in red. Focusing on this absorption region, it is clear that the greater the fat content of the sample, the larger the absorption peak.
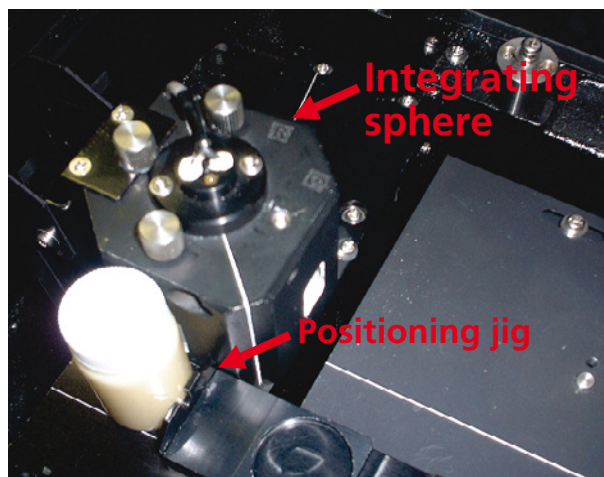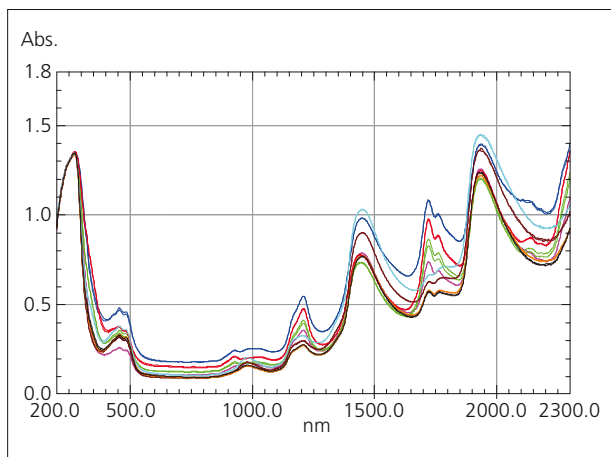
Table 1 Measured Mayonnaise Types (8 Kinds)

Sample	Fat Content Indicated on Label (g/15 g)
A	11.8
B	11.2
C	9.8
D	8.6
E	5.2
F	5.1
G	3.6
H	2.2

Table 2 Analytical Conditions

|	
Instrument	: UV-3600 Ultraviolet-Visible-Near Infrared Spectrophotometer, MPC-3100 Large-Sample Compartment (with built-in integrating sphere)
Measurement Wavelength Range	: 200 nm – 2300 nm
Scan Speed	: Medium
Sampling Pitch	: 2.0 nm
Photometric Value	: Reflectance
Slit Width	: (20) nm

Fig. 2 Total Luminous Measurement Spectra
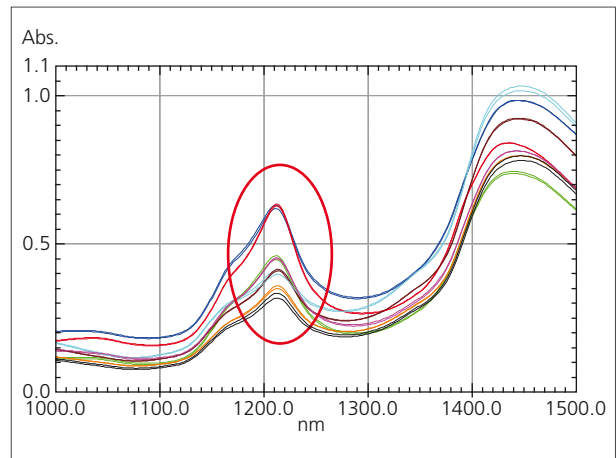**Red: A, Green: B, Blue: C, Purple: D, Black: E, Orange: F, Brown: G, Light Blue: H**
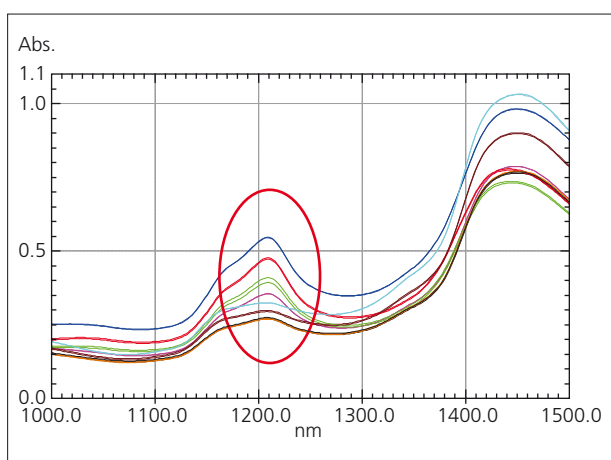
Fig. 3 Expanded Spectra of Fig. 2
Red: A, Green: B, Blue: C, Purple: D, Black: E, Orange: F, Brown: G, Light Blue: H

■ Results of Quantitative Analysis

Quantitation of the fat content was conducted by applying the multiple regression method and the PLS method of multivariate analysis on the obtained data. We created a calibration model for each of the methods based on the standard samples A, C, E, G and H of Table 1. We used the fat content values listed on the mayonnaise product labels as the true fat content values of the standard samples.

Samples B, D and F of Table 1 were used as verification samples for predicting the accuracy of the calibration model. Table 3 shows the results predicted for the fat content of the verification samples using each of the calibration models.

Comparing the results, there were no large differences in quantitation accuracy between the two methods, indicating good results. Here, the root mean square error of prediction (RMSEP) of Table 3 is an index that represents the mean difference between the predicted and actual results based on the values defined in Fig. 4. Calculations associated with the PLS method were conducted using The Unscrambler®[1] multivariate analysis software of CAMO Software company. In addition, regression analysis calculations for the multiple regression method were conducted using the "Regression Analysis" feature of the Microsoft Excel®[2] spreadsheet software.

Note: Four wavelengths, 1150 nm, 1210 nm, 1240 nm, and 1280 nm were used for the calculations by the multiple regression method. As for the PLS method, calculations were conducted by the center averaging process with respect to the total data between 1150 nm – 1280 nm.

Table 3 Prediction Results of Fat Calculated by Each Calibration Model for Validation Samples Measured Using Screw-Cap Vials

Sample	Fat Content Indicated on Label (g/15 g)	Predicted Results According to Multiple Regression Method	Predicted Results According to PLS Method
B (first)	11.2	10.17	10.02
B (second)	11.2	10.72	10.50
D (first)	8.6	8.05	8.23
D (second)	8.6	7.87	8.20
F (first)	5.1	4.90	4.89
F (second)	5.1	4.99	5.00
RMSEP		0.603	0.610

*RMSEP：Root Mean Square Error of Prediction

$$RMSEP = \sqrt{\frac{\sum\limits_{i=1}^{n}(y'_i - y_i)^2}{N}}$$

Where:
y'i : expected value
yi : actual value
N : number of evaluation samples

Fig. 4 Definition Formula for RMSEP

■ Measurement of Mayonnaise with Container

The container materials of the mayonnaise samples measured here all consisted of the polyethylene (PE) and ethylene-vinyl alcohol copolymer resin (EVOH). Focusing on that point, we then attempted measurement of the mayonnaise samples "as is" in their respective containers.

The mayonnaise container thickness varied depending on the sample. In this case, therefore, the influence of transmittance due to variation in container thicknesses should also be reflected in the data. This, in terms of multivariate analysis, means that an additional factor(s) may be needed to account for the noise added by the additional substance. Multivariate analysis permits correction for variation due to other components. Therefore, in this case, it means that variation due to thickness can be used for correction of the mayonnaise data.

A photograph of a sample set in the integrating sphere is shown in Fig. 5, and the measurement results for all the samples, A – H, are shown in Fig. 6. The measurement conditions are the same as those shown in Table 2. Each sample was measured twice, while repositioning it in the integrating sphere between measurements.

Fig. 7 shows an expanded view of the region of Fig. 6, and the region in which fat absorption occurs (in the vicinity of 1210 nm) is circled in red. Here, as well, it is clear that the greater the fat content in a sample, the larger the absorption peak in this region. Table 1 lists the fat content for each of the samples.
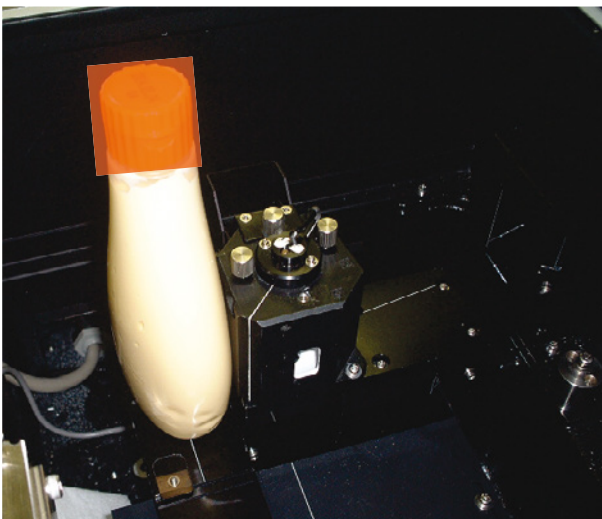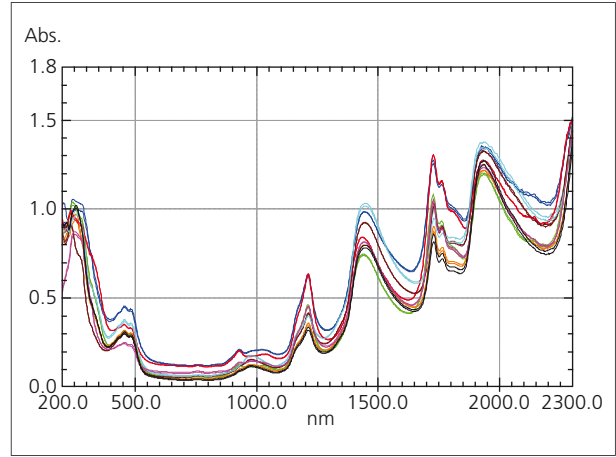
Fig. 6 Total Luminous Measurement Spectra
Red: A, Green: B, Blue: C, Purple: D, Black: E, Orange: F, Brown: G, Light Blue: H

Fig. 7 Expanded Spectra in Fig. 6
Red: A, Green: B, Blue: C, Purple: D, Black: E, Orange: F, Brown: G, Light Blue: H

Fig. 5 Sample Set in an Integrating Sphere

■ Results of Quantitative Analysis of Mayonnaise Measured "As Is" in its Container

Quantitation of fat content was conducted in the same way as that for the mayonnaise in screw-cap vials. The predicted results for each of the calibration models corresponding to validation sample are shown in Table 4. The data indicate that good results were obtained using both the multiple regression and PLS method.

Note: Data at 4 wavelengths, 1180 nm, 1210 nm, 1240 nm and 1300 nm, were used for calculation by the multiple regression method. With the PLS method, calculation was conducted by center averaging with respect to all data between 1100 nm – 1300 nm.

Table 4 Prediction Results for Fat Calculated by Each Calibration Model for Validation Samples Measured "As Is" in their Containers

Sample	Fat Content Indicated on Label (g/15 g)	Predicted Results According to Multiple Regression Method	Predicted Results According to PLS Method
B (first)	11.2	11.10	11.28
B (second)	11.2	10.96	11.25
D (first)	8.6	8.02	7.98
D (second)	8.6	8.17	8.18
F (first)	5.1	4.86	4.76
F(second)	5.1	4.95	4.83
RMSEP		0.334	0.355

■ Conclusion

We conducted measurement of mayonnaise with the samples transferred into screw-cap vials for measurement, in addition to measurement of the mayonnaises samples in their original containers. The measurement data were then subjected to multivariate analysis using both multiple regression and PLS analysis for determination of fat content. We also compared the quantitative accuracy obtained by these two methods. Good results were obtained using multivariate analysis and PLS analysis with respect to measurement using both the vials and the original containers.

Conventionally, highly viscous cream-state samples have been measured by the transmittance method with the samples coated on glass plates, etc., but measurement with this method has generally been difficult due to uneven coating, etc. Using the method presented here, however, it was found that measurement can be conducted easily and with good accuracy.

The results obtained here suggest that this technique is effective for quantitative analysis of creamy samples such as mayonnaise.

1) The Unscrambler is a registered trademark or trademark of CAMO.
2) Excel is a registered trademark or trademark of Microsoft Corporation.

SHIMADZU

Shimadzu Corporation

www.shimadzu.com/an/

Application News

Wine bottle measurement with UV-2600 and MPC-2600 Quality control of color

No. SCA-100-017

The packaging of food is of mayor interest since the modern world is using modern materials as factor of design for food. Should it be new style in carton (since 1977) or classical in glass (since 17th century)? In case of wine it seems that the classical glass wine bottle is still the most favorite packaging.

Fig. 1: Red wine Bottles from the Shimadzu Wine Edition I at left and Edition II at right side.

The glass appears transparent and emphasize a feeling of being clean, and the wine should be less influenced by additives

which can be result from the carton. The glass color can be blue, green, brown or white for liquids. It seems that glass which is not clear green or direct brown can be result of mixture caused by melting green and brown glass fraction in one or the adequate mixture of inorganic oxides causing such final color during the glass melting process. It is written in the literature that green glass can pick up to15% of other colors. And brown glass add up to 8%. For the human eye it is still in the category green and brown glass.

Fig. 2: Typical colors of wine bottles, the green glass is easy to identify, at the right side the color is subjective more brown green

It is difficult to judge for the human eye if the right bottle from figure 1 is a dark green, brown, or? To overcome such handicap the UV-VIS spectroscopy can be a neutral instrument to characterize the color of the glasses. The application shown in this experiment is a measurement through wine bottles.

■Experiment

The wine bottle in its appearance was completely set into the sample compartment of the MPC-2600. It was positioned so that the light energy could pass through the two

wine bottle walls, without touching the paper prints on the glass bottle wall. The UV-VIS spectra were recorded for the two bottles. By the presence of two thick bottle walls the ground absorbance of the glass spectrum resulted in a high baseline and high signal values. The measurement in this way was destroying free.
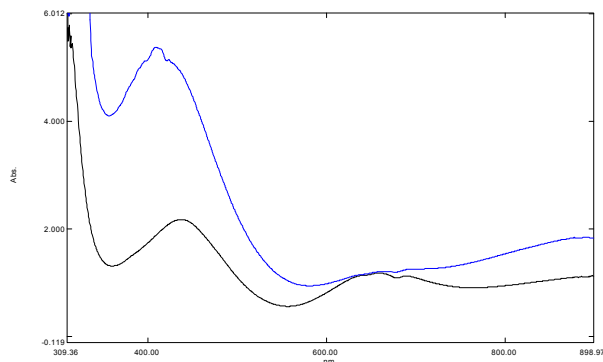
Fig. 3: blue line shows the UV-VIS spectrum from the brown-green glass and the black line is the spectrum from the green glass.

In figure 3 are shown two spectra from each sample. The range of interest is 310 to 890 nm. The green glass spectrum has two maxima ranges at around 650 and 440nm (black line). The blue lined spectrum has its maxima with a weak at 650nm and a very high at 410nm and a higher absorbance at >800nm. In detail it is at 650nm minimum a triplet signal or even a multiple which is saturated. With the help of the 2nd derivative spectroscopy it is possible to make this situation visible. The position of the maxima can be given as: 686.4, 669.9, 654.2, and 636 nm (Fig. 4). These absorbance maxima are typical signals belonging to Chromium 3$^+$ in form as Chromium oxide Cr_2O_3 (1). This oxide is used to generate green color in glass ware. The same profile but less in height is visible in the green-brown glass spectrum, but the mayor signal in the range of 400 is shifted from 440 to 410. A broad signal with an internal maximum at 410nm. Brown color

is result from the investigation of Manganese oxide (2). This is more present in the second sample because of less contents on Chromium oxide. A screening by Shimadzu EDX-7000 showed a factor of 3 lower contents of chromium in the brown-green sample.
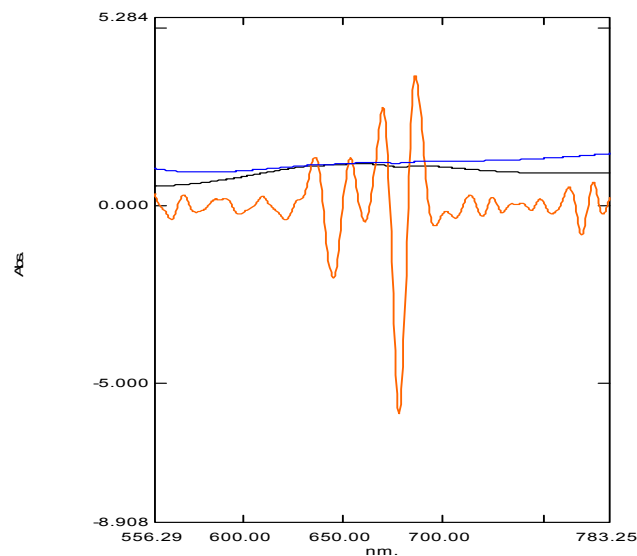
Fig. 4: 2nd derivative spectrum from the green glass spectrum (red), up to four signals can be separated at 650nm as characteristic for Cr_2O_3.

The manganese has influence on the redox process regards changes in the iron oxides under heat of melting. Absorption of yellow color falls into the visible spectrum. The presence of manganese oxide is also responsible for the more intense iron oxide signals at 380 to 430nm. The 2nd derivative spectrum extracts signals at. 420, 412, 400,390, 385 nm.

■ **Instrumentation**

UV-2600
MPC-2600 and Plane stage for a wine bottle

■ **Literature:**

(1) The effect of chromium oxide on optical spectroscopy of sodium silicate glasses, Bahman _Mirhadi, Behzad Mehdikhani, Journal of Optoelectronics and Advanced Materials, Vol. 13, No. 9, September 2011, p. 1067 -1070

(2) Effect on Manganese oxide on redox iron in sodium silicate glasses, Bahman _Mirhadi, Behzad Mehdikhani, Journal of Optoelectronics and Advanced Materials, Vol. 13, No. 10, October2011, p. 1309-1312

SHIMADZU
Excellence in Science

Application News

Spectrophotometric Analysis

No.A492

Simple Quantitative Analysis of Concentrated Suspension Drink by Spectroscopic Analysis

In the field of food beverages, many of the products sold, such as lactic acid beverages, consist of high-turbidity liquids. When conducting concentration management of such beverages during the production process, the use of direct conventional spectral transmission measurement of high-suspension beverages has been problematic unless considerable dilution, etc. is conducted as a pretreatment process. Therefore, we developed an analytical technique that combines the reflection method with multivariate analysis to achieve "as is measurement" of high-turbidity beverages. Here, we introduce an example of measurement of the concentration (dilution factor) of a lactic acid beverage.

■ Lactic Acid Beverage as a Sample

A commercially available lactic acid beverage was used as a high-turbidity sample. The beverage was diluted successively with deionized water to prepare twelve concentrations of the sample, ranging from 0 % to 100 %. The samples were divided into two groups as listed in Table 1 and Table 2, including standard samples for generating the calibration model, and validation samples for checking the calibration model, respectively. A photograph of the actual samples in their containers is shown in Fig. 1.

Table 1 Standard Samples

Standard Samples	Concentration (%)
①	100
②	90
③	80
⑤	60
⑥	50
⑦	40
⑨	20
⑩	10
⑫	0 (Purified water)

Table 2 Validation Samples

Standard Samples	Concentration (%)
④	70
⑧	30
⑪	5

Fig. 1 Lactic Acid Beverages

■ Instrument and Measurement Results

Measurements were conducted using the UV-2600 ultraviolet-visible spectrophotometer in combination with an integrating sphere attachment for analysis of high-turbidity samples. The samples, transferred into disposable screw cap sample vials, were set in the integrating sphere attachment as shown in Fig. 2, and the total reflectance was measured. As evident from Fig. 3, the greater the number of particles in the sample, the greater will be the percentage of light reflected in the vicinity of the liquid surface, thereby resulting in greater reflectance when using this technique.

Fig. 4 shows the twelve points of measurement results for the samples listed in Table 1 and Table 2, and Table 3 shows the measurement conditions used. Each sample was measured twice (12 data points × 2 = total of 24 data points), and the screw cap vial was replaced after each measurement. The results indicated a correlation of data with the sample concentration, such that the higher the sample concentration, the greater the reflectance, and the lower the concentration of the sample, the lower the reflectance.

As disposable screw cap cells were used in these measurements, tedious cleaning and storing of cells was not only unnecessary, it also eliminated the need for concern about carryover or contamination due to insufficient washing of the cells.

Fig. 2 Sample Set in Integrating Sphere Attachment

Light
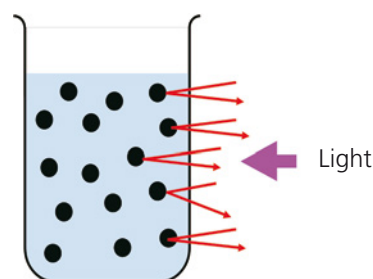
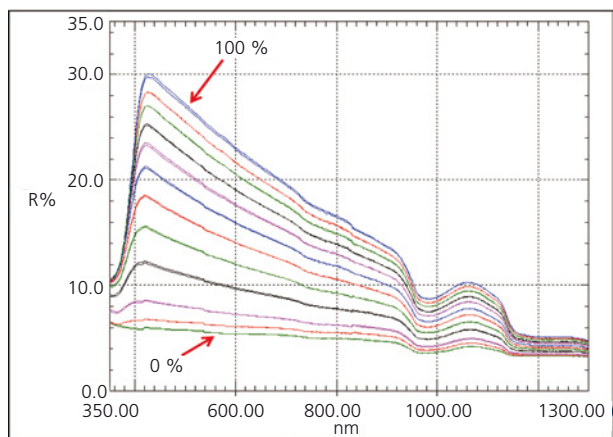**Fig. 3 Schematic Diagram of Reflection**

Fig. 4 Reflection Spectra

Table 3 Analytical Conditions

Instrument	: UV-2600 ultraviolet-visible spectrophotometer Integrating sphere attachment for high-turbidity analysis
Measurement Wavelength Range	: 350 nm - 1300 nm
Scan Speed	: High speed
Sampling Pitch	: 2.0 nm
Photometric Value	: Reflectance
Slit Width	: 5 nm

■ Results of Quantitative Analysis

Standard samples were used to set up calibration models for the single regression method and multiple regression method of multivariate analysis, and the validation sample was used to verify the prediction accuracies of the respective calibration models.

The regression equations for the respective models are shown in Table 4.

The reflectance values of the validation samples were applied to each of the calibration models (substituted into the regression equations), and the calculated concentration results are shown in Table 5. Clearly, the results obtained using the multiple regression method were superior to those obtained using the single regression method. While data at a single wavelength of 430 nm was used with the single regression method, data at three wavelengths, 430 nm, 500 nm, and 700 nm, were applied using the multiple regression method.

For the single regression method, quantitation was conducted using the calibration function included in UVProbe software. Analysis by the multiple regression method, however, was conducted using the Excel®[1] spreadsheet regression analysis function, and the obtained regression expression was entered into the UVProbe software to conduct quantitation.

As for the Root Mean Square Error Prediction (RMSEP) values shown in Table 5, these are defined indices that express the difference between the respective predicted values and true values. Therefore, it can be said that the smaller the RMSEP value, the better will be the accuracy of prediction.

Table 4 Respective Equations for Single Regression and Multiple Regression

Equation for Single Regression
    Conc = 4.107·A1 - 29.349
    A1: Absorbance at 430 nm
    Correlation coefficient: 0.9894

Equation for Multiple Regression
    Conc = -19.316·A1+21.651·A2+7.011·A3 - 46.346
    A1: Absorbance at 430 nm, A2: Absorbance at 500 nm,
    A3: Absorbance at 700 nm
    Multiple correlation coefficient: 0.9999

Table 5 Actual and Predicted Concentrations of Validation Samples Calculated Using Respective Calibration Models

Validation Samples	Actual Concentration (%)	Predicted Result (%) by Single Regression Method	Predicted Result (%) by Multiple Regression Method
④-1	70	73.53	69.98
④-2	70	73.93	68.60
⑧-1	30	33.43	30.54
⑧-2	30	33.91	30.20
⑪-1	5	-1.74	5.20
⑪-2	5	-1.69	5.20
RMSEP		4.92	0.63

• RMSEP: Root Mean Square Error of Prediction

$$RMSEP = \sqrt{\frac{\sum\limits_{i=1}^{n}(y_i' - y_i)^2}{N}}$$

y_i' is predicted value, y_i is actual value, and N is number of samples for evaluation.

Fig. 5 Expression Defining RMSEP

■ Conclusion

We developed a method that permits easy measurement of high-turbidity samples. Good results were obtained by applying this technique to lactic acid beverages. Although direct measurement of high-turbidity samples is generally difficult using the transmission method, the application of this technique permits quantitation that is both quick and simple.

1) Excel is a trademark or registered trademark of Microsoft Corporation in the United States and/or other countries.

SHIMADZU

Shimadzu Corporation

www.shimadzu.com/an/

Maple Syrup Color Analysis using the Shimadzu UV-2600 UV-Vis Spectrophotometer

Jeff Head, M.S., John Kinyanjui Ph.D., Mark Talbott, Ph.D.; Robert Clifford, Ph.D.

■ Introduction

UV-Visible spectrophotometry is a valuable tool in the laboratory for measuring the properties of various liquids and solids. One of the most common applications for QA/QC environments is Color Analysis and being able to assign a color value to finished products. The color value of a material can be obtained by collecting a % transmittance or reflectance spectrum of the sample under consideration. The Shimadzu UV-2600 spectrophotometer is ideal for making accurate color measurements due to the large photometric range of 5 abs. units. Therefore, dilution is not required for highly absorbing samples such as maple syrup. Samples can be analyzed neat without further dilution. The application illustrates the use of Shimadzu Color Analysis Software and the UV-2600 spectrophotometer for quick and easy spectral acquisition and interpretation into a meaningful color value.

■ Background

Maple syrup is one of the most commonly used sweeteners produced in the USA and Canada. Different grades of maple syrup are assigned primarily by color. The color of maple syrup is a result of the time of season that the maple sap is collected from maple trees. In general, the later in the season the sap is collected, the darker the color of the resulting maple syrup.

Currently, the United States has three categories of Grade A syrup referred to as Light, Medium, and Dark Amber. Light amber is the lightest of the three followed by Medium and then Dark. However, Vermont has a grade referred to as "Fancy", which has been reported to be lighter in color than the three U.S. Grade A classifications. An additional classification is Grade B, which is darker than Grade A Dark Amber and considered unsuitable for consumer labelling by some vendors. However, consumers are seeking ways to purchase the Grade B syrup because of its sweeter taste, leading to some manufacturers labelling it for sale and allowable for consumption purposes.

The United States Department of Agriculture is providing a path for a universal classification grading system, which is scheduled to be released and made active for consumers beginning in 2015. The new system will remove the Grade B classification and classify maple syrup as Golden Color, Amber Color, Dark Color, and Very Dark Color. Currently, U.S. grading classifications are made by comparing the maple syrup to color glass standards. In addition to the U.S. grade standards, some states use a spectroscopic method to determine the color of maple syrup. This spectroscopic method differentiates maple syrup grades by the % transmittance at a wavelength of 560 nm. Table 1 outlines the classifications of maple syrup both at a state and federal level, along with the proposed new rating program slated for implementation January 1st 2015[1].

Table 1: Federal and State Classifications of Maple Syrup[1]

Current U.S. Standard	Vermont and Ohio	New Hampshire	New York	Maine	Canada all Provinces	Proposed Option, Jan. 1st 2015
U.S. Grade A Light Amber	Vermont Fancy ≥ 75.0% T, Ohio Light	Grade A Light Amber	Grade A Light Amber	Grade A Light Amber ≥75.0%T	Canada No. 1 Extra Light ≥75.0%T	**Grade A Golden Delicate Taste ≥75.0%T**
U.S. Grade A Medium Amber	Grade A Medium Amber 60.5-74.9% T	Grade A Medium Amber	Grade A Medium Amber	Grade A Medium Amber 60.5-74.9%T	Canada No. 1 Light 60.5-74.9%T	**Grade A Amber Rich Taste 50-74.9%T**
U.S. Grade A Dark Amber	Grade A Dark Amber 44.0-60.4%	Grade A Dark Amber	Grade A Dark Amber	Grade A Dark Amber 44.0-60.4%T	Canada No. 1 Medium 44.0-60.4%T	**Grade A Dark Robust Taste 25-49.9%T**
U.S Grade B for Reprocessing	Grade B 27.0-43.9%T	Grade B	Extra Dark for Cooking or Grade B for Reprocessing	Grade A Extra Dark Amber 27.0-43.9%T	Canada No. 2 Amber 27.0-43.9%T	**Grade A Very Dark Strong Taste <25.0%T**
U.S. Grade B for Reprocessing	Commercial Grade <27.0%T	Grade B	Extra Dark for Cooking or Grade B for Reprocessing	Commercial Grade <27.0%T	Canada No. 3 Dark <27.0%T	**Processing Grade any Color Class, any off-flavored syrup.**

Color is a complex quality and may be more accurately interpreted by the concept of color scales rather than the %T value at a single wavelength. Multiple color scales are used in various lab settings depending on the user's protocol. One commonly used color scale is CIE $L*a*b*$. In this color scale, color values are calculated from a mathematical combination of %T. $L*$ out of the CIE $L*a*b*$ color scale measures the lightness of a sample. An $L*$ value of 100 represents the maximum brightness of a color, whereas an $L*$ value of 0 represents the minimum brightness of a color. $a*$ measures the red or green components of a given sample. Positive values of $a*$ represent a more red color component, whereas negative values lean more towards a dominant green component. Similarly, the $b*$ value measures the yellow or blue components of a sample. Positive values of $b*$ represent a stronger yellow, whereas negative values represent more blue in the sample[2].
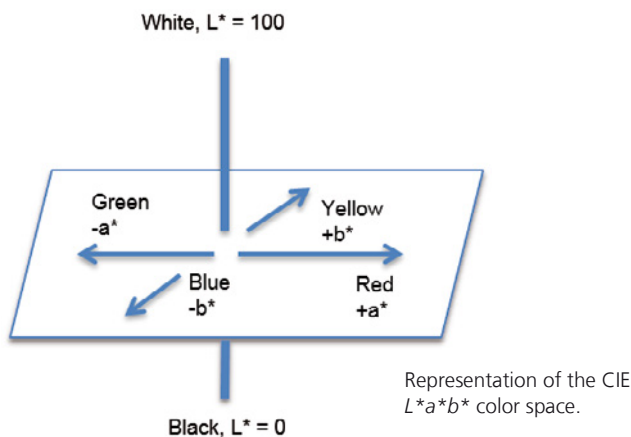
■ Experimental

Four separate samples labelled as "Vermont Fancy", "Grade A Medium Amber", "Grade A Dark Amber", and "Grade B", were received as is from a maple syrup sampling kit. Transmittance spectra were collected using standard 10 mm quartz cuvettes with an empty cuvette as a reference with no additional sample preparation. Along with the four samples obtained from the kit, ten commercial samples from different parts of the U.S. were analyzed.

Experimental parameters for the color calculation are given in Figure 1.
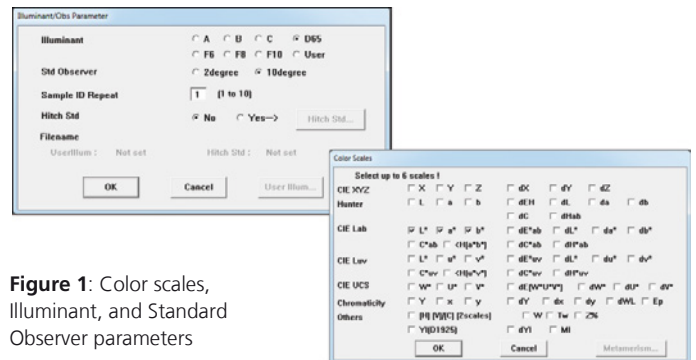
Figure 1: Color scales, Illuminant, and Standard Observer parameters

White, L* = 100

Green -a*   Yellow +b*

Blue -b*   Red +a*

Black, L* = 0

Representation of the CIE $L*a*b*$ color space.

■ Results and Discussion

Spectra of the four different pure maple syrup samples are shown in Figure 2, with corresponding CIE *L*a*b** values and the %T at 560 nm presented in Table 2. The transmittance spectra are similar in profile and demonstrate a decrease in magnitude going from the lighter Vermont Fancy to darker Grade B.
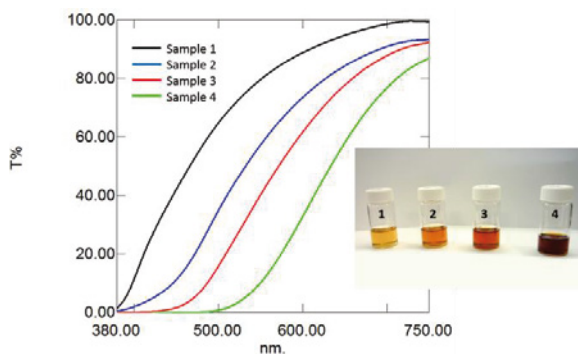
Figure 2: Transmittance spectra of maple syrup samples from sampling kit

As shown in Table 2, the %T at 560 nm decreases as the samples become darker. This trend is in good agreement as supported by the decreasing *L** values obtained, which indicate lightness. However, this alone does not offer any insight into the color of the sample.

Under the new classification system scheduled to go into effect in 2015, terms such as "Golden", "Amber", and "Dark" will be used to name the maple syrup. By visually inspecting the samples, the colors range from light yellow to a reddish brown between Vermont Fancy and Grade B. As previously discussed, positive *a** values indicate a more red component in the overall color determination, along with a positive *b** value, which corresponds with a more yellow sample. The color "Amber" is a yellowish-orange color and is halfway between yellow and orange on the color wheel. Thus, the values for *a** and *b** increase going from Vermont Fancy to Medium Amber and Dark Amber, as expected.

As shown in Table 2, the value of *b** for Grade B drops slightly as compared to Dark Amber, but rises significantly for *a** from 19.13 to 41.60. This is to be expected after visual inspection of Grade B since it is a dark color with a very intense red component, and less of a yellow component. This additional insight into the colors present in the maple syrup is gained through the use of the Shimadzu Color Analysis Software.

In addition to the samples analyzed from the sampling kit, ten separate commercial samples labelled as "Pure Maple Syrup" with various classification grades were analyzed for this Application News. Table 3 summarizes the results obtained for analyzing these products.

Table 2: *CIE L*a*b** values and %Transmittance (560 nm) for samples from sampling kit measured on the Shimadzu UV-2600

Sample ID	Sample Classification	*L**	*a**	*b**	%T at 560 nm
1	Vermont Fancy	90.49	0.40	33.31	81.61
2	Grade A Medium Amber	79.17	7.80	61.61	60.83
3	Grade A Dark Amber	69.33	19.13	83.67	44.64
4	Grade B	45.87	41.60	77.78	13.69

Table 3: CIE *L*a*b** values and %Transmittance (560 nm) for samples from sampling kit, along with commercial samples measured on the Shimadzu UV-2600

Sample ID	Sample Classification	*L**	*a**	*b**	%T at 560 nm
Sampling Kit					
1	Vermont Fancy	90.49	0.40	33.31	81.61
2	Grade A Medium Amber	79.17	7.80	61.61	60.83
3	Grade A Dark Amber	69.33	19.13	83.67	44.64
4	Grade B	45.87	41.60	77.78	13.69
Commercial Samples	**Classification Label**				
5	U.S. Grade A Light Amber	84.46	4.51	59.49	71.31
6	*Grade A Medium Amber*	*70.96*	*16.72*	*79.39*	*47.05*
7	U.S. Grade A Dark Amber	69.71	20.72	91.23	45.81
8	U.S. Grade A Dark Amber	67.26	16.97	83.47	41.73
9	U.S. Grade A Dark Amber	67.96	23.32	94.77	42.93
10	Grade A Dark Amber	70.38	19.77	88.68	46.78
11	U.S. Grade A Dark Amber	67.98	19.16	84.89	42.64
12	U.S. Grade A Dark Amber	66.32	18.05	82.72	40.07
13	U.S. Grade A Dark Amber	73.31	13.76	75.29	51.08
14	U.S. Grade B	52.62	22.69	79.41	22.75

Although the %T values are reported in Table 3, it is important to keep in mind that the majority of these samples were classified under the U.S. grading system. The U.S. system does not rely on %T for classifying maple syrup. Rather, the U.S. system relies on the color of the sample as compared to colored glass standards, which further supports the importance of color analysis[1].

The color results obtained for the commercial samples demonstrate that as the syrup becomes darker, the lightness value decreases. In addition to the lightness value, L*, it is observed that as the amber color darkens, the red component increases, and the yellow component decreases. Thus, a more complete picture of the color of the sample is established for each material.

Interestingly, sample #6, which is classified as "Grade A Medium Amber" on the packaged bottle, demonstrated transmittance and color values close to that of a dark amber maple syrup. More specifically, the color values and %T are similar to samples 3 and 7-13. Visually comparing the samples, #6 has the appearance of an Amber color more close to that of dark amber, rather than medium. The transmittance spectrum of sample 6 is shown in Figure 3, overlaid with the spectra from the sampling kit in Figure 2.
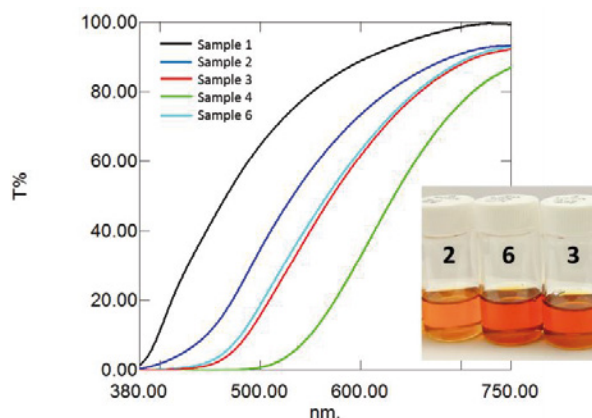
Figure 3: Transmittance spectra of maple syrup samples

■ **Conclusion**

The Shimadzu UV-2600 with Color Analysis software offers an accurate and effective means for obtaining a meaningful color value for maple syrup. The software and spectrophotometer together offer the ideal solution for any QA/QC laboratory requiring the analysis of finished products.

■ **References**

1. Federal Register/Vol. 79, No. 88/ Wednesday, May 7, 2014. "United States Standards of Maple Sirup".
2. Hunter, R.S., Harold, R.W. "The Measurement of Appearance". Second Edition. John Wiley & Sons.

Application News

No.A451

Spectrophotometric Analysis

Analysis of Contaminant Adhering to Frozen Pizza

The steady stream of consumer complaints related to foods reflects continuing high concern for food safety. To address these concerns and specific contamination-related complaints, it is important to quickly and accurately report the analysis results and clearly elucidate the contamination pathway. Here, using a Fourier transform infrared spectrometer (FTIR) and an energy dispersive X-ray fluorescence spectrometer (EDX), in addition to an electron probe micro analyzer (EPMA), we present the results of analysis of a contaminant adhering to the surface of frozen pizza.

■ Photograph of Contaminant Adhering to Surface Frozen Pizza

The photograph in Fig. 2 shows the site of contamination on the frozen pizza. It was discovered when the package of this commercially available frozen pizza was opened. The foreign substance was subjected to complex analysis using a Fourier transform infrared spectrometer (FTIR), an energy dispersive X-ray fluorescence spectrometer (EDX), and an electron probe micro analyzer (EPMA).

Fig. 1 Photograph of Contaminant Adhering to Frozen Pizza

■ Analysis by FTIR

Some of the foreign substance was scraped off the frozen pizza, and after rolling it onto the diamond cell, the infrared spectrum was measured by transmission infrared microscopy. Measurements were conducted at multiple sites on the contaminant. Fig. 2 shows a photograph indicating the measurement locations, and Fig. 3 shows the overlaid infrared spectra that were obtained at the respective sites. Measurements were conducted using 30 × 30 µm focal regions. The analytical conditions used are shown in Table 1.

Table 1 Instruments and Analytical Conditions

Instruments	: IRPrestige-21, AIM-8800
Resolution	: 4 cm^{-1}
Accumulation	: 45
Apodization	: Happ-Genzel
Detector	: MCT
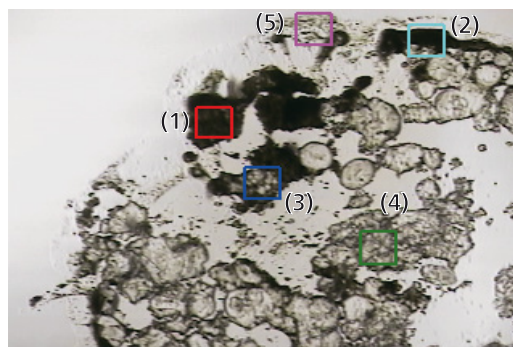
Fig. 2 Microscope Photograph of Measurement Sites
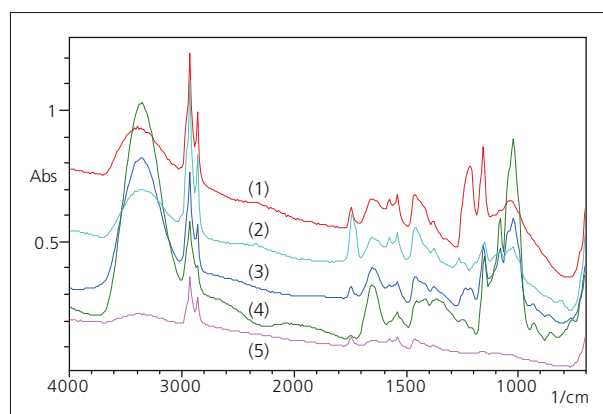
Fig. 3 Infrared Spectra of Contaminants

It is evident from Fig. 3 that the infrared spectra appear differently depending on the location. Among the spectra of Fig. 3, searches were conducted using the spectra (1), (4) and (5). The results are shown in Fig. 4 - Fig. 6.
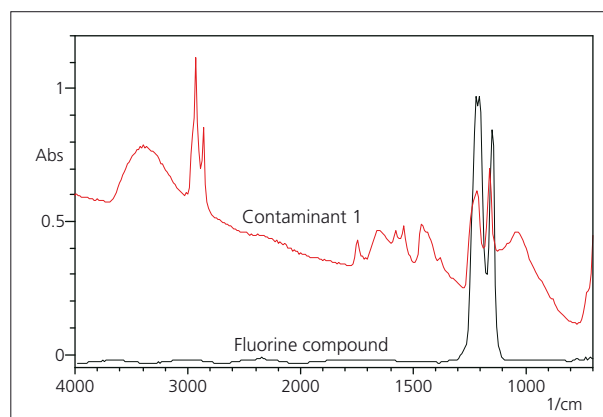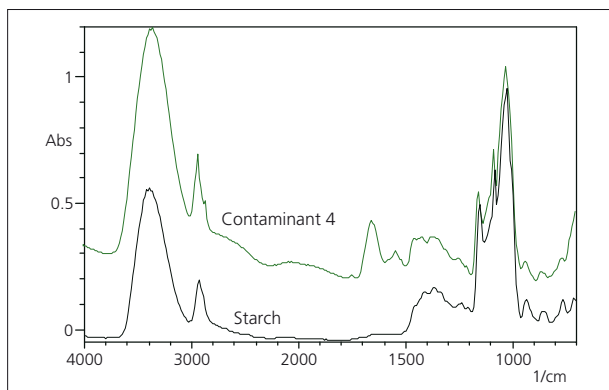

Fig. 4 Search Result 1
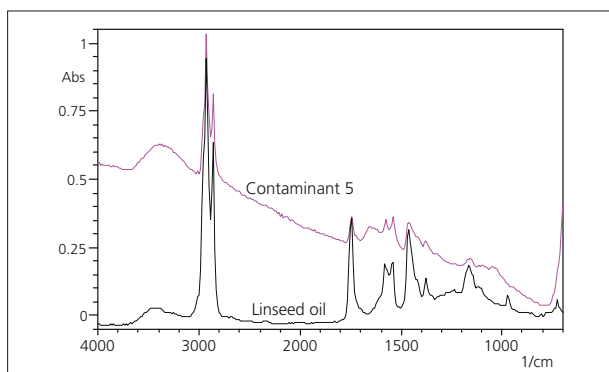
Fig. 5 Search Result 2

Fig. 6 Search Result 3

As can be seen from the respective search results, there were search hits on a fluorine compound, starch, and linseed oil. Of these, the starch and linseed oil are expected components of the pizza dough. The fluorine compound is an industrial product, and since it is also used in cooking utensils, it is apparently a contaminant derived from an external source.

■ Analysis by EDX

Analysis of the intact contaminant adhering to the frozen pizza was conducted using a 3 mm analysis diameter. Fig. 7 shows the qualitative results comparing the normal and contaminated parts of the frozen pizza. In addition, a comparative profile of the normal and contaminated sites of Fig. 7 was calculated, and quantitative analysis of the detected elements was conducted by the FP method. The obtained results are shown in Table 2.

- Normal Site
- Contaminated Site
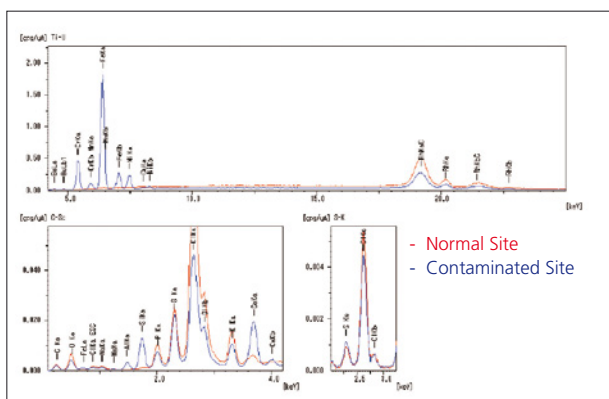
Fig. 7 $_6$C-$_{92}$U Qualitative Results for Contaminated and Normal Sites

Table 2 Quantitative Results for Contaminated Site by FP Method (%)

Fe	Cr	Ni	Si	Ca	Al	Ba	Mn
59.42	12.07	8.97	8.91	4.69	3.55	1.72	0.79

From the results shown in Fig. 7 in which Fe, Cr and Ni were detected in the contaminant as principal components, and considering the quantitative results, the contaminant is presumed to consist of stainless steel (SS). Further, since Al, Si, Ca and Ba were also detected, it is possible that a ceramic or other pigment-containing material may also be included. Since Na, P, S, Cl, K and Ca were also detected at the un-contaminated site, these are assumed to be of food origin. As for the F that is derived from the fluorine compound and was detected by FTIR, it was not clearly detected here, probably due to the small relative mass within the analysis radius and the overlap with the Fe$L\alpha$ line.

■ Analysis by EPMA

After scraping off a portion of the contaminant and coating its surface with gold, we conducted mapping of each element within a micro-region measuring 400 × 400 μm. Fig. 8 shows the mapping results for the principal elements that were detected.
The SS constituents Fe and Cr that were detected by EDX were detected over a wide range. In addition, the F that was detected by FTIR was detected in a localized perimeter. Thus, the results are consistent with the obtained FTIR and EDX results.
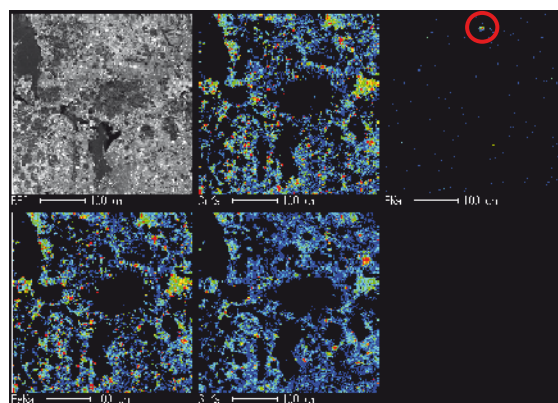

Fig. 8 Results of Elements Mapping for Contaminant Part

■ Conclusion

Complex qualitative analysis using FTIR, EDX and EPMA was conducted to identify a contaminant adhering to the surface of frozen pizza, and the results indicated detection of SS constituents and a fluorine compound. EPMA mapping results indicated that the SS constituents (Fe, Cr) were scattered over a region of approximately 10 μm.
On-site verification in the actual manufacturing process is essential to identify the source of contamination, but from the photograph of Fig. 1, the contaminant appears to be some type of burnt substance. The above analysis suggested that the contaminant consists of burnt cooking oil mixed with a fluorine compound originating from a cooking utensil or manufacturing machine, in addition to SS powder.

SHIMADZU

Shimadzu Corporation

www.shimadzu.com/an/

Application News

No. SCA-110-087

Analysis of bread with FTIR-ATR technique – View to the water content in different appearances of Bread

The infrared spectroscopy is a nice tool to make things visible which are not so easy to access. Without any sample treatment it is possible to go for identification. In the past the analysis with infrared and the classical analysis methods related to transmission spectroscopy needed prepared sample amounts free from water. That is not more needed with the ATR technique also humid sample, water based samples or water samples are possible. In this application the focus is set to the analysis of the daily bread. In Germany bread plays an important role. Nowhere in the world are more variation of bread available than in Germany.

■Bread analysis

A variety of fresh prepared bread is available also double baked bread, extra dry bread and the Scandinavian sorts named crisp bread (Knäcke-Brot, Smørebroed). These sorts of bread show the main difference in the water content. Double baked bread is with approximately 3% of water and Scandinavian dry bread with approx. 6% to 10% of water content. The standard bread will have higher content which is approx. 34 to 40% of water. The values are average values as found in

literature. Bread with all the materials is still a natural product. For the analysis three sorts of bread were analyzed. All three were used as they appeared, were placed on the measurement window of the single reflection ATR accessory and were measured. In figure one the infrared spectra from the three breads are shown.
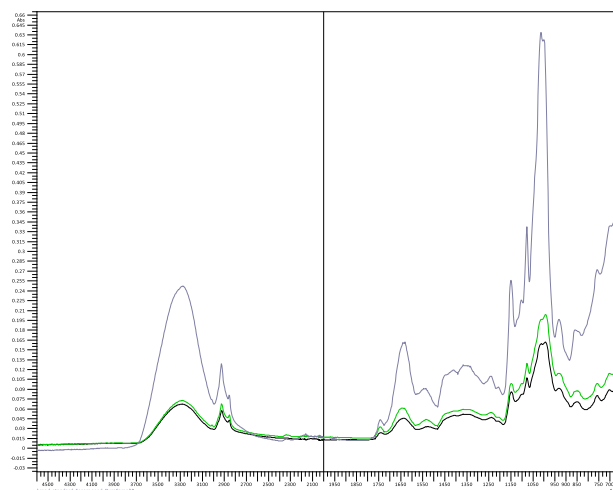
Fig.1: three infrared spectra showing different bread, black is the double baked, green the Scandinavian style and the grey is the fresh bread

The three spectra show different intensity but have similar shape. The difference in the intensity is result of the hardness of the bread. The contact from bread to the measurement crystal is different in all three cases. Best contact was realized with the fresh bread because it is very soft in comparison to hard bread variations. Thinking about the water content it is difficult to judge which one shows higher concentration. For solving such problem one idea is to use the superposition of the substance information in

each infrared signal. In case water is present then it should have strong signal at 3300cm^{-1}and at 1640cm^{-1}. The main signal of starch, sugar and cellulose which is around the 1000cm^{-1}, should show a difference in the ratio to the water based OH-signals.

literature. The values for the dried bread are higher than the one for the fresh bread. The signal 3300cm^{-1} is the –OH value, in case there is water inside the ratio to the vibrations modes of -CH, -CH2 should be lower than the one of the water. The range in which the water is most effective 3300cm^{-1} and the Hydrocarbon signals around the 2980cm^{-1} were used to built up a calibration using the area of the signal groups in ratio.

Table 1:
Analysis of the signal ratio from 3277cm^{-1} against the 1014cm^{-1} for bread infrared spectra

Bread	fresh	double baked	Crisp bread
At 1014cm^{-1}	0.635	0.2	0.16
At 3277cm^{-1}	0.248	0.074	0.068
Ratio	0.39	0.37	0.425

Fresh= bread_9, double baked= bread_1, crisp bread= bread_4

The result shown in table 1 is unexpected. The question is why such result is visible. The ratio of the two signals cannot make the water content visible. The crisp bread has same ratio as the fresh bread.

■What is the water content in bread at all and where is it in the bread?

First of all is to check the analysis technique itself. The ATR measurement is a surface measurement. The infrared beam will pass into the surface of a material with approximately 2µm. The beam will touch the starch and cellulose grating of the main materials of the bread. Sugar, starch, etc will have signals in the range of the water signal at 3300cm^{-1} too. More sensitive is the signal of 1640cm^{-1}.

The ratios in table 2 are better reflecting the actual situation as in comparison to the

Table 2:
Analysis of the signal ratio from 1640cm^{-1} against 1014cm^{-1} for bread infrared spectra

Bread	fresh	double baked	Crisp bread
At 1014cm^{-1}	0.635	0.2	0.16
At 1640cm^{-1}	0.164	0.064	0.046
Ratio	0.26	0.32	0.29

With the ratio of both signal groups the physical aspects are minimized. In this case it was the hardness/softness of the bread. The pressure of sample against the measurement window was in all cases the same.

Table 3:
Correlation model using the ratio areas of two signals and theoretical water content values using the approximations from the suppliers

Peak area	3020.526 - 3682.110cm^{-1}	
Reference	2974.234 - 2682.983cm^{-1}	
Spectrum	Concentration	Peak Area Ratio
bread_1	3	7.931
bread_9	30	20.287
bread_4	7	10.506

The quantitative model including the water area is most successful to determine the water content. Natural three standards are only a suggestion. More standards will improve the shape and truth of the calibration curve (Fig. 2).
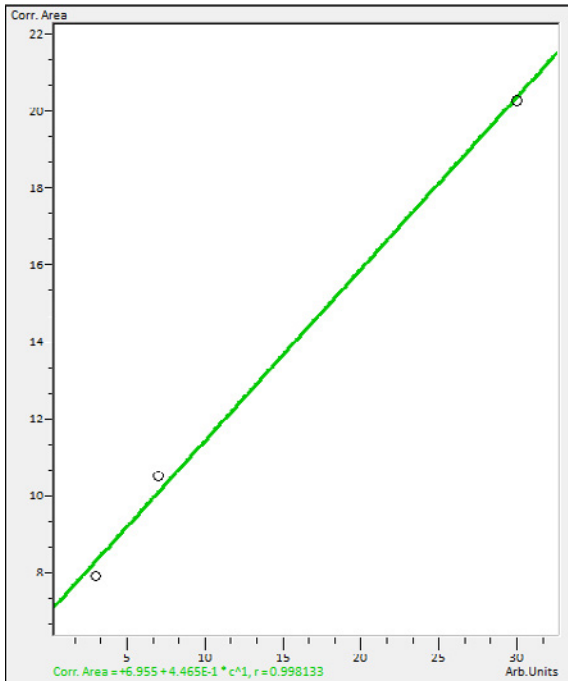

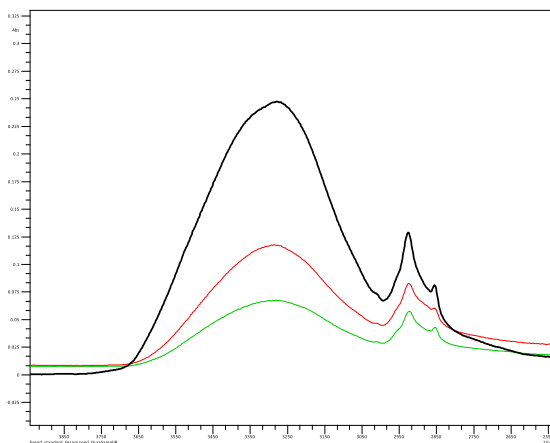Fig. 2: Correlation curve of the three samples, with a regression coefficient of R=0.998133.

Fig. 3: Infrared spectrum of the water signal at 3300cm-1 for three different bread samples.

■Conclusion

The analysis of water content in bread products is possible. The best analysis range combination is the water signal at 3300cm^{-1} and the region of deformation vibrations of -CH2, -CH3. The ratio is needed to exclude the physical situation of the sample, which is part of the spectrum shape. The –CH, -CH3 will represent the sugar molecule in the various substances which are part of the bread. The correlation at the selected position is most successful for the determination of the water contents with a single reflection accessory.

■Instrumentation

IRaffinity-1

DuraSamplIR

IRsolution: Quant program, MP calculation

Application News

Spectroscopy - FTIR

No. SCA-110-089

Packing made from Food Analysis of polymer chips With Infrared Spectroscopy

Polymer chips are widely used for the packing of materials which are sent to everywhere. Due to recycling matters and to fulfill environmental subjects the packing is changed to 100% recycling material. More and more such packing contain chips which are declared as to be food – eatable

Such eatable materials for packing are known in the catering area, as traditional the ice horns were used made from cookie tasting waffle. Earlier that time first plates for French fries or desserts appeared. New is to use food in form of a chip as packing. What makes the difference or is there a difference between the normal food like bread or bread like products and a chip for packing?

Fig. 1: Zoom on to a surface of a chip made from food

The appearance of such chips is very different. Some are declared to be eatable and others are prepared from food but not recommended to eat. The color of such chips can also vary. The chips discussed here have

in common that mixed with water they will change easily into a pulp and the volume is reduced to minimal.

■**Bread, Oblate or Chip**

Different food from the range of very dry bakery based on wheat, starch, etc. were compared to the industrial packing chips. As samples were used crisp bread, and oblate. Both are very dry materials which are result from their bakery style.
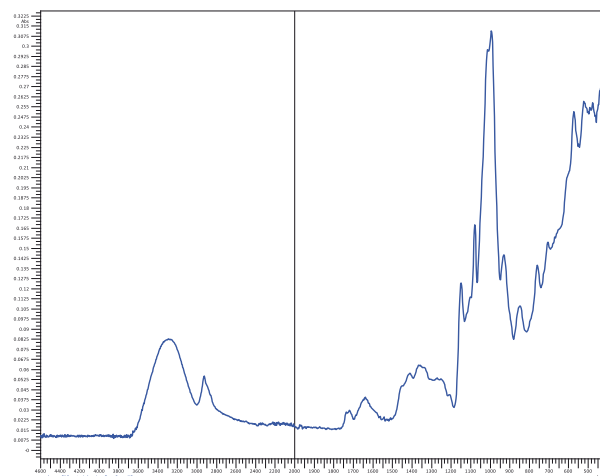
Fig. 2: Infrared spectrum of a packing chip, white colored, declared as eatable

The infrared spectra were measured using the single reflection ATR method. With this method the infrared beam will penetrate approx. 2μm into the sample surface. Due to the hardness of the bread and the oblate and the softness of the chips the intensity of the spectra are different.
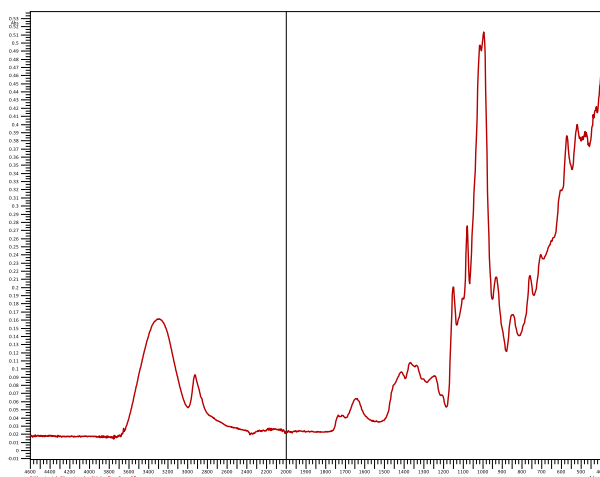
Fig. 3: Infrared spectrum of a packing chip declared to be from recycled paper mixed with starch
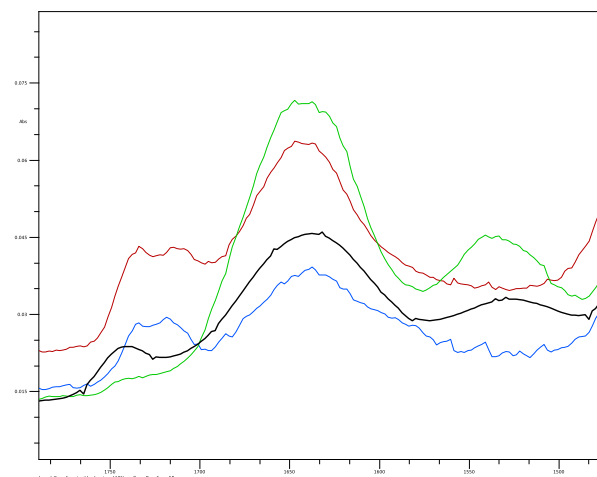

Fig. 5: In one view is shown the difference in the food as food and the chips as packing
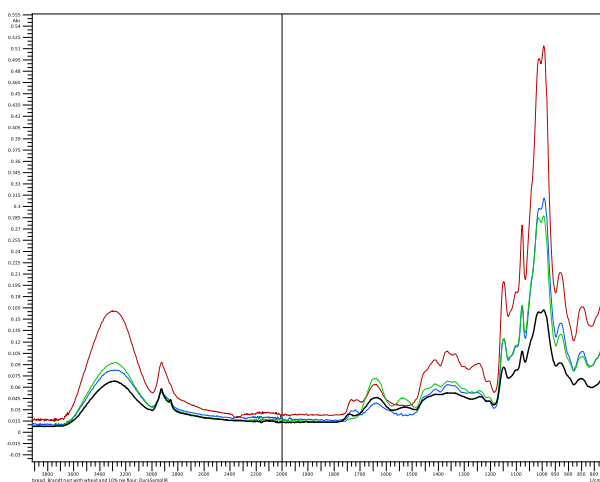

Fig. 4: Infrared spectra from crisp bread(black), oplate(green), eatable packing(blue) and packing from recycled paper(red)

As seen in figure 4 all spectra are showing the same base spectrum. Only little differences are detectable in a short range of the infrared spectra. The range which shows directly differences is shown in fig. 5.

■**Analysis of the result**

In the spectrum of the chips is missing a signal at 1540cm-1. In the range of 1700 to 1750 cm-1 is a difference in the –CO signal area. It is possible to detect the bread and to make the difference for the chip. It is as if the chip is fat free. On the other hand it seems that the chips contain some organics which are not belonging to the production of the bread and oblate shown here.

■**Instrumentation**

IRAffintiy-1

IRsolution software

DuraSamplIR

Application News

No. SCA-110-090

Coffee bean measurement under the pressure of the "Quest™" with Infrared Spectroscopy

For this application was of interest to see the infrared spectrum of a coffee bean under different hardness conditions using a single reflection ATR accessory made of diamond.

Fig. 1: Roasted coffee beans in different appearance depending on the roasting time

Coffee beans ready prepared for the coffee machines are from extraordinary hardness. By the roasting process the bean loses a lot of water, gets dry, hard and diverse brown colors (see Fig. 1). In figure 2 a short guide to bean colors gives an impression of the variation of the brewed coffee aromas which are behind the colors.

The yellow brown bean visible in the middle of figure 1 was used for this experiment. It is known that very hard material is very bad to measure with reflection techniques. In this case the focus was set to the single ATR measurement with a diamond optical element and diamond sample window.

Fig. 2: Typical colors of beans for different levels of roasting (from unroasted green, starting to pale, yellow tan, light brown, first crack, full city roast to Vienna French level).

For this measurement the QUEST™ from Specac was used. This is a full diamond single reflection accessory. The sample - the bean - was placed on top of the diamond window. With the flat anvil the bean was pressed against the diamond, the result is to see in figure 3. A very low spectrum of mainly polysaccharide and caramel products (see table 1) is visible.

Table 1: Average value of ingredients of Arabica coffee dry mass (1).

Substance	roasted coffee
Polysaccharide	35%
Lignin	3%
Fats	17%
Protein	7.5%
Caffeine	1.3%
Ash	4.5%
Caramel products	28.5%

A piece of the bean was pressed several time to the diamond window. With each repetition of the pressing procedure the piece was softer and the amount of details in the measured infrared spectrum got better. The softer part had much better contact to the diamond surface and transferred more product information into the spectrum. The

figure 3 shows three spectra, which reflect the hardness of the bean piece. The most soft bean fragment resulted in a high resolution spectrum - so far it is possible to talk about a high signal resolution in a mixture of substances shown in table 1 which resulted in a spectrum with broad signal groups.

The diamond ATR was used as a squeezer for the benefits of the spectrum resolution.
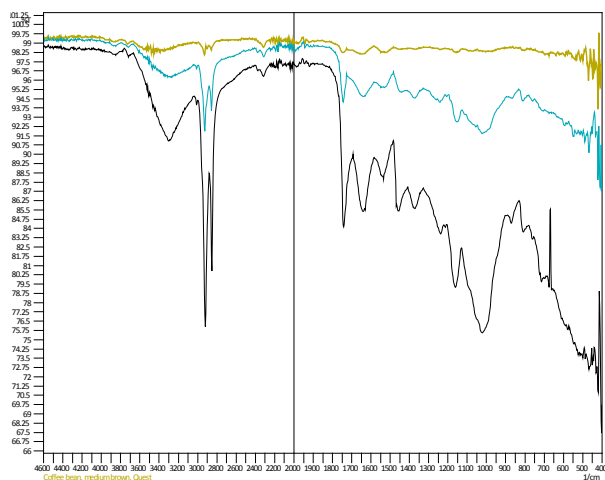

Fig. 3: Infrared spectrum of a coffee bean - hard coffee bean is the yellow-green line and the softest is presented by the black line.

Figure 3 shows clearly the growth in the signal shape caused by better sample contact to the optical element- in this case the diamond window. This is the benefits of a diamond window that it can be used for very hard material. You can press such materials directly to the surface without any chemical treatment.

■ The Quest ATR accessory

"This is an ATR accessory designed for the measurement range of 7800 to 400cm^{-1}. The ATR crystal is mounted in a durable stainless steel puck and held in place against a robust metal seal to ensure compatibility with a broad range of sample types." (2)

"Monolithic diamond ATR accessories are seen to benefit from the inherent robustness and durability of a solid diamond element, and are particularly resilient to high point loads typically encountered when analyzing hard irregularly-formed samples." (2)

Fig. 4: Single reflection ATR – The Quest, a full diamond ATR version from Specac, here shown as part of an IRAffinity-1 from Shimadzu

■ Instrumentation Package: FTIR-QUEST

IRAffintiy-1S
IRsolution software
Quest ATR accessory with monolithic diamond from Specac

■ Literature:

(1) St. Kaiser, I. Melle, H. J. Becker: *Zur Chemie des Kaffees,* Praxis der Naturwissenschaften – Chemie, 46. Jahrg. 1997, Nr. 6, S. 17–22, Aulis-Verlag; and Wikipedia, January 2013

(2) www.specac.com/userfiles/file/MD3Quest.pdf

Application News

Tea Bags in the focus of identification
Single reflection ATR measurements
With Infrared Spectroscopy

No. SCA-110-091

Tea is as hot and cold drink the next alternative to juice, water or coffee for refreshing the liquid household of the human body. Tea starts to get over the years also in Germany a strong competition to the coffee cooking. To attract possible consumers the supplier of tea work on the extraction and the presentation of the tea. A new package like a tetrahedron form is looking more exclusive than the standard bag to present the tea particles, it can have the function of an eye-catcher. The idea to use the tube form which can be used as spoon for stirring the tee is another trial. Diverse suppliers of tea invested into such new appearance of the tea.

Fig. 1: diverse tea packing from tetrahedron, stick to classical bag form from diverse suppliers

The nice appearance of the bags in all forms raised the question from what kind of material these bags are. Over the years the consumer was trained to the cellulose bags in its classical form as in Germany, pads in other countries, partly also tetrahedron forms seen in Japan. Doing the evaluation of this bags the thinking in cellulose or similar materials were the first idea.

Such identification of material can be easily done with the FTIR technique. With this analysis technique it is possible to analyze materials destroying free. The ATR measurement technique is a tool which helps to use the sample as it is. In this case simply the bags without tea particles were placed under anvil of the diamond based single reflection unit.

For this measurement the QUEST^{TM} from Specac was used. This is a full diamond single reflection accessory. The sample was placed on top of the diamond window. With the flat anvil the bag was pressed against the diamond.

Fig. 2: Single reflection ATR – The Quest, a full diamond ATR version from Specac, mounted to Shimadzu FTIR sample compartment

■Discussion of the analysis

In figure 3 are shown the reflection spectra of 5 different sources of tea bags:

1. Teekanne "Minze",
2. Teekanne Filter,
3. Bio Darjeeling, ALDI Süd
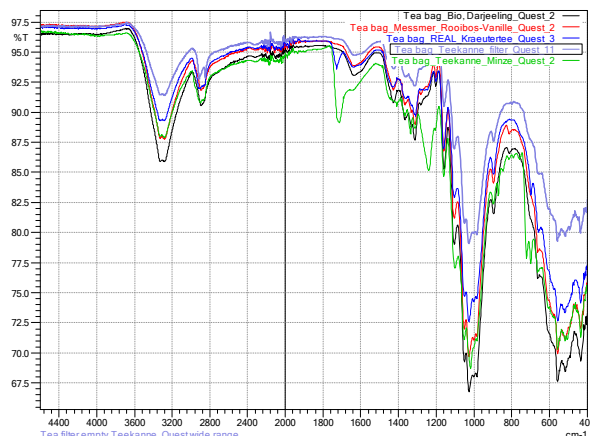4. REAL Kräutertee
5. Meßmer Rooibos Vanille

Fig. 3 Infrared spectra from 5 sources of tea bags in classical style. Two show significant differences caused by an additive (~1700cm-1 and ~1250cm-1 strong bands).

All spectra are dominated by the profile from cellulose as it is commonly used as material for tea bags. Two sources Teekanne Minze and REAL Kräutertee have an addon inside which is visible in a strong band in the CO vibration area (~1700, 1250cm-1).

Sample 2 the filter shows the expected hit quality when using the search in libraries.

Fig. 4: search result of the filter in the library collection, Cellulose was found with a match of 990. Score maximum is 1000.

The difference of the Teekanne cellulose is to see in the signals at 1716, 1333, 1240, 872, 846, 720 and 698 cm-1 which are broad and strong as well as small and sharper (Fig. 3 the green spectrum). With the subtraction of the Teekanne filter (fig.4) from the Teekanne Minze bag the following spectrum was received and this searchesd in libraries. The match is PET (Fig. 5).
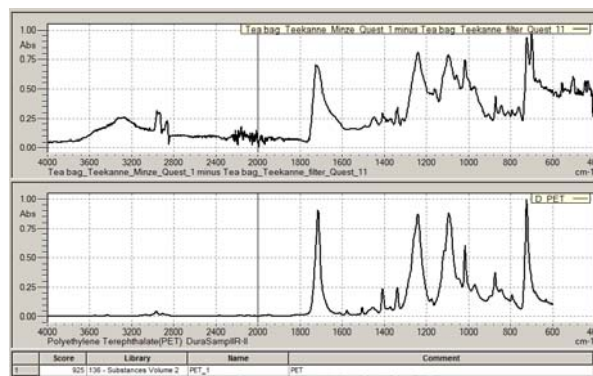

Fig. 5: Difference spectrum from two tea bags, which was used for the search in libraries, resulted in PET match with a score of 920, which is a good result.

The additive is PET as a thin layer covering the fabric. The signal size is roundabout 25 mAbs which is a very small signal

SHIMADZU

Shimadzu Europa GmbH
http://www.shimadzu.eu/home/

correlating to the thickness of the PET layer on the cellulose fabric. The penetration of the infrared beam into the fabric surface is approx. 2µm. In case the spectrum has the information from more than one substance the thickness discussion can start with having thickness of lower than 2µm. This is the discussion of the classical or regular teabags.

In the following the view is directed to the modern appearance of tetrahedron styled bags.

For this purpose several samples were collected:

1. Teekanne Assam Gold
2. Lipton Earl Grey
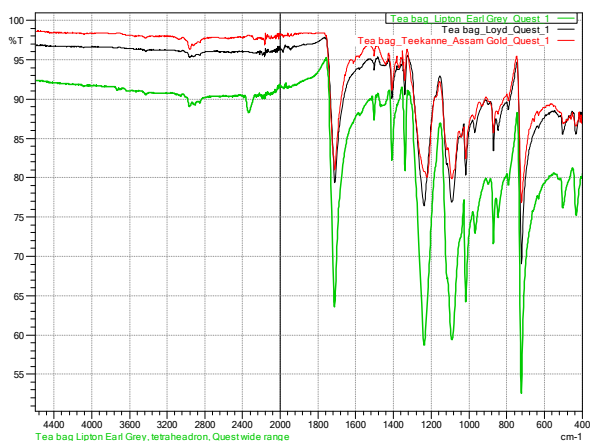3. Loyd Rosehip Apple

Fig. 6: Reflection infrared spectrum from three tetrahedron bags, the samples are from PET (polyethylene terephthalate)

In figure 6 are the infrared spectra from three bags of tetrahedron form. The baseline of the measurements is different in height. The position most nearest to the 100% of the baseline is correlating to the hardness and sum of contact to the measurement window of the accessory. By subjective view to the bags it is: red line, a more hard PET, signals are low because the contact of the PET net

from the bag is poor even when folded several times to get a more homogeneous fitting to the surface. Green line shows spectrum from the smoothest material with narrow grid lines used in the net of the bag. In this case a lot of fibers are filling up the measurement area from the diamond crystal and this result in higher spectrum signal.

■Conclusion

The infrared spectroscopy is able to identify the fiber and the polymer layer on a fiber with single reflection ATR method. It is easy and simple to handle. Very important is that the technic is destroying free in comparison to other analytical techniques in which first an extraction has to be done from the sample. Naturally with help of energy dispersive fluorescence (destroying free) or elemental analysis (AAS, ICP needs destroying) more details from such a tea bag can be evaluated. In the focus are rare earth and heavy metals in food.

■Instrumentation

- IRTracer-100
- LabSolutions IR software
- Quest ATR accessory with monolithic diamond from Specac
- Shimadzu Libraries

Application News

Spectrophotometric Analysis

Quantification of Natural Sugars in Baby Food Products by MID FTIR Spectroscopy

R.I. Clifford, Jeff Head, M.S., John Kinyanjui, Ph.D., Mark Talbott, Ph.D.

■ Introduction

No other food products focus consumer attention as those that are prepared for consumption by children. Of current interest are the natural and added sugar contents of processed baby foods and juices. Identification and quantification of natural sugars was investigated in baby food products by mid-IR Fourier Transform Infrared (FTIR) spectroscopy. Using Horizontal Attenuated Total Reflectance (HATR), neat baby food samples were analyzed without need for extensive sample preparation. By use of the HATR technique it was demonstrated that high sensitivity could be easily achieved without significant effect from water content. Factor space chemo-metric analysis was used to establish a robust method that allowed the confident measurement of sugar concentrations in these food products. The method was developed using a training matrix of three naturally occurring sugars, fructose, glucose, and sucrose. The method was confirmed using a verification matrix and was found to be readily applicable to the evaluation of sugar quantities occurring in commercial baby food products. Several commercial products were analyzed with this method and quantities of fructose, glucose, and sucrose were determined.

■ Analytical Concept – FTIR Analysis

Baby food samples pose a unique challenge for FTIR analysis because of the strong IR absorption by water. Figure 1 shows the FTIR absorption spectra of water (red) and a 5% aqueous glucose solution (black) acquired using a Horizontal Attenuated Total Reflection (HATR) accessory with a trough liquid plate.[1, 2, 3] The strong absorption bands due to water can be seen between 3800 – 2800, 1700 – 1550, and below 900 cm^{-1}. However, absorption from the glucose can be seen in the fingerprint region between 1486 and 963 cm^{-1}. This water-free absorption region suggests that quantitative sugar analysis in aqueous solutions may be feasible.
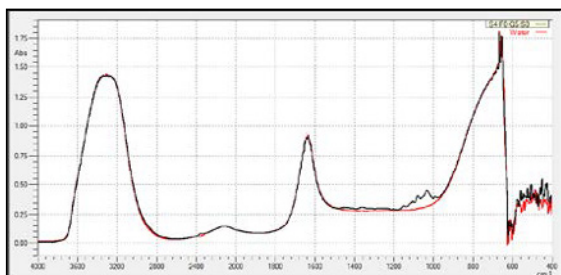
FTIR spectra of aqueous solutions of 5% fructose (blue), 5% glucose (green), and 5% sucrose (black) are shown in figure 2. The sugars have characteristic absorption bands that appear in the 1486 – 963 cm^{-1} range. The absorption bands overlap making quantitation by least squares or traditional multivariate analysis routines difficult.

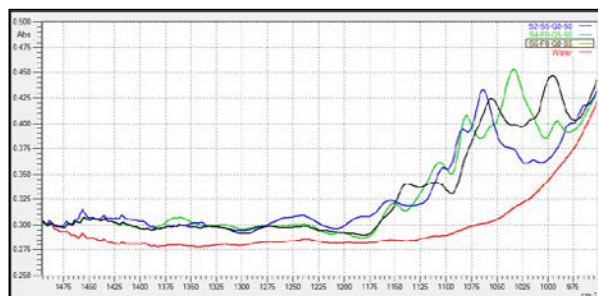**Figure 2**: FTIR spectra of 5% aqueous solutions of water (red), fructose (blue), glucose (green), and sucrose (black)

Figure 1: FTIR spectra for water and a 5% aqueous glucose

■ Analytical Concept – Factor Space

Chemometric factor-space analysis was utilized to establish simultaneous calibration curves for the three-sugar aqueous mixtures. Partial Least Squares (PLS) was selected as the factor-space routine of choice. The use of a factor-space analysis routine increased the number of dimensions in the analysis.[4] This allowed for each sugar component to be assigned to a specific dimension or factor-space. In addition, noise in the spectra (e.g. water absorption) was also treated by the additional dimensions. By using the factor-based routines, the components that attributed to analytical noise (e.g. water absorptions) could readily be identified and separated out in the quantitation.

A training set of samples was prepared to cover the full 3-dimensional quantitative space required for analysis of the baby foods. Since there were three sugar components of interest, fructose, glucose, and sucrose, a three dimensional training matrix was created (figures 3 and 4). Aqueous sugar samples were prepared to cover the eight corners of the matrix, the face centered positions of the matrix, and the matrix center.
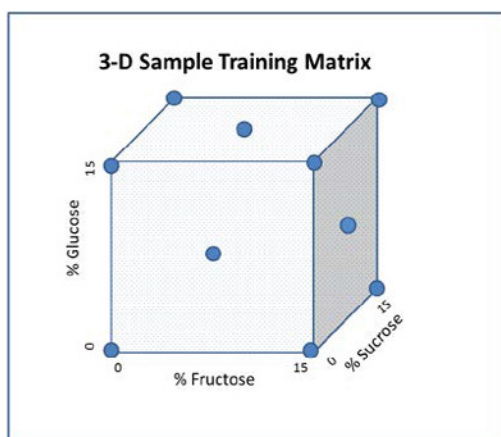

Figure 3: 3-Dimensional cube showing placement of training matrix calibration samples

In addition to the training matrix, a verification matrix (figure 5) of aqueous sugar samples was prepared using random concentrations of each of the three sugars, fructose, glucose, and sucrose. The verification matrix was used to evaluate the validity of the calibration method.

Sugar Concentration (Mass Percent)

Sample	Fructose	Glucose	Sucrose
1	0.00	0.00	0.00
2	5.08	0.00	0.00
3	10.06	0.00	0.00
4	0.00	5.00	0.00
5	0.00	10.22	0.00
6	0.00	0.00	4.97
7	0.00	0.00	9.94
8	4.92	4.91	0.00
9	0.00	5.10	4.95
10	4.95	0.00	4.91
11	10.10	10.55	0.00
12	0.00	9.83	9.88
13	10.21	0.00	10.03
14	5.10	5.06	5.04
15	10.11	9.84	9.94
16	3.84	7.83	2.68
17	7.94	5.03	1.75
18	1.83	4.67	0.73
19	0.48	2.94	3.07
20	4.95	6.39	1.47
21	3.99	2.66	7.21
22	3.56	3.53	9.63
23	4.97	4.96	9.95
24	10.13	5.05	5.05
25	4.92	9.84	4.94
26	14.95	0.00	0.00
27	0.00	14.99	0.00
28	0.00	0.00	14.72
29	15.14	15.26	0.00
30	15.31	0.00	15.24
31	0.00	15.15	15.16
32	14.97	14.98	7.59
33	14.89	7.45	14.97
34	7.53	15.14	15.21

Sugar Concentration (Mass Percent)

Sample	Fructose	Glucose	Sucrose
35	1.39	12.90	0.70
36	9.58	13.77	1.16
37	2.33	13.55	14.71
38	12.92	3.95	2.58
39	6.86	10.63	9.23
40	9.90	10.82	9.89

Figure 4 (top): Actual training matrix for aqueous sugar standards
Figure 5 (bottom): Verification matrix of random aqueous sugar standards

■ **Calibration Results**

FTIR Absorbance spectra were acquired of the training matrix standard samples using parameters of 4 cm^{-1} resolution, Happ-Genzel apodization, and the averaging of 32 scans. Figure 6 shows the spectra and demonstrates the complexity of the overlapping absorption bands.
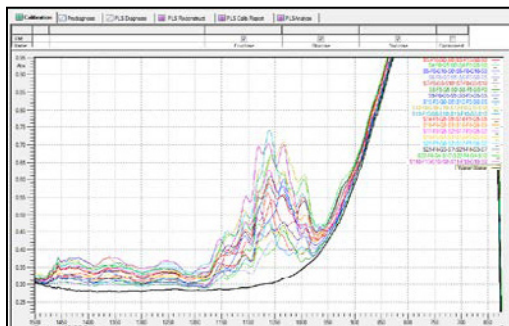

Figure 6: FTIR spectra of training matrix aqueous sugar standards

A Partial Least Squares (PLS) algorithm was utilized to establish a calibration curve for each of the three sugar components. It was found that good correlation could be achieved without the use of pre-processing methods such as smoothing, derivatives, or zero corrections. In addition, the use of five factors accounted for all of the noise in the spectra and provided good calibration curves with acceptable R^2 values (figure 7).

PLS Calibration Report			
Calibration Table:	Quant_1to25_a.irqc		
Algorithm:	PLS I		
Number of components:	3		
Number of references:	25		
Range[1]:	963.00 - 1486.00		
Preprocess:			
Scale:	None		
Component:	Fructose	Glucose	Sucrose
Number of factors:	5	5	5
Correlation coeff.:	0.999	0.9987	0.9986
Square of correlation coeff.:	0.998	0.9973	0.9973
MSEP:	0.0019	0.0026	0.0026
SEP:	0.0441	0.0506	0.0513
X Leverage warnings:	3	3	3
Y Residual warnings:	1	0	2

Figure 7: PLS Calibration Report showing R^2 values for each sugar calibration curve

To further demonstrate that the use of 5 factors was appropriate, the P Loadings for each sugar component were examined. As seen from the graphs (figure 8), the P Loading of the 5th factor resembles a random noise spectrum, suggesting that all of the spectral noise had been accounted for.
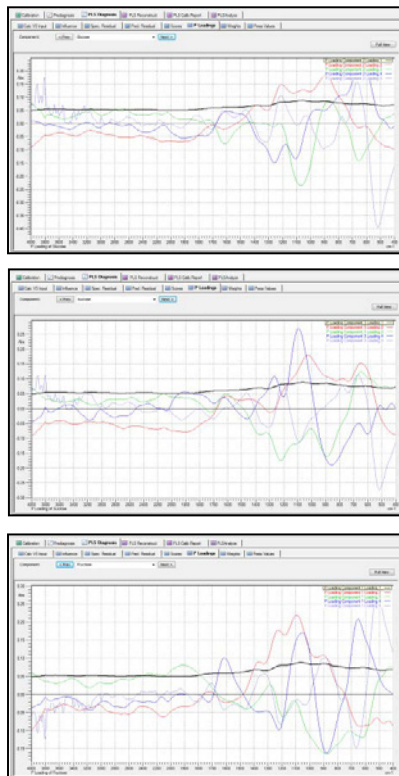
Figure 8: P Loading graphs for each sugar supporting the selection of five factors

■ **Calibration Validation**

Once the calibration curve for each sugar component were established, FTIR spectra were acquired of the verification matrix of samples using the same acquisition parameters as was used for the training matrix (figure 9).

Results of the verification matrix showed average residuals for each sugar of 0.004% and established that the calibration method was valid.

Spectrum	Fructose	Resid. 1	Glucose	Resid. 2	Sucrose	Resid. 3
S35-F1-G13-F1	1.638	0.005	13.088	0.005	1.076	0.005
S36-F10-G14-S1	9.41	0.003	14.036	0.003	1.762	0.003
S37-F2-G14-S15	1.589	0.005	13.591	0.005	15.156	0.005
S38-F13-G4-F3	12.189	0.006	3.411	0.006	2.642	0.006
S39-F7-G11-S9	6.636	0.002	10.813	0.002	9.655	0.002
S40-F10-G11-S10	9.213	0.003	11.151	0.003	10.175	0.003
Average		0.004		0.004		0.004

Figure 9: Verification Matrix results demonstrating the validation of the PLS calibration method

■ Sugar Component Analysis of Baby Foods

Commercial baby food samples from three major manufactures were acquired for fructose, glucose, and sucrose analysis. The baby foods selected consisted of pureed fruits and vegetables and fruit juices.

FTIR spectra for each baby food were acquired neat without any pretreatment using the HATR accessory and the spectral acquisition parameters noted previously (figure 10). The fructose, glucose, and sucrose sugar contents were calculated using the calibration established for each sugar from the factor-spaced analysis.
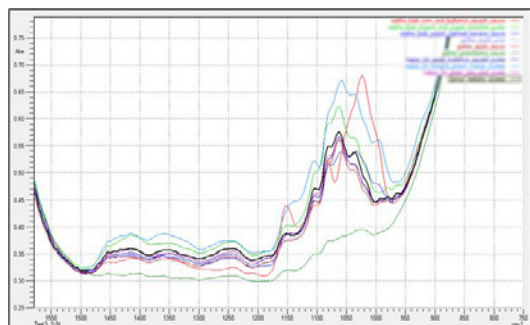

Figure 10: FTIR acquired for the neat commercial baby food samples

Examination of the calculated residuals from the calibration suggested very good fits with the various sugar calibration curves (figure 11). Baby foods that were more fruit based appeared to give better residual values, whereas baby foods that were more vegetable based generally gave higher residuals.

A total sugar concentration for each baby food was calculated from the sugar content provided on the nutrition label of each package. The calculated total sugar value from the nutritional label was compared to the total sugar value calculated from the FTIR quantitative spectral analysis. The measured total sugar values showed a high bias when compared to the reported total sugar values for all samples (figure 12).

Baby Food Analyzed	Measured % Fructose	Measured % Glucose	Measured % Sucrose	Total Measured Sugars (%)	Reported Total Sugar Conc. (%)
corn_and_butternut_squash_sauce	-3.25	10.55	4.52	11.82	2.65
organic_fruit_yogart_smoothie_puree	8.80	4.43	0.93	14.15	10.00
peach_oatmeal_banana_sauce	3.51	5.08	2.31	10.90	4.42
apple_sauce	7.01	2.79	1.45	11.24	9.73
greenbeans_sauce	0.68	2.34	0.36	3.37	2.65
banana_peach_mango_pureee	5.59	5.78	5.32	16.69	9.17
rasberry_pureee	7.12	4.29	0.66	12.06	9.17
apple_butternut_squash_puree	7.08	3.11	1.45	11.64	7.50
banana-peach-coconut_prune	6.90	7.61	3.38	17.88	10.00
green_pea_pear_puree	7.14	3.16	1.17	11.47	7.50
apple_juice	6.59	3.54	1.42	11.55	11.02

Figure 12: Total measured sugar comparison to that listed on the nutritional labels for each commercial baby food sample

Spectrum	Fructose	Resid. 1	Glucose	Resid. 2	Sucrose	Resid. 3
corn_and_butternut_squash_sauce	-3.25	0.05	10.55	0.05	4.52	0.05
organic_fruit_yogart_smoothie_puree	8.80	0.02	4.43	0.02	0.93	0.02
peach_oatmeal_banana_sauce	3.51	0.01	5.08	0.01	2.31	0.01
apple_sauce	7.01	0.01	2.79	0.01	1.45	0.01
greenbeans_sauce	0.68	0.01	2.34	0.01	0.36	0.01
banana_peach_mango_pureee	5.59	0.01	5.78	0.01	5.32	0.01
rasberry_pureee	7.12	0.01	4.29	0.01	0.66	0.01
apple_butternut_squash_puree	7.08	0.01	3.11	0.01	1.45	0.01
banana-peach-coconut_prune	6.90	0.01	7.61	0.01	3.38	0.01
green_pea_pear_puree	7.14	0.01	3.16	0.01	1.17	0.01
apple_juice	6.59	0.01	3.54	0.01	1.42	0.01

Figure 11: Measured sugar concentration results for the commercial baby food samples

■ Conclusion

FTIR Analysis, using a horizontal attenuated total reflection accessory, was demonstrated to be a suitable method to acquire FTIR spectra of commercial baby foods without sample pretreatment or concern for IR water absorption.

Chemometric Partial Least Squares (PLS) routines were used to establish and validate calibration curves for fructose, glucose, and sucrose concentrations in aqueous solutions.

Commercial baby food samples were analyzed for fructose, glucose, and sucrose sugar content. Residual data from the calibration suggested that the baby food samples were within the calibration algorithm's area of analysis. A comparison was made of the total sugars measured to those reported on the nutritional labels of the baby food packages.

This data demonstrates that FTIR analysis of baby foods offers a quick and efficient means of sugar analysis for QA/QC applications.

■ References

1. Jagdish, T., & Irudayaraj, J. (2004, June). Quantification of saccharides in multiple floral honeys using Fourier transform infrared microattenuated total reflectance spectroscopy. *J. Agric Food Chem*, *52*(11), 3237-43.
2. Tucker, M., Nguyen, Q., & Eddy, F. (2001). Fourier Transform Infrared Quantitative Analysis of Sugars and Lignin in Pretreated Softwood Solid Residues. *Applied Biochemistry and Biotechnology*, *91 - 93*, 51-61.
3. Cadet, F., & Offmann, B. (1997). Direct Spectroscopic Sucrose Determination of Raw Sugar Cane Juices. *J. Agric. Food chem.*, *45*(), 166-171.
4. Kramer, R. (1998). *Chemometric Techniques for Quantitative Analysis*. New York, NY: Marcel Dekker Inc.

First Edition: January 2014

SHIMADZU

![Shimadzu - Excellence in Science]

Application News

Spectrophotometric Analysis

Quantification and Identification of Various Sugars in Maple Syrup by MID FTIR Spectroscopy

Jeff Head, M.S., John Kinyanjui Ph.D., Mark Talbott, Ph.D.; Robert Clifford, Ph.D.

■ Introduction

Maple syrup is a commonly used sweetener that is heavily produced in the United States and Canada. Grocery stores keep their shelves well-stocked with multiple types and varieties for the average consumer. This food product can be purchased as either pure or as the cheaper alternative, which contains additives such as corn syrup. Corn syrup is a common additive to syrup products in the production process[1].

Pure maple syrup is comprised of various phenolics, flavor components, and sugars, mostly sucrose. In addition to sucrose, the sugars fructose and glucose may be present in smaller quantities. Typically, pure maple syrup contains 98% sucrose, and less than 2% fructose and glucose. Unlike maple syrup, corn syrup is comprised primarily of glucose. Figure 1 shows the FTIR spectra of the various sugars and syrups under consideration for this application news.
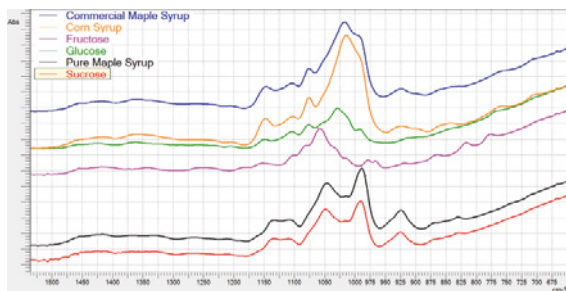

Figure 1: FTIR spectra of syrups and various sugars

Identification and quantification of natural sugars was investigated in maple syrup by MID FTIR spectroscopy. Using attenuated total reflectance (ATR) samples were analyzed with the Shimadzu IRTracer-100 FTIR spectrophotometer. Factor space chemometric analysis was used to establish a robust method that allowed the measurement of sugar concentrations in maple syrup. The method was developed and is discussed extensively in Application News No. FTIR-1401. Several types of maple syrup were analyzed with this method and quantities of fructose, glucose, and sucrose were determined.

IRTracer-100

■ Experimental

Maple syrup was diluted in water and dropped directly onto a ZnSe ATR crystal for analysis. During acquisition 32 spectra were averaged for each sample, using a resolution of 4 cm^{-1} on the Shimadzu IRTracer-100.

■ Results and Discussion

Using chemometric analysis, Table 1 summarizes the % W/W concentrations of sucrose, fructose, and glucose, present in various maple syrup samples.

For the commercial maple syrup, the amount of glucose present is significantly greater than that of the pure maple syrup, suggesting the presence of corn syrup. This is in good agreement with the ingredients label for each commercial sample which list corn syrup as a major component.

Table 1: Calculated concentrations of Fructose, Glucose, and Sucrose for various maple syrup samples

Sample ID	Sample Name	%Fructose (W/W)	%Glucose (W/W)	%Sucrose (W/W)
Vermont Sampling Kit				
1	Vermont Fancy	3.3%	0%	96.7%
2	Grade A Medium Amber	2.9%	0%	97.1%
3	Grade A Dark Amber	3.7%	0%	96.3%
4	Grade B	6.9%	0%	93.1%
Commercial Pure Maple Syrup				
5	U.S. Grade A Light Amber	0%	0%	100%
6	Grade A Medium Amber	0%	0%	100%
7	U.S. Grade A Dark Amber	3.2%	0%	96.8%
8	U.S. Grade A Dark Amber	5.8%	0%	94.2%
9	U.S. Grade A Dark Amber	8.9%	0%	91.1%
10	Grade A Dark Amber	5.4%	0%	95.5%
11	U.S. Grade A Dark Amber	6.1%	0%	93.9%
12	U.S. Grade A Dark Amber	6.4%	0%	93.6%
13	U.S. Grade A Dark Amber	0%	0%	100%
14	U.S. Grade B	4.5%	0%	95.5%
Commercial Maple Syrup				
15	Sample 1	0%	**68.1%**	31.9%
16	Sample 2	2.8%	**94.4%**	2.8%
17	Sample 3	8.1%	**87.7%**	4.2%
18	Sample 4	15.2%	**79.5%**	5.3%
19	Sample 5	23.4%	**58.9%**	17.7%

■ **Conclusion**

For the commercial maple syrup, the amount of glucose present is significantly greater than that of the pure maple syrup, suggesting the presence of corn syrup. This is in good agreement with the ingredients label for each commercial sample which list corn syrup as a major component.

This application news demonstrates that FTIR analysis is a viable tool for the quantification and identification of various natural sugars present in food products, such as maple syrup. Chemometric techniques allow for the quantitative analysis of fructose, glucose, and sucrose present, with minimal sample preparation. The IRTracer-100 coupled with an ATR accessory provides the ideal solution for any QA/QC environment requiring the quantitative analysis of components present in finished products.

■ **Reference**

1. Nollet, L.M.L. "Handbook of Food Analysis, Methods and Instruments in Applied Food Analysis". 2nd Edition, Revised and Expanded. Marcel Dekker, Inc. 2004.

4. Life Science
Lab Instruments

4. Life Science Lab Instruments

4.1 Electrophoresis

The MCE-202 "MultiNA" offers fully automated electrophoresis of DNA and RNA fragments based on reusable microchip technology. This enables not only high-speed analysis but also high separation performance and high reproducibility. Size determination and semi-quantification of any nucleic acids may therefore be used to detect biological contamination or to analyze the origin even of processed food products by genetic analysis.

C297-E080	Rapid identification of meat species with the MCE-202 "MultiNA"
SCA-210-012	Testing and analysis of genetically modified food
SCA-290-001	Identification of thunnus using PCR-RFLP method with MCE-202 "MultiNA"

Application News

Life Science

Rapid Identification of Meat Species with the MCE-202 "MultiNA"

No. C297-E080

Use of the MCE-202 "MultiNA" in combination with the Ampdirect® reagent kit not only simplifies the pre-processing and detection operations in the identification of meat species, but also enables convenient, accurate and rapid identification of each species.

■Introduction

With the increased concern over food safety and consumer awareness in recent years, there has been a demand for accurate, convenient, and rapid identification of the types of meat contained in meat food products. This need for meat species determination is met with the MCE-202 "MultiNA" DNA/RNA analyzer, which employs the multiplex PCR method.

■Results

Five types of individual meat samples (chicken, beef, mutton, pork, horse) and samples containing mixtures of these were prepared. Then, without con- ducting DNA refinement, the Ampdirect® reagent was used and PCR was performed. Results of the analysis using the MCE-202 "MultiNA" are shown in Fig. 1. The fragments were clearly separated according to species, with 218bp from chicken, 268bp from beef, 331bp from mutton, 359bp from pork, and 430bp from horse. Fig. 2 shows the results of species identification in varying mixtures of three types of meat. Detection was possible even for individual meats comprising just 1% of the mixture. It is clear that multiple species of meat can be rapidly identified with a single analysis.
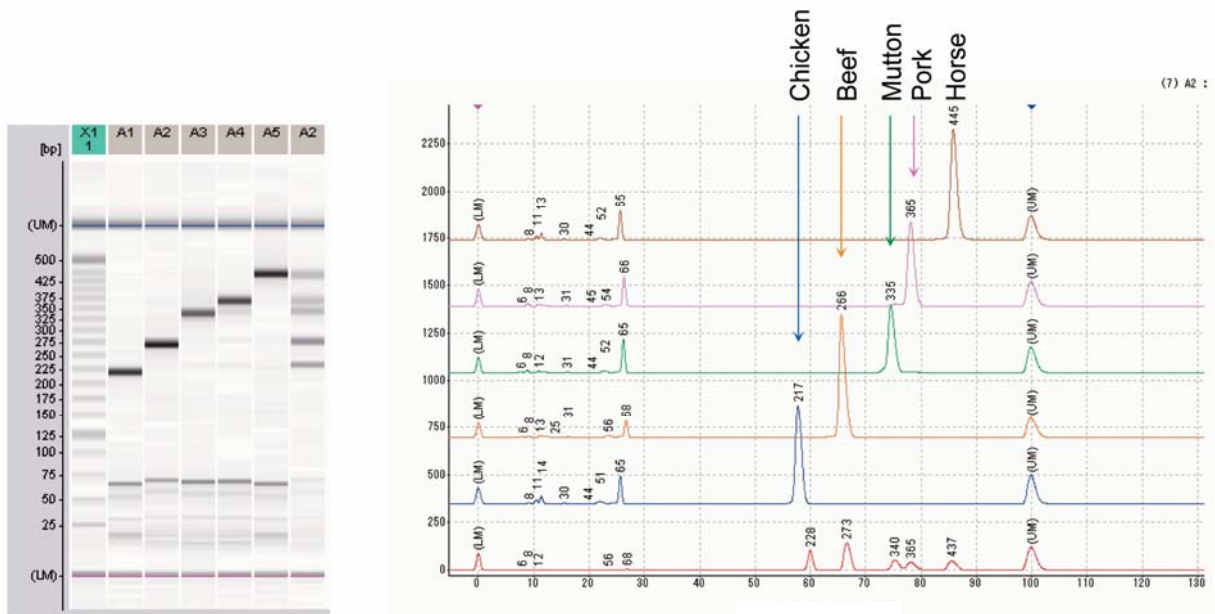

Fig. 1 Analytical results of multiplex PCR products of five meats amplified by Ampdirect®
(MultiNA gel image and electropherogram)

■Analytical Procedure

Analytical Instrument: MCE-202 "MultiNA"
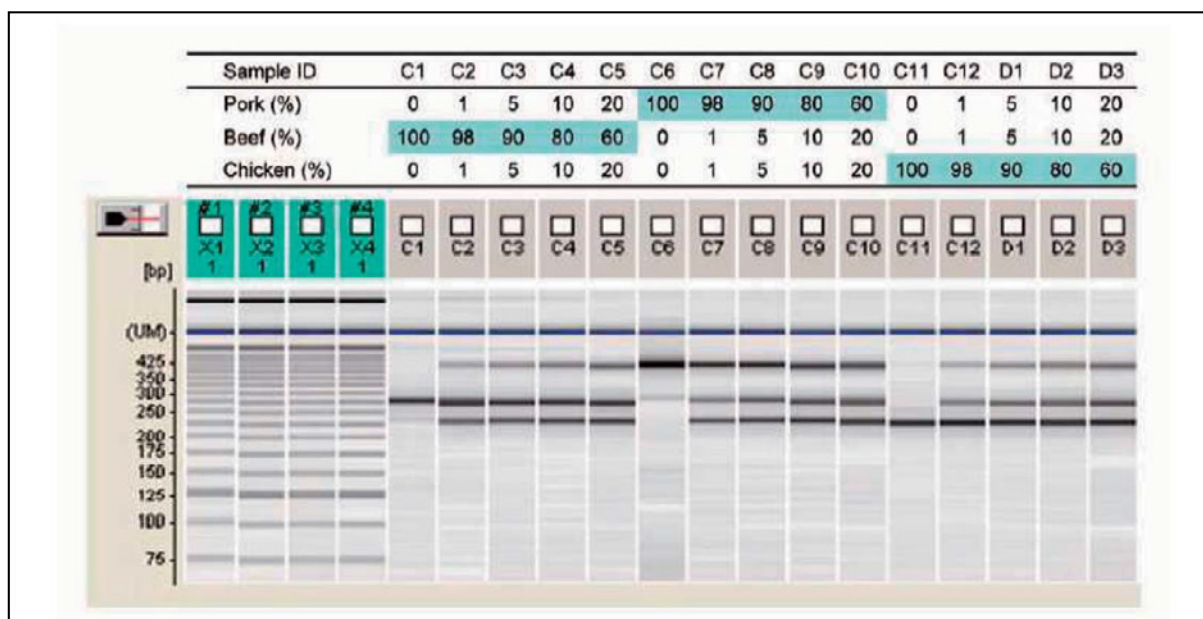Analysis Mode: DNA-500 Premix

Fig. 2 Analytical Results of Multiplex PCR Products of Three Meats at Various Mixing Ratios

PCR Primer: Based on the paper of Matsunaga, et. al. (Journal of Japanese Food Science and Engineering, 46(3), 187, 1999), some modifications were made to the base array.

Reagents:

- Ampdirect®
- DNA-500 Reagent Kit for MultiNA
  (by Shimadzu Corporation)
- SYPR® Gold nucleic acid gel stain
  (by Invitrogen Corporation)
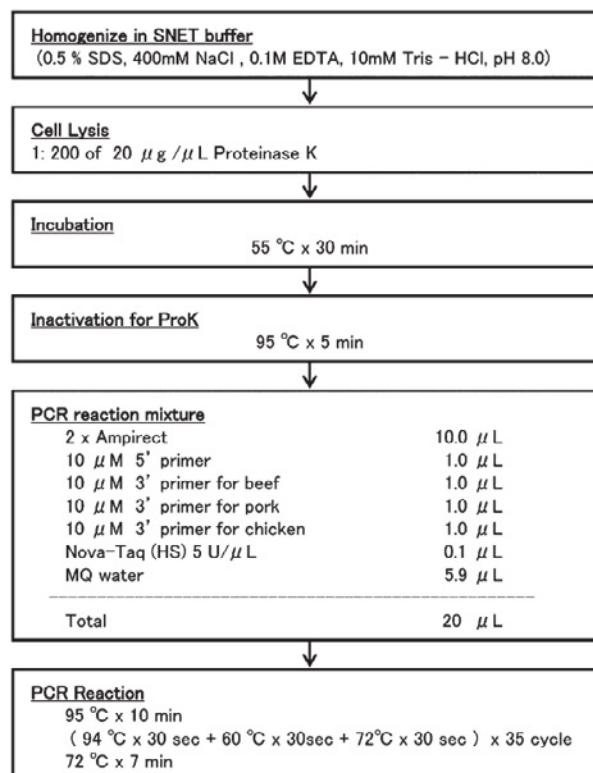- 25bp DNA ladder
  (by Invitrogen Corporation)

Fig. 3 Sample Preparation and Reaction Conditions

Application News

Life Sciences - MultiNA

Testing and Analysis of Genetically Modified Food

No. SCA-210-012

Genetically modified organism (GMO) has burgeoned over the years in order to satiate the global appetite or to add value to natural agriculture products. Technology to increase crop yields has been a constant demand, and the introduction and success of increased agricultural yield by using gene recombinant technology has indeed increased productivity in crop yields. On the other hand, the question arises as to whether these genetically modified food sources are safe to eat, and are nutritionally beneficial compared to natural products? The necessity to protect consumers while assisting agricultural food producers is a challenge for regulatory agencies globally, requiring that they keep up with quickly evolving technology and increasing genetically modified foods. In this environment, various regulations are conducted in many countries. Consumers tend to avoid such genetically modified foods though many GMO food have been approved by the safety assessment, the cultivation and circulation of foods developed using gene recombinant technology are currently rare in some countries. However, genetically modified organisms are actively cultivated globally, and large quantities of genetically modified organisms and their processed foods spread all over the world.

■ Test procedures of genetically modified foods

Analytical tests for recombinant genes in food products can be classified to qualitative testing to determine the presence or absence of genetically modified organisms (GMO) and quantitative testing to determine the ratio of genetically modified organisms to non-genetically modified organisms (GMO content). The methods adopted for qualitative testing include lateral flow immunoassay, qualitative PCR, and the GUS gene test, while quantitative PCR and ELISA (enzyme-linked immunosorbent assay) are adopted for quantitative testing.

Since the ELISA and lateral flow immunoassay methods are based on antigen-antibody reactions, they are not applicable to testing for processed foods because antigenicity is lost due to protein denaturation during heat processing, etc. DNA exhibits superior stability to protein because DNA has better thermal stability and is more tolerant to decomposition and denaturation upon heating or other processes.

■ Analysis of Genetically Modified Corn (MON810)

Here we introduce an analysis of genetically modified corn (MON810) as an example of genetically modified food analysis. After extracting DNA from 3 powdered samples consisting of genetically modified corn (MON810) having GMO content of 0 %, 1 % and 5 %, respectively, the extracted DNA from each of the samples was used as a template. PCR was then conducted using a primer for endogenous gene SSIIb-3 detection and a primer for the genetically modified MON810 detection. Electrophoretic analysis of the obtained PCR products is conducted using the 'MCE-202' MultiNA microchip electrophoresis system, and the

L : 25 bp DNA Ladder
1-3 : MON810 0 % GMO content sample
4-6 : MON810 1 % GMO content sample
7-9 : MON810 5 % GMO content sample
10 : Negative control (without template DNA)
11 : Negative control (without primer)
12 : Positive control plasmid

Fig. 1: Analysis of genetically modified corn (MON810) using MultiNA

presence or absence of PCR products corresponding to the target region is confirmed. The electrophoretic analysis of PCR product using the MultiNA are shown in Fig. 1. In analysis of the PCR products using corresponding to SSIIb-3 was detected in all of the samples except for the negative control. The endogenous gene SSIIb-3 is a gene that is specific to corn, and detection of the endogenous gene in a sample means PCR testing of the recombinant gene in that sample is effective. On the other hand, in analysis of the PCR products using the primer for the genetically modified MON810 detection, the PCR product (113 bp) corresponding to MON810 was detected in the 1 % and 5 % GMO content samples, as well as in the positive control sample.

■ **Detection of Genetically Modified DNA (GA21) in Processed Corn**

Here we introduce an example of analysis of genetically modified DNA in processed corn using qualitative PCR. DNA was extracted from 4 types of processed corn products (2 types of canned corn, 1 type of popcorn, 1 type of corn starch), and the DNA extracted from each of the samples was used as a template. PCR was conducted using a primer for the endogenous gene SSIIb detection and

a primer for the genetically modified GA21 detection. Next, the obtained PCR products were analyzed using the MultiNA. The analysis results are shown in Fig. 2. In PCR using the primer for the endogenous gene SSIIb detection, the PCR product (151 bp) corresponding to SSIIb was detected in all of the processed food samples and in the positive control plasmid. If damage to DNA derived from processed food is considerable due to heating during processing,the endogenous genes will not be detected. In samples where the endogenous gene is not detected, qualitative testing for genetically modified genes in these samples is regarded as invalid. On the other hand, in analysis of the PCR products using the primer for the genetically modified GA21 detection, the PCR product (133 bp) corresponding to GA21 was detected only in the positive control plasmid, and was not detected in the 4 types of processed food samples, which were labeled as "Non-GMO". As shown in the electropherograms of the negative and positive controls, the SSIIb gene (151 bp) and GA21 gene (133 bp) are clearly detected using only 20 copies of the positive control plasmid. Thus, high-sensitivity qualitative PCR analysis of genetically modified food is clearly achieved using the MultiNA.
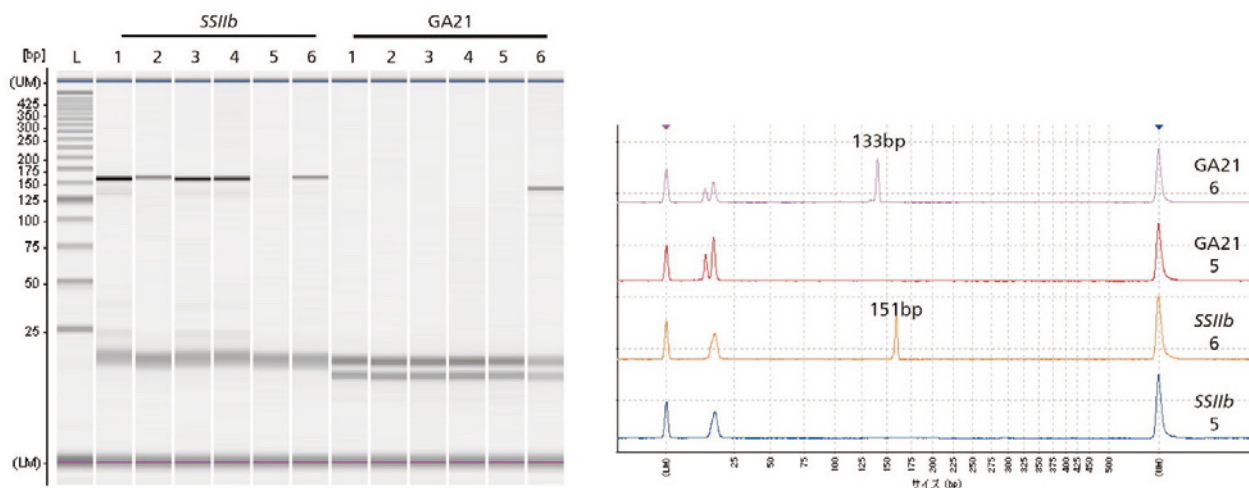
Fig. 2: Analysis of genetically modified gene (GA21) in processed corn food products using MultiNA.

Left side: Gel image showing the ladder (lane L). 4 types of processed corn food samples (lanes 1-4), negative control (lane 5) and positive control (lane 6)

Right side: electropgerograms showing the negative controls (5) and positive control plasmid (6)

MultiNA Features

High Analysis Performance
Compared with agarose gel electrophoresis, the microchip electrophoretic analysis with the MultiNA delivers excellent sensitivity, separation, repeatability and quantitation performance.

Automated Operation for up to 120 Analyses
Simply set up the samples and the separation buffer for automated analysis of up to 120 analyses. The parallel processing for analysis pretreatment and electrophoresis permits a processing speed of just 80 seconds per analysis.

Maximum Ease of Use
Analysis operation with the MultiNA is extremely simple. Just set up the analysis schedule, and then simply load the reagents and samples and click the [Start] button.

Reduce Analysis Costs
The reusable, high-performance microchip achieves lower running costs per analysis than agarose gel electrophoresis.

Application News

Identification of Thunnus Using PCR-RFLP Method with MCE-202 "MultiNA"

No. SCA_290_001

Consumer concern over food safety has steadily risen in recent years. Responding to this concern, the Japanese Agricultural Standard (Law Concerning Standardization and Proper Labeling of Agricultural and Forestry Products) was revised. The Quality Labeling Standard System was established, requiring the clear and accurate display of food product name, country of origin, etc. It is the responsibility of the manufacturer or the distributor to accurately convey this information as a product selection guideline to consumers. For example, seafood belonging to the tuna species, which is consumed in large quantities by the Japanese, is difficult to distinguish among the various types when presented in the fresh or processed seafood state. Therefore, misidentification, inaccurate labeling and disguise during the distribution process are considered to be social problems, therefore requiring a technique that can quickly, simply and accurately distinguish among product varieties. Here we introduce the procedure for distinguishing the differences among fish stock of Atlantic bluefin tuna (Thunnus thynnus), southern bluefin tuna (T. maccoyii), α and β bigeye tuna (T. obesus), yellowfin tuna (T. albacares), and albacore tuna (T. alalunga) using the PCR-RFLP (Polymerase Chain Reaction - Restriction Fragment Length Polymorphism) method as described in the manual produced by the Food and Agricultural Materials Inspection Center and the National Research Institute of Fisheries Science, Fisheries Research Agency. The MCE-202 "MultiNA" microchip electrophoresis analyzer was used for detection of the separation patterns of the PCR-RFLP products used for distinguishing the differences between these types of fish stocks.

■Experimental Procedure

The DNA extraction and PCR conditions conformed to those presented in the Manual for Distinguishing Among Tuna Fish Stocks produced by the Food and Agricultural Materials Inspection Center and the National Research Institute of Fisheries Science, Fisheries Research Agency. DNA was extracted from pieces of Atlantic bluefin

tuna, southern bluefin tuna, α and β bigeye tuna, yellowfin tuna and albacore tuna. PCR was conducted using the DNA extracted from the various types of tuna as templates. Primers specific to the tuna mitochondrial DNA were used for PCR amplification. The obtained PCR products were processed using restriction enzymes (Alu I, Mse I, Tsp509 I). Electrophoresis of the obtained enzyme digest fragments was conducted using the MultiNA, and the fish varieties were distinguished based on the differences in the fragment patterns.

■Reagents / Kits

DNA-500 Kit (Shimadzu)
SYBR® Gold nucleic acid gel stain (Invitrogen)
25 bp DNA Ladder (Invitrogen)
DNeasy Blood & Tissue Kit (Qiagen)
Alu I (New England Biolabs Japan)
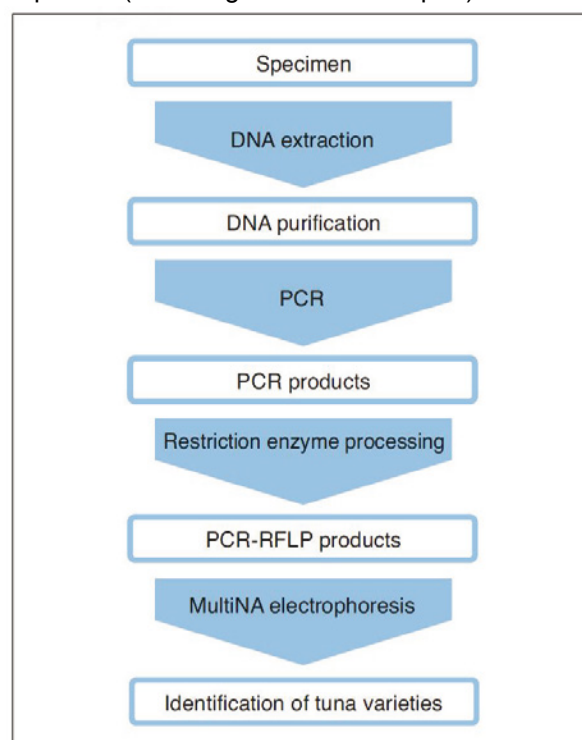Mse I (New England Biolabs Japan)
Tsp 509 I (New England Biolabs Japan)

Fig.1: Experimental procedure of identification of Thunnus using PCR-RFLP method

■**Analytical Conditions for PCR-RFLP Products**

Instrument: MCE-202 "MultiNA"
Analysis Mode: DNA-500 on-chip mode

■**Results**

Fig. 2 shows the results of analysis of the PCR-RFLP products from Atlantic bluefin tuna (Thunnus thynnus), southern bluefin tuna (T. maccoyii), α and β bigeye tuna (T. obesus), yellowfin tuna (T. albacares), and albacore tuna (T. alalunga) by MultiNA. The Atlantic bluefin tuna, β bigeye tuna, and albacore tuna show distinctive fragment patterns as a result of Alu I restriction enzyme processing, allowing them to be distinguished (Alu I processing marked with★ in Fig. 2).

However, the southern bluefin tuna, α bigeye tuna, and yellowfin tuna show the same fragmentation pattern. Therefore, we next performed restriction enzyme processing using Mse I. The southern Bluefin tuna showed a distinct fragmentation pattern as a result of restriction enzyme processing using Mse I, allowing its identification (Mse I processing marked with★ in Fig. 2). As for the remaining α bigeye tuna and yellowfin tuna, 2 types of distinct fragmentation patterns were observed as a result of Tsp 509 I restriction enzyme processing, allowing these to be easily distinguished (Tsp 509 I processing marked with★ in Fig. 2). The excellent sensitivity, separation and repeatability of the analysis data obtained with the MultiNA demonstrate that it is a powerful and fully automated tool for determining intra-species genetic variation.
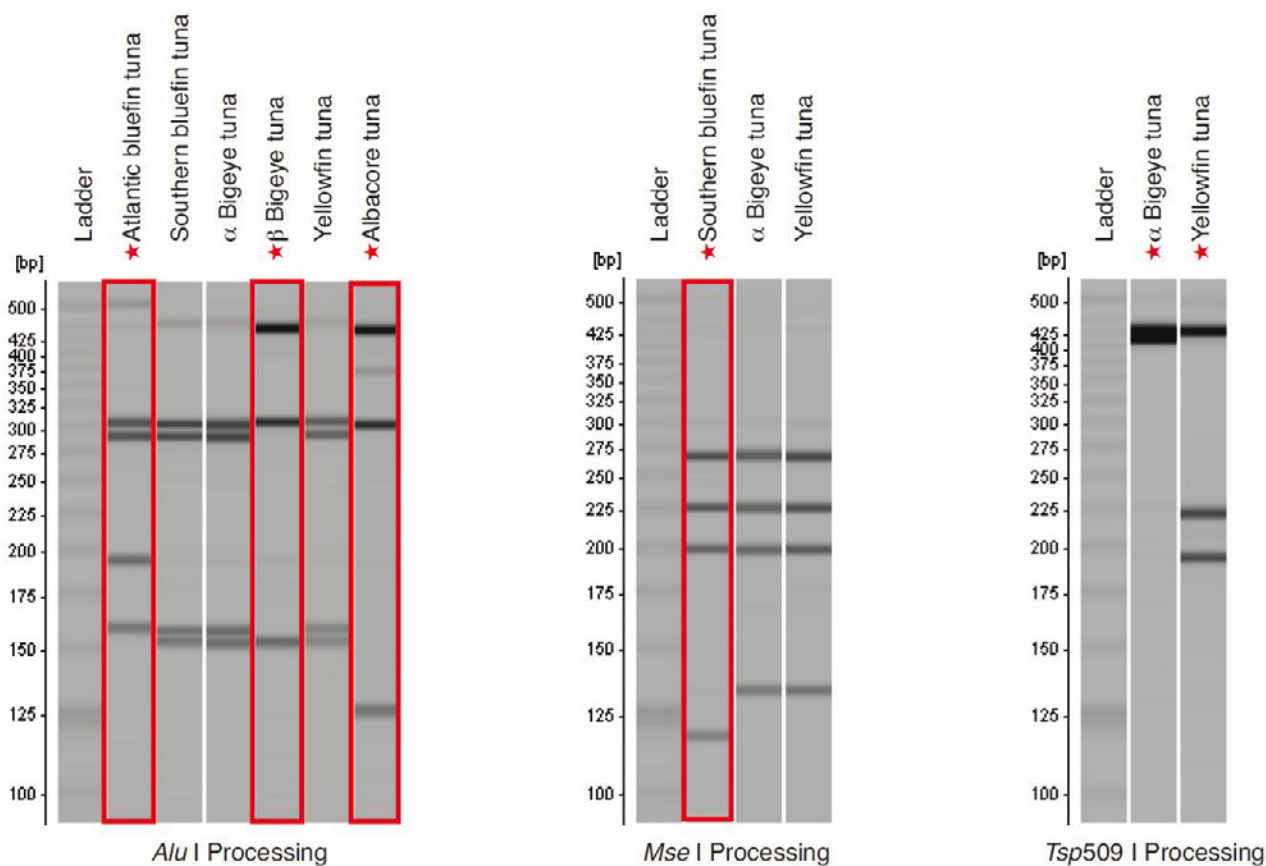
Fig.2: Analytical results for PCR-RFLP products from Thunnus

SHIMADZU

Shimadzu Europa GmbH
www.shimadzu.eu

4. Life Science Lab Instruments

4.2 MALDI-TOF Mass Spectrometry

The MALDI-TOF (Matrix Assisted Laser Desorption Ionization – Time of Flight) technology offers multiple options for profiling of proteins. This enables identification of contamination, differentiation of bacteria, fungi, yeasts and much more. MALDI-TOF can also be applied to check authenticity, e.g. profiling of milk used in dairy products. It is a robust and easy technology that fits in routine labs for quick control.

MO398   Milk and dairy product profiling using iD^{plus}

![SHIMADZU — Excellence in Science]

No.MO398 | Milk and Dairy Product Profiling Using iD^{plus}

- Foodstuff authenticity screening
- Effective detection of adulteration in dairy products
- Molecular profiling with minimal sample preparation
- Patented SuperSpectrum™ concept
- High degree of flexibility: customizable open database
- Visualization, clustering and dendrogramming tools for simple interpretation of results

Introduction

iD^{plus}™ is an established MALDI-TOF MS based platform in microbial identification but it is far from limited to this application. The flexibility of the open database associated with iD^{plus} allows the use of the platform for molecular profiling experiments and differentiation of related samples based on the unique features in their profile. New custom sample-specific entries (SuperSpectra) can be added to the existing microbial database to create a sub-database relevant to a particular area of research. This has been reported in areas as diverse as cell line identification, entomology, zooplankton research, fish speciation and the study of food-borne bacteria (ref 1-7).

Adulteration of dairy products is a significant problem in the food industry. Methods for the detection of fraudulent addition of cows' milk to other more expensive types of milk, such as goat or sheep, is important to eradicate economically motivated milk adulteration. This illegal practice, however, is not limited solely to milk production: other areas of the dairy industry such as cheese manufacture have also been targeted.

For example: the European protected designation of origin (PDO) legislation protects highly sought-after buffalo mozzarella from the Campania region of Italy (Mozzarella di Bufala Campana). While mozzarella can be made from cows' milk, it would not receive PDO certification and would be a significantly cheaper product. This has led to widespread fraudulent attempts to misrepresent cow mozzarella as buffalo mozzarella, a practice highlighted in 2010 when checks of PDO-protected Mozzarella di Bufala Campana by the ministry of agriculture in Italy found that at least 25% contained cows' milk.

This work demonstrates the effectiveness of the iD^{plus} platform for rapid differentiation of dairy products and identification of fraudulent practices. Proof of principle of this technique is demonstrated using milk profiling from several different species. The established method is then applied to foodstuff authentication using mozzarella cheese as a model product.

The SuperSpectrum Concept

SuperSpectra are database entries within the iD^{plus} database (SARAMIS™) that represent a typical population of a species or sample. They are computed from multiple mass spectra (Reference Spectra) acquired from a given sample that are combined into a consensus spectrum weighted by specificity. The weighting algorithm favors sample-specific peaks and devalues common-feature peaks, further increasing confidence when using database matching. The diagram in figure 1 illustrates the process used to create a SuperSpectrum.
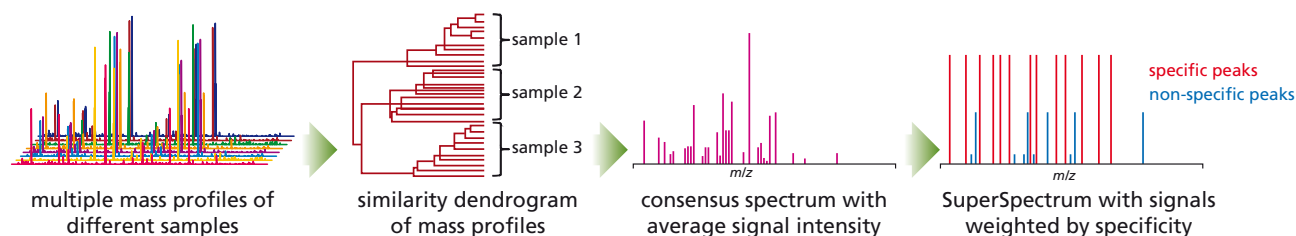
Figure 1: Creation of a SuperSpectrum

Experimental

Three types of milk (cow, buffalo and goat) and two types of mozzarella cheese (cow and buffalo) were obtained from several sources (table 1). Multiple reference spectra were acquired and combined into a characteristic SuperSpectrum for each milk product to populate a custom dairy-specific database.

Briefly, each of the milk samples was diluted 10-fold into 0.1% aqueous TFA. 1 µL of this solution was then deposited onto the target plate and left until almost dry before adding 1 µL of CHCA matrix. For the mozzarella samples, a small amount of the cheese was smeared directly onto the FlexiMass-DS™ target surface using an inoculation loop before adding 1 µL of CHCA matrix. Spectra were acquired across the m/z range 2000 to 20 000.

Product Name	Product Type	Species
Tesco Semi-skimmed	Milk	Cow
Tesco Pure Filtered Semi-skimmed	Milk	Cow
Tesco Jersey & Guernsey Cow	Milk	Cow
Delamere Sterilized Whole	Milk	Cow
Laverstock Park Semi-skimmed	Milk	Buffalo
Laverstock Park Whole	Milk	Buffalo
St Helen's Farm Semi-skimmed	Milk	Goat
Galbani	Mozzarella	Cow
Waitrose Italian	Mozzarella	Cow
Cantile	Mozzarella	Buffalo
Laverstock Park	Mozzarella	Buffalo
Garofalo	Mozzarella	Buffalo

Table 1: Summary of the milk and mozzarella samples

Results

Proof of Principle

The different types of milk analyzed (cow, goat and buffalo) generated highly taxon-specific mass profiles exhibiting many species-specific masses. Figure 2 highlights the differences observed between these profiles.
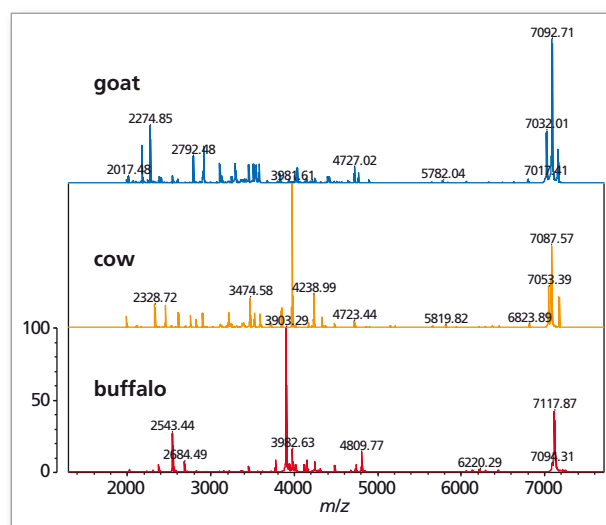

Figure 2: iD^{plus} mass profiles for goat, cow and buffalo milk

Additional samples of cow, buffalo and goat milk were analyzed and processed for cluster analysis. The dendrogram results obtained confirmed effective differentiation of the milk samples (figure 3).
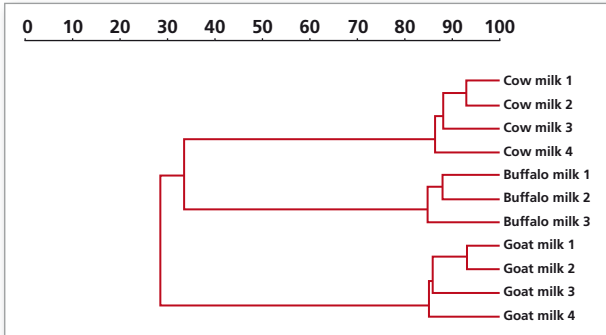

Figure 3: Cluster analysis of milk originating from cow, buffalo and goat

Food Adulteration Detection

Similarly to milk, the different types of mozzarella cheese generated distinguishable mass profiles exhibiting many product specific masses (figure 4).
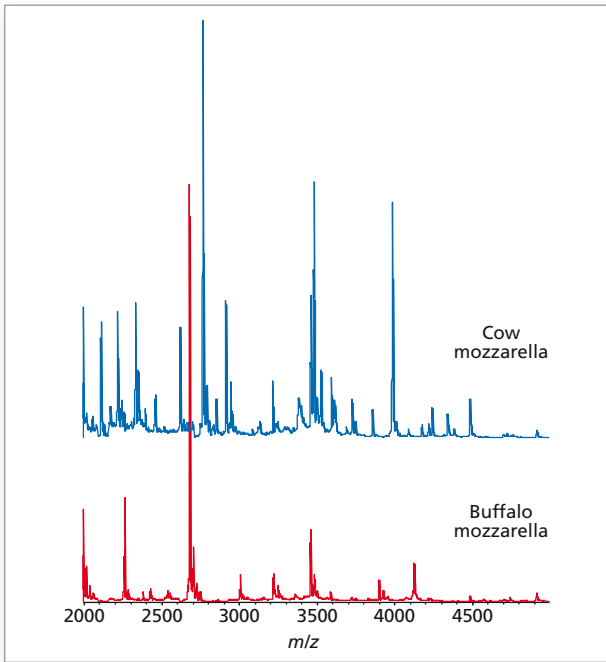

Figure 4: iD^{plus} mass profiles for cow and buffalo mozzarella cheese

To simulate adulteration of a mozzarella sample, Mozzarella di Bufala Campana cheese was mixed with cow mozzarella and prepared in the same manner as previously. The mass profile obtained for the adulterated sample is shown in figure 5 and clearly exhibits mass signals from both taxa.
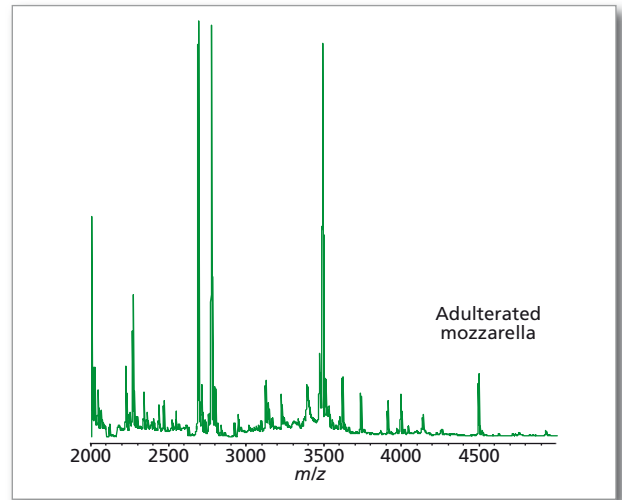
Figure 5: iD^{plus} mass profiles for adulterated mozzarella cheese

When the adulterated mozzarella sample results were submitted to search the custom dairy database an unambiguous identification was not achieved (result flagged in red in figure 6). Further inspection of the detailed result showed that the sample had matched both cow and buffalo mozzarella in the database, a clear indication of an adulterated sample (figure 6).

Figure 6: Search result confirming mozzarella adulteration

Further adulterated mozzarella samples were analyzed. Cluster analysis of the results clearly displayed three distinct groups: buffalo mozzarella, cow mozzarella and adulterated mozzarella (cow and buffalo mix) confirming that the iD^{plus} system can be applied to dairy foodstuff adulteration detection (figure 7).
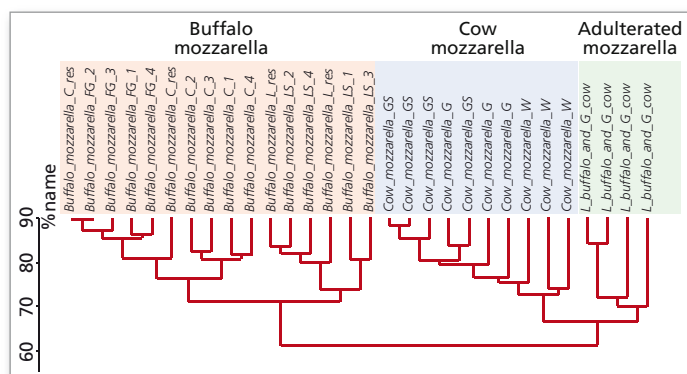

**Figure 7: Cluster analysis of buffalo, cow and adulterated mozzarella**

Conclusion

Foodstuff adulteration is a prevalent problem within the industry. It comprises both misrepresentation of products and deliberate contamination with lesser ingredients. The results shown here demonstrate effective detection of adulteration in dairy products. Construction of custom databases is straightforward and provides a very high level of confidence due to the use of the patented SuperSpectrum concept and the cluster analysis tool provides a simple graphical representation of the results obtained. The iD^{plus} is an ideal platform for simple and efficient foodstuff adulteration detection and authenticity screening.

References
(1)   Vogel *et al*, *BMC Proceedings.* 2011; **5(suppl 8)**: p45.
(2)   Muller P *et al*, *PLoS ONE.* **8(2)**: e57486.
(3)   Kaufmann C *et al*, *Parasitology.* 2012; **139**: 248-258.
(4)   Kaufmann C *et al*, *Medical and Veterinary Entomology.* 2011; **25**: 32-38.
(5)   Riccardi N *et al*, *Journal of Plankton Research.* 2012; **34**: 6, 484-492.
(6)   Volta P *et al*, *J. Limnol.* 2012; **71(1)**: 164-169.
(7)   Stephan R *et al*, *Journal of Microbiological Methods.* 2011; **87**: 150-153.

SHIMADZU

SHIMADZU Corporation

www.shimadzu.com/an/

5. Sum Parameter (TOC/TN)
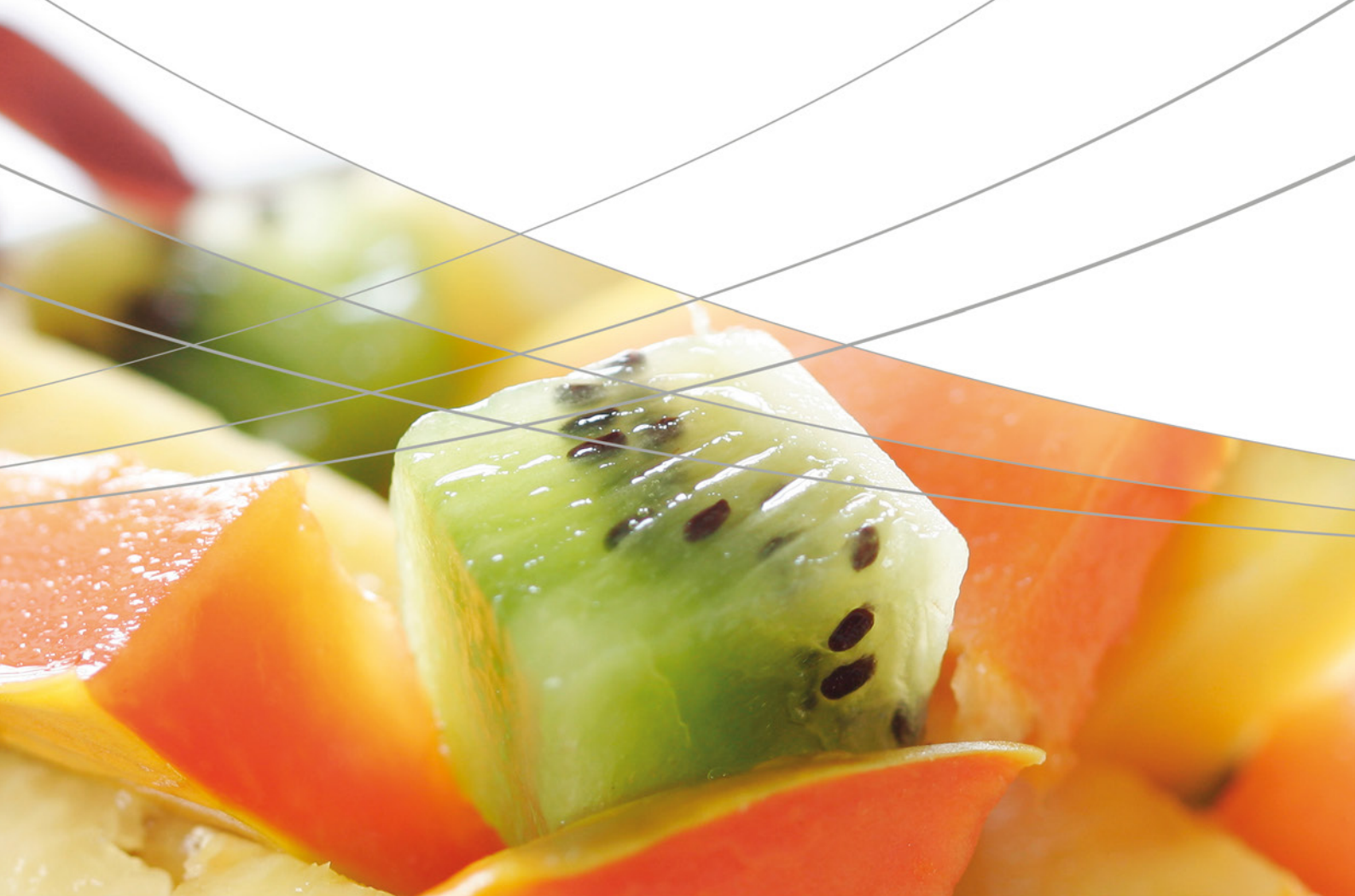
5. Sum Parameter (TOC/TN)

5.1 Total Organic Carbon Lab Analyzers

The TOC sum parameter determines organic compounds in different matrixes, especially in all kinds of water. In the food and beverage industry, water is used as solvent, product or rinsing solution. In addition, the TOC-Analyzer can help in special applications such as CO_2 determination in beer.

O47	Measurement of TOC in mineral water
SCA-130-101	TOC – determination in drinking water
SCA-130-403	Carbon dioxide determination in beer

![SHIMADZU logo] **SHIMADZU**
Excellence in Science

Application News

No.O47

Total Organic Carbon Analysis

Measurement of TOC in Mineral Water

Mineral water and soft drinks use water as their raw material, but the quality of that water may have a significant impact on the quality of the final water product.

The water quality standard of the Water Supply Act was amended in 2005 in Japan, and TOC (total organic carbon) was adopted as an indicator of organic matter in tap water. Similarly, organic matter included in mineral water and source water can also be evaluated using a TOC analyzer.

Here, we introduce an example in which the TOC-L$_{CPH}$ total organic carbon analyzer was used to conduct TOC measurements of commercially available mineral water.

Mineral Water Samples

Sample name	Source Designation
A	Deep well water
B	Deep well water
C	Spring water
D	Mineral water
E	Mineral water
F	Mineral water

■ Measurement Method

The samples, consisting of 6 types of commercially available mineral water in plastic bottles, were analyzed using the Shimadzu TOC-L$_{CPH}$ total organic carbon analyzer. The instrument was calibrated according to the "Total Organic Carbon Analyzer Measurement Method: Calibration Curve Generation" method specified in the Water Supply Act using aqueous solutions of potassium hydrogen phthalate at concentrations of 0, 0.3, 1.0, 2.0 and 3.0 mgC/L (carbon concentration 3.0 mg/L), and a calibration curve was generated. To eliminate the influence of the carbon content in the pure water used to prepare the standard solutions, the calibration curve was corrected by shifting it so as to pass through the origin.

■ Calibration Curve

The generated 5-point calibration curve is shown in Fig. 1.
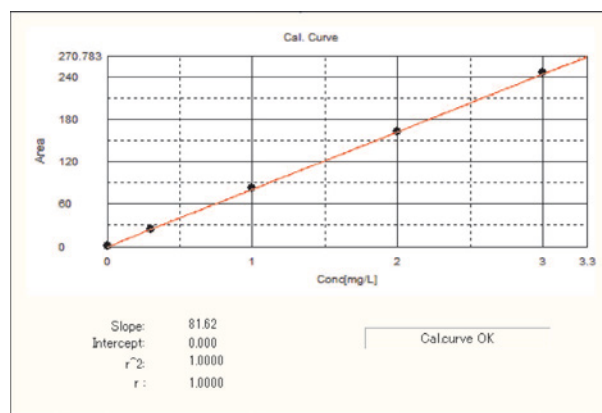
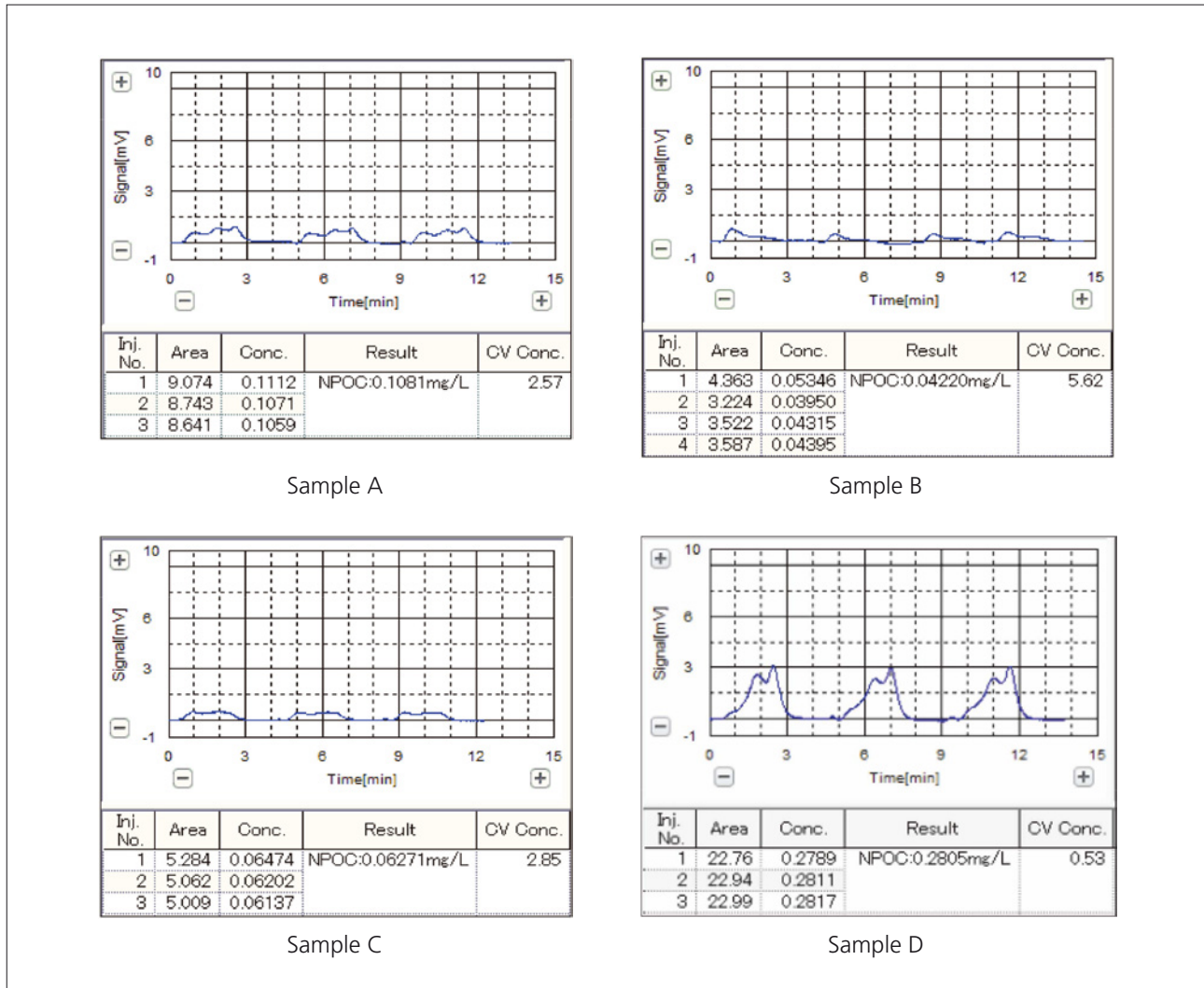**Fig. 1 Calibration Curve Data**

Measurement Conditions

Analyzer	: Shimadzu TOC-L$_{CPH}$ Total Organic Carbon Analyzer
Catalyst	: High Sensitivity Catalyst
Injection volume	: 1000 μL
Measurement item	: TOC (= NPOC: TOC by acidification and sparging)
Calibration curve	: 5-point calibration curve using aqueous solutions of potassium hydrogen phthalate at carbon concentrations of 0 – 0.3 – 1.0 – 2.0 – 3.0 mgC/L
Samples	: Commercially available plastic bottles of mineral water

■ Results

The TOC analysis results obtained using 6 types of bottled mineral water are shown in Table 1 and Fig. 2. The TOC values of the samples were low, ranging from 0.04 to 0.3 mgC/L, but the measurements were conducted with good accuracy.

Table 1 TOC Measurement Results for Mineral Water

Sample name	TOC Concentration [mgC/L]
A	0.108
B	0.042
C	0.063
D	0.281
E	0.089
F	0.333

Inj. No.	Area	Conc.	Result	CV Conc.
1	9.074	0.1112	NPOC:0.1081mg/L	2.57
2	8.743	0.1071		
3	8.641	0.1059		

Sample A

Inj. No.	Area	Conc.	Result	CV Conc.
1	4.363	0.05346	NPOC:0.04220mg/L	5.62
2	3.224	0.03950		
3	3.522	0.04315		
4	3.587	0.04395		

Sample B

Inj. No.	Area	Conc.	Result	CV Conc.
1	5.284	0.06474	NPOC:0.06271mg/L	2.85
2	5.062	0.06202		
3	5.009	0.06137		

Sample C

Inj. No.	Area	Conc.	Result	CV Conc.
1	22.76	0.2789	NPOC:0.2805mg/L	0.53
2	22.94	0.2811		
3	22.99	0.2817		

Sample D

Fig. 2 TOC Measurement Data for Mineral Water

SHIMADZU

Shimadzu Corporation

www.shimadzu.com/an/

Application News

Sum parameter – Total Organic Carbon

TOC –Determination in drinking water

No. SCA-130-101

Drinking water is one of the main important and life-sustaining food stuffs and is essential to the survival of all known organism. It is a crucial component for metabolic processes and serves as solvent for many bodily solutes. Water for human consumption must be free from pathogens, pleasant to drink and pure. Continuous monitoring is carried out according to European Drinking Water Regulation to ensure the greatest possible security

■ European Drinking Water Directive
The Directive is intended to protect human health by laying down healthiness and purity requirements which must be met by drinking water within the European Union (EU).
The directive applies to all water intended for human consumption apart from natural mineral waters and water which are medicinal products.
The European drinking water directive includes the category of indicator parameter value specifications. These are not directly linked to health problems but have an indicator function.

This list of indicator parameters also includes the TOC value (total organic carbon), which has not been assigned a limiting value or criterion but can be considered as a cautionary warning for action under unusual circumstances. Another indicator parameter included in the list is oxidizability. This is a measure for the sum of all chemically oxidizable organically bound compounds present in water.
With reference to drinking water limiting values, this parameter is no cause for direct health concern but can lead to regermination or undesirable disinfection byproducts. Oxidizability is proportional to the sum of organically bound carbons that are determined as DOC (dissolved organic carbon) or TOC. Oxidizability can therefore be replaced by the TOC parameter. The frequency of determination of the parameter indicators depends on the volume of water that is produced or released in a water supply area.

■ TOC determination in drinking water
When examining carbon compounds in drinking water, it is apparent that the amount of inorganic carbons, such as carbonates and hydrogen carbonates, is much higher than the organic fraction.

The organic fraction is only 1% of the total carbons. A TOC determination via the difference method (TOC = TC - IC) will not be appropriate in this case, as the calculated TOC value is prone to large statistical errors.

Example:
TC = 100 mg/l (RSD = 2%) ± 2 mg/l
(98 – 102 mg/l)
IC = 98 mg/l (RSD = 2%) ± 1,96 mg/l
(96,04 – 99,96mg/l)

Based on error propagation the total error is ± 3,96 mg/l

TOC (calc.) = 2 mg/l ± 3,96mg/l
(- 1,96 - 5,96 mg/l)

The total error is bigger than the TOC-result, negative results are possible.

According to European Standardization EN 1484 (instructions for the determination of total organic carbon and dissolved organic carbon), the difference method can only be applied when the TIC value (total inorganic carbon) is smaller than the TOC value.
For drinking water analysis the NPOC method (non purgeable organic carbon) is therefore used. The drinking water sample is first acidified to a pH value of 2. This way the carbonates and hydrogen carbonates are transformed into carbon dioxide. The CO_2 is then removed via sparging with carrier gas. The amount of volatile and therefore purgeable organic carbon can be disregarded in drinking water. What remains is a solution of non-volatile organic carbon compounds. These can be oxidized to CO_2 and detected via NDIR.

■ **TOC-L Series**
The sample preparation for the NPOC method (acidification and sparging) is automatically done in the TOC-L analyzer. The removing of the TIC can be performed either in the syringe of the ISP-Module or in the autosampler with the external spare kit.
The ISP (integrated sample preparation) module consists of an 8-port valve and a syringe with sparging gas connection. In addition to acidification and sparging in the syringe, the ISP also enables automatic dilution. This feature facilitates an extended measuring range, dilution of highly contaminated samples and the preparation of a series of calibration samples from a stock solution. The ISP module can therefore considerably reduce time-consuming sample handling steps.

■ **Example of drinking water analysis:**
NPOC-Method
Acidification: 1,5%
Sparge time: 5 minutes
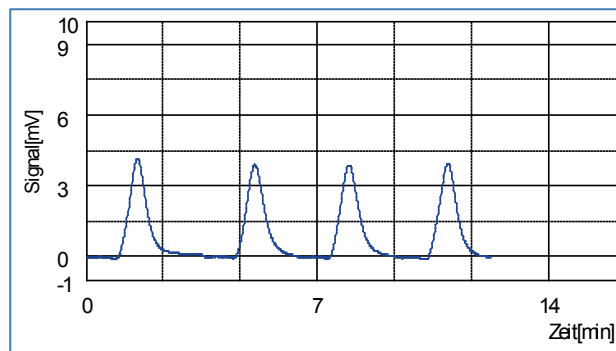
■ **Recommended analyzer / Configuration**
TOC-L $_{CPH}$
ASI-L (40ml), External Sparge-Kit.

TOC-V$_{WP}$ with ASI-V (40ml)

SHIMADZU

Shimadzu Europa GmbH
www.shimadzu.eu

Application News

Carbon dioxide determination in beer

No. SCA-130-403

Carbon dioxide is an important ingredient in many soft drinks. This is also the case for beer. It creates a sparkling and refreshing (tangy) taste and is important for the formation of foam.

The CO_2 content of a beer affects the threshold values for various fragrance and aroma components. In addition, bottling under CO_2 increases the shelf life of beer..

In the manual of the 'central- European brewery technological analysis commission)' (MEBAK) various methods for the determination of CO_2 are listed. These are generally based on manometric or titrimetric method, or they are methods that use specialized detectors.

Disadvantages of these methods are often the lack of selectivity for CO_2 (other gases or substances are also determined), high expenditure in terms of personnel and time, and the lack of possibilities for automation.

In order to develop a method that does not have these disadvantages, a TOC analyzer was used.

■ Innovative methods

In this method, the sample (beer) is directly placed in a 40 mL autosampler vial. 5 mL of a 32% NaOH solution was added to the autosampler vial to preserve the CO_2.

The sample is subsequently added directly to the autosampler and the IC (inorganic carbon) content is measured.

Preservation step:

$$CO_2 + OH^- \rightarrow HCO_3^-$$

$$CO_2 + 2\,OH^- \rightarrow CO_3^{2-} + H_2O$$
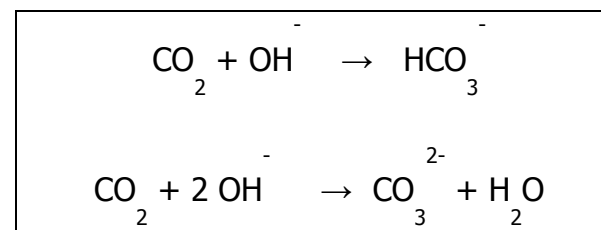
In the TOC analyzer, the sample is injected in a concentrated phosphoric acid solution (25%). The CO_2 is subsequently released again and is transferred via the carrier gas to a CO_2-selective NIDR detector where it is detected.

Displacement reaction: (the strong acid displaces the weak acid from its salt)

$$HCO_3^- + H^+ \rightarrow H_2O + CO_2$$

$$CO_3^{2-} + 2H^+ \rightarrow H_2O + CO_2$$
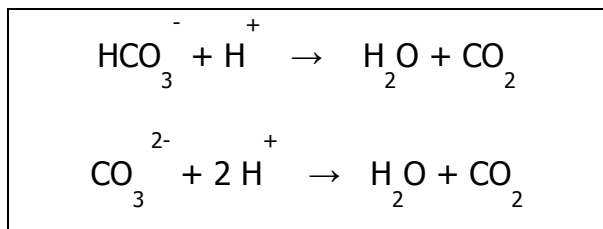
To calculate the results, the IC function of the TOC system is calibrated using a sodium hydrogen carbonate standard in the range of 100 – 1000 mg/L. The dilution of the individual calibration points is performed automatically via the dilution function of the instrument.

■ **Advantages of this method**
- can be automated to a high degree
- fast
- good reproducibility and high accuracy (precision)
- multiple determinations from one sample is possible
- effortless calibration
- simple operation
- highly specific

Using the modern TOC-L software, evaluation can be carried out automatically or can be recalculated manually. Another function enables further processing of the measurement results. This way the carbon dioxide content can be directly presented in the desired dimension. Due to the possibility for multiple injections, the evaluation contains all the important statistical quantities

Another sample preparation variant is to be carried out during the determination of carbon dioxide in bottled or canned beer. In this step, 5 mL of a 32% solution of NaOH was directly added to the freshly opened bottle or can for preservation.
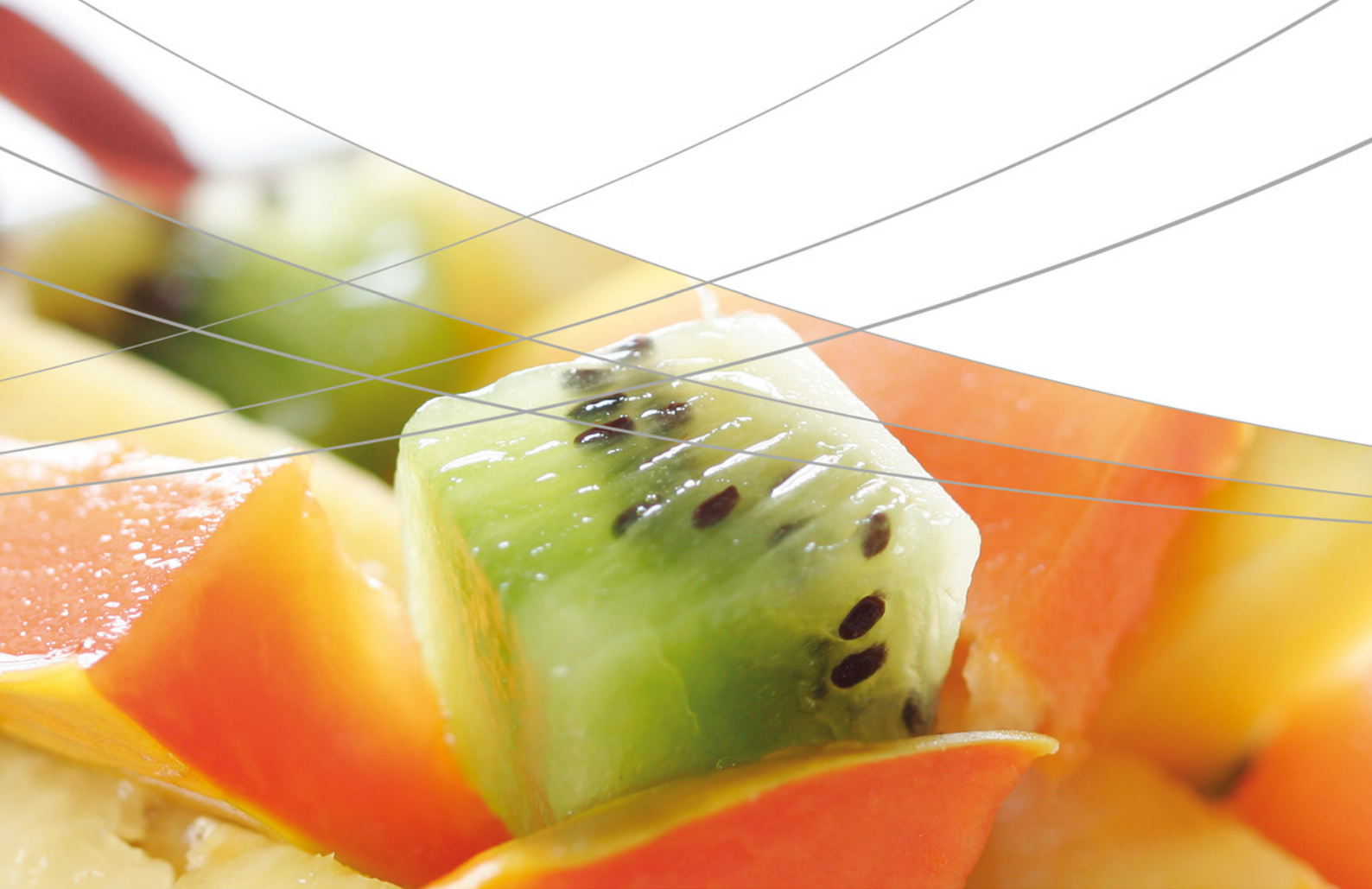
■ **Comparison of the methods**
The following graph shows the good agreement between the TOC method (blue bars) and the Corning method (green bars).
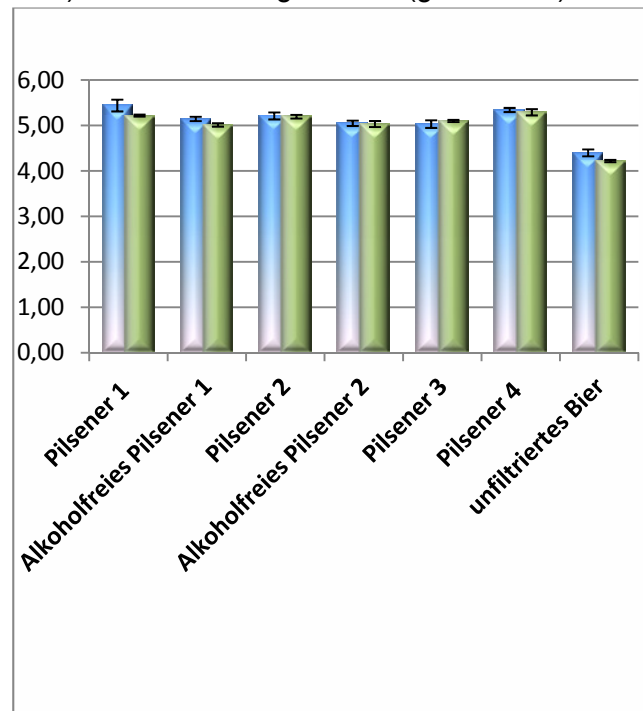
■ **Recommended Analyzer / Configuration**
TOC-L CPH
ASI-L (40ml)

6. Materials Testing & Inspection

6. Materials Testing & Inspection

6.1 Universal Testing

In addition to food flavor, another important factor that affects how good a food tastes is food texture, such as crispiness, glutinousness, feel on tooth and tongue. Shimadzu provides complete solutions including soft- and hardware to evaluate physical properties of food. Other areas of importance for testing in the food industry are packaging materials such as plastics, aluminium foils and papers.
Shimadzu has solutions for tensile and compression testing of all materials, hardness testing of metals, box compression testing tools for food container testing and much more.

No. 11	Evaluation of foods for people with dysphagia
No. 12	Evaluation of food texture

SHIMADZU
Excellence in Science

Application Data Sheet No.11	EZTest Compact Table-Top Universal Tester

Material Testing & Inspection

Evaluation of Foods for People with Dysphagia

Consumer Affairs Agency, Government of Japan, Food Labeling Notification No. 277
(Permission of Labeling for Foods for Special Dietary Uses)

Introduction

Foods for people with dysphagia are easy to swallow, and intended to prevent pulmonary aspiration and suffocation. In recent years, there has been an increase in people with dysphagia due to an aging population, so the demand for these commodities has increased. In the home medical care context, selecting appropriate meals is important, and using foods for people with dysphagia is one aspect of this. This article introduces a system for measuring hardness, adhesion, and agglomeration, evaluation items based on the Consumer Affairs Agency of Japan's Food Labeling Notification No. 277 (Permission of Labeling for Foods for Special Dietary Uses).

<div align="right">F. Yano</div>

Measurements and Jigs

Fig. 1 shows a schematic diagram of the tools used in evaluating foods for people with dysphagia. The sample is used to fill a container with a diameter of 40 mm to a height of 15 mm. Compression measurement is then done twice using a resin plunger with a diameter of 20 mm and a height of 8 mm, at a compression speed of 10 mm/sec and a clearance of 5 mm. For foods that are chilled or eaten at room temperature, the test is conducted at 10 °C ± 2 °C and 20 °C ± 2 °C. For foods that are eaten warmed, the test is conducted at 20 °C ±2 °C and 45 °C ± 2 °C.
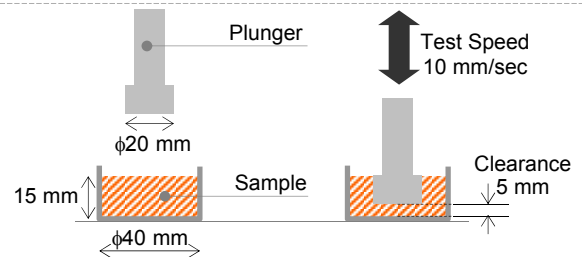

Fig. 1: Schematic Diagram of the Evaluation Test for Foods for People with Dysphagia
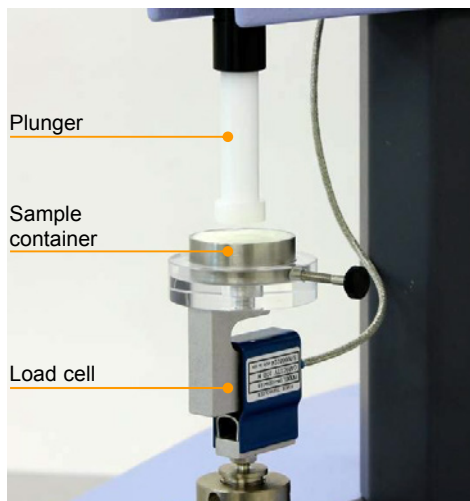
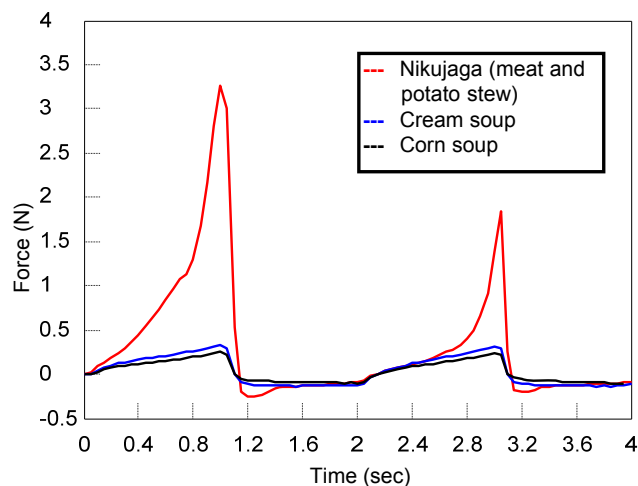## Measurement Results

Fig. 2: Food Test Evaluation Jigs

Fig. 3: Food Test Evaluation Results

Table 1: Test Conditions

Item	Set Value
Test Speed	10 mm/s
Clearance	5 mm
No. of Repetitions	2
Test Temperature	20 °C

Table 2: Test Results

Sample	Hardness (N/m^2)	Adhesion (J/m^3)	Agglomeration	Standard (judgment)
Nikujaga (meat and potato stew)	1.04×10^4	0.246×10^3	0.21	III
Cream soup	1.07×10^3	0.206×10^3	0.78	II
Corn soup	0.81×10^3	0.129×10^3	0.78	III

Evaluation System for Foods for People with Dysphagia

Tester: EZ-SX

Load Cell: 50 N

Test Jig: Universal Design Food Test Set

Software: TRAPEZIUM X Texture

Thermostat: Thermo-constant cooler/heater (separately installed)

EZTest Compact Table-Top Universal Tester

Features

■ Light and compact
  The compact size fits easily on tables. Testing can be performed in a corner of the office.

■ A high-precision load cell is adopted. (The high-precision type is class 1; the standard-precision type is class 0.5.)
  Accuracy is guaranteed over a wide range, from 1/500 to 1/1 of the load cell capacity. This supports highly reliable test evaluations.

■ Jog controller (optional)
  This allows hand-held control of the crosshead position. Fine position adjustment is possible using the jog dial.

■ TRAPEZIUM X Texture operational software
  This is the optimal software for a variety of pharmaceutical and cosmetic quality evaluations and physical characteristics measurements, as well as food texture measurements. It can create flexible control patterns and data processing items specific to foods, including hardness, brittleness, and energy.

■ A wealth of specialized jigs
  Supporting the many needs of our customers with special jigs and applications for a number of fields, including foods, pharmaceuticals, electrical machinery & electronics, and plastics.

SHIMADZU

Shimadzu Corporation

www.shimadzu.com/an/

SHIMADZU
Excellence in Science

Application Data Sheet

No.12

EZTest Compact Table-Top Universal Tester
Material Testing & Inspection

Evaluation of Food Texture

Introduction

Universal Design Foods is a term for foods that have been designed with consideration to texture or being easy to eat, and which can be used for everything from everyday meals to nursing-care foods. In Japan, with its rapidly aging society, a variety of nursing-care foods are currently available, and such meals must be suitable for patients.
The Japan Care Food Conference has established the Universal Design Foods concept, which is classified into 4 categories by hardness and viscosity. In this article, we introduce a system for measuring hardness.   F. Yano

Measurements and Jigs

Fig. 1 shows a schematic diagram of the test jigs used to evaluate the texture of foods. A cycle of compression and unloading is used to measure the hardness. Table 1 shows the relationship between the categories and the hardness upper limit values.
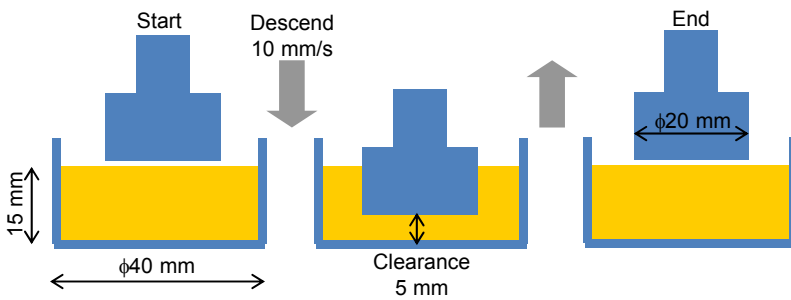

Fig. 1: Schematic Diagram of Universal Design Food Hardness Test

Table 1: Universal Design Food Categories and Upper Limit Values

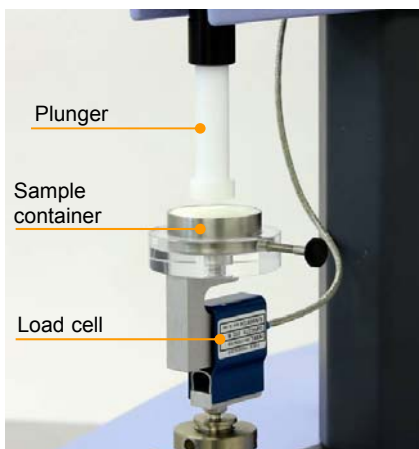| Category	Hardness Upper Limit (N/m2)
1 (Easy to chew)	5×10^5
2 (Can be broken up using the gums)	5×10^4
3 (Can be broken up by the tongue)	Sol: 1×10^4 Gel: 2×10^4
4 (Does not need chewing)	Sol: 3×10^3 Gel: 3×10^3

Measurement Results

Fig. 2: Food Test Evaluation Jigs
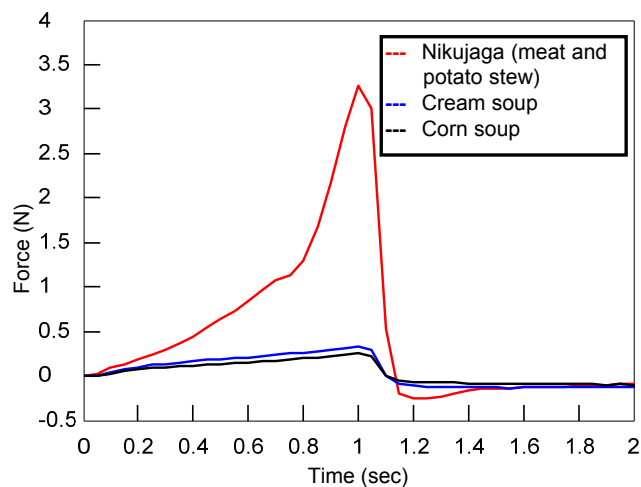
Fig. 3: Food Test Evaluation Results

Table 2: Test Conditions

Item	Set Value
Test Speed	10 mm/s
Clearance	5 mm
Test Temperature	20 °C

Table 3: Results for Food Hardness and Categories

Sample	Hardness (N/m^2)	Classification
Nikujaga (meat and potato stew)	1.04×10^4	2
Cream soup	1.07×10^3	4
Corn soup	0.81×10^3	4

Food Hardness Evaluation System

Tester: EZ-SX

Load Cell: 50 N

Test jig: Universal Design Food Test Set

Software: TRAPEZIUM X Texture

Thermostat: Thermo-constant cooler/heater (separately installed)
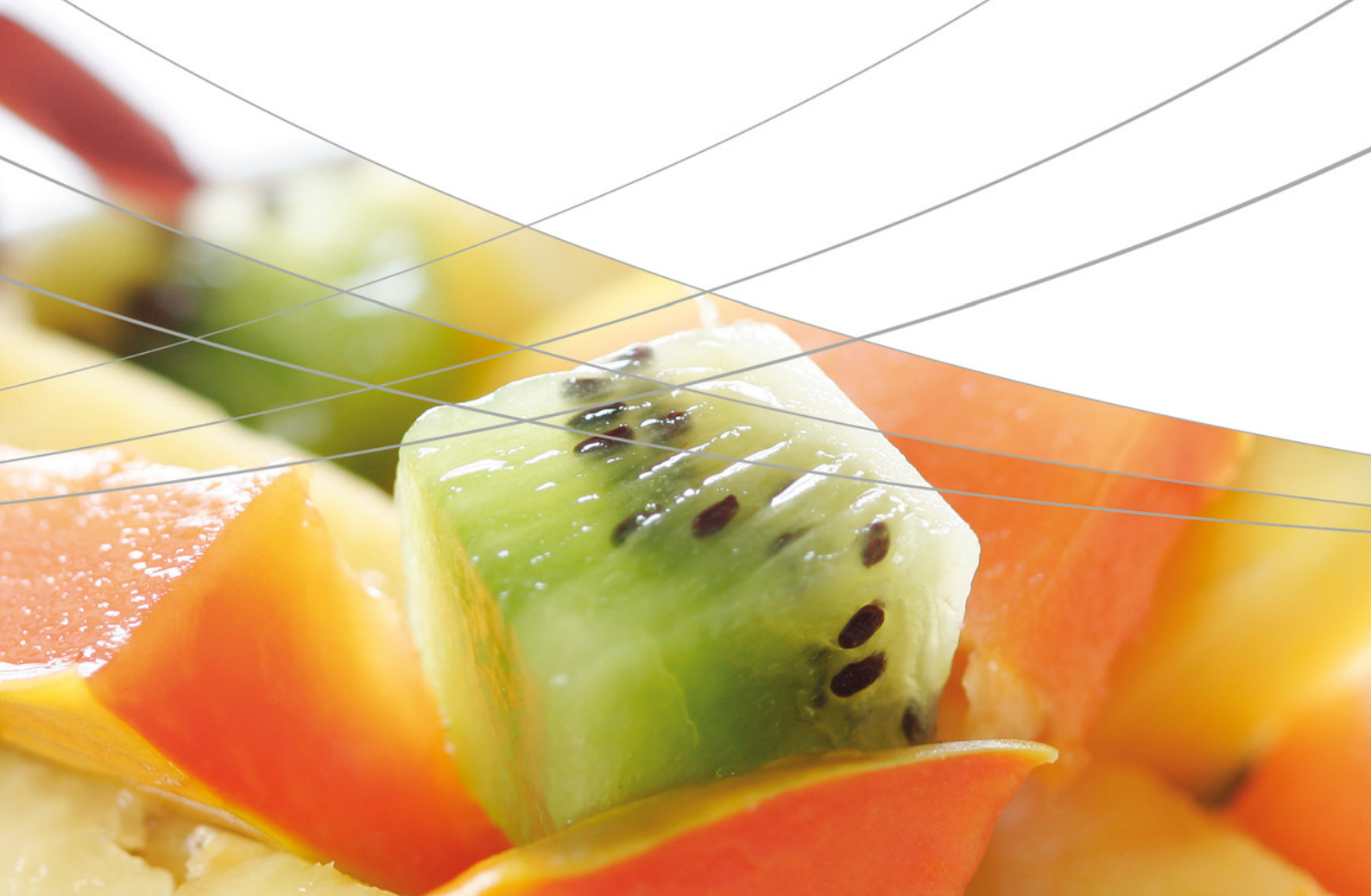
EZTest Compact Table-Top Universal Tester

Features

■ Light and compact
The compact size fits easily on tables. Testing can be performed in a corner of the office.

■ A high-precision load cell is adopted. (The high-precision type is class 1; the standard-precision type is class 0.5.)
Accuracy is guaranteed over a wide range, from 1/500 to 1/1 of the load cell capacity. This supports highly reliable test evaluations.

■ Jog controller (optional)
This allows hand-held control of the crosshead position. Fine position adjustment is possible using the jog dial.

■ TRAPEZIUM X Texture operational software
This is the optimal software for a variety of pharmaceutical and cosmetic quality evaluations and physical characteristics measurements, as well as food texture measurements. It can create flexible control patterns and data processing items specific to foods, including hardness, brittleness, and energy.

■ A wealth of specialized jigs
Supporting the many needs of our customers with special jigs and applications for a number of fields, including foods, pharmaceuticals, electrical machinery & electronics, and plastics.

SHIMADZU

Shimadzu Corporation

www.shimadzu.com/an/

7. Particle Size

7. Particle Size

7.1   Laser Diffraction Particle Size Measurement

Many food products include powdered ingredients. The mouth, tooth, and tongue feel and other characteristics of bread, cakes, pasta, etc. depend on the particle size distribution. Also, controlling the particle size distribution in beverages is important to ensure consistent quality. For example, smaller particle sizes are used in milk and lactic acid beverages to prevent differences in concentration and taste between the upper and lower portions of the container. For this reason, particle size distribution must be measured when handling powders, suspensions and emulsions.

Q112   Particle size distribution measurement of chocolate

Q113   Particle size distribution measurement of powdered young leaf blade of barley

![SHIMADZU - Excellence in Science]

Application News

No.Q112

Powder Property Analysis

Particle Size Distribution Measurement of Chocolate

■ Introduction

There are several possible parameters for expressing the taste of a piece of chocolate. For example, it can be described in terms of taste characteristics such as sweetness or bitterness, but it is also possible to characterize chocolate in terms of its texture in the mouth, for instance, how readily it melts in the mouth. Included in such parameters is "tongue texture," for which particle size distribution provides a potential index for expressing this parameter in numeric terms. This article describes the use of a SALD-2300 laser diffraction particle size analyzer to measure the size distribution of particles in chocolate. Chocolate is a mixture of cocoa mass, which consists of ground cocoa beans mixed with milk, sugar, cocoa butter, and other ingredients. This can be considered as a mixture of various particles in fat. Consequently, the particle size distribution presumably varies depending on the dispersion conditions. In this example, isopropanol at about 45 °C was used as the dispersant.

Fig. 1 SALD-2300 Laser Diffraction Particle Size Analyzer

Table 1 Measurement Conditions

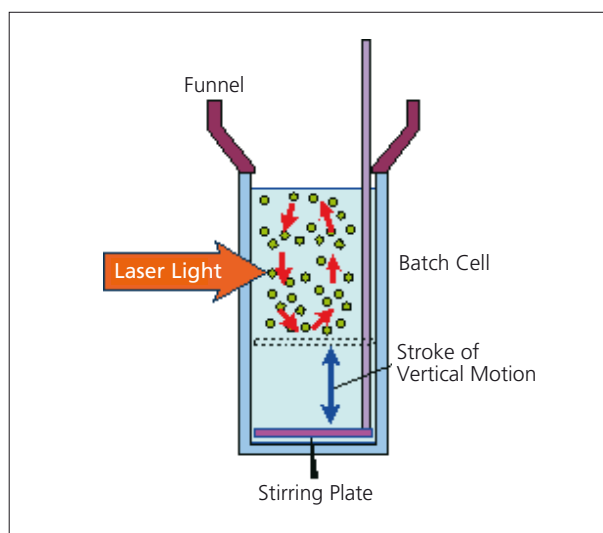|	
Dispersant	: Isopropanol (45 °C)
Dispersing Agent	: None
Dispersing Method	: Stirred using a magnetic stirrer
Refractive Index	: 1.70-0.05i

Fig. 2 Batch Cell

■ **Test Samples and Results**

Three kinds of chocolate were prepared as samples. Sample A was milk chocolate, B was milk chocolate from a different manufacturer, and C was chocolate removed from a chocolate chip cookie.

Each sample was cut into thin pieces with a box cutter knife and placed in a 50 mL beaker. Then 45 °C isopropanol was added to dissolve (disperse) the samples into a suspension, which was stirred for about 2 minutes with a magnetic stirrer. This suspension was used as the stock solution. Part of this stock solution was sampled and added to a batch cell filled with ambient-temperature isopropanol until the appropriate concentration was achieved. Figure 3 shows the particle size distribution results obtained from measurement of the samples as described above.

The results indicate that C contains larger particles than B and B contains larger particles than A. When the samples were actually eaten, the mouth texture of Sample A was extremely smooth, B was slightly less smooth than A, and C felt clearly grainy on the tongue. Put simply, the results indicate that an adequately smooth mouth texture can be achieved if all the particles are smaller than 50 μm in diameter. In contrast, chocolate containing particles with diameters larger than 100 μm clearly imparts a grainy sensation.

Of course, smoothness on the tongue is not the only factor that determines how good a chocolate product tastes, but this example shows how measuring the particle size distribution provides a measurement scale that can be used for evaluation.
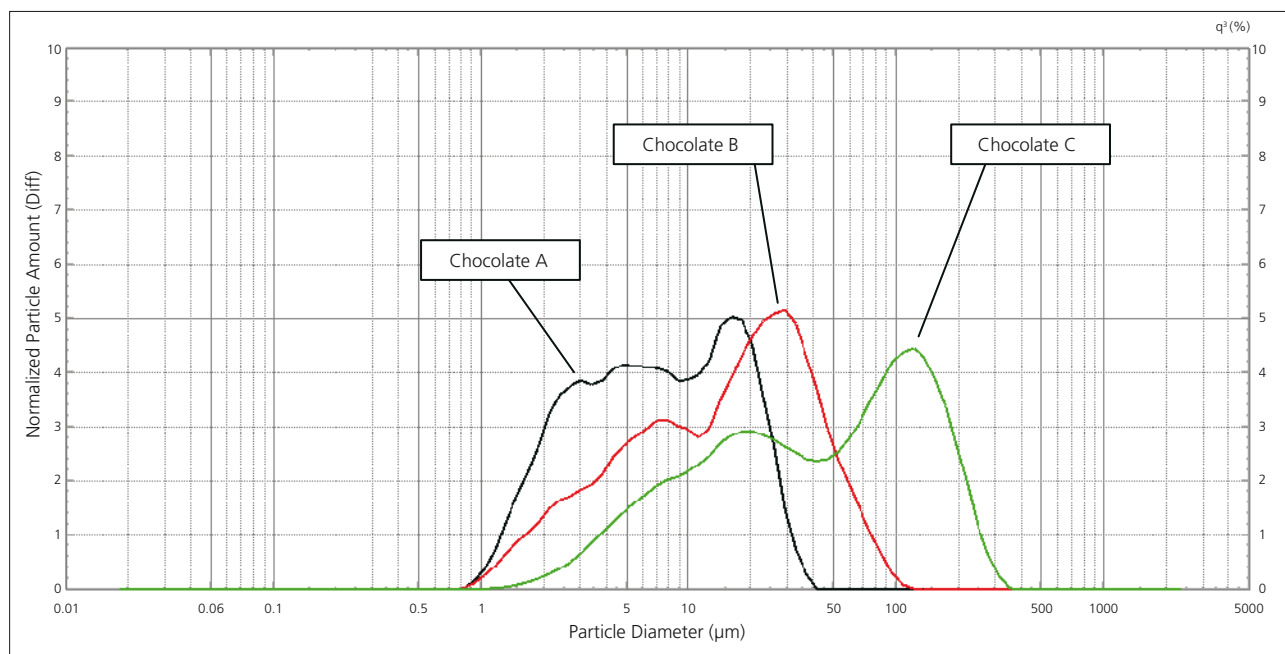
	File Name	Sample ID	Sample #	Absorbance	Refractive Index
1	A	A	bc ipa st2m	0.10	1.60-0.02i
2	B	B	bc ipa st2m	0.08	1.60-0.02i
3	C	C	bc ipa st2m	0.12	1.60-0.02i

	Median D (μm)	Modal D (μm)	Mean V (μm)	Std Dev	10 %D (μm)	50 %D (μm)	90 %D (μm)	0 %D (μm)	0 %D (μm)	0 %D (μm)	0 %D (μm)	0 %D (μm)	0 %D (μm)
1	6.969	14.994	6.771	0.377	2.049	6.969	20.764	0.000	0.000	0.000	0.000	0.000	0.000
2	15.895	30.617	13.265	0.449	2.906	15.895	45.539	0.000	0.000	0.000	0.000	0.000	0.000
3	42.862	127.664	36.861	0.534	6.351	42.862	163.880	0.000	0.000	0.000	0.000	0.000	0.000

Fig. 3 Particle Size Distributions of Several Kinds of Chocolate

SHIMADZU

Shimadzu Corporation

www.shimadzu.com/an/

Application News

No.Q113

Particle Size Distribution Measurement of Powdered Young Leaf Blade of Barley

■ Introduction

Powdered barley grass is often used in health food products. At the distribution stage, it is packaged in dry powdered form, but it is normally mixed with water, milk, or other liquids, to form a suspension for actual consumption. In other words, from the time it is shipped until it is consumed, the barley grass exists in a variety of different states.
Particle size distribution is a physical property that is dependent on the dispersion status.

Given the same sample, measurement results can differ depending on how the particles are dispersed. This article describes the results obtained from measuring the particle size distribution of the same sample in which the particles were dispersed using three different dispersion methods. Note the difference in particle size distributions, depending on the dispersion conditions. Measurements were obtained using a Shimadzu SALD-2300 laser diffraction particle size analyzer.

Wet Measurement System

Dry Measurement System

Fig. 1 SALD-2300 Laser Diffraction Particle Size Analyzer

Table 1 Measurement Conditions (wet)

Dispersant	: Purified water, Isopropanol
Dispersing Agent	: None
Dispersing Method	: Sonicated for 3 minutes in 100 W ultrasonic bath
Refractive Index	: 1.70-0.05 i

Table 2 Measurement Conditions (dry)

Injection Type	: Cyclone
Pressure	: 0.3 MPa
Refractive Index	: 1.70-0.05 i

■ Test Samples and Results

Purified water was used as a dispersant for measuring samples in a wet batch cell. Measurement conditions are indicated in Table 1. A dispersion solution was prepared in a 50 mL beaker as the stock solution. A portion of that solution was sampled, placed in a batch cell, and measured.

The measurement results are shown in Figure 2. Of the two particle size distributions, one was obtained following measurement immediately after dispersion, whereas measurement of the other was conducted about five minutes after dispersion. The results show that the particles were larger when measured five minutes after dispersion.

Next, samples were measured with isopropanol (IPA) used as the dispersant, but with all other conditions and procedures kept the same. Just as with the purified water dispersant, samples were sampled and measured twice at least five minutes apart. Unlike the purified water, however, there was no time-dependent variation in particles sizes, as shown in Figure 3.

These results suggest that the barley grass particles swell in water.

The same sample was then measured using a dry method. The sample was dispersed by spraying it as a dry powder in air, and then measured.

Figure 4 shows a comparison of results from the wet dispersion in purified water, wet dispersion in IPA, and dry dispersion methods. The results from dry dispersion were roughly consistent with the IPA dispersion results, except for the apparent presence of particle clusters included in the large particle region.

Presumably, these are from particles that dispersed in IPA, but did not quite disperse in air.

Based on the above results, the wet IPA method appears to be preferable for determining the original primary particle diameters, the dry method for determining the particle size distribution close to the dry powdered state with aggregations, and the wet water method for determining the distribution of particles close to their slightly swollen state when they are actually consumed.

Therefore, it is probably best to select the dispersion method, or even the measurement system, based on the state of the particles for which the particle distribution is to be measured.
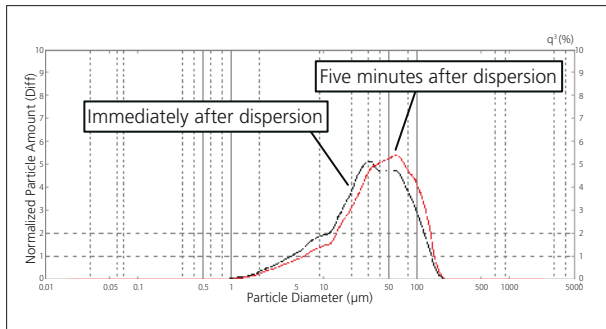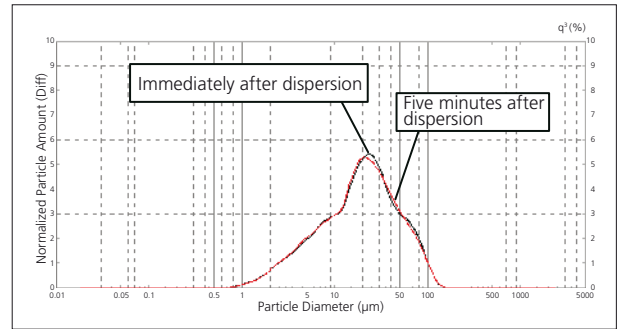

Fig. 2 Measurement Result of Barley Dispersed in Water

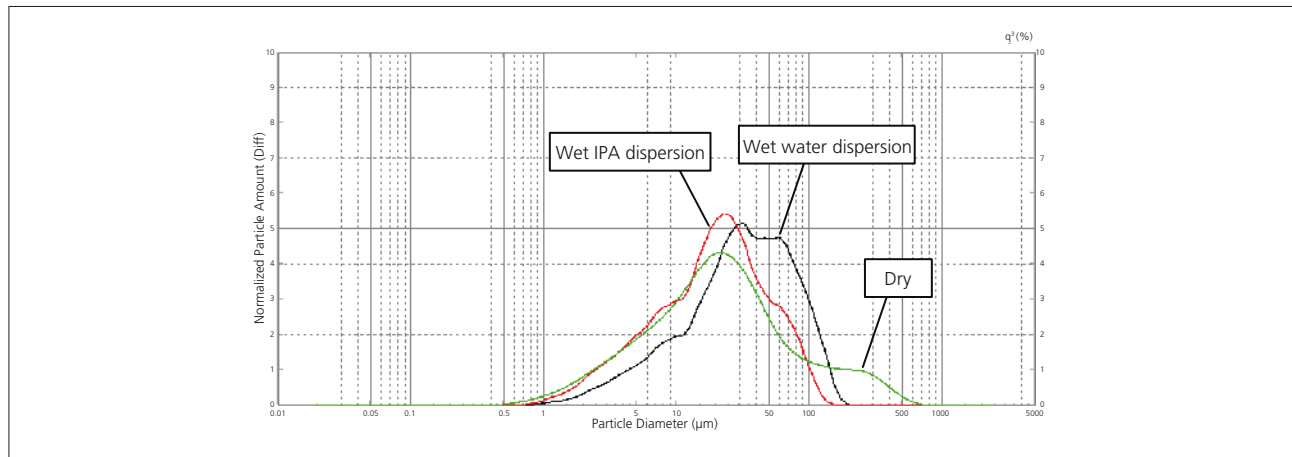**Fig. 3 Measurement Result of Barley Dispersed in Isopropanol**

	File Name	Sample ID	Sample #	Median D (µm)	Modal D (µm)	Mean V (µm)	Std Dev	Refractive Index
1	BG-2300bc-w-0001	Barley Grass		31.408	30.617	27.723	0.428	1.60-0.05i
2	BG-2300bc-IPA-0001	Barley Grass		19.476	24.133	17.262	0.433	1.60-0.05i
3	BG-2300DS5-2001	Barley Grass		20.161	19.023	20.482	0.567	1.60-0.01i

Fig. 4 Overlay Graph of Particle Size Distributions of Barley Dispersed in Different Methods

SHIMADZU

Shimadzu Corporation

www.shimadzu.com/an/

Founded in 1875, Shimadzu Corporation, a leader in the development of advanced technologies, has a distinguished history of innovation built on the foundation of contributing to society through science and technology. We maintain a global network of sales, service, technical support and applications centers on six continents, and have established long-term relationships with a host of highly trained distributors located in over 100 countries.

For information about Shimadzu, and to contact your local office, please visit our website at www.shimadzu.eu

SHIMADZU